Advances in Experimental Medicine and Biology 767

Maria Spies *Editor*

DNA Helicases and DNA Motor Proteins

Springer

Advances in Experimental Medicine and Biology

For further volumes:
http://www.springer.com/series/5584

Maria Spies
Editor

DNA Helicases and DNA Motor Proteins

Springer

Editor
Maria Spies
Department of Biochemistry
University of Iowa Carver College of Medicine
Iowa City, IA, USA

ISSN 0065-2598
ISBN 978-1-4614-5036-8 ISBN 978-1-4614-5037-5 (eBook)
DOI 10.1007/978-1-4614-5037-5
Springer New York Heidelberg Dordrecht London

Library of Congress Control Number:2012950410

Printed on acid-free paper

Springer is part of Springer Science+Business Media (www.springer.com)

Preface

A plethora of molecular motors hustle and bustle along the chromosomes of all living cells. Distinct among them are helicases, classified by the presence of the so-called helicase signature motifs in their amino acid sequences. Helicases were discovered in the 1970s and were reputed to be the enzymes that "unwind" duplex nucleic acids in an energy-dependent manner. The transient separation of DNA duplexes allows cellular machines of DNA replication, recombination, repair, and transcription to access the encoded information and is thereby an essential process required for all aspects of cellular DNA metabolism. An explosion of the helicase-related research was prompted by the paramount importance to understand at the molecular level the fundamental cellular processes that depend on helicase activities. Recent methodological advances allowed for critical breakthroughs in understanding the helicase structure and function. Numerous proteins containing the helicase signature motifs have been identified and extensively studied. Many of these proteins do, indeed, display *bona fide* strand separation activity. An important realization, however, came when the helicase family was expanded by the discovery of proteins that, despite the presence of the conserved signature motifs, lack duplex unwinding activity. It became clear that the helicase signature motifs define a generic motor core, which enables ATP- (or NTP-)driven conformational changes that allow the enzyme to translocate along nucleic acids. The mechanistic underpinnings of this process have been pondered, debated, and only recently agreed upon. Whether the same mechanism underlies "useful" activities of the helicases, however, is still an unresolved question. Unidirectional translocation of a helicase or a helicase-like translocase may be coupled to other thermodynamically unfavorable processes including separation of DNA duplexes, packaging of viral genomes, DNA segregation after replication, and disassembly and rearrangement of protein–nucleic acid complexes. The distinct mechanistic properties can be endowed to a structurally and mechanistically conserved motor core in part through unique auxiliary domains or interacting partners that provide additional functions allowing the helicase/translocase to perform a diverse set of activities. Moreover, interactions with different substrates, protein partners, and/or posttranslational modification readily convert a helicase into a translocase and a translocase into a helicase.

Each cell contains numerous DNA helicases, RNA helicases, helicase-like translocases, and molecular switches. Some of them function independently, some are integrated into larger macromolecular assemblies orchestrating complex nucleoprotein remodeling events, while others can participate in different cellular pathways guided by posttranslational modifications or by the presence of distinct interacting partners.

The field of DNA helicase research has reached a stage when the studies of molecular mechanisms and basic biology of helicases can and shall be integrated with the studies of development, cancer, and longevity. The objective of this book is to provide the first systematic overview of structure, function, and regulation of DNA helicases and related molecular motors. The chapters in this book are written by leading experts in the growing field of DNA helicase research. By integrating the knowledge obtained through diverse technical approaches ranging from single-molecule biophysics to cellular and molecular biological studies the 13 chapters comprising this volume aim at providing a unified view on how helicases function in the cell, are regulated in response to different cellular stresses, and are integrated into large macromolecular assemblies to form a complex and adaptive living system.

Wu and Spies start this volume by introducing in Chap. 1 the diverse substrates that DNA helicases act upon: duplex and single-stranded DNA, chromatin, and various nucleoprotein complexes. This chapter will also provide a historic outlook on discovery of DNA helicases, classification into superfamilies, and on the evolution of our understanding of what helicases are and what functions they perform. Chapters 2, 3, and 4 comprehensively review the state of the art in our knowledge of the structure, function, and mechanisms of translocation and duplex unwinding by major helicase superfamilies. In Chap. 3 Aarattuthodiyil, Byrd, and Raney introduce Superfamily 1 helicases; in Chap. 4 Beyer, Ghoneim and Spies Describe Superfamily 2; and in Chap. 4 Medagli and Onesti discuss hexameric DNA helicases. These chapters provide a mechanistic platform for understanding the assembly, function, and regulation of the molecular machines, which incorporate the helicase-like motor components. In Chap. 5, McGlynn describes how individual helicases introduced in the previous chapters cooperate at the replication fork to maintain an uninterrupted progression of the delicate machinery of the replisome.

One of the major consequences of cellular dependence on DNA helicases is that the absence of, or defects in, these enzymes often lead to cellular dysfunction and cause a broad spectrum of human disorders, usually characterized by premature aging, susceptibility to cancers, and other diseases normally associated with aging, immunodeficiency, or mental retardation. Expression of some DNA helicases is upregulated in proliferating cells, providing a diagnostic marker for malignant cells and presenting an attractive target for development of anticancer therapeutics. In Chap. 6 Suhasini and Brosh discuss these biomedically important helicases and their potential as targets for novel anticancer therapeutics and adjuvants of the standard treatments. Viral helicases serve as another potential drug target highlighted by the recent development of several specific inhibitors targeting the association of the helicase/primase encoded by herpes simplex virus. In Chap. 7,

Field and Mickleburgh provide an account of, so far, the only successful drug discovery campaign targeting a DNA helicase.

The next three chapters focus on the DNA helicases functioning in the cellular processes vital for maintaining the integrity of the genome. In Chap. 8, Larsen and Hickson discuss RecQ helicases, which are probably the most extensively studied family of caretaker helicases to date. In Chap. 9, Daley, Niu and Sung discuss DNA helicases and translocases that control, both positively and negatively, the processes of homologous recombination and homology-directed DNA repair. DNA helicases participating in the nucleotide excision, base excision, and mismatch repair are covered in Chap. 10 by Kuper and Kisker.

The subjects of the three final chapters are helicase-like proteins that do not require a bona fide strand separation activity to perform their cellular roles. In Chap. 11, Szczelkun highlights the similarities between some helicase-like proteins and other hydrolysis-driven molecular switches. The theme of dsDNA translocases is further elaborated in Chap. 12, where Demarre, Galli and Barre discuss FtsK, a complex motor involved in bacterial division. In the last chapter, Yodh talks about dsDNA translocating motors incorporated into the chromatin assembly and remodeling complexes.

In recent years, a number of groundbreaking structural and mechanistic studies deepened our understanding of helicase mechanisms and established new approaches for their analyses. Many fundamental mechanistic questions, however, remain to be answered. These questions range from the mechanism of force generation and mechanochemical coupling to distinct mechanisms by which the same enzyme translocates on DNA removing obstacles, unwinds DNA, and/or remodels nucleoprotein complexes. It is even less understood how the helicase motors are regulated and incorporated into a wide range of genome maintenance and repair machines.

It is our hope that this book will become a key reference to the researchers with expertise in diverse fields who study DNA helicases, inspiring collaborative and multidisciplinary approaches to many unresolved questions in the helicase field. This book will also be a useful starting point for graduate, medical, and advanced undergraduate students who look to extend their knowledge of these exciting enzymes beyond standard and often outdated textbook information. Finally, we hope that this book will provide a valuable resource for medicinal chemists seeking new targets for development of novel anticancer and antiviral therapeutics.

Iowa City, IA, USA Maria Spies

Contents

Contributors

Suja Aarattuthodiyil Department of Biochemistry and Molecular Biology, University of Arkansas for Medical Sciences, Little Rock, AR, USA

François-Xavier Barre Centre de Génétique Moléculaire, CNRS, Gif sur Yvette , Cedex, France

David C. Beyer Department of Biochemistry, University of Iowa Carver College of Medicine, Iowa City, IA, USA

Robert M. Brosh Jr Laboratory of Molecular Gerontology, National Institute on Aging, National Institutes of Health, NIH Biomedical Research Center, Baltimore, MD, USA

Alicia K. Byrd Department of Biochemistry and Molecular Biology, University of Arkansas for Medical Sciences, Little Rock, AR, USA

James M. Daley Molecular Biophysics and Biochemistry, Yale University School of Medicine, New Haven, CT, USA

Gaëlle Demarre Centre de Génétique Moléculaire, CNRS, Gif sur Yvette, Cedex, France

Hugh J. Field Queens' College, Cambridge, UK

Elisa Galli Centre de Génétique Moléculaire, CNRS, Gif sur Yvette, Cedex, France

Mohamed Karem Ghoneim Center for Biophysics and Computational Biology, University of Illinois Urbana-Champaign, Urbana, IL, USA

Ian D. Hickson Nordea Center for Healthy Ageing, Department of Cellular and Molecular Medicine, University of Copenhagen, Copenhagen, Denmark

Caroline Kisker Rudolf Virchow Center for Experimental Biomedicine, University of Würzburg, Würzburg, Germany

Jochen Kuper Rudolf Virchow Center for Experimental Biomedicine, University of Würzburg, Würzburg, Germany

Nicolai Balle Larsen Nordea Center for Healthy Aging, Department of Cellular and Molecular Medicine, University of Copenhagen, Copenhagen, Denmark

Peter McGlynn Department of Biology, University of York, York, Yorkshire, UK

Barbara Medagli Structural Biology, Sincrotrone Trieste (Elettra), Trieste, Italy

Ian Mickleburgh Department of Biochemistry, University of Cambridge, Cambridge, UK

Hengyao Niu Molecular Biophysics and Biochemistry, Yale University School of Medicine, New Haven, CT, USA

Silvia Onesti Structural Biology, Sincrotrone Trieste (Elettra), Trieste, Italy

Kevin D. Raney Department of Biochemistry and Molecular Biology, University of Arkansas for Medical Sciences, Little Rock, AR, USA

Maria Spies Department of Biochemistry, University of Iowa Carver College of Medicine, Iowa City, IA, USA

Avvaru N. Suhasini Laboratory of Molecular Gerontology, National Institute on Aging, National Institutes of Health, NIH Biomedical Research Center, Baltimore, MD, USA

Patrick Sung Molecular Biophysics and Biochemistry, Yale University School of Medicine, New Haven, CT, USA

Mark D. Szczelkun School of Biochemistry, University of Bristol, Bristol, UK

Colin G. Wu Department of Biochemistry, University of Iowa Carver College of Medicine, Iowa City, IA, USA

Jaya Yodh Department of Physics, University of Illinois at Urbana-Champaign, Urbana, IL, USA

Chapter 1
Overview: What Are Helicases?

Colin G. Wu and Maria Spies

Abstract First discovered in the 1970s, DNA helicases were initially described as enzymes that use chemical energy to separate (i.e., to unwind) the complementary strands of DNA. Because helicases are ubiquitous, display a range of fascinating biochemical activities, and are involved in all aspects of DNA metabolism, defects in human helicases are linked to a variety of genetic disorders, and helicase research continues to be important in understanding the molecular basis of DNA replication, recombination, and repair. The purpose of this book is to organize this information and to update the traditional view of these enzymes, because it is now evident that not all helicases possess bona fide strand separation activity and may function instead as energy-dependent switches or translocases. In this chapter, we will first discuss the biochemical and structural features of DNA—the lattice on which helicases operate—and its cellular organization. We will then provide a historical overview of helicases, starting from their discovery and classification, leading to their structures, mechanisms, and biomedical significance. Finally, we will highlight several key advances and developments in helicase research, and summarize some remaining questions and active areas of investigation. The subsequent chapters will discuss these topics and others in greater detail and are written by experts of these respective fields.

DNA: The Source of Genetic Information

DNA is the "blueprint of life" and stores within the necessary instructions for living cells to grow and to function. The existence of DNA has been known since 1869. It took, however, almost a century to discern DNA structure and its role in the

C.G. Wu • M. Spies (✉)
Department of Biochemistry, University of Iowa Carver College of Medicine,
Iowa City, IA, USA
e-mail: maria-spies@uiowa.edu

M. Spies (ed.), *DNA Helicases and DNA Motor Proteins*, Advances in Experimental Medicine and Biology, DOI 10.1007/978-1-4614-5037-5_1,

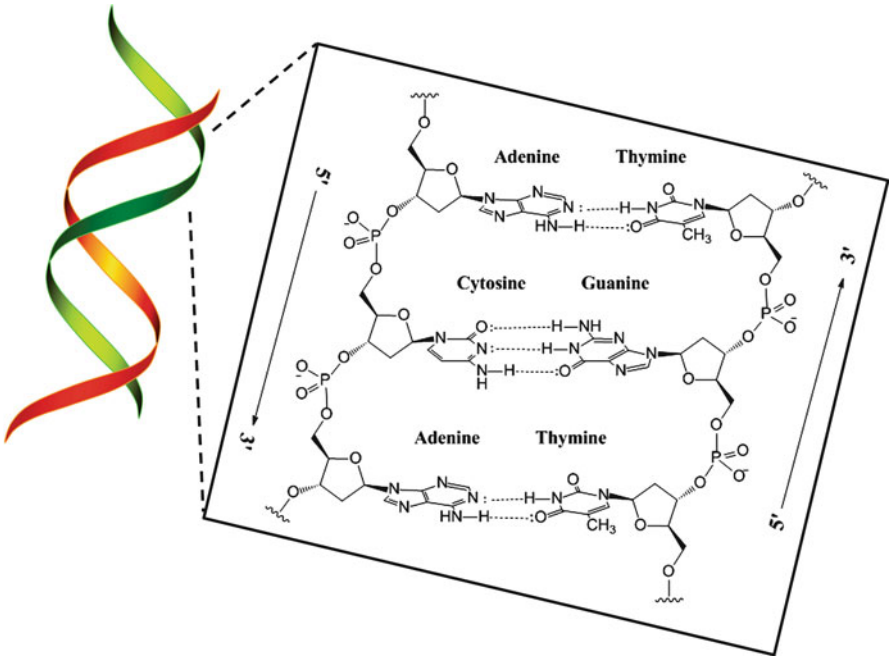

Fig. 1.1 Schematic of a DNA double helix. The two antiparallel strands of a DNA double helix are shown as *green* and *red ribbons*. The detailed positioning of the phosphate backbone, ribose sugar, and nitrogenous bases as well as the hydrogen bonding network is shown in the magnified inset

storage of genetic information. One of the first well-reasoned theoretical predictions that stimulated the search for genetic molecule can be attributed to the ideas introduced by Erwin Schrödinger in his popular book *What Is life* in 1944. Schrödinger proposed that the chromosomes, which were known at that time to be the information carriers, are the "aperiodic crystals" where covalent chemical bonds are utilized to enhance the genetic information. The search for the genetic molecule culminated in 1953 with the discovery of DNA structure by James Watson and Francis Crick [1]. In 1962, Watson, Crick, and Maurice Wilkins were awarded Nobel Prize in Physiology and Medicine for their discoveries concerning the molecular structure of nucleic acids and its significance for information transfer in living material. This information is written in a code composed of a four-letter alphabet system which must be duplicated accurately as cells divide in order to maintain genomic integrity. DNA is a polymer of nucleotides, where each building block consists of a phosphate group, a five-carbon sugar (deoxyribose), and one of four nitrogenous bases (*A*denine, *G*uanine, *C*ytosine, and *T*hymine).

The structure of DNA proposed in 1953 by James Watson and Francis Crick, and also Rosalind Franklin and Maurice Wilkins, has been paramount in facilitating nucleic acid research. The structure revealed that two strands of DNA intertwine to form a right-handed "double helix" (Fig. 1.1). The backbone of the helix is formed by alternating units of the phosphate and carbon groups while the nitrogenous bases point

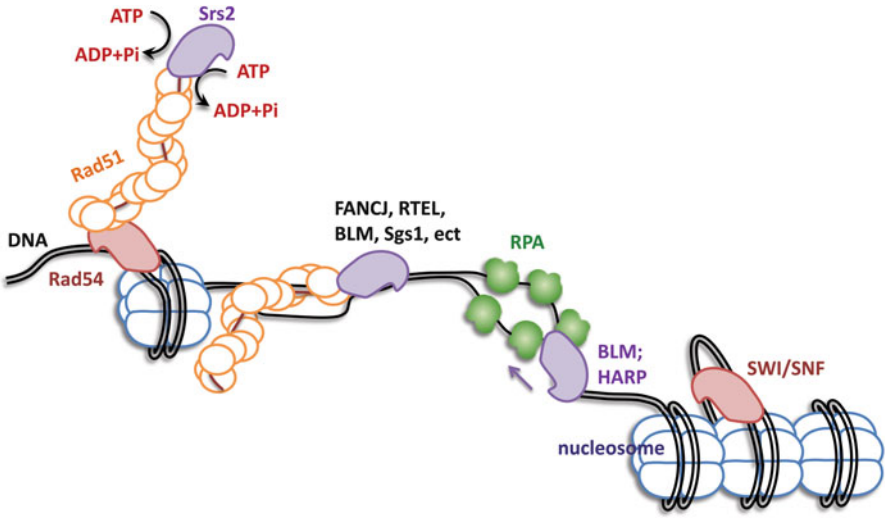

Fig. 1.2 DNA helicases, helicase-like motors, and their diverse substrates. Eukaryotic genomic DNA is organized in a chromatin, where an approximately 146 bp of DNA is wrapped around each histone octamer (*blue*), which consists of two copies of H2A, H2B, H3, and H4 histone proteins. Adjacent nucleosome core particles are tethered together by linker DNA and forms a "beads on a string" structure. Examples of other important DNA replication, recombination, and repair machinery are also shown and include SWI/SNF family chromatin remodeler, which repositions nucleosomes and enables the access to genetic information to the transcription and repair systems, DNA annealing helicases BLM and HARP, anti-recombinases Srs2, FANCJ, RTEL, BLM and Sgs1, and the Rad54 protein, which has both pro-recombinogenic and chromatin remodeling functions

towards the center of the helical axis. The sequential arrangement of these bases is how genetic information is written and stored. Only specific pairs of bases can properly bond together between the two DNA strands without perturbing the double-stranded helix (adenine with thymine and cytosine with guanine); hence, if the base sequence of one DNA chain is known, then the identity of bases on the other strand can be determined empirically. The double helix structure of DNA and the hydrogen bonding patterns of the nitrogenous bases have provided invaluable insight into how the genetic code is replicated—the two strands of the double helix must be first separated and then the replication machinery can read the sequence of the template bases and incorporate the corresponding partner bases to regenerate the DNA duplex. Although this is simple conceptually, DNA replication is highly regulated in order to maintain genomic stability. During semiconservative replication [2], the complete DNA content of the cell has to be duplicated in a timely manner and exactly once.

In addition, DNA is a large macromolecule and the human genome, which is on the order of ~3,000 million base pairs in length and arranged into 23 distinct chromosomes. To cope with its enormous length, genomic DNA is tightly packaged and stored, an arrangement that allows the control of the accessibility of this information.

DNA in each chromosome is packaged as protein–DNA complexes called chromatin, and the basic structural unit of chromatin is a nucleosome [3] (Fig. 1.2) (see Chap. 13). One purpose of these complex arrangements is to package the vast

amount of genetic material (almost 2 m in length) within the nucleus inside which space is limited (roughly 10 μm in diameter). To do so, the DNA is wrapped around a core of histone proteins in each nucleosome, much like how thread is spun around a spindle (Fig. 1.2). Histones comprise the majority of protein found in chromatin, and ~146 bp of DNA can be wrapped around each histone core in the nucleosome. These tightly arranged protein–DNA complexes condense to form chromatin and are further organized into chromosomes. As described above, access to genetic information is tightly controlled and genetic DNA is protected and stored as chromatin. These protein–DNA complexes must be "remodeled" in order to gain access to the genetic code. Chromatin assembly and remodeling will be discussed in greater detail in Chap. 13.

Cellular DNA undergoes harmful modifications every day as a result of exposure to UV light, environmental stress, and toxic chemicals. DNA damage can also result from errors during DNA synthesis. Damaged DNA must be repaired promptly and efficiently; otherwise, the replication machinery can incorporate the wrong nitrogenous base, leave nicks and gaps, and stall or disengage during subsequent rounds of DNA synthesis, resulting in deleterious mutations and chromosomal instability. The cell utilizes a number of repair pathways to prevent the loss of genetic information. The enzymes that are involved in the repair process are specific to the type of DNA damage encountered and depend on the stage of the cell cycle. Not surprisingly, defects in key components of these systems in humans are associated with a broad spectrum of disorders, usually characterized by premature aging, susceptibility to cancers, and other diseases bearing hallmarks of aging, immunodeficiency, or mental retardation (see Chap. 6). Similar to DNA replication, in order for the DNA repair machinery to gain access to the genetic code, the two strands of the double helix must first be "unwound." In some cases, because DNA is tightly packaged in chromatin, these protein–DNA complexes need to be restructured to expose the DNA region of interest. The enzymes which couple chemical energy to unwind the DNA duplex are commonly referred to as helicases. Related motors also work as chromatin remodelers, which restructure chromosome organization and thereby enabling or restricting access to DNA.

DNA Helicases: Ubiquitous Molecular Motors

The first DNA helicase, *Escherichia coli* TraI (helicase I), was purified and characterized in 1976 [4, 5]. As more helicases were identified and reported in the literature, helicase "signature motifs" were identified [6]. These highly conserved amino acid domains are involved in the binding and hydrolysis of nucleoside triphosphate (NTP), the energy source required to separate the stable double-stranded DNA (dsDNA). So far hundreds of helicases have been identified across different organisms. It is estimated that approximately 1% of the prokaryotic and eukaryotic genomes encode for proteins containing helicase signature motifs. Helicases have been classified into superfamilies (SF) and families based on amino acid patterns and the presence of the

helicase motifs, with a majority of enzymes falling into SF1 and SF2 [6]. However, this original classification scheme was developed when biochemical and structural data were limited; therefore, bioinformatics-based analysis and nomenclature often fail to provide a reliable mechanistic insight into how a helicase might function. Recently, a new classification approach has been proposed to differentiate between enzymes that move along single-stranded DNA (ssDNA) (type A) and dsDNA (type B) with either 3′–5′ (type α) or 5′–3′ (type β) directionality [7]. This book will mainly focus on discussing the features and characteristics of DNA helicases although we note that there are many enzymes that act on RNA duplexes and RNA–DNA hybrids. The properties of these RNA helicases and their role in RNA metabolism and diseases are well reviewed in the following literature [8, 9].

Mechanistic Considerations

The DNA double helix is thermodynamically stable under normal physiological conditions. Therefore, energy input is required to destabilize the duplex. Helicase activity is defined as the ability to use energy from nucleotide binding and hydrolysis to separate dsDNA into ssDNA. This unique activity is quite distinct, at least at a first glance, from duplex melting by the ssDNA binding proteins, which can destabilize short DNA duplexes transiently simply because they bind and capture ssDNA with high affinity and selectivity. A processive helicase is an enzyme that unwinds many base pairs per binding event. In contrast, a distributive helicase unwinds only a limited region of dsDNA before dissociating and typically separates the duplex by virtue of binding to it akin to the ssDNA binding proteins that destabilize duplexes exclusively at the expense of the potential energy. An important distinction, however, is that the distributive helicases still require ATP hydrolysis, which supplies the free energy to recycle the helicase and reset it for the next binding/melting event. In order for a helicase to unwind DNA processively, it must also be able to move along the DNA filament (i.e., to translocate) and couple this directional motion along the DNA lattice to strand separation activity. While processive helicase activity certainly requires processive translocation, the reverse is not necessarily true—a protein that translocates along DNA processively may not have robust helicase activity; therefore, it is more appropriate to refer to such enzymes as translocases. Examples of such motors include the *E. coli* Rep and UvrD enzymes as well as *Bacillus stearothermophlius* PcrA [10–13], which are reviewed in Chap. 2 as well as dsDNA translocases reviewed in Chaps. 12 and 13. Since helicases are identified and classified based on the presence of conserved signature motifs, it is not known whether a helicase would have bona fide strand separation activity or translocase activity solely based on amino acid patterns. In fact, it is now evident that there are some enzymes that are classified as helicases but function instead as molecular switches and remodel protein–DNA complexes without moving along nucleic acid, while others act on substrates that are not nucleic acids at all [14–16]. Hence, the presence of these conserved helicase motifs only designates these enzymes as

nucleic acid-stimulated NTPases, and their exact function(s) must be examined experimentally.

Processive DNA unwinding requires a helicase to undergo a series of repeated "steps" along the DNA lattice until the duplex is fully unwound [17, 18]. Each step involves a number of processes such as NTP binding, hydrolysis, phosphate release, base pair melting or capturing of the spontaneously melted bases, and translocation. The physical step size of a helicase is defined as the mean distance change of the center of mass of the enzyme in between two repeated rounds of DNA unwinding or per NTP molecule hydrolyzed. This is a useful and informative parameter because it not only gives a helicase a physical characteristic but also provides a mechanistic constraint for its function. However, it is not always possible to measure the physical step size directly since high resolution techniques and a suitable helicase model system are both required. Using high precision single-molecule approaches, the kinesin motor has been shown to take discrete 8 nm steps along microtubules [19]. Similar optical trapping methods have revealed that the Hepatitis C virus (HCV) NS3 RNA helicase takes large steps of about 11 bp and that DNA unwinding occurs in smaller ~1 bp substeps [20]. Alternatively, DNA unwinding can also be expressed as a multistep process involving the cycling of a series of repeated rate-limiting steps. Since it is not known a priori which physical process is rate limiting in the unwinding mechanism (e.g., NTP binding, base pair melting, translocation), the kinetic step size refers to the average movement of the enzyme in between two successive rate-limiting steps of the reaction. While they are conceptually similar, the kinetic step size could differ from the physical step size [21]. For example, a helicase can unwind DNA in discrete physical steps of 1 bp per step but may need to undergo a slow step after every X base pairs are unwound as a result of molecular rearrangement, phosphate release, etc. In this case, the observed kinetic step size will be X bp even though the actual physical step size is 1 bp.

Another important parameter is the stepping rate, which is defined as the number of steps a helicase takes per second. Depending on the helicase system and the type of experiment, the stepping rate and step size could be measured for DNA unwinding and/or translocation. The product of the step size and the stepping rate is the macroscopic rate of unwinding or translocation and has units of bp (or nt) per second. In the extreme case, the *E. coli* TraI and RecBCD helicases can unwind dsDNA with high processivity and with rates of over 1,000 bp/s [22–24]. In contrast, the *E. coli* RepΔ2B monomer only unwinds dsDNA with a rate of 226 ± 28 bp/s and limited processivity [10]. It is important to note that translocase and helicase activities are strongly sensitive to solution conditions (temperature, pH, salt concentration, salt type, NTP concentration, etc.), and one must keep this in mind when making quantitative comparisons between different studies.

Mechanistic models by which helicases unwind and translocate along DNA will be discussed in more detail in the subsequent chapters. Two limiting mechanisms have been suggested for DNA unwinding—active and passive [17, 25–28]. A passive helicase simply translocates along ssDNA with a directional bias. When it encounters a ds/ssDNA junction, the enzyme is stopped and must wait for the duplex to open through transient thermal fluctuations. Exploiting this phenomenon, a passive helicase

will eventually advance into the partially open duplex using its translocase activity, capture the spontaneously open fork, and prevent the two ssDNA strands from reannealing. In contrast, an active helicase directly interacts and destabilizes the DNA duplex and lowers the free energy of the fork. Therefore, the ssDNA translocation rate of a passive enzyme is predicted to be much faster than its unwinding rate since it has to wait for the DNA duplex to open transiently. In contrast the active unwinding model predicts this enzyme will have an unwinding rate similar to its rate of ssDNA translocation. The terms active and passive simply define the two extremes of a scale and there is an entire spectrum of possibilities in between. Under solution conditions similar to that of *E. coli* (pH 7.0, 3 mM Mg^{2+}, 0.2 M K^{+}, 8 mM ATP, 1 mM ADP, 8 mM P_i), ΔG_{ATP} is ~−13 kcal mol^{-1} at 25 °C while $\Delta G_{base\ pair}$ is ~1–1.5 kcal mol^{-1}. Therefore, if the coupling of ATP hydrolysis to DNA unwinding is 100% efficient, ~9–12 bp can be melted per molecule of ATP hydrolyzed [17]. Efforts have been made to quantify the "activeness" of a helicase based on its unwinding and translocation rates and to estimate NTP consumption during these processes [27–29].

There are several models with which the duplex strand separation is described. In the *E. coli* RecBCD enzyme, a "separation pin" in the RecC subunit was proposed to function as a molecular wedge [30]. This aromatic amino acid forms base stacking interactions with the DNA duplex, and base pair melting is achieved as a result of the RecB (a 3′–5′ helicase) and RecD (a 5′–3′ helicase) motors translocating along two strands of DNA. However, RecBCD is able to use its binding free energy to melt out 5–6 bp of DNA upon binding to a DNA end, and the RecB monomer, devoid of the separation pin, is able to unwind short DNA duplexes [31, 32]. The RecB subunit also has an "arm" domain which forms contact with the duplex ahead of the ds/ss junction. Taken together, RecBCD may be able to directly interact with the duplex and destabilize the fork [33]. In the case of ring-shaped hexameric helicases (i.e., DnaB, T7), strand exclusion models have been proposed in which the hexameric ring encircles one strand of the DNA duplex via a single-stranded loading region [34–36] (see also Chap. 5). Upon strand separation, the hexamer advances into the fork and the opposite strand is sterically excluded from the ring. Notably, various "pin" and "wedge" structures have been implicated in the dsDNA unwinding by virtually every non-hexameric helicase independent on where it lies of the passiveness continuum.

Brownian Ratchet vs. Powerstroke

Two distinct mechanisms utilized by helicases to ensure directional translocation have been considered: Brownian ratchet and powerstroke. A Brownian motor (thermal ratchet) is driven by thermal fluctuations. Directional movement of this "ratchet" is achieved as a result of an anisotropic energy potential across the DNA lattice although the nature and the origin of this asymmetry is not well understood and is likely to vary in different enzymes. However, in such a model system, the helicase only needs to switch between two conformational states (i.e., high and low affinity for DNA) which could be triggered by NTP binding and hydrolysis, and the helicase

will travel along the path of the anisotropic potential akin to guided diffusion. This model requires simply one DNA binding site on the helicase, and predicts low translocation and unwinding processivity since NTP hydrolysis is loosely coupled to movement.

In contrast, a powerstroke motor or stepping motor requires at least two DNA binding sites on the helicase. The best example of this is a molecular "inch worm" mechanism described for several SF1 helicases [37] in which translocation is driven by movements of the 1A and 2A subdomains. Nucleotide is bound in a cleft between these two RecA-like motifs and the state of the cofactor leads to a series of conformational changes that move the two subdomains closer together. In such an inch worm mechanism, the leading domain is always in the front and similarly the trailing domain always follows behind. Directionality is achieved in the initiation complex as a result of binding orientation [38, 39]. In contract, in a hand-over-hand stepping model like in the kinesin family motors, movement is similar to walking where the leading domain becomes the trailing domain in the next cycle and vice versa [40].

Structures of DNA Helicases

There are a number of high resolution structures of DNA helicases either in the apo form or bound to a DNA substrate with (or without) a nucleotide cofactor. A common structural feature is the motor core domain, which adopts two RecA-like folds (Fig. 1.3). Chapters 2 and 3 will discuss in detail the structural features as well as mechanisms of SF1 and SF2 helicases, respectively. The canonical motor core consists of two globular subdomains 1A and 2A, and the nucleotide cofactor binds in a cleft in between these two regions. Although the motor core is conserved amongst helicases, their diversity stems from a number of factors such as oligomeric state, presence of accessory and regulatory domains, and DNA substrate specificity. For example, the XPD helicase, which is an SF2Aβ enzyme, possesses two auxiliary domains in addition to the canonical helicase motor core: an Arch domain and an iron-sulfur cluster (FeS) domain. Both of these regions are necessary for unwinding activity and may be involved in stabilizing the interaction between XPD and the ds/ssDNA junction [38, 41]. In *E. coli* Rep, an SF1Aα enzyme, the presence of a 2B subdomain has an auto-inhibitory effect which may play a regulatory role in its translocation and unwinding activities [10]. Rep monomers can translocate rapidly and processively along ssDNA in vitro but are unable to unwind even short DNA duplexes. Rep helicase activity can be stimulated by removing the 2B subdomain artificially, thus forming the RepΔ2B monomer, or the wild-type enzyme can undergo dimerization to promote DNA unwinding. The presence of modular accessory domains can provide an extra level of control and regulation of helicase and translocase activities in vivo, and in some systems these accessory domains can target the enzymes to specific DNA structures, or they can be scaffolds for forming higher ordered complexes with mediator proteins. Helicases do indeed come in all

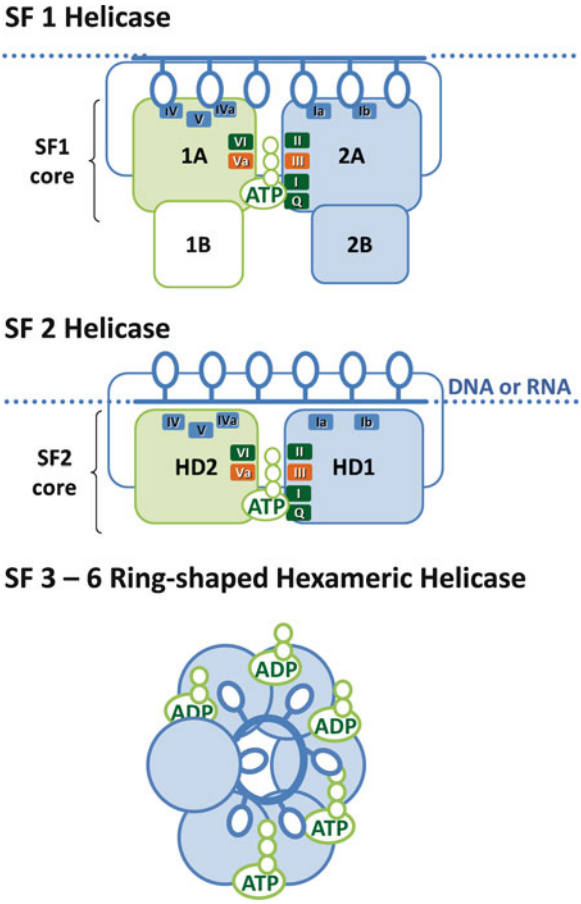

Fig. 1.3 Cartoon representations of DNA helicases from different superfamilies. Schematics of an SF1, SF2, and ringed-shaped hexameric helicase are shown. For SF1 helicases, the subdomains are as indicated, and the 1A and 2A subdomains form a motor core and adopt a "RecA"-like fold. The same is true for HD1 and HD2 in SF2 helicases. Nucleotide cofactor is bound in a cleft between these two subdomains. In a ring-shaped hexameric helicase, the hexamer encircles the DNA in the center pore and one strand of the nucleic acid is excluded from the helicase as it unwinds the duplex. Nucleotide cofactor is bound at the subunit interfaces. Because there are six potential nucleotide binding sites, these sites can have different nucleotide cofactor states (ATP bound, ADP, empty, etc.) depending on whether the helicases uses a random or ordered mechanism for ATP binding and hydrolysis

shapes and sizes. Some are monomeric while others function as homodimers or heterodimers. Other enzymes form ring-shaped hexamers (Fig. 1.3 and Chap. 4), and some are integral parts of complex transcription and replication machinery.

Helicases can modulate their activities not only through protein–protein interactions but also through posttranslational modifications (PTMs) such as phosphorylation, ubiquitylation, and sumoylation. Modified helicases can possess intrinsically different properties (i.e., unwinding and translocation activities), and PTMs can enable interactions with other protein partners, and target the helicase to certain sites for function. For example, the FANCJ helicase, upon phosphorylation on S990, enables interaction with the BRCA1 tumor suppressor protein [42, 43]. How this interaction influences FANCJ unwinding, translocation, and its ability to disrupt holiday junctions and G-quadruplexes is still not well understood. Since many mammalian helicases are subject to PTMs, it has become increasingly important to understand the functional roles of these modifications as an additional component to mechanistic studies of DNA helicases.

Assays for Helicase Activity

When helicases were first identified, DNA unwinding activity was inferred by coupling the strand separation reaction with nuclease digestion [44]. If a helicase unwinds dsDNA in the presence of NTP, then the newly generated ssDNA will be sensitive to nuclease degradation, and the cleavage products can be analyzed by scintillation counting. A more direct and the most widely used approach is a strand displacement experiment in which one strand of the DNA duplex is either radiolabeled with ^{32}P or fluorescently labeled with a fluorophore so that this strand can be detected when the duplex is unwound and the ssDNA is displaced into solution [45, 46]. Since the labeled reporter strand can hybridize with the other unlabeled unwound ssDNA product to form the original duplex, excess unlabeled ssDNA can be added to capture this other strand and thereby preventing reannealing. Strand displacement assays can be either discontinuous or continuous [21]. In a discontinuous assay, an initiation complex is formed between the helicase and duplex DNA substrate in the absence of nucleotide cofactor. DNA unwinding is then initiated with the addition of NTP and an unlabeled ssDNA trap. The reaction is quenched in a series of predetermined time intervals and the products from each time point can be separated by gel electrophoresis and analyzed using autoradiography. This type of a gel-based assay is "all or none" because at any given time point only the fully unwound product and the original duplex can be detected. Any partially unwound intermediates will "re-zip" and form the fully base-paired duplex when the reaction is quenched. However, as discussed later below, information regarding these transient intermediate species can be extracted from such an all or none experiment. In a continuous assay, DNA unwinding is monitored in real time continuously. Each of these approaches has distinct advantages and limitations. A discontinuous assay allows one to analyze the reaction products at each time point and thus the extent of DNA unwinding can be directly measured. Also, the gel-based assay can resolve different types of products that are formed. This is especially important when a helicase acts on a complex multi-strand substrate (e.g., replication fork, holiday junction, four-way junction), since one can unambiguously define its substrate preference by separating and directly observing the unwinding products. However, due to the discontinuous nature of the experiment, the number of data points one can collect within a reasonable amount of time is limited. Therefore, it is difficult to construct a detailed time course and to examine DNA unwinding as a function of different reaction conditions.

In contrast, in a continuous unwinding experiment, many data points can be obtained for a given time course, and different DNA substrates and solution conditions can be examined readily. However, a continuous unwinding experiment typically requires a difference in spectroscopic signal coming from either the protein or the DNA molecule when the DNA is unwound; hence, the relationship between this signal change and unwound DNA products need to be determined and calibrated independently in order to determine the extent of DNA unwinding. While all gel-based discontinuous assays are "all or none," continuous unwinding assays can be either depending on how the DNA substrate is constructed and how DNA unwinding

is monitored. Analogous all or none experiments can be performed in a continuous assay in which a pair of fluorescent dyes can be placed across the DNA duplex on the two strands. These two fluorophores can undergo Forster Resonance Energy Transfer (FRET) in the duplex since they are in close proximity. Because FRET efficiency is initially high, the donor fluorophore is quenched by the presence of the acceptor fluorophore as a result of non-radiative transfer of energy; however, when the two strands are unwound, separated, and displaced into solution, FRET efficiency decreases and the quantum yield of the donor fluorophore increases. In the case of RAD3 family helicases (e.g., XPD, FANCJ, RTEL), which possess an innate FeS cluster, this domain quenches fluorescence as a function of distance and therefore can be used to monitor either DNA unwinding or ssDNA translocation. Variations to continuous ensemble unwinding experiments include coupling the unwinding reaction with the binding of fluorescently labeled *E. coli* single-stranded binding protein (SSB), which undergoes a change in fluorescence intensity when it binds to ssDNA rapidly and with high affinity [47]. Alternatively, fluorescent dyes which intercalate between the nitrogenous bases can also be used to monitor DNA unwinding since they are either displaced upon strand separation or have different fluorescence properties when bound to ssDNA vs. dsDNA [48]. Since intercalating agents can have adverse effects on helicase activity, gel-based unwinding experiments should be carried out as an important control experiment. Continuous and discontinuous assays have different strengths and limitations, and they complement each other in the type of information each provides. Fluorescence-based continuous methods give better estimates of kinetic parameters since many data points can be collected for a given time course while gel-based discontinuous methods give better insight into the extent of DNA unwinding and the types of products that are formed.

The average kinetic step size of a helicase can be estimated using either continuous or discontinuous "all or none" strand displacement methods. As discussed above, in such an experiment, only the fully unwound DNA duplex is detected. Since helicase-catalyzed DNA unwinding is a multistep process in which the helicase undergoes a series of repeated steps along the DNA substrate until it is unwound and because only the fully unwound DNA product is monitored in an "all or none" experiment, a lag in product formation is observed in the beginning of the unwinding time course. The duration of this lag phase is proportional to the number of steps the helicase must take to fully unwind the DNA and therefore it is sensitive to the duplex length. By repeating the unwinding experiment as a function of increasing duplex length, the longer DNA substrates will exhibit longer lag phases in the unwinding time courses and these lag kinetics can be globally analyzed to estimate the average kinetic step size for DNA unwinding [21, 49].

With the recent advances and developments of instrumentation, there are now several "single-molecule" techniques with which a single DNA or a single helicase molecule can be observed. Several distinct single-molecule unwinding assays have been used to study many DNA helicases [50]. In total internal reflection fluorescence (TIRF) microscopy, DNA or helicase molecules are tethered onto a microscope slide surface and either moiety can be fluorescently labeled. By using low concentrations of materials as well as evanescent wave excitation, the unwinding or translocation

activities of individual helicase molecules can be observed by using FRET or protein-induced fluorescence enhancement (or quenching) as a metric of distance. Alternatively, conformation dynamics of helicase–DNA interactions or inter-domain movements can also be examined.

Another single-molecule approach is the use of high precision optical trap(s), and there are several variations of instrumentation used in these experiments. One example is the use of dual optical traps in which a DNA substrate has two handles, typically polystyrene beads, that are each held in place by the laser traps [51]. The forces exerted on the beads as well as their relative positions to the center of each trap can be measured and detected with high precision and accuracy. The DNA substrate held by the "optical tweezer" can be pulled and stretched by moving the position of one of the traps. Typically, a force vs. ssDNA extension curve is experimentally determined independently in order to convert the measured forces in an unwinding experiment to the number of bases unwound. If a DNA hairpin is held via the two handles on the optical traps, then as a helicase unwinds the hairpin substrate, 2 nts are released per base pair unwound. Therefore, the extent of DNA unwinding is calculated from the calibration curve after the relationship between force and extension (position) is established. Under high forces (>12 pN), force vs. ssDNA extension can be modeled using a freely jointed chain model. Under very lower forces (2 pN), secondary structure in the ssDNA may form and the worm-like chain model would be a poor representation of force vs. extension [52]. Despite this ambiguous representation, the compactness of ssDNA at low applied forces provides a second regime where ssDNA products of the helicase-catalyzed unwinding can be distinguished from the duplex substrate [27].

Alternatively, ssDNA translocation can be examined by using a duplex DNA substrate with a nick, and ssDNA can be generated by "pulling" on one of the handles thereby ripping open a region of the duplex mechanically. The helicase then be able to bind to the newly generated ssDNA region and translocate along the tract until it reaches the duplex upon which DNA unwinding occurs and the force exerted on the polystyrene bead changes. At this point another region of ssDNA can be generated mechanically again to observe another round of translocation. Although ssDNA translocation is not monitored directly in such an experiment, translocation activity can be inferred by determining the length of the ssDNA region opened mechanically, and the time it takes before unwinding is detected. These types of experiments have been used to examine the translocation and unwinding activities of the bacteriophage T7 helicase and also the HCV NS3 RNA helicase. One advantage of these optical tweezer experiments is that forward and reverse motions, and also pausing events, can be detected [53–55]. Since these events are stochastic in nature, it is not possible to detect them using traditional ensemble methods described above. In addition, DNA unwinding and ssDNA translocation can be examined in a single experiment under the same conditions [27], which enables one to compare these two activities and determine whether the helicase functions as an active or passive motor.

Another type of optical trap experiment employs the use of a single optical trap. A long piece of DNA (e.g., bacteriophage λ) is held by the trap on one end via a polystyrene bead. Instead of holding the DNA at another end, flow is applied to the system

so that the DNA is stretched in the direction of flow. A DNA intercalating dye (e.g., YOYO-1) is used to visualize the nucleic acid. When a helicase binds and unwinds the DNA, the dye is displaced and a loss of fluorescence signal is observed. *E. coli* RecBCD has been shown using such an experiment to pause at Chi regulatory DNA sequences (5′-GCTGGTGG-3′) [22, 24, 54]. Building upon this concept, a series of hundreds of trapped DNA molecules can be lined up and stretched, thereby forming a "DNA curtain" [56, 57]. This method allows one to examine the activities of many more helicase molecules simultaneously, and RecBCD has been shown to disrupt RNA polymerase, lac repressor, and other protein–DNA complexes including nucleosomes [58].

Helicases in Diseases

The genetic code is written as the sequences of the nitrogenous bases in DNA. This information is stored within duplex DNA, which is thermodynamically stable. In order to access the genetic information, dsDNA must first be unwound; hence, helicase activity is required during DNA replication, recombination, and repair. Mutations in human helicases such as BLM, WRN, and XPD can result in Bloom's syndrome, Werner's syndrome, and Xeroderma pigmentosum, respectively. These diseases are characterized by signs of premature aging as a result of genetic instability. Defects in the FANCJ helicase is linked to Fanconi anemia, a chromosomal instability disorder which results in bone marrow failure and susceptibility to breast cancer, ovarian cancer, and acute myeloid leukemia. The molecular basis and mechanisms by which the malfunctions of these enzymes result in diseases remain unclear. This is because helicases are involved in an intricate network of DNA metabolic enzymes and mediator proteins, and it is not known specifically which interactions are functionally important. In Chap. 6, DNA helicases associated with cancer, aging, and other genetic instability disorders will be discussed in detail; potential drug targets and therapeutics will also be described.

Remaining Questions

Although the field of DNA helicases research has matured immensely over the last decade or so, a number of gaps in our understanding of structure functional relationships, regulation, and integration of DNA helicases remain wide open. Recent advancements in instrumentation and method development have enabled researchers to monitor DNA unwinding at a single-molecule level with up to one base pair resolution. We are now poised to better address some fundamental questions of DNA helicases—how the NTP binding and hydrolysis are coupled to base pair melting and translocation, and how do helicases unwind and move along DNA? There are a number of detailed biochemical and structural studies using bacterial helicases as model systems in effort to address these questions. However, mechanistic

studies of mammalian helicases and our understanding of these enzymes are limited to this date. One research challenge is that these mammalian enzymes are typically more complex since they may possess multiple motor subunits or may be a part of complicated replication and recombination machinery. Furthermore, these helicases are often regulated by posttranslational modifications (PTMs) or interaction with regulatory factors. As a result, it has been difficult to reconstitute these systems for traditional bulk phase studies in vitro. One way to overcome this obstacle is to bypass this problem altogether. For example, using powerful single-molecule methods, it is possible to tether the entire cellular pool of a helicase of interest on a microscope slide. Enzymes possessing PTMs and the PTM type can be identified on the slide surface using fluorescence probes specific for the PTM. This enables all positions of modified and unmodified enzymes to be identified and then subsequent studies of helicase activity or translocase activity can be correlated to the PTMs. Powerful microscopy approaches have also been used to visualize movements of helicase subdomains. Continual effort is made to correlate these movements to DNA binding as well as nucleotide binding/hydrolysis. These types of experiments combined with classical mechanistic studies will provide a better understanding of how helicases harness chemical energy to do mechanical work, and how defects of helicase function are associated with genetic diseases.

Acknowledgements We are gratefully acknowledge support by the American Cancer Society (RSG-09-182-01-DMC to MS and PF-11-243-01-DMC to CGW) and Howard Hughes Medical Institute (Early Career Scientist Award).

References

1. Watson JD, Crick FH. Molecular structure of nucleic acids; a structure for deoxyribose nucleic acid. Nature. 1953;171(4356):737–8.
2. Meselson M, Stahl FW. The replication of DNA in Escherichia coli. Proc Natl Acad Sci U S A. 1958;44(7):671–82.
3. Andrews AJ, Luger K. Nucleosome structure(s) and stability: variations on a theme. Annu Rev Biophys. 2011;40:99–117.
4. Abdel-Monem M, Durwald H, Hoffmann-Berling H. Enzymic unwinding of DNA. 2. Chain separation by an ATP-dependent DNA unwinding enzyme. Eur J Biochem. 1976;65(2):441–9.
5. Abdel-Monem M, Hoffmann-Berling H. Enzymatic unwinding of DNA. 1. Purification and characterization of a DNA-dependent ATPase from Escherichia coli. Eur J Biochem. 1976;65(2):431–40.
6. Gorbalenya AE, Koonin EV. Helicases: amino acid sequence comparisons and structure-function relationships. Curr Opin Struct Biol. 1993;3:419–29.
7. Singleton MR, Dillingham MS, Wigley DB. Structure and mechanism of helicases and nucleic acid translocases. Annu Rev Biochem. 2007;76:23–50.
8. Jankowsky E, Fairman ME. RNA helicases—one fold for many functions. Curr Opin Struct Biol. 2007;17(3):316–24.
9. Jankowsky E, Fairman ME, Yang Q. RNA helicases: versatile ATP-driven nanomotors. J Nanosci Nanotechnol. 2005;5(12):1983–9.
10. Brendza KM, et al. Autoinhibition of *Escherichia coli* Rep monomer helicase activity by its 2B subdomain. Proc Natl Acad Sci U S A. 2005;102(29):10076–81.

11. Maluf NK, Fischer CJ, Lohman TM. A dimer of *Escherichia coli* UvrD is the active form of the helicase in vitro. J Mol Biol. 2003;325(5):913–35.
12. Niedziela-Majka A, et al. Bacillus stearothermophilus PcrA monomer is a single-stranded DNA translocase but not a processive helicase in vitro. J Biol Chem. 2007;282(37): 27076–85.
13. Tomko EJ, et al. A nonuniform stepping mechanism for E. coli UvrD monomer translocation along single-stranded DNA. Mol Cell. 2007;26(3):335–47.
14. Park SK, et al. RNA helicase activity of *Escherichia coli* SecA protein. Biochem Biophys Res Commun. 1997;235:593–7.
15. Gelis I, et al. Structural basis for signal-sequence recognition by the translocase motor SecA as determined by NMR. Cell. 2007;131(4):756–69.
16. Martin A, Baker TA, Sauer RT. Rebuilt AAA+ motors reveal operating principles for ATP-fuelled machines. Nature. 2005;437(7062):1115–20.
17. Lohman TM, Bjornson KP. Mechanisms of helicase-catalyzed DNA unwinding. Annu Rev Biochem. 1996;65:169–214.
18. Patel SS, Donmez I. Mechanisms of helicases. J Biol Chem. 2006;281(27):18265–8.
19. Schnitzer MJ, Block SM. Kinesin hydrolyses one ATP per 8-nm step. Nature. 1997;388: 386–90.
20. Cheng W, et al. Single-base pair unwinding and asynchronous RNA release by the hepatitis C virus NS3 helicase. Science. 2011;333(6050):1746–9.
21. Lucius AL, et al. General methods for analysis of sequential "n-step" kinetic mechanisms: application to single turnover kinetics of helicase-catalyzed DNA unwinding. Biophys J. 2003;85(4):2224–39.
22. Bianco PR, et al. Processive translocation and DNA unwinding by individual RecBCD enzyme molecules. Nature. 2001;409:374–8.
23. Sikora B, et al. DNA unwinding by Escherichia coli DNA helicase I (TraI) provides evidence for a processive monomeric molecular motor. J Biol Chem. 2006;281(47):36110–6.
24. Spies M, et al. RecBCD enzyme switches lead motor subunits in response to chi recognition. Cell. 2007;131(4):694–705.
25. Betterton MD, Julicher F. Opening of nucleic-acid double strands by helicases: active versus passive opening. Phys Rev E Stat Nonlin Soft Matter Phys. 2005;71(1):011904.
26. Delagoutte E, von Hippel PH. Helicase mechanisms and the coupling of helicases within macromolecular machines. Part I: structures and properties of isolated helicases. Q Rev Biophys. 2002;35(4):431–78.
27. Johnson DS, et al. Single-molecule studies reveal dynamics of DNA unwinding by the ring-shaped T7 helicase. Cell. 2007;129(7):1299–309.
28. Manosas M, et al. Active and passive mechanisms of helicases. Nucleic Acids Res. 2010;38(16):5518–26.
29. Byrd AK, et al. Dda helicase tightly couples translocation on single-stranded DNA to unwinding of duplex DNA: Dda is an optimally active helicase. J Mol Biol. 2012;420(3):141–54.
30. Singleton MR, et al. Crystal structure of RecBCD enzyme reveals a machine for processing DNA breaks. Nature. 2004;432(7014):187–93.
31. Farah JA, Smith GR. The RecBCD enzyme initiation complex for DNA unwinding: enzyme positioning and DNA opening. J Mol Biol. 1997;272:699–715.
32. Wong CJ, Lucius AL, Lohman TM. Energetics of DNA end binding by *E. coli* RecBC and RecBCD helicases indicate loop formation in the 3′-single-stranded DNA tail. J Mol Biol. 2005;352(4):765–82.
33. Wu CG, Bradford C, Lohman TM. Escherichia coli RecBC helicase has two translocase activities controlled by a single ATPase motor. Nat Struct Mol Biol. 2010;17(10):1210–7.
34. Ahnert P, Patel SS. Asymmetric interactions of hexameric bacteriophage T7 DNA helicase with the 5′- and 3′-tails of the forked DNA substrate. J Biol Chem. 1997;272(51):32267–73.
35. Hacker KJ, Johnson KA. A hexameric helicase encircles one DNA strand and excludes the other during DNA unwinding. Biochemistry. 1997;36:14080–7.

36. Galletto R, Jezewska MJ, Bujalowski W. Unzipping mechanism of the double-stranded DNA unwinding by a hexameric helicase: the effect of the 3′ arm and the stability of the dsDNA on the unwinding activity of the *Escherichia coli* DnaB helicase. J Mol Biol. 2004;343(1):101–14.
37. Eoff RL, Raney KD. Helicase-catalysed translocation and strand separation. Biochem Soc Trans. 2005;33(Pt 6):1474–8.
38. Pugh RA, Wu CG, Spies M. Regulation of translocation polarity by helicase domain 1 in SF2B helicases. EMBO J. 2012;31(2):503–14.
39. Saikrishnan K, et al. DNA binding to RecD: role of the 1B domain in SF1B helicase activity. EMBO J. 2008;27(16):2222–9.
40. Tomishige M, Stuurman N, Vale RD. Single-molecule observations of neck linker conformational changes in the kinesin motor protein. Nat Struct Mol Biol. 2006;13(10):887–94.
41. Kuper J, et al. Functional and structural studies of the nucleotide excision repair helicase XPD suggest a polarity for DNA translocation. EMBO J. 2012;31(2):494–502.
42. Cantor SB, et al. BACH1, a novel helicase-like protein, interacts directly with BRCA1 and contributes to its DNA repair function. Cell. 2001;105(1):149–60.
43. Clapperton JA, et al. Structure and mechanism of BRCA1 BRCT domain recognition of phosphorylated BACH1 with implications for cancer. Nat Struct Mol Biol. 2004;11(6):512–8.
44. Kuhn B, Abdel-Monem M, Hoffmann-Berling H. DNA helicases. Cold Spring Harb Symp Quant Biol. 1979;43(Pt 1):63–7.
45. Venkatesan M, Silver LL, Nossal NG. J Biol Chem. 1982;257:12426–34.
46. Matson SW, Tabor S, Richardson CC. The gene 4 protein of bacteriophage T7. Characterization of helicase activity. J Biol Chem. 1983;258:14017–24.
47. Dillingham MS, et al. Fluorescent single-stranded DNA binding protein as a probe for sensitive, real-time assays of helicase activity. Biophys J. 2008;95(7):3330–9.
48. Eggleston AK, Rahim NA, Kowalczykowski SC. A helicase assay based on the displacement of fluorescent, nucleic acid-binding ligands. Nucleic Acids Res. 1996;24:1179–86.
49. Ali JA, Lohman TM. Kinetic measurement of the step size of DNA unwinding by Escherichia coli UvrD helicase. Science. 1997;275(5298):377–80.
50. Yodh JG, Schlierf M, Ha T. Insight into helicase mechanism and function revealed through single-molecule approaches. Q Rev Biophys. 2010;43(2):185–217.
51. Comstock MJ, Ha T, Chemla YR. Ultrahigh-resolution optical trap with single-fluorophore sensitivity. Nat Methods. 2011;8(4):335–40.
52. Dessinges MN, et al. Stretching single stranded DNA, a model polyelectrolyte. Phys Rev Lett. 2002;89(24):248102.
53. Perkins TT, et al. Forward and reverse motion of single RecBCD molecules on DNA. Biophys J. 2004;86(3):1640–8.
54. Spies M, et al. A molecular throttle: the recombination hotspot chi controls DNA translocation by the RecBCD helicase. Cell. 2003;114(5):647–54.
55. Sun B, et al. ATP-induced helicase slippage reveals highly coordinated subunits. Nature. 2011;478(7367):132–5.
56. Fazio TA, et al. Fabrication of nanoscale “curtain rods” for DNA curtains using nanoimprint lithography. J Vac Sci Technol A. 2009;27(6):3095–8.
57. Fazio T, et al. DNA curtains and nanoscale curtain rods: high-throughput tools for single molecule imaging. Langmuir. 2008;24(18):10524–31.
58. Finkelstein IJ, Visnapuu ML, Greene EC. Single-molecule imaging reveals mechanisms of protein disruption by a DNA translocase. Nature. 2010;468(7326):983–7.

Chapter 2
Structure and Mechanisms of SF1 DNA Helicases

Kevin D. Raney, Alicia K. Byrd, and Suja Aarattuthodiyil

Abstract Superfamily I is a large and diverse group of monomeric and dimeric helicases defined by a set of conserved sequence motifs. Members of this class are involved in essential processes in both DNA and RNA metabolism in all organisms. In addition to conserved amino acid sequences, they also share a common structure containing two RecA-like motifs involved in ATP binding and hydrolysis and nucleic acid binding and unwinding. Unwinding is facilitated by a "pin" structure which serves to split the incoming duplex. This activity has been measured using both ensemble and single-molecule conditions. SF1 helicase activity is modulated through interactions with other proteins.

Introduction

Helicases are molecular motor proteins present in viruses, bacteria, and eukaryotes [1, 2]. They harness the chemical energy of ATP hydrolysis to break the energetically stable hydrogen bonding between the duplex DNA. By doing so, helicases allow access to the genetic information locked in the duplex DNA. Helicases participate in various aspects of nucleic acid metabolism such as DNA replication, recombination, repair, transcription, translation, and splicing of RNA transcripts [3–13].

S. Aarattuthodiyil • A.K. Byrd • K.D. Raney (✉)
Department of Biochemistry and Molecular Biology,
University of Arkansas for Medical Sciences,
Little Rock, AR, USA
e-mail: raneykevind@uams.edu; akbyrd@uams.edu; baarattuthodiyil@uams.edu

M. Spies (ed.), *DNA Helicases and DNA Motor Proteins*, Advances in Experimental Medicine and Biology, DOI 10.1007/978-1-4614-5037-5_2,

Mutations in helicase genes involved in DNA repair processes have been linked to numerous human diseases [14–17] in which genomic instability, immunodeficiency, mental retardation, premature aging, and predisposition to cancer are common features [14, 15, 18–21]. Some of the diseases caused by defective helicases are xeroderma pigmentosum, Cockayne Syndrome, trichothiodystrophy, Werner's syndrome, Bloom's syndrome, and alpha-thalassemia mental retardation on the X chromosome [22–30]. A mutation in superfamily 1 (SF1) helicase Pif1 results in breast cancer predisposition [31]. Mutations in SetX helicase, involved in RNA splicing and termination, cause juvenile amyotrophic lateral sclerosis [32] and ataxia-ocular apraxia 2 [33], while mutations in IGHMBP2 (Smubp2), involved in translation [34], result in distal spinal muscular atrophy [35]. The diverse disease abnormalities caused by defective helicases suggest that multiple aspects of DNA and RNA metabolism are affected [18].

In some aggressive cancers, the activity of helicases in DNA repair reduces the efficacy of anticancer agents, because many of these agents are targeted to DNA. Studies have shown that the efficacy of chemotherapeutic agents could be increased by administering drugs that target helicases along with the anticancer drugs [36]. Helicases encoded by herpes simplex virus [37–39], West Nile virus, dengue virus, and hepatitis C virus [40] are targets for antiviral drug development [38, 41]. Some bacterial helicases such as Rep from *Legionella pneumophilia* are required for infection of mammalian cells [42]. The importance of helicases in the fundamental aspects of nucleic acid metabolism and the association of human, bacterial, and viral helicases in human diseases makes the study of helicases critical. This also makes it essential to understand the mechanisms by which helicases perform different biochemical functions so that the relationship between mutations and specific disease states can be understood at the molecular level.

Functions of Helicases

Unwinding of duplex or structured nucleic acids by helicases provides the ssNA intermediates required for metabolism of DNA and RNA [43–45]. *In vivo*, DNA unwinding is coupled to the action of many proteins such as primases, ssDNA-binding proteins, polymerases, and other factors depending on the functions of a particular helicase. Many of the biological functions of various helicases are listed in Table 2.1. Helicases are implicated in processes ranging from replication to translation [8, 10–12, 46–49] and also in ATP-dependent chromatin remodeling [50, 51]. Replicative helicases deal with the process of nucleic acid replication (initiation, elongation, and termination). Helicases play an important role in DNA repair, as these are frequently the first proteins that encounter DNA damage [13, 19, 52–54]. During DNA repair, the damaged area on the DNA has to be unwound before repair can proceed as most DNA repair processes require ssDNA. Helicases play roles in both initiation and branch migration during recombination [21, 25, 28, 55–60].

Table 2.1 Biological functions carried out by various helicases

Biological function	Helicase
Replicative helicases	PcrA1, RepA, UvrD, Dda, HSV UL5, HSV UL9, DnaB, PriA, T7gp4A and 4B, T4gp41, SV40, TAG, Polyoma TAG, BPV E1, MCM 4/6/7, Dna2, FFA-1, RecD, TraI, NS3, RecQL4
Repair helicases	UvrD, UvrAB, PcrA, Rad3, helicase E, XPD, XPB, Dna2, RecD2, BACH1, HDH II, RecQ, WRN, Rtel1, BLM, RuvB, Mph 1, CHD4
Recombination helicases	RecBCD, RecG, RecQ, RuvAB, PriA, UvrD, T4 UvsW, HDH II, HDH IV, WRN, Tra I, Rho, PDH65, BLM, Srs2, Sgs1, Rtel1
Other functions of helicases	
Transcription	SWI2, SNF2, TFIIH, Rho, Factor 2, TRCF, RecQL5, ERCC6/RAD26
Translation	HSV UL5, eIF4A, RHA, Ded1p, vasa
Chromatin remodeling	Rad54, ATRX, BLM, CHD4
Maintenance of telomeres	Pif1, Dna2, Rtel 1, WRN, BLM, FANC
Okazaki fragment maturation	Dna2, Pif1, WRN

References are cited within [19, 21, 24, 28, 55–58, 61, 63–65, 90–92, 135, 150, 159, 163, 179, 191, 198–226]

Helicases alter DNA and RNA structures, remodel chromatin [24, 51, 61–65], and modulate access to the DNA template by transcriptional machinery. RNA polymerases that are involved in the elongation of RNA transcripts have been considered as helicases that unwind the dsDNA to expose the ssDNA strand that serves as the template for RNA synthesis [2]. Helicases thus play a role in most transcriptional processes including activation (TFIIH), initiation (TFIIH, SNF2), maintenance (SW1), DNA repair (TFIIH, ERCC6/RAD26), and termination (Factor 2, Rho) [49, 66–72].

Properties of Helicases

Some of the fundamental properties exhibited by helicases are nucleic acid binding, ATP binding and hydrolysis, translocation, unwinding of duplex nucleic acids, and displacement of proteins bound to the nucleic acid substrate (Fig. 2.1), although not all helicases are able to perform all of these activities. Helicases unwind DNA with a unique directionality (either from 5′ to 3′ or from 3′ to 5′) relative to the strand of DNA that is bound by the enzyme. RecBCD exhibits bipolar enzyme activity, where RecB and RecD components of the complex unwind DNA in 3′–5′ and 5′–3′ directions, respectively [73]. Other bipolar helicases are *Bacillus anthracis* PcrA [74] and *Sulfolobus acidocaldarius* HerA helicase [75].

Most helicases require a short stretch of ssDNA as a loading strand *in vitro*, and they show a preference for binding to ssDNA over dsDNA. Many helicases

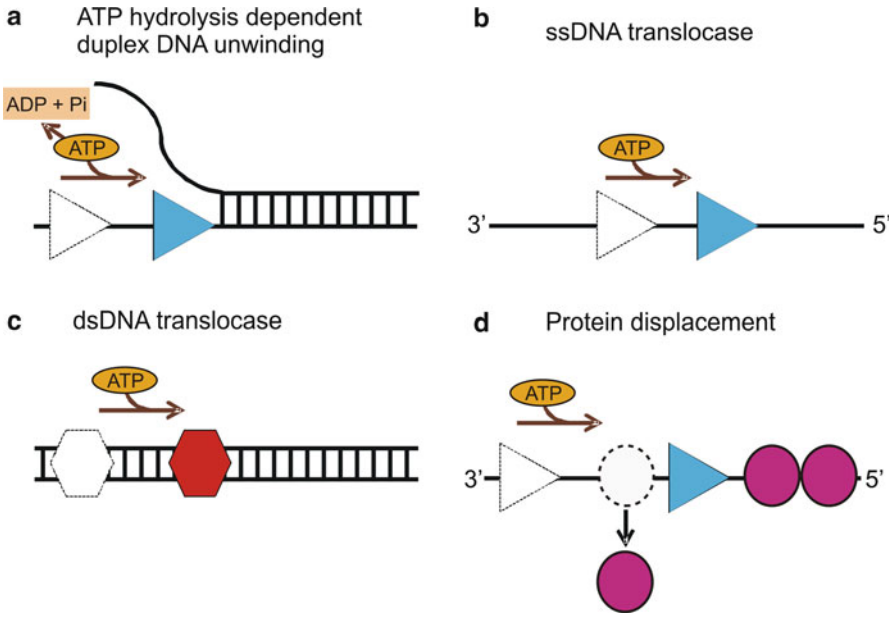

Fig. 2.1 Biochemical properties of helicases: (**a**) ATP hydrolysis-dependent unwinding of duplex DNA by helicase (*blue triangle*). The movement of helicase along the DNA utilizing the energy from ATP hydrolysis separates the duplex nucleic acid into single strands. (**b**) An ssDNA translocase (*blue triangle*) moves with biased directionality along the DNA powered by ATP binding and hydrolysis. The directionality of translocation can be 3′–5′ or 5′–3′. (**c**) A dsDNA translocase (*red hexagon*) moves along dsDNA. (**d**) Helicases can displace proteins (*magenta circles*) bound to the DNA strand as a result of their biased directional movement (adapted from ref. [45])

(Rep, UvrD, PcrA, Dda, and HSV-UL5) are generally considered to be ssDNA translocases, while other helicases (eIF4A, RecG, and PriA) are dsDNA translocases [76, 77]. Some helicases need a replication fork-like structure on the substrate for optimum unwinding, whereas other DNA helicases can initiate unwinding from blunt-ended duplex DNA, such as RecBCD, UvrD, Rep, and RecQ [77–79]. While the ATPase activity of helicases is low in the absence of DNA, presence of ssDNA stimulates this activity [80].

Superfamily 1 Helicases

Helicases are divided into six superfamilies (SF1–6) based on the sequence identity among the conserved helicase motifs [1, 43, 47, 81]. Superfamily 1 is one of the largest classes of helicases with members that participate in virtually all steps in DNA or RNA metabolism [82–85]. SF1 includes three families (Rep/UrvD, Pif1/RecD, and Upf1 like) [86] and can be divided into groups based on the direction of translocation on ssDNA: 3′–5′ for SF1A helicases and 5′–3′ for SF1B helicases [43]. Some of the well-characterized SF1A helicases are PcrA, Rep, and UvrD T[87–92].

Table 2.2 Superfamily 1A (3′–5′) and SF1B (5′–3′) helicases

Helicase	Source	Biological function	Active form	Polarity
PcrA	*Bacillus stearothermophilus*	DNA repair and rolling replication of plasmids	Monomer	3′–5′
Rep	*Escherichia coli*	DNA replication	Dimer	3′–5′
RecB	*Escherichia coli*	DNA recombination	Monomer	3′–5′
UvrD	*Escherichia coli*	DNA replication, recombination, and repair of UV damage and mismatched base pairs	Dimer	3′–5′
Pif1	*Saccharomyces cerevisiae*	Maintenance of telomeres, ribosomal DNA replication, processing of Okazaki fragments	Monomer	5′–3′
Dna2	*Saccharomyces cerevisiae*	Maintenance of telomeres, Okazaki fragment maturation, double strand break repair, aging	Monomer	5′–3′
Dda	Bacteriophage T4	DNA replication initiation, and recombination	Monomer	5′–3′
UL5	Herpes simplex virus	Viral DNA replication	Dimer	5′–3′
RecD2	*Deinococcus radiodurans*	DNA repair	Monomer	5′–3′
TraI	*Escherichia coli*	DNA transfer during conjugation, DNA nicking	Monomer	5′–3′

References are cited within [90–92, 135, 150, 163, 191, 198, 200–203, 205, 209, 211, 212, 214, 215, 218, 219, 225, 227–233]

Well-characterized members of SF1B include RecD and Dda [93, 94] (He et al., in press). The biological functions, polarity, and active forms of some of the SF1 helicases are listed (Table 2.2).

Helicase Motifs

A characteristic feature of helicases is the presence of highly conserved amino acid sequences termed the "helicase motifs" [46, 47, 95–98]. Based on their sequence similarity and organization, these motifs are useful in the grouping of helicases into different families. SF1 and SF2 contain at least seven conserved amino acid motifs whose sequences, organization, and secondary structures are, in general, very similar [43, 46]. SF1 (Rep and PcrA) and SF2 (NS3) helicases differ primarily in motifs III and IV. In NS3, motif IV makes contacts with the DNA backbone and is not in the same relative position as motif IV of Rep and PcrA. While motif III of Rep contacts the bound ssDNA molecule, this motif in NS3 does not [99, 100]. The SF1A and SF1B helicases also show differences with motifs Ia and III being particularly characteristic for each class. These motifs are usually clustered in a core region of 200–700 amino acids, separated by stretches of low sequence but high length conservation [79]. In contrast, the N-terminal and C-terminal regions of helicases are characterized by a high degree of sequence and length variability. The divergent regions are responsible for individual protein functions, whereas the highly conserved motifs are involved in ATP binding and hydrolysis or binding and unwinding of nucleic acids.

Helicase motifs involved in ATP binding are located at the interface between two RecA-like domains [43, 46, 47, 95, 96, 101] in the structures of SF1 and SF2 helicases [48, 102–104]. Figure 2.2 shows the conserved sequence of the motifs (Q, I, Ia, II, III, IV, V, and VI) of the SF1 helicase family and their location in PcrA. The biochemical functions of these motifs are described below.

Q Motif

The Q of the Q motif [101] is conserved among all SF1 helicases [86]. This motif coordinates the adenine base and is less conserved among those helicase families which do not show specificity for ATP [86]. Mutagenesis suggests that the Q motif is required for viability and plays a role in orienting ATP for hydrolysis [101, 105].

Motif I (Walker A)

The consensus sequence of this motif is AxxGxGKT [46]. It is present in many nucleotide-binding proteins and forms a phosphate-binding loop [106]. The residues "GKT" are required for the interaction of the protein with Mg^{2+} and ATP [107]. The conserved G in GKT helps to maintain the flexible loop conformation [46].

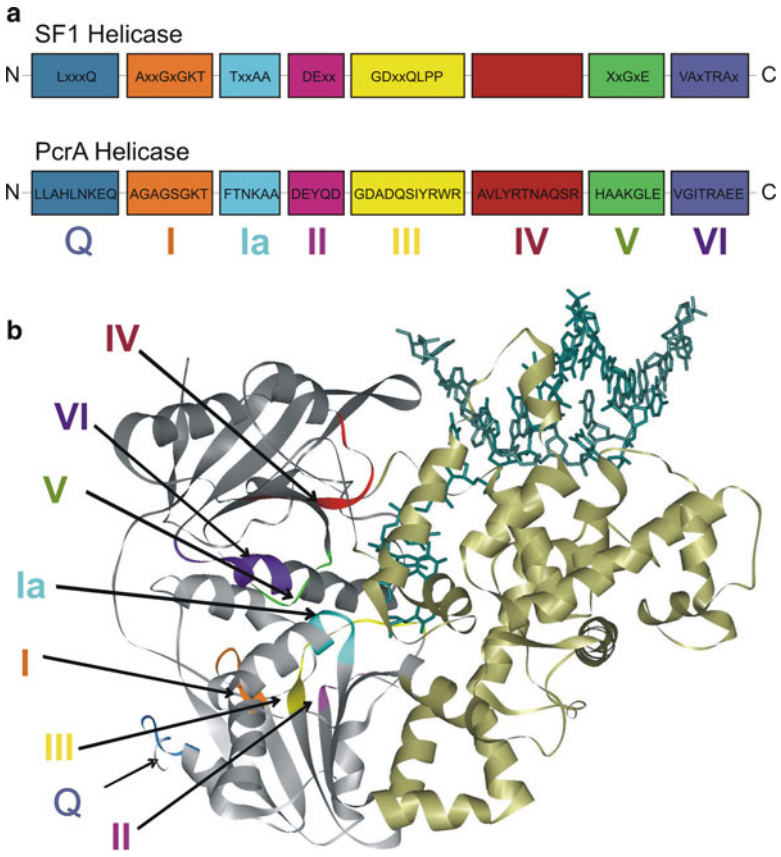

Fig. 2.2 Schematic representation of the motifs of SF1 helicases: (**a**) The consensus sequences for the conserved helicase motifs of SF1 helicases and PcrA are shown. The N-terminus of the protein is on the *left* and C-terminus is on the *right* side. Labels below the boxes are the names assigned to the motifs (motifs Q, I, Ia, II–VI). The relative positions of motifs and spacing between motifs are arbitrary. The consensus amino acid sequences of PcrA are taken from refs. [46, 89]. (**b**) The crystal structure of PcrA helicase (Protein Data Bank code 3PJR) [87, 89] bound to DNA (*dark green*) illustrating the different conserved motifs. The helicase motifs are in the cleft formed between the two RecA-like domains (*grey*). The colors of different motifs in the structure are as follows: motif Q, *blue*; motif I, *orange*; motif Ia, *cyan*; motif II, *magenta*; motif III, *yellow*; motif IV, *red*; motif V, *green*; motif VI, *purple*

Motif Ia

The consensus sequence for motif Ia is TxxAA. It has been suggested that this motif is involved in ssDNA binding [89] and energy transduction from the ATP-binding site to the DNA-binding site [86]. For the SF1 helicases (UvrD, Rep, Pif1), motifs Ia and III have been proposed to play important roles in defining translocation polarity [94].

Motif II (Walker B) [108]

This motif, DExx, is involved in NTP hydrolysis [46, 76, 86]. The D and E residues coordinate the ATP-associated Mg^{2+} and activate the attacking water molecule, respectively [109, 110]. Mutation of these residues reduces ATPase and helicase reactivity [111–113].

Motif III

The consensus sequence for motif III is GDxxQLPP [86]. It functions in DNA binding through base stacking and hydrogen bonding with the bases [76]. The close proximity of some residues in motifs III to that in motif II suggests that motif III transduces the energy of ATP hydrolysis to the DNA [88]. Motif III mutants of UL5, UvrD, and eIF-4A exhibited uncoupling of ATPase and helicase activities [79, 110, 114]. The highly conserved Q in motif III contacts the γ-phosphate of the bound nucleotide in PcrA [89], UvrD, and UL5 [113, 115]. These results imply a role for motif III in coupling ATP hydrolysis with the unwinding of duplex DNA.

Motif IV

The consensus sequence for this motif varies among the three families within SF1. Motif IV supplies a stacking platform (conserved Y) for the adenine base [88] as well as direct contact with the γ-phosphate, suggesting that it may be involved directly in hydrolysis of the NTP [89].

Motif V

This motif interacts with the sugar-phosphate backbone of the DNA. Motif V mutants of UL5 exhibited reduced affinity for ssDNA and reduced rates of ATP hydrolysis [116].

Motif VI

The consensus sequence for this motif is VA(L/Y)TRA(K/R) [86]. It is proposed to be a part of the ATP-binding cleft and is involved in coupling the helicase and ATPase activities of the protein [88]. Several helicases exhibited nucleic acid binding defects when motif VI residues were altered [110]. Motif VI mutants of UvrD exhibited reduced ssDNA binding, ATP hydrolysis rate, and ligand-induced conformational changes [117]. In motif VI mutants of UL5, an uncoupling of

ATPase and helicase activity was observed [113]. Studies on PcrA [89] and Upf1p [112, 113, 117] suggest that motif VI, by virtue of its close proximity to the NTP- and DNA-binding sites, mediates ligand-induced conformational changes, which are essential for the helicase to move along the nucleic acid substrate [88].

The conserved motifs bind and hydrolyze ATP and transduce the resulting energy to cause conformational changes in the helicase. These motifs function together to drive directional movement along ssDNA or dsDNA. They participate in the communication between nucleic acid and ATP-binding sites [118]. The ability to unwind dsDNA appears to be provided by additional protein domains which do not contain the helicase motifs [48].

Helicase Structure

SF1 helicases constitute one of the best structurally characterized helicase families. The crystal structures have revealed that the helicase motifs are clustered together in two RecA-like domains, forming an ATP-binding pocket between them and a part of the nucleic acid-binding site. The nonconserved regions may contain specific domains such as protein–protein interaction domains, cellular localization domains, and DNA-recognition domains specific to individual helicases. Several helicase structures have been solved in the last decade contributing significantly to the overall understanding of the mechanism of SF1 helicases. Figure 2.3 shows the structures of two SF1A and two SF1B helicases [87–89, 93, 94, 103] (He et al., in press).

Structure of SF1A Helicases (PcrA and UvrD)

The first helicase structure to be solved was that of PcrA from *B. stearothermophilus* [87, 89]. PcrA is composed of four domains (1A, 2A, 1B, and 2B) (Fig. 2.3a), resembling other SF1 helicases [119–121]. The ATP-binding site is situated in a cleft between the RecA-like domains (1A and 2A). This cleft opens and closes in response to nucleotide binding and hydrolysis suggesting how translocation could occur [88, 89]. In UvrD (SF1A helicase), binding of an ATP analog, AMPPNP, in the cleft between domains 1A and 2A (Fig. 2.4) induces a 20° rotation between domain 2A and the remaining three domains (1A, 1B, and 2B). Upon AMPPNP binding, the duplex moves domains 1A/1B/2B towards 2A leading to untwisting of the duplex DNA as single-stranded DNA is pulled through the active site [122]. The structural data for UvrD, as for PcrA, predict one nt translocated and one bp unwound per ATP hydrolyzed.

Structure of SF1B Helicases (RecD2 and Dda)

A crystal structure of *Deinococcus radiodurans* RecD2 helicase with ssDNA [93] is shown in Fig. 2.3c. RecD2 comprises five domains: the N-terminal, 1A, 1B, 2A, and

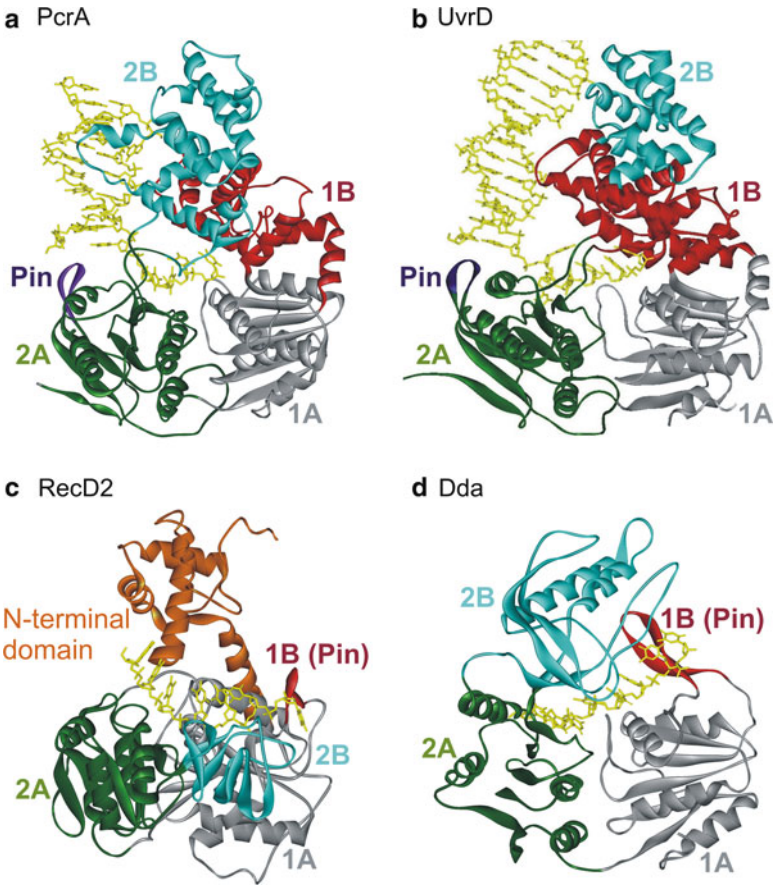

Fig. 2.3 Crystal structures of SF1A (PcrA, UvrD) and SF1B (RecD2, Dda) helicases: (**a**) Ribbon diagram of PcrA helicase from *Bacillus stearothermophilus* (Protein Data Bank code 3PJR) [87, 89]. The RecA-like domains 1A and 2A are shown in *grey* and *green* colors, respectively. The structure shows the *red* 1B domain and the pin (*purple*) separating the strands of duplex DNA. The 2B domain is shown in *cyan*. (**b**) Structure of *Escherichia coli* UvrD helicase (PDB code 2IS1 [122]). Domains are colored as in (**a**). (**c**) Structure of RecD2 helicase from *Deinococcus radiodurans* (PDB code 3GPL [93]). Domains 1A, 2A, and 2B are colored as in (**a**). The beta-hairpin (1B) is *red*. The N-terminal domain is colored *orange*. (**d**) Structure of bacteriophage T4 Dda helicase bound to ssDNA (PDB id: 3UPU) (He et al., in press). The domains are colored as in (**c**). Nucleic acid is colored *yellow* in all structures

2B domains. Domains 1A and 2A have the RecA-like fold seen in all SF1 and SF2 helicases [48]. Domain 1B forms a rigid β-hairpin that protrudes from the surface of domain 1A, and the 2B domain has an SH3 fold [93]. The ssDNA-binding site runs in a 5′–3′ direction along a channel across the top of domains 2A and 1A. The DNA is also contacted by the 1B and 2B domains that form the sides of the channel.

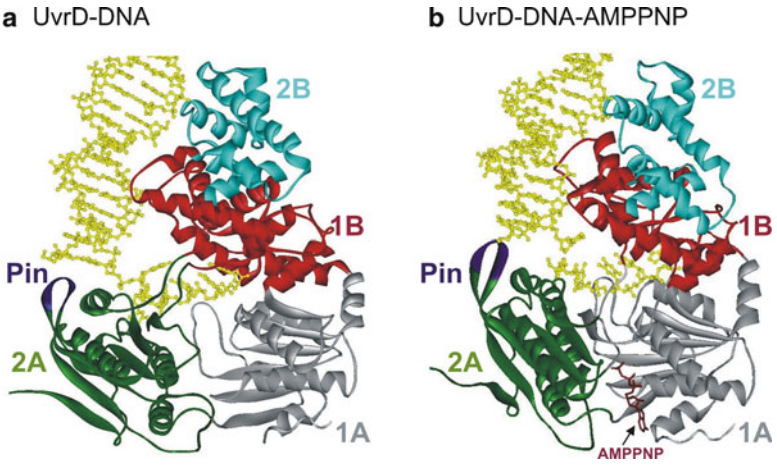

Fig. 2.4 Crystal structures of (**a**) UvrD–DNA and (**b**) UvrD–DNA–AMPPNP complexes [122]. The four domains (1A, 1B, 2A, and 2B) are colored *grey*, *red*, *green*, and *cyan*, respectively. The Pin region is shown in *purple*. The 3′-ssDNA tail is bound across domains 1A and 2A. Domains 1B and 2B interact with the DNA duplex. Binding of AMPPNP (*brown*) induces domains 2A and 1A to rotate towards each other by 20°

Although the location of the ssDNA-binding site is similar in SF1A and SF1B helicases [88, 89], the contacts between the protein and the DNA and conformation of the DNA are different. PcrA interacts with the DNA through stacking of aromatic side chains with the DNA bases and there are relatively few contacts with the DNA backbone [89]. In contrast, the majority of protein–DNA contacts in RecD2 are via the phosphodiester backbone [93]. The bound ssDNA is in a configuration more similar to that found in a DNA duplex, with the bases stacked against one another, unlike the extended conformation observed in PcrA. Interestingly, the RecD2 mode of binding is more similar to that seen in SF2 enzymes such as NS3, Rad54, Vasa, and Hel308 [104, 123–125] rather than SF1A helicases [126].

Even though there is significant structural similarity between SF1A and SF1B enzymes, they translocate in opposite directions. Comparison of the structures of PcrA and RecD2 shows that both SF1A and SF1B helicases bind the ssDNA in the same orientation (2A domain on the 5′ side of the DNA, 1A domain on the 3′ side of the DNA) [89, 94], and reveals how directionality is determined (Fig. 2.5a, b) [89, 94, 127]. Opening and closing of the cleft between the 1A and 1B domains in the presence and absence of ATP appears to provide the means of translocation [89]. The RecA-like domains bind to DNA and upon binding to ATP, the more weakly bound domain shifts towards the more tightly bound domain. For PcrA (SF1A), domain 1A moves towards domain 2A upon ATP binding, resulting in translocation in the 3′–5′ direction [94, 127]. For RecD2 (SF1B), ATP binding causes movement of domain 2A towards domain 1A, resulting in 5′–3′ translocation [94]. The net forward movement occurs in one nt physical steps with each ATP hydrolyzed. The efficiency of helicases may vary, with some ATP hydrolysis events being uncoupled

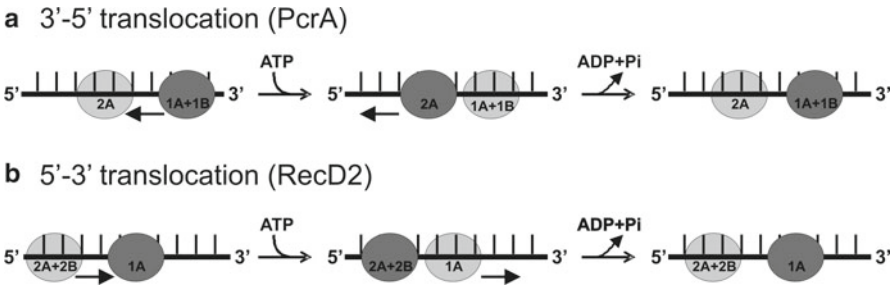

Fig. 2.5 Comparison of the translocation mechanism of SF1A (PcrA) and SF1B (RecD2) helicases: In both enzyme classes, a cycle of ATP binding and hydrolysis induces conformational changes that result in translocation of the protein along DNA, but in opposite directions. *Dark grey circles* represent domains that have a tight grip on the ssDNA, and *light grey circles* represent domains that have a weaker grip and can slide along the DNA. Conversion between tight and weak grip (*dark* and *light grey circles*) is indicated by *arrows*. (**a**) The translocation mechanism of PcrA is shown in cartoon form demonstrating the change in affinity for ssDNA of domains 1A and 2A during translocation. Prior to ATP binding, ssDNA is bound to the enzyme spanning the 1A and 2A domains. Binding of ATP induces closure of the cleft between 1A and 2A domains. At this point, the grip is tightest on the 2A domain, causing the DNA to slide across the 1A/1B domains. Upon ATP hydrolysis, bind to ssDNA in 1A becomes tighter, whereas binding of ssDNA in 2A becomes weaker, releasing ssDNA. The domains also move apart, due to domain 2A sliding forward, causing the ssDNA to be pulled along the DNA-binding channel relative to the domain 2A. The result is translocation along the DNA in a 3′–5′ direction (indicated by *black arrows*). (**b**) Translocation mechanism of RecD2 helicase. When ATP binds to the enzyme, the cleft closes between 1A and 2A motor domains, causing domains 2A and 2B to slide along the DNA backbone (*black arrows*). The contacts between domain 1A and the DNA remain tight to anchor the DNA as domains 2A and 2B slide along it. When the conformational change is complete, the grip of domain 1A on the DNA is loosened. Then, ATP hydrolysis takes place, allowing the cleft to relax to the open conformation. The DNA is pulled back by domains 2A and 2B, which now have a tighter grip on bound DNA than domain 1A. This causes the DNA to slide across the surface of domain 1A as it moves away from domains 2A and 2B. The result is translocation by one base in a 5′–3′ direction (*black arrows*) during a single round of ATP binding and hydrolysis (adapted from ref. [94])

from movement. Despite being in the same superfamily, SF1A and SF1B helicases exhibit significantly different mechanisms.

Duplex DNA Is Split by the Pin Region

In addition to the RecA-like 1A and 2A domains containing the conserved helicase motifs, all SF1 helicases contain accessory domains which can vary in structure. One common feature of these domains is the presence of a pin or wedge which functions to split the incoming DNA. The pin was first discovered in the SF2 helicase Hel308 from *Archaeoglobus fulgidus* [125]. A pin splitting the DNA was observed previously in RecC [103], the Chi recognition protein of the RecBCD helicase complex and in RuvA [128, 129], which along with RuvB and RuvC catalyzes branch migration resulting in Holliday junction resolution.

The location of the pin varies to correspond with the direction of translocation. For SF1A helicases, the 2A domain leads during unwinding in the 3′–5′ direction. In the structures of PcrA with DNA bound (Fig. 2.3a) [89] a pin is visible, positioned at the junction of the duplex and ssDNA. For SF1B helicases, 1A is the leading RecA-like domain, and an insertion in this domain, domain 1B, serves as the pin (Fig. 2.3c, d) [93]. In each case, the pin is positioned appropriately to split the incoming duplex during translocation along the ssDNA. Based on the structure of RecD2 bound to DNA, a mutant lacking the pin was designed which was completely devoid of unwinding activity although it hydrolyzed ATP at the same rate as wt RecD2 [93].

A recent report demonstrates that the mere presence of the pin is not sufficient for helicase activity (He et al., in press). Specific residues in the pin may be necessary for helicase activity. For the SF1B helicase Dda, mutation of a single F residue in the pin which stacks with the ssDNA completely eliminates strand separation although translocation on ssDNA is unaffected. In the case of RecD2 [93], the pin is short and it appears to function only in splitting the incoming duplex. Dda contains a long β-hairpin which is anchored at its tip by electrostatic interactions to domain 2B, allowing it to function not only directly in splitting the dsDNA but also in coupling ATP hydrolysis to unwinding (He et al., in press). Like Dda, the hepatitis C virus NS3 helicase (SF2) contains an extended pin [100], and mutation of conserved residues with this pin also uncouples ATP hydrolysis from unwinding [130].

Ensemble Kinetics for Helicase-Catalyzed DNA Unwinding of dsDNA and Translocation on ssDNA

SF1 helicases unwind the DNA in a stepwise manner so that more steps are required to unwind longer duplexes. Unwinding of duplexes of varying length has led to several descriptors of the kinetic and physical constants associated with helicases. One of the most discussed values relates to the "step size." The kinetic step size refers to the number of base pairs unwound prior to a rate-limiting kinetic step. This value can be determined by measuring unwinding of increasing length duplexes [131]. The kinetic step sizes for some SF1 helicases are shown in Table 2.3. The physical step size refers to the number of base pairs that are unwound simultaneously. Single-molecule approaches have provided direct measures of the physical step size for a number of helicases (see below). The relationship between the kinetic step and the physical step size may be complex. A helicase might unwind one base pair at a time (physical step of one), but then proceed through a slow conformational change that occurs every three base pairs, resulting in a kinetic step size of three bps. The chemical step size refers to the number of base pairs unwound per ATP hydrolyzed. In the simplest case, all of these values are equal to one. However, there may be differences and care must be taken to distinguish between these values when comparing the activity of one helicase to another.

Table 2.3 Kinetic constants for select SF1 helicases

Helicase	Kinetic step size for unwind (bp)	Kinetic step size for trans (nt)	Unwind rate (bp/s)	Trans. rate (nt/s)	Unwinding processivity (bp)	Trans. processivity (nt)
wtRep—monomer	N.D.[a]	N.D.	N.D.	298 [155]	0 [119]	700 [155]
wtRep—EE[b]	4[c] [119]	N.D.	57 [119]	N.D.	N.D.	N.D.
ReΔ2B—monomer	4[c] [155]	N.D.	226 [155]	530 [155]	<21 [155]	800 [155]
UvrD—monomer	N.D.	4–5 [92, 156, 234]	N.D.	200 [92, 156, 234]	<18 bp [156]	240 [92, 234]
UvrD—EE	4.4 [131]	N.D.	73.4 [131]	N.D.	10 [131]	N.D.
RecBCD EE	3–4 [235–238]	N.D.[d]	700–1,350 [235–239]	N.D.[d]	30,000 [183]	N.D.
PcrA—monomer	N.D.	4.0 [145]	N.D.	234 [145]	<18 [145]	248 [145]
PcrA—EE	4 [240]	N.D.	31 [145, 240]	N.D.	N.D.	N.D.
Dda—monomer	2.8 [241, 242]	N.D.	262 [136, 241, 242]	267 [136]	19 [242]	N.D.
Dda—EE	3.4 [242]	N.D.	257 [242]	N.D.	64 [242]	N.D.
TraI—monomer	6.2 [159]	N.D.	1,085 [159]	N.D.	N.D.	N.D.
TraI EE	8.2 [159]	N.D.	1,120 [159]	N.D.	>850 [243]	N.D.

[a]Not determined
[b]Excess enzyme—enzyme concentration is in excess of substrate
[c]Step size for ReΔ2B is assumed based on the duplex length and the number of steps in the kinetic mechanism
[d]Kinetic step size and rates of translocation have been measured for RecB and RecBC, but not for RecBCD [244]

Similar to the unwinding studies, translocation can be examined by measuring the time needed to reach the end of varying lengths of ssDNA. The lag phase for these measurements provides kinetic information that can give rise to kinetic step sizes, rates of translocation, and coupling efficiencies when combined with ATP hydrolysis measurements. One assay that provided a breakthrough in helicase ATPase studies was the development of the phosphate-binding protein for measuring phosphate release kinetics [91]. This assay has been instrumental in relating the rates and efficiencies of ATPase activity to movement on ssDNA. However, it has not been generally applied, as yet, to understanding unwinding of dsDNA.

Helicases can be described as acting by an active or passive mechanism in reference to whether they actively separate the duplex or simply trap single-stranded intermediates that form as a result of thermal fraying [132, 133]. One suggestion for classifying active vs. passive helicases relies on comparing the ratio of the velocity for translocation on ssDNA to the velocity for unwinding of dsDNA [133]. If this ratio falls between 0.25 and 1, then a helicase can be considered as active. Most helicases likely fall between these extremes, and for some SF1 helicases, comparison of unwinding and translocation rates is complicated by oligomerization that occurs during unwinding [119, 134, 135]. However, bacteriophage T4 Dda has been shown to unwind duplex DNA and translocate on ssDNA at the same rate suggesting that it functions by a completely active mechanism [136].

Single-Molecule Methods Provide New Insights into SF1 Helicases

Breakthroughs in technology have resulted in corresponding breakthroughs in biology, and this theme has held true in understanding helicase mechanisms. Single-molecule Förster resonance energy transfer (smFRET) as well as laser tweezers or magnetic tweezers have been extensively applied to the study of helicases during the past decade [137, 138]. These techniques are particularly useful for visualizing kinetic events that are “hidden” within ensemble experiments. Recognition of the Chi sequence in DNA causes RecBCD to pause and reduce its translocation rate to approximately one-half the initial rate [139–141] resulting in a switch in motor usage with RecD being the lead motor prior to Chi and RecB after the Chi sites [142]. Magnetic tweezer analysis reported the average unwinding rate by RecBCD to be 900 bp/s [143] and the processivity of the complex to be ~1.

The physical step size can be directly observed in some cases using smFRET or laser tweezers. Single-molecule studies of PcrA reported the unwinding step size to be one nt [144], whereas a kinetic step size of four nts for translocation was estimated from ensemble experiments [145]. The larger kinetic step size determined from ensemble analysis could be an overestimation due to the presence of static disorder. In the case of Dda, single-molecule and ensemble experiments reported the unwinding rate to be ~250 bp/s and the rate varied little for forces ranging from 5 to 13 pN [136].

The mechanisms by which helicases catalyze protein displacement are beginning to be explored [146]. Single-molecule studies revealed the repetitive movements of Rep, PcrA, and UvrD helicases on the same stretch of DNA. The *in vitro* smFRET studies showed that the shuttling of the Rep monomer on ssDNA can prevent RecA filament formation [147], and that PcrA reeling in ssDNA can remove a preformed RecA filament [144]. Two other SF1 helicases, yeast Srs2 [148, 149] and UvrD [150], can displace Rad51 and RecA presynaptic filaments from ssDNA, respectively. Single-molecule studies offer insight into why many helicases display only limited unwinding processivity *in vitro*. For Rep, the reduced processivity *in vitro* is due to the relative instability of the functional complex [120]. The open and closed conformational states of Rep helicase undergoing ATP hydrolysis while bound to DNA were studied using smFRET [151]. The biological significance of having multiple conformations might be to regulate the helicase activity. Recent developments in three (or more)-color FRET [152, 153] should enable one to obtain simultaneous information on more than one activity, for example, ATP cycling and movement on DNA.

Protein–Protein Interactions That Regulate Helicase Activity

Helicases translocate along nucleic acids while separating dsDNA into single strands. Translocase activity alone is, in some cases, insufficient for helicase activity. In these cases, oligomerization and/or interactions with other proteins can regulate their translocase and helicase activities. Oligomerization can affect their NTPase, DNA-binding and -unwinding activities [45]. The monomeric forms of some SF1 enzymes, Rep [119, 120, 147, 154, 155], UvrD [121, 134, 156], and PcrA [89, 91, 127, 145], are processive translocases [91, 92, 156, 157], but do not display DNA unwinding activity *in vitro* [147]. On the other hand, the SF1 helicases Dda [158] and TraI [159] are able to function as monomeric helicases *in vitro*, b. But with the exception of the TraI, the SF1 helicases, when examined by themselves, generally unwind DNA with low processivity *in vitro*.

The nucleic acid unwinding processivity of some SF1 helicases can be increased significantly either through self-assembly or interactions with accessory proteins [119, 121, 134, 135, 160]. Rep helicase (SF1A) exists as a monomer in the absence of DNA [161]. However, Rep undergoes a DNA-induced dimerization upon binding either ss or dsDNA [132, 162], and the dimer appears to be the active form of the Rep helicase [119, 132, 161, 163–165]. Single turnover kinetic studies of UvrD-catalyzed DNA unwinding suggested that dimers are the minimal oligomeric form needed for optimal helicase activity [121, 134, 135]. In the case of Pif1, binding of ssDNA induces protein dimerization [166]. Oligomerization provides the active helicase with multiple DNA- and NTP-binding sites that are necessary for optimal DNA unwinding activity.

Regulation of helicase activity through protein–protein interactions may occur by altering conformations of the helicase. Crystal structures of Rep bound to ssDNA

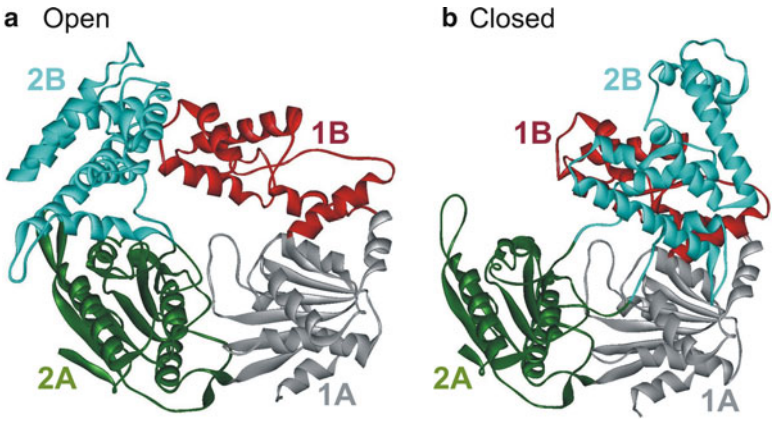

Fig. 2.6 Crystal structure of *E. coli* Rep helicase (PDB code 1UAA [88]) in the open and closed conformations. Rep consists of four domains 1A, 1B, 2A, and 2B which are colored *grey*, *red*, *green,* and *cyan,* respectively. The open (**a**) and closed (**b**) conformations differ by rotations of around 130° of the 2B domain about a hinge region connecting it to the 2A domain [167]. The other domains are unchanged in both forms

showed open and closed forms that differ in the 2B domain orientation [88] (Fig. 2.6). Deletion of the 2B domain in Rep was found to activate the helicase activity [154, 155]. Although, earlier smFRET studies have suggested the closed form of Rep to be an inhibited form [167], later detailed studies revealed two distinct Rep-partial-duplex DNA conformations in the ATPγS and ADP states. Here the primary conformation is found to be similar to the closed form, and in the secondary conformation the duplex DNA and 2B domain are rotated relative to the rest of the protein [151]. The multiple conformations may provide a mechanism of regulation of helicase activity whereby interactions between Rep and other proteins may determine the relative conformational states of domain 2B.

In addition to helicases interacting among themselves, they can interact with other helicases to modulate their activity. It has been reported that Pif1 helicase activity is essential in *top3* mutants in an Sgs1-dependent manner [168]. Pif1 has been suggested to strip Sgs1 from DNA, thereby downregulating the activity of Sgs1. Srs2 helicase has been reported to have a similar role in the disassembly of Rad51 filaments [148, 149]. Interaction between Rep and DnaB has been suggested to promote fork progression along protein-bound DNA [169].

Many SF1 enzymes are poor helicases *in vitro*; therefore, it is not surprising that their activities are enhanced through interactions with accessory proteins. Several helicases from prokaryotes and eukaryotes interact with other proteins to stimulate helicase activity [170–174]. The phage Φx174 gene A protein increases the helicase processivity of Rep [175–178]. PcrA is a nonprocessive helicase with difficulty unwinding even short lengths of duplex DNA [145], but the presence of plasmid replication initiator protein, RepD, enables PcrA to separate duplexes with high processivity [160, 179, 180].

The RecBCD holoenzyme contains two motors RecB (SF1A) and RecD (SF1B) in addition to the Chi recognition protein RecC [142]. RecBCD is compared to the world's fastest supercar [181], since with the RecB and RecD helicase motors [73, 182], RecBCD is capable of moving along DNA at over 1,000 base pairs per second [183]. RecBCD is able to switch which of the two motors takes the lead, thereby regulating the translocation velocity of the complex [142] following the recognition of recombination hotspots called Chi sites [184, 185]. RecB helicase is activated through an interaction with RecC. RecB is a poor helicase by itself [186], but in complex with RecC is highly processive [139, 182, 183, 187]. Interaction with the accessory protein RecC is suggested to relieve an inhibitory function of the 2B subdomain of RecB [188]. Similarly, the inability of Rep monomers to function as helicases *in vitro* seems to be the result of an autoinhibitory effect of its subdomain 2B, and the deletion of this domain stimulates helicase activity of the Rep monomer [155].

Increased helicase processivity has been linked to helicase–SSB interactions [173, 189]. Rep and UvrD advance movement of replisomes blocked by nucleoprotein complexes *in vitro* [190]. Here the binding of successive monomers of Rep or UvrD at a blocked fork could facilitate protein displacement. Okazaki fragment processing in eukaryotes can occur either by the FEN1-only pathway or the two-nuclease pathway [191]. It has been reported that Dna2, Pif1, and RPA, the proteins of the two-nuclease pathway, stimulate FEN1 acting in the one-nuclease pathway [192]. Interactions with these proteins may change the conformation of FEN1 to optimally function on the substrate [192].

Saccharomyces Rrm3 helicase (SF1B) promotes replication fork progression through telomeric and subtelomeric DNA. Rrm3 is telomere-associated *in vivo*, suggesting a direct role in telomere replication [193]. Rrm3 is also needed for the timely replication of the entire genome, possibly through its role in promoting fork progression through difficult-to-replicate sites [194]. Rrm3 interacts with the catalytic subunit of DNA polymerase epsilon as it moves through both Rrm3p-dependent and -independent sites [194].

In addition to the stimulatory effects, some helicase-accessory protein interactions reduce the helicase activity. Through structural, biochemical, and functional studies, it was shown that the Srs2 helicase interacts with SUMO-PCNA thereby suppressing the Rad52-dependent recombinational repair pathway [195]. Also, Pif1 helicase negatively regulates telomere lengths by catalytically inhibiting telomerase activity [196–198].

Conclusion

The overall view from these studies is that SF1 helicases have multiple DNA-binding sites and that the entire enzyme does not move as a single unit, but instead different domains of the enzyme move at different times during the translocation–unwinding cycle as a function of ATP binding and hydrolysis. The description of this movement as an "inchworm" appears to hold true. Although the structures and

helicase motifs are quite similar, the *in vivo* activities vary, which are likely achieved through structural differences outside of the 1A and 2A (RecA-like) domains. These variations can affect how the helicase interacts with the DNA substrate and how it interacts with other proteins which regulate its activity.

Despite the impressive progress made in understanding the kinetic and chemical mechanisms of helicases, there is much to be learned. The specific mechanism(s) by which most helicases actively pry apart the duplex remain to be determined. The specific step in the overall mechanism that limits the rate of the reaction is generally not known. Some data suggest that steps in the ATP hydrolysis cycle such as release of phosphate may limit the overall rate of DNA unwinding. The interactions between protein and DNA with the loading strand (or translocase strand) have been defined but interactions with the displaced strand largely remain a mystery. The role of protein–protein interactions in helicase mechanisms and other regulatory mechanisms remains to be uncovered. Finally, the specific mechanisms whereby helicases displace other proteins from DNA remain to be determined. There are certainly many unanswered questions that will require continued growth in the field.

Acknowledgements Funding for this work was provided by NIH R01 GM098922 (K.D.R.).

References

1. Caruthers JM, McKay DB. Helicase structure and mechanism. Curr Opin Struct Biol. 2002;12:123–33.
2. Delagoutte E, von Hippel PH. Helicase mechanisms and the coupling of helicases within macromolecular machines. Part II: integration of helicases into cellular processes. Q Rev Biophys. 2003;36:1–69.
3. Matson SW, Kaiser-Rogers KA. DNA helicases. Annu Rev Biochem. 1990;59:289–329.
4. Schmid SR, Linder P. D-E-A-D protein family of putative RNA helicases. Mol Microbiol. 1992;6:283–91.
5. Matson SW, Bean DW, George JW. DNA helicases: enzymes with essential roles in all aspects of DNA metabolism. Bioessays. 1994;16:13–22.
6. Alberts B. The cell as a collection of protein machines: preparing the next generation of molecular biologists. Cell. 1998;92:291–4.
7. Li J, Tang H, Mullen TM, Westberg C, Reddy TR, Rose DW, et al. A role for RNA helicase A in post-transcriptional regulation of HIV type 1. Proc Natl Acad Sci USA. 1999;96:709–14.
8. Linder P, Yeast RNA. helicases of the DEAD-box family involved in translation initiation. Biol Cell. 2003;95:157–67.
9. Bennett RJ, Keck JL. Structure and function of RecQ DNA helicases. Crit Rev Biochem Mol Biol. 2004;39:79–97.
10. Sangrithi MN, Bernal JA, Madine M, Philpott A, Lee J, Dunphy WG, et al. Initiation of DNA replication requires the RECQL4 protein mutated in Rothmund-Thomson syndrome. Cell. 2005;121:887–98.
11. Hartman TR, Qian S, Bolinger C, Fernandez S, Schoenberg DR, Boris-Lawrie K. RNA helicase A is necessary for translation of selected messenger RNAs. Nat Struct Mol Biol. 2006;13:509–16.

12. Matsuno K, Kumano M, Kubota Y, Hashimoto Y, Takisawa H. The N-terminal noncatalytic region of Xenopus RecQ4 is required for chromatin binding of DNA polymerase alpha in the initiation of DNA replication. Mol Cell Biol. 2006;26:4843–52.
13. Hu Y, Raynard S, Sehorn MG, Lu X, Bussen W, Zheng L, et al. RECQL5/Recql5 helicase regulates homologous recombination and suppresses tumor formation via disruption of Rad51 presynaptic filaments. Genes Dev. 2007;21:3073–84.
14. Modrich P. Mismatch repair, genetic stability, and cancer. Science. 1994;266:1959–60.
15. Sancar A. Mechanisms of DNA excision repair. Science. 1994;266:1954–6.
16. Andressoo JO, Hoeijmakers JH, de Waard H. Nucleotide excision repair and its connection with cancer and ageing. Adv Exp Med Biol. 2005;570:45–83.
17. Stevnsner T, Muftuoglu M, Aamann MD, Bohr VA. The role of Cockayne syndrome group B (CSB) protein in base excision repair and aging. Mech Ageing Dev. 2008;129:441–8.
18. Ellis NA. DNA helicases in inherited human disorders. Curr Opin Genet Dev. 1997;7:354–63.
19. Andressoo JO, Hoeijmakers JH. Transcription-coupled repair and premature ageing. Mutat Res. 1997;577:179–94.
20. Brosh Jr RM, Bohr VA. Human premature aging, DNA repair and RecQ helicases. Nucleic Acids Res. 2007;35:7527–44.
21. Ouyang KJ, Woo LL, Ellis NA. Homologous recombination and maintenance of genome integrity: cancer and aging through the prism of human RecQ helicases. Mech Ageing Dev. 2008;129:425–40.
22. German J. Bloom's syndrome. Dermatol Clin. 1995;13:7–18.
23. Shen JC, Gray MD, Oshima J, Kamath-Loeb AS, Fry M, Loeb LA. Werner syndrome protein. I. DNA helicase and dna exonuclease reside on the same polypeptide. J Biol Chem. 1998;273:34139–44.
24. Gibbons RJ, Bachoo S, Picketts DJ, Aftimos S, Asenbauer B, Bergoffen J, et al. Mutations in transcriptional regulator ATRX establish the functional significance of a PHD-like domain. Nat Genet. 1997;17:146–8.
25. Prince PR, Emond MJ, Monnat Jr RJ. Loss of Werner syndrome protein function promotes aberrant mitotic recombination. Genes Dev. 2001;15:933–8.
26. Saintigny Y, Makienko K, Swanson C, Emond MJ, Monnat Jr RJ. Homologous recombination resolution defect in werner syndrome. Mol Cell Biol. 2002;22:6971–8.
27. Hickson ID. RecQ helicases: caretakers of the genome. Nat Rev Cancer. 2003;3:169–78.
28. Sharma S, Doherty KM, Brosh Jr RM. Mechanisms of RecQ helicases in pathways of DNA metabolism and maintenance of genomic stability. Biochem J. 2006;398:319–37.
29. Ozgenc A, Loeb LA. Werner syndrome, aging and cancer. Genome Dyn. 2006;1:206–17.
30. Muftuoglu M, Oshima J, von Kobbe C, Cheng WH, Leistritz DF, Bohr VA. The clinical characteristics of Werner syndrome: molecular and biochemical diagnosis. Hum Genet. 2008;124:369–77.
31. Chisholm KM, Aubert SD, Freese KP, Zakian VA, King MC, Welcsh PL. A genomewide screen for suppressors of Alu-mediated rearrangements reveals a role for PIF1. PLoS One. 2012;7:e30748.
32. Chen YZ, Bennett CL, Huynh HM, Blair IP, Puls I, Irobi J, et al. DNA/RNA helicase gene mutations in a form of juvenile amyotrophic lateral sclerosis (ALS4). Am J Hum Genet. 2004;74:1128–35.
33. Moreira MC, Klur S, Watanabe M, Nemeth AH, Le Ber I, Moniz JC, et al. Senataxin, the ortholog of a yeast RNA helicase, is mutant in ataxia-ocular apraxia 2. Nat Genet. 2004;36:225–7.
34. Guenther UP, Handoko L, Laggerbauer B, Jablonka S, Chari A, Alzheimer M, et al. IGHMBP2 is a ribosome-associated helicase inactive in the neuromuscular disorder distal SMA type 1 (DSMA1). Hum Mol Genet. 2009;18:1288–300.
35. Grohmann K, Schuelke M, Diers A, Hoffmann K, Lucke B, Adams C, et al. Mutations in the gene encoding immunoglobulin mu-binding protein 2 cause spinal muscular atrophy with respiratory distress type 1. Nat Genet. 2001;29:75–7.

36. Aggarwal M, Brosh Jr RM. Hitting the bull's eye: novel directed cancer therapy through helicase-targeted synthetic lethality. J Cell Biochem. 2009;106:758–63.
37. Lehman IR, Boehmer PE. Replication of herpes simplex virus DNA. J Biol Chem. 1999;274:28059–62.
38. Kleymann G. Novel agents and strategies to treat herpes simplex virus infections. Expert Opin Investig Drugs. 2003;12:165–83.
39. Kleymann G. New antiviral drugs that target herpesvirus helicase primase enzymes. Herpes. 2003;10:46–52.
40. Kim DW, Gwack Y, Han JH, Choe J. C-terminal domain of the hepatitis C virus NS3 protein contains an RNA helicase activity. Biochem Biophys Res Commun. 1995;215:160–6.
41. De FR, Rice CM. New therapies on the horizon for hepatitis C: are we close? Clin Liver Dis. 2003;7:211–42, xi.
42. Harb OS, Abu KY. Essential role for the Legionella pneumophila rep helicase homologue in intracellular infection of mammalian cells. Infect Immun. 2000;68:6970–8.
43. Singleton MR, Dillingham MS, Wigley DB. Structure and mechanism of helicases and nucleic acid translocases. Annu Rev Biochem. 2007;76:23–50.
44. Enemark EJ, Joshua-Tor L. On helicases and other motor proteins. Curr Opin Struct Biol. 2008;18:243–57.
45. Lohman TM, Tomko EJ, Wu CG. Non-hexameric DNA helicases and translocases: mechanisms and regulation. Nat Rev Mol Cell Biol. 2008;9:391–401.
46. Gorbalenya AE, Koonin EV, Donchenko AP, Blinov VM. Two related superfamilies of putative helicases involved in replication, recombination, repair and expression of DNA and RNA genomes. Nucleic Acids Res. 1989;17:4713–30.
47. Gorbalenya AE, Koonin EV. Helicases: amino acid sequence comparisons and structure-function relationships. Curr Opin Struct Biol. 1993;3:419–29.
48. Singleton MR, Wigley DB. Modularity and specialization in superfamily 1 and 2 helicases. J Bacteriol. 2002;184:1819–26.
49. von Hippel PH, Delagoutte E. Macromolecular complexes that unwind nucleic acids. Bioessays. 2003;25:1168–77.
50. Becker PB, Horz W. ATP-dependent nucleosome remodeling. Annu Rev Biochem. 2002;71:247–73.
51. Lusser A, Kadonaga JT. Chromatin remodeling by ATP-dependent molecular machines. Bioessays. 2003;25:1192–200.
52. Petkovic M, Dietschy T, Freire R, Jiao R, Stagljar I. The human Rothmund-Thomson syndrome gene product, RECQL4, localizes to distinct nuclear foci that coincide with proteins involved in the maintenance of genome stability. J Cell Sci. 2005;118:4261–9.
53. Sharma S, Brosh Jr RM. Human RECQ1 is a DNA damage responsive protein required for genotoxic stress resistance and suppression of sister chromatid exchanges. PLoS One. 2007;2:e1297.
54. Larsen DH, Poinsignon C, Gudjonsson T, Dinant C, Payne MR, Hari FJ, et al. The chromatin-remodeling factor CHD4 coordinates signaling and repair after DNA damage. J Cell Biol. 2010;190:731–40.
55. Raynard S, Bussen W, Sung P. A double Holliday junction dissolvasome comprising BLM, topoisomerase IIIalpha, and BLAP75. J Biol Chem. 2006;281:13861–4.
56. Wu L, Bachrati CZ, Ou J, Xu C, Yin J, Chang M, et al. BLAP75/RMI1 promotes the BLM-dependent dissolution of homologous recombination intermediates. Proc Natl Acad Sci U S A. 2006;103:4068–73.
57. Barber LJ, Youds JL, Ward JD, McIlwraith MJ, O'Neil NJ, Petalcorin MI, et al. RTEL1 maintains genomic stability by suppressing homologous recombination. Cell. 2008;135:261–71.
58. Singh TR, Ali AM, Busygina V, Raynard S, Fan Q, Du CH, et al. BLAP18/RMI2, a novel OB-fold-containing protein, is an essential component of the Bloom helicase-double Holliday junction dissolvasome. Genes Dev. 2008;22:2856–68.

59. Bugreev DV, Brosh Jr RM, Mazin AV. RECQ1 possesses DNA branch migration activity. J Biol Chem. 2008;283:20231–42.
60. Uringa EJ, Youds JL, Lisaingo K, Lansdorp PM, Boulton SJ. RTEL1: an essential helicase for telomere maintenance and the regulation of homologous recombination. Nucleic Acids Res. 2011;39:1647–55.
61. Picketts DJ, Tastan AO, Higgs DR, Gibbons RJ. Comparison of the human and murine ATRX gene identifies highly conserved, functionally important domains. Mamm Genome. 1998;9:400–3.
62. Travers A. Chromatin modification by DNA tracking. Proc Natl Acad Sci USA. 1999;96:13634–7.
63. Alexeev A, Mazin A, Kowalczykowski SC. Rad54 protein possesses chromatin-remodeling activity stimulated by the Rad51-ssDNA nucleoprotein filament. Nat Struct Biol. 2003;10:182–6.
64. Zhang Z, Fan HY, Goldman JA, Kingston RE. Homology-driven chromatin remodeling by human RAD54. Nat Struct Mol Biol. 2007;14:397–405.
65. Srivastava V, Modi P, Tripathi V, Mudgal R, De S, Sengupta S. BLM helicase stimulates the ATPase and chromatin-remodeling activities of RAD54. J Cell Sci. 2009;122:3093–103.
66. Troelstra C, van Gool A, de Wit J, Vermeulen W, Bootsma D, Hoeijmakers JH. ERCC6, a member of a subfamily of putative helicases, is involved in Cockayne's syndrome and preferential repair of active genes. Cell. 1992;71:939–53.
67. Evans E, Fellows J, Coffer A, Wood RD. Open complex formation around a lesion during nucleotide excision repair provides a structure for cleavage by human XPG protein. EMBO J. 1997;16:625–38.
68. Eisen A, Lucchesi JC. Unraveling the role of helicases in transcription. Bioessays. 1998;20:634–41.
69. Moreland RJ, Tirode F, Yan Q, Conaway JW, Egly JM, Conaway RC. A role for the TFIIH XPB DNA helicase in promoter escape by RNA polymerase II. J Biol Chem. 1999;274:22127–30.
70. Fuller-Pace FV. DExD/H box RNA helicases: multifunctional proteins with important roles in transcriptional regulation. Nucleic Acids Res. 2008;34:4206–15.
71. Aygun O, Svejstrup J, Liu Y. A RECQ5-RNA polymerase II association identified by targeted proteomic analysis of human chromatin. Proc Natl Acad Sci U S A. 2008;105:8580–4.
72. Izumikawa K, Yanagida M, Hayano T, Tachikawa H, Komatsu W, Shimamoto A, et al. Association of human DNA helicase RecQ5beta with RNA polymerase II and its possible role in transcription. Biochem J. 2008;413:505–16.
73. Dillingham MS, Spies M, Kowalczykowski SC. RecBCD enzyme is a bipolar DNA helicase. Nature. 2003;423:893–7.
74. Naqvi A, Tinsley E, Khan SA. Purification and characterization of the PcrA helicase of Bacillus anthracis. J Bacteriol. 2003;185:6633–9.
75. Constantinesco F, Forterre P, Koonin EV, Aravind L, Elie C. A bipolar DNA helicase gene, herA, clusters with rad50, mre11 and nurA genes in thermophilic archaea. Nucleic Acids Res. 2004;32:1439–47.
76. Hall MC, Matson SW. Helicase motifs: the engine that powers DNA unwinding. Mol Microbiol. 1999;34:867–77.
77. Tuteja N, Tuteja R. Prokaryotic and eukaryotic DNA helicases. Essential molecular motor proteins for cellular machinery. Eur J Biochem. 2004;271:1835–48.
78. Lohman TM. Escherichia coli DNA helicases: mechanisms of DNA unwinding. Mol Microbiol. 1992;6:5–14.
79. Tuteja N, Tuteja R. Unraveling DNA helicases. Motif, structure, mechanism and function. Eur J Biochem. 2004;271:1849–63.
80. Bird LE, Subramanya HS, Wigley DB. Helicases: a unifying structural theme? Curr Opin Struct Biol. 1998;8:14–8.
81. Iyer LM, Leipe DD, Koonin EV, Aravind L. Evolutionary history and higher order classification of AAA+ ATPases. J Struct Biol. 2004;146:11–31.

82. Kadare G, Haenni AL. Virus-encoded RNA helicases. J Virol. 1997;71:2583–90.
83. Cordin O, Banroques J, Tanner NK, Linder P. The DEAD-box protein family of RNA helicases. Gene. 2006;367:17–37.
84. Jankowsky E, Fairman ME. RNA helicases—one fold for many functions. Curr Opin Struct Biol. 2007;17:316–24.
85. Pyle AM. Translocation and unwinding mechanisms of RNA and DNA helicases. Annu Rev Biophys. 2008;37:317–36.
86. Fairman-Williams ME, Guenther UP, Jankowsky E. SF1 and SF2 helicases: family matters. Curr Opin Struct Biol. 2010;20:313–24.
87. Subramanya HS, Bird LE, Brannigan JA, Wigley DB. Crystal structure of a DExx box DNA helicase. Nature. 1996;384:379–83.
88. Korolev S, Hsieh J, Gauss GH, Lohman TM, Waksman G. Major domain swiveling revealed by the crystal structures of complexes of E. coli Rep helicase bound to single-stranded DNA and ADP. Cell. 1997;90:635–47.
89. Velankar SS, Soultanas P, Dillingham MS, Subramanya HS, Wigley DB. Crystal structures of complexes of PcrA DNA helicase with a DNA substrate indicate an inchworm mechanism. Cell. 1999;97:75–84.
90. Soultanas P, Dillingham MS, Wiley P, Webb MR, Wigley DB. Uncoupling DNA translocation and helicase activity in PcrA: direct evidence for an active mechanism. EMBO J. 2000;19:3799–810.
91. Dillingham MS, Wigley DB, Webb MR. Demonstration of unidirectional single-stranded DNA translocation by PcrA helicase: measurement of step size and translocation speed. Biochemistry. 2000;39:205–12.
92. Tomko EJ, Fischer CJ, Niedziela-Majka A, Lohman TM. A nonuniform stepping mechanism for E. coli UvrD monomer translocation along single-stranded DNA. Mol Cell. 2007;26:335–47.
93. Saikrishnan K, Griffiths SP, Cook N, Court R, Wigley DB. DNA binding to RecD: role of the 1B domain in SF1B helicase activity. EMBO J. 2008;27:2222–9.
94. Saikrishnan K, Powell B, Cook NJ, Webb MR, Wigley DB. Mechanistic basis of 5′–3′ translocation in SF1B helicases. Cell. 2009;137:849–59.
95. Gorbalenya AE, Koonin EV, Donchenko AP, Blinov VM. A novel superfamily of nucleoside triphosphate-binding motif containing proteins which are probably involved in duplex unwinding in DNA and RNA replication and recombination. FEBS Lett. 1988;235:16–24.
96. Gorbalenya AE, Koonin EV, Donchenko AP, Blinov VM. A conserved NTP-motif in putative helicases. Nature. 1988;333:22.
97. Hodgman TC. A new superfamily of replicative proteins. Nature. 1988;333:22–3.
98. Ilyina TV, Koonin EV. Conserved sequence motifs in the initiator proteins for rolling circle DNA replication encoded by diverse replicons from eubacteria, eucaryotes and archaebacteria. Nucleic Acids Res. 1992;20:3279–85.
99. Korolev S, Yao N, Lohman TM, Weber PC, Waksman G. Comparisons between the structures of HCV and Rep helicases reveal structural similarities between SF1 and SF2 super-families of helicases. Protein Sci. 1998;7:605–10.
100. Kim JL, Morgenstern KA, Griffith JP, Dwyer MD, Thomson JA, Murcko MA, et al. Hepatitis C virus NS3 RNA helicase domain with a bound oligonucleotide: the crystal structure provides insights into the mode of unwinding. Structure. 1998;6:89–100.
101. Tanner NK. The newly identified Q motif of DEAD box helicases is involved in adenine recognition. Cell Cycle. 2003;2:18–9.
102. Bernstein DA, Zittel MC, Keck JL. High-resolution structure of the E. coli RecQ helicase catalytic core. EMBO J. 2003;22:4910–21.
103. Singleton MR, Dillingham MS, Gaudier M, Kowalczykowski SC, Wigley DB. Crystal structure of RecBCD enzyme reveals a machine for processing DNA breaks. Nature. 2004; 432:187–93.
104. Durr H, Korner C, Muller M, Hickmann V, Hopfner KP. X-ray structures of the Sulfolobus solfataricus SWI2/SNF2 ATPase core and its complex with DNA. Cell. 2005;121:363–73.

105. Rozen F, Pelletier J, Trachsel H, Sonenberg N. A lysine substitution in the ATP-binding site of eucaryotic initiation factor 4A abrogates nucleotide-binding activity. Mol Cell Biol. 1989;9:4061–3.
106. Tanner NK, Linder P. DExD/H box RNA helicases: from generic motors to specific dissociation functions. Mol Cell. 2001;8:251–62.
107. Walker JE, Saraste M, Runswick MJ, Gay NJ. Distantly related sequences in the alpha- and beta-subunits of ATP synthase, myosin, kinases and other ATP-requiring enzymes and a common nucleotide binding fold. EMBO J. 1982;1:945–51.
108. Venkatesan M, Silver LL, Nossal NG. Bacteriophage T4 gene 41 protein, required for the synthesis of RNA primers, is also a DNA helicase. J Biol Chem. 1982;257:12426–34.
109. Story RM, Steitz TA. Structure of the recA protein-ADP complex. Nature. 1992; 355:374–6.
110. Pause A, Sonenberg N. Mutational analysis of a DEAD box RNA helicase: the mammalian translation initiation factor eIF-4A. EMBO J. 1992;11:2643–54.
111. Brosh Jr RM, Matson SW. Mutations in motif II of Escherichia coli DNA helicase II render the enzyme nonfunctional in both mismatch repair and excision repair with differential effects on the unwinding reaction. J Bacteriol. 1995;177:5612–21.
112. Weng Y, Czaplinski K, Peltz SW. Genetic and biochemical characterization of mutations in the ATPase and helicase regions of the Upf1 protein. Mol Cell Biol. 1996;16:5477–90.
113. Graves-Woodward KL, Gottlieb J, Challberg MD, Weller SK. Biochemical analyses of mutations in the HSV-1 helicase-primase that alter ATP hydrolysis, DNA unwinding, and coupling between hydrolysis and unwinding. J Biol Chem. 1997;272:4623–30.
114. Brosh Jr RM, Matson SW. A point mutation in Escherichia coli DNA helicase II renders the enzyme nonfunctional in two DNA repair pathways. Evidence for initiation of unwinding from a nick in vivo. J Biol Chem. 1997;272:572–9.
115. Brosh Jr RM, Matson SW. A partially functional DNA helicase II mutant defective in forming stable binary complexes with ATP and DNA. A role for helicase motif III. J Biol Chem. 1996;271:25360–8.
116. Graves-Woodward KL, Weller SK. Replacement of gly815 in helicase motif V alters the single-stranded DNA-dependent ATPase activity of the herpes simplex virus type 1 helicase-primase. J Biol Chem. 1996;271:13629–35.
117. Hall MC, Ozsoy AZ, Matson SW. Site-directed mutations in motif VI of Escherichia coli DNA helicase II result in multiple biochemical defects: evidence for the involvement of motif VI in the coupling of ATPase and DNA binding activities via conformational changes. J Mol Biol. 1998;277:257–71.
118. Banroques J, Cordin O, Doere M, Linder P, Tanner NK. A conserved phenylalanine of motif IV in superfamily 2 helicases is required for cooperative, ATP-dependent binding of RNA substrates in DEAD-box proteins. Mol Cell Biol. 2008;28:3359–71.
119. Cheng W, Hsieh J, Brendza KM, Lohman TM. E. coli Rep oligomers are required to initiate DNA unwinding in vitro. J Mol Biol. 2001;310:327–50.
120. Ha T, Rasnik I, Cheng W, Babcock HP, Gauss GH, Lohman TM, et al. Initiation and re-initiation of DNA unwinding by the Escherichia coli Rep helicase. Nature. 2002;419:638–41.
121. Maluf NK, Ali JA, Lohman TM. Kinetic mechanism for formation of the active, dimeric UvrD helicase-DNA complex. J Biol Chem. 2003;278:31930–40.
122. Lee JY, Yang W. UvrD helicase unwinds DNA bone base pair at a time by a two-part power stroke. Cell. 2006;127:1349–60.
123. Yao N, Hesson T, Cable M, Hong Z, Kwong AD, Le HV, et al. Structure of the hepatitis C virus RNA helicase domain. Nat Struct Biol. 1997;4:463–7.
124. Sengoku T, Nureki O, Nakamura A, Kobayashi S, Yokoyama S. Structural basis for RNA unwinding by the DEAD-box protein Drosophila Vasa. Cell. 2006;125:287–300.
125. Buttner K, Nehring S, Hopfner KP. Structural basis for DNA duplex separation by a superfamily-2 helicase. Nat Struct Mol Biol. 2007;14:647–52.
126. Singleton MR, Scaife S, Wigley DB. Structural analysis of DNA replication fork reversal by RecG. Cell. 2001;107:79–89.

127. Soultanas P, Wigley DB. DNA helicases: 'inching forward'. Curr Opin Struct Biol. 2000;10:124–8.
128. Hargreaves D, Rice DW, Sedelnikova SE, Artymiuk PJ, Lloyd RG, Rafferty JB. Crystal structure of E. coli RuvA with bound DNA Holliday junction at 6 A resolution. Nat Struct Biol. 1998;5:441–6.
129. Ariyoshi M, Nishino T, Iwasaki H, Shinagawa H, Morikawa K. Crystal structure of the Holliday junction DNA in complex with a single RuvA tetramer. Proc Natl Acad Sci USA. 2000;97:8257–62.
130. Lam AM, Keeney D, Frick DN. Two novel conserved motifs in the hepatitis C virus NS3 protein critical for helicase action. J Biol Chem. 2003;278:44514–24.
131. Ali JA, Lohman TM. Kinetic measurement of the step size of DNA unwinding by Escherichia coli UvrD helicase. Science. 1997;275:377–80.
132. Wong I, Lohman TM. Allosteric effects of nucleotide cofactors on Escherichia coli Rep helicase-DNA binding. Science. 1992;256:350–5.
133. Manosas M, Xi XG, Bensimon D, Croquette V. Active and passive mechanisms of helicases. Nucleic Acids Res. 2010;38:5518–26.
134. Ali JA, Maluf NK, Lohman TM. An oligomeric form of E. coli UvrD is required for optimal helicase activity. J Mol Biol. 1999;293:815–34.
135. Maluf NK, Fischer CJ, Lohman TM. A dimer of Escherichia coli UvrD is the active form of the helicase in vitro. J Mol Biol. 2003;325:913–35.
136. Byrd AK, Matlock DL, Bagchi D, Aarattuthodiyil S, Harrison D, Croquette V, et al. Dda helicase tightly couples translocation on single-stranded dna to unwinding of duplex DNA: Dda is an optimally active helicase. J Mol Biol. 2012;420(3):141–54.
137. Myong S, Ha T. Stepwise translocation of nucleic acid motors. Curr Opin Struct Biol. 2010;20:121–7.
138. Ha T, Kozlov AG, Lohman TM. Single-molecule views of protein movement on single-stranded DNA. Annu Rev Biophys. 2012;41:295–319.
139. Bianco PR, Brewer LR, Corzett M, Balhorn R, Yeh Y, Kowalczykowski SC, et al. Processive translocation and DNA unwinding by individual RecBCD enzyme molecules. Nature. 2001;409:374–8.
140. Dohoney KM, Gelles J. Chi-sequence recognition and DNA translocation by single RecBCD helicase/nuclease molecules. Nature. 2001;409:370–4.
141. Spies M, Bianco PR, Dillingham MS, Handa N, Baskin RJ, Kowalczykowski SC. A molecular throttle: the recombination hotspot chi controls DNA translocation by the RecBCD helicase. Cell. 2003;114:647–54.
142. Spies M, Amitani I, Baskin RJ, Kowalczykowski SC. RecBCD enzyme switches lead motor subunits in response to [chi] recognition. Cell. 2007;131:694–705.
143. Rasnik I, Myong S, Ha T. Unraveling helicase mechanisms one molecule at a time. Nucleic Acids Res. 2006;34:4225–31.
144. Park J, Myong S, Niedziela-Majka A, Lee KS, Yu J, Lohman TM, et al. PcrA helicase dismantles RecA filaments by reeling in DNA in uniform steps. Cell. 2010;142:544–55.
145. Niedziela-Majka A, Chesnik MA, Tomko EJ, Lohman TM. Bacillus stearothermophilus PcrA monomer is a single-stranded DNA translocase but not a processive helicase in vitro. J Biol Chem. 2007;282:27076–85.
146. Antony E, Tomko Q, Xiao L, Krejci L, Lohman TM, Ellengerger T. Srs2 disassembles Rad51 filaments by a protein-protein interaction triggering ATP turnover and dissociation of Rad51 from DNA. Mol Cell. 2009;35:105–15.
147. Myong S, Rasnik I, Joo C, Lohman TM, Ha T. Repetitive shuttling of a motor protein on DNA. Nature. 2005;437:1321–5.
148. Krejci L, Van KS, Li Y, Villemain J, Reddy MS, Klein H, et al. DNA helicase Srs2 disrupts the Rad51 presynaptic filament. Nature. 2003;423:305–9.
149. Veaute X, Jeusset J, Soustelle C, Kowalczykowski SC, Le CE, Fabre F. The Srs2 helicase prevents recombination by disrupting Rad51 nucleoprotein filaments. Nature. 2003;423:309–12.

150. Veaute X, Delmas S, Selva M, Jeusset J, Le CE, Matic I, et al. UvrD helicase, unlike Rep helicase, dismantles RecA nucleoprotein filaments in Escherichia coli. EMBO J. 2005;24:180–9.
151. Balci H, Arslan S, Myong S, Lohman TM, Ha T. Single-molecule nanopositioning: structural transitions of a helicase-DNA complex during ATP hydrolysis. Biophys J. 2011; 101:976–84.
152. Hohng S, Joo C, Ha T. Single-molecule three-color FRET. Biophys J. 2004;87:1328–37.
153. Clamme JP, Deniz AA. Three-color single-molecule fluorescence resonance energy transfer. Chemphyschem. 2005;6:74–7.
154. Cheng W, Brendza KM, Gauss GH, Korolev S, Waksman G, Lohman TM. The 2B domain of the Escherichia coli Rep protein is not required for DNA helicase activity. Proc Natl Acad Sci U S A. 2002;99:16006–11.
155. Brendza KM, Cheng W, Fischer CJ, Chesnik MA, Niedziela-Majka A, Lohman TM. Autoinhibition of Escherichia coli Rep monomer helicase activity by its 2B subdomain. Proc Natl Acad Sci U S A. 2005;102:10076–81.
156. Fischer CJ, Maluf NK, Lohman TM. Mechanism of ATP-dependent translocation of E. coli UvrD monomers along single-stranded DNA. J Mol Biol. 2004;344:1287–309.
157. Dillingham MS, Wigley DB, Webb MR. Direct measurement of single-stranded DNA translocation by PcrA helicase using the fluorescent base analogue 2-aminopurine. Biochemistry. 2002;41:643–51.
158. Nanduri B, Byrd AK, Eoff RL, Tackett AJ, Raney KD. Pre-steady-state DNA unwinding by bacteriophage T4 Dda helicase reveals a monomeric molecular motor. Proc Natl Acad Sci U S A. 2002;99:14722–7.
159. Sikora B, Eoff RL, Matson SW, Raney KD. DNA unwinding by Escherichia coli DNA helicase I (TraI) provides evidence for a processive monomeric molecular motor. J Biol Chem. 2006;281:36110–6.
160. Zhang W, Dillingham MS, Thomas CD, Allen S, Roberts CJ, Soultanas P. Directional loading and stimulation of PcrA helicase by the replication initiator protein RepD. J Mol Biol. 2007;371:336–48.
161. Chao KL, Lohman TM. DNA-induced dimerization of the Escherichia coli Rep helicase. J Mol Biol. 1991;221:1165–81.
162. Wong I, Chao KL, Bujalowski W, Lohman TM. DNA-induced dimerization of the Escherichia coli rep helicase. Allosteric effects of single-stranded and duplex DNA. J Biol Chem. 1992;267:7596–610.
163. Amaratunga M, Lohman TM. Escherichia coli rep helicase unwinds DNA by an active mechanism. Biochemistry. 1993;32:6815–20.
164. Bjornson KP, Amaratunga M, Moore KJ, Lohman TM. Single-turnover kinetics of helicase-catalyzed DNA unwinding monitored continuously by fluorescence energy transfer. Biochemistry. 1994;33:14306–16.
165. Bjornson KP, Moore KJ, Lohman TM. Kinetic mechanism of DNA binding and DNA-induced dimerization of the Escherichia coli Rep helicase. Biochemistry. 1996;35:2268–82.
166. Barranco-Medina S, Galletto R. DNA binding induces dimerization of Saccharomyces cerevisiae Pif1. Biochemistry. 2010;49(39):8445–54.
167. Rasnik I, Myong S, Cheng W, Lohman TM, Ha T. DNA-binding orientation and domain conformation of the E. coli rep helicase monomer bound to a partial duplex junction: single-molecule studies of fluorescently labeled enzymes. J Mol Biol. 2004;336:395–408.
168. Wagner M, Price G, Rothstein R. The absence of Top3 reveals an interaction between the Sgs1 and Pif1 DNA helicases in Saccharomyces cerevisiae. Genetics. 2006;174:555–73.
169. Atkinson J, Gupta MK, Rudolph CJ, Bell H, Lloyd RG, McGlynn P. Localization of an accessory helicase at the replisome is critical in sustaining efficient genome duplication. Nucleic Acids Res. 2011;39(3):949–57.
170. Korhonen JA, Gaspari M, Falkenberg M. TWINKLE Has 5′ -> 3′ DNA helicase activity and is specifically stimulated by mitochondrial single-stranded DNA-binding protein. J Biol Chem. 2003;278:48627–32.

171. Cadman CJ, McGlynn P. PriA helicase and SSB interact physically and functionally. Nucleic Acids Res. 2004;32:6378–87.
172. Shereda RD, Bernstein DA, Keck JL. A central role for SSB in Escherichia coli RecQ DNA helicase function. J Biol Chem. 2007;282:19247–58.
173. Rajagopal V, Patel SS. Single strand binding proteins increase the processivity of DNA unwinding by the hepatitis C virus helicase. J Mol Biol. 2008;376:69–79.
174. Sowd G, Wang H, Pretto D, Chazin WJ, Opresko PL. Replication protein A stimulates the Werner syndrome protein branch migration activity. J Biol Chem. 2009;284:34682–91.
175. Scott JF, Eisenberg S, Bertsch LL, Kornberg A. A mechanism of duplex DNA replication revealed by enzymatic studies of phage phi X174: catalytic strand separation in advance of replication. Proc Natl Acad Sci U S A. 1977;74:193–7.
176. Eisenberg S, Griffith J, Kornberg A. phiX174 cistron A protein is a multifunctional enzyme in DNA replication. Proc Natl Acad Sci U S A. 1977;74:3198–202.
177. Yarranton GT, Gefter ML. Enzyme-catalyzed DNA unwinding: studies on Escherichia coli rep protein. Proc Natl Acad Sci U S A. 1979;76:1658–62.
178. Reinberg D, Zipursky SL, Weisbeek P, Brown D, Hurwitz J. Studies on the phi X174 gene A protein-mediated termination of leading strand DNA synthesis. J Biol Chem. 1983;258:529–37.
179. Soultanas P, Dillingham MS, Papadopoulos F, Phillips SE, Thomas CD, Wigley DB. Plasmid replication initiator protein RepD increases the processivity of PcrA DNA helicase. Nucleic Acids Res. 1999;27:1421–8.
180. Slatter AF, Thomas CD, Webb MR. PcrA helicase tightly couples ATP hydrolysis to unwinding double-stranded DNA, modulated by the initiator protein for plasmid replication, RepD. Biochemistry. 2009;48(27):6326–34.
181. Wigley DB. RecBCD: the supercar of DNA repair. Cell. 2007;131:651–3.
182. Taylor AF, Smith GR. RecBCD enzyme is a DNA helicase with fast and slow motors of opposite polarity. Nature. 2003;423:889–93.
183. Roman LJ, Eggleston AK, Kowalczykowski SC. Processivity of the DNA helicase activity of Escherichia coli recBCD enzyme. J Biol Chem. 1992;267:4207–14.
184. Lam ST, Stahl MM, McMilin KD, Stahl FW. Rec-mediated recombinational hot spot activity in bacteriophage lambda. II. A mutation which causes hot spot activity. Genetics. 1974;77:425–33.
185. Anderson DG, Kowalczykowski SC. The recombination hot spot chi is a regulatory element that switches the polarity of DNA degradation by the RecBCD enzyme. Genes Dev. 1997;11:571–81.
186. Boehmer PE, Emmerson PT. The RecB subunit of the Escherichia coli RecBCD enzyme couples ATP hydrolysis to DNA unwinding. J Biol Chem. 1992;267:4981–7.
187. Bianco PR, Kowalczykowski SC. Translocation step size and mechanism of the RecBC DNA helicase. Nature. 2000;405:368–72.
188. Rigden DJ. An inactivated nuclease-like domain in RecC with novel function: implications for evolution. BMC Struct Biol. 2005;5:9.
189. Marsh VL, McGeoch AT, Bell SD. Influence of chromatin and single strand binding proteins on the activity of an archaeal MCM. J Mol Biol. 2006;357:1345–50.
190. Guy CP, Atkinson J, Gupta MK, Mahdi A, Gwynn EJ, Rudolph CJ, et al. Rep provides a second motor at the replisome to promote duplication of protein-bound DNA. Mol Cell. 2009;36:654–66.
191. Bae SH, Seo YS. Characterization of the enzymatic properties of the yeast dna2 helicase/endonuclease suggests a new model for Okazaki fragment processing. J Biol Chem. 2000;275:38022–31.
192. Henry RA, Balakrishnan L, Ying-Lin ST, Campbell JL, Bambara RA. Components of the secondary pathway stimulate the primary pathway of eukaryotic Okazaki fragment processing. J Biol Chem. 2010;285:28496–505.
193. Ivessa AS, Zhou JQ, Schulz VP, Monson EK, Zakian VA. Saccharomyces Rrm3p, a 5′ to 3′ DNA helicase that promotes replication fork progression through telomeric and subtelomeric DNA. Genes Dev. 2002;16:1383–96.

194. Azvolinsky AS, Dunaway S, Torres JZ, Bessler JB, Zakian VA. The S. cerevisiae Rrm3p DNA helicase moves with the replication fork and affects replication of all yeast chromosomes. Genes Dev. 2006;20:3104–16.
195. Armstrong AA, Mohideen F, Lima CD. Recognition of SUMO-modified PCNA requires tandem receptor motifs in Srs2. Nature. 2012;483:59–63.
196. Schulz VP, Zakian VA. The Saccharomyces PIF1 DNA helicase inhibits telomere elongation and de novo telomere formation. Cell. 1994;76:145–55.
197. Zhou J, Monson EK, Teng SC, Schulz VP, Zakian VA. Pif1p helicase, a catalytic inhibitor of telomerase in yeast. Science. 2000;289:771–4.
198. Boule JB, Vega LR, Zakian VA. The yeast Pif1p helicase removes telomerase from telomeric DNA. Nature. 2005;438:57–61.
199. Jongeneel CV, Bedinger P, Alberts BM. Effects of the bacteriophage T4 dda protein on DNA synthesis catalyzed by purified T4 replication proteins. J Biol Chem. 1984;259:12933–8.
200. Amundsen SK, Taylor AF, Chaudhury AM, Smith GR. recD: the gene for an essential third subunit of exonuclease V. Proc Natl Acad Sci U S A. 1986;83:5558–62.
201. Lahue EE, Matson SW. Purified Escherichia coli F-factor TraY protein binds oriT. J Bacteriol. 1990;172:1385–91.
202. Iordanescu S, Bargonetti J. Staphylococcus aureus chromosomal mutations that decrease efficiency of Rep utilization in replication of pT181 and related plasmids. J Bacteriol. 1989;171:4501–3.
203. Dodson MS, Lehman IR. Association of DNA helicase and primase activities with a subassembly of the herpes simplex virus 1 helicase-primase composed of the UL5 and UL52 gene products. Proc Natl Acad Sci U S A. 1991;88:1105–9.
204. Rong L, Palladino F, Aguilera A, Klein HL. The hyper-gene conversion hpr5-1 mutation of Saccharomyces cerevisiae is an allele of the SRS2/RADH gene. Genetics. 1991;127:75–85.
205. Gauss P, Park K, Spencer TE, Hacker KJ. DNA helicase requirements for DNA replication during bacteriophage T4 infection. J Bacteriol. 1994;176:1667–72.
206. Bjornson KP, Wong I, Lohman TM. ATP hydrolysis stimulates binding and release of single stranded DNA from alternating subunits of the dimeric E. coli Rep helicase: implications for ATP-driven helicase translocation. J Mol Biol. 1996;263:411–22.
207. Budd ME, Campbell JL. A yeast replicative helicase, Dna2 helicase, interacts with yeast FEN-1 nuclease in carrying out its essential function. Mol Cell Biol. 1997;17:2136–42.
208. Bird LE, Brannigan JA, Subramanya HS, Wigley DB. Characterisation of Bacillus stearothermophilus PcrA helicase: evidence against an active rolling mechanism. Nucleic Acids Res. 1998;26:2686–93.
209. Dao V, Modrich P. Mismatch-, MutS-, MutL-, and helicase II-dependent unwinding from the single-strand break of an incised heteroduplex. J Biol Chem. 1998;273:9202–7.
210. Petit MA, Dervyn E, Rose M, Entian KD, McGovern S, Ehrlich SD, et al. PcrA is an essential DNA helicase of Bacillus subtilis fulfilling functions both in repair and rolling-circle replication. Mol Microbiol. 1998;29:261–73.
211. Bruand C, Ehrlich SD. UvrD-dependent replication of rolling-circle plasmids in Escherichia coli. Mol Microbiol. 2000;35:204–10.
212. Ivessa AS, Zhou JQ, Zakian VA. The Saccharomyces Pif1p DNA helicase and the highly related Rrm3p have opposite effects on replication fork progression in ribosomal DNA. Cell. 2000;100:479–89.
213. Wang SW, Goodwin A, Hickson ID, Norbury CJ. Involvement of Schizosaccharomyces pombe Srs2 in cellular responses to DNA damage. Nucleic Acids Res. 2001;29:2963–72.
214. Choe W, Budd M, Imamura O, Hoopes L, Campbell JL. Dynamic localization of an Okazaki fragment processing protein suggests a novel role in telomere replication. Mol Cell Biol. 2002;22:4202–17.
215. Lesur I, Campbell JL. The transcriptome of prematurely aging yeast cells is similar to that of telomerase-deficient cells. Mol Biol Cell. 2004;15:1297–312.
216. Ding H, Schertzer M, Wu X, Gertsenstein M, Selig S, Kammori M, et al. Regulation of murine telomere length by Rtel: an essential gene encoding a helicase-like protein. Cell. 2004;117:873–86.

217. Opresko PL, Otterlei M, Graakjaer J, Bruheim P, Dawut L, Kolvraa S, et al. The Werner syndrome helicase and exonuclease cooperate to resolve telomeric D loops in a manner regulated by TRF1 and TRF2. Mol Cell. 2004;14:763–74.
218. Budd ME, Reis CC, Smith S, Myung K, Campbell JL. Evidence suggesting that Pif1 helicase functions in DNA replication with the Dna2 helicase/nuclease and DNA polymerase delta. Mol Cell Biol. 2006;26:2490–500.
219. Liao S, Toczylowski T, Yan H. Identification of the Xenopus DNA2 protein as a major nuclease for the 5′->3′ strand-specific processing of DNA ends. Nucleic Acids Res. 2008;36:6091–100.
220. Rossi ML, Pike JE, Wang W, Burgers PM, Campbell JL, Bambara RA. Pif1 helicase directs eukaryotic Okazaki fragments toward the two-nuclease cleavage pathway for primer removal. J Biol Chem. 2008;283:27483–93.
221. London TB, Barber LJ, Mosedale G, Kelly GP, Balasubramanian S, Hickson ID, et al. FANCJ is a structure-specific DNA helicase associated with the maintenance of genomic G/C tracts. J Biol Chem. 2008;283:36132–9.
222. Wu Y, Shin-ya K, Brosh Jr RM. FANCJ helicase defective in Fanconia anemia and breast cancer unwinds G-quadruplex DNA to defend genomic stability. Mol Cell Biol. 2008;28:4116–28.
223. Pike JE, Burgers PM, Campbell JL, Bambara RA. Pif1 helicase lengthens some Okazaki fragment flaps necessitating Dna2 nuclease/helicase action in the two-nuclease processing pathway. J Biol Chem. 2009;284:25170–80.
224. Ghosh A, Rossi ML, Aulds J, Croteau D, Bohr VA. Telomeric D-loops containing 8-oxo-2′-deoxyguanosine are preferred substrates for Werner and Bloom syndrome helicases and are bound by POT1. J Biol Chem. 2009;284:31074–84.
225. Burgers PM. Polymerase dynamics at the eukaryotic DNA replication fork. J Biol Chem. 2009;284:4041–5.
226. Chakraborty P, Grosse F. WRN helicase unwinds Okazaki fragment-like hybrids in a reaction stimulated by the human DHX9 helicase. Nucleic Acids Res. 2010;38:4722–30.
227. van de Putte P, van Sluis CA, van Dillewijn J, Rorsch A. The location of genes controlling radiation sensitivity in Escherichia coli. Mutat Res. 1965;2:97–110.
228. Ogawa H, Shimada K, Tomizawa J. Studies on radiation-sensitive mutants of E. coli. I. Mutants defective in the repair synthesis. Mol Gen Genet. 1968;101:227–44.
229. Arthur HM, Lloyd RG. Hyper-recombination in uvrD mutants of Escherichia coli K-12. Mol Gen Genet. 1980;180:185–91.
230. Jongeneel CV, Formosa T, Alberts BM. Purification and characterization of the bacteriophage T4 dda protein. A DNA helicase that associates with the viral helix-destabilizing protein. J Biol Chem. 1984;259:12925–32.
231. Jongeneel CV, Formosa T, Munn M, Alberts BM. Enzymological studies of the T4 replication proteins. Adv Exp Med Biol. 1984;179:17–33.
232. Bjornson KP, Hsieh J, Amaratunga M, Lohman TM. Kinetic mechanism for the sequential binding of two single-stranded oligodeoxynucleotides to the Escherichia coli Rep helicase dimer. Biochemistry. 1998;37:891–9.
233. Sikora B, Chen Y, Lichti CF, Harrison MK, Jennings TA, Tang Y, et al. Hepatitis C virus NS3 helicase forms oligomeric structures that exhibit optimal DNA unwinding activity in vitro. J Biol Chem. 2008;283:11516–25.
234. Tomko EJ, Fischer CJ, Lohman TM. Single-stranded DNA translocation of E. coli UvrD monomer is tightly coupled to ATP hydrolysis. J Mol Biol. 2012;418:32–46.
235. Lucius AL, Wong CJ, Lohman TM. Fluorescence stopped-flow studies of single turnover kinetics of E. coli RecBCD helicase-catalyzed DNA unwinding. J Mol Biol. 2004;339:731–50.
236. Lucius AL, Lohman TM. Effects of temperature and ATP on the kinetic mechanism and kinetic step-size for E. coli RecBCD helicase-catalyzed DNA unwinding. J Mol Biol. 2004;339:751–71.
237. Lucius AL, Vindigni A, Gregorian R, Ali JA, Taylor AF, Smith GR, et al. DNA unwinding step-size of E. coli RecBCD helicase determined from single turnover chemical quenched-flow kinetic studies. J Mol Biol. 2002;324:409–28.

238. Wu CG, Lohman TM. Influence of DNA end structure on the mechanism of initiation of DNA unwinding by the Escherichia coli RecBCD and RecBC helicases. J Mol Biol. 2008;382:312–26.
239. Dillingham MS, Webb MR, Kowalczykowski SC. Bipolar DNA translocation contributes to highly processive DNA unwinding by RecBCD enzyme. J Biol Chem. 2005;280:37069–77.
240. Yang Y, Dou SX, Ren H, Wang PY, Zhang XD, Qian M, et al. Evidence for a functional dimeric form of the PcrA helicase in DNA unwinding. Nucleic Acids Res. 2008;36:1976–89.
241. Eoff RL, Raney KD. Intermediates revealed in the kinetic mechanism for DNA unwinding by a monomeric helicase. Nat Struct Mol Biol. 2006;13:242–9.
242. Eoff RL, Raney KD. Kinetic mechanism for DNA unwinding by multiple molecules of Dda helicase aligned on DNA. Biochemistry. 2010;49:4543–53.
243. Lahue EE, Matson SW. Escherichia coli DNA helicase I catalyzes a unidirectional and highly processive unwinding reaction. J Biol Chem. 1988;263:3208–15.
244. Wu CG, Bradford C, Lohman TM. *Escherichia coli* RecBC helicase has two translocase activities controlled by a single ATPase motor. Nat Struct Mol Biol. 2010;17(10):1210–7.

Chapter 3
Structure and Mechanisms of SF2 DNA Helicases

David C. Beyer*, Mohamed Karem Ghoneim*, and Maria Spies

Abstract Effective transcription, replication, and maintenance of the genome require a diverse set of molecular machines to perform the many chemical transactions that constitute these processes. Many of these machines use single-stranded nucleic acids as templates, and their actions are often regulated by the participation of nucleic acids in multimeric structures and macromolecular assemblies that restrict access to chemical information. Superfamily II (SF2) DNA helicases and translocases are a group of molecular machines that remodel nucleic acid lattices and enable essential cellular processes to use the information stored in the duplex DNA of the packaged genome. Characteristic accessory domains associated with the subgroups of the superfamily direct the activity of the common motor core and expand the repertoire of activities and substrates available to SF2 DNA helicases, translocases, and large multiprotein complexes containing SF2 motors. In recent years, single-molecule studies have contributed extensively to the characterization of this ubiquitous and essential class of enzymes.

* These authors contributed equally to this work.

D.C. Beyer • M. Spies (✉)
Department of Biochemistry, University of Iowa Carver College of Medicine, Iowa City, IA, USA
e-mail: maria-spies@uiowa.edu

M.K. Ghoneim
Center for Biophysics and Computational Biology, University of Illinois Urbana-Champaign, Urbana, IL, USA

M. Spies (ed.), *DNA Helicases and DNA Motor Proteins*, Advances in Experimental Medicine and Biology, DOI 10.1007/978-1-4614-5037-5_3,

Superfamily II Helicases and Translocases

Helicases are a subset of nucleic acid (NA) translocases, enzymes that convert the energy of ATP hydrolysis into directional motion along polar NA substrates [1–6]. Superfamily II (SF2) helicases and translocases make up the largest and most structurally diverse group of these motor proteins [1]. Much like SF1 enzymes (see Chap. 2), SF2 proteins are so grouped owing to a common set of "helicase signature motifs" [4–8]. Further structural and functional studies have shown, however, that the two conserved domains containing the signature motifs form a general-purpose motor core, the primary biochemical function of which being the transduction of energy produced through ATP binding and hydrolysis into directional motion along a NA lattice [1, 9]. This motor core consists of two RecA-like folds termed helicase domain 1 (HD1) and helicase domain 2 (HD2); HD1 and HD2 correspond to RecA-like folds 1A and 2A in SF1 motors [1, 10]. Changing affinities of the two motor domains for DNA during the ATPase cycle bias the energy landscape and enables directional translocation. Helicase activity itself results from the actions of accessory domains unique to each enzyme that couple the biochemical activity of NA strand separation to the translocating action of the motor core [4–6]. Interestingly, SF2 enzymes exhibit a range of modular accessory domain architectures that expand the repertoire of the superfamily to include such diverse activities as replication fork reversal, chromatin remodeling, and even peptide export, all coupled to the action of the conserved motor core [11–13]. Recent sequence analysis of SF2 proteins identified six major families involved in DNA metabolism, each named after their archetypal member (RecG, RIG-I, RecQ, Rad3, Ski2, and Swi/Snf); these families within SF2 are the foci of this chapter [1].

Figure 3.1a shows the relative composition of SF2, grouped by substrate specificity [1, 4–6]. RNA helicases make up a clear majority of SF2 proteins when sorted this way, with the DEAD-box family of these enzymes being particularly numerous. *Bona fide* DNA helicases make up the next largest group, followed by ss- and dsDNA-specific translocases. Singleton et al. proposed a system for classifying helicases with respect to translocation direction, or polarity [5]. The orientation of the SF2 motor core to its NA substrate within the context of this system is shown in Fig. 3.1b: motors that operate in the 3′–5′ and 5′–3′ directions are classified as SF2A and SF2B, respectively. Although SF1 and SF2 bind NA lattices in the same relative orientation, that is, with HD1 oriented towards the 5′ end of the translocation strand, SF2 enzymes interact primarily with the phosphodiester backbone of their NA substrates while SF1 helicases intercalate the nucleobases in specific pockets of the motor core enabling a "Mexican wave"-like translocation (see Chap. 2) [4–6, 8, 14, 15]. The motor domain orientation and interaction of SF2 motors with the phosphodiester backbone is reflected in the B-form conformation of the NA lattice in first three panels of Fig. 3.1b. Many DEAD-box helicases are hypothesized to dismantle secondary structures present at sites essential to RNA quality control [16]. This highly local helicase function requires relatively limited processivity; structural and functional studies have shown that these enzymes make more extensive contacts with the heterocyclic bases of their NA substrates, a situation that would necessarily hinder the progress of an SF2 motor core optimized for back-

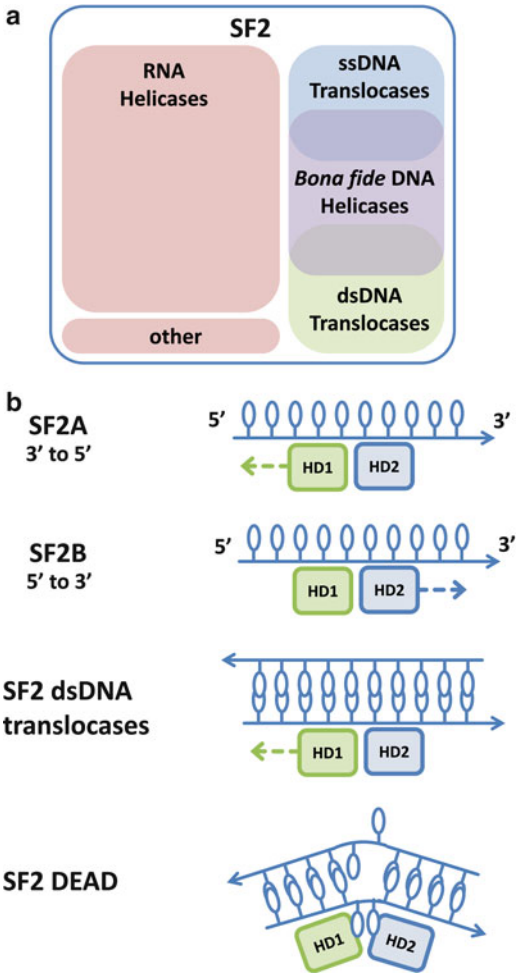

Fig. 3.1 Superfamily II, a varied class of NA motor proteins. (**a**) Shows the major groups of SF2 grouped by substrate specificity. RNA helicases make up the largest portion, with DNA helicases and translocases making up (roughly) the other half. (**b**) Displays the binding modes of SF2A and SF2B enzymes as described by Singleton et al. [5]. The *lower panels* show the orientation of the helicase domains in SF2 dsDNA translocases and DEAD-box proteins

bone-mediated translocation [4–6, 8, 16]. A diagram representing DNA binding by this group is shown in the last panel of Fig. 3.1b.

The SF2 Motor Core

Translocation of SF2 motor cores along NA lattices is accomplished by the concerted action of the HD1 and HD2 moieties [2, 4–6, 8]. Current data suggest this action mirrors the "inchworm" model of translocation proposed for other helicase superfamilies (Chaps. 1 and 2) [2, 4–6, 9, 16]. Containing 11 conserved motifs

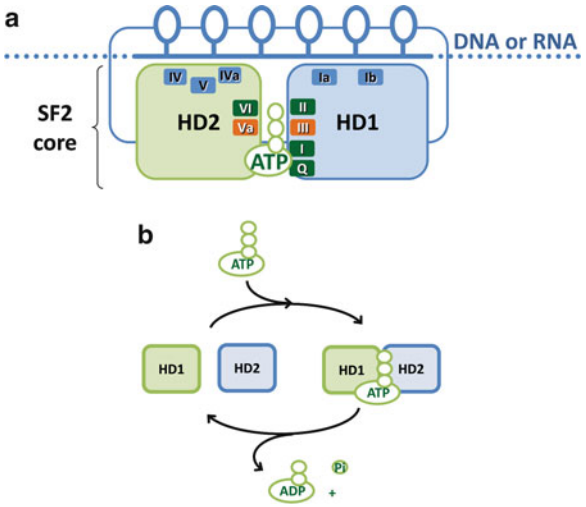

Fig. 3.2 The SF2 motor: its structure and behavior during ATP binding and hydrolysis. (**a**) Shows the orientation of the helicase signature motifs within the motor core and their relationship to the NA lattice when bound to ATP. (**b**) Shows the relative positions of HD1 and HD2 through the course of the ATP hydrolysis cycle

(Q, I, Ia, Ib, II, III, IV, IVa, V, Va, and VI), the SF2 helicase domains are diagrammed in Fig. 3.2a [1]. A subset of the P-loop NTPases, SF2 enzymes use the sterically optimized Walker A and B motifs to hydrolyze NTPs [2]. The SF2 DNA translocases and processive helicases possess a Q motif that confers specificity for ATP [17]. Helicase motifs I and II, containing the Walker A and B boxes, are among the most conserved motifs across the superfamily [1]. Motif VI is also involved in the coordination and hydrolysis of NTPs [2, 18, 19]. Located at the interface between the RecA-like folds, motifs I and II—along with motifs Q, III, Va, and VI—compose a pocket formed when the helicase domains are brought into close proximity upon ATP binding [2, 5, 6, 14]. This process is depicted in Fig. 3.2b. The subsequent hydrolysis of ATP to ADP and inorganic phosphate collapses this pocket and allows the separation of the helicase domains. Motifs III and Va contact both DNA-binding and NTP hydrolysis moieties within HD1 and HD2 (respectively) and are believed to play an essential role in transmitting the energy of ATP hydrolysis into motor function [2, 18, 19].

Motifs Ia, Ib, IV, IVa, and V make extensive contacts with the phosphodiester backbone of the DNA lattice [4, 14]. The tuned affinities of these motifs for NA substrates are believed to be the antecedents of helicase polarity [5, 6]. Furthermore, the inchworm model of translocation predicts that these affinities are dynamic through the course of the ATP hydrolysis cycle; however, the details of how this variation is tied to specific conformational transitions of the helicase domains remain poorly understood, mainly due to the dearth of structural information from SF2 enzymes [2, 9, 16].

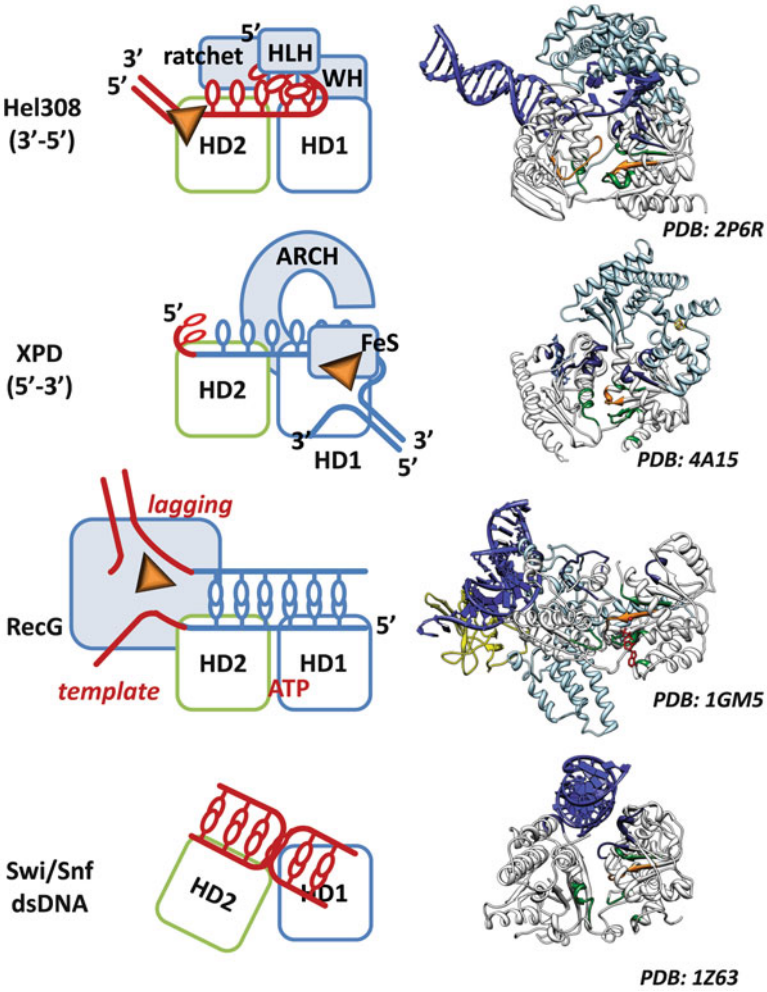

Fig. 3.3 Structures of several representative SF2 motors. The high-resolution crystal structures (from indicated PDB entries) of several SF2 motors are shown alongside diagrammatic representations. Substrate nucleic acids are shown in *violet* in the crystal structures and *red*/*blue* in the diagrams. Motifs in the crystal structures are color coded as follows: *green*—ATP binding; *dark blue*—DNA binding; *orange*—involved in the communication between ATP- and DNA-binding sites. HD1 and HD2 are *white* and are aligned the same as on the cartoon. In the diagrams, the auxiliary domains are in *light blue* (pin/wedge structures are shown in *yellow*)
ATP adenosine triphosphate; *SF1* superfamily I; *NTP* nucleoside triphosphate; *FRET* Förster resonance energy transfer; *GC* guanine-cytosine; *TIRFM* total internal reflection fluorescence microscopy; *OB* oligonucleotide binding fold; *bp* base pair

Accessory Domains Dictate Biological Function

The helicase domains of SF2 motors often contain long insertions that are believed to function in coupling ATP hydrolysis and translocation activities to accessory biochemical function [1]. These regions act in concert with accessory domains separate from the motor core to enable the in vivo functions of SF2 proteins. An example of this phenomenon is the presence of a protruding region of β-hairpin secondary structure between motifs Va and VI in the Ski2-like helicase Hel308 [20]. Structural data for this enzyme indicate that this structure may function as a "pin" that separates substrate NA strands and thus plays a crucial role in coupling translocation to helicase activity. Similarly, accessory NA-binding domains facilitate Hel308's unwinding of duplex DNA [20]. Figure 3.3 shows the domain orientation of several SF2 proteins for which structural data are available. These examples—Hel308 and members of the Rad3, RecG, and Swi/Snf families—show explicitly the degree to which domains outside of the motor core influence the nucleoprotein interactions within the SF2 core and beyond to yield the intermediates required for essential processes in NA metabolism including DNA cross-link repair, replication fork rescue, and chromatin remodeling.

RecG Family Helicases: Bacterial First Responders

Packed tightly inside the bacterial envelope, even the simplest DNA lattices form highly heterogeneous manifolds. Replete with stable nucleoprotein complexes and persistent NA structures, even these relatively simple genomes can prove resistant to the efficient progress of the replisome. In the case of a replication fork stall caused by a difficult element of the lattice or a collision with another DNA-translocating machine or otherwise tightly bound protein, there exist robust mechanisms for the origin-independent rescue of replication. Regression of the replication fork from the site of replisome dissociation is often the first step in these processes [21, 22]. Stalled replication fork regression is performed in prokaryotes by SF2 helicases of the RecG family [23]. Belonging to SF2A, RecG proteins translocate along dsDNA in the 3′–5′ direction while primarily contacting the DNA along the phosphodiester backbone of the template for the nascent lagging strand (see Fig. 3.3) [4]. Topologically, these proteins consist of an accessory "wedge" domain at the N-terminus linked to the conserved SF2 motor core, with this assembly capped by a short accessory domain at the C-terminus [1].

Structural and Mechanistic Insights from Thermotoga maritima

A crystal structure of RecG from *Thermotoga maritima* represents the only published structural information for this helicase family [4]. Solved in a complex with ADP and a three-way DNA junction, this structure provides valuable insight into the detailed

mechanism of SF2 motor-coupled replication fork reversal. It is hypothesized from the structural data that RecG translocation is facilitated by protein–DNA contacts at the branch point of the parent strands [24]. The contacts at the parent strand branch point occur in a dsDNA-binding conduit separating the motor core and the wedge domain, a substantial gap bridged by a 41-residue α-helical linker [4]. Several residues of the C-terminal accessory domain form a pin structure that inserts prominently into this channel. The pin structure makes contact with the DNA backbone and is linked to motif VI of the motor core by a network of hydrogen bonds. Alteration of this network as a consequence of the ATP hydrolysis cycle is believed to drive RecG translocation. Directional movement of the motor core along the dsDNA lattice brings the nascent strands of the stalled fork structure into contact with the wedge domain; it is in this way that translocation is coupled to helicase activity. The wedge domain is believed to separate the nascent DNA strands from the parental components of the stalled fork during translocation by steric exclusion of the nascent strands from a set of diverging ssDNA channels. Interestingly, the wedge domain's contacts with the liberated DNA strands facilitate the simultaneous reannealing of the fork's parental strands in its wake and the formation of a "nascent strand duplex" at its prow. Thus, the concerted action of the accessory domains during dsDNA translocation forms the Holliday junction structures typical of RecG processing of stalled replication forks [4, 20].

The In Vivo Role of RecG

A variety of in vitro studies have observed a strong preference among RecG proteins to bind dsDNA substrates possessing 3′ ssDNA branches (as shown in Fig. 3.3) [25–27]. This class of substrates includes Holliday junctions, D-loops, and R-loops—the usual suspects for recombination-mediated repair processes. The affinities of RecG proteins for these structures and the fork-like junctions that result from replisome collapse place the RecG family at the interface of DNA replication, recombination, and repair. dsDNA translocation is coupled to helicase activity through the accessory domains to yield a Holliday junction from the stalled fork [28]. The formation of these junctions may permit origin-independent replication fork restoration by the bacterial recombination machinery [29, 30]. Conversely, these Holliday junctions may also be substrates for direct resolution pathways [23]. Though it is clear that RecG proteins act as first responders at stalled forks, at this time the precise methods by which these structures are ultimately resolved are poorly understood [27, 28].

Although RecG is an exclusively bacterial helicase, regression of stalled replication forks into a "chicken foot" structure is important in all organisms [21]. Evidence of fork regression activity exists for human BLM and FANCM helicases [31, 32]. Much like RecG, FANCM is an SF2A dsDNA translocase that uses specific accessory domains to perform branch migration on a variety of three- and four-way DNA junctions [31].

RIG-I Translocases: Guides of Branched DNAs in Archaea and Eukarya

SF2 translocases often perform the initial steps in processing branched DNA structures [30]. Three- and four-way junction structures are frequent intermediates of DNA damage repair. If not processed in a timely manner, these structures can cause genome instability [33]. In most cases, the intermediates produced by SF2 translocases are subsequently modified via biochemical activities unrelated to NA translocation. The RIG-I family translocases have been linked to the resolution of many of the three- and four-way branched DNA structures observed in Archaea and Eukarya including D-loops, R-loops, Holliday junctions, and aberrant fork structures [30, 34]. Named for a human RNA translocase implicated in viral recognition, the RIG-I SF2 enzymes exhibit a wide range of biochemical activities united by common domain architecture [1]. Archaeal members of the RIG-I family possess terminal accessory domains that cleave the branched intermediates produced by the coupled action of the motor core and helicase domains [31]. These enzymes physically link the primary and secondary responses to stalled replication forks and other events yielding branched DNAs in vivo. In eukaryotes, the downstream processing of three- and four-way DNA junctions frequently occurs within macromolecular assemblies recruited by RIG-I proteins [29, 33, 35, 36]. A discrete set of mutations to the terminal accessory regions of eukaryotic RIG-I translocases abolishes their nuclease activity [31]. Interestingly, these same mutations facilitate the participation of eukaryotic RIG-I translocases in a range of macromolecular assemblies. Severing the physical link between branch point migration and downstream processing establishes a modular paradigm in eukaryotes where RIG-I translocases tune their recruitment of protein partners to their substrates, allowing them to facilitate a variety of DNA transactions essential for genome maintenance and concomitant regulation of the cell cycle [30, 31, 33].

Hef: An Archaeal Model for RIG-I Action

Isolated from *Pyrococcus furiosus*, *h*elicase-associated *e*ndonuclease for *f*ork-structured DNA (Hef) is the only available structural model for RIG-I DNA translocases [37]. Though Hef functions quite differently from its eukaryotic brethren, RIG-I translocases share a highly conserved domain architecture that permits a certain degree of generalization [1, 31]. The helicase activity that drives branch point migration by RIG-I enzymes is believed to be coupled to the action of the SF2 core by an Mph1-like accessory domain present at the N-terminus, though the detailed mechanism of this coupling is unknown [36, 37]. RIG-I proteins are SF2A enzymes that perform dsDNA translocation [1, 5]. A “family-specific” accessory domain bisects the RecA-like folds of the motor core. Containing a network of positively charged residues, this accessory domain shares marked characteristics with the DNA-binding

"thumb" domains of A-family DNA polymerases [1, 31]. The details of how this domain aligns branched DNA substrates are unclear from the available *apo*-structure, but this region is believed to recruit Hef to specific DNA junctions. Hef's C-terminal ERCC4 and helix-turn-helix domains are responsible for the cleavage of forked DNAs in a manner similar to nuclease ERCC4 (MUS81) [31, 36, 37]. In vitro observations suggest that RIG-I helicase activity stimulates nuclease action, suggesting that the activities act in concert in vivo. Human RIG-I DNA translocases retain these nuclease domains, but the deletion of a single lysine in the ERCC4 domain abrogates their nuclease activity [31].

Human RIG-I Translocase FANCM

The terminal helix-turn-helix motif of Fanconi Anemia Complementation Group M protein (FANCM) facilitates its interaction with the Fanconi Anemia core complex (see Chap. 9) [1, 31, 33]. FA-associated protein FAAP24 possesses inactive ERCC4 and helix-turn-helix domains that dimerize with identical domains in FANCM and link the RIG-I translocase to the FA core complex. The dimerization of these proteins is believed to activate FANCM's branch point migration activity and recruit the FA core to branch point sites made labile by RIG-I helicase activity. Branched DNA structures that stimulate FANCM helicase activity often indicate the necessity for initiating repair processes, many of which are regulated by the FA core [30, 31]. Recruitment of the core by FANCM has been further linked to the S-phase DNA damage checkpoint. FANCM's affinity for a variety of three- and four-way junctions makes it an excellent indicator of the repair status of the genome. The participation of the human FANCM in a number of FA complexes allows it to tune the cellular response to branched DNA structures and guide their processing in a way that responsively maintains genomic stability and ensures the proper progress of the cell cycle [29, 31].

The RecQ Family

Originally identified almost 30 years ago, RecQ translocases have since been identified in all three kingdoms of life and are among the best-studied SF2 proteins (see Chap. 8) [38, 39]. In vivo, RecQ helicases participate in replication fork rescue, telomere maintenance, homologous recombination, and DNA damage checkpoint signaling (see Chaps. 6, 8 and 9) [40]. There are five human RecQ helicases, and mutations in three of their genes are associated with cancer predisposition and/or premature aging as expressed in Bloom syndrome, Werner syndrome, and Rothmun-Thomson syndrome [32, 41, 42]. In contrast, bacteria and lower eukaryotes have a single RecQ family member. RecQ helicases unwind DNA with a 3′–5′ polarity and

are capable of unwinding or remodeling a variety of DNA structures in vitro. These structures include forked duplexes, D-loops, triple helices, four-way junctions, and G-quadruplex DNA. The activities of RecQ family members are often tuned by integration into macromolecular complexes catalyzing multiple enzymatic activities (discussed in detail in Chap. 8).

In addition to a common SF2A motor core, RecQ helicases contain several characteristic accessory domains. Immediately downstream of the RecA-like regions, these enzymes carry a highly conserved RecQ-C-terminal (RQC) domain [39, 43–45]. This region contains a zinc-binding domain and a winged-helix (WH) domain and is present in all RecQ helicases, save for RecQ4. Mutagenesis studies on some members of this helicase family have shown that the zinc-binding domain is likely involved in maintaining the structural stability of the protein [46, 47]. The WH domain is important for dsDNA recognition and may also be involved in protein–protein interactions [39]. At their C-termini, RecQ helicases possess a relatively varied accessory region termed the helicase-and-RNaseD-like-C-terminal (HRDC) domain. This region has been implicated in substrate recognition. These modular accessory domains (RQC and HRDC) position the SF2 core and tune its action to give rise to the varied substrate specificities and enzymatic activities of the RecQ family.

BLM: A Human Model for RecQ Action

Among human RecQ helicases, BLM (Bloom Syndrome protein) is probably the most extensively studied. Not surprisingly, it is discussed extensively in several chapters of this book (Chaps. 6, 8 and 9). Bloom Syndrome is the disease caused by a BLM deficiency [32]. This disease is associated with chromosomal abnormalities and defective response to replication stress, both due to extraordinarily high levels of homologous recombination (HR).

BLM's ability to regulate HR results primarily from the augmentation of basic SF2A translocation activity by its accessory domains. The RQC's zinc-binding region has been shown to stabilize BLM and facilitate DNA binding [32]. Similarly, the WH region of the RQC confers BLM's ability to bind G-quadruplex DNA [39]. While not essential for forked-duplex unwinding or ATP hydrolysis, the HRDC domain plays an important role in Holliday junction unwinding and, more importantly, double Holliday junction dissolution, an activity exclusive to BLM among human RecQ helicases. Sato et al. recently demonstrated that isolated HRDC alone could not bind substrate DNA [48]. Both RQC and HDRC domains together are necessary for interaction with telomere-associated protein TRF2, a factor that stimulates the BLM-mediated unwinding of telomeres. BLM's unique N-terminal regions are likely involved in macromolecular interactions of still unknown significance. Full-length BLM was found to form hexameric ring structures, while the isolated BLM helicase core was found to be active in monomeric form even under conditions that strongly favor oligomerization [49]. When studied in isolation, the helicase core domain showed low processivity, a moderate unwinding rate, and, surprisingly, an ability to

"measure" the length of the duplex it unwound (see single-molecule section below) [50]. Although numerous biochemical studies of BLM exist, the mechanochemistry and detailed coupling mechanisms between ATP hydrolysis, translocation, and other activities of BLM remain unresolved. What is clear, however, is that the protein's accessory domains dictate its substrate specificity and biochemical activity.

Rad3 Family Helicases

The Rad3 family (also known as XPD-like) is the only family of SF2 helicases shown thus far to translocate on ssDNA in the 5′–3′ direction. It is named after yeast Rad3, the first identified member of this family [51]. Members of the Rad3 family are found in all domains of life and are involved in several genome maintenance pathways [52–54]. There are typically two Rad3 helicases in bacteria, one in archaea and yeast, and four have been identified in humans (XPD, FANCJ, RTEL, and CHLR1) [55]. A distinct structural feature of this family is the presence of a large insertion in HD1's Walker A motif split into two accessory domains, the iron-sulfur (FeS) cluster-containing domain and the arch domain [52, 56, 57]. Because of the important, but still debated, roles Rad3 helicases play in genome maintenance, many members of this family are discussed in detail in later chapters (Chaps. 6, 9 and 10). Here, we will use XPD, a model Rad3 helicase, to discuss how the structural features of Rad3 enzymes enable 5′–3′ translocation on crowded lattices and concomitant duplex unwinding.

XPD: A Model SF2B Enzyme

In humans, XPD (Xeroderma pigmentosum complementation group D) helicase is one of the most important subunits of TFIIH (Transcription Factor II-H complex), an essential element of the nucleotide excision repair (NER) machinery [58–60]. Four published crystal structures of XPD helicases from three different archaeal organisms make up the body of Rad3 structural data [60–63]. Three structures are without DNA or ATP and share a common topology. The most recent structure was obtained from a complex of XPD and a short DNA fragment [60]. XPD contains two modular domains incorporated into the motor core, an FeS-cluster containing domain and an arch domain [57]. The 4Fe-4S cluster is coordinated to four cysteine residues, three of which are important for the integrity of the cluster, folding of the FeS domain, and XPD activity [64]. Situated on the other side of the Walker A box, the arch domain is composed of two sets of alpha-helices arrayed with 60° between them, their relative orientation giving rise to an arch-like structure (Fig. 3.3). All published models predict that ssDNA passes first through the groove between the HD2 and arch domains, moving then through a hole encircled by the arch, FeS-cluster, and HD1 domains. Two recent studies identified the polarity of the translocation strand as

bound by XPD and provided insights into how the enzyme achieves its directionality on the NA lattice [60, 65]. These studies also identified the FeS-cluster domain as a wedge structure involved in duplex separation.

In isolation, XPD functions quite poorly as a helicase; on the other hand, in distributive processes like transcription and NER, this could be an asset. *Ferroplasma acidarmanus* XPD can unwind forked DNA as a monomer when assisted by RPA2, one of the cognate ssDNA-binding proteins. RPA2 stimulates DNA unwinding by XPD through a novel mechanism by providing a helix-destabilizing function [66]. Honda et al. demonstrated that XPD moves along ssDNA coated with RPA2 without displacing or stepping over it [67, 68]. Taken together, these data suggest a model whereby XPD helicase recognizes forked DNA substrates decorated with RPA2 (common structures in transcription and NER) and uses its FeS-containing domain to orient itself at the fork. RPA2 then melts the duplex ahead of the helicase, allowing XPD to advance forward and to trap the newly open bases. Retaining contact with the translocation strand, RPA2 then plays an additional supporting role by stabilizing the product(s) of helicase activity.

As yet, the other human Rad3 helicases (FANCJ, RTEL, CHLR1) and their homologs have proved resistant to high-resolution structural studies. However, based on amino acid sequence alignment, all of these helicases should have an SF2B motor core similar to that of XPD, an FeS-containing domain, and an arch domain. Additional domains integrated into or found at the termini of the motor core are involved in the interactions of each family member with its specific protein partners in the cell [53, 54]. Forthcoming structural data may elucidate how these domains work together to render the biological functions carried out by these enzymes.

The Hel308 Helicases of the Ski2 Family

Though named for an RNA-specific enzyme, the Ski2 family of SF2 helicases contains the Hel308 subfamily [1]. Exhibiting primary domain architecture nearly superimposable with both the RecQ and DEAH/RHA families, the Hel308 helicases have been identified in many archaeal and eukaryotic organisms. Implicated in several DNA repair pathways, these enzymes are believed to act primarily through processes involving recombinase nucleoprotein filaments at sites of DNA damage [33, 69, 70]. In metazoans, Hel308 enzymes are believed to function in the Fanconi Anemia (FA) pathway of recombination-mediated repair and in the regulation of RAD51 foci generated during meiosis [33].

Structural Lessons from Archaeal Hel308 Helicases

Both high-resolution structures available for the Hel308 subfamily are archaeal in origin, derived from crystallized complexes of *Sulfolobus solfataricus* and *Archaeoglobus fulgidus* helicases with partially unwound DNA structures [69, 70].

The crystallographic data suggest that Hel308 helicases bind specifically to fork-like structures possessing a 3′ overhang, a specificity enforced by their accessory domains. In addition to the conserved SF2A motor core, the Hel308 helicases possess three C-terminal accessory domains (as shown in Fig. 3.3) [1]. A β-hairpin motif inserted between motifs V and VI of HD2 is believed to act as a pin structure, coupling helicase activity to 3′–5′ ssDNA translocation by direct insertion into the duplex interface [1, 69, 70]. Interactions with the "ratchet" accessory domain are believed to facilitate strand separation by the pin structure. This domain is situated directly opposite the motor core-duplex interface and may stabilize released ssDNA, easing strand separation. Nearest to the motor core, the winged helix (WH) domain is also observed in the RecQ-like and DEAH/RHA translocases, and the folded orientation of the WH domain relative to the motor core is conserved across the Ski2, RecQ, and DEAH/RHA families [1]. The WH domain makes extensive orienting contacts with branched structures and may function as a "hinge," allowing Hel308 helicases to bind and then close tightly around substrate DNA [69, 70]. Capping the Hel308 helicases at the C-terminal is a helix-loop-helix (HLH) domain that exhibits typical DNA-binding activity and a strong affinity for ssDNA. The HLH domain is believed to function in vivo as a "brake," grasping the freed translocation strand and limiting the processivity of Hel308 helicases on branched substrates [70]. Taken together, the actions of accessory domains appear to orient Hel308 helicases to specific branched substrates and to couple their translocation along these substrates to self-limiting helicase activity.

The Role of Hel308 Helicases In Vivo

The in vivo role of Hel308 helicases has been extensively investigated [33]. Studies of *Caenorhabditis elegans* show that its Hel308 helicase, HELQ, is recruited to replication forks in response to crosslinking DNA damage. Real-time studies of U2OS cultures under crosslinking conditions support this result in human cells and agree with worm-based results placing Hel308 helicases in the FA repair pathway. Further genetic studies in *Drosophila* have shown Hel308 enzymes to play an essential role in the modulation of meiotic recombination. Interestingly, biochemical studies have shown Hel308 helicases to specifically disrupt dsDNA-RAD51 filaments, implicating these enzymes along with Rad54 translocase as postsynaptic regulators of recombination, a finding further supported by genetic results in *C. elegans*. Furthermore, Hel308 helicases have been shown in vitro to displace DNA-binding proteins via direct, though helicase-activity independent, interactions. Surprisingly, the in vitro ability of HELQ to remove RAD51 was observed to be ATPase independent. Taken together, the genetic and biochemical data suggest that Hel308 helicases act to assist the recombination-mediated repair of DNA damage encountered during replication and meiosis by resolving post-synaptic Rad51 complexes. The detailed pathway of RAD51 locus regulation, a pathway proceeding through Hel308 enzymes that provides resistance to cross-linking DNA damage and ensures proper levels of meiotic recombination, however remains unclear [29, 33].

Future work will resolve the relationship between the observed architecture of Hel308 enzymes, their observed in vitro activities, and the growing body of genetic studies placing these enzymes in essential genome maintenance pathways.

SF2 Chromatin Remodelers

Eukaryotic chromosomal DNA is packaged into a condensed structure known as chromatin [71, 72]. The basic unit of chromatin is the nucleosome, which consists of 146 bp of dsDNA wrapped around a histone protein octamer [73, 74]. Highly condensed chromatin packs and organizes dsDNA within the nucleus. On the other hand, however, nucleosomes restrict access to the templating information required by the molecular machines tasked with DNA replication, repair, recombination, and transcription [72, 75]. Chromatin remodeling complexes are multisubunit enzymes that use the energy of ATP hydrolysis to reposition, destabilize, eject, or restructure nucleosomes, thereby rendering nucleosomal DNA accessible. The importance of chromatin remodelers can be illustrated by their absolute requirement for embryonic development and their governing role in cell cycle progression [76].

The essential unit of chromatin remodeling is a single nucleosome bound by a single remodeler driven by an SF2 motor [77, 78]. While a unified model of chromosome immobilization remains elusive (see Chap. 13), many recent models support the notion that the remodeler binds to the nucleosome particle via accessory moieties, and then the motor core binds DNA at a location inside the nucleosome [75]. The translocase domain, tightly anchored to the nucleosome core, then induces directional DNA translocation, generating a remodeling strain within the nucleosome particle. This process may occur by sequential or concerted action of two domains: a DND (DNA-binding domain) that pushes DNA into the nucleosome, creating small DNA loop, and a Tr (translocation) domain that pumps the DNA loop outward.

There are four families of chromatin remodelers: Swi/Snf, ISWI, CHD, and INO80 [72, 75, 79]. Remodelers in all these families possess a Swi2/Snf2 family ATPase core (or subunit), a version of the SF2 motor core containing DExx and HELICc domains. What differentiates these families from each other is the presence of accessory domains incorporated into, or adjacent to, the SF2 translocase core. The Swi/Snf, ISWI, and CHD families each have a short insertion within the SF2 motor, while remodelers of INO80 family have a long insertion. These insertions form the accessory domains that regulate the enzymatic activity of the complex, facilitate interactions with transcription factors or other chromatin-associated enzymes, or target the complex to DNA and histones.

The Swi/Snf Family

Swi/Snf (Switching defective/Sucrose nonfermenting) chromatin remodelers are multiprotein complexes composed of 8–14 subunits [80]. Many of the activities carried out by this family serve to enable genome maintenance and

transcription machines' access to genetic information. Different Swi/Snf remodelers slide, unwrap, and eject nucleosomes at many loci and mediate dimer exchange and/or dimer swapping [75]. The Swi/Snf family can be subdivided into two groups, and both play distinct roles in DNA repair [77, 79]. Powered by ATP hydrolysis, Swi/Snf protein complexes carry out directional translocation on dsDNA [81]. This activity destroys histone–DNA contacts, and, according to the loop capture model, creates a transient DNA loop that propagates around the nucleosome and resolves when it reaches the other side of the nucleosome, a process that leads to nucleosome repositioning. It is not yet known whether the loop is large (>100 bp) or small (1–12 bp), but it is clear that during remodeling the contacts between histones and DNA are broken and reformed along the length of the nucleosome.

The ISWI and CHD Families

ISWI (Imitation Switch) family remodeling complexes are typically smaller than Swi/Snf assemblies, containing two to four subunits. Some members of this family optimize the spacing between nucleosomes to promote chromatin assembly and the repression of transcription, while other members randomize nucleosome spacing [82]. Much like ISWI proteins, the CHD (Chromodomain, Helicase, DNA binding) family participates in chromatin organization. Some members of this family slide or eject nucleosomes to promote transcription, while others have repressive roles. CHD remodelers may consist of a helicase subunit in lower eukaryotes but are large complexes in vertebrates [75, 83].

INO80 Remodeling Factors

Finally, the INO80 (Inositol-requiring 80) family complexes contain more than ten subunits, often with a long insertion present in the middle of the SF2 helicase domain [84]. Functionally, this family is diverse; INO80 enzymes perform a variety of transactions involved in transcriptional activation and DNA repair. SWR1 proteins are often classified as INO80 remodelers, but their functions are different from most INO80 family members in that they are able to remodel the nucleosome [72, 75].

Despite the diverse set of activities attributed to the four families of chromatin remodelers, they all contain an SF2 helicase motor essential for the remodeling activity. The varied accessory domains that interact with nucleosome, directing SF2 motor action and carrying additional enzymatic activities, bring about the diverse functions of this family.

Insights into SF2 Biochemistry from Single-Molecule Studies

In recent years, the emergence of single-molecule (SM) techniques has contributed powerfully to the study of SF2 [9, 16, 85, 86]. The ability to address the behaviors of individual molecular motors provides unprecedented insights into their function [87]. This holds particularly true in the cases where the same enzyme may perform different functions in different contexts. For example, human RecQ family helicase BLM participates in the macromolecular RTR complex to dissolve double Holliday junctions (see Chap. 8). Proper function of the RTR complex depends on the integrity of BLM HRDC domain and thereby on its oligomerization. BLM helicase has several additional roles in controlling and promoting recombination which may have different oligomeric forms or binding partners [88].

Single-Molecule Studies of RecQ Helicases

In the absence of a unified mechanism for DNA unwinding, the accurate assignment of activities to a distinct physiologically relevant form of a helicase is of paramount importance. A single-molecule FRET study on BLM helicase showed that this enzyme undertakes repetitive unwinding attempts on forked DNA substrates [50]. This behavior was observed for wild-type BLM and a mutant that lacks an oligomerization domain. In addition, unwinding time was found to be protein concentration independent, which suggested that repetitive low-processivity unwinding events on the same DNA molecule can be attributed to a single BLM monomer. Reannealing time was found to be ATP dependent, a behavior that was interpreted as strand switching by the helicase motor and translocation on the opposite (complementary) arm of the fork in the 3′–5′ direction allowing the strands to reanneal. From the FRET change histogram analysis, Yodh and colleagues concluded that BLM unwinds a well-defined length of DNA, leading to the interpretation that BLM helicase is able to "measure" the number of base-pairs unwound, and once it reaches a specific length, it rapidly reverses unwinding by switching the strand. Another interesting finding of this SM-FRET study was that the repetitive unwinding pattern persisted in the presence of human replication factor A (RPA) with only a limited increase in unwinding processivity per cycle and no effect on reannealing time. This was unexpected since RPA is known to enhance the processivity of BLM helicase on long duplex regions [89]. Furthermore, RPA significantly increased the waiting time before repeating unwinding for catalytic core BLM (lacking the RPA-binding domain). These results indicated that RPA facilitates BLM transfer back to the tracking strand and reinitiation of unwinding via direct physical interaction between the two proteins.

Another important feature of the helicase mechanism that can be definitively addressed in the single-molecule experiments is whether the enzyme is an active or a passive helicase [7, 8, 90]. This again is particularly important for helicases whose motor cores translocate along the phosphodiester backbone of ssDNA or dsDNA and therefore may be prone to slipping and back stepping [91].

Escherichia coli RecQ was one of the model helicases that were compared in a magnetic tweezer study targeted at establishing a physical reference value/parameter to judge whether a specific helicase unwinds dsDNA in an active or passive manner [92]. The theoretical approach adopted to find this reference parameter was based on comparing translocation velocity (V_{trans}) on ssDNA vs. unwinding rate (V_{un}) of dsDNA using DNA substrates of different GC contents, and with different tension forces. An active helicase destabilizes the fork, resulting in similar unwinding and translocation rates. In contrast, a passive helicase is slowed down by the presence of the dsDNA fork, which leads to a much slower unwinding rate compared to the translocation rate. Furthermore, because a passive helicase advances by trapping the spontaneously melted base pairs, its unwinding rate is expected to be sensitive to dsDNA sequence and tension applied to the two ssDNA tails of a fork. Manosas and colleagues proposed that for a helicase taking 1 bp steps and no slippage or back steps, the value of $V_{un}/V_{trans} = 0.25$ can be a good reference to judge whether a helicase is passive (<0.25) or active (>0.25). Surprisingly, RecQ was found to have V_{un}/V_{trans} values ranging from 0.9 to 0.7 under all GC ratios and tension forces tested in this study, suggesting that RecQ is an extremely active helicase (compared to the passive T4 gp41 helicase, which has values of 0.1 or less, and showed strong GC content and tension force dependence). It is important to note that all experiments on RecQ were done under monomeric conditions (picomolar concentration range), supporting previous studies suggesting that RecQ can unwind dsDNA as a monomer.

In a different FRET-based single-molecule study, the Dou and Xi groups noticed a lag in the initiation of unwinding by RecQ for longer ssDNA tails of an overhang DNA structure at a low ATP concentration [93]. At a high ATP concentration, the unwinding initiation rate was similar for longer and shorter tails of overhang DNA structures. The authors suggested that this behavior is an indicator of mutual inhibition by RecQ molecules. To prove that this is indeed the case, Pan and colleagues carried out experiments at low and high enzyme concentrations and observed that delayed initiation disappeared at low helicase concentration in the presence of a long tail overhang structure. They proposed that the mutual inhibition is due to a forced closure of the cleft between RecA-like domains HD1 and HD2 of a leading monomer by a trailing monomer before binding of ATP. Notably, preincubation of RecQ and DNA with a non-hydrolysable ATP analog before initiating the unwinding reaction prevented the unnatural closure of the cleft and alleviated the mutual inhibition effect by higher concentrations of RecQ. This phenomenon was observed in a stopped-flow experiment conducted under single-turnover conditions.

Single-Molecule Studies of Rad3 Helicases

Due to the lack of structural information from Rad3 helicases, SM studies have been particularly useful in addressing the mechanisms of their activity [67]. The first SM study of XPD helicase combined the well-known SM-TIRFM technique with distance-dependent quenching of fluorescent dyes by the iron-sulfur cluster observed in all members of the Rad3 helicase family [94]. The ability to follow helicase movement

by monitoring the FeS-mediated fluorescence quenching allowed Honda and colleagues to address an intriguing question: what happens when a translocating helicase encounters a roadblock [68]. The main finding of this multiparameter SM study was that distinct ssDNA binding proteins had a differential effect on the translocation activity of XPD helicase. RPA1 (a homodimeric ssDNA-binding protein) competed with XPD for ssDNA access, while RPA2 (an ssDNA-binding protein containing a single OB fold) targeted XPD to the RPA2-ssDNA complex. In a pseudo-tricolor experiment, Honda and colleagues directly observed that XPD was able to share the lattice with RPA2 and to bypass this ssDNA-binding protein without displacing it from ssDNA. RPA2 was found, however, to significantly slow down XPD translocation. The authors proposed that the ability of XPD to translocate on protein-coated ssDNA depends on the high flexibility of the relative position of the arch domain with respect to iron-sulfur domain, which may permit an opening motion to accommodate the protein–DNA complex into the hole made by the arch and iron-sulfur domains and HD1 (Fig. 3.3). Whether this is indeed the case remains to be determined and will likely require further development of novel SM techniques.

A recent atomic force microscopy (AFM) study by the Tainer and Barton groups showed that XPD helicase may cooperate with other proteins that are efficient in DNA charge transfer (CT) in order to localize to the vicinity of damage in DNA [95]. XPD helicase was found to redistribute on kilobase DNA substrates in the vicinity of a lesion which prevents CT, while a CT interaction-deficient mutant of XPD did not have this redistribution ability. The authors proposed that the ability of redox sensitive proteins like XPD to redistribute in the vicinity of lesions might be a good strategy to reduce the search process required to find lesions across the genome.

Insights into SF2 Chromatin Remodeling Activities

Single-molecule analyses have been particularly useful in discriminating between a number of models proposed to explain the activities of the Swi/Snf family of DNA translocases and nucleosome remodeling motors. One member of this family, Rad54 (see Chap. 9), is an important player in homologous recombination and in the recombination-mediated repair of broken chromosomes [96, 97]. The enzyme remodels DNA structures (including nucleosomes), assists Rad51-mediated strand invasion into nucleosome bound DNA, and facilitates disassembly of Rad51 nucleoprotein filaments from dsDNA. The first indirect indication that hRad54 (human Rad54) moves on dsDNA came from the observation that it generates supercoils on closed circular DNA [98]. It was a much later SM study, however, which unambiguously revealed the motion of Rad54 molecules, decorated with fluorescently labeled antibodies, on lambda dsDNA (approximately 50 kb long) stretched by hydrodynamic flow [99]. Rad54 was observed to bind DNA randomly and with no particular preference for substrate orientation. The observed velocity of translocation (~300 bp/s) was much faster than the movements usually detected during remodeling processes and was ATP dependent. Translocation rates were varied widely, with a tenfold difference between the slowest and fastest molecules. Rad54

processivity was remarkably high (~11 kb) and, unexpectedly, it was independent of ATP concentration, a behavior opposite to that observed in many other DNA motor proteins. A number of peculiar features of the Rad54 translocation were observed. These included pausing, direction reversal, and velocity change. The small sample size, however, prevented firm conclusions. In summation, the authors proposed that there is a change in the molecular species undertaking the translocation after pausing or direction reversal, which could reflect a multimeric Rad54 complex with a different monomer being used after the translocation restart since there was no observed correlation between velocity before and after a pause or directional reversal. Another interesting observation reported in this study was that at least half of the molecules exhibited a "lag" phase before starting translocation. Furthermore, the duration of this lag was reduced with increasing ATP concentration. This behavior may originate from a rate-limiting ATP-induced structural transition necessary for starting translocation.

In a following study, the same group used a very similar experimental approach to monitor the activity of yeast Tid1, a Rad54 homolog, which interacts with the meiotic recombinase Dmc1 [100]. Tid1 displayed more complex translocation behavior than Rad54 with most of the molecules showing the characteristic velocity change. In addition, the average translocation rate was two- to fourfold slower than Rad54; however, their processivities were similar. Similar to Rad54, Tid1 showed uncorrelated translocation rates before and after pauses and reversals, a finding indicative of a multimeric active form of this motor protein. Finally, Tid1 showed a wide distribution of translocation rates with a tenfold difference between the fastest and the slowest molecules.

The observed ATP dependence of the lag phase can be at least in part explained by the observations from another single-molecule study. Lewis et al. investigated the conformational transitions of an archaeal Rad54 catalytic core (Rad54-cc) [101]. Previous crystallographic studies showed that, in the absence of ATP, the Rad54 catalytic core adopts an open conformation with or without substrate DNA [102]. Ensemble FRET results showed that the catalytic core closes upon binding to DNA, while subsequent ATP binding did not change FRET [101]. Interestingly, a detectable conformational transition occurred after ATP hydrolysis but before ADP release (as inferred from FRET measurements in the presence of ATP, ADP, and an analog of the ATP hydrolysis transition state). In the same study, SM-FRET measurements performed on immobilized Rad54-cc showed that the protein is free to open and close in the presence of DNA. It was unclear, however, whether these conformational transitions corresponded to DNA molecule binding and dissociation. FRET histogram analysis revealed that the equilibrium between open and closed states was shifted towards a lower FRET state (open) in the absence of DNA, and towards a higher FRET state (closed) in the presence of DNA, though the FRET distributions in both cases were remarkably broad. Repeated SM-FRET measurements with freely diffusing protein molecules led to the same FRET distributions. Additionally, no discernible differences in conformational states were detected in the presence of DNA and in the presence and absence of ATP. Notably, the FRET-based study, which utilized truncated Rad54cc, did not produce any evidence of the multimeric

forms of active Rad54 complex, which contrasted with the observations made in the optical tweezer study of full length yeast Rad54 [99]. This discrepancy may be due to the omission of modular auxiliary domains responsible for protein oligomerization in the second study.

Recently, a sub-second AFM study was performed on full-length human RAD54 [103]. Based on volume measurements, the authors concluded that RAD54 functions as a monomer. Diffusion of the protein molecules in the absence of DNA was found to be six orders of magnitude slower than theoretically expected for a monomer, which could either indicate multimerization or surface interaction effects. Consistent with the SM-FRET studies, adding ATP or a non-hydrolyzable analog led to an increase in diffusion coefficient. RAD54 molecules were one order of magnitude faster in the presence of DNA than proteins alone on the imaging surface. Surprisingly, adding ATP in the presence of DNA did not lead to any detectable enhancement of Rad54 mobility on the NA chain.

ACF is another member of Swi/Snf family that is involved in chromatin remodeling and gene silencing (see Chap. 13) [104]. It repositions nucleosomes to create evenly spaced assemblies. These evenly spaced assemblies are critical for higher order chromatin folding, a process associated with long-term transcriptional repression. Blosser et al. studied the dynamics of nucleosome remodeling by human ACF using SM-FRET [105]. The authors adopted a three-color assay in which the nucleosome was labeled with a FRET donor–acceptor pair, while ACF was labeled with another, orthogonal dye. This experimental strategy allowed the authors to monitor simultaneously the events of nucleosome remodeling by FRET and the binding events of ACF and to correlate the dynamics of both entities. It was found that the gradual translocation of nucleosomes by ACF is interrupted by well-defined pauses. Surprisingly, several aspects of the remodeling process were found to be ATP-dependent: the binding of ACF, translocation of the nucleosome, and pauses. When the nucleosome was positioned at the end of DNA, the first pause occurred after 7 bp of translocation. Subsequent pauses were separated by 3–4 bp. The same behavior was observed when the nucleosome was positioned centrally, which means that this behavior may be a fundamental characteristic of remodeling by ACF. The authors suggested that the origin of these pauses is an ATP-dependent conformational transition of the enzyme that prepares the nucleosome for the next round of DNA translocation. Experiments with centrally positioned nucleosomes showed that ACF complex can translocate the histone octamer back and forth a total distance of more than 200 bp and switch directions more than 20 times. Statistical analysis of the fluorescence intensity and photobleaching behavior of the labeled ACF showed that when ACF binding events lead to bidirectional remodeling, there is always a dimer of ACF molecules. Conversely, binding events associated with unidirectional remodeling were observed to be due to ACF monomers. Interestingly, another study published at the same time used biochemical data and electron microscopy to show that ACF acts as a dimeric motor to separate nucleosomes [104].

SM tools can directly observe (and often in real time) details of the chromatin remodeling process including the structure of the nucleosome after remodeling and the displacement range per remodeling event. Yeast Swi/Snf is a transcriptional

activator that uses the energy of ATP hydrolysis to regulate the accessibility of the genetic code by changing chromatin structure [106]. By unzipping single DNA molecules using an optical trapping setup, Shundrovsky et al. probed some of the finer details of yeast Swi/Snf complex action [107]. Remodeling by Swi/Snf occurred in both directions on dsDNA. In addition, remodeled nucleosomes showed a continuous distribution of relocation sites around their original positions on DNA. The novel aspect of this SM approach is that it can directly detect the precise locations of the DNA-histone contacts, while the ordinary end-to-end stretching approach detects only the relative locations of the interactions. Unfortunately, the shapes of the response curves modeling the relationship of applied force to the number of unzipped DNA bases (or "disruption signature") in the presence of nucleosomes were similar with and without Swi/Snf (i.e. any structural changes to the nucleosomes were not stable enough to be detected). This result was used as evidence that the nucleosome resumes its classical structure after remodeling under the selected experimental conditions and spatial resolution of the technique used in this study. This study, however, did not show in any way that nucleosome structure is unchanged during the remodeling process [71]. Applications of this method to other systems may lead to more informative results.

RSC, or Remodels the Structure of Chromatin, is about tenfold more abundant in the cell than Swi/Snf [108]. It has been implicated in transcriptional regulation, sister chromatid cohesion, chromosome stability, and DNA repair. Two SM studies of RSC (and Swi/Snf) were published in 2006, both showing very interesting aspects of the remodeling process [81, 109]. The two studies were complementary to each other: one of them done on bare DNA without nucleosomes [109], while the other was done with nucleosomal DNA [81]. The experimental design of both studies was based on detecting changes in the length of single DNA molecules fixed at both ends.

In the former study [109], RSC was found to induce transient DNA length shortening (which was confirmed by AFM). This was interpreted as translocation of RSC on DNA resulting in a loop generation. Both ATP concentration and tension force affected the size of the translocated loop. The extent of underwinding during loop formation differed between (−) and (+) supercoiled DNA (scDNA); this was explained as a consequence of either the difference in the size of the DNA loop formed on (+/−) scDNA or the difference in the number of generated negative supercoils. The authors noted that loop formation was associated more closely with the underwinding of DNA, though a combination of both supercoiling processes is also possible. Notably, the generation of supercoils on a topologically closed DNA by a translocating SF2 motor has also been observed for hRad54. Based on the Worm-like Chain (WLC) model, the authors estimated that RSC generates much less than one turn of loop per every 10.5 bp of (−) scDNA translocated. The amount of negative rotation generated was between −0.15 and −0.04 rotations per 10.5 bp translocated, perhaps because the motion of RSC along DNA might be broken down into steps of ~12 bp in length. Interestingly, although the length of the translocated loop assumed a Gaussian distribution, the time taken to form the loop could be modeled by an exponential distribution. This difference in statistical behavior may reflect a change in RSC remodeling activity in response to tensile load during translocation.

The authors thus proposed a “thermal ratchet model” to describe RSC translocation. In this model, the RSC–DNA complex proceeds upon ATP binding into active translocation mode, with at least two contacts between DNA and RSC. Most of the loops formed due to translocation of DNA by RSC are removed in an ATP-dependent manner, probably due to translocation in the opposite direction. Sometimes, the loop collapses rapidly, either due to translocase disengagement or due to losing another contact that constrains the DNA.

Zhang et al. found that both RSC and yeast Swi/Snf switch translocation direction on DNA that has nucleosomes, but with a lower probability compared to their behavior on bare DNA [81]. Loop formation on bare DNA occurs only at very low DNA tension (<1 pN), while on DNA with a nucleosome present it could be observed at much higher tensions (1–6 pN). The average loop size on bare DNA was significantly larger than the average loop size observed on nucleosomal DNA (~100 bp). Following the same trend, the translocation rate on nucleosomal DNA substrates was much slower than on bare DNA (12 bp/s). Another interesting observation in the experiments done with nucleosomal DNA was the occurrence of a burst of loop formation and dissipation activity, a behavior that was not observed on bare DNA.

The differences between the studies of RSC were ultimately suggested to reflect a specific recognition of the nucleosome by the remodeler and a strong coupling between nucleosome association and remodeler translocation. It is important to note that the SM approach used in both studies cannot directly discriminate between nucleosome mobilization due to loop formation and that achieved by another mobilization mechanism; however, there were clear similarities observed between the translocation activities of Swi/Snf and RSC complexes that may represent general features of chromatin remodeling by Swi/Snf-like enzymes.

Concluding Remarks

Clearly, the emergence of SM methods has contributed extensively to the characterization of SF2 helicases and translocases. Without a doubt, the maturation of these techniques will provide many more useful findings. Future work with SF2 enzymes must place particular emphasis on building a more detailed mechanism of duplex separation and filling the great need for high-resolution structural data. Progress in these areas will advance the larger goal of a deepened understanding of translocation and helicase activities in biological contexts and the regulation of these activities within the macromolecular complexes in which they so often play central roles. A deeper understanding of SF2 enzymes will no doubt shed light on many essential cellular processes and enrich the larger picture of NA metabolism.

Acknowledgements We are gratefully acknowledge support by the American Cancer Society (RSG-09-182-01-DMC) and Howard Hughes Medical Institute (Early Career Scientist Award).

References

1. Fairman-Williams ME, Guenther U-P, Jankowsky E. SF1 and SF2 helicases: family matters. Curr Opin Struct Biol. 2010;20(3):313–24.
2. Lohman TM, Bjornson KP. Mechanisms of helicase-catalyzed DNA unwinding. Annu Rev Biochem. 1996;65:169–214.
3. Lohman TM, Tomko EJ, Wu CG. Non-hexameric DNA helicases and translocases: mechanisms and regulation. Nat Rev Mol Cell Biol. 2008;9(May):391–401.
4. Singleton MR, Scaife S, Wigley DB. Structural analysis of DNA replication fork reversal by RecG. Cell. 2001;107(1):79–89.
5. Singleton MR, Dillingham MS, Wigley DB. Structure and mechanism of helicases and nucleic acid translocases. Annu Rev Biochem. 2007;76:23–50.
6. Singleton M. Modularity and specialization in superfamily 1 and 2 helicases. J Bacteriol. 2002;184(7):1819–26.
7. Delagoutte E, von Hippel PH. Helicase mechanisms and the coupling of helicases within macromolecular machines. Q Rev Biophys. 2003;36(1):1–69.
8. Delagoutte E, von Hippel PH. Helicase mechanisms and the coupling of helicases within macromolecular machines Part I: structures and properties of isolated helicases. Q Rev Biophys. 2002;35(4):431–78.
9. Myong S, Ha T. Stepwise translocation of nucleic acid motors. Curr Opin Struct Biol. 2010;20(1):121–7.
10. von Hippel PH, Delagoutte E. A general model for nucleic acid helicases and their "coupling" within macromolecular machines. Cell. 2001;104(2):177–90.
11. Karamanou S, Gouridis G, Papanikou E, Sianidis G, Gelis I, Keramisanou D, et al. Preprotein-controlled catalysis in the helicase motor of SecA. EMBO J. 2007;26(12):2904–14.
12. Petermann E, Helleday T. Pathways of mammalian replication fork restart. Nat Rev Mol Cell Biol. 2010;11(10):683–7.
13. Suhasini AN, Brosh RM. Mechanistic and biological aspects of helicase action on damaged DNA. Cell Cycle. 2010;9(12):2317–29.
14. Bochkarev A, Bochkareva E, Frappier L, Edwards AM. The crystal structure of the complex of replication protein A subunits RPA32 and RPA14 reveals a mechanism for single-stranded DNA binding. EMBO J. 1999;18(16):4498–504.
15. Velankar SS, Soultanas P, Dillingham MS, Subramanya HS, Wigley DB. Crystal structures of complexes of PcrA DNA helicase with a DNA substrate indicate an inchworm mechanism. Cell. 1999;97(1):75–84.
16. Pyle AM. Translocation and unwinding mechanisms of RNA and DNA helicases. Annu Rev Biophys. 2008;37:317–36.
17. Tanner NK, Cordin O, Banroques J, Doère M, Linder P. The Q motif: a newly identified motif in DEAD box helicases may regulate ATP binding and hydrolysis. Mol Cell. 2003;11(1):127–38.
18. Zhang X, Wigley DB. The "glutamate switch" provides a link between ATPase activity and ligand binding in AAA+ proteins. Nat Struct Mol Biol. 2008;15(11):1223–7.
19. Zittel MC, Keck JL. Coupling DNA-binding and ATP hydrolysis in Escherichia coli RecQ: role of a highly conserved aromatic-rich sequence. Nucleic Acids Res. 2005;33(22):6982–91.
20. Büttner K, Nehring S, Hopfner KP. Structural basis for DNA duplex separation by a superfamily-2 helicase. Nat Struct Mol Biol. 2007;14(7):647–52.
21. Atkinson J, McGlynn P. Replication fork reversal and the maintenance of genome stability. Nucleic Acids Res. 2009;37(11):3475–92.
22. Briggs GS, Mahdi A, Weller GR, Wen Q, Lloyd RG. Interplay between DNA replication, recombination and repair based on the structure of RecG helicase. Philos Trans R Soc Lond B Biol Sci. 2004;359(1441):49–59.
23. Dillingham MS, Kowalczykowski SC. A step backward in advancing DNA replication: rescue of stalled replication forks by RecG. Mol Cell. 2001;8(4):734–6.

24. McGlynn P, Lloyd RG. Rescue of stalled replication forks by RecG: simultaneous translocation on the leading and lagging strand templates supports an active DNA unwinding model of fork reversal and Holliday junction formation. Proc Natl Acad Sci USA. 2001;98(15):8227–34.
25. Buss JA, Kimura Y, Bianco PR. RecG interacts directly with SSB: implications for stalled replication fork regression. Nucleic Acids Res. 2008;36(22):7029–42.
26. Gregg AV, McGlynn P, Jaktaji RP, Lloyd RG. Direct rescue of stalled DNA replication forks via the combined action of PriA and RecG helicase activities. Mol Cell. 2002;9(2):241–51.
27. Rudolph CJ, Upton AL, Briggs GS, Lloyd RG. Is RecG a general guardian of the bacterial genome? DNA Repair. 2010;9(3):210–23.
28. Rudolph CJ, Mahdi AA, Upton AL, Lloyd RG. RecG protein and single-strand DNA exonucleases avoid cell lethality associated with PriA helicase activity in Escherichia coli. Genetics. 2010;186(2):473–92.
29. Heyer W-D. Biochemistry of eukaryotic homologous recombination. Top Curr Genet. 2007;17:95–133.
30. Yusufzai T, Kadonaga JT. Branching out with DNA helicases. Curr Opin Genet Dev. 2011;21(2):214–8.
31. Whitby MC. The FANCM family of DNA helicases/translocases. DNA Repair. 2010;9(3):224–36.
32. Wu L. Role of the BLM helicase in replication fork management. DNA Repair. 2007;6(7):936–44.
33. Adelman CA, Boulton SJ. Metabolism of postsynaptic recombination intermediates. FEBS Lett. 2010;584(17):3709–16.
34. He Y, Andersen GR, Nielsen KH. Structural basis for the function of DEAH helicases. EMBO Rep. 2010;11(3):180–6.
35. Muzzolini L, Beuron F, Patwardhan A, Popuri V, Cui S, Niccolini B, et al. Different quaternary structures of human RECQ1 are associated with its dual enzymatic activity. PLoS Biol. 2007;5(2):12.
36. Prakash R, Krejci L, Van Komen S, Anke Schürer K, Kramer W, Sung P. Saccharomyces cerevisiae MPH1 gene, required for homologous recombination-mediated mutation avoidance, encodes a 3′ to 5′ DNA helicase. J Biol Chem. 2005;280(9):7854–60.
37. Nishino T, Komori K, Tsuchiya D, Ishino Y, Morikawa K. Crystal structure and functional implications of Pyrococcus furiosus hef helicase domain involved in branched DNA processing. Structure. 2005;13(1):143–53.
38. Nakayama H, Nakayama K, Nakayama R, Irino N, Nakayama Y, Hanawalt PC. Isolation and genetic characterization of a thymineless death-resistant mutant of Escherichia coli K12: identification of a new mutation (recQ1) that blocks the RecF recombination pathway. Mol Gen Genet. 1984;195(3):474–80.
39. Vindigni A, Hickson ID. RecQ helicases: multiple structures for multiple functions? HFSP J. 2009;3(3):153–64.
40. Bachrati CZ, Hickson ID. RecQ helicases: guardian angels of the DNA replication fork. Chromosoma. 2008;117(3):219–33.
41. Bernstein KA, Gangloff S, Rothstein R. The RecQ DNA helicases in DNA repair. Annu Rev Genet. 2010;44:393–417.
42. Wu Y, Brosh RM. Distinct roles of RECQ1 in the maintenance of genomic stability. DNA Repair. 2010;9(3):315–24.
43. Bernstein DA. Domain mapping of Escherichia coli RecQ defines the roles of conserved N- and C-terminal regions in the RecQ family. Nucleic Acids Res. 2003;31(11):2778–85.
44. Bernstein DA, Zittel MC, Keck JL. High-resolution structure of the E. coli RecQ helicase catalytic core. EMBO J. 2003;22(19):4910–21.
45. Vindigni A, Marino F, Gileadi O. Probing the structural basis of RecQ helicase function. Biophys Chem. 2010;149(3):67–77.
46. Guo R, Rigolet P, Zargarian L, Fermandjian S, Xi XG. Structural and functional characterizations reveal the importance of a zinc binding domain in Bloom's syndrome helicase. Nucleic Acids Res. 2005;33(10):3109–24.

47. Liu JL, Rigolet P, Dou S-X, Wang P-Y, Xi XG. The zinc finger motif of Escherichia coli RecQ is implicated in both DNA binding and protein folding. J Biol Chem. 2004;279(41):42794–802.
48. Sato A, Mishima M, Nagai A, Kim S-Y, Ito Y, Hakoshima T, et al. Solution structure of the HRDC domain of human Bloom syndrome protein BLM. J Biochem. 2010;148(4):517–25.
49. Yang Y, Dou S-X, Xu Y-N, Bazeille N, Wang P-Y, Rigolet P, et al. Kinetic mechanism of DNA unwinding by the BLM helicase core and molecular basis for its low processivity. Biochemistry. 2010;49(4):656–68.
50. Yodh JG, Stevens BC, Kanagaraj R, Janscak P, Ha T. BLM helicase measures DNA unwound before switching strands and hRPA promotes unwinding reinitiation. EMBO J. 2009;28(4):405–16.
51. Deschavanne PJ, Harosh I. The Rad3 protein from Saccharomyces cerevisiae: a DNA and DNA:RNA helicase with putative RNA helicase activity. Mol Microbiol. 1993;7(6):831–5.
52. Rudolf J, Rouillon C, Schwarz-Linek U, White MF. The helicase XPD unwinds bubble structures and is not stalled by DNA lesions removed by the nucleotide excision repair pathway. Nucleic Acids Res. 2010;38(3):931–41.
53. White MF. Structure, function and evolution of the XPD family of iron-sulfur-containing 5′–3′ DNA helicases. Biochem Soc Trans. 2009;37(Pt 3):547–51.
54. Wu Y, Brosh RM. DNA helicase and helicase-nuclease enzymes with a conserved iron-sulfur cluster. Nucleic Acids Res. 2012;40(10):1–14.
55. Wolski SC, Kuper J, Kisker C. The XPD helicase: XPanDing archaeal XPD structures to get a grip on human DNA repair. Biol Chem. 2010;391(7):761–5.
56. Hiom K. FANCJ: solving problems in DNA replication. DNA Repair. 2010;9(3):250–6.
57. Rudolf J, Makrantoni V, Ingledew WJ, Stark MJR, White MF. The DNA repair helicases XPD and FancJ have essential iron-sulfur domains. Mol Cell. 2006;23(6):801–8.
58. Fuss JO, Tainer JA. XPB and XPD helicases in TFIIH orchestrate DNA duplex opening and damage verification to coordinate repair with transcription and cell cycle via CAK kinase. DNA Repair. 2011;10(7):697–713.
59. Kuper J, Kisker C. Damage recognition in nucleotide excision DNA repair. Curr Opin Struct Biol. 2012;22(1):88–93.
60. Kuper J, Wolski SC, Michels G, Kisker C. Functional and structural studies of the nucleotide excision repair helicase XPD suggest a polarity for DNA translocation. EMBO J. 2012;31(2):494–502.
61. Fan L, Fuss JO, Cheng QJ, Arvai AS, Hammel M, Roberts V, et al. XPD helicase structures and activities: insights into the cancer and aging phenotypes from XPD mutations. Cell. 2008;133(5):789–800.
62. Liu H, Rudolf J, Johnson KA, McMahon S, Oke M, Carter L, et al. Structure of the DNA repair helicase XPD. Cell. 2008;133(5):801–12.
63. Wolski SC, Kuper J, Hänzelmann P, Truglio JJ, Croteau DL, Van Houten B, et al. Crystal structure of the FeS cluster-containing nucleotide excision repair helicase XPD. PLoS Biol. 2008;6(6):e149.
64. Pugh RA, Honda M, Leesley H, Thomas A, Lin Y, Nilges MJ, et al. The iron-containing domain is essential in Rad3 helicases for coupling of ATP hydrolysis to DNA translocation and for targeting the helicase to the single-stranded DNA-double-stranded DNA junction. J Biol Chem. 2008;283(3):1732–43.
65. Pugh RA, Wu CG, Spies M. Regulation of translocation polarity by helicase domain 1 in SF2B helicases. EMBO J. 2011;31(2):1–12.
66. Pugh RA, Lin Y, Eller C, Leesley H, Cann IKO, Spies M. Ferroplasma acidarmanus RPA2 facilitates efficient unwinding of forked DNA substrates by monomers of FacXPD helicase. J Mol Biol. 2008;383(5):982–98.
67. Honda M, Park J, Pugh RA, Ha T, Spies M. Single-molecule analysis reveals differential effect of ssDNA-binding proteins on DNA translocation by XPD helicase. Mol Cell. 2009;35(5):694–703.

68. Spies M, Ha T. Inching over hurdles: how DNA helicases move on crowded lattices. Cell Cycle. 2010;9(9):1742–9.
69. Büttner K, Nehring S, Hopfner K-P. Structural basis for DNA duplex separation by a superfamily-2 helicase. Nat Struct Mol Biol. 2007;14(7):647–52.
70. Richards JD, Johnson KA, Liu H, McRobbie A-M, McMahon S, Oke M, et al. Structure of the DNA repair helicase hel308 reveals DNA binding and autoinhibitory domains. J Biol Chem. 2008;283(8):5118–26.
71. Andrews AJ, Luger K. Nucleosome structure(s) and stability: variations on a theme. Annu Rev Biophys. 2011;40:99–117.
72. Hargreaves DC, Crabtree GR. ATP-dependent chromatin remodeling: genetics, genomics and mechanisms. Cell Res. 2011;21(3):396–420.
73. Kornberg RD. Chromatin structure: a repeating unit of histones and DNA. Science. 1974;184(139):868–71.
74. Luger K, Mäder AW, Richmond RK, Sargent DF, Richmond TJ. Crystal structure of the nucleosome core particle at 2.8 A resolution. Nature. 1997;389(6648):251–60.
75. Clapier CR, Cairns BR. The biology of chromatin remodeling complexes. Annu Rev Biochem. 2009;78(1):273–304.
76. Ko M, Sohn DH, Chung H, Seong RH. Chromatin remodeling, development and disease. Mutat Res. 2008;647(1–2):59–67.
77. Liu N, Balliano A, Hayes JJ. Mechanism(s) of SWI/SNF-induced nucleosome mobilization. Chembiochem. 2010;12(2):196–204.
78. Saha A, Wittmeyer J, Cairns BR. Chromatin remodelling: the industrial revolution of DNA around histones. Nat Rev Mol Cell Biol. 2006;7(6):437–47.
79. Tang L, Nogales E, Ciferri C. Structure and function of SWI/SNF chromatin remodeling complexes and mechanistic implications for transcription. Prog Biophys Mol Biol. 2010;102(2–3):122–8.
80. Mohrmann L, Verrijzer CP. Composition and functional specificity of SWI2/SNF2 class chromatin remodeling complexes. Biochim Biophys Acta. 2005;1681(2–3):59–73.
81. Zhang Y, Smith CL, Saha A, Grill SW, Mihardja S, Smith SB, et al. DNA translocation and loop formation mechanism of chromatin remodeling by SWI/SNF and RSC. Mol Cell. 2006;24(4):559–68.
82. Corona DFV, Tamkun JW. Multiple roles for ISWI in transcription, chromosome organization and DNA replication. Biochim Biophys Acta. 2004;1677(1–3):113–9.
83. Marfella CGA, Imbalzano AN. The Chd family of chromatin remodelers. Mutat Res. 2007;618(1–2):30–40.
84. Bao Y, Shen X. INO80 subfamily of chromatin remodeling complexes. Mutat Res. 2007;618(1–2):18–29.
85. Bianco PR, Brewer LR, Corzett M, Balhorn R, Yeh Y, Kowalczykowski SC, et al. Processive translocation and DNA unwinding by individual RecBCD enzyme molecules. Nature. 2001;409(6818):374–8.
86. Hopfner K-P, Michaelis J. Mechanisms of nucleic acid translocases: lessons from structural biology and single-molecule biophysics. Curr Opin Struct Biol. 2007;17(1):87–95.
87. Yodh JG, Schlierf M, Ha T. Insight into helicase mechanism and function revealed through single-molecule approaches. Q Rev Biophys. 2010;43(2):185–217.
88. Karow JK, Newman RH, Freemont PS, Hickson ID. Oligomeric ring structure of the Bloom's syndrome helicase. Curr Biol. 1999;9(11):597–600.
89. Garcia PL, Bradley G, Hayes CJ, Krintel S, Soultanas P, Janscak P. RPA alleviates the inhibitory effect of vinylphosphonate internucleotide linkages on DNA unwinding by BLM and WRN helicases. Nucleic Acids Res. 2004;32(12):3771–8.
90. Betterton M, Jülicher F. Opening of nucleic-acid double strands by helicases: active versus passive opening. Phys Rev E. 2005;71(1):1–11.
91. Dumont S, Cheng W, Serebrov V, Beran RK, Tinoco I, Pyle AM, et al. RNA translocation and unwinding mechanism of HCV NS3 helicase and its coordination by ATP. Nature. 2006;439(7072):105–8.

92. Manosas M, Xi XG, Bensimon D, Croquette V. Active and passive mechanisms of helicases. Nucleic Acids Res. 2010;38(16):5518–26.
93. Pan B-Y, Dou S-X, Yang Y, Xu Y-N, Bugnard E, Ding X-Y, et al. Mutual inhibition of RecQ molecules in DNA unwinding. J Biol Chem. 2010;285(21):15884–93.
94. Pugh RA, Honda M, Spies M. Ensemble and single-molecule fluorescence-based assays to monitor DNA binding, translocation, and unwinding by iron-sulfur cluster containing helicases. Methods. 2010;51(3):313–21.
95. Sontz P, Mui T, Fuss J, Tainer JA, Barton JK. DNA charge transport as a first step in coordinating the detection of lesions by repair proteins. Proc Natl Acad Sci U S A. 2012;109(6): 1856–61.
96. Heyer W-D, Li X, Rolfsmeier M, Zhang X-P. Rad54: the Swiss Army knife of homologous recombination? Nucleic Acids Res. 2006;34(15):4115–25.
97. Mazin AV, Mazina OM, Bugreev DV, Rossi MJ. Rad54, the motor of homologous recombination. DNA Repair. 2010;9(3):286–302.
98. Ristic D, Wyman C, Paulusma C, Kanaar R. The architecture of the human Rad54–DNA complex provides evidence for protein translocation along DNA. Proc Natl Acad Sci USA. 2001;98(15):8454–60.
99. Amitani I, Baskin RJ, Kowalczykowski SC. Visualization of Rad54, a chromatin remodeling protein, translocating on single DNA molecules. Mol Cell. 2006;23(1):143–8.
100. Nimonkar AV, Amitani I, Baskin RJ, Kowalczykowski SC. Single molecule imaging of Tid1/Rdh54, a Rad54 homolog that translocates on duplex DNA and can disrupt joint molecules. J Biol Chem. 2007;282(42):30776–84.
101. Lewis R, Dürr H, Hopfner K-P, Michaelis J. Conformational changes of a Swi2/Snf2 ATPase during its mechano-chemical cycle. Nucleic Acids Res. 2008;36(6):1881–90.
102. Dürr H, Flaus A, Owen-Hughes T, Hopfner K-P. Snf2 family ATPases and DExx box helicases: differences and unifying concepts from high-resolution crystal structures. Nucleic Acids Res. 2006;34(15):4160–7.
103. Sanchez H, Suzuki Y, Yokokawa M, Takeyasu K, Wyman C. Protein–DNA interactions in high speed AFM: single molecule diffusion analysis of human RAD54. Integr Biol. 2011;21(4):546–56.
104. Racki LR, Yang JG, Naber N, Partensky PD, Acevedo A, Purcell TJ, et al. The chromatin remodeller ACF acts as a dimeric motor to space nucleosomes. Nature. 2009;462(7276):1016–21.
105. Blosser TR, Yang JG, Stone MD, Narlikar GJ, Zhuang X. Dynamics of nucleosome remodelling by individual ACF complexes. Nature. 2009;462(7276):1022–7.
106. Dechassa ML, Hota SK, Sen P, Chatterjee N, Prasad P, Bartholomew B. Disparity in the DNA translocase domains of SWI/SNF and ISW2. Nucleic Acids Res. 2012;40(10):4412–21.
107. Shundrovsky A, Smith CL, Lis JT, Peterson CL, Wang MD. Probing SWI/SNF remodeling of the nucleosome by unzipping single DNA molecules. Nat Struct Mol Biol. 2006;13(6):549–54.
108. Van Vugt JJFA, Ranes M, Campsteijn C, Logie C. The ins and outs of ATP-dependent chromatin remodeling in budding yeast: biophysical and proteomic perspectives. Biochim Biophys Acta. 2007;1769(3):153–71.
109. Lia G, Praly E, Ferreira H, Stockdale C, Tse-Dinh YC, Dunlap D, et al. Direct observation of DNA distortion by the RSC complex. Mol Cell. 2006;21(3):417–25.

Chapter 4
Structure and Mechanism of Hexameric Helicases

Barbara Medagli and Silvia Onesti

Abstract Hexameric helicases are responsible for many biological processes, ranging from DNA replication in various life domains to DNA repair, transcriptional regulation and RNA metabolism, and encompass superfamilies 3–6 (SF3–6).

To harness the chemical energy from ATP hydrolysis for mechanical work, hexameric helicases have a conserved core engine, called ASCE, that belongs to a subdivision of the P-loop NTPases. Some of the ring helicases (SF4 and SF5) use a variant of ASCE known as RecA-like, while some (SF3 and SF6) use another variant known as AAA+ fold. The NTP-binding sites are located at the interface between monomers and include amino-acid residues coming from neighbouring subunits, providing a mean for small structural changes within the ATP-binding site to be amplified into large inter-subunit movement.

The ring structure has a central channel which encircles the nucleic acid. The topological link between the protein and the nucleic acid substrate increases the stability and processivity of the enzyme. This is probably the reason why within cellular systems the critical step of unwinding dsDNA ahead of the replication fork seems to be almost invariably carried out by a toroidal helicase, whether in bacteria, archaea or eukaryotes, as well as in some viruses.

Over the last few years, a large number of biochemical, biophysical and structural data have thrown new light onto the architecture and function of these remarkable machines. Although the evidence is still limited to a couple of systems, biochemical and structural results suggest that motors based on RecA and AAA+ folds have converged on similar mechanisms to couple ATP-driven conformational changes to movement along nucleic acids.

B. Medagli • S. Onesti (✉)
Structural Biology, Sincrotrone Trieste (Elettra),
Area Science Pk, Basovizza, Trieste, Italy
email: e-mail: silvia.onesti@elettra.trieste.it; barbara.medagli@elettra.trieste.it

M. Spies (ed.), *DNA Helicases and DNA Motor Proteins*, Advances in Experimental Medicine and Biology, DOI 10.1007/978-1-4614-5037-5_4,

Overall Architecture

Although helicases have been classified into six different superfamilies [1] (SF1–6), a main distinction can be drawn between those working as monomers or dimers (belonging to superfamilies SF1 and SF2) and those forming toroidal rings (SF3–6). The ring-forming helicases are responsible for a huge variety of biological processes, ranging from DNA replication in various life domains to DNA repair, transcriptional regulation and RNA metabolism. In particular, within cellular systems, the critical step of unwinding dsDNA ahead of the replication fork seems to be almost invariably carried out by a toroidal helicase, whether in bacteria, archaea or eukaryotes, as well as some viruses (see also Chap. 5).

To harness the chemical energy from ATP hydrolysis for mechanical work, hexameric helicases have a conserved core engine, known as ASCE, that belongs to a subdivision of the P-loop NTPases. Some of the ring helicases use a variant of the ASCE fold first visualised in the RecA recombinase, and therefore known as RecA-like fold, while some use another variant known as AAA+ fold. SF1 (discussed in Chap. 2) and SF2 (discussed in Chap. 3) polypeptides typically contain tandem ASCE folds and bind the nucleotide at the interface between the two domains (Fig. 4.1), with the N-terminal half providing the Walker A and Walker B motif, and the C-terminal domain providing other elements that are critical for the mechanism of action. In contrast, oligomeric helicases contain only a single ASCE domain (either with a RecA or a AAA+ fold) per monomer, with the ATP site at the interface between adjacent subunits, and rely on the interaction with neighbouring subunits to provide the full nucleotide-binding pocket. Whereas most of the interactions with the nucleotide are therefore provided by one subunit (such as the Walker A and B, acting in *cis*), some of the necessary amino-acid side chains come from the neighbouring monomer and are therefore said to act in *trans* (Fig. 4.1).

The ring structure provides a central channel where the nucleic acid substrate is supposed to thread. The size of the channel can be very variable, ranging from 13 Å [2, 3] up to more than 50 Å [4–6]. Larger channels can therefore accommodate not only single-stranded oligonucleotides, but also double-stranded ones. Whereas some dsDNA translocases clearly bind and walk along dsDNA, the situation is less clear for bona fide helicases, and in some cases there is some uncertainty as to the nature of the physiological substrate [7–10].

The toroidal architecture presents both advantages and disadvantages. The topological link between the protein and the nucleic acid substrate increases the stability of the complex and therefore the processivity of the helicase. This is probably the reason why helicases involved in cellular DNA replication, which must continuously unwind long stretches of dsDNA ahead of the replication fork, are invariably ring helicases (see also Chap. 5). On the other hand the circular architecture creates a topological problem during loading, since the helicase ring needs to open up to correctly bind the substrate within the channel. This can be achieved in multiple ways, either through an intrinsic plasticity of the ring (with the presence of C-shaped, partially opened rings assemblies), or through a specialised loading machinery, such as DnaA/DnaC in bacteria, the Cdc6/Orc1 system in archaea and the pre-replicative complex (including the Orc1-6 complex, Cdt1, Cdc6, beside the Mcm2-7 helicase)

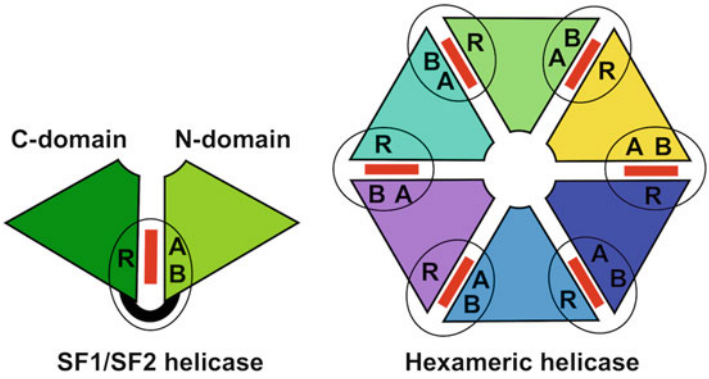

Fig. 4.1 General architecture of helicases. On the *left* is a schematic representation of helicases belonging to the SF1 and SF2 family: the enzymes are typically monomeric (although may work as dimers) and fold into two structurally similar domains, each similar to a RecA monomer, with the ATP-binding site (depicted as a *red bar*) sandwiched between the domains, the Walker A and Walker B domains provided by the N-terminal half of the protein (*light green*), and additional elements necessary for hydrolysis (such as an arginine finger R) provided by the C-terminal portion (*dark green*). On the *right* is a schematic diagram of the architecture of hexameric helicases: six monomers (either RecA or AAA+ folds) assemble into a ring, with the ATP sandwiched between adjacent subunits. Each monomer thus contains both the Walker A and Walker B domain on one side, and the arginine finger necessary for the activity on the opposite side. A central cavity in the middle binds the nucleic acid substrate, which is therefore "trapped" within the ring

in eukaryotes. Although undoubtedly a complication, elaborated loading mechanisms ensures that the critical step of processive DNA unwinding occurs in a carefully controlled way, and can be the target of multiple levels of regulation.

The ring can move along the nucleic acid either in the 3′→5′ or in the 5′→3′ direction. Within the well-studied ring helicases, those belonging to the RecA-like group translocate in the 5′→3′ direction, whereas the AAA+ enzymes have the opposite polarity (3′→5′). Whether this is a general rule and reflects a conserved and distinct mechanism of action or it is simply due to the relatively small number of enzymes that have been fully characterised needs to be ascertained.

Hexameric helicases include both DNA and RNA helicases, as well as a variety of dsDNA translocases and DNA/RNA packaging motors. However, all eukaryotic RNA helicases studied to date belong to the SF1 and SF2 family, whereas toroidal RNA helicases are less common, and are only found in bacteria and viruses [11, 12]. Although the subject of the present book is limited to DNA helicases, we will include a discussion on the RNA helicase Rho, as it provides essential insights into the mechanisms of action of hexameric helicases.

The Basic Units: RecA and AAA+ Folds

As helicases couple NTP (typically ATP) hydrolysis to movement along nucleic acid, they belong to the general division of P-loop NTPases, identified by the presence of a Walker A (the "P loop") and Walker B motifs. More specifically, the core of a helicase

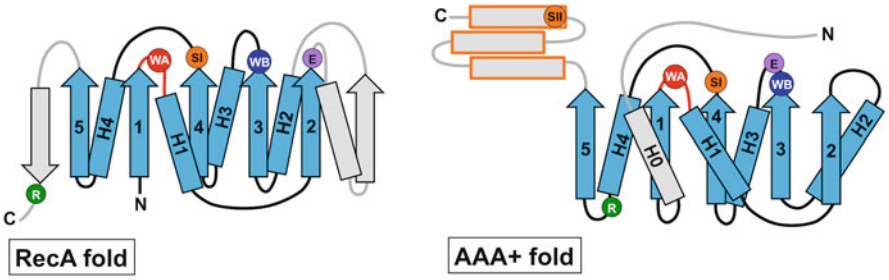

Fig. 4.2 A comparison between the RecA and the AAA+ folds. Both RecA and AAA+ belong to the ASCE subgroup of the P loop NTPases, and comprise a 5-stranded parallel β-sheet, flanked by helices both in front and behind the plane of the sheet. The secondary structure elements that are common to the ASCE proteins are shown in *blue*: the P loop containing the Walker A motif (WA) is shown in *red*, the Walker B motif in *dark blue*, the catalytic glutamate in *violet* (E), the arginine finger (R) in *green* and the Sensor I (SI) and Sensor II (SII) in *orange*. The AAA+ is characterised by a C-terminal α-helical domains (in *orange*)

motor is built around a ubiquitous fold known as ASCE (*A*dditional *S*trand *C*atalytic *E*), belonging to the class of P-loop NTPases, but characterised by the insertion of an additional strand (strand 4) between the Walker A and Walker B motifs and by the presence of a catalytic glutamate [13]. The ASCE fold thus comprises an α/β core with five parallel β-strands (51432 topology, with strands 1 and 3 carrying the Walker A and Walker B motif), flanked by α-helices on both sides (Fig. 4.2). A characteristic of ASCE ATPases is that they are active only in tandem, with at least two domains assembling so as to form a fully functional ATP-Mg-binding site (Fig. 4.1).

The Walker A (or P-loop) is a glycine-rich loop interacting with the phosphate moiety of the ATP located at the end of strand 1, while the Walker B (at the end of strand 4) motif contains a conserved aspartate coordinating the divalent cation (Mg^{2+}). ASCE proteins are then characterised by a conserved glutamate, which is involved in catalysis by activating a water molecule acting as the nucleophile in the hydrolysis reaction. Other two conserved features are the presence of a polar residue at the end of strand 4, which could act as a sensor of the nucleotide state, and a conserved arginine residue (arginine finger) that interacts with the nucleotide of the neighbouring subunit to couple ATP hydrolysis to inter-subunit conformational changes. Both the catalytic glutamate and the arginine finger may come from different topological positions.

Within the ASCE group various subdivisions can be identified, including the RecA-like ATPases and the AAA+ proteins [13–15]. Some confusion in the nomenclature arises from the fact that "RecA fold" was historically used (and sometimes still is) to indicate the whole ASCE group, rather than the specific subtype. Here we are following the classification suggested by Iyer et al. [14].

RecA proteins and their close homologues are characterised by two extensions on both side of the ASCE middle β-sheet: a helix-strand addition after strand 2, and a C-terminal β-hairpin after strand 5 (Fig. 4.2), therefore generating a 7-stranded central β-sheet. A conserved arginine residue is often found in the C-terminal

β-hairpin addition; in the RecA-like hexameric structures this arginine directly coordinates the γ-phosphate of the ATP bound to an adjacent subunit, thus acting as an arginine finger. Beside RecA, one of the best studied proteins of this class is the F1 ATP synthase. This is a protein made up of six RecA-like domains, alternating three catalytically active subunits with three subunits lacking the ATP-binding site: the rotation of a helical shaft in the central pore controls the exact configuration of the three active sites which sequentially change from empty to ADP-bound to ATP-bound [16–18].

AAA+ ATPases (ATPases Associated with various cellular Activities) are enzymes which utilise the energy released by ATP hydrolysis to do mechanical work, and can be found in a diverse range of processes such as protein transport, folding and degradation, membrane fusion, microtubule dynamics, transcription, DNA repair and recombination, as well as DNA replication. AAA+ proteins generally assemble as higher order oligomers, with a strong preference for hexameric rings [15, 19]. The monomers are characterised by a two-domain structure: the catalytic α/β ASCE domain has an additional helix before strand 1 (H0, Fig. 4.2) and contains a number of conserved motifs. The catalytic glutamate is part of the Walker B motif (hhhhD**E**) and the arginine finger is located between helix H4 and strand 5. This domain is followed by a helical (or "lid") domain, made up of 3 or 4 helices and containing a sensor II motif, typically including another conserved arginine. This residue also interacts with the ATP, and undergoes a conformational change upon the ATP→ADP transition, therefore "sensing" the nucleotide state. A conserved polar residue (known as "glutamate switch") sequesters the catalytic glutamate in the absence of nucleic acid, ensuring that ATP hydrolysis is activated only in the presence of the correct substrate [20].

AAA+ ATPases have been classified in various clades, based on various criteria (sequence or structural analysis) with different, and sometimes contrasting, results [15, 21, 22]. Following the structure-based analysis [15, 21], a class has been identified that is characterised by the insertion of a β-hairpin before sensor I (pre-sensor I β-hairpin, PS1BH, Fig. 4.2). All AAA+ helicases belong to the PS1BH superclade and in some cases the PS1BH has been shown to be critical for DNA binding and translocation [2, 23, 24].

Hexameric Helicase Superfamilies: An Overview

Whereas superfamilies SF1 and SF2 are clearly distinct and comprise a large number of proteins (see Chaps. 2 and 3, respectively), the situation for hexameric helicases is rather more blurred. When the first classification of helicases was proposed [25], three superfamilies were described, including the monomeric SF1 and SF2, and the hexameric SF3, consisting of a relatively small number of enzymes involved in replication of viral genomes, as well as two minor groups covering DnaB-like and Rho helicases. Subsequent bioinformatic, structural and biochemical studies have highlighted the relationship between various enzymes, so that a more recent

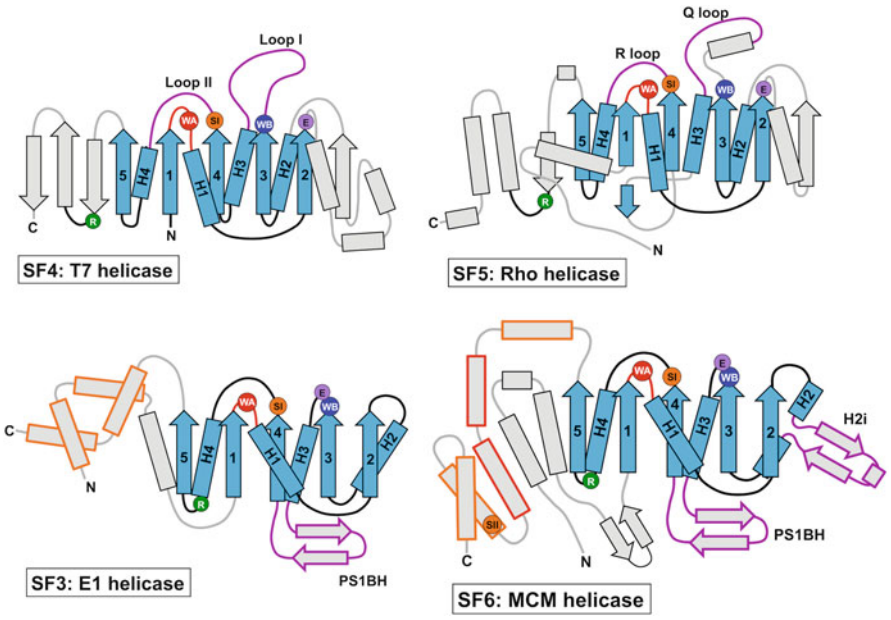

Fig. 4.3 Topology diagrams for SF3–6 families of hexameric helicases. A schematic representation of the topology of representatives of superfamilies SF4 (gp4 helicase from bacteriophage T7), SF5 (transcription termination factor Rho), SF3 (E1 helicase from papilloma virus) and SF6 (MCM helicase) are shown. SF4 and SF5 proteins share a RecA fold, whereas SF3 and SF6 share an AAA+ fold. The colour-code is the same as in Fig. 4.2; DNA-binding loops/regions are shown in *purple*. RecA-like hexameric helicases bind DNA through loops located at the *top* (C-terminal edge) of the β-sheet, whereas AAA+ helicases bind DNA via β-hairpins emanating from the *bottom* (N-terminal edge) of the β-sheet, and probably (in the case of MCM) from the H2 insertion. With respect to the canonical AAA+ fold (Fig. 4.2) the SF3 helicases lack the C-terminal α-helical domain, but have a helical bundle that is formed by both N-terminal and C-terminal elements. MCM helicases do possess a standard α-helical domain, but a long helical insertion (in *red*) reorients it in such a way that Sensor II becomes a *trans* rather than a *cis* residue

analysis defined three more superfamilies (SF4–6) bringing to 6 the total number of groups, with four (SF3–6, Fig. 4.3) consisting of hexameric enzymes [1]. Within the four hexameric superfamilies, two (SF4, SF5) are based on the RecA fold, and share a variety of structural features, including a similar location of the nucleic acid-binding loops, and a similar orientation of the fold in the context of the hexamer. The other two instead (SF3 and SF6) belong to the AAA+ division, and in particular to the PS1BH superclade. Below is a brief overview of the salient features of each family.

Superfamily SF3 includes proteins found in the genome of small DNA and RNA viruses and are involved in various stages of the viral replication cycle, from origin recognition, to origin melting and unwinding, therefore incorporating in one polypeptide both the function of an initiator protein and replicative helicase, as well as having additional roles such as inactivation of cellular tumour suppressors. The polypeptide chain contains multiple domains, typically including an origin

DNA-binding domain and a C-terminal helicase domain. The best studied members of the group are the large T antigen (LTag) from the simian virus 40 (SV40) and the E1 protein from the papilloma virus, but the superfamily also includes other members, such as the Rep helicases from adeno-associated virus (AAV), helicases from parvovirus Rep/NS1, polyoma virus large T antigen, etc. All the proteins that have been biochemically characterised have a 3′→5′ polarity.

From a structural point of view, the SF3 helicase domain folds around an α/β core that closely resembles that of AAA+ proteins (Fig. 4.3). However the classification of SF3 proteins is contentious: whereas the original report that identified the key similarities between AAA+ proteins such as MCM and the σ54-dependent transcriptional activators did indeed include SF3 helicases [26], other bioinformatic analysis do not include them within the AAA+ group, based on the lack of a "canonical" α domain [22]. However, despite the divergence of the domain, structure-based approaches identify a clear correlation between the topology of the α/β domain of SF3 helicases and the AAA+ fold, and especially the presence of the PS1BH insertion and the conserved position of the arginine finger [15, 21].

A number of crystal structures for this superfamilies have been reported, including the SV40 LTag in the apo form and in the presence of various nucleotides [27]; the papilloma virus E1 helicase in the presence of nucleotide and ssDNA [2] and the AAV Rep40 helicase [28].

The PS1BH insertions are located close to the central pore and in a number of cases have been shown to change orientation depending on the ATP state of the enzyme, thus linking ATP turnover to nucleic acid translocation. This is illustrated very clearly both in the symmetric structure of the SV40 LTag, where the β-hairpins assume a different concerted orientation in the apo, ATP and ADP forms [27], and even more in the crystal structure of the E1 helicase [2], where each hairpin has a different vertical position depending on the exact nucleotide state, forming a spiral staircase that is likely to chaperone each DNA unit.

Superfamily SF4 comprises a variety of helicases from various systems, including proteins from bacteriophages (T7 gp4, SPP1 GP40) and bacteria (the replicative DnaB helicase), as well as eukaryotic mitochondrial helicases TWINKLE [29]. Some confusion can arise from the fact that in Gram-negative bacteria the helicase is called DnaB and is loaded on the origin via the help of an AAA+ protein called DnaC, while in Gram-positive bacteria the DnaB-like helicase is actually named DnaC.

Often SF4 helicase domains are closely associated with a primase, either via a fusion event so that the primase and helicase are located in the same polypeptide [30], or by a strong physical interaction with a primase domain, as seen in the bacterial systems [5, 31].

Most of the biochemical and structural studies have focussed on the T7 helicase and the bacterial DnaB helicase. A number of crystal structures and electron microscopy reconstructions have been reported for the T7 helicase [30, 32–34], as well as a large amount of biochemical studies [35]. Similarly well studied are the bacterial DnaB-like helicases, both from the biochemical and structural point of view [5, 6, 36–41]. The core of the enzymes is a RecA-like fold [42] with the DNA-binding loops emerging from the C-terminal ends of the central β-strands (Fig. 4.3). The proteins move along the DNA in the 5′→3′ direction.

Superfamily SF5 includes only the bacterial transcription termination factors Rho. This protein binds to a transcription terminator pause site, then translocates along the transcript and unwinds the DNA/RNA hybrid. Although the sequence of Rho proteins is rather divergent from other helicases, their basic fold closely resembles members of the SF4 family. As SF4 members, Rho has a 5′→3′ polarity, is built around a RecA-like fold, and binds DNA with loops that are structurally and topologically equivalent.

The protein has been thoroughly dissected, making it one of the best studied hexameric helicases [11, 43–47].

Superfamily SF6 includes the archaeal and eukaryotic MCM proteins, as well as the RuvB proteins. MCM proteins are conserved between archaea and eukaryotes, with most archaea possessing a single copy forming homomeric rings, while eukaryotes have at least six different paralogs (MCM2-7) assembling into a multimeric complex [48]. A growing body of evidence confirmed the role of MCM proteins as the replicative helicase in both archaea and eukaryotes [49, 50]. Whereas the archaeal proteins display helicase activity [50], the activity of the MCM2-7 complex requires the presence of additional factors (such as Cdc45 and GINS) and post-translational modifications [51]; this is probably due to the more complex regulation of DNA replication in eukaryotes, where sophisticated cell-cycle control mechanisms ensure the ordered succession of DNA synthesis and cell division and the coordination of a large number of origins. The bacterial RuvB proteins, also classified within the SF6 family, work as a dsDNA translocase and, together with RuvA and RuvC, process Holliday junctions [52]. The so-called eukaryotic homologues of RuvB (variously cited as RvB1/2, RuvBL1/2, Tip49/48, Pontin/Reptin) lack a series of specific features, most notably the PS1BH insertion, making it unlikely that these proteins are true orthologues of RuvB [21]. Although it has been suggested that they may belong to a novel hexameric helicase superfamily [53], data regarding the helicase activity of the complex are rather contradictory [54, 55].

SF6 helicases share a similar AAA+ α/β core, and contain a PS1BH insertion. In RuvB the PS1BH interact with RuvA, rather than the nucleic acid substrate [56]. In the MCM proteins, in addition to the PS1BH, a second insertion emerges from helix H2, forming a long β-hairpin capped by a short helix (H2i, Fig. 4.3). Mutagenesis studies of both the PS1BH [23] and H2i [24] have demonstrated their crucial role in DNA binding and helicase activity.

Structural information on SF6 proteins is still patchy and no crystal structure for a hexameric form is available. There are various crystal structures of the monomeric form of RuvB [56–58], but we need to rely on low resolution electron microscopy reconstructions to build a hexamer [59, 60]. Even more complex is the situation with MCM helicases: although two crystal structures are available for the AAA+ motor domain of archaeal proteins, one is from an inactive protein [61] that lacks most of the functional elements (Walker A, Walker B, sensor I, arginine finger); the other is of a functional protein, but the crystals diffracted to low resolution, thus allowing only an approximate polyalanine model to be built [62]. The crystal structures show an unusual reorganisation of the α-helical domain, which moves from the canonical AAA+ fold position (Fig. 4.2), in such a way that sensor II

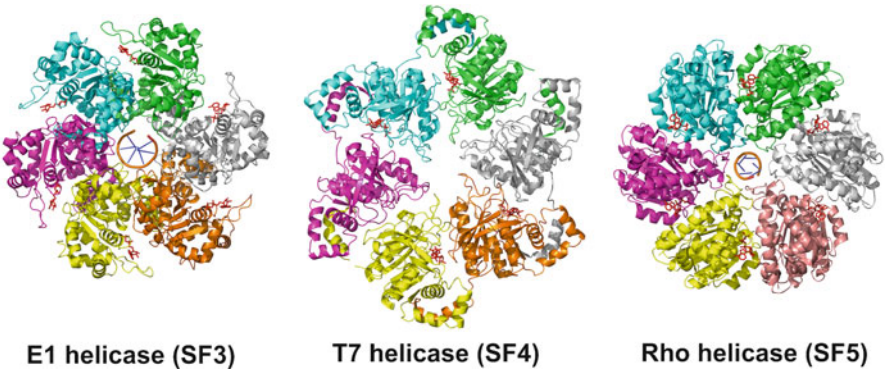

Fig. 4.4 The atomic structures of the crystallographic hexamers for representative member of the SF3–5 family. For the SF4 family we choose the hexameric crystal structure of the T7 helicase domain in an asymmetric configuration [33] (PDB code: 1E0J); for the SF5 family, the structure of the Rho hexamers in the presence of ADP•BeF_3 and ssRNA [3] (PDB code: 3ICE); for the E1 helicase, the crystal structure of the hexamer in the presence of ADP and ssDNA [2] (PDB code: 2GXA). No crystallographic model is available for an SF6 helicase in hexameric form. The nucleotide bound to the catalytic site is shown in *red* as ball-and-stick representation. Where available (Rho and E1) the nucleic acid bound to the central channel is shown

becomes a *trans*, rather than a *cis* residue (Fig. 4.3). A number of electron microscopy reconstructions, both of archaeal and eukaryotic MCM complexes, show a large degree of polymorphism [4, 63–67].

The Quaternary Structure

Although the basic ATPase ASCE fold is shared between RecA and AAA+ proteins, and the central β-sheet and the conserved motifs can be overlapped, the relative orientation of the fold within the hexamer is very different within the two classes of hexameric helicases, placing the substrate-binding channels in distinct orientation with respect to the basic fold [68] (Figs. 4.5 and 4.6).

More puzzling, a variety of stoichiometries and symmetries have been described for proteins belonging to the same superfamily, or even for the same protein. For example, the T7 helicase has been reported to form symmetric hexameric rings, distorted hexameric rings, heptameric rings, trimers of dimers and helical assemblies [30, 32–34, 69, 70]. The bacterial DnaB-like helicases have also been visualised as trimers, hexamers, distorted hexamers and dodecamers [5, 6, 38–41]. An even more striking example is provided by the archaeal MCM helicases, where single hexamers, single heptamers, double hexamers, double heptamers, open rings, as well as helical fibres have been observed by electron microscopy [4, 64–67, 71].

One obvious question is the functional relevance of the heptameric arrangements. For T7 helicase it has been shown that the heptameric ring is able to translocate

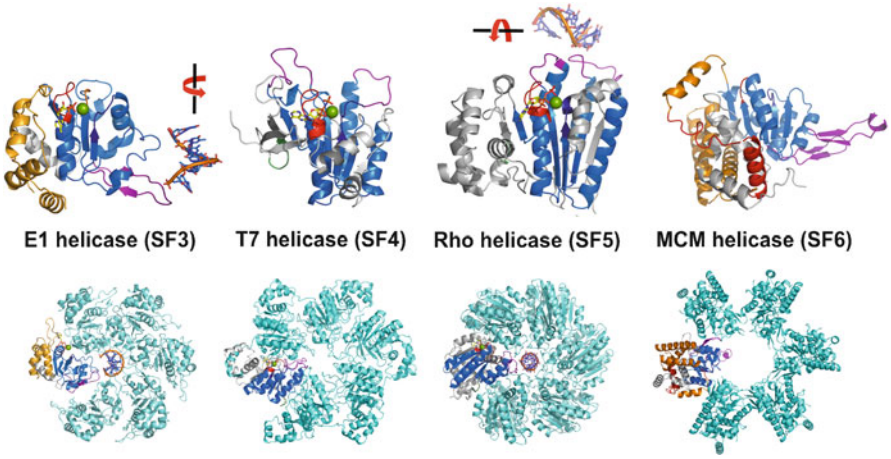

Fig. 4.5 Crystal structures of the monomers of members of the SF3–6 family. For SF3–5 the choice of crystal structure is the same as in Fig. 4.4. For the SF6 family we have built a hybrid model, with the overall framework based on the more accurate crystal structure of the *M. kandleri* MCM AAA+ domain [61] (PDB code: 38FT), and the functional elements (PS1BH, H2i) from the low resolution structure of the AAA+ domain from *S. sulfolobus* [62] (PDB code: 3F9V). All the monomers are rotated so that the ASCE core is in a similar orientation. The colour code is the same as in Fig. 4.2, showing in *blue* the secondary structure elements that are shared within the ASCE fold, in *red* the Walker A, in *dark blue* the Walker B, in *green* the arginine finger, in *orange* sensor I and sensor II motifs. The nucleotide bound to the ATP site is shown as ball-and-stick representation, with the carbon atoms in *yellow*; the Mg atom is a *light green* sphere. The nucleic acid binding loops are shown in *purple*. Both ssRNA (Rho) and ssDNA (E1) bind in a helical conformation. As expected from the very different positions of the DNA binding loops between RecA and AAA+ helicases, the nucleic acid binds in a very different location and the helical ssDNA/ssRNA axis (whose axis roughly coincides with the hexameric axis—shown by a *red arrow*) makes an angle of roughly 90° (see Fig. 4.6). Below each monomer is a representation of the hexamer, with a monomer highlighted, so as to visualise all the key element in their context. An approximate model of an MCM AAA+ hexamer has been built using the *M. kandleri* atomic coordinates of the AAA+, based on the hexameric arrangement of the N-terminal domain [75] (not shown)

along dsDNA but does not possess helicase activity [70]; in some cases the transition from hexameric to heptameric rings was nucleotide-dependent [65, 66, 70] or depended on the exact construct/mutant used [30, 72]. Invariably, protein–DNA complexes display hexameric symmetry [2, 3, 59, 65] strongly suggesting that the active helicase requires a hexameric assembly.

One possibility is that the heptameric rings may be in vitro artefacts. Alternatively, it has been suggested that the heptameric rings may represent intermediate states which have a role in loading or in dsDNA translocation [35, 48, 70, 73]. The most likely explanation however is that the existence heptameric rings is symptomatic of the ability of the subunit interface to assume diverse configurations, going from "open" to fully "closed", and may also reflect the ability of these proteins to assume an open-ring or lock-washer configuration [45, 74].

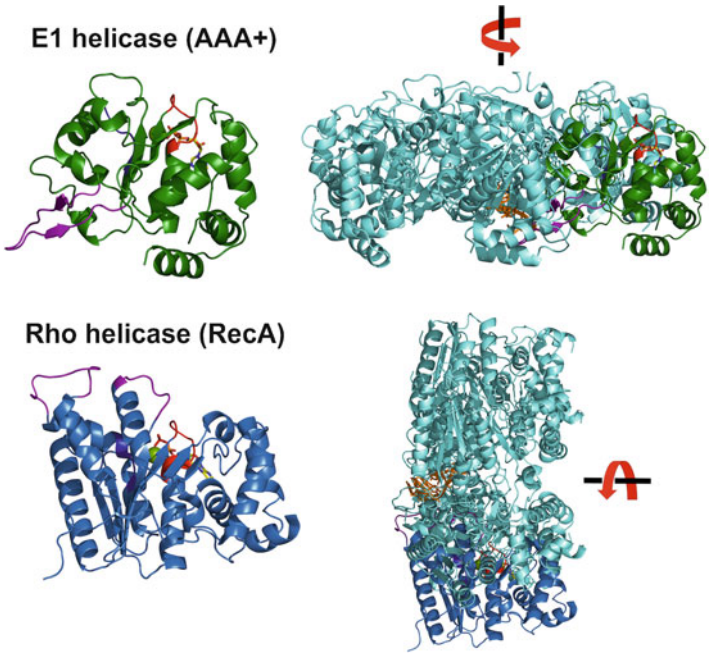

Fig. 4.6 Relative orientation of the AAA+ and RecA hexameric ring. A monomer of the E1 helicase [2] (PDB code: 2GXA) is shown in *green*, and below is a monomer of the Rho helicase [3] (PDB code: 3ICE, in *blue*), oriented so as to match the ASCE fold. On the *right side* of the picture are shown the full hexameric structures, with the single monomers highlighted in *green* and *blue*, respectively, and the nucleic acid substrate in *orange*. The plane of the rings is rotated of almost 90° (a the *black line with a arrow* shows the position of the pseudo-hexameric axes)

More contentious is the presence of double-ring arrangements. Double hexameric (and sometimes double heptameric) structures have been detected for a large number of hexameric helicases, including SV40 LTag, MCM helicases and DnaB-like helicases [7, 41, 64–66, 75, 76]. In some cases, notably for some SF3 helicases such as LTag and Rep, the proposed mechanism of action involve the double-ring structure [7]; in some systems, biochemical experiments trying to assess the physiological role of the double hexamers provided contradictory results [72, 77–79]. Here again, the evidence suggests that all these architectures are more likely to be involved in intermediate stages of the process (i.e. loading, DNA melting, etc.), whereas the active helicase is a single hexamer [2, 74].

The ATP-Binding Site

The main characteristic of helicases (and in general molecular motors) is to have an ATP-binding site wedged between two adjacent subunits/domains (Fig. 4.1). This architecture provides a way to amplify relatively small conformational changes

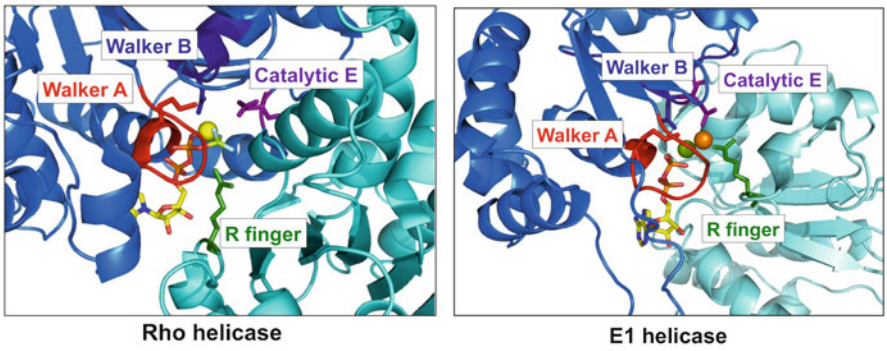

Fig. 4.7 The nucleotide-binding site. The ATP-binding site is shown for a RecA-like helicase [3] (Rho; PDB code: 3ICE) and an AAA+ helicase [2] (E1, PDB code: 2GXA). The site is located at the interface between two subunits, in *blue* and *cyan*, respectively. For the sake of clarity, only the most important motifs are shown. The *blue* subunit provides most of the nucleotide contacts, with the Walker A motif shown in *red* (with the critical lysine side chain shown), the Walker B in *dark blue* (with the conserved aspartate) and catalytic glutamate (in *purple*). The arginine finger (in *green*) is provided by the neighbouring subunit. The nucleotide bound to the ATP (ADP BeF_3 for Rho, and ADP for E1) site is shown as ball-and-stick representation, with the carbon atoms in *yellow*; the Mg atom is a *light green* sphere; in the crystal structure of E1 a chlorine ion (in *orange*) is supposed to take the place of the γ-phosphate

upon ATP binding and/or hydrolysis by changing the relative orientation of the subunits/domains. Binding of ATP and a divalent cation (Mg^{2+}) is achieved through a number of motifs that are conserved in most ASCE members (Walker A, Walker B, catalytic glutamate, arginine finger), as well as through motifs that are peculiar to each class (Fig. 4.7).

The Walker A and Walker B are essential sequence motifs common to all the P-loop proteins: the Walker A motif (GxxxxGK[S/T]) is located between strand 1 and helix H1 and is involved in positioning the triphosphate moiety of the NTP, while the Walker B motif (hhhhD) coordinates an Mg^{2+} ion. In ASCE proteins, a glutamate contributes to catalysis by priming a water molecule for the nucleophilic attack on the γ-phosphate of the NTP. Despite the conserved role and three-dimensional location, the catalytic glutamate does not necessarily come from the same secondary structure elements: in some families (most of the RecA-like proteins) it is located at the end of strand 2, whereas in others (such as the AAA+ proteins) it immediately follows the Walker B aspartate (hhhhD**E**). In addition to Walker A and B, most ASCE proteins carry a polar residue at the tip of strand 4, which appears to be required for sensing the triphosphate of the bound nucleotide and trigger the hydrolysis. For analogy with the nomenclature of the AAA+ ATPase, we use the name "sensor I".

A conserved arginine residue is often found adjacent to the ATP-binding site of the neighbouring subunit: in the hydrolysis-ready configuration it binds the ATP γ-phosphate, thus acting similarly to the arginine fingers of GTPase-activating proteins [80] and promoting inter-subunit cooperation upon hydrolysis. This ensures the crosstalk between subunit interfaces and ATP hydrolysis: the state of

the ATP-binding site affects the interface, but at the same time the details of the interface (which may depend on the interaction with the nucleic acid substrates and the fine tuning of the subunit interactions) affect the capacity of triggering ATP hydrolysis [2, 3].

AAA+ proteins are further characterised by a second conserved positive charge located on the α-helical domain, which is part of the sensor II motif, and interacts with the γ-phosphate of the adjacent ATP molecule [15]. Another general feature of AAA+ domains is the so-called glutamate switch: to ensure that ATP hydrolysis is activated only in the presence of the correct substrate (in the case of helicases, the nucleic acid), a polar residue (typically an asparagine) located at the end of strand 2 makes a hydrogen bond with the catalytic glutamate in the absence of the substrate, keeping it in an "off" conformation [20].

Mechanism of Action of Hexameric Helicases

Helicases are molecular engines that translocate along nucleic acid substrates using ATP (or, more generally, NTP) as a source of energy. They therefore need to transform the chemical energy of ATP hydrolysis into mechanical work so as to move unidirectionally along the DNA or RNA. An interesting analogy has been proposed between multimeric helicases and combustion engines [9], with each subunit acting as a single cylinder going through a continuous cycle of ATP binding (fuel injection), active site rearrangement (compression), hydrolysis (combustion) and product release (exhaust). The main questions are therefore how is the coupling between hydrolysis and movement achieved and how the subunits are coordinated.

A variety of mechanism has been suggested (Fig. 4.8). At one end of the spectrum there is a stochastic mechanism, where each subunit acts independently and no coordination exists between subunits. Although this has been proposed for an AAA+ ATPase such as ClpX protein unfoldase [81], there is no suggestion that it may apply to a helicase. Consistently, for most helicases ATP binding has been shown to be cooperative, and the presence of a small amount of inactive subunits to have a non-linear effect on the activity, confirming the presence of mechanisms of cross-communication between subunits [70, 82–84].

At the other end of the spectrum there is a fully concerted mechanism, where all six subunits bind and hydrolyse ATP in a synchronous way (Fig. 4.8). A crystallographic analysis of the SV40 LTag in three distinct nucleotide states (apo, ATP, ADP) revealed highly symmetrical structures, where all six subunits displayed identical conformation and nucleotide state [27]. An interesting feature of this system is that the position of the PS1BH hairpins correlates with the nucleotide state, so that in the presence of ATP the hairpins are at the top of the channel, and in the empty state at the bottom.

However, a growing body of evidence suggests that most helicases work through a sequential mechanism. The prototype of such scheme is the F1 ATP synthase/ATPase that shares a number of similarities (and a likely evolutionary link) with the SF4 helicases, and whose mode of action has been thoroughly dissected [17, 18].

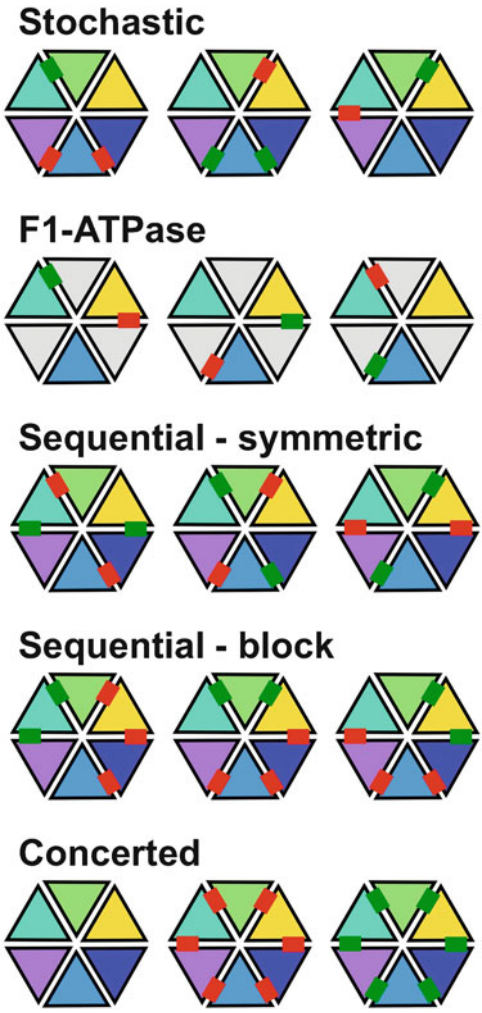

Fig. 4.8 A schematic diagram of the putative mechanisms for subunit coordination. Many mechanisms have been proposed for sequence of catalytic events around the hexameric ring, from a purely stochastic mechanisms, where each subunits randomly fires, without any communication with the neighbours, to a fully concerted mechanism, where all subunits bind and hydrolyse ATP in synch. Both structural and biochemical data seem to rather support sequential mechanisms of hydrolysis, where a "wave" of ATP binding, active site rearrangement, ATP hydrolysis and product release goes around the ring in an ordered manner. These mechanisms share some similarity with the ATP synthesis cycle of the F1 ATPase. There are various ways of conceiving a sequential mechanism, from a twofold symmetric model (as suggested for the T7 helicase [33]) to an asymmetric one [2]. The six subunit of hexameric helicases are coloured as in Fig. 4.1, while the non-catalytic β-subunit of F1-ATPase are shown in *grey*. A *red bar* indicates the ATP bound at the interface between subunits, and a *green bar* indicated ADP

The exact F1 scheme is not easily applicable to homo-hexamers, as the synthase has only three catalytic subunits, and therefore retains only three ATP sites out of six (Fig. 4.8). A conceptually similar mechanism, although with six, rather than three active sites, was proposed based on the crystal structure of the helicase domain of the bacteriophage T7 gp4 protein in the presence of the ATP analogue AMP-PNP [33]. The symmetry of the hexameric ring was broken, with two half rings having opposite spiral configurations. The six ATP sites showed three different configurations, ranging from empty, to ATP-like to ADP+Pi-like. The three configurations are then repeated by a crystallographic twofold axis, so that the sequence of sites around the hexameric ring would be empty/ATP/ADP+Pi/empty/ATP/ADP+Pi (Fig. 4.8, Sequential-symmetric). Remarkably, the ATP site configuration is correlated with the vertical position of the DNA-binding loops, so that the loops form two half spiral within the protein channel, providing a mechanism for the sequential translocation of an ssDNA molecule with a spiral conformation. The reorientation of the loops is not achieved through a hinge-like movement, but rather by the relative rotation of one subunit with respect to the neighbouring one by about 15° along an axis parallel to the plane of the ring.

More recently the crystal structures of two helicases have been determined in the presence of single-stranded nucleic acid, providing a clear picture of the translocation mechanism. The structure of E1 helicase, in the presence of ADP and ssDNA [2], shows a completely asymmetric arrangement, with different modes of nucleotide coordination along the ring, which appear to show a full cycle of hydrolysis around the ring. The interface between subunits and the detailed interactions made by each nucleotide vary along the ring: "ATP-like" sites are characterised by a well-ordered nucleotide with the exact positioning of all the motifs involved in catalysis (both *cis* and *trans*) and a tight subunit–subunit interface; "ADP-like" sites are less compact, while "apo-like" sites are characterised by a larger gap, and are either empty or with a nucleotide completely "disengaged" from the neighbouring subunit. Similarly to what observed in the T7 helicase, the vertical position of the DNA-binding hairpins are highly correlated with the nucleotide states, with a highest position for the ATP states, and a lowest one for the empty state. The hairpins are therefore arranged as a spiral staircase: the ssDNA bound to the central channel assumes a right-handed helical conformation with the 5′ end at the "top" that mirrors the hairpins' helical arrangement. This model strongly supports a sequential block scheme (Figs. 4.8 and 4.9) with a "coordinated escort" mechanism, so that the subunit that has just bound an ATP molecule moves up so as to grab a DNA phosphate; the sequential rearrangement of the active site and the ATP hydrolysis is correlated with the downward movement of the hairpin, which chaperones a DNA base towards the bottom of the ring; upon ADP and Pi release, the subunit is then free to bind a new ATP molecule, which brings the hairpin up again, ready to grab a new base and start a new cycle. In addition to the nucleotide state of the subunit, the position of the hairpin is also modulated by the interaction with the hairpins of the adjacent monomers, further highlighting the cooperativity within the ring [2, 9].

The crystal structure of the RNA helicase Rho, in a complex with ssRNA and ADP·BeF_3 shows a strikingly similar situation, with an analogous sequence of ATP-like,

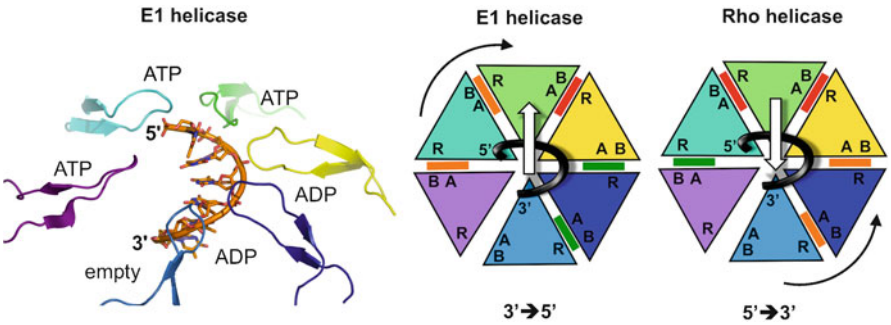

Fig. 4.9 Mechanism for directional translocation. *On the left* is a close up of the DNA-binding region of the E1 helicase [2] (PDB code: 2GXA): the PS1BH loops are shown in different colours, with the ssDNA in *orange*. The helicase moves along the DNA from the 3′ to the 5′ direction (i.e. the enzyme moves up, pushing the DNA towards the bottom). The nucleotide configuration found at the interface between the two subunits is schematically shown as "ATP", "ADP" and "empty". With the exception of the violet subunit, the other five loops form a spiral staircase that follow closely the pitch of the DNA helix, and is stabilised by a network of inter-loop interactions, suggesting a "coordinated escort" mechanism. After reaching the bottom upon ADP+Pi release, the subunit rebinds ATP and moves up again, ready to catch another DNA base: the violet subunit, disengaged from DNA, is probably on its way "up" to restart the cycle. As in the E1 helicase crystal two independent hexamers are present, with slightly different nucleotide configuration sequences, only the configuration of hexamer 1 is shown here. *On the right* is a schematic comparison between the crystal structures of E1 helicase bound to ssDNA, and Rho helicase bound to ssRNA [3] (PDB code: 3ICE). Single-stranded nucleic acid is shown as a *black spiral*, with the 5′ end coming up towards the viewer. *Orange bars* represent ATP molecules loosely bound, *red bars* the ATP after the correct rearrangement for hydrolysis (ATP*), *green bars* represent the ADP+Pi after hydrolysis has occurred. The *white arrow* represents the translocation of the protein ring along the nucleic acid; the *circular black arrow* indicates the sequence of events during ATP hydrolysis (i.e. ATP, ATP*, ADP+Pi, empty)

ADP-like and empty active sites, and a corresponding spiral staircase of the DNA-binding loops [3]. Rho binds the nucleic acid with the same orientation, but the subunits "fire" in the opposite order, therefore explaining the opposite polarity (Rho walks in the 5′ →3′ direction rather than in the 3′ →5′ direction as E1 [85]) (Fig. 4.9).

A General Mechanism?

The variety of biochemical and structural results obtained for different hexameric helicases raises the problem of how universal are the above results. The considerable similarity observed between the E1 and Rho appears highly significant for a number of reasons: Rho and E1 not only belong to different classes (SF5 vs. SF3), but are built around a different fold (RecA vs. AAA+, Fig. 4.3), with a very different architecture of the hexameric ring (Fig. 4.6), hydrolyse ATP with the assistance of an arginine finger emanating from a different region of the fold, translocate along different classes of nucleic acids (ssRNA vs. ssDNA) and bind their substrates with

loops emerging from different position within the ASCE fold (Fig. 4.6). Despite all these differences, the enzymes have converged towards an apparently similar mechanism of coupling ATP hydrolysis to nucleic acid translocation [2, 3] (Fig. 4.9), which strongly suggests that it may be a general model for hexameric helicase function.

The fact that other crystal and electron microscopy structures show other configurations and/or symmetries (from the perfect hexamers of SV40 LTag [27], to the trimeric/hexameric structures of DnaB helicase [5, 6, 38–41], to the helical or twofold symmetric structures of T7 helicases [32, 33]) can be explained in various ways. One argument is that the real functional state of the helicase is only achieved when bound to the nucleic acid substrate and to a nucleotide, whereas the more symmetric configurations can represent intermediate/alternative states before loading and/or activation of the enzymatic activity. The high sequence and structural similarity between E1 and LTag helicases suggest that the two proteins work with very similar mechanisms: it is therefore possible that upon binding an asymmetric substrate such as ssDNA the symmetric hexamer seen for LTag [27] may change conformation to act as a helicase.

There are also technical considerations that can explain the variety of structural biology results: electron microscopy reconstructions only provide low resolution pictures, are often obtained by imposing rotational symmetry and can therefore "mask" the true architecture of a slightly asymmetric multimeric protein. Indeed, not only biochemical data had suggested that T7 helicase binds ssDNA at a single monomer, but a careful analysis of the EM projection without symmetry applied confirms a small but significant variation from hexameric symmetry in the presence of the substrate [86]. Crystallisation may also be biased towards more symmetric arrangements, which are easier to pack within a three-dimensional lattice: if a mixture of symmetric and asymmetric states is present in solution, it is possible that the most symmetric are more prone to form well-ordered crystals, therefore shifting the equilibrium towards the most "regular" architecture.

However, there are a number of other considerations that need to be taken into account. Some biochemical results suggest that even in the presence of a sequential mechanism some system may have a higher degree of tolerance than other, compatible with a certain degree of disruption in some active sites [70, 83, 84]. Slippage of a hexameric ring has also been observed for the T7 helicase in single-molecule experiments [82], opening up the possibility that there may be competing processes at work, and bulk biochemical data may be not always suited to capture more complex behaviours [87]. In some cases it is not easy to reconcile the structural results with the biochemical data. For example, a biochemical study using nucleotide analogue interference mapping suggests that the Rho helicase contacts the RNA 2′ OH every seventh nucleotide [88], in contrast with the crystal structure [3] where every nucleotide appears to be actively escorted through the central channel. Moreover, the action of hexameric helicases is tightly regulated by the presence of accessory factors [51, 89, 90] and by the interaction of other proteins [31, 90–92], especially in the context of the replisome.

A combination of detailed biochemical analysis, high resolution structural studies and single-molecule approaches on multiple systems are therefore still needed to thoroughly dissect the mechanisms of action of these complex machines and to establish the similarities and peculiarities of the various hexameric helicase families.

References

1. Singleton MR, Dillingham MS, Wigley DB. Structure and mechanism of helicases and nucleic acid translocases. Annu Rev Biochem. 2007;76:23–50.
2. Enemark EJ, Joshua-Tor L. Mechanism of DNA translocation in a replicative hexameric helicase. Nature. 2006;442:270–5.
3. Thomsen ND, Berger JM. Running in reverse: the structural basis for translocation polarity in hexameric helicases. Cell. 2009;139:523–34.
4. Pape T, Meka H, Chen S, Vicentini G, van Heel M, Onesti S. Hexameric ring structure of the full-length archaeal MCM protein complex. EMBO Rep. 2003;4:1079–83.
5. Bailey S, Eliason WK, Steitz TA. Structure of hexameric DnaB helicase and its complex with a domain of DnaG primase. Science. 2007;318:459–63.
6. Lo YH, Tsai KL, Sun YJ, Chen WT, Huang CY, Hsiao CD. The crystal structure of a replicative hexameric helicase DnaC and its complex with single-stranded DNA. Nucleic Acids Res. 2009;37:804–14.
7. Li D, Zhao R, Lilyestrom W, Gai D, Zhang R, DeCaprio JA, et al. Structure of the replicative helicase of the oncoprotein SV40 large tumour antigen. Nature. 2003;423:512–8.
8. Takahashi TS, Wigley DB, Walter JC. Pumps, paradoxes and ploughshares: mechanism of the MCM2-7 DNA helicase. Trends Biochem Sci. 2005;30:437–44.
9. Enemark EJ, Joshua-Tor L. On helicases and other motor proteins. Curr Opin Struct Biol. 2008;18:243–57.
10. Fu YV, Yardimci H, Long DT, Ho TV, Guainazzi A, Bermudez VP, et al. Selective bypass of a lagging strand roadblock by the eukaryotic replicative DNA helicase. Cell. 2011;146:931–41.
11. Rabhi M, Tuma R, Boudvillain M. RNA remodeling by hexameric RNA helicases. RNA Biol. 2010;7:655–66.
12. Jankowsky E. RNA helicases at work: binding and rearranging. Trends Biochem Sci. 2011;36:19–29.
13. Leipe DD, Koonin EV, Aravind L. Evolution and classification of P-loop kinases and related proteins. J Mol Biol. 2003;333:781–815.
14. Iyer LM, Makarova KS, Koonin EV, Aravind L. Comparative genomics of the FtsK-HerA superfamily of pumping ATPases: implications for the origins of chromosome segregation, cell division and viral capsid packaging. Nucleic Acids Res. 2004;32:5260–79.
15. Erzberger JP, Berger JM. Evolutionary relationships and structural mechanisms of AAA+ proteins. Annu Rev Biophys Biomol Struct. 2006;35:93–114.
16. Abrahams JP, Leslie AG, Lutter R, Walker JE. Structure at 2.8 Å resolution of F1-ATPase from bovine heart mitochondria. Nature. 1994;370:621–8.
17. Boyer PD. The ATP synthase—a splendid molecular machine. Annu Rev Biochem. 1997;66:717–49.
18. Leslie AG, Abrahams JP, Braig K, Lutter R, Menz RI, Orriss GL, et al. The structure of bovine mitochondrial F1-ATPase: an example of rotary catalysis. Biochem Soc Trans. 1999;27:37–42.
19. Ogura T, Wilkinson AJ. AAA+ superfamily ATPases: common structure–diverse function. Genes Cells. 2001;6:575–97.
20. Zhang X, Wigley DB. The 'glutamate switch' provides a link between ATPase activity and ligand binding in AAA+ proteins. Nat Struct Mol Biol. 2008;15:1223–7.
21. Iyer LM, Leipe DD, Koonin EV, Aravind L. Evolutionary history and higher order classification of AAA+ ATPases. J Struct Biol. 2004;146:11–31.

22. Ammelburg M, Frickey T, Lupas AN. Classification of AAA+ proteins. J Struct Biol. 2006;156:2–11.
23. McGeoch AT, Trakselis MA, Laskey RA, Bell SD. Organization of the archaeal MCM complex on DNA and implications for the helicase mechanism. Nat Struct Mol Biol. 2005;12:756–62.
24. Jenkinson ER, Chong JP. Minichromosome maintenance helicase activity is controlled by N- and C-terminal motifs and requires the ATPase domain helix-2 insert. Proc Natl Acad Sci USA. 2006;103:7613–8.
25. Gorbalenya AE, Koonin EV. Helicases: amino acid sequence comparisons and structure–function relationship. Curr Opin Struct Biol. 1993;3:419–29.
26. Koonin EV. A common set of conserved motifs in a vast variety of putative nucleic acid-dependent ATPases including MCM proteins involved in the initiation of eukaryotic DNA replication. Nucleic Acids Res. 1993;21:2541–7.
27. Gai D, Zhao R, Li D, Finkielstein CV, Chen XS. Mechanisms of conformational change for a replicative hexameric helicase of SV40 large tumor antigen. Cell. 2004;119:47–60.
28. James JA, Escalante CR, Yoon-Robarts M, Edwards TA, Linden RM, Aggarwal AK. Crystal structure of the SF3 helicase from adeno-associated virus type 2. Structure. 2003;11:1025–35.
29. Moraes CT. A helicase is born. Nat Genet. 2001;28:200–1.
30. Toth EA, Li Y, Sawaya MR, Cheng Y, Ellenberger T. The crystal structure of the bifunctional primase-helicase of bacteriophage T7. Mol Cell. 2003;12:1113–23.
31. Corn JE, Berger JM. Regulation of bacterial priming and daughter strand synthesis through helicase-primase interactions. Nucleic Acids Res. 2006;34:4082–8.
32. Sawaya MR, Guo S, Tabor S, Richardson CC, Ellenberger T. Crystal structure of the helicase domain from the replicative helicase-primase of bacteriophage T7. Cell. 1999;99:167–77.
33. Singleton MR, Sawaya MR, Ellenberger T, Wigley DB. Crystal structure of T7 gene 4 ring helicase indicates a mechanism for sequential hydrolysis of nucleotides. Cell. 2000;101:589–600.
34. Egelman EH, Yu X, Wild R, Hingorani MM, Patel SS. Bacteriophage T7 helicase/primase proteins form rings around single-stranded DNA that suggest a general structure for hexameric helicases. Proc Natl Acad Sci USA 1995;92:3869–73.
35. Donmez I, Patel SS. Mechanisms of a ring shaped helicase. Nucleic Acids Res. 2006;34:4216–24.
36. LeBowitz JH, McMacken R. The Escherichia coli dnaB replication protein is a DNA helicase. J Biol Chem. 1986;261:4738–48.
37. Kaplan DL, O'Donnell M. DnaB drives DNA branch migration and dislodges proteins while encircling two DNA strands. Mol Cell. 2002;10:647–57.
38. Yang S, Yu X, VanLoock MS, Jezewska MJ, Bujalowski W, Egelman EH. Flexibility of the rings: structural asymmetry in the DnaB hexameric helicase. J Mol Biol. 2002;321:839–49.
39. San Martin MC, Stamford NP, Dammerova N, Dixon NE, Carazo JM. A structural model for the Escherichia coli DnaB helicase based on electron microscopy data. J Struct Biol. 1995;114:167–76.
40. Wang G, Klein MG, Tokonzaba E, Zhang Y, Holden LG, Chen XS. The structure of a DnaB-family replicative helicase and its interactions with primase. Nat Struct Mol Biol. 2008;15:94–100.
41. Stelter M, Gutsche I, Kapp U, Bazin A, Bajic G, Goret G, et al. Architecture of a dodecameric bacterial replicative helicase. Structure. 2012;20:554–64.
42. Leipe DD, Aravind L, Grishin NV, Koonin EV. The bacterial replicative helicase DnaB evolved from a RecA duplication. Genome Res. 2000;10:5–16.
43. Yu X, Horiguchi T, Shigesada K, Egelman EH. Three-dimensional reconstruction of transcription termination factor rho: orientation of the N-terminal domain and visualization of an RNA-binding site. J Mol Biol. 2000;299:1279–87.
44. Richardson JP. Loading Rho to terminate transcription. Cell. 2003;114:157–9.
45. Skordalakes E, Berger JM. Structure of the Rho transcription terminator: mechanism of mRNA recognition and helicase loading. Cell. 2003;114:135–46.
46. Skordalakes E, Berger JM. Structural insights into RNA-dependent ring closure and ATPase activation by the Rho termination factor. Cell. 2006;127:553–64.

47. Boudvillain M, Walmacq C, Schwartz A, Jacquinot F. Simple enzymatic assays for the in vitro motor activity of transcription termination factor Rho from Escherichia coli. Methods Mol Biol. 2010;587:137–54.
48. Costa A, Onesti S. Structural biology of MCM helicases. Crit Rev Biochem Mol Biol. 2009;44:326–42.
49. Boos D, Frigola J, Diffley JF. Activation of the replicative DNA helicase: breaking up is hard to do. Curr Opin Cell Biol. 2012;24:423–30.
50. Sakakibara N, Kelman LM, Kelman Z. Unwinding the structure and function of the archaeal MCM helicase. Mol Microbiol. 2009;72:286–96.
51. Ilves I, Petojevic T, Pesavento JJ, Botchan MR. Activation of the MCM2-7 helicase by association with Cdc45 and GINS proteins. Mol Cell. 2010;37:247–58.
52. West SC. Processing of recombination intermediates by the RuvABC proteins. Annu Rev Genet. 1997;31:213–44.
53. Berger JM. SnapShot: nucleic acid helicases and translocases. Cell. 2008;134: 888–888.e1
54. Jha S, Dutta A. RVB1/RVB2: running rings around molecular biology. Mol Cell. 2009;34:521–33.
55. Grigoletto A, Lestienne P, Rosenbaum J. The multifaceted proteins Reptin and Pontin as major players in cancer. Biochim Biophys Acta. 2011;1815:147–57.
56. Yamada K, Miyata T, Tsuchiya D, Oyama T, Fujiwara Y, Ohnishi T, et al. Crystal structure of the RuvA-RuvB complex: a structural basis for the Holliday junction migrating motor machinery. Mol Cell. 2002;10:671–81.
57. Yamada K, Kunishima N, Mayanagi K, Ohnishi T, Nishino T, Iwasaki H, et al. Crystal structure of the Holliday junction migration motor protein RuvB from Thermus thermophilus HB8. Proc Natl Acad Sci USA 2001;98:1442–7.
58. Putnam CD, Clancy SB, Tsuruta H, Gonzalez S, Wetmur JG, Tainer JA. Structure and mechanism of the RuvB Holliday junction branch migration motor. J Mol Biol. 2001;311:297–310.
59. Miyata T, Yamada K, Iwasaki H, Shinagawa H, Morikawa K, Mayanagi K. Two different oligomeric states of the RuvB branch migration motor protein as revealed by electron microscopy. J Struct Biol. 2000;13:83–9.
60. Chen YJ, Yu X, Egelman EH. The hexameric ring structure of the Escherichia coli RuvB branch migration protein. J Mol Biol. 2002;319:587–91.
61. Bae B, Chen YH, Costa A, Onesti S, Brunzelle JS, Lin Y, et al. Insights into the architecture of the replicative helicase from the structure of an archaeal MCM homolog. Structure. 2009;17:211–22.
62. Brewster AS, Wang G, Yu X, Greenleaf WB, Carazo JM, Tjajadi M, et al. Crystal structure of a near-full-length archaeal MCM: functional insights for an AAA+ hexameric helicase. Proc Natl Acad Sci USA 2008;105:20191–6.
63. Yu X, VanLoock MS, Poplawski A, Kelman Z, Xiang T, Tye BK, et al. The Methanobacterium thermoautotrophicum MCM protein can form heptameric rings. EMBO Rep. 2002;3:792–7.
64. Gómez-Llorente Y, Fletcher RJ, Chen XS, Carazo JM, San Martín C. Polymorphism and double hexamer structure in the archaeal minichromosome maintenance (MCM) helicase from Methanobacterium thermoautotrophicum. J Biol Chem. 2005;280:40909–15.
65. Costa A, Pape T, van Heel M, Brick P, Patwardhan A, Onesti S. Structural studies of the archaeal MCM complex in different functional states. J Struct Biol. 2006;156:210–9.
66. Costa A, Pape T, van Heel M, Brick P, Patwardhan A, Onesti S. Structural basis of the Methanothermobacter thermautotrophicus MCM helicase activity. Nucleic Acids Res. 2006;34:5829–38.
67. Costa A, van Duinen G, Medagli B, Chong J, Sakakibara N, Kelman Z, et al. Cryo-electron microscopy reveals a novel DNA-binding site on the MCM helicase. EMBO J. 2008;27:2250–8.
68. Wang J. Nucleotide-dependent domain motions within rings of the RecA/AAA(+) superfamily. J Struct Biol. 2004;148:259–67.
69. Yu X, Jezewska MJ, Bujalowski W, Egelman EH. The hexameric E. coli DnaB helicase can exist in different quaternary states. J Mol Biol. 1996;259:7–14.

70. Crampton DJ, Ohi M, Qimron U, Walz T, Richardson CC. Oligomeric states of bacteriophage T7 gene 4 primase/helicase. J Mol Biol. 2006;360:667–77.
71. Chen YJ, Yu X, Kasiviswanathan R, Shin JH, Kelman Z, Egelman EH. Structural polymorphism of Methanothermobacter thermautotrophicus MCM. J Mol Biol. 2005;346:389–94.
72. Jenkinson ER, Costa A, Leech AP, Patwardhan A, Onesti S, Chong JP. Mutations in subdomain B of the minichromosome maintenance (MCM) helicase affect DNA binding and modulate conformational transitions. J Biol Chem. 2009;284:5654–61.
73. Costa A, Onesti S. The MCM complex: (just) a replicative helicase? Biochem Soc Trans. 2008;36:136–40.
74. Costa A, Ilves I, Tamberg N, Petojevic T, Nogales E, Botchan MR, et al. The structural basis for MCM2-7 helicase activation by GINS and Cdc45. Nat Struct Mol Biol. 2011;18:471–7.
75. Fletcher RJ, Bishop BE, Leon RP, Sclafani RA, Ogata CM, Chen XS. The structure and function of MCM from archaeal M. thermoautotrophicum. Nat Struct Biol. 2003;10:160–7.
76. Remus D, Beuron F, Tolun G, Griffith JD, Morris EP, Diffley JF. Concerted loading of Mcm2-7 double hexamers around DNA during DNA replication origin licensing. Cell. 2009;139:719–30.
77. Smelkova NV, Borowiec JA. Dimerization of simian virus 40 T-antigen hexamers activates T-antigen DNA helicase activity. J Virol. 1997;71:8766–73.
78. Fletcher RJ, Shen J, Gómez-Llorente Y, Martín CS, Carazo JM, Chen XS. Double hexamer disruption and biochemical activities of Methanobacterium thermoautotrophicum MCM. J Biol Chem. 2005;280:42405–10.
79. Shin JH, Heo GY, Kelman Z. The Methanothermobacter thermautotrophicus MCM helicase is active as a hexameric ring. J Biol Chem. 2009;284:540–6.
80. Ahmadian MR, Stege P, Scheffzek K, Wittinghofer A. Confirmation of the arginine-finger hypothesis for the GAP-stimulated GTP-hydrolysis reaction of Ras. Nat Struct Biol. 1997;4:686–9.
81. Martin A, Baker TA, Sauer RT. Rebuilt AAA+ motors reveal operating principles for ATP-fuelled machines. Nature. 2005;437:1115–20.
82. Sun B, Johnson DS, Patel G, Smith BY, Pandey M, Patel SS, et al. ATP-induced helicase slippage reveals highly coordinated subunits. Nature. 2011;478:132–5.
83. Crampton DJ, Guo S, Johnson DE, Richardson CC. The arginine finger of bacteriophage T7 gene 4 helicase: role in energy coupling. Proc Natl Acad Sci USA 2004;101:4373–8.
84. Moreau MJ, McGeoch AT, Lowe AR, Itzhaki LS, Bell SD. ATPase site architecture and helicase mechanism of an archaeal MCM. Mol Cell. 2007;28:304–14.
85. Lyubimov AY, Strycharska M, Berger JM. The nuts and bolts of ring-translocase structure and mechanism. Curr Opin Struct Biol. 2011;21:240–8.
86. Yu X, Hingorani MM, Patel SS, Egelman EH. DNA is bound within the central hole to one or two of the six subunits of the T7 DNA helicase. Nat Struct Biol. 1996;3:740–3.
87. Hopfner KP, Michaelis J. Mechanisms of nucleic acid translocases: lessons from structural biology and single-molecule biophysics. Curr Opin Struct Biol. 2007;17:87–95.
88. Schwartz A, Rabhi M, Jacquinot F, Margeat E, Rahmouni AR, Boudvillain M. A stepwise 2′-hydroxyl activation mechanism for the bacterial transcription termination factor Rho helicase. Nat Struct Mol Biol. 2009;16:1309–16.
89. Kang YH, Galal WC, Farina A, Tappin I, Hurwitz J. Properties of the human Cdc45/Mcm2-7/GINS helicase complex and its action with DNA polymerase epsilon in rolling circle DNA synthesis. Proc Natl Acad Sci USA 2012;109:6042–7.
90. Zhou B, Arnett DR, Yu X, Brewster A, Sowd GA, Xie CL, et al. Structural basis for the interaction of a hexameric replicative helicase with the regulatory subunit of human DNA polymerase alpha-primase. J Biol Chem. 2012;387(32):26854–66.
91. Patel SS, Pandey M, Nandakumar D. Dynamic coupling between the motors of DNA replication: hexameric helicase, DNA polymerase, and primase. Curr Opin Chem Biol. 2011;15:595–605.
92. Manosas M, Spiering MM, Ding F, Croquette V, Benkovic SJ. Collaborative coupling between polymerase and helicase for leading-strand synthesis. Nucleic Acids Res. 2012;40(13):6187–98.

Chapter 5
Helicases at the Replication Fork

Peter McGlynn

Abstract Helicases are fundamental components of all replication complexes since unwinding of the double-stranded template to generate single-stranded DNA is essential to direct DNA synthesis by polymerases. However, helicases are also required in many other steps of DNA replication. Replicative helicases not only unwind the template DNA but also play key roles in regulating priming of DNA synthesis and coordination of leading and lagging strand DNA polymerases. Accessory helicases also aid replicative helicases in unwinding of the template strands in the presence of proteins bound to the DNA, minimising the risks posed by nucleoprotein complexes to continued fork movement. Helicases also play critical roles in Okazaki fragment processing in eukaryotes and may also be needed to minimise topological problems when replication forks converge. Thus fork movement, coordination of DNA synthesis, lagging strand maturation and termination of replication all depend on helicases. Moreover, if disaster strikes and a replication fork breaks down then reloading of the replication machinery is effected by helicases, at least in bacteria. This chapter describes how helicases function in these multiple steps at the fork and how DNA unwinding is coordinated with other catalytic processes to ensure efficient, high fidelity duplication of the genetic material in all organisms.

Introduction

A need for enzymes that unwind double-stranded DNA into two single strands is perhaps most apparent during the process of DNA replication. A requirement to expose the bases within each strand for use as templates for DNA polymerases

P. McGlynn (✉)
Department of Biology, University of York, York, Yorkshire, UK
e-mail: peter.mcglynn@york.ac.uk

M. Spies (ed.), *DNA Helicases and DNA Motor Proteins*, Advances in Experimental Medicine and Biology, DOI 10.1007/978-1-4614-5037-5_5,

means that the entire genome of every cell must be unwound during every cell cycle. One requirement of replicative helicases is therefore very high processivity, enabling a single replication initiation event to result in synthesis of many thousands, perhaps millions, of base pairs. The central role of replicative helicases in genome duplication is also reflected in their functioning as moving platforms for the association of other components of the replisome, facilitating coordination of the multiple catalytic processes that must occur during both leading and lagging strand synthesis at the fork. However, recent years have uncovered many additional functions for other helicases at the replication fork. These additional functions are still emerging but include helicases that aid strand separation within the context of protein-bound DNA, processing of Okazaki fragments, convergence of replication forks and targeting of stalled forks to facilitate the reinitiation of DNA replication. Multiple roles for different helicases also imply exquisite coordination of these catalytic activities at the replication fork, not only to ensure efficient movement of the fork during genome duplication but also to avoid unscheduled unwinding of strands that could result in potentially catastrophic genome instability. However, whilst much is known about how replicative helicase activity in bacteria and their viruses is controlled, there is little information available concerning how other helicases at the fork are coordinated.

This chapter describes helicases at the replication fork that are critical for completion of genome duplication, illustrating the central role played by helicases in all aspects of replication.

Replicative Helicases

Replicative helicases are most commonly hexameric, homohexameric in prokaryotes and heterohexameric in eukaryotes, forming a ring structure that encircles DNA (see Chap. 4) (Fig. 5.1). Nucleotide binding and hydrolysis occur at the interfaces between monomers and drives conformational changes within the subunits that results in movement of nucleic acid within the ring with respect to the subunits [1, 2]. The toroidal nature of replicative helicases has likely evolved to minimise the rate at which the helicase dissociates from the DNA, a key requirement during genome duplication given that the helicase has to translocate along many thousands of bases. However, it should be noted that the very high processivity required of a replicative helicase may not necessarily be conferred solely by a toroidal quaternary structure. The *Escherichia coli* replicative helicase, DnaB, can unwind ≈ 85 kbp in vitro within the context of the replisome [3–5] but in isolation DnaB has modest processivity [6]. Encirclement of the DNA strand might therefore be necessary but not sufficient to confer high processivity on replicative helicases. There might also be other advantages in replicative helicases having a hexameric ring structure. The disposition of DNA binding loops projecting into the central channel of replicative helicases suggests that there might be very little rotation of the helicase around the DNA strand, potentially reducing supercoiling problems during replication [7].

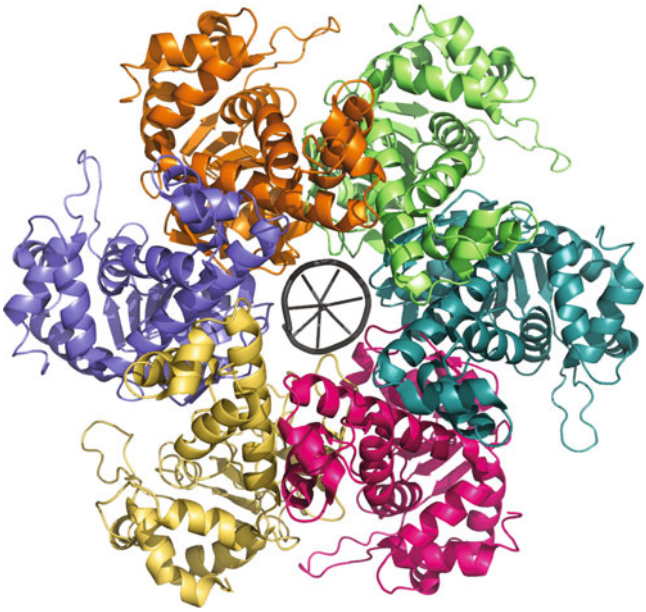

Fig. 5.1 Structure of the replicative helicase of papilloma virus (PDB ID: 2GXA). Six monomers, indicated by different colours, form a hexameric ring that encircles a single strand of DNA

Replicative helicases also act as platforms for assembly of other components of the replisome via multiple protein–protein interactions and having six subunits may facilitate organisation of the replisome. A clear example of this are the multiple primase molecules that interact with the bacterial replicative helicase DnaB in a cooperative manner to coordinate primer synthesis (see below).

Mechanisms of DNA Unwinding

The primary function of replicative helicases is to unwind duplex DNA to generate single-stranded templates for DNA polymerase. Chromosomal origins of replication require the assembly of two replication forks and hence two replicative polymerases must be loaded at each origin. Bacterial and bacteriophage replicative helicases are loaded onto ssDNA and translocate in the 5′–3′ direction [8] as does the human mitochondrial replicative helicase Twinkle [9]. The other DNA strand is excluded from the central cavity within the hexameric ring and so translocation 5′–3′ along the ssDNA results in unwinding of the parental dsDNA via a “steric exclusion” mechanism [10–15] (Fig. 5.2). However, whether this mechanism is active or passive is still the subject of debate and may also vary between different helicases (see Chap. 4).

Multiple different mechanisms have been suggested for unwinding by the eukaryotic nuclear and archaeal replicative helicases (the heterohexameric MCM2-7 and

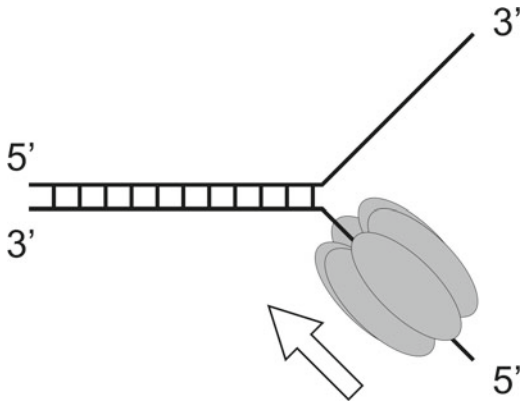

Fig. 5.2 Translocation 5′–3′ by bacterial and bacteriophage replicative helicases along the lagging strand template at a fork results in DNA unwinding since the second DNA strand is excluded from the hexameric ring

homohexameric MCM complexes, respectively). The MCM complex differs substantially at the structural level from bacterial and bacteriophage replicative helicases [1], a difference that is reflected in the 3′–5′ polarity of translocation of MCM complexes [16, 17], raising the possibility that steric exclusion is not necessarily a ubiquitous feature of replicative helicases. Moreover, the MCM complex belongs to a family of AAA+ hexameric helicases [18] that includes some members that may translocate along dsDNA rather than ssDNA [19] whilst the MCM complex itself interacts with dsDNA during initiation of replication [20, 21]. These suggestive findings led to models of MCM-catalysed unwinding that envisaged translocation along dsDNA rather than ssDNA [19]. However, an MCM sub-complex (a hexamer composed of only three of the six MCM subunits but which still forms a ring helicase) can unwind DNA by steric exclusion [22] whilst selective inhibition of *Xenopus* replication fork movement using DNA strand-specific blocks provides strong support for a steric exclusion mechanism of DNA unwinding by MCM2-7 within the context of the replisome [23]. It is likely therefore that most, if not all, hexameric helicases unwind DNA via steric exclusion. Variations on this general mechanism are emerging, though. The 5′ ssDNA arm displaced by the archaeal *Sulfolobus solfataricus* MCM complex wraps around a positively charged region on the outside of the MCM ring, an interaction that may facilitate DNA unwinding by prevention of reannealing of the ssDNA strands [24].

Although most if not all types of replicative helicase translocate along ssDNA and unwind dsDNA at the replication fork via steric exclusion, it is still also possible that dsDNA translocation by these helicases could have functions in vivo. Bacterial, bacteriophage and eukaryotic replicative helicases can translocate along duplex regions upon encountering a ssDNA/dsDNA junction [14, 25, 26] (Fig. 5.3). Such activity can displace proteins bound to duplex DNA and also drive branch migration of Holliday junctions in vitro [25] implying that replicative helicases may have multiple functions inside a cell in addition to the well-characterised role at the replication fork. However, loading of replicative helicases onto DNA is a tightly

Fig. 5.3 Hexameric replicative helicases can accommodate more than one DNA strand within the central cavity. Such helicases can therefore translocate over dsDNA if an ssDNA/dsDNA junction is encountered whilst translocating along ssDNA

regulated process in all organisms as this is a key step in the initiation of DNA replication. Moreover, there may be mechanisms to specifically inhibit translocation along dsDNA by replicative helicases. The helicase loader in *E. coli*, DnaC (see below), inhibits DnaB translocation along dsDNA but not ssDNA, raising doubts about whether this dsDNA translocation can occur in vivo [27]. Although these ring helicases can therefore catalyse a variety of unwinding/displacement reactions in vitro, their function is likely restricted to the replication fork in vivo.

Helicase Loading onto DNA

Encirclement of DNA within a ring helicase creates a requirement for some mechanism to load the ring onto the DNA and a remarkable variety of different mechanisms have evolved to accomplish this task. Loading of a ring helicase onto DNA could occur by opening of a pre-assembled hexamer to allow entry of DNA followed by ring closure. Alternatively, helicase monomers or other subassemblies could associate into a hexamer on the DNA. Both ring opening and ring assembly processes have been characterised and loading via either mechanism can occur with the assistance of accessory factors (assisted loading) or of accessory domains within subunits of the helicase (self-assisted loading) [28].

Loading of bacterial replicative helicases occurs via the initiator protein DnaA, a DNA sequence-specific binding protein that recognises the origin of replication *oriC* [29–31]. These initiators promote melting of dsDNA at *oriC* by ATP-dependent formation of DnaA oligomers that bind to and remodel the DNA backbone of one of the strands [32–34], aided by other factors that destabilise dsDNA such as negative supercoiling and nucleoid-associated proteins [35, 36]. Helicase loader proteins then facilitate the ATP-dependent loading of the replicative helicase onto the exposed ssDNA, either via ring opening or ring assembly mechanisms [28], although helicase loaders may not be employed by some bacteria such as *Helicobacter pylori* [37]. Loading of two DnaB hexamers, one on each exposed ssDNA, directs the assembly of other replisome components to form two replication forks that initiate bidirectional replication from *oriC* [38, 39].

Initiation of bacterial chromosomal replication occurs therefore upon loading of the replicative helicase onto ssDNA, with control of this process governed primarily via regulation of DnaA activity (reviewed in ref. [31]). In contrast, both

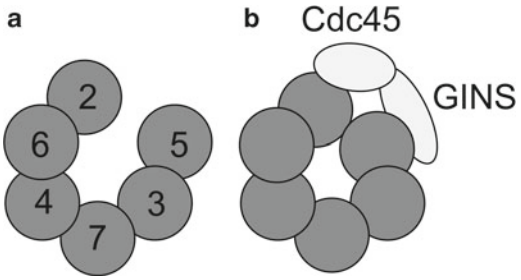

Fig. 5.4 The MCM2-7 complex forms a gapped ring structure (**a**) but the gap is closed upon interaction with Cdc45, GINS and ATP (**b**). This closed ring has two cavities that have each been proposed to accommodate a single DNA strand. The *numbers* in (**a**) indicate the identities of each MCM subunit

helicase loading and subsequent assembly of a competent replication fork are tightly regulated processes in eukaryotes. The MCM2-7 complex is loaded initially as a catalytically inactive double hexamer around dsDNA via the concerted action of the origin recognition complex (ORC), Cdc6 and Cdt1 in an ATP-dependent process during late M and G1 phases [20, 21, 40]. This initial loading step is regulated via inhibition by cyclin-dependent kinase-dependent and -independent mechanisms to ensure loading occurs only at the end of mitosis and during G1 [41]. Upon entry into S-phase these inactive MCM2-7 complexes become activated via phosphorylation and also by recruitment of Cdc45 and the GINS tetramer to form the CMG helicase complex [17, 42], an association that is also regulated by kinase activity [41, 43]. The two helicases then dissociate and translocate away from the origin to form two independent replisomes [44]. This CMG complex is likely the functional form of the 3′–5′ helicase that drives template DNA unwinding within the replisome progression complex (RPC) [45–47] since, although MCM2-7 by itself is an active helicase [48], the CMG complex is a considerably more robust helicase [46]. This activation depends at least in part on the ability of GINS and Cdc45, together with ATP binding, to promote closure of a gap in the MCM2-7 ring [49] (Fig. 5.4). This gap in the ring may be critical in initial assembly of the MCM double hexamer onto dsDNA, allowing dsDNA to enter into the MCM ring, but bridging this gap by Cdc45 and GINS implies that closure facilitates unwinding [48, 49]. Conversion of the single large pore within MCM2-7 into two smaller pores within the CMG complex, together with the inability of the CMG complex to bind dsDNA [20, 21, 46], is also consistent with a model in which dsDNA within MCM2-7 is destabilised upon association of Cdc45 and GINS, with the two single strands partitioned in the two different pores within CMG [49] (Fig. 5.4b). Such a model implies that there are two modes of unwinding via steric exclusion, one in which one of the DNA strands is completely excluded from the replicative helicase ring (bacteria and bacteriophage) and one in which both DNA strands remain within the helicase complex but are segregated into two different channels (eukaryotes and archaea).

Links Between Replicative Helicases and DNA Polymerases

Physical and functional coupling between DNA polymerases and replicative helicases is critical for observed rates of DNA synthesis. At the *E. coli* replication fork the τ subunit of the clamp loader complex interacts physically with both the replicative helicase and DNA polymerase, facilitating rapid fork movement [50–52]. In the absence of the τ-DnaB interaction the polymerase follows the helicase at the slow rate of unwinding displayed by the helicase alone [50]. Physical and functional interactions between DNA polymerase and the replicative helicase are a conserved feature in replisomes in bacteriophages [53–57] and in mitochondria [58]. Moreover, interaction of the helicase and polymerases at replication forks results not only in accelerated fork movement but also in enhanced processivity of DNA synthesis in bacteria, bacteriophages and mitochondria [58–60].

Interaction between the replicative helicase and DNA polymerase may also be a feature of eukaryotic forks within the nucleus, with the leading strand polymerase associating with the GINS complex [61, 62], although whether such physical interactions result in functional coupling remains unclear. Indeed, the 3′–5′ polarity of the eukaryotic replicative helicase means that the leading strand DNA polymerase and helicase translocate along the same DNA strand at the fork, in contrast to bacterial, bacteriophage and mitochondrial replication forks. It is unlikely therefore that any functional coupling between the replicative helicase and leading strand DNA polymerase at eukaryotic forks in the nucleus would occur by the same mechanism(s) operative at forks where the replicative helicase translocates along the lagging strand template.

Increasing numbers of protein–DNA contacts within a complex provide a simple explanation of enhanced processivities via coupling of replicative helicases and polymerases at forks. However, the basis of accelerated rates of replication fork movement is less clear. DNA synthesis has been shown to be the means by which the replicative helicase within the bacteriophage T7 replication fork is accelerated tenfold, probably by prevention of reannealing of ssDNA at the fork by DNA synthesis [56]. Such a mechanism implies that the helicase undergoes slippage during unwinding resulting in backwards sliding of the helicase along ssDNA and subsequent reannealing of DNA at the fork if leading strand DNA synthesis is not ongoing [56, 63]. However, whether such slippage occurs sufficiently frequently to account for polymerase-directed stimulation of fork movement is not clear.

Coupling of helicase and polymerase activities is also critical for lagging strand DNA synthesis. The lagging strand DNA polymerase in *E. coli* is, like the leading strand polymerase, connected to the replicative helicase via one of the three τ subunits within the clamp loader [51, 64–66]. This coupling of two DNA polymerases and helicase ensures coupling of leading and lagging strand synthesis at the fork, facilitating rapid, complete duplication of both parental strands and minimisation of the amount of ssDNA exposed at any one time. Coupling leading and lagging strand synthesis is a conserved feature of genome duplication, although different organisms display variations on this theme. For example, the two bacteriophage T4 polymerases

not only interact indirectly with the helicase via the gp59 helicase loader but are also covalently linked together at the fork via two cysteine residues [57].

Links Between Replicative Helicases and Primases

Interaction between the replicative helicase and a specialised RNA polymerase, primase, is also critical for DNA synthesis since DNA polymerases cannot initiate polymerisation de novo. Synthesis of short RNA primers must occur at origins of replication to initiate leading strand synthesis and subsequently at moving forks to continually re-prime lagging strand DNA synthesis. Association of primase with DnaB in *E. coli* is also critical in the re-priming of leading strand synthesis downstream of polymerase-blocking lesions to allow fork movement to continue along a damaged template [67]. Helicase–primase interactions ensure primer synthesis occurs within the vicinity of the replisome, with bacterial and bacteriophage primases acting on the lagging strand template along which the replicative helicase also translocates. In contrast, eukaryotic/archaeal primases must operate on the strand opposite the replicative helicase since the MCM complex translocates along the leading strand template. Association of primase with helicase occurs via relatively unstable noncovalent interactions in *E. coli* [68–70], via stable noncovalent interactions in *Bacillus stearothermophilus* and bacteriophage T4 [71–73] and also by the presence of both helicase and primase domains within a single protein in bacteriophage T7 [74]. The archaeal and eukaryotic primase complexes also form a relatively stable non-covalent interaction with GINS within the CMG replicative helicase complex [75, 76]. Thus, even though helicase and primase act on different template strands at the archaeal/eukaryotic fork, the helicase–primase interaction is conserved.

Multiple primases can associate with the replicative helicase regardless of whether these activities associate covalently or non-covalently [71, 77, 78]. Primase associates with the trailing face of the helicase ring in bacteria and bacteriophage to direct priming activity at the ssDNA emerging from the rear of the helicase [74, 79] (Fig. 5.5). The relative disposition of helicase and primase in archaea and eukaryotes is not clear but is likely to differ from that found in bacteria since priming occurs on the strand along which the replicative helicase does not translocate along.

Primase/replicative helicase interactions may also modulate the functions of both enzymes. Primase–helicase interactions can activate both the ATPase and unwinding activities of the bacterial replicative helicase [71] and also stimulate primase activity, the length of primers synthesised and primase initiation specificity [68, 80, 81]. How primase stimulates replicative helicase activity in bacteria and bacteriophage is unclear but binding of primase to DnaB might stabilise the DnaB hexamer, thus activating helicase function [79]. Activation of bacterial/phage primase activity may occur simply by increasing the local concentration of primase at the fork but interaction of multiple primases with the helicase may also increase cooperativity between primase monomers (reviewed in ref. [78]). Localisation of primases to the replicative helicase may therefore ensure that primase-directed initiation of DNA synthesis occurs only at the replication fork, minimising the chance of unprogrammed

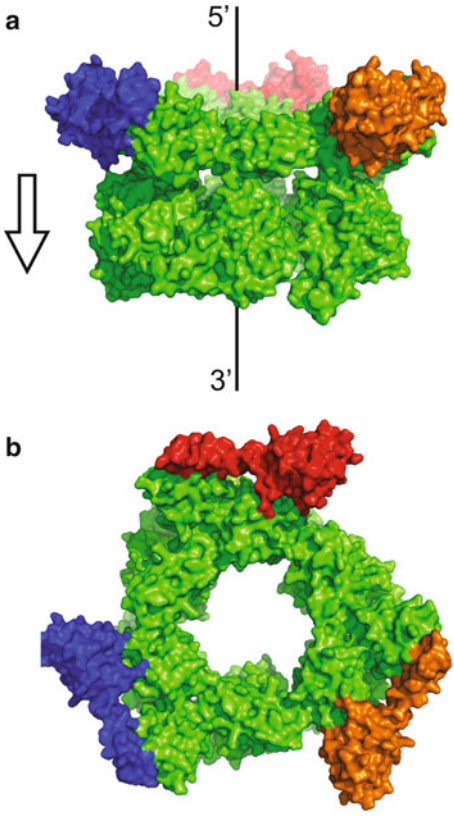

Fig. 5.5 Structure of the *Bacillus stearothermophilus* DnaB hexameric ring (*green*) in complex with three monomers of the helicase binding domain of DnaG (*red*, *blue* and *orange*) (PDB ID 2R6C). (**a**) Side view of the DnaB–DnaG complex illustrating interaction of the primase domains with the N-terminus of DnaB. The 5′–3′ polarity of translocation of DnaB is indicated. (**b**) View of the N-terminal face of the DnaB hexamer in complex with the helicase binding domains of three DnaG monomers

initiation of replication at other stretches of ssDNA within the genome [82]. The impact of the helicase–primase interaction on enzyme function is less clear in archaea and eukaryotes but, given the opposite polarities of replicative helicases at the fork in eukaryotes vs. bacteria, any modulation of eukaryotic/archaeal helicase and primase functions via this interaction may differ mechanistically to the bacterial/phage systems.

Accessory Replicative Helicases

Hexameric replicative helicases drive strand separation at the replication fork and act as organising platforms for other catalytic functions within the replisome. However, the substrate for replicative helicases is protein-coated rather than naked DNA and nucleoprotein complexes, especially those associated with transcription, pose barriers to unwinding by helicases [83–86]. Blockage of the replicative helicase results in stalling of the replication fork which can lead to incomplete genome

duplication or to genome rearrangements initiated by processing of the stalled fork [87, 88]. Adjacent origin firing in eukaryotes, an option not available in bacteria, might be able to rescue forks stalled at nucleoprotein barriers [89, 90]. However, evidence is accumulating that nucleoprotein complexes present replicative barriers even in mammals [91–93] indicating that multiple origins cannot fully address the dangers of replicating protein-bound DNA.

Although protein–DNA complexes present barriers to unwinding by helicases, multiple helicases can cooperate functionally to minimise the inhibitory effects of nucleoprotein complexes on DNA unwinding [94]. However, the necessity to tightly control the loading of replicative helicases onto DNA means that there is no mechanism to load multiple replicative helicases at the fork in order to aid protein displacement. One solution to blockage of the replicative helicase would be to employ other types of helicase at the fork that could aid protein displacement [83, 95] without acting as initiators of replisome assembly, thus avoiding the problem of unprogrammed replication initiation. Such accessory replicative helicases have been identified. The *E. coli* 3′–5′ Superfamily 1 helicase Rep can promote fork movement along protein-bound DNA in vitro and in vivo [96, 97], an activity that depends on physical interaction with the replicative helicase DnaB [96, 98, 99]. The interaction of Rep and DnaB, 3′–5′ and 5′–3′ helicases respectively, also results in cooperative unwinding of dsDNA in the absence of other replisome components [96]. This Rep accessory helicase activity is critical for the maintenance of genome stability [100, 101] and for wild type rates of genome duplication [98, 102]. Interaction with hexameric DnaB creates the potential for up to six monomers of Rep to be located at the replisome, although the stoichiometry of the Rep–DnaB interaction is unknown. If more than one Rep monomer does associate with DnaB then this may provide functional cooperativity with the opportunity for multiple Rep monomers translocating 3′–5′ along the leading strand template to aid protein displacement ahead of the fork. Rep also has low processivity [103] which would limit translocation by Rep ahead of the fork, ensuring that extensive unwinding of parental DNA does not occur ahead of the replisome. Two other *E. coli* helicases, UvrD and DinG, have also been implicated as accessory replicative helicases [97]. However, UvrD, a 3′–5′ Superfamily 1 helicase homologous to Rep, is likely only to act as an accessory helicase in the absence of Rep by virtue of its high intracellular concentration [96]. DinG, a 5′–3′ Superfamily 2 helicase, plays a critical role in fork movement through highly transcribed operons [97] but physical association with ribosomes suggests an indirect role in removal of replicative barriers [104].

Saccharomyces cerevisiae Rrm3, a 5′–3′ Superfamily 1 helicase, also promotes fork movement through non-histone protein–DNA complexes [105, 106], an activity that contributes to the maintenance of genome stability [107–109]. Rrm3 also localises to the replisome via an interaction with the leading strand DNA polymerase [110] and/or PCNA [111] although whether such colocalisation is critical for Rrm3 function is unknown. Accessory replicative helicases in bacteria and lower eukaryotes are therefore Superfamily 1 helicases that translocate along

ssDNA and localise to the replisome. Moreover, the primary and accessory replicative helicases translocate along opposing template strands at the fork in both systems. Whether this disposition of helicases at the fork is a universal feature must await identification of accessory helicases in other organisms. However, translocation along opposing template strands might provide a mechanism for functional cooperativity between the two types of helicase during protein displacement [96, 99].

Okazaki Fragment Processing

Discontinuous lagging strand synthesis creates a requirement for RNA primer excision, gap filling and ligation. This processing in bacteria is not thought to require helicase activity since the 5′–3′ exonuclease activity of DNA polymerase I can efficiently remove RNA from a downstream Okazaki fragment whilst simultaneously extending the 3′ end of the upstream fragment, leaving a ligatable nick between the two strands (Fig. 5.6a). However, UvrD helicase and other nucleotide excision repair proteins in *E. coli* can provide an alternative Okazaki fragment processing system if the normal DNA polymerase I-dependent pathway is absent [112]. This alternative pathway may involve UvrAB-dependent recognition of strand discontinuities between Okazaki fragments followed by directed loading of UvrD onto the template strand [112, 113]. The 3′–5′ helicase activity of UvrD could then displace the 5′ end of the downstream Okazaki fragment to promote removal of the RNA primer by unidentified nucleases and subsequent gap filling by DNA polymerases (Fig. 5.6b).

Okazaki fragment maturation in eukaryotes differs substantially from bacteria since there is no DNA polymerase with a 5′–3′ exonuclease activity equivalent to that of bacterial DNA polymerase I. Eukaryotes employ two pathways to process Okazaki fragments. One pathway relies on coupled extension of the upstream DNA strand and displacement of the 5′ end of the downstream Okazaki fragment by the lagging strand DNA polymerase δ followed by targeting of the resultant short flaps by FEN1 nuclease resulting in a ligatable nick between the two Okazaki fragments [114] (Fig. 5.7). However, if flaps longer than 25–30 nucleotides are generated then binding of the flap by single-strand binding protein RPA inhibits FEN1 cleavage [115]. In such circumstances Dna2, a 5′–3′ Superfamily 2 helicase that also possesses endonuclease activity, binds to the free 5′ ssDNA end of the flap and translocates towards the base of the flap [116–118]. This translocation displaces RPA and is coupled to repeated RPA-stimulated cleavage of the ssDNA by Dna2 to leave a short 5–10 nucleotide flap [119] (Fig. 5.7). RPA cannot bind such short regions of ssDNA and so FEN1 cleavage can now occur to generate a nick that can be ligated. Efficient Okazaki fragment processing requires therefore the combined activities of a flap endonuclease and a helicase/endonuclease with coordination of this processing likely depending on interactions between Dna2 and FEN1, Polδ and RPA.

A second helicase is also implicated in eukaryotic Okazaki fragment processing. The lethality associated with absence of Dna2 in *S. cerevisiae* can be suppressed by

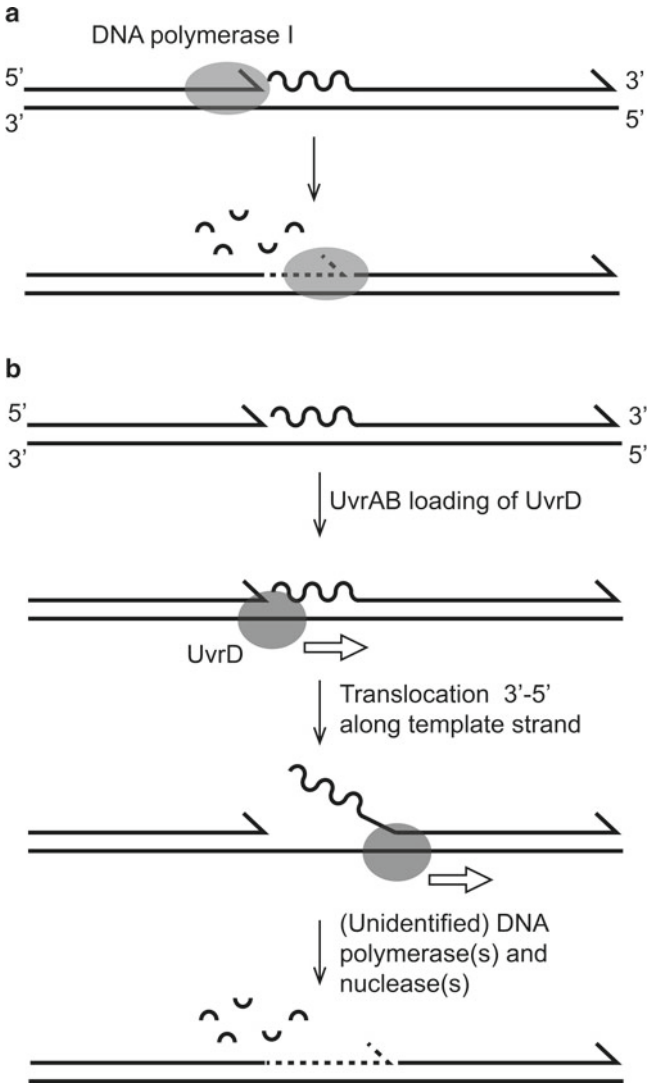

Fig. 5.6 Okazaki fragment processing in *Escherichia coli*. (**a**) In wild type cells DNA polymerase I degrades the RNA primer (a *wavy line*) via a 5′–3′ exonuclease activity and simultaneously extends the 3′ end of the upstream lagging strand to generate a nicked duplex that can be sealed by DNA ligase. (**b**) In the absence of DNA polymerase I cells might survive by UvrAB-directed loading of UvrD helicase at strand discontinuities between adjacent Okazaki fragments and subsequent unwinding of the 5′ end of the downstream Okazaki fragment. Degradation of the flap and DNA synthesis would then result in generation of a nicked duplex that could be sealed by DNA ligase

deletion of another helicase *pif1* [120]. This suppression implies that Pif1, a 5′–3′ Superfamily 1 helicase with homology to Rrm3 [121, 122], generates long flaps during Okazaki fragment processing by translocating 5′–3′ from the ends of short

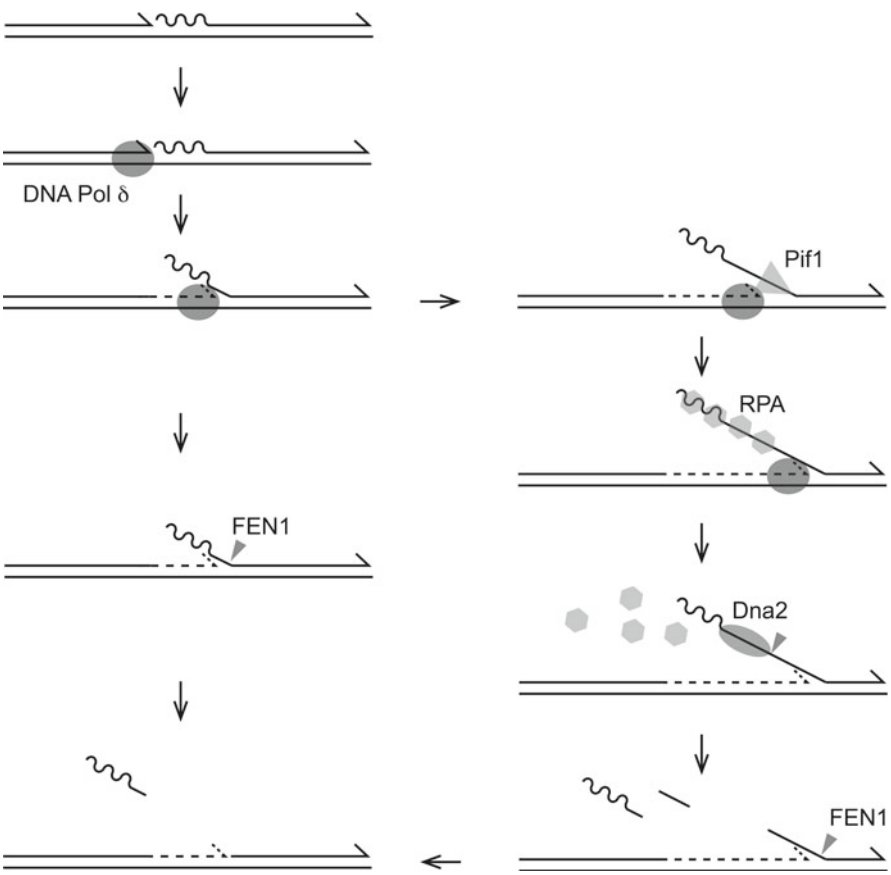

Fig. 5.7 Okazaki fragment processing in eukaryotes. DNA synthesis and strand displacement by DNA polymerase δ generate a short RNA/DNA flap that can be cleaved by FEN1 endonuclease resulting in removal of the RNA primer and generation of a nicked duplex. However, Pif1 helicase may target some flaps created by DNA polymerase δ to generate a longer ssRNA/DNA region that can be bound by the single-strand binding protein RPA. RPA inhibits cleavage by FEN1, necessitating targeting of the flap by Dna2. The helicase activity of Dna2 displaces RPA whilst the endonucleolytic activity cleaves the ssDNA to leave a short flap that can now be cleaved by FEN1

flaps created by Polδ [123, 124] (Fig. 5.7). Thus Dna2 may be required to counter the deleterious effects of Pif1 activity, a helicase that has multiple roles in both the nucleus and mitochondria (reviewed in ref. [122]). However, Pif1 might also have a positive role in Okazaki fragment processing. This positive function is currently unclear but could be to unwind secondary structures within the 5′ flap that might inhibit both Dna2 and FEN1 [125]. The high specific activity of Pif1 in unwinding G-quadruplex (G4) structures [126, 127], four-stranded structures formed by Hoogsteen G–G base pairs, and the physical association and functional linkage between Pif1 and G4 sites in *S. cerevisiae* [128] support a potential role for Pif1 in resolving G4 structures during Okazaki fragment maturation. However, the exact context in which Pif1 might resolve G4 structures is still unknown.

Fork Convergence

All cells contain topoisomerases to relieve the positive supercoiling generated by parental DNA unwinding during replication. Converging forks present a particular topological challenge since as the length of DNA separating the two forks decreases, the probability of type II topoisomerases (that cleave both strands within a duplex) binding to this region decreases, inhibiting resolution of positive supercoils between the forks. One resolution mechanism could involve a type I topoisomerase (that cleaves single DNA strands) acting on ssDNA on the lagging strand template thus bypassing any need for targeting of the parental duplex sandwiched between two converging forks [129]. Alternatively, helicase-catalysed unwinding of the parental strands between converging forks followed by topoisomerase I-directed unlinking of the resultant single strands could allow fork convergence to go to completion [130]. Biochemical and genetic evidence indicates that a type I topoisomerase in *E. coli*, topoisomerase III, cooperates with a 3′–5′ Superfamily 2 helicase, RecQ, in resolving converging forks via this second resolution mechanism [131, 132]. Although RecQ and topo III do not interact physically, both proteins interact with the acidic C terminus of SSB [133, 134] and these interactions are critical for resolution of converging forks [131]. RecQ family helicases are ubiquitous and play critical roles in genome maintenance in bacteria and eukaryotes (see Chap. 8). The functions of eukaryotic RecQ helicases are also linked to type I topoisomerases and single-stranded DNA binding proteins (Chap. 8) whilst in hyperthermophiles a RecQ-like helicase domain and a type I topoisomerase domain are found within the same polypeptide [135], indicating a conserved linkage between these different enzyme activities. However, whether this helicase–topoisomerase combination promotes fork convergence in organisms other than bacteria is unclear.

Replisome Reloading

Although replisomes have high processivity, there are many potential barriers such as DNA lesions and nucleoprotein complexes encountered in vivo that can halt replisome progression [136]. If halted, replication must be restarted to complete chromosome duplication and avoid genome instability. Many halted replisomes might simply pause before continuing, thus avoiding any need to reload replication enzymes onto the chromosome. For example, DNA lesions can be bypassed by re-priming DNA synthesis downstream of the lesion regardless of whether the damage is in the leading or lagging strand template [67, 137–139] whilst protein–DNA barriers can be cleared by accessory replicative helicases to allow resumption of replication by the original replisome (see above). However, bypass of lesions on the leading strand template is not 100 % efficient [67] whilst nucleoprotein barriers such as arrays of stalled RNA polymerases on highly transcribed genes [140] may present long-lived

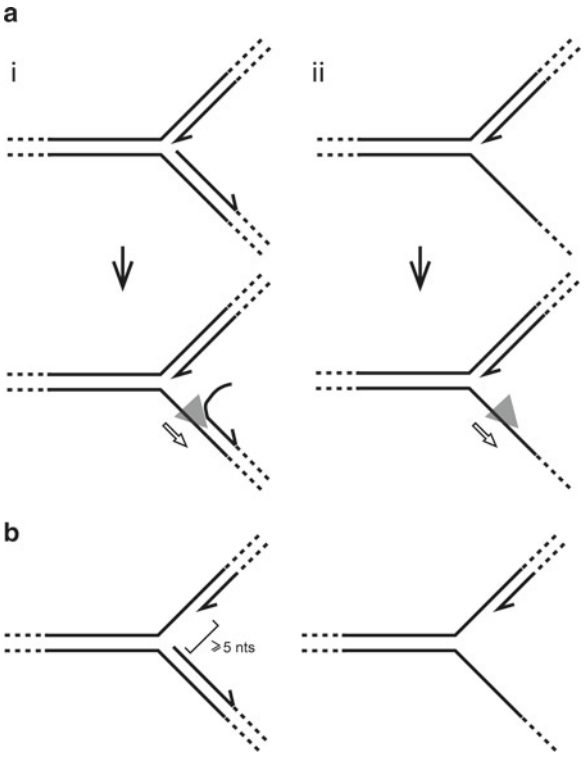

Fig. 5.8 (**a**) High affinity forked DNA substrates for PriA helicase in which the 3′ OH group of the leading strand is located near the branch point. PriA helicase translocates 3′–5′ along the lagging strand template upon binding to such forks resulting in unwinding of any lagging strand DNA present near the branch point. Note that it is currently not known whether PriA maintains contact with the branch point whilst simultaneously translocating along the lagging strand template. (**b**) Forked substrates bound with high affinity by PriC

barriers that outlast the functional lifetime of a blocked replisome [141, 142]. Mechanisms that reassemble replisomes back onto chromosomes but away from normal origins of replication are therefore required [143, 144]. This reloading can occur at stalled forks that have been processed by enzymes such as helicases and nucleases but can also occur at D-loop recombination intermediates generated by strand exchange after processing of stalled forks [88] (see also Chap. 9).

Mechanisms that facilitate fork restart away from normal origins exist in lower and higher eukaryotes [144, 145] but the means by which replisome components in eukaryotes are reassembled onto DNA is not known. In certain contexts, eukaryotic replisomes might only partially disassemble upon blockage [146]. Multiple mechanisms might therefore exist in eukaryotes to effect reloading of different subsets of replisome proteins depending upon the nature of the initial block. In contrast, fork restart mechanisms in bacteria result ultimately in reloading of the replicative helicase DnaB onto ssDNA [147, 148], implying that bacterial replisomes do not partially dissociate but require a complete rebuild. DnaB reloading is achieved by two mechanisms in *E. coli*, each of which preferentially targets a different set of forked DNA substrates. PriA is a 3′–5′ Superfamily 2 helicase [149, 150] that preferentially binds to forked DNA possessing a leading strand 3′ OH less than six nucleotides from the branch point [151–154] with the orientation of binding directing PriA translocation along the lagging strand template [147, 155] (Fig. 5.8a). PriA

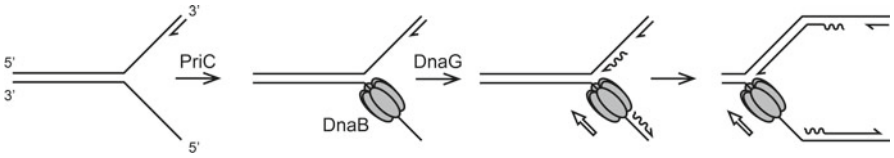

Fig. 5.9 PriC-directed loading of DnaB onto forks without a leading strand 3′ OH group near the branch point results in priming of both leading and lagging strand DNA synthesis upon association of DnaG with DnaB at the fork. For clarity only DnaB is illustrated

also interacts physically with the acidic C-terminus of SSB, an interaction that localises PriA to structures containing ssDNA such as forks and recombination intermediates and stimulates PriA helicase activity [156, 157]. Initial binding of PriA to DNA exposes a binding site on PriA for PriB, a dimeric ssDNA binding protein, allowing PriB binding both to PriA and to single-stranded lagging strand template [158–162]. This ssDNA is already present at D-loop recombination intermediates and may be present at stalled forks but the helicase activity of PriA can also unwind any nascent lagging strand present to expose ssDNA for PriB binding [162] (Fig. 5.8ai). The ssDNA within the PriA.PriB.DNA complex results in increased affinity of DnaT for PriB, resulting in a PriA.PriB.DnaT.DNA complex that facilitates loading of DnaB onto the single-stranded lagging strand template [148, 162]. Thus the specificity of PriA binding to branched DNA and unwinding of the lagging strand template acts as a regulatory switch to ensure that DnaB loading is restricted to recombination intermediates and forks and occurs only on the lagging rather than the leading strand template [162].

PriC provides a second fork reloading system in *E. coli* and binds preferentially to branched DNA with more than 5 nucleotides of ssDNA exposed on the leading strand template at the fork, a specificity opposite to that of PriA [163] (Fig. 5.8b). PriC binding results in loading of DnaB onto single-stranded lagging strand template without a need for PriB or DnaT [163] but the mechanism by which PriC directs DnaB binding is unclear. Absence of a leading strand 3′ OH at forks preferentially bound by PriC inhibits continued elongation of the pre-existing leading strand. However, loading of DnaB and subsequent association of primase with the replicative helicase facilitate re-priming of both leading and lagging strand synthesis to leave a gap in the leading strand to be repaired later [164] (Fig. 5.9).

PriC is not a helicase, in contrast to PriA, and so cannot itself generate ssDNA on the lagging strand template for DnaB loading [165]. However, both genetic and biochemical data indicate functional interactions between PriC and PriA and also between PriC and Rep helicase activities implying that PriA and Rep might be able to unwind lagging strand duplex DNA to facilitate PriC-directed loading of DnaB [165–168]. PriA might therefore be both a replication initiator in its own right and also an accessory factor for PriC-directed DnaB reloading [165]. However, identification of Rep as an accessory replicative helicase [96, 97] complicates interpretation of any Rep–PriC interaction. Genetic interactions between *rep* and *priC* [169] might reflect increased fork stalling in cells lacking Rep rather than Rep-

promoted DnaB loading whilst stimulation of Rep helicase by PriC in vitro [165, 168] might be via non-specific binding of ssDNA by PriC.

In what contexts do the complementary fork substrate specificities of PriA and PriC act to reload DnaB? Processing of stalled forks in the absence of recombination could generate the preferred substrates for either PriA or PriC [143]. Fork processing, possibly via fork regression, could also result in recombination to form a D-loop (reviewed in ref. [88]). However, efficient DnaB reloading onto a D-loop would require PriA rather than PriC due to the presence of a leading strand 3′ OH near the branch point. The severe recombination defects in Δ*priA* but not Δ*priC* cells is consistent with targeting of D-loops by PriA but not PriC [170, 171]. The relative balance between multiple blocked fork processing pathways in wild type cells is unclear but the extreme viability and DNA repair defects observed in Δ*priA* but not Δ*priC* cells [171–173] suggests PriA-dependent fork repair predominates. The high conservation of PriA but not PriC in bacteria [174] (Gary Sharples, personal communication) also supports a dominant role for PriA. Alternatively, PriC might be engaged frequently in DnaB reloading in wild type *E. coli* but fork processing, possibly via D-loop formation, might allow blocked forks in Δ*priC* cells to be converted ultimately into substrates for PriA-directed restart whereas PriA substrates cannot be converted into substrates for PriC in Δ*priA* cells. Indeed, recombination and D-loop formation might provide a general means to restart replication when other fork processing pathways are defective. A helicase-defective PriA retains the ability to reload DnaB at D-loops because ssDNA is already available for DnaB reloading [175]. Cells possessing this helicase-defective PriA have a phenotype very similar to wild type cells [167, 170, 176], consistent with PriA-directed loading of DnaB onto recombination intermediates providing an efficient fork rescue pathway. However, regardless of the relative balance between PriA- and PriC-directed restart, the inviability of *E. coli* lacking both enzymes highlights the critical importance of replisome reloading away from normal origins of replication [169].

References

1. Singleton MR, Dillingham MS, Wigley DB. Structure and mechanism of helicases and nucleic acid translocases. Annu Rev Biochem. 2007;76:23–50.
2. Patel SS, Pandey M, Nandakumar D. Dynamic coupling between the motors of DNA replication: hexameric helicase, DNA polymerase, and primase. Curr Opin Chem Biol. 2011;15:595–605.
3. Mok M, Marians KJ. The Escherichia coli preprimosome and DnaB helicase can form replication forks that move at the same rate. J Biol Chem. 1987;262:16644–54.
4. Tanner NA, Loparo JJ, Hamdan SM, Jergic S, Dixon NE, van Oijen AM. Real-time single-molecule observation of rolling-circle DNA replication. Nucleic Acids Res. 2009;37:e27.
5. Yao NY, Georgescu RE, Finkelstein J, O'Donnell ME. Single-molecule analysis reveals that the lagging strand increases replisome processivity but slows replication fork progression. Proc Natl Acad Sci USA. 2009;106:13236–41.
6. Galletto R, Jezewska MJ, Bujalowski W. Unzipping mechanism of the double-stranded DNA unwinding by a hexameric helicase: quantitative analysis of the rate of the dsDNA unwinding,

processivity and kinetic step-size of the Escherichia coli DnaB helicase using rapid quench-flow method. J Mol Biol. 2004;343:83–99.
7. Singleton MR, Sawaya MR, Ellenberger T, Wigley DB. Crystal structure of T7 gene 4 ring helicase indicates a mechanism for sequential hydrolysis of nucleotides. Cell. 2000;101:589–600.
8. Benkovic SJ, Valentine AM, Salinas F. Replisome-mediated DNA replication. Annu Rev Biochem. 2001;70:181–208.
9. Korhonen JA, Gaspari M, Falkenberg M. TWINKLE has 5′ -> 3′ DNA helicase activity and is specifically stimulated by mitochondrial single-stranded DNA-binding protein. J Biol Chem. 2003;278:48627–32.
10. Hacker KJ, Johnson KA. A hexameric helicase encircles one DNA strand and excludes the other during DNA unwinding. Biochemistry. 1997;36:14080–7.
11. Ahnert P, Patel SS. Asymmetric interactions of hexameric bacteriophage T7 DNA helicase with the 5′- and 3′-tails of the forked DNA substrate. J Biol Chem. 1997;272:32267–73.
12. Jezewska MJ, Rajendran S, Bujalowska D, Bujalowski W. Does single-stranded DNA pass through the inner channel of the protein hexamer in the complex with the Escherichia coli DnaB Helicase? Fluorescence energy transfer studies. J Biol Chem. 1998;273:10515–29.
13. Jezewska MJ, Rajendran S, Bujalowski W. Complex of Escherichia coli primary replicative helicase DnaB protein with a replication fork: recognition and structure. Biochemistry. 1998;37:3116–36.
14. Kaplan DL. The 3′-tail of a forked-duplex sterically determines whether one or two DNA strands pass through the central channel of a replication-fork helicase. J Mol Biol. 2000;301:285–99.
15. Galletto R, Jezewska MJ, Bujalowski W. Unzipping mechanism of the double-stranded DNA unwinding by a hexameric helicase: the effect of the 3′ arm and the stability of the dsDNA on the unwinding activity of the Escherichia coli DnaB helicase. J Mol Biol. 2004;343:101–14.
16. Chong JP, Hayashi MK, Simon MN, Xu RM, Stillman B. A double-hexamer archaeal minichromosome maintenance protein is an ATP-dependent DNA helicase. Proc Natl Acad Sci USA. 2000;97:1530–5.
17. Moyer SE, Lewis PW, Botchan MR. Isolation of the Cdc45/Mcm2-7/GINS (CMG) complex, a candidate for the eukaryotic DNA replication fork helicase. Proc Natl Acad Sci USA. 2006;103:10236–41.
18. Neuwald AF, Aravind L, Spouge JL, Koonin EV. AAA+: a class of chaperone-like ATPases associated with the assembly, operation, and disassembly of protein complexes. Genome Res. 1999;9:27–43.
19. Takahashi TS, Wigley DB, Walter JC. Pumps, paradoxes and ploughshares: mechanism of the MCM2-7 DNA helicase. Trends Biochem Sci. 2005;30:437–44.
20. Remus D, Beuron F, Tolun G, Griffith JD, Morris EP, Diffley JF. Concerted loading of Mcm2-7 double hexamers around DNA during DNA replication origin licensing. Cell. 2009;139:719–30.
21. Evrin C, Clarke P, Zech J, et al. A double-hexameric MCM2-7 complex is loaded onto origin DNA during licensing of eukaryotic DNA replication. Proc Natl Acad Sci USA. 2009;106:20240–5.
22. Kaplan DL, Davey MJ, O'Donnell M. Mcm4,6,7 uses a "pump in ring" mechanism to unwind DNA by steric exclusion and actively translocate along a duplex. J Biol Chem. 2003;278:49171–82.
23. Fu YV, Yardimci H, Long DT, et al. Selective bypass of a lagging strand roadblock by the eukaryotic replicative DNA helicase. Cell. 2011;146:931–41.
24. Graham BW, Schauer GD, Leuba SH, Trakselis MA. Steric exclusion and wrapping of the excluded DNA strand occurs along discrete external binding paths during MCM helicase unwinding. Nucleic Acids Res. 2011;39:6585–95.
25. Kaplan DL, O'Donnell M. DnaB drives DNA branch migration and dislodges proteins while encircling two DNA strands. Mol Cell. 2002;10:647–57.

26. Kaplan DL, O'Donnell M. Twin DNA pumps of a hexameric helicase provide power to simultaneously melt two duplexes. Mol Cell. 2004;15:453–65.
27. Gupta MK, Atkinson J, McGlynn P. DNA structure specificity conferred on a replicative helicase by its loader. J Biol Chem. 2010;285:979–87.
28. Soultanas P. Loading mechanisms of ring helicases at replication origins. Mol Microbiol. 2012;84(1):6–16.
29. Kaguni JM. DnaA: controlling the initiation of bacterial DNA replication and more. Annu Rev Microbiol. 2006;60:351–75.
30. Mott ML, Berger JM. DNA replication initiation: mechanisms and regulation in bacteria. Nat Rev Microbiol. 2007;5:343–54.
31. Katayama T, Ozaki S, Keyamura K, Fujimitsu K. Regulation of the replication cycle: conserved and diverse regulatory systems for DnaA and oriC. Nat Rev Microbiol. 2010;8:163–70.
32. Speck C, Messer W. Mechanism of origin unwinding: sequential binding of DnaA to double- and single-stranded DNA. EMBO J. 2001;20:1469–76.
33. Sutton MD, Carr KM, Vicente M, Kaguni JM. Escherichia coli DnaA protein. The N-terminal domain and loading of DnaB helicase at the E. coli chromosomal origin. J Biol Chem. 1998;273:34255–62.
34. Duderstadt KE, Chuang K, Berger JM. DNA stretching by bacterial initiators promotes replication origin opening. Nature. 2011;478:209–13.
35. Bramhill D, Kornberg A. Duplex opening by dnaA protein at novel sequences in initiation of replication at the origin of the E. coli chromosome. Cell. 1988;52:743–55.
36. Kowalski D, Eddy MJ. The DNA unwinding element: a novel, cis-acting component that facilitates opening of the Escherichia coli replication origin. EMBO J. 1989;8:4335–44.
37. Soni RK, Mehra P, Mukhopadhyay G, Dhar SK. Helicobacter pylori DnaB helicase can bypass E. coli DnaC function in vivo. Biochem J. 2005;389:541–8.
38. Fang L, Davey MJ, O'Donnell M. Replisome assembly at oriC, the replication origin of E. coli, reveals an explanation for initiation sites outside an origin. Mol Cell. 1999;4:541–53.
39. Johnson A, O'Donnell M. Cellular DNA replicases: components and dynamics at the replication fork. Annu Rev Biochem. 2005;74:283–315.
40. Bowers JL, Randell JC, Chen S, Bell SP. ATP hydrolysis by ORC catalyzes reiterative Mcm2-7 assembly at a defined origin of replication. Mol Cell. 2004;16:967–78.
41. Remus D, Diffley JF. Eukaryotic DNA replication control: lock and load, then fire. Curr Opin Cell Biol. 2009;21:771–7.
42. Gambus A, Jones RC, Sanchez-Diaz A, et al. GINS maintains association of Cdc45 with MCM in replisome progression complexes at eukaryotic DNA replication forks. Nat Cell Biol. 2006;8:358–66.
43. Labib K. How do Cdc7 and cyclin-dependent kinases trigger the initiation of chromosome replication in eukaryotic cells? Genes Dev. 2010;24:1208–19.
44. Yardimci H, Loveland AB, Habuchi S, van Oijen AM, Walter JC. Uncoupling of sister replisomes during eukaryotic DNA replication. Mol Cell. 2010;40:834–40.
45. Calzada A, Hodgson B, Kanemaki M, Bueno A, Labib K. Molecular anatomy and regulation of a stable replisome at a paused eukaryotic DNA replication fork. Genes Dev. 2005;19:1905–19.
46. Ilves I, Petojevic T, Pesavento JJ, Botchan MR. Activation of the MCM2-7 helicase by association with Cdc45 and GINS proteins. Mol Cell. 2010;37:247–58.
47. Pacek M, Tutter AV, Kubota Y, Takisawa H, Walter JC. Localization of MCM2-7, Cdc45, and GINS to the site of DNA unwinding during eukaryotic DNA replication. Mol Cell. 2006;21:581–7.
48. Bochman ML, Schwacha A. The Mcm2-7 complex has in vitro helicase activity. Mol Cell. 2008;31:287–93.
49. Costa A, Ilves I, Tamberg N, et al. The structural basis for MCM2-7 helicase activation by GINS and Cdc45. Nat Struct Mol Biol. 2011;18:471–7.

50. Kim S, Dallmann HG, McHenry CS, Marians KJ. Coupling of a replicative polymerase and helicase: a t-DnaB interaction mediates rapid replication fork movement. Cell. 1996;84:643–50.
51. Gao D, McHenry CS. Tau binds and organizes Escherichia coli replication proteins through distinct domains. Domain IV, located within the unique C terminus of tau, binds the replication fork, helicase, DnaB. J Biol Chem. 2001;276:4441–6.
52. Gao D, McHenry CS. t binds and organizes Escherichia coli replication through distinct domains. Partial proteolysis of terminally tagged t to determine candidate domains and to assign domain V as the a binding domain. J Biol Chem. 2001;276:4433–40.
53. Notarnicola SM, Mulcahy HL, Lee J, Richardson CC. The acidic carboxyl terminus of the bacteriophage T7 gene 4 helicase/primase interacts with T7 DNA polymerase. J Biol Chem. 1997;272:18425–33.
54. Delagoutte E, von Hippel PH. Molecular mechanisms of the functional coupling of the helicase (gp41) and polymerase (gp43) of bacteriophage T4 within the DNA replication fork. Biochemistry. 2001;40:4459–77.
55. Lee SJ, Marintcheva B, Hamdan SM, Richardson CC. The C-terminal residues of bacteriophage T7 gene 4 helicase-primase coordinate helicase and DNA polymerase activities. J Biol Chem. 2006;281:25841–9.
56. Stano NM, Jeong YJ, Donmez I, Tummalapalli P, Levin MK, Patel SS. DNA synthesis provides the driving force to accelerate DNA unwinding by a helicase. Nature. 2005;435:370–3.
57. Ishmael FT, Trakselis MA, Benkovic SJ. Protein-protein interactions in the bacteriophage T4 replisome. The leading strand holoenzyme is physically linked to the lagging strand holoenzyme and the primosome. J Biol Chem. 2003;278:3145–52.
58. Korhonen JA, Pham XH, Pellegrini M, Falkenberg M. Reconstitution of a minimal mtDNA replisome in vitro. EMBO J. 2004;23:2423–9.
59. Hamdan SM, Johnson DE, Tanner NA, et al. Dynamic DNA helicase-DNA polymerase interactions assure processive replication fork movement. Mol Cell. 2007;27:539–49.
60. Tanner NA, Hamdan SM, Jergic S, Schaeffer PM, Dixon NE, van Oijen AM. Single-molecule studies of fork dynamics in Escherichia coli DNA replication. Nat Struct Mol Biol. 2008;15:170–6.
61. Takayama Y, Kamimura Y, Okawa M, Muramatsu S, Sugino A, Araki H. GINS, a novel multiprotein complex required for chromosomal DNA replication in budding yeast. Genes Dev. 2003;17:1153–65.
62. Muramatsu S, Hirai K, Tak YS, Kamimura Y, Araki H. CDK-dependent complex formation between replication proteins Dpb11, Sld2, Pol (epsilon), and GINS in budding yeast. Genes Dev. 2010;24:602–12.
63. Sun B, Johnson DS, Patel G, et al. ATP-induced helicase slippage reveals highly coordinated subunits. Nature. 2011;478:132–5.
64. Studwell-Vaughan PS, O'Donnell M. Constitution of the twin polymerase of DNA polymerase III holoenzyme. J Biol Chem. 1991;266:19833–41.
65. McInerney P, Johnson A, Katz F, O'Donnell M. Characterization of a triple DNA polymerase replisome. Mol Cell. 2007;27:527–38.
66. Reyes-Lamothe R, Sherratt DJ, Leake MC. Stoichiometry and architecture of active DNA replication machinery in Escherichia coli. Science. 2010;328:498–501.
67. Yeeles JT, Marians KJ. The Escherichia coli replisome is inherently DNA damage tolerant. Science. 2011;334:235–8.
68. Lu YB, Ratnakar PV, Mohanty BK, Bastia D. Direct physical interaction between DnaG primase and DnaB helicase of Escherichia coli is necessary for optimal synthesis of primer RNA. Proc Natl Acad Sci USA. 1996;93:12902–7.
69. Biswas EE, Biswas SB. Mechanism of DnaB helicase of Escherichia coli: structural domains involved in ATP hydrolysis, DNA binding, and oligomerization. Biochemistry. 1999;38:10919–28.

70. Oakley AJ, Loscha KV, Schaeffer PM, et al. Crystal and solution structures of the helicase-binding domain of Escherichia coli primase. J Biol Chem. 2005;280:11495–504.
71. Bird LE, Pan H, Soultanas P, Wigley DB. Mapping protein-protein interactions within a stable complex of DNA primase and DnaB helicase from Bacillus stearothermophilus. Biochemistry. 2000;39:171–82.
72. Thirlway J, Turner IJ, Gibson CT, et al. DnaG interacts with a linker region that joins the N- and C-domains of DnaB and induces the formation of 3-fold symmetric rings. Nucleic Acids Res. 2004;32:2977–86.
73. Norcum MT, Warrington JA, Spiering MM, Ishmael FT, Trakselis MA, Benkovic SJ. Architecture of the bacteriophage T4 primosome: electron microscopy studies of helicase (gp41) and primase (gp61). Proc Natl Acad Sci USA. 2005;102:3623–6.
74. Toth EA, Li Y, Sawaya MR, Cheng Y, Ellenberger T. The crystal structure of the bifunctional primase-helicase of bacteriophage T7. Mol Cell. 2003;12:1113–23.
75. Marinsek N, Barry ER, Makarova KS, Dionne I, Koonin EV, Bell SD. GINS, a central nexus in the archaeal DNA replication fork. EMBO Rep. 2006;7:539–45.
76. De Falco M, Ferrari E, De Felice M, Rossi M, Hubscher U, Pisani FM. The human GINS complex binds to and specifically stimulates human DNA polymerase alpha-primase. EMBO Rep. 2007;8:99–103.
77. Valentine AM, Ishmael FT, Shier VK, Benkovic SJ. A zinc ribbon protein in DNA replication: primer synthesis and macromolecular interactions by the bacteriophage T4 primase. Biochemistry. 2001;40:15074–85.
78. Corn JE, Berger JM. Regulation of bacterial priming and daughter strand synthesis through helicase-primase interactions. Nucleic Acids Res. 2006;34(15):4082–8.
79. Bailey S, Eliason WK, Steitz TA. Structure of hexameric DnaB helicase and its complex with a domain of DnaG primase. Science. 2007;318:459–63.
80. Bhattacharyya S, Griep MA. DnaB helicase affects the initiation specificity of Escherichia coli primase on single-stranded DNA templates. Biochemistry. 2000;39:745–52.
81. Johnson SK, Bhattacharyya S, Griep MA. DnaB helicase stimulates primer synthesis activity on short oligonucleotide templates. Biochemistry. 2000;39:736–44.
82. Corn JE, Pease PJ, Hura GL, Berger JM. Crosstalk between primase subunits can act to regulate primer synthesis in trans. Mol Cell. 2005;20:391–401.
83. Yancey-Wrona JE, Matson SW. Bound Lac repressor protein differentially inhibits the unwinding reactions catalyzed by DNA helicases. Nucleic Acids Res. 1992;20:6713–21.
84. Mackintosh SG, Raney KD. DNA unwinding and protein displacement by superfamily 1 and superfamily 2 helicases. Nucleic Acids Res. 2006;34:4154–9.
85. Trautinger BW, Jaktaji RP, Rusakova E, Lloyd RG. RNA polymerase modulators and DNA repair activities resolve conflicts between DNA replication and transcription. Mol Cell. 2005;19:247–58.
86. Azvolinsky A, Giresi PG, Lieb JD, Zakian VA. Highly transcribed RNA polymerase II genes are impediments to replication fork progression in Saccharomyces cerevisiae. Mol Cell. 2009;34:722–34.
87. Aguilera A, Gomez-Gonzalez B. Genome instability: a mechanistic view of its causes and consequences. Nat Rev Genet. 2008;9:204–17.
88. Atkinson J, McGlynn P. Replication fork reversal and the maintenance of genome stability. Nucleic Acids Res. 2009;37:3475–92.
89. Blow JJ, Ge XQ. A model for DNA replication showing how dormant origins safeguard against replication fork failure. EMBO Rep. 2009;10:406–12.
90. Kawabata T, Luebben SW, Yamaguchi S, et al. Stalled fork rescue via dormant replication origins in unchallenged S phase promotes proper chromosome segregation and tumor suppression. Mol Cell. 2011;41:543–53.
91. Jacome A, Fernandez-Capetillo O. Lac operator repeats generate a traceable fragile site in mammalian cells. EMBO Rep. 2011;12:1032–8.
92. Klein IA, Resch W, Jankovic M, et al. Translocation-capture sequencing reveals the extent and nature of chromosomal rearrangements in B lymphocytes. Cell. 2011;147:95–106.

93. Chiarle R, Zhang Y, Frock RL, et al. Genome-wide translocation sequencing reveals mechanisms of chromosome breaks and rearrangements in B cells. Cell. 2011;147:107–19.
94. Byrd AK, Raney KD. Protein displacement by an assembly of helicase molecules aligned along single-stranded DNA. Nat Struct Mol Biol. 2004;11:531–8.
95. Bonne-Andrea C, Wong ML, Alberts BM. In vitro replication through nucleosomes without histone displacement. Nature. 1990;343:719–26.
96. Guy CP, Atkinson J, Gupta MK, et al. Rep provides a second motor at the replisome to promote duplication of protein-bound DNA. Mol Cell. 2009;36:654–66.
97. Boubakri H, de Septenville AL, Viguera E, Michel B. The helicases DinG, Rep and UvrD cooperate to promote replication across transcription units in vivo. EMBO J. 2010;29(1):145–57.
98. Atkinson J, Gupta MK, Rudolph CJ, Bell H, Lloyd RG, McGlynn P. Localization of an accessory helicase at the replisome is critical in sustaining efficient genome duplication. Nucleic Acids Res. 2011;39:949–57.
99. Atkinson J, Gupta MK, McGlynn P. Interaction of Rep and DnaB on DNA. Nucleic Acids Res. 2011;39:1351–9.
100. Uzest M, Ehrlich SD, Michel B. Lethality of rep recB and rep recC double mutants of Escherichia coli. Mol Microbiol. 1995;17:1177–88.
101. Seigneur M, Bidnenko V, Ehrlich SD, Michel B. RuvAB acts at arrested replication forks. Cell. 1998;95:419–30.
102. Lane HE, Denhardt DT. The rep mutation. IV. Slower movement of replication forks in Escherichia coli rep strains. J Mol Biol. 1975;97:99–112.
103. Smith KR, Yancey JE, Matson SW. Identification and purification of a protein that stimulates the helicase activity of the Escherichia coli Rep protein. J Biol Chem. 1989;264:6119–26.
104. Costes A, Lecointe F, McGovern S, Quevillon-Cheruel S, Polard P. The C-terminal domain of the bacterial SSB protein acts as a DNA maintenance hub at active chromosome replication forks. PLoS Genet. 2010;6:e1001238.
105. Ivessa AS, Zhou JQ, Schulz VP, Monson EK, Zakian VA. Saccharomyces Rrm3p, a 5′ to 3′ DNA helicase that promotes replication fork progression through telomeric and subtelomeric DNA. Genes Dev. 2002;16:1383–96.
106. Ivessa AS, Lenzmeier BA, Bessler JB, Goudsouzian LK, Schnakenberg SL, Zakian VA. The Saccharomyces cerevisiae helicase Rrm3p facilitates replication past nonhistone protein-DNA complexes. Mol Cell. 2003;12:1525–36.
107. Keil RL, McWilliams AD. A gene with specific and global effects on recombination of sequences from tandemly repeated genes in Saccharomyces cerevisiae. Genetics. 1993;135:711–8.
108. Schmidt KH, Kolodner RD. Requirement of Rrm3 helicase for repair of spontaneous DNA lesions in cells lacking Srs2 or Sgs1 helicase. Mol Cell Biol. 2004;24:3213–26.
109. Torres JZ, Schnakenberg SL, Zakian VA. Saccharomyces cerevisiae Rrm3p DNA helicase promotes genome integrity by preventing replication fork stalling: viability of rrm3 cells requires the intra-S-phase checkpoint and fork restart activities. Mol Cell Biol. 2004;24:3198–212.
110. Azvolinsky A, Dunaway S, Torres JZ, Bessler JB, Zakian VA. The S. cerevisiae Rrm3p DNA helicase moves with the replication fork and affects replication of all yeast chromosomes. Genes Dev. 2006;20:3104–16.
111. Schmidt KH, Derry KL, Kolodner RD. Saccharomyces cerevisiae RRM3, a 5′ to 3′ DNA helicase, physically interacts with proliferating cell nuclear antigen. J Biol Chem. 2002;277:45331–7.
112. Moolenaar GF, Moorman C, Goosen N. Role of the Escherichia coli nucleotide excision repair proteins in DNA replication. J Bacteriol. 2000;182:5706–14.
113. Atkinson J, Guy CP, Cadman CJ, Moolenaar GF, Goosen N, McGlynn P. Stimulation of UvrD helicase by UvrAB. J Biol Chem. 2009;284:9612–23.

114. Garg P, Stith CM, Sabouri N, Johansson E, Burgers PM. Idling by DNA polymerase delta maintains a ligatable nick during lagging-strand DNA replication. Genes Dev. 2004;18:2764–73.
115. Bae SH, Bae KH, Kim JA, Seo YS. RPA governs endonuclease switching during processing of Okazaki fragments in eukaryotes. Nature. 2001;412:456–61.
116. Bae SH, Seo YS. Characterization of the enzymatic properties of the yeast dna2 Helicase/endonuclease suggests a new model for Okazaki fragment processing. J Biol Chem. 2000;275:38022–31.
117. Kao HI, Campbell JL, Bambara RA. Dna2p helicase/nuclease is a tracking protein, like FEN1, for flap cleavage during Okazaki fragment maturation. J Biol Chem. 2004;279:50840–9.
118. Balakrishnan L, Polaczek P, Pokharel S, Campbell JL, Bambara RA. Dna2 exhibits a unique strand end-dependent helicase function. J Biol Chem. 2010;285:38861–8.
119. Kao HI, Veeraraghavan J, Polaczek P, Campbell JL, Bambara RA. On the roles of Saccharomyces cerevisiae Dna2p and Flap endonuclease 1 in Okazaki fragment processing. J Biol Chem. 2004;279:15014–24.
120. Budd ME, Reis CC, Smith S, Myung K, Campbell JL. Evidence suggesting that Pif1 helicase functions in DNA replication with the Dna2 helicase/nuclease and DNA polymerase delta. Mol Cell Biol. 2006;26:2490–500.
121. Lahaye A, Stahl H, Thines-Sempoux D, Foury F. PIF1: a DNA helicase in yeast mitochondria. EMBO J. 1991;10:997–1007.
122. Bochman ML, Sabouri N, Zakian VA. Unwinding the functions of the Pif1 family helicases. DNA Repair (Amst). 2010;9:237–49.
123. Rossi ML, Pike JE, Wang W, Burgers PM, Campbell JL, Bambara RA. Pif1 helicase directs eukaryotic Okazaki fragments toward the two-nuclease cleavage pathway for primer removal. J Biol Chem. 2008;283:27483–93.
124. Pike JE, Burgers PM, Campbell JL, Bambara RA. Pif1 helicase lengthens some Okazaki fragment flaps necessitating Dna2 nuclease/helicase action in the two-nuclease processing pathway. J Biol Chem. 2009;284:25170–80.
125. Pike JE, Henry RA, Burgers PM, Campbell JL, Bambara RA. An alternative pathway for Okazaki fragment processing: resolution of fold-back flaps by Pif1 helicase. J Biol Chem. 2010;285:41712–23.
126. Ribeyre C, Lopes J, Boule JB, et al. The yeast Pif1 helicase prevents genomic instability caused by G-quadruplex-forming CEB1 sequences in vivo. PLoS Genet. 2009;5:e1000475.
127. Sanders CM. Human Pif1 helicase is a G-quadruplex DNA-binding protein with G-quadruplex DNA-unwinding activity. Biochem J. 2010;430:119–28.
128. Paeschke K, Capra JA, Zakian VA. DNA replication through G-quadruplex motifs is promoted by the Saccharomyces cerevisiae Pif1 DNA helicase. Cell. 2011;145:678–91.
129. Minden JS, Marians KJ. Escherichia coli topoisomerase I can segregate replicating pBR322 daughter DNA molecules in vitro. J Biol Chem. 1986;261:11906–17.
130. Rothstein R, Gangloff S. Hyper-recombination and Bloom's syndrome: microbes again provide clues about cancer. Genome Res. 1995;5:421–6.
131. Suski C, Marians KJ. Resolution of converging replication forks by RecQ and topoisomerase III. Mol Cell. 2008;30:779–89.
132. Nurse P, Levine C, Hassing H, Marians KJ. Topoisomerase III can serve as the cellular decatenase in Escherichia coli. J Biol Chem. 2003;278:8653–60.
133. Butland G, Peregrin-Alvarez JM, Li J, et al. Interaction network containing conserved and essential protein complexes in Escherichia coli. Nature. 2005;433:531–7.
134. Shereda RD, Bernstein DA, Keck JL. A central role for SSB in Escherichia coli RecQ DNA helicase function. J Biol Chem. 2007;282:19247–58.
135. Nadal M. Reverse gyrase: an insight into the role of DNA-topoisomerases. Biochimie. 2007;89:447–55.

136. Mirkin EV, Mirkin SM. Replication fork stalling at natural impediments. Microbiol Mol Biol Rev. 2007;71:13–35.
137. Higuchi K, Katayama T, Iwai S, Hidaka M, Horiuchi T, Maki H. Fate of DNA replication fork encountering a single DNA lesion during oriC plasmid DNA replication in vitro. Genes Cells. 2003;8:437–49.
138. Pagès V, Fuchs RP. Uncoupling of leading- and lagging-strand DNA replication during lesion bypass in vivo. Science. 2003;300:1300–3.
139. McInerney P, O'Donnell M. Functional uncoupling of twin polymerases: mechanism of polymerase dissociation from a lagging-strand block. J Biol Chem. 2004;279:21543–51.
140. Merrikh H, Machon C, Grainger WH, Grossman AD, Soultanas P. Co-directional replication-transcription conflicts lead to replication restart. Nature. 2011;470:554–7.
141. Marians KJ, Hiasa H, Kim DR, McHenry CS. Role of the core DNA polymerase III subunits at the replication fork. α is the only subunit required for processive replication. J Biol Chem. 1998;273:2452–7.
142. McGlynn P, Guy CP. Replication forks blocked by protein-DNA complexes have limited stability in vitro. J Mol Biol. 2008;381:249–55.
143. Heller RC, Marians KJ. Replisome assembly and the direct restart of stalled replication forks. Nat Rev Mol Cell Biol. 2006;7:932–43.
144. Petermann E, Helleday T. Pathways of mammalian replication fork restart. Nat Rev Mol Cell Biol. 2010;11:683–7.
145. Llorente B, Smith CE, Symington LS. Break-induced replication: what is it and what is it for? Cell Cycle. 2008;7:859–64.
146. Hashimoto Y, Puddu F, Costanzo V. RAD51- and MRE11-dependent reassembly of uncoupled CMG helicase complex at collapsed replication forks. Nat Struct Mol Biol. 2012;19:17–24.
147. Jones JM, Nakai H. Duplex opening by primosome protein PriA for replisome assembly on a recombination intermediate. J Mol Biol. 1999;289:503–16.
148. Liu J, Marians KJ. PriA-directed assembly of a primosome on D loop DNA. J Biol Chem. 1999;274:25033–41.
149. Lee MS, Marians KJ. Escherichia coli replication factor Y, a component of the primosome, can act as a DNA helicase. Proc Natl Acad Sci USA. 1987;84:8345–9.
150. Lasken RS, Kornberg A. The primosomal protein n′ of Escherichia coli is a DNA helicase. J Biol Chem. 1988;263:5512–8.
151. McGlynn P, Al-Deib AA, Liu J, Marians KJ, Lloyd RG. The DNA replication protein PriA and the recombination protein RecG bind D-loops. J Mol Biol. 1997;270:212–21.
152. Nurse P, Liu J, Marians KJ. Two modes of PriA binding to DNA. J Biol Chem. 1999;274:25026–32.
153. Sasaki K, Ose T, Okamoto N, et al. Structural basis of the 3′-end recognition of a leading strand in stalled replication forks by PriA. EMBO J. 2007;26:2584–93.
154. Tanaka T, Mizukoshi T, Sasaki K, Kohda D, Masai H. Escherichia coli PriA protein, two modes of DNA binding and activation of ATP hydrolysis. J Biol Chem. 2007;282:19917–27.
155. Gregg AV, McGlynn P, Jaktaji RP, Lloyd RG. Direct rescue of stalled DNA replication forks via the combined action of PriA and RecG helicase activities. Mol Cell. 2002;9:241–51.
156. Cadman CJ, McGlynn P. PriA helicase and SSB interact physically and functionally. Nucleic Acids Res. 2004;32:6378–87.
157. Lecointe F, Serena C, Velten M, et al. Anticipating chromosomal replication fork arrest: SSB targets repair DNA helicases to active forks. EMBO J. 2007;26:4239–51.
158. Ng JY, Marians KJ. The ordered assembly of the fX174-type primosome. I. Isolation and identification of intermediate protein-DNA complexes. J Biol Chem. 1996;271:15642–8.
159. Liu J, Nurse P, Marians KJ. The ordered assembly of the phiX174-type primosome. III. PriB facilitates complex formation between PriA and DnaT. J Biol Chem. 1996;271:15656–61.

160. Lopper M, Holton JM, Keck JL. Crystal structure of PriB, a component of the Escherichia coli replication restart primosome. Structure (Camb). 2004;12:1967–75.
161. Cadman CJ, Lopper M, Moon PB, Keck JL, McGlynn P. PriB stimulates PriA helicase via an interaction with single-stranded DNA. J Biol Chem. 2005;280:39693–700.
162. Lopper M, Boonsombat R, Sandler SJ, Keck JL. A hand-off mechanism for primosome assembly in replication restart. Mol Cell. 2007;26:781–93.
163. Heller RC, Marians KJ. The disposition of nascent strands at stalled replication forks dictates the pathway of replisome loading during restart. Mol Cell. 2005;17:733–43.
164. Heller RC, Marians KJ. Replication fork reactivation downstream of a blocked nascent leading strand. Nature. 2006;439:557–62.
165. Heller RC, Marians KJ. Unwinding of the nascent lagging strand by Rep and PriA enables the direct restart of stalled replication forks. J Biol Chem. 2005;280:34143–51.
166. Sandler SJ, Marians KJ. Role of PriA in replication fork reactivation in Escherichia coli. J Bacteriol. 2000;182:9–13.
167. Sandler SJ, McCool JD, Do TT, Johansen RU. PriA mutations that affect PriA-PriC function during replication restart. Mol Microbiol. 2001;41:697–704.
168. Heller RC, Marians KJ. Non-replicative helicases at the replication fork. DNA Repair (Amst). 2007;6:945–52.
169. Sandler SJ. Multiple genetic pathways for restarting DNA replication forks in Escherichia coli K-12. Genetics. 2000;155:487–97.
170. Kogoma T, Cadwell GW, Barnard KG, Asai T. The DNA replication priming protein, PriA, is required for homologous recombination and double-strand break repair. J Bacteriol. 1996;178:1258–64.
171. Sandler SJ, Marians KJ, Zavitz KH, Coutu J, Parent MA, Clark AJ. dnaC mutations suppress defects in DNA replication- and recombination- associated functions in priB and priC double mutants in Escherichia coli K-12. Mol Microbiol. 1999;34:91–101.
172. Nurse P, Zavitz KH, Marians KJ. Inactivation of the Escherichia coli priA DNA replication protein induces the SOS response. J Bacteriol. 1991;173:6686–93.
173. Lee EH, Kornberg A. Replication deficiencies in priA mutants of Escherichia coli lacking the primosomal replication n′ protein. Proc Natl Acad Sci USA. 1991;88:3029–32.
174. Rocha EP, Cornet E, Michel B. Comparative and evolutionary analysis of the bacterial homologous recombination systems. PLoS Genet. 2005;1:e15.
175. Liu J, Xu L, Sandler SJ, Marians KJ. Replication fork assembly at recombination intermediates is required for bacterial growth. Proc Natl Acad Sci USA. 1999;96:3552–5.
176. Zavitz KH, Marians KJ. ATPase-deficient mutants of the Escherichia coli DNA replication protein PriA are capable of catalyzing the assembly of active primosomes. J Biol Chem. 1992;267:6933–40.

Chapter 6
DNA Helicases Associated with Genetic Instability, Cancer, and Aging

Avvaru N. Suhasini and Robert M. Brosh Jr.

Abstract DNA helicases have essential roles in the maintenance of genomic stability. They have achieved even greater prominence with the discovery that mutations in human helicase genes are responsible for a variety of genetic disorders and are associated with tumorigenesis. A number of missense mutations in human helicase genes are linked to chromosomal instability diseases characterized by age-related disease or associated with cancer, providing incentive for the characterization of molecular defects underlying aberrant cellular phenotypes. In this chapter, we discuss some examples of clinically relevant missense mutations in various human DNA helicases, particularly those of the Iron-Sulfur cluster and RecQ families. Clinically relevant mutations in the XPD helicase can lead to Xeroderma pigmentosum, Cockayne's syndrome, Trichothiodystrophy, or COFS syndrome. FANCJ mutations are associated with Fanconi anemia or breast cancer. Mutations of the Fe-S helicase ChlR1 (DDX11) are linked to Warsaw Breakage syndrome. Mutations in the RecQ helicases BLM and WRN are linked to the cancer-prone disorder Bloom's syndrome and premature aging condition Werner syndrome, respectively. RECQL4 mutations can lead to Rothmund-Thomson syndrome, Baller-Gerold syndrome, or RAPADILINO. Mutations in the Twinkle mitochondrial helicase are responsible for several neuromuscular degenerative disorders. We will discuss some insights gained from biochemical and genetic studies of helicase variants, and highlight some hot areas of helicase research based on recent developments.

A.N. Suhasini • R.M. Brosh Jr. (✉)
Laboratory of Molecular Gerontology, National Institute on Aging, National Institutes of Health, NIH Biomedical Research Center, Baltimore, MD, USA
e-mail: BroshR@grc.nia.nih.gov

M. Spies (ed.), *DNA Helicases and DNA Motor Proteins*, Advances in Experimental Medicine and Biology, DOI 10.1007/978-1-4614-5037-5_6,

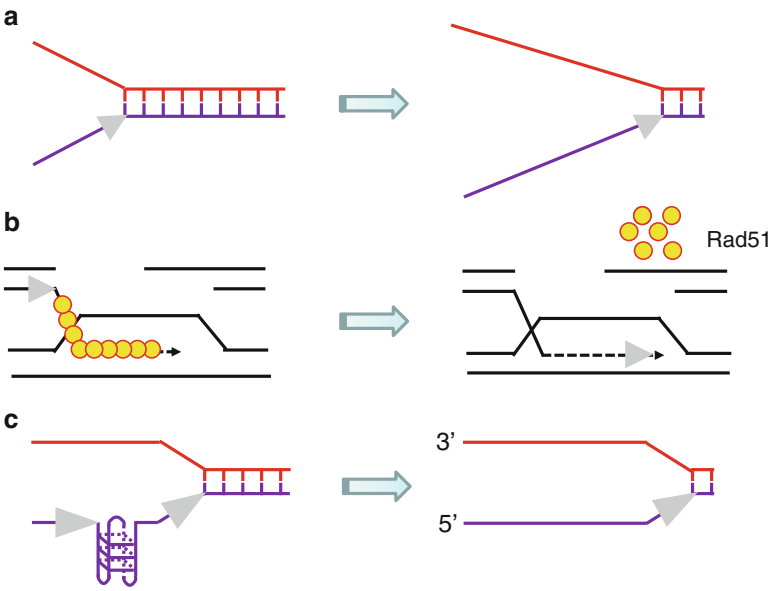

Fig. 6.1 Depending on their specialty, DNA helicases use the energy of ATP hydrolysis to perform multiple functions. (**a**) A DNA helicase can disrupt noncovalent hydrogen bonds between complementary strands of the DNA double helix to form transient single-stranded DNA tracts. (**b**) A DNA helicase can strip proteins (e.g., Rad51) off DNA to regulate HR. (**c**) A DNA helicase can resolve alternate DNA structures (e.g., G-quadruplex) to enable smooth progression of the replication fork

DNA Helicases: A Specialized Class of Molecular Motors

Helicases are molecular motors that couple nucleoside triphosphate (NTP) hydrolysis (typically ATP) to the unwinding of polynucleic acid structures [1, 2]. Helicases have multifaceted roles in virtually all aspects of nucleic acid metabolism, including replication, DNA repair, recombination, transcription, chromosome segregation, and telomere maintenance [2–6]. ATP-dependent DNA or RNA unwinding enzymes exist; however, certain helicases can act upon both DNA and RNA [6]. Although DNA helicases are conventionally known to unwind B-form DNA double helical molecules, some are specialized such that they can catalytically disrupt alternate DNA structures (e.g., D-loop, Holliday junction (HJ), triplex, G-quadruplex), strip proteins bound to either single-stranded or double-stranded DNA, perform chromatin remodeling, and/or anneal complementary single-strands [7–10] (Fig. 6.1).

Hereditary DNA Helicase Disorders

An increasing number of genetic diseases characterized by chromosomal instability are linked to mutations in DNA helicase genes. Many of these diseases are very rare, and inherited by autosomal homozygous recessive mutations. In certain cases,

mutations in human helicase genes are linked to premature aging or age-related diseases, whereas some helicase mutations have been associated with cancer. In addition to these, hereditary dominant mutations have been identified in the mitochondrial DNA helicase which lead to neuromuscular degenerative diseases. We will provide an overview on the clinical disorders associated with mutations in DNA helicase genes.

Iron-Sulfur Cluster DNA Helicase Diseases

A prominent family of DNA helicases with a linkage to human diseases that has acquired a great deal of interest is the so-called Iron-Sulfur (Fe-S) cluster helicases, named after a conserved metal binding domain in the helicase core [11, 12]. These helicases belong to the Superfamily 2 (SF2) grouping of DNA helicases which share sequence homology within the helicase core domain. Mutations in the Fe-S cluster helicase XPD, a key factor of the TFIIH complex implicated in transcription and nucleotide excision repair (NER), can give rise to multiple rare autosomal recessive clinical disorders: xeroderma pigmentosum (XP), XP combined with Cockayne's syndrome (CS), Trichothiodystrophy (TTD), and Cerebro-oculo-facial-skeletal (COFS) syndrome (for a recent review, see ref. [13]). Photosensitivity, neurological/developmental abnormalities, and skin cancer can be used to distinguish between XP, TTD, and CS; however, related or overlapping clinical features can arise from *XPD* mutations. XPD unwinds duplex DNA with a 5′–3′ directionality, and together with the SF2 XPB helicase (which lacks an Fe-S cluster) is required for NER and transcription [14]. Operating as components of the TFIIH complex, two DNA helicases XPD and XPB with opposite translocation polarities are responsible for unwinding duplex DNA in the vicinity of the lesion to create a bubble containing the lesion, a prerequisite for proper removal of the damaged fragment [14]. In contrast to XPD where helicase activity is indispensable for NER, only XPB ATPase is necessary for the pathway to remove bulky lesions and UV photoproducts. XPB ATPase activity is also necessary for DNA opening for transcription to occur, but its helicase activity is important for promoter escape during transcription (for review, see ref. [15]).

Homozygous recessive mutations in the *FANCJ* gene encoding the FANCJ Fe-S cluster DNA helicase (also called BACH1 or BRIP1), and at least 14 other genes, are responsible for Fanconi anemia (FA), a disorder characterized by congenital defects, progressive bone marrow failure, cancer accompanied by chromosomal instability, and hypersensitivity to agents that induce DNA interstrand cross-links (ICLs) [16, 17]. Notably, *FANCJ* mutations have also been associated with breast cancer [18]. Indeed, FANCJ was originally discovered by its association with the tumor suppressor protein BRCA1 [19]. In addition to its role in ICL repair, FANCJ helps cells to maintain genomic stability by resolving G-quadruplex (G4) DNA structures [20, 21], suggesting a more general role of the helicase in the response to replication stress.

The latest Fe-S cluster helicase implicated in a genetic disease is ChlR1, also known as DDX11, which is linked to Warsaw Breakage syndrome (WABS), a unique disease with cellular features of both FA and the cohesinopathy Roberts syndrome [22]. The clinical features of the single WABS patient reported include severe microcephaly, pre- and postnatal growth retardation, and abnormal skin pigmentation. Cells from the WABS patient display defective sister chromatid cohesion, a finding that is consistent with studies of mutant versions of ChlR1 homologs in yeast [23] and mouse [24] which also showed cohesion defects. The Lahti lab showed that depletion of human ChlR1 by RNA interference resulted in abnormal sister chromatid cohesion and a prometaphase delay leading to mitotic failure [25]. ChlR1 has a role in heterochromatin organization [26]; however, it is still unclear how the helicase is important for the cohesion process. Since cohesion is widely thought to be coupled to cellular DNA replication, it may be that ChlR1 is necessary for smooth replication fork progression through its catalytic activity and protein interactions, and that in its absence the cohesion proteins are not assembled properly; however, this may be an over simplistic assessment. Clearly further studies are necessary to understand the precise functions of ChlR1 required for chromosomal stability.

RecQ DNA Helicase Diseases

In addition to the Fe-S cluster DNA helicases, the SF2 RecQ DNA helicases are important for genomic stability and have been implicated in hereditary disorders. Homozygous recessive mutations in the *BLM* gene encoding a DNA helicase are responsible for Bloom's syndrome [27]. BS patients are highly sensitive to sunlight, immunodeficient, and display a broad spectrum of cancers early in life. The hallmark of BS is an elevated rate of sister chromatid exchange (SCE) [28]. BLM is believed to function in homologous recombination (HR) repair to maintain genomic stability. A model for the role of BLM in SCE suppression was proposed in which a BLM protein complex containing topoisomerase IIIα, RPA, RMI, and RMI2 dissolves double HJ structures which may form during recombination or the convergence of replication forks [29, 30]. BLM helicase activity working in concert with topoisomerase cleavage/ligation is required for the double HJ dissolution reaction. In addition to this function, BLM is believed to have other roles (early and late) in homologous recombination (HR) repair of double strand breaks (DSBs) [31, 32] and helping cells to deal with replication stress [33].

A second RecQ helicase disorder known as Werner syndrome (WS) is characterized by premature aging features and the early onset of age-related diseases such as cardiovascular disorders, diabetes mellitus (Type II), osteoporosis, and sarcoma and mesenchymal tumors. WS is characterized by genomic instability, sensitivity to DNA damaging agents, elevated recombination, and replication defects. The *WRN* gene encodes an RecQ 3′–5′ DNA helicase and 3′–5′ exonuclease that is proposed to play a role in regulation of recombination events, primarily HR [3, 34]. It may be

that WRN has a specialized function when the replication fork encounters a blocking lesion or alternate DNA structure. WRN interacts with a number of nuclear proteins, and these interactions are believed to facilitate genomic stability in various capacities including telomere maintenance, replication, and DNA repair [34, 35].

Mutations in a third RecQ family member, *RECQL4*, can lead to three distinct genetic disorders, namely Rothmund-Thomson syndrome (RTS), Baller-Gerold syndrome (BGS), and RAPADILINO (radial hypoplasia/aplasia, patellae hypoplasia/aplasia, cleft or highly arched palate, diarrhea, dislocated joints, little size (height at least 2 S.D. smaller than the average height) and limb malformation, nose slender, and normal intelligence) syndrome [36]. RTS patients are stunted in growth, and characterized by photosensitivity with poikiloderma, early graying and hair loss, juvenile cataracts, and osteogenic sarcomas. BGS is characterized by radial aplasia/hypoplasia and craniosynostosis, but not the poikiloderma typical of RTS patients [37]. Recent work form the Bohr lab has provided evidence that RECQL4 has pleiotropic roles in cellular DNA metabolism that include DSB repair [38] and telomere maintenance [39]. RECQL4 can be found in mitochondria where it helps to preserve the mitochondrial genome [40] and recruit p53 [41].

In addition to WRN, BLM, and RECQL4, two other human RecQ helicases, RECQL1 (RECQ1) and RECQL5 (RECQ5), are not yet linked to a disease; but it seems likely that these helicases will also play a role in cancer predisposition or a hereditary disorder characterized by chromosomal instability [42]. Indeed, studies of primary fibroblasts from RECQ1-knockout mice [43] and human cells depleted of RECQ1 by RNA interference [44] show chromosomal instability. Recent evidence has implicated distinct roles of RECQ1 (and RECQL4) in DNA replication initiation [45]. RECQ5 was found to be associated with RNA polymerase and may help to maintain genomic stability during transcription [46, 47]. RECQ5 also participates in DNA decatenation through its cooperation with Topoisomerase II alpha [48].

Twinkle Mitochondrial DNA Helicase

Aside from the Fe-S and RecQ DNA helicases, mutation of the Twinkle mitochondrial DNA helicase co-segregates with a number of diseases with mitochondrial defects including adult-onset progressive external ophthalmoplegia, hepatocerebral syndrome with mtDNA depletion syndrome, and infantile-onset spinocerebellar ataxia [49]. Twinkle is required for replication of human mitochondrial DNA, and mutations in the C10orf2 gene encoding Twinkle helicase can lead to mitochondrial deletions in post-mitotic tissues. Work from several laboratories demonstrated that Twinkle is an oligomeric helicase that unwinds double-stranded DNA molecules [50–52], and can also catalyze strand annealing [51], a function that is also observed for a number of the RecQ helicases [42]. It is yet unclear what the biological significance of helicase-catalyzed strand annealing truly is, but may play a role when replication forks are stalled or during DSB repair.

Hereditary Missense Mutations in DNA Helicase Disorders

Structural and biochemical analyses of purified recombinant DNA helicase proteins has sparked tremendous interest in understanding the molecular pathology behind disease-causing mutations in this specialized class of molecular motor ATPases. Disease-causing missense mutations result in single amino acid substitutions have been identified in DNA helicase disorders, which may be insightful for understanding biochemical mechanism and cellular function. In the following section, we will discuss some basic lessons from the spectrum of clinically relevant missense mutations in human DNA helicase genes, highlighting some unique aspects and potential areas of investigation.

Disease-Causing Missense Mutations in Iron-Sulfur Cluster DNA Helicases

XPD Missense Mutations

Missense mutations in the *XPD* gene are linked to four hereditary diseases: XP, XP combined with CS, TTD, and COFS syndrome with some cases of partially overlapping clinical features [13] (Fig. 6.2). *XPD* mutations responsible for XP are located mainly in the helicase core domain, and either significantly reduce or completely inactivate helicase function. The XP-causing *XPD* mutations do not affect basal transcription [53], consistent with a requirement of XPD ATPase/helicase activity for NER, but not transcription. As components of the TFIIH complex, XPD helicase operating in conjunction with the opposite polarity XPB helicase unwinds double-stranded DNA in the vicinity of the helix distorting lesion to create a bubble that can be acted upon by structure-specific nucleases to remove a short (~30 nt) single-stranded fragment containing the damage. Repair synthesis and ligation complete the steps of NER.

XPD mutations responsible for XP/CS also reside within or near the conserved helicase motifs as well (Fig. 6.2). However, XPD missense mutations causing XP/CS are believed to interfere with XPD protein interactions within the TFIIH complex. Unlike the *XPD* mutations implicated in XP or XP/CS which are only found in or very near the helicase core domain, *XPD* mutations responsible for TTD can also be found in the C-terminal region of the protein (Fig. 6.2). The C-terminus of XPD is important for interaction with other proteins (e.g., p44 subunit of TFIIH), which can be critical for optimal XPD helicase activity and/or stability of the TFIIH complex (for review, see ref. [54]). Such mutations in *XPD* reduce DNA repair activity and basal transcription [55]. Several *XPD* missense mutations linked to TTD that have been examined inhibit basal transcription, suggesting a molecular defect distinct from that of XP.

The heterozygous *XPD* mutations identified in a COFS syndrome patient were a *R616W* null mutation previously observed in an XP patient and a unique *D681N*

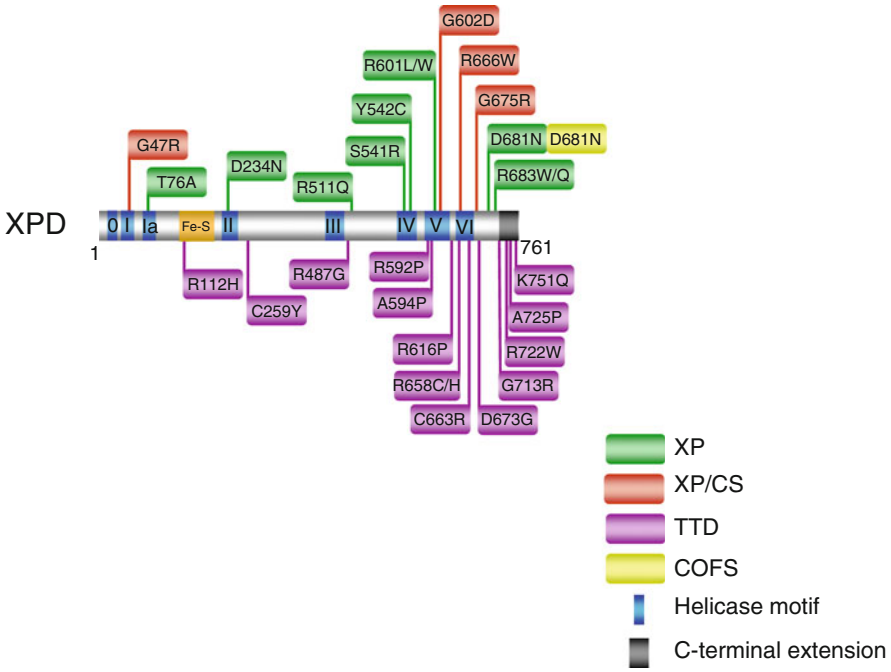

Fig. 6.2 Clinically relevant missense mutations in XPD helicase responsible for Xeroderma pigmentosum, Xeroderma pigmentosum combined with Cockayne syndrome, Trichothiodystrophy, and COFS Syndrome. See text for details. For discussion of *XPD* mutations and genetic heterogeneity, see ref. [13]. *XPD-D681N* mutation is associated with XP and COFS syndrome

mutation residing on the C-terminal side of motif VI [56] (Fig. 6.2). The aspartic acid (D681) is highly conserved in all known *XPD* genes. UV survival assays performed with COFS syndrome patient cells showed UV sensitivity comparable to that of cells from an XP-A patient with severe XP. It is unclear how the *XPD-D681N* mutation can result in distinct clinical phenotypes of COFS syndrome vs. XP. The wide spectrum of *XPD* missense mutations resulting in heterogeneity in clinical phenotype prompt continued interest to characterize the molecular and cellular defects of XPD variants to acquire a better understanding of the relevant diseases.

FANCJ Missense Mutations

The great majority of *FANCJ* missense mutations genetically linked to FA or associated with breast cancer reside in the N-terminal portion of the protein where the helicase core domain is located (Fig. 6.3), suggesting that ATP-dependent DNA unwinding by FANCJ is required for its function in the FA pathway of DNA repair and its involvement as a tumor suppressor. The requirement of FANCJ helicase

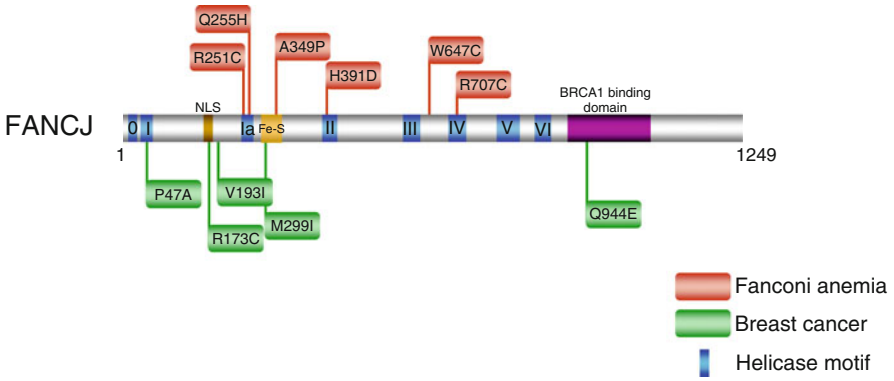

Fig. 6.3 Clinically relevant missense mutations in FANCJ helicase responsible for Fanconi Anemia complementation group J and associated with breast cancer. See text for details. For a comprehensive listing of *FANCJ* mutations, see The Rockefeller University-Fanconi anemia mutation database www.rockefeller.edu/fanconi/mutate; also see ref. [18]

activity for proper operation of the FA pathway is consistent with genetic complementation studies in human cells which show that cross-link resistance is dependent on catalytically active FANCJ protein [57].

A FANCJ missense mutation linked to FA of particular interest is an alanine-to-proline substitution in the Fe-S domain at residue 349 immediately adjacent to a highly conserved cysteine that is important for binding an iron atom [58] (Fig. 6.4). Inheritance of the paternal *FANCJ-A349P* missense allele and a maternal truncating *R798X* allele resulted in phenotypic abnormalities, including intrauterine growth failure and death as a stillborn fetus with a gestational age of 22 weeks [58]. Biochemical analysis of purified recombinant FANCJ-A349P protein demonstrated that it was defective in coupling ATP-dependent DNA translocase activity to unwinding duplex DNA or displacing proteins bound to DNA [59] (Fig. 6.4). From a genetic standpoint, expression of the *FANCJ-A349P* mutant allele failed to rescue sensitivity of FANCJ null cells to a DNA cross-linking agent or the G-quadruplex (G4) binding drug telomestatin, indicating that it was unable to perform its role in ICL repair or resolution of G4 DNA [59]. In addition, expression of the *FANCJ-A349P* allele in a wild-type background exerted a dominant negative effect on resistance to DNA cross-linkers or telomestatin. Thus, the ability of FANCJ to couple ATP hydrolysis and DNA translocase activity to higher order functions such as unwinding structured nucleic acids or stripping protein from DNA is essential for its biological roles.

There is one FANCJ missense mutation, Q944E, identified in a breast cancer patient that is positioned outside the helicase core domain (Fig. 6.3). The Q944E mutation resides in the BRCA1 binding domain located in the C-terminal region of FANCJ (Fig. 6.2). Given the relatively close linear proximity of residue Q944 to S990, the site for FANCJ phosphorylation required for the physical interaction between FANCJ and BRCA1 [60], it will be of interest to determine if the BRCA1

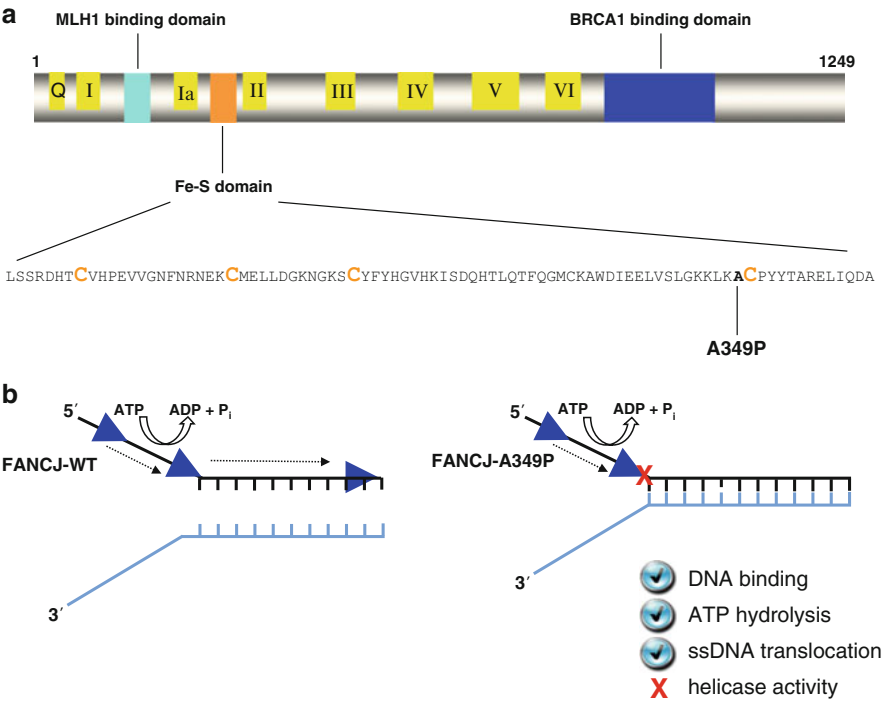

Fig. 6.4 An FA complementation group J patient mutation (A349P) in the conserved Fe-S domain uncouples DNA ATPase and translocase activities from strand separation (helicase) activity. (**a**) FANCJ protein with the conserved helicase core domain, key protein interaction domains, and the Fe-S cluster. The conserved helicase motifs are indicated by *yellow boxes*, and the protein interaction domains for MLH1 and BRCA1 are shown by *aqua green* and *blue boxes*, respectively. The expanded Fe-S domain shows the locations for conserved cysteine residues in *orange*, and the A349P missense mutation of a FANCJ patient in *bold*. (**b**) The purified recombinant FANCJ-A349P protein fails to couple ATPase and single-stranded DNA translocase activity to unwinding duplex DNA. See text and ref. [59] for details

binding to FANCJ is affected by the Q944E mutation. Such a FANCJ missense mutation may influence the molecular mechanism employed for DNA repair, as it was recently shown that disruption of the FANCJ-BRCA1 interaction blocks DNA repair by homologous recombination and promotes polη-dependent bypass [61].

DDX11 (ChlR1) Single Amino Acid Deletion Mutation

Mutations in the ChlR1 helicase (also named DDX11) are genetically linked to the chromosomal instability disorder WABS [22]. The WABS patient is characterized by a compound heterozygous *K897del* mutation in trans with a maternally inherited splice site mutation in an intron that leads to a truncated protein, leading to

nonsense-mediated decay of the maternal allele and monoallelic expression of the *K897del*-containing paternal allele. The *K897del* mutation results in a single amino acid deletion of a lysine residue that resides ten amino acids from the C-terminus of the protein. The endogenous hChlR1-K897del protein was poorly detected by immunoblot analysis of lysates from fibroblasts or lymphoblasts of the affected individual [22]. Cells from the patient exhibit chromosomal instability characterized by sister cohesion defects, chromosomal breakage, and sensitivity to the DNA cross-linking agent mitomycin and topoisomerase inhibitor camptothecin. Based on the cellular phenotypes, it was suggested that WABS is a unique disease with cellular features of both FA and the cohesinopathy Roberts syndrome.

Biochemical analysis of the purified recombinant ChlR1 protein demonstrated that it possesses a DNA-dependent ATPase activity and a 5′–3′ helicase activity [62, 63]. The purified recombinant hChlR1-K897del protein was dramatically inhibited for DNA binding and DNA-dependent ATPase activity compared to the wild-type recombinant ChlR1 protein [64], suggesting an important role of the extreme C-terminus of the protein for its stable interaction with nucleic acid. Further cellular and biochemical studies are likely to yield insight to the proposed role of the ChlR1 helicase to allow smooth replication fork progression necessary for proper sister chromatid cohesion during mitosis [62]. The strong preference of ChlR1 to unwind G4 DNA may be important for stability at particular genomic loci [64]. Greater insight to the disease will likely be gained from more biochemical and genetic studies, including the identification and characterization of other mutant *ChlR1* alleles.

Disease-Causing Missense Mutations in RecQ DNA Helicases

BLM Missense Mutations

Inspection of the clinical spectrum of Bloom's syndrome patient missense mutations reveals that the ones identified to date reside in the helicase core domain or the adjacent RecQ C-terminal region (RQC) [65] (Fig. 6.5). This mutational pattern strongly suggests that BLM helicase activity is required for suppression of the BS disease phenotype, a result that is consistent with the observation that expression of an engineered Walker A box (motif I) catalytically inactive BLM protein failed to complement the genomic instability of BS cells; moreover, the helicase-dead BLM protein exerted a dominant negative effect on cell viability in a wild-type background [66]. In fact, all of the BS patient-derived helicase domain mutant proteins that have been biochemically characterized show defects in ATP or DNA binding, which result in low or no detectable helicase activity [66–69].

The conserved RQC region in BLM, found in many RecQ helicases, consists of a Zn^{2+} binding domain and a winged helix domain. Two of the cysteine residues (C1036 and C1055) residing in the RQC region and responsible for binding Zn^{2+} are mutated in BS (Fig. 6.5). Five different amino acids substitutions (S, G, R, V, and Y)

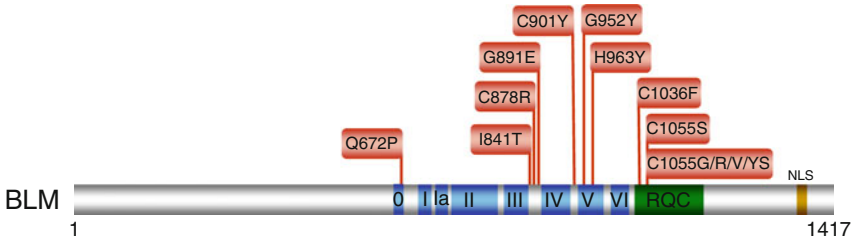

Fig. 6.5 Clinically relevant missense mutations in BLM helicase responsible for Bloom's syndrome. See text for details. For a comprehensive listing of *BLM* mutations, see The Bloom's Syndrome Registry www.med.cornell.edu/bsr/; also see ref. [65]

resulting from BLM patient mutations occur at C1055, suggesting that this particular locus in the BLM Zn^{2+} domain may be a hotspot for mutation and that the cysteine residue is highly important for BLM structure and function. Biochemical characterization of the purified recombinant BLM-C1055S mutant protein showed that it lacked ATPase and helicase activity [66, 67]. Expression of the BLM-C1055S mutant protein in vivo failed to rescue the p53-mediated apoptosis defect of BS fibroblasts [70]. Collectively, the location of the BLM missense mutations and their molecular analysis demonstrate that BLM helicase activity is required for its in vivo function to suppress BS phenotypes.

RECQL4 Missense Mutations

The RECQL4 helicase is distinct from other human RecQ helicases because three distinct genetic disorders can be attributed to mutations in the *RECQL4* gene: RTS, RAPADILINO, and BGS [36]. Unlike BLM, missense mutations for all three RECQL4 diseases have been identified in regions outside the conserved helicase domain shared by the other RecQ helicases [36] (Fig. 6.6). RTS missense mutations are found in the C-terminal region, N-terminal region, and the helicase core domain. Only two RAPADILINO missense mutations have been reported, one in the N-terminal region and one in the helicase core domain. For BGS, a single patient missense mutation (R1021W) is known that resides in the C-terminal region. Interestingly, the C-terminal *R1021W* mutation was genetically linked to both BGS and RTS. The effects of the *R1021W* mutation, as well as all of the other mutations in the *RECQL4* gene, on the biochemical functions of the RECQ4 helicase protein have not yet been determined.

WRN Missense Mutations

The discovery that mutations in the *WRN* gene are linked to a premature aging disorder [71] sparked a tremendous amount of interest in understanding the

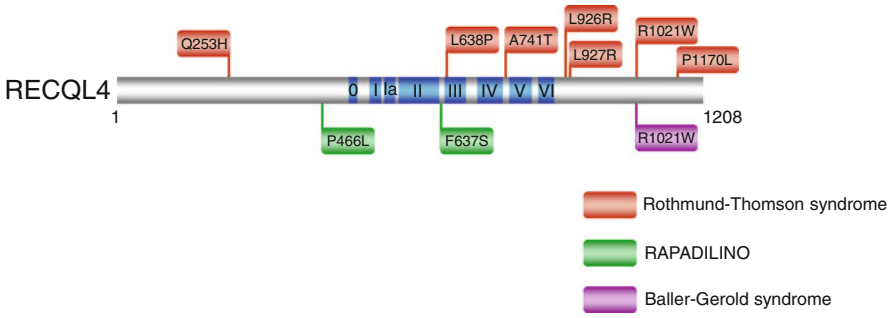

Fig. 6.6 Clinically relevant missense mutations in RECQL4 helicase responsible for Rothmund-Thomson syndrome, Baller-Gerold syndrome, and RAPADILINO. See text for details. For comprehensive listing of *RECQL4* mutations, see ref. [36]. RECQL4-R1021W is associated with both RTS and BGS

pathological basis for the disease on a molecular level; however, the clinical spectrum of WS mutations was rather uninformative because those identified resulted in truncated proteins. Since the nuclear localization sequence (NLS) of WRN protein residing in the extreme C-terminus, it would be predicted that these WRN protein fragments would fail to localize to the nucleus where WRN is required to preserve genomic stability [72]. However, more recently a small number of *WRN* missense mutations have been identified (Fig. 6.6). One of these, the *M1350R* missense mutation would be predicted to interfere with the ability of the WRN protein to effectively localize to nuclei since it resides immediately N-terminal to the NLS of WRN [73].

Two missense mutations reside in the N-terminal exonuclease domain of WRN were shown to result in WRN protein instability [74]. From a research standpoint, this is unfortunate because if the mutant WRN proteins had been selectively inactivated for exonuclease function, they may have been useful for understanding the molecular importance of that catalytic function. Two additional WRN missense mutations were found in the helicase domain, one in the Walker A box (motif I) (G574R) [73] just three amino acids away from the invariant lysine residue implicated in nucleotide binding and the other (R637W) [75] very near helicase motif V. Although not yet biochemically characterized, these two helicase core domain mutants would be predicted to interfere with normal ATPase and helicase function. If this were true, they may constitute separation of function mutations that would be valuable for assessing the relative importance of WRN helicase vs. exonuclease activity to suppress the cellular phenotypes associated with WS. Genetic and biochemical studies suggest the dual importance of balanced and concerted WRN helicase and exonuclease activities [76–78]; however, there is still much to learn precisely how WRN helicase or exonuclease activities suppress the disease phenotypes of WS.

Disease-Causing Missense Mutations in the XPB and Twinkle DNA Helicases

XPB Missense Mutations

The *XPB* gene encodes a DNA helicase with opposite polarity to that of XPD that is also found in the TFIIH complex, and *XPB* mutations can lead to multiple clinical disorders including XP/CS, XP with neurological abnormalities, and TTD [13]. In contrast to XPD where helicase activity is indispensable for NER, only XPB ATPase is necessary for the pathway to remove bulky lesions and UV photoproducts. XPB ATPase activity is also necessary for DNA opening for transcription to occur, but its helicase activity is important for promoter escape during transcription (for review, see ref. [15]). It is generally believed that the phenotypic heterogeneity of XPB is attributed to missense mutations which only partially affect XPB biochemical and cellular function in mild XP/CS, whereas severe XP/CS is associated with nonsense mutations in both *XPB* alleles, resulting in altered and reduced XPB protein [79]. A causative mutation in the XPB helicase resulting in a single amino acid substitution (T119P) in the N-terminus of the protein prior to the conserved helicase motifs was identified in a patient with mild versions of both TTD and photosensitivity [80]. Cellular studies from the Sarasin lab demonstrated that the *XPB-T119P* allele is associated with moderately defective DNA repair [81]. This is in contrast to *XPB-F99S* allele (also located in the N-terminus) of an XP/CS patient which is profoundly reduced in its DNA repair function [81]. Interestingly, both the T119P and F99S mutations in XPB do not impair TFIIH helicase activity [15]; however, the F99S substitution was shown to impair the interaction of XPB with p52, one of the subunits of the TFIIH complex [55]. Collectively, the studies of TFIIH and clinical spectrum of mutations in the XPB and XPD helicases have helped to dissect the complex heterogeneity of DNA repair-transcription syndromes.

Twinkle Missense Mutations

As mentioned earlier, missense mutations in the human *C10orf2* mitochondrial helicase gene encoding Twinkle DNA helicase are linked to several neuromuscular degenerative disorders. Expression of patient-derived Twinkle mutant proteins in normal cells or transgenic mice led to the accumulation of mitochondrial DNA replication intermediates and mitochondrial DNA depletion [82–84], consistent with the idea that dysfunctional Twinkle helicase can cause mitochondrial replication forks to stall. The reduction in Twinkle helicase activity for those variants that were examined correlated to the extent of mitochondrial DNA depletion and accumulation of replication intermediates [82]. Biochemical analysis of 20 disease variants of the human mitochondrial DNA helicase showed that the mutations are quite

heterogeneous in terms of their molecular effects on ATPase and helicase function as well as effects in some cases on protein stability [85]. All 20 mutant Twinkle variants retained at least partial helicase activity, leading the authors to propose that these defects are consistent with the delayed presentation of mitochondrial diseases associated with the *c10orf2* mutations.

Recent Advances and Research Directions for DNA Helicases Implicated in Disease

The helicase field is moving at a brisk pace, with the development of new technologies and a greater understanding of their biological roles. In the following section, we will highlight some interesting developments from our viewpoint. These emerging stories, as well as others discussed in the accompanying chapters, convey a very exciting era for the scientific community beyond the scope of DNA metabolism because there are rippling implications for the fields of aging, disease, and cancer.

Communication Between Redox Active DNA Repair Proteins

Nearly all DNA repair pathways share a few common steps: (1) initial detection of a DNA lesion; (2) processing of the damaged DNA nucleotide/strand; (3) removal of the damaged nucleotide/strand; (4) replacement of the damaged nucleotide/strand with correct nucleotide/sequence; (5) sealing the nick(s) by ligation. Of these steps, initial detection of the lesion is critical and can be rate-limiting due to low copy number of DNA damage recognition proteins and lack of preferential DNA binding affinity for the lesion compared to undamaged sequence. Recent experimental evidence supports a model that DNA charge transport is a signaling mechanism for the recruitment of redox active DNA repair proteins to the vicinity of DNA damage ([86, 87], and for review see ref. [88]). In the latest development, Sontz et al. [89] provide experimental evidence that coordinated DNA charge transport between DNA repair proteins with redox active Fe-S clusters, the XPD NER helicase and EndoIII base excision DNA glycosylase, can occur to enable efficient redistribution of the repair proteins to the location of DNA damage within a vast excess of undamaged nucleotides. Thus, DNA repair proteins (or proteins involved in other aspects of DNA metabolism such as replication or gene expression) conventionally thought to operate in distinct pathways might collaborate with each other in an unexpected way by their ability to participate in DNA charge transport chemistry. Although there is evidence for cross-talk between DNA repair pathways and also with replication

[90–93], the ability of redox active proteins to collaborate by DNA charge transport broadens the scope of possibilities since the proteins do not necessarily need to physically interact with one another. This is highly provocative for the potential synergy that might exist between redox active DNA interacting proteins that influence diverse pathways previously thought to function independently of one another. Research that further explores the collaboration between proteins able to perform DNA charge transport will likely have important implications for molecular gerontology and cancer biology.

Coordination of End-Processing Proteins in Double Strand Break Repair Resection

DSBs can be highly poisonous and lethal to cells; therefore, several DNA repair pathways including nonhomologous end-joining and homologous recombination exist to join ends back together again. In replicating cells, the preferred mechanism of DSB repair is by homologous recombination because it occurs with high fidelity, using the sister chromatid duplex as a template. Based on experimental evidence, BLM is implicated in an early stage of DSB repair in which strand resection from a DNA end occurs to provide a 3′ single-stranded DNA tail for RAD51-mediated strand invasion into recipient duplex [32, 94, 95]. Strand resection is much more complex than previously thought, and requires a battalion of helicases, nucleases, DNA binding proteins, and additional accessory factors. The BLM helicase promotes access of the DNA end to either DNA2 or EXO-1, enabling processive catalytic removal of one strand to produce the 3′ single-stranded DNA tail.

Another layer of complexity for the involvement of BLM in strand resection was suggested by the discovery that BLM interacts with FANCJ [96], which is associated with BRCA1, a tumor suppressor molecule implicated in DSB repair [19]. FANCJ-deficient cells have a defect in DSB-induced HR and show delayed resolution of DSBs following ionizing radiation [97]. Moreover, FANCJ and certain other HR proteins function downstream of FANCD2/I mono-ubiquitination in ICL repair to presumably repair the processed DNA cross-link by an HR-mediated pathway. We propose a model in which strand resection is facilitated by FANCJ and BLM helicases translocating on opposite strands of the broken double-stranded DNA end to promote access to structure-specific nucleases (EXO-1, DNA2) [98]. The FANCJ-BLM partnership may facilitate resection at chemically modified blocked DNA ends or through G-rich sequences prone to form G-quadruplex (G4) structures. This model for the dual collaboration of FANCJ and BLM in DSB repair can be tested by a combination of genetic and biochemical approaches. DNA end resection assays in a reconstituted system with chromatinized templates may help to elucidate the functional importance of the FANCJ-BLM interaction in DSB repair in a biological context.

Structural Determinants of XPD Helicase Function and Translocation Polarity

Recent progress in understanding the molecular architecture of Fe-S cluster DNA helicases has come from several labs working on archaeal XPD proteins. This effort began with the discovery that XPD bears an Fe-S cluster metal binding site essential for its DNA unwinding activity, but not necessary for binding single-stranded DNA or ATP hydrolysis [99]. Crystal structures solved independently by three research groups confirmed the existence of a novel Fe-S domain [100–102]. The XPD structure contains two Rad51/RecA-like domains (HD1 and HD2) with two additional domains, the Fe-S and Arch domains, inserted between adjacent β-strands of the central β-sheet of HD1. ATP binding and hydrolysis controls the conformational state of the Fe-S and Arch domains in conjunction with the conserved helicase motifs that comprise the helicase core domain. The Fe-S domain was proposed to form a wedge with the nearby Arch domain to separate the DNA duplex as the enzyme translocates in an ATP-dependent manner. Mutations introduced to the Fe-S domain, including the conserved cysteines, abolished XPD helicase activity and/or destabilized tertiary structure [99, 100], attesting to the structural importance of the Fe-S domain. Biochemical studies demonstrated that the integrity of the XPD Fe-S domain is required for the proper folding and structural stability, and is important for coupling ATP hydrolysis to unidirectional translocation [103]. Furthermore, the Fe-S cluster serves to stabilize elements of protein secondary structure and target the helicase to the single-stranded/double-stranded DNA junction [103].

The structure of XPD in complex with a short DNA fragment was recently reported [104]. This provided a working model for the mechanism of translocation by Fe-S cluster DNA helicases. The XPD-DNA crystal structure, combined with a mutational and biochemical analysis of XPD, revealed how the 5′–3′ directionality of translocation along DNA is achieved and suggested how the XPD enzyme might act upon a DNA substrate harboring a helix-distorting lesion susceptible to NER. These conclusions on how regulation of translocation polarity by XPD helicase is achieved were further supported by another very recent study using proteolytic DNA and mutational analysis of XPD [105]. Based on these two studies, it was suggested that Fe-S domain helicases achieve a polarity of ATP-driven translocation opposite to that of 3′–5′ helicases by conformational changes within the motor domain rather than binding single-stranded DNA with an opposite orientation. It is plausible that the Fe-S redox activity may provide an additional mechanism for FANCJ and other DNA repair molecules to communicate with each other and sense DNA-mediated charge transport such that they cooperate with each other to assemble and/or translocate with a defined polarity and in a regulated manner [106]; however, this hypothesis remains to be experimentally tested.

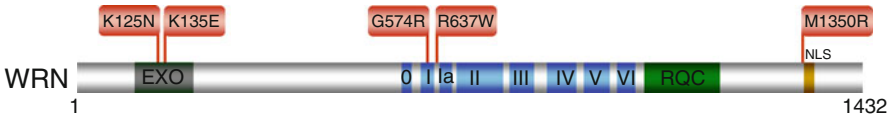

Fig. 6.7 Clinically relevant missense mutations in WRN helicase-nuclease responsible for Werner syndrome. See text for details. For a comprehensive listing of *WRN* mutations, see The International Registry of Werner Syndrome www.wernersyndrome.org; also see ref. [73]

Small Molecule Inhibitors of DNA Helicases

Understanding the precise molecular-genetic defects of helicase disorders in some cases such as the RecQ diseases can be challenging. Partial functional redundancy between DNA helicases as well as backup pathways make it difficult to establish cause and effect relationships between a helicase defect and biological outcome. Since DNA helicases provide essential functions in multiple steps of DNA damage response and repair pathways, it will be highly informative to precisely characterize their functions in vivo. This information will lead to new insight to their roles in prevention or correction of genomic DNA damage that is a causative force for cellular senescence and contributes to organismal decline associated with aging. Use of small molecules to target human helicases for inhibition (or activation) in a cell-based model system is a novel approach to the problem of assigning specific helicase functions in vivo. In addition to the new insight to the roles of helicases in DNA damage response and repair to prevent age-associated phenotypes, this work will also be informative for the development of anticancer strategies which target DNA repair proteins/processes [107].

Recently, a small molecule (NSC 19630) from the NCI Diversity Set was identified that inhibited WRN helicase activity, but not other DNA helicases tested, suggesting specificity [108]. Human cells exposed to NSC 19630 were dramatically impaired in their growth and proliferation, and displayed elevated apoptosis in a WRN-dependent manner, suggesting an effect of the small molecule that mimicked expression of a helicase-dead protein. Furthermore, cellular exposure to the WRN helicase inhibitor resulted in elevated γ-H2AX and proliferating cell nuclear antigen (PCNA) foci, and delayed S-phase progression, consistent with the accumulation of stalled replication forks. Exposure to NSC 19630 sensitized cancer cells to agents that induce replication stress or interfere with DNA repair. We anticipate that the WRN helicase inhibitor molecule may be helpful in understanding WRN-mediated pathway(s) important for the response to DNA damage and replication stress (Fig. 6.7).

Summary

In this chapter, we have attempted to provide an overview of hereditary helicase disorders, with a particular emphasis on clinically relevant missense mutations as these may prove to be valuable in understanding pathway dysfunction. In addition,

we have highlighted some hot topics in helicase research that we believe will be important for future studies. Clearly, progress in understanding the biochemical and genetic functions of RecQ and Fe-S cluster helicases will serve as a springboard for new investigations. In addition, the recent progress in understanding the molecular basis for Twinkle mitochondrial helicase disorders has created a lot of excitement in the field. Contributions from an increasing number of scientists will continue to unveil new insights to the roles of DNA helicases in suppressing genomic instability, cancer, and age-related diseases.

Acknowledgments This research was supported by the Intramural Research Program of the NIH, National Institute on Aging and the Fanconi Anemia Research Fund (RMB). We apologize to helicase researchers whose work was not cited due to space limitations.

References

1. Lohman TM, Tomko EJ, Wu CG. Non-hexameric DNA helicases and translocases: mechanisms and regulation. Nat Rev Mol Cell Biol. 2008;9:391–401.
2. Singleton MR, Dillingham MS, Wigley DB. Structure and mechanism of helicases and nucleic acid translocases. Annu Rev Biochem. 2007;76:23–50.
3. Brosh Jr RM, Bohr VA. Human premature aging, DNA repair and RecQ helicases. Nucleic Acids Res. 2007;35:7527–44.
4. Lohman TM, Bjornson KP. Mechanisms of helicase-catalyzed DNA unwinding. Annu Rev Biochem. 1996;65:169–214.
5. Patel SS, Donmez I. Mechanisms of helicases. J Biol Chem. 2006;281:18265–8.
6. Pyle AM. Translocation and unwinding mechanisms of RNA and DNA helicases. Annu Rev Biophys. 2008;37:317–36.
7. Bernstein KA, Gangloff S, Rothstein R. The RecQ DNA helicases in DNA repair. Annu Rev Genet. 2010;44:393–417.
8. Dillingham MS, Superfamily I. helicases as modular components of DNA-processing machines. Biochem Soc Trans. 2011;39:413–23.
9. Singh DK, Ghosh AK, Croteau DL, Bohr VA. RecQ helicases in DNA double strand break repair and telomere maintenance. Mutat Res. 2012;736:15–24.
10. Wu Y, Suhasini AN, Brosh RM. Welcome the family of FANCJ-like helicases to the block of genome stability maintenance proteins. Cell Mol Life Sci. 2009;66:1209–22.
11. White MF. Structure, function and evolution of the XPD family of iron-sulfur-containing 5′–>3′ DNA helicases. Biochem Soc Trans. 2009;37:547–51.
12. White MF, Dillingham MS. Iron-sulphur clusters in nucleic acid processing enzymes. Curr Opin Struct Biol. 2012;22:94–100.
13. Digiovanna JJ, Kraemer KH. Shining a light on xeroderma pigmentosum. J Invest Dermatol. 2012;132:785–96.
14. Egly JM, Coin F. A history of TFIIH: two decades of molecular biology on a pivotal transcription/repair factor. DNA Repair (Amst). 2011;10:714–21.
15. Oksenych V, Coin F. The long unwinding road: XPB and XPD helicases in damaged DNA opening. Cell Cycle. 2010;9:90–6.
16. Crossan GP, Patel KJ. The Fanconi anaemia pathway orchestrates incisions at sites of cross-linked DNA. J Pathol. 2012;226:326–37.
17. Deans AJ, West SC. DNA interstrand crosslink repair and cancer. Nat Rev Cancer. 2011;11:467–80.
18. Cantor SB, Guillemette S. Hereditary breast cancer and the BRCA1-associated FANCJ/BACH1/BRIP1. Future Oncol. 2011;7:253–61.

19. Cantor SB, Bell DW, Ganesan S, et al. BACH1, a novel helicase-like protein, interacts directly with BRCA1 and contributes to its DNA repair function. Cell. 2001;105:149–60.
20. London TB, Barber LJ, Mosedale G, et al. FANCJ is a structure-specific DNA helicase associated with the maintenance of genomic G/C tracts. J Biol Chem. 2008;283:36132–9.
21. Wu Y, Shin-Ya K, Brosh Jr RM. FANCJ helicase defective in Fanconia anemia and breast cancer unwinds G-quadruplex DNA to defend genomic stability. Mol Cell Biol. 2008;28:4116–28.
22. van der LP, Chrzanowska KH, Godthelp BC, et al. Warsaw breakage syndrome, a cohesinopathy associated with mutations in the XPD helicase family member DDX11/ChlR1. Am J Hum Genet. 2010;86:262–6.
23. Skibbens RV. Chl1p, a DNA helicase-like protein in budding yeast, functions in sister-chromatid cohesion. Genetics. 2004;166:33–42.
24. Inoue A, Li T, Roby SK, et al. Loss of ChlR1 helicase in mouse causes lethality due to the accumulation of aneuploid cells generated by cohesion defects and placental malformation. Cell Cycle. 2007;6:1646–54.
25. Parish JL, Rosa J, Wang X, Lahti JM, Doxsey SJ, Androphy EJ. The DNA helicase ChlR1 is required for sister chromatid cohesion in mammalian cells. J Cell Sci. 2006;119:4857–65.
26. Inoue A, Hyle J, Lechner MS, Lahti JM. Mammalian ChlR1 has a role in heterochromatin organization. Exp Cell Res. 2011;317:2522–35.
27. Ellis NA, Groden J, Ye TZ, et al. The Bloom's syndrome gene product is homologous to RecQ helicases. Cell. 1995;83:655–66.
28. Chaganti RS, Schonberg S, German J. A manyfold increase in sister chromatid exchanges in Bloom's syndrome lymphocytes. Proc Natl Acad Sci USA. 1974;71:4508–12.
29. Bachrati CZ, Hickson ID. Dissolution of double Holliday junctions by the concerted action of BLM and topoisomerase IIIalpha. Methods Mol Biol. 2009;582:91–102.
30. Wu L, Hickson ID. The Bloom's syndrome helicase suppresses crossing over during homologous recombination. Nature. 2003;426:870–4.
31. Chu WK, Hanada K, Kanaar R, Hickson ID. BLM has early and late functions in homologous recombination repair in mouse embryonic stem cells. Oncogene. 2010;29:4705–14.
32. Nimonkar AV, Genschel J, Kinoshita E, et al. BLM-DNA2-RPA-MRN and EXO1-BLM-RPA-MRN constitute two DNA end resection machineries for human DNA break repair. Genes Dev. 2011;25:350–62.
33. Chan KL, Palmai-Pallag T, Ying S, Hickson ID. Replication stress induces sister-chromatid bridging at fragile site loci in mitosis. Nat Cell Biol. 2009;11:753–60.
34. Monnat Jr RJ. Human RECQ helicases: roles in DNA metabolism, mutagenesis and cancer biology. Semin Cancer Biol. 2010;20:329–39.
35. Rossi ML, Ghosh AK, Bohr VA. Roles of Werner syndrome protein in protection of genome integrity. DNA Repair (Amst). 2010;9:331–44.
36. Larizza L, Roversi G, Volpi L. Rothmund-Thomson syndrome. Orphanet J Rare Dis. 2010;5:2.
37. Van Maldergem L, Siitonen HA, Jalkh N, et al. Revisiting the craniosynostosis-radial ray hypoplasia association: Baller-Gerold syndrome caused by mutations in the RECQL4 gene. J Med Genet. 2006;43:148–52.
38. Singh DK, Karmakar P, Aamann M, et al. The involvement of human RECQL4 in DNA double-strand break repair. Aging Cell. 2010;9:358–71.
39. Ghosh AK, Rossi ML, Singh DK, et al. RECQL4, the protein mutated in Rothmund-Thomson syndrome, functions in telomere maintenance. J Biol Chem. 2012;287:196–209.
40. Croteau DL, Rossi ML, Canugovi C, et al. RECQL4 localizes to mitochondria and preserves mitochondrial DNA integrity. Aging Cell. 2012;11(3):456–66.
41. De S, Kumari J, Mudgal R, et al. RECQL4 is essential for the transport of p53 to mitochondria in normal human cells in the absence of exogenous stress. J Cell Sci. 2012;125:2509–22.
42. Sharma S, Doherty KM, Brosh Jr RM. Mechanisms of RecQ helicases in pathways of DNA metabolism and maintenance of genomic stability. Biochem J. 2006;398:319–37.

43. Sharma S, Stumpo DJ, Balajee AS, et al. RECQL, a member of the RecQ family of DNA helicases, suppresses chromosomal instability. Mol Cell Biol. 2007;27:1784–94.
44. Sharma S, Brosh Jr RM. Human RECQ1 is a DNA damage responsive protein required for genotoxic stress resistance and suppression of sister chromatid exchanges. PLoS One. 2007;2:e1297.
45. Thangavel S, Mendoza-Maldonado R, Tissino E, et al. The human RECQ1 and RECQ4 helicases play distinct roles in DNA replication initiation. Mol Cell Biol. 2010;30:1382–96.
46. Aygun O, Svejstrup J, Liu Y. A RECQ5-RNA polymerase II association identified by targeted proteomic analysis of human chromatin. Proc Natl Acad Sci USA. 2008;105:8580–4.
47. Kanagaraj R, Huehn D, MacKellar A, et al. RECQ5 helicase associates with the C-terminal repeat domain of RNA polymerase II during productive elongation phase of transcription. Nucleic Acids Res. 2010;38:8131–40.
48. Ramamoorthy M, Tadokoro T, Rybanska I, et al. RECQL5 cooperates with topoisomerase II alpha in DNA decatenation and cell cycle progression. Nucleic Acids Res. 2012;40:1621–35.
49. Copeland WC. Defects in mitochondrial DNA replication and human disease. Crit Rev Biochem Mol Biol. 2012;47:64–74.
50. Korhonen JA, Gaspari M, Falkenberg M. TWINKLE Has 5′ -> 3′ DNA helicase activity and is specifically stimulated by mitochondrial single-stranded DNA-binding protein. J Biol Chem. 2003;278:48627–32.
51. Sen D, Nandakumar D, Tang GQ, Patel SS. The human mitochondrial DNA helicase TWINKLE is both an unwinding and an annealing helicase. J Biol Chem. 2012;287(18):14545–56.
52. Ziebarth TD, Gonzalez-Soltero R, Makowska-Grzyska MM, Nunez-Ramirez R, Carazo JM, Kaguni LS. Dynamic effects of cofactors and DNA on the oligomeric state of human mitochondrial DNA helicase. J Biol Chem. 2010;285:14639–47.
53. Dubaele S, De Proietti SL, Bienstock RJ, et al. Basal transcription defect discriminates between xeroderma pigmentosum and trichothiodystrophy in XPD patients. Mol Cell. 2003;11:1635–46.
54. Lehmann AR. XPD structure reveals its secrets. DNA Repair (Amst). 2008;7:1912–5.
55. Coin F, Oksenych V, Egly JM. Distinct roles for the XPB/p52 and XPD/p44 subcomplexes of TFIIH in damaged DNA opening during nucleotide excision repair. Mol Cell. 2007;26:245–56.
56. Graham Jr JM, Nyane-Yeboa K, Raams A, et al. Cerebro-oculo-facio-skeletal syndrome with a nucleotide excision-repair defect and a mutated XPD gene, with prenatal diagnosis in a triplet pregnancy. Am J Hum Genet. 2001;69:291–300.
57. Peng M, Litman R, Xie J, Sharma S, Brosh Jr RM, Cantor SB. The FANCJ/MutLalpha interaction is required for correction of the cross-link response in FA-J cells. EMBO J. 2007;26:3238–49.
58. Levran O, Attwooll C, Henry RT, et al. The BRCA1-interacting helicase BRIP1 is deficient in Fanconi anemia. Nat Genet. 2005;37:931–3.
59. Wu Y, Sommers JA, Suhasini AN, et al. Fanconi anemia Group J mutation abolishes its DNA repair function by uncoupling DNA translocation from helicase activity or disruption of protein-DNA complexes. Blood. 2010;116:3780–91.
60. Yu X, Chini CC, He M, Mer G, Chen J. The BRCT domain is a phospho-protein binding domain. Science. 2003;302:639–42.
61. Xie J, Litman R, Wang S, et al. Targeting the FANCJ-BRCA1 interaction promotes a switch from recombination to poleta-dependent bypass. Oncogene. 2010;29:2499–508.
62. Farina A, Shin JH, Kim DH, et al. Studies with the human cohesin establishment factor, ChlR1. Association of ChlR1 with Ctf18-RFC and Fen1. J Biol Chem. 2008;283:20925–36.
63. Hirota Y, Lahti JM. Characterization of the enzymatic activity of hChlR1, a novel human DNA helicase. Nucleic Acids Res. 2000;28:917–24.
64. Wu Y, Sommers JA, Khan I, De Winter JP, Brosh Jr RM. Biochemical characterization of warsaw breakage syndrome helicase. J Biol Chem. 2012;287:1007–21.

65. German J, Sanz MM, Ciocci S, Ye TZ, Ellis NA. Syndrome-causing mutations of the BLM gene in persons in the Bloom's Syndrome Registry. Hum Mutat. 2007;28:743–53.
66. Neff NF, Ellis NA, Ye TZ, et al. The DNA helicase activity of BLM is necessary for the correction of the genomic instability of bloom syndrome cells. Mol Biol Cell. 1999;10:665–76.
67. Bahr A, De Graeve F, Kedinger C, Chatton B. Point mutations causing Bloom's syndrome abolish ATPase and DNA helicase activities of the BLM protein. Oncogene. 1998;17:2565–71.
68. Guo RB, Rigolet P, Zargarian L, Fermandjian S, Xi XG. Structural and functional characterizations reveal the importance of a zinc binding domain in Bloom's syndrome helicase. Nucleic Acids Res. 2005;33(10):3109–24.
69. Guo RB, Rigolet P, Ren H, et al. Structural and functional analyses of disease-causing missense mutations in Bloom syndrome protein. Nucleic Acids Res. 2007;35:6297–310.
70. Wang XW, Tseng A, Ellis NA, et al. Functional interaction of p53 and BLM DNA helicase in apoptosis. J Biol Chem. 2001;276:32948–55.
71. Yu CE, Oshima J, Fu YH, et al. Positional cloning of the Werner's syndrome gene. Science. 1996;272:258–62.
72. Suzuki T, Shiratori M, Furuichi Y, Matsumoto T. Diverged nuclear localization of Werner helicase in human and mouse cells. Oncogene. 2001;20:2551–8.
73. Friedrich K, Lee L, Leistritz DF, et al. WRN mutations in Werner syndrome patients: genomic rearrangements, unusual intronic mutations and ethnic-specific alterations. Hum Genet. 2010;128:103–11.
74. Huang S, Lee L, Hanson NB, et al. The spectrum of WRN mutations in Werner syndrome patients. Hum Mutat. 2006;27:558–67.
75. Uhrhammer NA, Lafarge L, Dos SL, et al. Werner syndrome and mutations of the WRN and LMNA genes in France. Hum Mutat. 2006;27:718–9.
76. Swanson C, Saintigny Y, Emond MJ, Monnat Jr RJ. The Werner syndrome protein has separable recombination and survival functions. DNA Repair (Amst). 2004;3:475–82.
77. Chen L, Huang S, Lee L, et al. WRN, the protein deficient in Werner syndrome, plays a critical structural role in optimizing DNA repair. Aging Cell. 2003;2:191–9.
78. Opresko PL, Otterlei M, Graakjaer J, et al. The Werner syndrome helicase and exonuclease cooperate to resolve telomeric D loops in a manner regulated by TRF1 and TRF2. Mol Cell. 2004;14:763–74.
79. Oh KS, Khan SG, Jaspers NG, et al. Phenotypic heterogeneity in the XPB DNA helicase gene (ERCC3): xeroderma pigmentosum without and with Cockayne syndrome. Hum Mutat. 2006;27:1092–103.
80. Weeda G, Eveno E, Donker I, et al. A mutation in the XPB/ERCC3 DNA repair transcription gene, associated with trichothiodystrophy. Am J Hum Genet. 1997;60:320–9.
81. Riou L, Zeng L, Chevallier-Lagente O, et al. The relative expression of mutated XPB genes results in xeroderma pigmentosum/Cockayne's syndrome or trichothiodystrophy cellular phenotypes. Hum Mol Genet. 1999;8:1125–33.
82. Goffart S, Cooper HM, Tyynismaa H, Wanrooij S, Suomalainen A, Spelbrink JN. Twinkle mutations associated with autosomal dominant progressive external ophthalmoplegia lead to impaired helicase function and in vivo mtDNA replication stalling. Hum Mol Genet. 2009;18:328–40.
83. Tyynismaa H, Mjosund KP, Wanrooij S, et al. Mutant mitochondrial helicase Twinkle causes multiple mtDNA deletions and a late-onset mitochondrial disease in mice. Proc Natl Acad Sci USA. 2005;102:17687–92.
84. Wanrooij S, Goffart S, Pohjoismaki JL, Yasukawa T, Spelbrink JN. Expression of catalytic mutants of the mtDNA helicase Twinkle and polymerase POLG causes distinct replication stalling phenotypes. Nucleic Acids Res. 2007;35:3238–51.
85. Longley MJ, Humble MM, Sharief FS, Copeland WC. Disease variants of the human mitochondrial DNA helicase encoded by C10orf2 differentially alter protein stability, nucleotide hydrolysis, and helicase activity. J Biol Chem. 2010;285:29690–702.
86. Boal AK, Genereux JC, Sontz PA, Gralnick JA, Newman DK, Barton JK. Redox signaling between DNA repair proteins for efficient lesion detection. Proc Natl Acad Sci USA. 2009;106:15237–42.

87. Romano CA, Sontz PA, Barton JK. Mutants of the base excision repair glycosylase, endonuclease III: DNA charge transport as a first step in lesion detection. Biochemistry. 2011;50:6133–45.
88. Merino EJ, Boal AK, Barton JK. Biological contexts for DNA charge transport chemistry. Curr Opin Chem Biol. 2008;12:229–37.
89. Sontz PA, Mui TP, Fuss JO, Tainer JA, Barton JK. DNA charge transport as a first step in coordinating the detection of lesions by repair proteins. Proc Natl Acad Sci USA. 2012;109:1856–61.
90. Constantinou A. Rescue of replication failure by Fanconi anaemia proteins. Chromosoma. 2012;121:21–36.
91. Hakem R. DNA-damage repair; the good, the bad, and the ugly. EMBO J. 2008;27:589–605.
92. Lagerwerf S, Vrouwe MG, Overmeer RM, Fousteri MI, Mullenders LH. DNA damage response and transcription. DNA Repair (Amst). 2011;10:743–50.
93. Wilson III DM, Seidman MM. A novel link to base excision repair? Trends Biochem Sci. 2010;35:247–52.
94. Gravel S, Chapman JR, Magill C, Jackson SP. DNA helicases Sgs1 and BLM promote DNA double-strand break resection. Genes Dev. 2008;22:2767–72.
95. Nimonkar AV, Ozsoy AZ, Genschel J, Modrich P, Kowalczykowski SC. Human exonuclease 1 and BLM helicase interact to resect DNA and initiate DNA repair. Proc Natl Acad Sci USA. 2008;105:16906–11.
96. Suhasini AN, Rawtani NA, Wu Y, et al. Interaction between the helicases genetically linked to Fanconi anemia group J and Bloom's syndrome. EMBO J. 2011;30:692–705.
97. Litman R, Peng M, Jin Z, et al. BACH1 is critical for homologous recombination and appears to be the Fanconi anemia gene product FANCJ. Cancer Cell. 2005;8:255–65.
98. Suhasini AN, Brosh Jr RM. Fanconi anemia and Bloom's syndrome crosstalk through FANCJ-BLM helicase interaction. Trends Genet. 2012;28:7–13.
99. Rudolf J, Makrantoni V, Ingledew WJ, Stark MJ, White MF. The DNA repair helicases XPD and FancJ have essential Iron-Sulfur domains. Mol Cell. 2006;23:801–8.
100. Fan L, Fuss JO, Cheng QJ, et al. XPD helicase structures and activities: insights into the cancer and aging phenotypes from XPD mutations. Cell. 2008;133:789–800.
101. Liu H, Rudolf J, Johnson KA, et al. Structure of the DNA repair helicase XPD. Cell. 2008;133:801–12.
102. Wolski SC, Kuper J, Hanzelmann P, et al. Crystal structure of the FeS cluster-containing nucleotide excision repair helicase XPD. PLoS Biol. 2008;6:e149.
103. Pugh RA, Honda M, Leesley H, et al. The iron-containing domain is essential in Rad3 helicases for coupling of ATP hydrolysis to DNA translocation and for targeting the helicase to the single-stranded DNA-double-stranded DNA junction. J Biol Chem. 2008;283:1732–43.
104. Kuper J, Wolski SC, Michels G, Kisker C. Functional and structural studies of the nucleotide excision repair helicase XPD suggest a polarity for DNA translocation. EMBO J. 2011;31:494–502.
105. Pugh RA, Wu CG, Spies M. Regulation of translocation polarity by helicase domain 1 in SF2B helicases. EMBO J. 2011;31:503–14.
106. Wu Y, Brosh Jr RM. DNA helicase and helicase-nuclease enzymes with a conserved iron-sulfur cluster. Nucleic Acids Res. 2012;40(10):4247–60.
107. Aggarwal M, Brosh Jr RM. Hitting the bull's eye: novel directed cancer therapy through helicase-targeted synthetic lethality. J Cell Biochem. 2009;106:758–63.
108. Aggarwal M, Sommers JA, Shoemaker RH, Brosh Jr RM. Inhibition of helicase activity by a small molecule impairs Werner syndrome helicase (WRN) function in the cellular response to DNA damage or replication stress. Proc Natl Acad Sci USA. 2011;108:1525–30.

Chapter 7
The Helicase–Primase Complex as a Target for Effective Herpesvirus Antivirals

Hugh J. Field and Ian Mickleburgh

Abstract Herpes simplex virus and varicella-zoster virus have been treated for more that half a century using nucleoside analogues. However, there is still an unmet clinical need for improved herpes antivirals. The successful compounds, acyclovir; penciclovir and their orally bioavailable prodrugs valaciclovir and famciclovir, ultimately block virus replication by inhibiting virus-specific DNA-polymerase. The helicase–primase (HP) complex offers a distinctly different target for specific inhibition of virus DNA synthesis. This review describes the synthetic programmes that have already led to two HP-inhibitors (HPI) that have commenced clinical trials in man. One of these (known as AIC 316) continues in clinical development to date. The specificity of HPI is reflected by the ability to select drug-resistant mutants. The role of HP-antiviral resistance will be considered and how the study of cross-resistance among mutants already shows subtle differences between compounds in this respect. The impact of resistance on the drug development in the clinic will also be considered. Finally, herpesvirus latency remains as the most important barrier to a therapeutic cure. Whether or not helicase primase inhibitors alone or in combination with nucleoside analogues can impact on this elusive goal remains to be seen.

Herpesvirus Chemotherapy—A Historical Perspective

Since the advent of antiviral chemotherapy, several herpesviruses have been successfully treated. Indeed, the successful treatment of herpes simplex eye disease (herpes keratitis) was among the first proofs-of-principle that a virus infection could

H.J. Field (✉)
Queens' College, Cambridge, UK
e-mail: hjf10@cam.ac.uk

I. Mickleburgh
Department of Biochemistry, University of Cambridge,
Cambridge, UK

M. Spies (ed.), *DNA Helicases and DNA Motor Proteins*, Advances in Experimental Medicine and Biology, DOI 10.1007/978-1-4614-5037-5_7,

Table 7.1 Features of herpseviruses important for the development of antivirals

Virus characteristics	Consequences for antiviral chemotherapy
Large double-stranded genome coding for more than 70 polypeptides including many enzyme functions	Many potential targets for inhibition of virus replication
Easy to culture	Easy to titrate in few days
Clear cytopathic effects in culture	Easy to screen for inhibitors of virus replication over relatively short time scale
Many well-characterised laboratory animal infection models available	Efficacy can be demonstrated *in vivo* at an early stage of drug development
Produce characteristic clinical signs	Clinical benefit readily measured
Extremely common with up to 100% infection rates in population	Potential market large for therapy and prevention
Establish latency with recurrent infection/ lesions	Stable market with long-term prospects

be treated with specific antiviral compounds. Since the early 1960s, the conditions of labial and ocular herpes caused by herpes simplex virus type 1 (HSV-1), genital herpes (HSV-2), chickenpox-shingles (varicella-zoster virus; VZV) and cytomegalovirus (CMV) infections in the immunocompromised have all been shown to respond to antiviral chemotherapy with considerable benefit to the patient. The likely reasons why members of the Herpesviridae were in the vanguard of the new discipline of antiviral research are listed (Table 7.1).

However, despite this early success, the current antiviral agents used to control herpesvirus infections do not provide ideal medication for a number of reasons that will be outlined below. Patients require better treatments and, from the pharmaceutical perspective, there remains a large potential market for improved herpesvirus antivirals. These should be more effective and/or more convenient for the patient or broaden the spectrum of treatable conditions. To date, the most successful compounds used to treat herpesvirus infections by specifically blocking virus replication, all work by interfering with virus DNA synthesis. Since the first publication of 5-iodo-2′-deoxyuridine in 1959 [1] the chemotherapy of herpesviruses has been dominated by nucleoside analogues that interact with virus-specific enzymes and in particular with herpesvirus thymidine kinase (TK) and DNA-polymerase (DNA-pol). Although there are many other gene products involved in virus DNA synthesis, all the useful nucleoside analogues with a selective mode of action have been shown to interact with one or both of these two key enzymes. (An important exception being ganciclovir which has been shown to be phosphorylated by CMV protein kinase.) The three compounds most widely used in the therapy and prevention of HSV, VZV and CMV diseases are all guanosine-related nucleoside analogues, namely acyclovir (ACV) penciclovir (PCV) and ganciclovir (GCV). The first two are notable for their remarkable lack of toxic side-effects and over a period of more than 30 years they have proved to be entirely safe such that they are prescribed for suppression of disease in patients who suffer frequent recurrences of HSV. However a major drawback of these guanosine nucleoside analogues is that they have a very short half-life in tissue following oral administration. This led to the development of the nucleoside

prodrugs valaciclovir (VACV) famciclovir (FCV) and valganciclovir [2] all of which have high oral bioavailability that provides more sustained levels of the nucleoside analogue following administration, allowing trough levels to remain above the theoretical level for inhibition of virus replication during a course of therapy.

The Search for Improved Inhibitors of Herpesviruses

Having originally proved the potential value of antiviral chemotherapy against herpesviruses by means of targeting DNA-pol, the focus of antiviral research moved to HIV, influenza and more recently hepatitis B and hepatitis C. The enormous injection of funds into these problems has led to the discovery of many new alternative strategies for attacking viruses by means of antiviral chemotherapy. Furthermore, the existing nucleoside analogues (ACV and PCV) currently used for treating common HSV diseases are not fully effective. Problems with these compounds include delayed lesion healing, breakthrough of lesions during suppression therapy and virus replication continuing despite therapy, such that transmission to a new susceptible host can take place [3]. Moreover, therapy or prophylaxis involves frequent administration of these compounds. Of the many theoretical enzyme targets, helicase–primase has recently come to the fore and may represent the first of a new era of herpes antiviral chemotherapy with small molecule inhibitors other than nucleoside analogues.

Helicase–Primase as a Target for Herpes Antiviral Chemotherapy

The discovery and characterization of the HSV helicase–primase (HP) enzyme complex, covered in depth elsewhere in this volume, led to the quest for inhibitors of these functions that are essential for virus replication. Once inhibitors are identified they can be used to select for resistance mutations which can then inform the mechanistic studies. Furthermore, the discovery of potent inhibitors of an essential virus function leading to selective inhibition of virus replication can provide a path to successful antiviral chemotherapy. Several HP-inhibitors (HPI) with therapeutic potential have been discovered. The first of these resulted from rationale drug design programmes based on the screening of libraries of compounds in *in vitro* enzyme assays. However, ironically the current leading HPI undergoing clinical trials resulted from classical screening for inhibitors of virus replication that were serendipitously shown to be HPI.

Enzyme Screens

Crute et al., published a seminal paper in 1989 describing the purification and characterization of the HSV-1-induced DNA helicase [4]. The generation of three

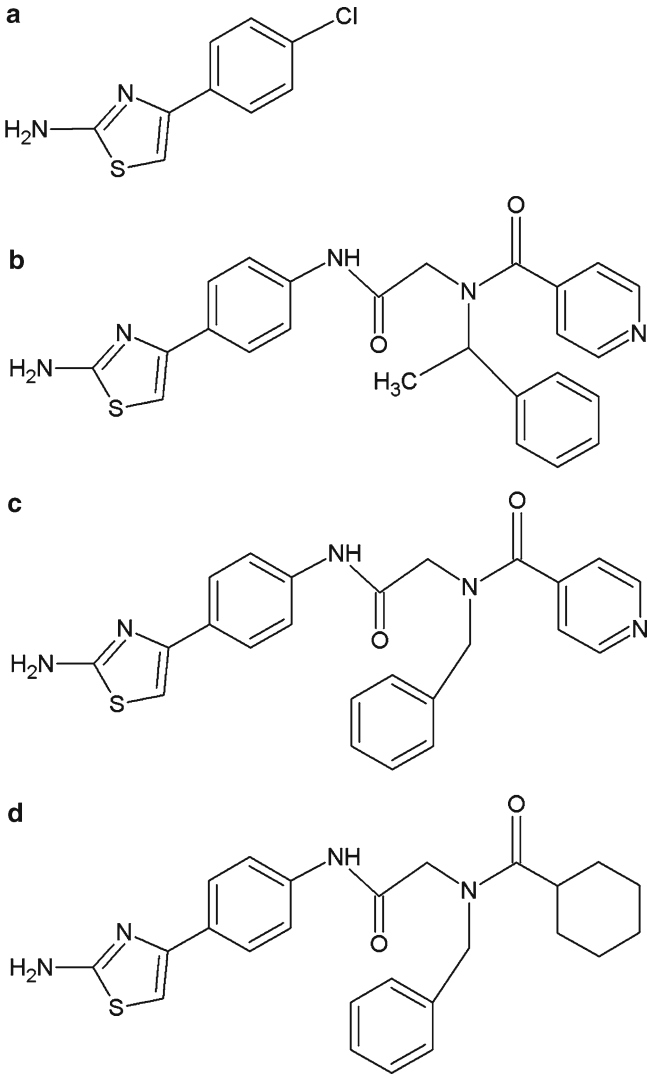

Fig. 7.1 The first compounds shown to be specific inhibitors of HSV helicase–primase showing their structural relationship. (**a**) T 157602. (**b**) BILS 179 BS. (**c**) BILS 45 BS. (**d**) BILS 22 BS

protein subunits comprising the gene products of *UL5*, *UL52* and *UL8* with helicase–primase activity *in vitro* provided a basis for screening potential inhibitors of these functions. This rational approach was soon to bear fruit and among the first successes to exploit this new target was reported by Spector et al. [5]. Using the *in vitro* HP assay, a library of >190,000 random pure chemicals and natural products were screened. Several 2-amino thiazole compounds e.g. T157602 (Fig. 7.1a) were found to inhibit both helicase (IC_{50} = 5 mM) and primase (IC_{50} = 5 mM) activities with approximately 30-fold selectivity index. Furthermore, the latter compound was

specific for HSV and did not inhibit the growth of VZV or CMV. Importantly T157602 also inhibited virus replication under one-step growth conditions with an IC_{90} = 3 mM. Drug-resistant mutants were selected by culturing HSV in the presence of the inhibitor. A few years previously, Zhu and Weller [6] had defined six highly conserved functional domains in the helicase protein and the T157602-resistance mutations all mapped to a position just downstream from the fourth functional domain [6]. These first reported HPI mutations were M354T, K355N and E399T and the authors estimated that they occurred as polymorphisms in the virus stock with a frequency in the order of 10^{-7}. The putative mechanism proposed for inhibition was that the compound stabilised the HP–DNA complex effectively trapping the enzyme complex on the DNA substrate. The three substituted residues leading to drug resistance involved shorter side chains possibly leading to reduced drug binding. The 2-amino thiazole compounds, however, did not progress as medicinal compounds but this was the first published evidence that HPI may have utility as effective herpes antivirals.

The BILS Series of HPI

Crute and coworkers in the laboratories of Boehringer Ingleheim Pharmaceuticals similarly used the HP *in vitro* enzyme system to screen a Boehringer Ingleheim library of compounds [7]. This led to the identification a series of thiozolyl phenyl-containing compounds with anti-herpesvirus activity. Structure-activity studies were carried out to optimise the compounds for further development and subsequently several compounds were pursued; the first to be published was the lead compound BILS 179 BS (Fig. 7.1b). BILS 179 BS was reported to be approximately tenfold more active than ACV in an HSV plaque-reduction assay with an EC_{50} value of approximately 100 nM against both HSV-1 and HSV-2. Biochemical studies confirmed that the mechanism-of-action was specifically directed at HP; furthermore, amino acid substitutions at residue K356 of *UL5* were found to confer resistance. The compound was, as expected, active against ACV-resistant strains but was reportedly inactive against other herpesviruses (VZV, human CMV and murine CMV). A cytotoxicity assay based on mitochondrial function (MTT assay) suggested a 50% toxic concentration of the order of 36 μM, although this depended on cell type. Encouragingly, the compound was shown to be extremely effective in murine infection models for cutaneous and genital HSV where oral dosing led to marked dose-dependent improvements in clinical signs including mortality and reductions of several orders of magnitude in infectious virus in tissues.

This chemical series, which included a number of active compounds, clearly posed a challenge to the medicinal chemist, and it was reported that liver microsome metabolism studies led to the identification of further modifications including the closely related compound, BILS 45 BS (Fig. 7.1c) [8]. This compound was also reported to be more potent than ACV with activity against HSV-1

and HSV-2 in tissue culture $EC_{50} = 0.15$ μM. The BILS 45 BS derivative was also effective in a murine infection model using oral therapy ($ED_{50} = 56$ mg/kg) with bioavailability in the order of 50%. Finally, analogue BILS 22 BS (Fig. 7.1d) was also shown to be a very promising potent inhibitor of HSV. However the problems that had beset this group of aminothiazole-phenyl compounds were too great and this ground-breaking development programme was terminated. The close similarity between the three compounds mentioned above may be seen in the figure (Fig. 7.1a–d).

Whole Virus Screens

BAY 57-1293

In the same issue of Nature Medicine that reported the first description of the BILS series of compounds, a paper by Kleymann et al. [9] disclosed a different series of compounds that had been developed in the laboratories of Bayer Pharmaceuticals. In this case, the antiviral activity was discovered by means of an innovative cell-based virus replication assay (reviewed [10]). Approximately 400,000 compounds in the company's library were tested at 10 μM using this fluorometric, high-throughput screen. The identification of a hit followed by further synthesis in a structure-activity study eventually led to the compound BAY 57-1293 (AIC 316). The compound is a stable white powder, *N*-[5-(aminosulfonyl)-4-methl-1,3-thiazole-2-yl]-*N*-2[4-(pyridinyl)phenyl]acetamide (Fig. 7.2a) with a molecular mass of 402 (almost twice that of ACV at 225). BAY 57-1293 inhibited HSV-1 and HSV-2 replication with $EC_{50} = 0.01–0.02$ μM with only weak activity against VZV and human CMV. Evidence obtained from the study of resistance mutations pointed to HP as the site of action for the thiazolylamide compounds. Gene sequencing of the HSV genes coding for DNA replication enzymes showed that mutations in *UL5* helicase gene at amino acid residues G352, M355 and K356 accounted for resistance and this was confirmed in subsequent enzyme studies.

Efficacy of AIC316 in Animal Infection Models

Like the BILS compounds, BAY 57-1293 was also demonstrated to be efficacious in several different laboratory HSV infection models. Betz et al. [11] clearly demonstrated that the compound is highly effective in rodents infected with either HSV-1 or HSV-2. One model employed a lethal intranasal inoculation that provides rapid virus access to the central nervous system with a distribution of infection that resembles herpes encephalitis in man [12]. Oral therapy three times a day from 6 h after inoculation for 5 days was extremely effective; preventing death and reducing other clinical signs of disease. The ED_{50} under these conditions was 0.5 mg/kg rising to 3 mg/kg/day when dosing was reduced to once a day. A higher dose (15 mg/kg/day) for 4 days reduced

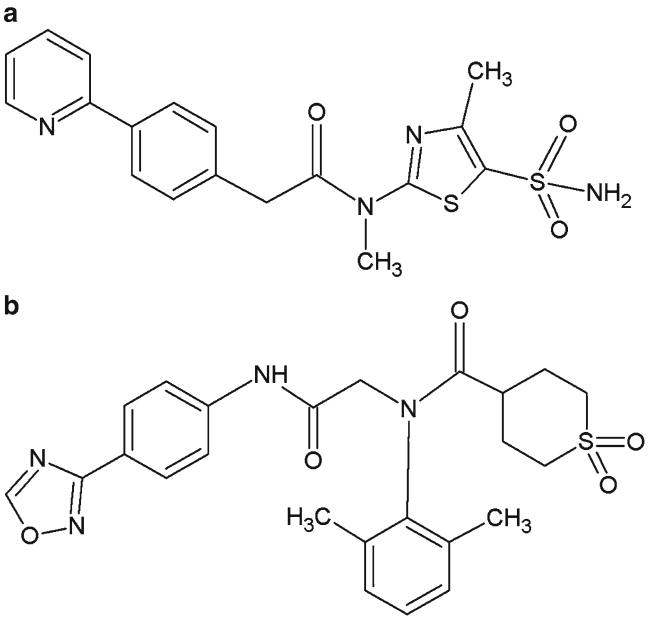

Fig. 7.2 Effective HPI that have entered clinical trials in man. (**a**) BAY 57-1293 (AIC 316); active against HSV-1 and HSV-2. (**b**) ASP 2151 (amenamevir); active against HSV and VZV

infectious virus in the tissues by several orders of magnitude. It was also reported by Betz et al. [11], that similar results were obtained in intranasally inoculated rats. Betz et al. also published data obtained from a zosteriform infection model in mice [11]. In this case virus was inoculated into the skin whereupon virus translocates, via sensory nerves, to the dorsal root ganglia. Subsequently a characteristic zosteriform distribution of skin lesions is produced, first visible 3 or 4 days after inoculation. Using this model, oral therapy with BAY 57-1293 at 15 mg/kg three times per day starting on day 3 prevented mortality and again produced marked reductions in virus replication and clinical signs. In both models the experimental therapy was superior to VACV and it was particularly notable that, following cessation of VACV therapy, there was a rebound of virus replication in the nervous system and lesion development whereas this did not occur following cessation of BAY 57-1293 treatment.

Baumeister et al. [13] also published extremely encouraging *in vivo* data on the same inhibitor. In this case the well-established female HSV-2 guinea pig infection model was employed. BAY 57-1293 was given orally two or three times per day starting from 6 h after virus inoculation. A clear dose-response was obtained and 20 mg/kg was found to significantly decrease lesion development and reduce infectious virus in the tissues. A 1,000-fold reduction in infectious virus was recorded in the dorsal root ganglia at 7 days post-infection. It was concluded that this resulted in a reduced burden of latent virus and that this was the most probable explanation for the observed reduction in frequency of recurrent lesions following therapy. In further experiments, the onset of therapy was delayed until 4 days post-infection,

when 20 mg/kg twice a day was administered for 2 weeks. Again this led to significant reductions in clinical signs, including the suppression of recurrent lesions. This infection model is well-documented and is regarded as being suitable for the study of HSV reactivation and recurrent genital lesions. Accordingly, the same authors delayed the onset of therapy until day 20. The animals were then treated from day 20 until day 30 post-infection and observations were continued up until day 80. Again there was good suppression of recurrent lesions during the therapy and the reduction was superior to VACV. However, comparison with VACV in this model should be treated with caution since it is known that guinea pig cells are unusual with respect to the activity of ACV [14, 15] and may unduly bias results against the latter compound.

Finally, Biswas and Field [16] published the results of further *in vivo* studies that generally supported these findings. Using a zosteriform HSV-1 infection model in BALB/c mice, an oral or intraperitoneal dose of 15 mg/kg once a day starting on day 1 post-infection for 4 days protected mice from death and produced a significant reduction in other clinical signs. Infectious virus in the skin at the inoculation site, nervous system and ear pinna (secondary site following zosteriform spread) were all reduced to below the level of detection and there was no recurrence on cessation of therapy. In these experiments BAY 57-1293 therapy was reported to be superior to oral FCV that previously had been shown to be the most effective therapy in this model. In agreement with Betz's experiments [11], it was found that the ED_{50} for once daily oral administration was approximately 5 mg/kg/day (Field and Biswas, unpublished). Using a small number of athymic nude mice on a BALB/c background, Biswas et al. also showed that one or two single doses of BAY 57-1293 given on day 3 or day 4 (i.e. well after infection was present in the nervous system) was effective; this being a model for HSV infection in an immunocompromised host [16].

Helicase–Primase Inhibitors as Antiviral Agents in Man

At least two HPI have entered human clinical trials in man. These include BAY 57-1293 (referred to in the trials as AIC 316) and the compound ASP 2151 (amenamevir) (Fig. 7.2b). Following the normal safety testing in the requisite animal species, AIC 316 was tested in man in a series of six phase-I trials involving more than 150 healthy subjects. No adverse changes were observed and the compound was found to be safe with no obvious side-effects during the course of the studies. The behaviour of the compound *in vivo* looked very promising with favourable pharmacodynamics. It appeared that tissue concentrations above the EC_{50} value that had been derived from cell culture experiments could easily be achieved and maintained *in vivo* [17]. Potentially antiviral plasma levels were reached after a single administration and the steady state remained above the EC_{90} for 24 h [18]. Phase II clinical trials were commenced and a randomised, parallel, double-blind, placebo-controlled trial involving more than 150 subjects was completed in December 2010. The subjects in this trial suffered from genital herpes with between 1 and 9 recurrences of HSV-2 per year.

Oral doses of 5, 25 and 75 mg once per day were tested as well as the higher oral dose of 400 mg just once per week. Clinical signs were scored and patient swabs were tested for evidence of virus using a PCR-based method. The results were promising with highly significant dose-dependent effects being recorded. Particularly notable was the reported suppression of virus shedding including that seen following the single 400 mg weekly dose and no safety issues were reported following the trial [19]. Thus the results described in several reports concerning the administration of BAY 57-1293 to HSV-infected patients that have been presented at scientific meetings are extremely encouraging. However, proper evaluation of these data awaits publication in journals following peer review and independent scrutiny of the data.

ASP 2151: Second of Example of an HPI to Reach Clinical Trials in Man

The compound, ASP 2151 originated in Japan from a medicinal chemistry programme based on the known 2-aminothiazole-containing HPI [20]. The new compounds, discovered by workers at Yamanouchi Co (later Astellas Pharma inc) contained the oxadiazolyl-phenyl moiety. The structure-activity studies employed an assay comprising the HSV-1 UL5–UL52–UL8 complex. The most promising compound, ASP 2151 (amenamevir) was active in the assay at approximately 0.1 μM. Furthermore, the compound was reported to inhibit virus replication at 0.036 and 0.028 μM for HSV-1 and HSV-2 respectively. Of particular interest was the reported finding that this compound, unlike BAY 57 1293, was also a potent inhibitor of VZV (ED_{50}=0.047 M) [21]. This and further publications demonstrated the compound to be highly effective in a murine HSV infection model using doses of 1–10 mg/kg twice per day and in HSV-2-infected guinea pigs [22]. ASP 2151 was actually the first HPI to progress to human trials. Initially, no toxic side-effects were encountered and HSV and VZV-infected subjects were recruited for trials from 2007 [23, 24]. However, it appears that adverse events were encountered and the development of ASP 2151 is currently suspended. Notwithstanding, the preliminary results obtained with this interesting HPI provide further evidence that the compounds in the HPI class do have real clinical potential.

As mentioned above, evidence for a selective mechanism for antiviral action is often dependent on the selection of resistance mutations. As drugs enter clinical trials the potential for the development antiviral of drug resistance is also a matter of great practical importance [25].

Mutations Conferring Resistance to HPI

Drug resistance is seen in herpes viruses against nucleoside analogues, normally at a rate of ~10^{-4} in the form of null mutations in TK, which is required to activate these drugs [26, 27], but is not essential for virus replication. There are also nucleoside analogue-resistance mutations in the DNA-polymerase, but at a much lower

rate ($<10^{-6}$) [28]. Such resistant mutants have not been shown to be a widespread problem in immunocompetent individuals (with the possible exception of ocular herpes antiviral resistance) but can be in immunocompromised patients with persistent infections, although resistance has typically been found in <5% of cases [25, 29, 30]. As expected, TK and DNA-pol mutants are found not to be cross-resistant to HPI because they act through a different target.

In the case of HPI resistance (selected in tissue culture) the majority of mutations conferring resistance have been located to a group of residues just downstream from functional motif IV in the helicase (*UL5*) gene as defined by Zho and Weller [6] between amino acid residues 342–356 or 341–355 for HSV-1 or HSV-2 respectively ([31]; reviewed [32, 33]). Rarely, substitution of the first amino acid of motif IV (residue 342 in HSV-1 and 341 in HSV-2) has also shown this to be a potential site for resistance-conferring substitutions as well as residue 899 in HSV-1 *UL52* primase gene. The role of these substitutions in resistance to HPI will be further discussed below.

Prevalence of HPI-Resistance Mutations

The first reports of HPI-resistance mutations detected in laboratory strains and clinical isolates suggested that they occur at frequencies (10^{-6}); lower than seen for nucleoside analogues [5, 9, 31]. Early work on HPI resistance was performed on HSV laboratory stocks by serial passage in the presence of HPI so that resistant mutants could be isolated and characterised. However, it soon became apparent that mutants could be isolated readily following a single passage in the presence of BAY 57-1293. Biswas et al. [34] reported that there were already HPI-resistant mutants present in laboratory working stocks of HSV-1 strain Cl (101) known as PDK at approximately 4×10^{-4} and in the well-characterised laboratory strain of HSV-1, SC16 ($>10^{-5}$). Although most SC16 mutants were not highly resistant (e.g. approximately 15-fold: *UL5* A199T) with more highly resistant mutants (e.g. approximately 100-fold: *UL5* K356T or K356Q) occurring at a frequency of ~10^{-6}, which is similar to background and consistent with the rate of spontaneous mutation. However, the more common PDK resistant mutants typically had >50-fold resistance to BAY 57-1293 (*UL5* M355T, a mutation reported earlier by Kleymann et al. [9]). Plaque-purified clones of these stocks showed BAY 57-1293-resistance selection reduced to a frequency of approximately 10^{-6}, providing further evidence that the higher frequencies of resistance mutation were not caused by incubation with the HPI but were merely selected for in its presence.

It is important to look at clinical isolates, because laboratory stocks may not properly represent the natural populations of HSVs. Biswas et al. [35] reported the highly HPI-resistant HSV-1 *UL5* K356N mutation in two of ten clinical isolates; in each case at a frequency of approximately 10^{-4}. The authors suggest that this could be explained by the K356N mutation having a neutral effect on virus growth and pathogenicity under most conditions, and possibly providing a growth advantage in some circumstances.

A study reported by Sukla et al. [36] using an "intentional mismatch PCR" (IMP) technique on 30 clinical isolates of HSV-1 appears to show that five of these isolates contained resistance mutations to BAY 57-1293 in *UL5* at 10–100 times the expected frequency. However, the IMP method only analyzes viral DNA, which does not necessarily originate from viable viral particles. Similar work analysing HSV-2 clinical isolates has shown that some of these viruses also contained BAY 57-1293-resistance at the higher frequency (HJF, unpublished data). It is important to note that in all these studies virus isolates under investigation were obtained prior to the introduction of any HPI to the clinic and therefore were obtained from patients who had no prior exposure to HPI, again suggesting that the resistance mutations (polymorphisms) must be pre-existing. Furthermore, all the clinical virus isolates, to date are universally sensitive to HPI as measured by a plaque-reduction assay.

We emphasise that clinical trials of BAY 57-1293 to date have not shown any evidence that rapid development of resistance to this compound is going to be a problem and experiments in mice [37] have indicated that an infection with a mixture of highly resistant mutant and parental virus does not lead to rapid emergence of resistance *in vivo*.

HPI-Resistance Mutations in Helicase and Primase

Early mechanistic studies on the BILS series of compounds [7] suggested that they act by inhibiting recycling of HP complex through stabilising its interaction with DNA, shown by a DNA docking assay measured by fluorescence anisotropy. The HSV-1 *UL5* (K356N) mutant did not have higher affinity for ssDNA substrate in the presence of BILS 103 BS and the frequency of HPI resistance in lab stocks of the HSV-1 KOS strain was approximately 10^{-6}. Liuzzi et al. [31] isolated three HSV-1 KOS mutants by serial passage in the presence of BILS 22 BS, which had similar growth properties to the wild type *in vitro*. All three mutants had single amino acid substitutions in the *UL5* protein: K356N (2,500-fold resistant), G352V (316-fold) and G352C (38-fold). These authors measured activities (DNA-dependent ATPase, DNA helicase and RNA primase) of the K356N H–P complex *in vitro* using purified mutant expressed in baculovirus and found no significant difference to wild-type virus. Isolation of resistant mutants confirmed mode-of-action of BILS 22 BS and again showed the mutation rate to be an estimated 10^{-6}. These mutants (K356N and G352V) did not revert to wild type in the absence of HPI, suggesting they were not detrimental to viral replication. They also confirmed the results of Betz et al. [11] reporting that the K356N resistance mutation did not alter *in vitro* viral replication rates or murine pathogenicity. Similar results were reported later [38, 39] for the HSV-1 SC16 mutant containing the same resistance substitution.

The HPI, BAY 57-1293 was initially identified by high-throughput screening of compounds with HSV inhibitory activity, but its mechanism-of-action was only established after isolating resistant HSV-1 viruses, sequencing one of their genomes and complementation analysis [9]. It was found that almost all of the resistance

mutations to BAY 57-1293 and its related compounds were in the *UL5* helicase protein downstream of motif IV, similar to the resistant mutants obtained with the previously reported BILS compounds. However, an A to T resistance mutation was also discovered in the *UL52* primase protein at residue A897 (this residue being equivalent to A899T in HSV-1 SC16 and PDK). It is of interest that these mutants are not co-resistant to the alternative HPI, BILS 179 BS [10]. The lack of cross-resistance was confirmed by Biswas et al. [40] and recently a similar lack of co-resistance has been shown with amenamevir (ASP 2151) suggesting an important difference between the different classes of HPI [41].

As mentioned above, the majority of HPI-resistance mutations reported thus far in both HSV-1 and 2 have been in the region just downstream of the helicase motif IV in the UL5 protein. The asparagine-to-lysine mutation found at the start of motif IV in HSV-1 (N342K) and HSV-2 (N341K) has also been shown to confer resistance to the HPI, but this mutation appears to cause a decrease in the viral fitness in terms of its growth rate and pathogenicity in mice, possibly due to steric/allosteric hindrance to the UL5–UL52 interaction [42]. The equivalent mutation in VZV (ORF55 N336K), isolated after serial passage in the presence of ASP 2151, has a similar effect on viral fitness [21]. To the best of our knowledge, no resistance mutations in the *UL8* gene have been isolated to date, suggesting that the HPI may not interact with this subunit of the H–P complex.

Different Sensitivities of Mutants to the 3 HPI

It appears that most HPI-resistance mutants are cross-resistant to BILS, BAY 57-1293 and ASP 2151 but, as mentioned above, there are some interesting exceptions and the resistance mutation to BAY 57-1293 isolated in the HSV-1 primase gene (*UL52*), causing the A899T amino acid change, is sensitive to BILS and ASP 2151 [40]. However, we have recently discovered a primase mutation in HSV-2 conferring resistance to BAY 57-1293, which comprises the deletion of a lysine residue at position 905 that is equivalent to 898 in HSV-1, that retains resistance to ASP 2151 [41].

Although the three classes of HPI discussed—BILS compounds, BAY 57-1293 and ASP 2151—target the same enzyme complex, they clearly interact with it in subtly different ways. ASP 2151 is the only one of the three that inhibits the VZV HP complex. The A899T primase mutation in HSV-1 only confers resistance to BAY 57-1293, but the HSV-2 K905 primase deletion is resistant to BAY 57-1293 and ASP 2151. More investigation into how the HPI interact with the amino acids of the HP complex components needs to be carried out to discover the complete mechanism-of-action of these compounds, but the resistance mutants give important clues to this. Molecular modelling of the BAY 57-1293–UL5–UL52 interaction shows that the BAY 57-1293 molecule sits in a pocket formed by UL5 and UL52, which perhaps reduces the movement in this dynamic interface [42].

The Prospects for HPI for Treatment or Prevention of Herpesvirus Diseases

Nucleoside analogues have enjoyed supremacy for treating or suppressing herpes infections for more than 50 years. ACV and PCV and their orally bioavailable prodrugs may not be fully effective antivirals but they have been remarkably free from any toxic side-effects. No serious problems have been encountered throughout their history apart from occasional damage arising from low solubility that can be avoided. It will be very difficult for the new compounds to match this enviable record and already several HPI that looked very promising in their early development have not progressed because of safety concerns. However, on the positive side the compound currently undergoing Phase II clinical trials (AIC 316) appears to be an extremely effective antiviral for treatment or suppression of HSV and, importantly, it offers the prospect of much longer intervals between dosing. Hopefully this will translate into more convenience for the patient (leading to improved compliance) and the potential for better suppression of subclinical virus replication and transmission.

Latency remains the major hurdle to curing recurrent HSV. Whether or not the early indications from animal models that BAY 57-1293 may impact on the frequency of recurrences in the guinea pig infection model [9] can be confirmed in further human trial remains to be seen. Further work is required using quantitative laboratory infection models to establish the effects, if any, on the establishment and maintenance of latent foci and their potential for reactivation.

In any case, the above compound has already provided proof-of-principle that it is an effective antiviral for HSV in man and there is no doubt that this and other HPI will now be developed as medicines for use either alone or in combination with the existing nucleoside analogue inhibitors such as ACV. Finally, having successfully exploited the helicase–primase as a target for inhibition of HSV and VZV, virus-specific helicase is now the focus of attention in the search for inhibitors of viruses (e.g. hepatitis C) from completely different families and there is no doubt in our minds that we are at the advent of a new era in antiviral chemotherapy.

References

1. Field HJ, De Clercq E. Antiviral drugs: a short history of their discovery and development. Microbiol Today. 2004;31:58–61.
2. De Clercq E, Field HJ. Antiviral prodrugs - the development of successful prodrug strategies for antiviral chemotherapy. Br J Pharmacol. 2006;147:1–11.
3. Harmenberg JG, Awan AR, Alenius S, Stahle L, Erlandsson AC, Lekare G, et al. ME-609: a treatment for recurrent herpes simplex virus infections. Antivir Chem Chemother. 2003;14:205–15.
4. Crute JJ, Tsurumi T, Zhu L, Weller SK, Olivo PD, Challberg MD, et al. Herpes simplex virus 1 helicase-primase: a complex of three herpes-encoded gene products. Proc Natl Acad Sci USA. 1989;86:2186–9.

5. Spector FC, Liang L, Giordano H, Sivaraja M, Peterson MG. Inhibition of herpes simplex virus replication by a 2-amino thiazole via interactions with the helicase component of the UL5-UL8-UL52 complex. J Virol. 1998;72:6979–87.
6. Zhu L, Weller SK. The six conserved helicase motifs of the UL5 gene product, a component of the herpes simplex virus type 1 helicase-primase, are essential for its function. J Virol. 1992;66:469–79.
7. Crute JJ, Grygon CA, Hargrave KD, Simoneau B, Faucher A-M, Bolger G, et al. Herpes simplex virus helicase-primase inhibitors are active in animal models of human disease. Nat Med. 2002;8:386–91.
8. Duan J, Liuzzi M, Paris W, Liard F, Browne A, Dansereau N, et al. Oral bioavailability and *in vivo* efficacy of the helicase-primase inhibitor BILS 45 BS against acyclovir-resistant herpes simplex virus type 1. Antimicrob Agents Chemother. 2003;47:1798–804.
9. Kleymann G, Fischer R, Betz UA, Hendrix M, Bender W, Schneider U, et al. New helicase-primase inhibitors as drug candidates for the treatment of herpes simplex disease. Nat Med. 2002;8:392–8.
10. Kleymann G. New antiviral drugs against herpesviruses. Herpes. 2003;10:46–52.
11. Betz UAK, Fischer R, Kleymann G, Hendrix M, Rübsamen-Waigmann H. Potent *in vivo* antiviral activity of the herpes simplex virus primase-helicase inhibitor BAY57-1293. Antimicrob Agents Chemother. 2002;4:1766–72.
12. Anderson JR, Field HJ. The distribution of herpes simplex type 1 antigen in mouse central nervous system after different routes of inoculation. J Neurol Sci. 1983;60:181–95.
13. Baumeister J, Fischer R, Eckenberg P, Henninger K, Ruebsamen-Waigmann H, Kleymann G. Superior efficacy of helicase-primase inhibitor BAY 57-1293 for herpes infection and latency in the guinea pig model of human genital herpes disease. Antivir Chem Chemother. 2007;18:35–48.
14. Harmenberg J, Abele G, Malm M. Deoxythymidine pools in animal and human skin with reference to antiviral drugs. Arch Dermatol Res. 1985;277:402–3.
15. Harmenberg J, Abele G, Wahren B. Nucleoside pools of acyclovir-treated herpes simplex type 1 infected cells. Antiviral Res. 1985;5:75–81.
16. Biswas S, Jennens L, Field HJ. The helicase primase inhibitor, BAY57-1293 shows potent therapeutic antiviral activity superior to famciclovir in BALB/c mice infected with herpes simplex virus type 1. Antiviral Res. 2007;75:30–5.
17. Birkmann A, Hewlett G, Rubsamen-Schaeff H, Zimmermann H. Helicase primase inhibitors as the potential next gerneration of highly active drugs against herpes simplex viruses. Future Virol. 2011;6:1199–209.
18. Birkman A, Kropeit D, Biswas S, Paulsen D, Sukla S, Field HJ. PK/PD evaluation of AIC316, a novel herpes simplex virus inhibitor currently in clinical development. Presented at Antivirals congress, Amsterdam, The Netherlands; 7–9 Nov 2010.
19. Wald A, Stoellben S, Tyring S, Warren T, Johnston C, Huang M-L, et al. Impact of AIC316, a novel antiviral helicase-primase inhibitor, on genital HSV shedding: randomized, double-blind, placebo-controlled trial. Presented at 19th Biennial conference of the International Society of Sexually Transmitted Diseases Research (ISSTDR) Quebec City, QC, Canada; 10–13 July 2011.
20. Chono K, Katsumata K, Kontani T, Kobayashi M, Sudo K, Yokota T, et al. ASP2151, a novel helicase–primase inhibitor, possesses antiviral activity against varicella-zoster virus and herpes simplex virus types 1 and 2. J Antimicrob Chemother. 2010;65:1733–41.
21. Chono K, Katsumata K, Kontani T, Kobayashi M, Sudo K, Yokata T, et al. ASP2151, a novel helicase-primase inhibitor, possesses antiviral activity against varicella-zoster virus and herpes simplex virus types 1 and 2. J Antimicrob Chemother. 2010;65:1733–41.
22. Katsumata K, Chono K, Sudo K, Shimizu Y, Kontani T, Suzuki H. Effect of ASP2151, a herpesvirus helicase-primase inhibitor, in a guinea pig model of genital herpes. Molecules. 2011;16:7210–23.
23. ClinicalTrials.gov. Dose-finding study of ASP2151 in subjects with herpes zoster. http://clinicaltrials.gov/ct2/show/NCT00487682; http://clinicaltrials.gov/ct2/show/NCT00487682.
24. ClinicalTrials.gov. A study with ASP2151 in subjects with recurrent episodes of genital herpes. http://clinicaltrials.gov/ct2/show/NCT00486200; http://clinicaltrials.gov/ct2/show/NCT00486200.

25. Field HJ. Herpes simplex virus antiviral drug resistance-current trends and future prospects. J Clin Virol. 2001;21:261–9.
26. Bacon TH, Levin MJ, Leary JJ, Sarisky RT, Sutton D. Herpes simplex virus resistance to acyclovir and penciclovir after two decades of antiviral therapy. Clin Microbiol Rev. 2003;16:114–28.
27. Parris DS, Harrington JE. Herpes simplex virus variants resistant to high concentrations of acyclovir exist in clinical isolates. Antimicrob Agents Chemother. 1982;22:71–7.
28. Gilbert C, Bestman-Smith J, Boivin G. Resistance of herpesviruses to antiviral drugs: clinical impacts and molecular mechanisms. Antiviral Res. 2002;5:88–114.
29. Christophers J, Clayton J, Craske J, Ward R, Collins P, Trowbridge M, et al. Survey of resistance of herpes simplex virus to acyclovir in northwest England. Antimicrob Agents Chemother. 1998;42:868–72.
30. Christophers J, Sutton RN. Characterization of acyclovir-resistant and sensitive clinical isolates of herpes simplex virus isolates from an immunocompromised patient. J Antimicrob Chemother. 1987;20:389–98.
31. Liuzzi M, Kibler P, Bousquet C, Harji F, Bolger G, Garneau M, et al. Isolation and characterization of herpes simplex virus type 1 resistant to aminothiazolylphenyl-based inhibitors of the viral helicase-primase. Antiviral Res. 2004;64:161–70.
32. Field HJ, Biswas S. Antiviral drug resistance and helicase-primase inhibitors of herpes simplex virus. Drug Resist Updat. 2011;14:45–51.
33. Biswas S, Field HJ. Helicase-primase inhibitors: a new approach to combat herpes simplex virus and varicella-zoster virus. In: De Clercq E, editor. Antiviral drug strategies. Weinheim: Wiley; 2011. p. 129–45.
34. Biswas S, Swift M, Field HJ. High frequency of spontaneous helicase-primase inhibitor (BAY 57-1293) drug-resistant variants in certain laboratory isolates of HSV-1. Antivir Chem Chemother. 2007;18:13–23.
35. Biswas S, Smith C, Field HJ. Detection of HSV-1 variants highly resistant to the helicase-primase inhibitor BAY 57-1293 at high frequency in two of ten recent clinical isolates of HSV-1. J Antimicrob Chemother. 2007;60:274–9.
36. Sukla S, Biswas S, Birkmann A, Lischka P, Zimmermann H, Field H. Mismatch primer-based PCR reveals that helicase-primase inhibitor resistance mutations pre-exist in herpes simplex virus type 1 clinical isolates and are not induced during incubation with the inhibitor. J Antimicrob Chemother. 2010;65:1347–52.
37. Sukla S, Biswas S, Birkmann A, Lischka P, Ruebsamen-Schaeff H, Zimmermann H, et al. Effects of therapy using a helicase-primase inhibitor (HPI) in mice infected with deliberate mixtures of wild-type HSV-1 and an HPI-resistant UL5 mutant. Antiviral Res. 2010;87:67–73.
38. Biswas S, Jennens L, Field HJ. Single amino acid substitutions in the HSV-1 helicase protein that confer resistance to the helicase-primase inhibitor BAY 57-1293 are associated with increased or decreased virus growth characteristics in tissue culture. Arch Virol. 2007;152:1489–500.
39. Biswas S, Tiley LS, Zimmermann H, Birkmann A, Field HJ. Mutations close to functional motif IV in HSV-1 UL5 helicase that confer resistance to HSV helicase-primase inhibitors, variously affect virus growth rate and pathogenicity. Antiviral Res. 2008;80:81–5.
40. Biswas S, Kleymann G, Swift M, Tiley LS, Lyall J, Aguirre-Hernández J, et al. A single drug-resistance mutation in HSV-1 UL52 primase points to a difference between two helicase-primase inhibitors in their mode of interaction with the antiviral target. J Antimicrob Chemother. 2008;61:1044–7.
41. Field HJ, Mickelburgh I, Huang M-L, Tiley L, Wald A, Ruebsamen-Schaeff H, et al. Sensitivity of Clinical isolates to helicase primase inhibitors and no detection of resistance mutations above background frequency. In: Twenty fifth international conference on antiviral research, Sapporo, Japan; 2012, Abstract 46.
42. Biswas S, Miguel RN, Sukla S, Field HJ. A mutation in helicase motif IV of herpes simplex virus type 1 UL5 that results in reduced growth *in vitro* and lower virulence in a murine infection model is related to the predicted helicase structure. J Gen Virol. 2009;90:1937–42.

Chapter 8
RecQ Helicases: Conserved Guardians of Genomic Integrity

Nicolai Balle Larsen and Ian D. Hickson

Abstract The RecQ family of DNA helicases is highly conserved throughout evolution, and is important for the maintenance of genome stability. In humans, five RecQ family members have been identified: BLM, WRN, RECQ4, RECQ1 and RECQ5. Defects in three of these give rise to Bloom's syndrome (BLM), Werner's syndrome (WRN) and Rothmund–Thomson/RAPADILINO/Baller–Gerold (RECQ4) syndromes. These syndromes are characterised by cancer predisposition and/or premature ageing. In this review, we focus on the roles of BLM and its *S. cerevisiae* homologue, Sgs1, in genome maintenance. BLM/Sgs1 has been shown to play a critical role in homologous recombination at multiple steps, including end-resection, displacement loop formation, branch migration and double Holliday junction dissolution. In addition, recent evidence has revealed a role for BLM/Sgs1 in the stabilisation and repair of replication forks damaged during a perturbed S-phase. Finally BLM also plays a role in the suppression and/or resolution of ultra-fine anaphase DNA bridges that form between sister-chromatids during mitosis.

Introductory Remarks

The ability to repair damage to cellular DNA is of paramount importance for the maintenance of a stable genome. Therefore, cells have evolved multiple pathways to repair the various kinds of DNA lesions that can occur spontaneously or following exposure to a DNA damaging agent. These repair pathways involve multiple

N.B. Larsen • I.D. Hickson (✉)
Nordea Center for Healthy Ageing, Department of Cellular and Molecular Medicine, University of Copenhagen, 2200N Copenhagen, Denmark
e-mail: iandh@sund.ku.dk

M. Spies (ed.), *DNA Helicases and DNA Motor Proteins*, Advances in Experimental Medicine and Biology, DOI 10.1007/978-1-4614-5037-5_8,

enzymatic activities including DNA helicases, nucleases, ligases and topoisomerases. The RecQ helicase family is an example of one such group of DNA repair helicases. The RecQ proteins represent one of the most highly conserved families throughout evolution. Unicellular organisms generally have a single RecQ helicase gene, while humans have five: *BLM*, *WRN*, *RECQ4*, *RECQ1* and *RECQ5*. Mutations in three of these have been found to cause disease in humans, resulting in Bloom's syndrome (*BLM*), Werner's syndrome (*WRN*), and Rothmund–Thomson, RAPADILINO and Baller–Gerold syndromes (all *RECQ4*). The clinical features of these syndromes have recently been reviewed [1–3] (see also Chap. 8) and will not be discussed further here. In this review, we will focus our attention on BLM, because in humans it appears that BLM functionally fulfils most of the roles described for RecQ homologues from model organisms. In humans, Bloom's syndrome is characterised by a predisposition to early development of all forms of cancer [4], illustrating the prime importance of BLM in the maintenance of genome stability. BLM-deficient cells display chromosome instability with increased chromatid gaps and breaks, as well as large scale rearrangements [5]. The diagnostic feature is a tenfold increase in sister chromatid exchanges (SCEs), which are thought to arise by an increase in so-called crossover events during homologous recombination [6], which will be described in more detail later in this article.

Structural Features of RecQ Helicases

The RecQ helicase family is named after the prototypical member, the *Escherichia coli* RecQ helicase. *Ec*RecQ protein consists of three functional domains: the helicase domain and the RecQ carboxy-terminal (RQC) domain, both of which are unique to RecQ helicases, and the Helicase and RNase D C-terminal (HRDC) domain, which is also found in other DNA binding proteins. All three domains are also conserved in RecQ homologues from other species, with the notable exception of human RECQ1, RECQ4 and RECQ5 (Fig. 8.1). The helicase domain defines RecQ as a member of the SF2 superfamily of helicases, which all contain seven conserved helicase motifs coupling NTP hydrolysis to double stranded DNA (dsDNA) strand separation [7] (see also Chap. 3). The helicase and RQC domains form the ~59 kDa catalytic core of *Ec*RecQ, and this fragment is sufficient to catalyse single stranded DNA (ssDNA) binding and 3′ 5′ helicase activity in vitro with the same specific activity as full-length *Ec*RecQ [8]. This core fragment has been crystallised and shown to form a monomer with four distinct subdomains: the helicase domain is made up of the two N-terminal RecA-like subdomains with the ATP and ssDNA binding sites sandwiched between them. This serves as the "motor" of the helicase [9]. Helicase activity is crucial for RecQ helicase function in vivo, and inactivating point-mutations in this domain lead to a mutant phenotype in *Saccharomyces cerevisiae* [10, 11], mice [12] and humans [13]. The C-terminal subdomains of the catalytic core, which are contributed by the RQC domain, consist of a Zn^{2+}-binding subdomain and a β-hairpin winged-helix (WH) subdomain that together form a dsDNA

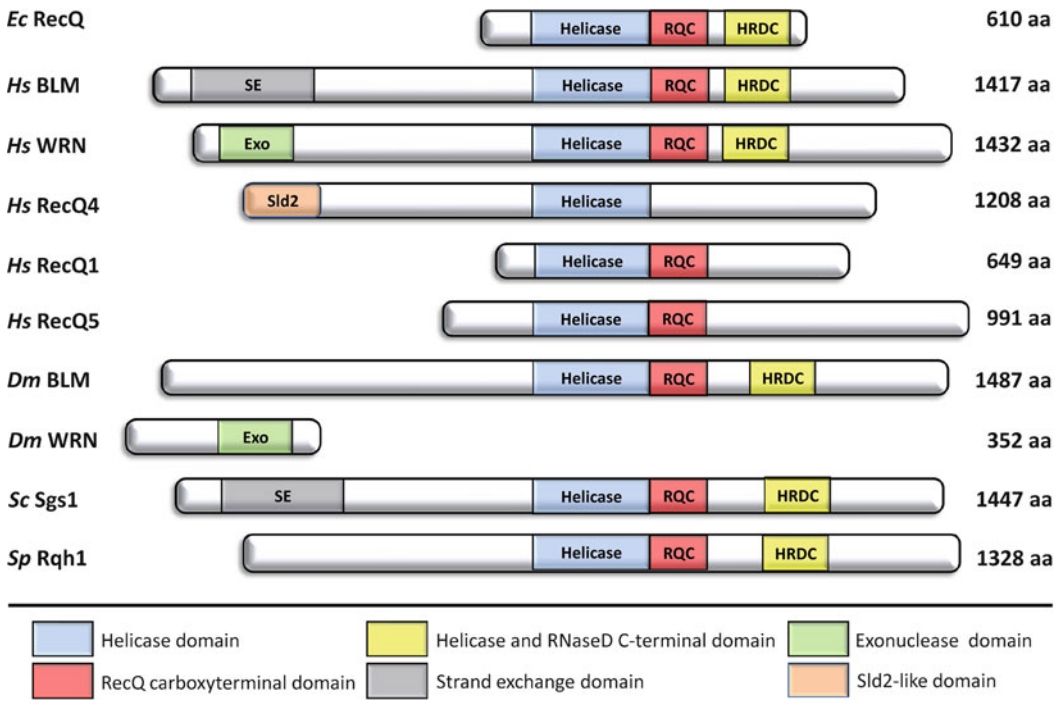

Fig. 8.1 Structural features of the RecQ helicase family. Several defining domains are conserved in RecQ family helicases from bacteria to man. The helicase domain is conserved in all family members, and the RQC and HRDC domains are found in the vast majority. In higher organisms, which have multiple RecQ family members, a larger degree of structural variation is seen. WRN has acquired a unique exonuclease domain, while others, like RECQ1 and RECQ5, have lost the HRDC domain, and RecQ4 has lost both the RQC and HRDC domains. The number of amino acids in each protein is indicated on the right. Abbreviations on the *left* are as follows: *Ec E. coli*; *Sc S. cerevisiae*; *Sp S. pombe*; *Hs H. sapiens*; *Dm D. melanogaster*

binding domain [9]. Substitution of Zn^{2+} coordinating Cysteine residues in *Ec*RecQ revealed that the Zn^{2+} binding domain is essential for stable DNA binding (and thus helicase function) and for protein stability [14]. Mutations affecting Zn^{2+} coordinating Cysteines in BLM and RecQ5 generated similar results, strongly indicating that this function is evolutionarily conserved [15, 16].

A near full-length, helicase-proficient fragment of human RECQ1 has been crystallised as a monomer and shown to have the same overall architecture as that of *Ec*RecQ [17]. However the WH-subdomain of RECQ1 is longer than that of *Ec*RecQ and adopts a different conformation, which brings it into contact with the DNA strand-separation point [17]. Mutation of a conserved aromatic residue (Tyr in RECQ1) at the tip of a β-hairpin region severely compromises the DNA unwinding activity of RECQ1, but not *Ec*RecQ [17]. The importance of the β-hairpin and the conserved Tyr residue has since been confirmed using the full length RECQ1 protein [18].

Co-crystallisation of the RQC fragment of WRN with duplex DNA showed that the β-hairpin directly binds to dsDNA ends and melts the hydrogen bonds between the first base-pair [19]. This functional separation of the unpairing activity (in the RQC subdomain) from the translocase activity (in the helicase subdomain) provides a structural explanation for the ability of RecQ helicases to migrate branched and forked DNA structures [19]. In addition, the RQC domain may also function as a DNA structure-specific binding motif for a subset of substrates. The RQC domain containing fragment of *Ec*RecQ binds to G4 DNA and forked structures with virtually the same affinity as does the full length protein, however it is unable to bind Holliday junctions (HJs), which the full length protein does [20].

The most C-terminal of the conserved RecQ domains, the HRDC domain, exhibits the highest degree of variation between different family members. The approximately 10 kDa HRDC domain consists of a basic bundle of five α-helices with varying surface charge distribution in the different family members studied so far [21–25]. It functions as an auxiliary DNA binding domain; however, its substrate specificity and exact function varies between different RecQ family members. In *S. cerevisiae* Sgs1, the HRDC domain fragment binds to ssDNA and to dsDNA with a ssDNA overhang [21]. In contrast, the *Ec*RecQ HRDC fragment only binds ssDNA [22]. In the context of full-length *Ec*RecQ, mutation of a single residue in the HRDC ssDNA interacting surface, or removal of the entire domain, abrogates partial duplex DNA binding, but increases binding to HJ-like substrates [8, 22]. However, the core helicase activity remains unaffected in both mutants [8, 22]. The isolated HRDC domain of BLM also only binds to ssDNA, but with much lower affinity than does the *Ec*RecQ HRDC domain, as determined using an electrophoretic mobility shift assay [24]. However, a second study on essentially the same HRDC BLM fragment failed to show DNA binding activity when using a fluorescence polarisation assay [25]. Truncation of the HRDC containing C-terminal of BLM has been shown to specifically abrogate double-Holliday junction (dHJ) dissolution activity (which will be discussed below) without affecting helicase activity on forked duplex structures [20]. Loss of activity was attributed to the failure of BLM to bind dHJs in

the absence of the HRDC domain. Furthermore, mutation of a single conserved lysine residue in the HRDC domain to the same loss of function is seen in the truncation mutant [20]. Intriguingly, the structure of the BLM HRDC domain shows that this apparently crucial residue is not situated close to the ssDNA binding region [24]. In vivo studies have shown that the HRDC domain-containing C-terminal region is necessary and sufficient for recruitment of BLM to laser-induced dsDNA breaks (DSBs) [26]. In contrast, the HRDC domain fragment of WRN seems to lack DNA binding activity, despite displaying the same overall fold [23]. However, a C-terminal fragment of WRN containing the HRDC domain together with the remainder of the C-terminal region can bind HJs, forked DNA and duplex DNA with ssDNA overhangs, but not dsDNA or ssDNA [27]. Taken together, these data indicate that the HRDC domain functions as a structure-specific DNA binding domain. The variation in sequence and binding affinities between family members may direct individual family members to a specific subset of DNA substrates and thus underlie the functional diversity of RecQ helicases.

With the clear exceptions of human WRN and RECQ4, the N- and C-terminal regions of RecQ helicases do not contain other clearly-defined functional domains, despite displaying areas of high sequence conservation between family members, mostly in the form a blocks of acidic residues [28]. WRN contains a well-defined exonuclease domain in its N-terminal. The crystal structure of the WRN exonuclease domain reveals a high degree of architectural conservation with the DnaQ exonuclease family that is often involved in DNA proofreading activities [29]. WRN displays exonuclease activity against forked dsDNA structures and dsDNA with ssDNA overhangs, structures that are also substrates for the helicase activity [30]. An exonuclease-dead WRN fails to rescue non-homologous end-joining defects seen in *WRN* cells [29]. In addition, flies expressing an exonuclease defective WRN display high levels of mitotic recombination [31]. Taken together, these data show that exonuclease activity is required for correct WRN function. The N-terminal domain of human RECQ4 contains a region with weak sequence similarity to a region of *S. cerevisiae* Sld2 protein. Sld2 is required for the initiation of DNA replication, and studies in *Drosophila* and chicken cells strongly suggest that RECQ4 is required for this process too [32–34].

The N-terminal region of Sgs1, BLM and *Drosophila melanogaster* BLM contains a conserved, but poorly characterised, ssDNA strand annealing (SA) domain [35]. In addition, this domain catalyses strand exchange between homologous ssDNA and a dsDNA duplex, a reaction that is entirely inhibited by the presence of a single mismatch [35]. The conservation of this function across RecQ family members suggests that this activity constitutes an additional conserved strand exchange (SE) functional domain. Mutant forms of Sgs1 that lack the SE domain are unable to suppress the hyper-recombination phenotype of *Δsgs1* cells in vivo, showing that this domain is essential for proper function [35]. In addition, Sgs1 lacking the SE domain phenocopies a *Δtop3* mutant, suggesting that the function of SE is closely linked to the "dissolvasome" complex function [35].

Functionally Important Binding Partners of RecQ Helicases

*Ec*RecQ functions in concert with several partner proteins. *Ec*RecQ helicase activity is strongly stimulated in vitro by SSB [36], via both trapping of ssDNA and preventing the formation of non-catalytic ssDNA–RecQ complexes [37]. This interaction is mediated by a conserved RecQ-binding domain in the C-terminal section of SSB, which binds directly to the WH domain of *Ec*RecQ [38, 39]. In addition, *Ec*RecQ acts in concert with Top3, a type IA topoisomerase can cleave ssDNA, to promote catenation/decatenation of circular dsDNA substrates in vitro [40]. The helicase activity of RecQ can unwind small segments of duplex DNA creating negatively supercoiled DNA that Top3 then acts upon. Finally, *Ec*RecQ and SSB also act in close concert with RecA, providing an ssDNA substrate for RecA to assemble upon in vitro [41]. These interaction partners are conserved throughout evolution. In yeast, the RecQ homologues Sgs1 (*S. cerevisiae*) and Rqh1 (*S. pombe*) both interact with Top3 [42, 43]. For Sgs1, the Top3 binding domain has been mapped to the first 158 residues and the interaction was shown to be very strong in vitro [44]. Truncation of the N-terminal region of Sgs1 and thus abrogation of Top3 interaction, leads to a *Δsgs1* phenotype, showing that this interaction is crucial for function [45]. A similar N-terminal binding domain is seen in Rqh1, which binds to Top3 via the first 322 residues [43]. Sgs1-Top3 also interacts directly with an OB-fold containing protein, Rmi1 and *Δrmi1* cells show many of the same phenotypes as *Δtop3* cells [46]. Rmi1 binds directly to both Top3 and to the N-terminal part of Sgs1, and can stimulate the ssDNA binding activity of Top3 fivefold [47]. Sgs1 also binds directly to Rad51 in vitro via its C-terminal region [48]. Unlike in *E. coli*, no direct interaction between Sgs1 and RPA (the eukaryote SSB homologue) has been mapped. However, the enzymatic activity of Sgs1-Top3 is stimulated approximately tenfold by RPA in vitro, showing that the three proteins act in concert [49]. Among the human RecQ helicases, only BLM forms an enzymatic complex with a type IA topoisomerase and a homologue of Rmi1, strongly suggesting that BLM is the functional homologue of *Ec*RecQ and Sgs1, at least for those processes that involve the action of Top3 and Rmi1. BLM contains two independent TOPOIIIα binding sites, one located in the N-terminal (residues 1–212) and one in the C-terminal (residues 1266–1417) [50]. BLM also binds directly to the human Rmi1 homologue, which is required for the in vivo stability of the BLM-TOPOIIIα complex [51]. The N-terminal region of RMI1 (residues 150–211) binds directly to both BLM and TOPOIIIα, while the C-terminal harbours a ssDNA binding domain [52]. In addition, the BLM-TOPOIIIα-RMI1 complex also binds to a second OB-fold containing protein RMI2, which is not found in yeast [53, 54]. RMI2 lacks DNA-binding activity, and may slightly stimulate the enzymatic action of BLM-TOPOIIIα-RMI1 in vitro [54]. In addition, depletion or complete deletion of RMI2 in vertebrate cells leads to increased chromosome breakage and SCE, respectively, showing that RMI2 is essential for BLM-TOPOIIIα-RMI1 function in vivo [53, 54]. In vivo, these four proteins form a tight and functional complex, in which all components can be co-immunoprecipitated

with each other, which we will refer to as the RTR complex [54]. The crystal structure of RMI1-RMI2 reveals a strong structural similarity between this dimer and RPA [55]. Like *Ec*RecQ, BLM also binds directly to RPA, which stimulates the helicase activity of BLM in vitro [56]. Finally BLM also interacts directly with RAD51 via two independent binding sites, one in the N-terminal and one in the C-terminal [48]. Further refinement of the binding sites has mapped the sites to residues 100–124 and 1317–1367, which interestingly overlap with proposed ssDNA specific binding domains [57].

DNA Substrate Requirements for RecQ Helicases

BLM is capable of unwinding a number of different substrates, the majority of which are intermediates in the process of homologous recombination (HR) (Fig. 8.2) (see also Chap. 9). In vitro, BLM does not unwind blunt-ended duplex DNA or DNA containing an internal nick [58]; instead, it requires the presence of one of several "non-duplex" DNA features for loading. The simplest of such structures is a ssDNA overhang. Sgs1 is capable for unwinding dsDNA with a 3′ overhang of at least three nucleotides, via recognition of the ssDNA/dsDNA junction [59]. DNA with a 3′ ssDNA overhang is, however, a relatively poor substrate for both BLM and WRN, suggesting a more complex mode of substrate recognition than simple recognition of the dsDNA–ssDNA junction [58]. BLM unwinds bubble structures with an internal bubble of four nucleotides or larger, forked duplex structures and X-shaped, 4-way junctions, which are all characterised by the presence of internal recognition structures with junctions between dsDNA and two single strands [58].

In vitro, a preferred substrate for both Sgs1 and BLM is G4-DNA structures in which Hoogsteen bonding between four guanines form a planar quartet structure [60, 61]. In competition assays, BLM preferentially unwinds G4 DNA, even in the presence of excess forked DNA structures [60]. In addition, determination of kinetic parameters for BLM showed that while the K_m values for G4 DNA, a partial duplex and a forked DNA structure are similar, only G4 DNA was capable of forming a very stable protein–substrate complex with BLM [62].

BLM shows limited in vitro processivity with the structures mentioned above, with the notable exception of closed Holliday junction containing structures, in which the junction is efficiently branch migrated over long distances [63]. BLM has also been shown to very efficiently disrupt mobile D-loops formed by RecA catalysed invasion of a single strand into a negatively supercoiled plasmid [64]. Complete unwinding of this structure was seen as protein concentrations capable of also catalysing complete unwinding of G4 DNA, while 4-way junctions required higher concentrations, suggesting that mobile D-loops are a preferred substrate for BLM [64]. BLM also efficiently disrupts D-loops in which the invading strand is coated with Rad51, a structure that more closely resembles the in vivo situation during the initial stages of HR [65]. Hence, BLM substrates are not limited to "naked" DNA structures, but also

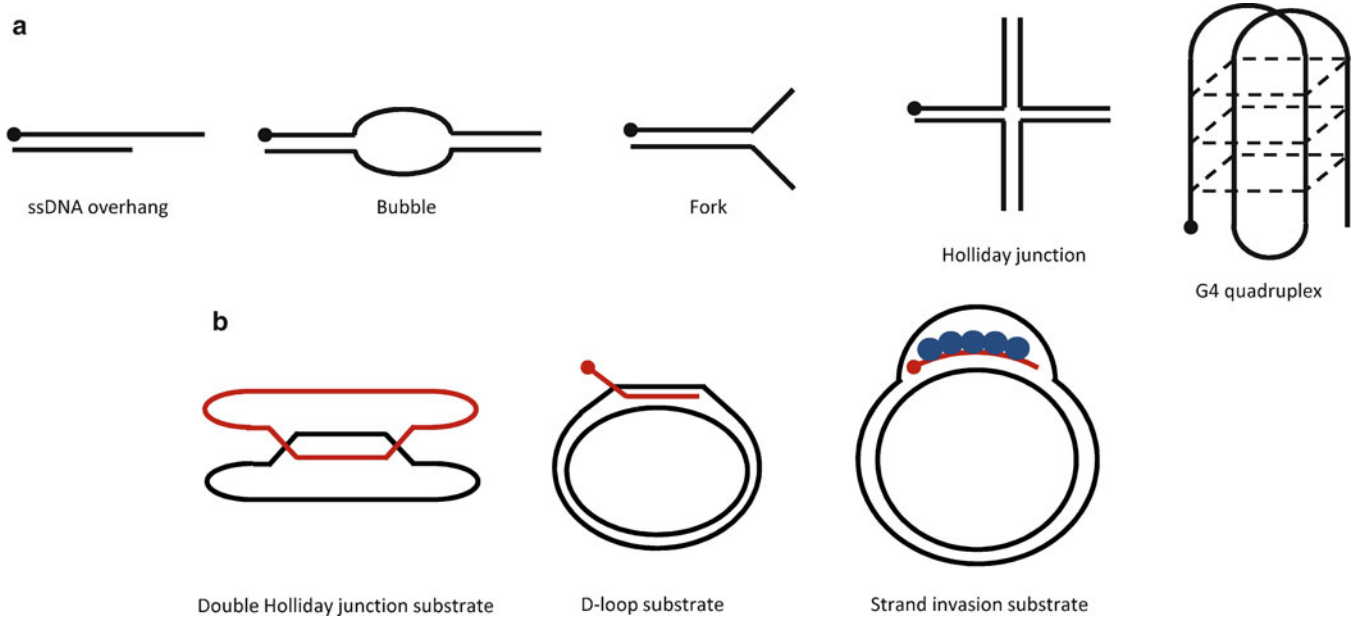

Fig. 8.2 DNA substrates for the RecQ family. The 5′ end of the DNA in each case is marked with a black circle. (**a**) BLM unwinds all of the structures indicated, with increasing efficiency from *left* to *right*. (**b**) Schematic representation of structures of more complex DNA substrates for RecQ helicase. BLM catalyses the disruption of the G-quadruplex, dissolution of the double Holliday junction, and the displacement of the D-loop. In the strand invasion substrate, the invading strand is coated by a RAD51 filament, indicated by *blue circles*

include DNA–protein filaments. In vitro, BLM is capable of removing RAD51 (the human RecA ortholog) filaments from ssDNA, if RAD51 is in its inactive ADP bound form [65]. In contrast, BLM stimulates D-loop formation with the active ATP-bound form of RAD51, by stimulating the homology search and strand exchange step [66]. In these experiments, BLM was capable of simulating D-loop formation involving templates with up to 10% mismatches, albeit at a slower rate [66].

Double Holliday Junction Dissolution, a Conserved Function That Limits Crossing Over

As described earlier, BLM forms a stable RTR-complex in vivo, which displays unique enzymatic activities. BLM and TOPOIIIα alone are capable of catalysing double Holliday junction (dHJ) dissolution in vitro [67]. The substrate used initially for this reaction comprised two, interlinked, covalently-closed oligonucleotides that contain two Holliday junctions separated by a 14 nucleotide heteroduplex region (Fig. 8.2). The dHJ dissolution reaction results in the unlinking of the two molecules without any exchange of sequences between the oligonucleotides and is dependent on BLM ATPase activity and TOPOIIIα catalytic activity [67]. BLM branch migrates the two Holliday junctions towards each other, converting them into a hemi-catenane structure, which can be unlinked by the single strand passage activity of TOPOIIIα. Further characterisation of this reaction revealed that the dHJ dissolution activity is highly specific for BLM and TOPOIIIα and cannot be catalysed by other human RecQ helicases [68] or *E. coli* Top3 [69]. Moreover, dissolution is an evolutionarily conserved function of the RTR complex. *S. cerevisiae* Sgs1 and Top3 alone are also capable of catalysing dHJ dissolution [49]. *D. melanogaster* BLM and Top3α also catalyse dHJ dissolution in vitro [70]. Furthermore, the HRDC domain is essential for the reaction, mutation of a single conserved lysine residue (position 1329) reduced dHJ dissolution activity without affecting unwinding activity on a partial duplex substrate [68]. Although they are not strictly required for dHJ dissolution activity in vitro, both RMI1 and RMI2 modulate the activity. Addition of RMI1 leads to a >10-fold increase in dHJ dissolution activity in the assay system described above [71]. RMI1 physically interacts with TOPOIIIα, leading to an increase in TOPOIIIα binding to dHJ structures [71]. Mutational studies show that only the N-terminal region of RMI1, which contains the BLM and TOPOIIIα(alpha) interacting domains, is required for this stimulation [52]. The Rmi1 stimulatory effect is also seen with Sgs1-Top3 dHJ dissolution, where Rmi1 directly stimulates Top3 decatenation activity, without affecting HJ branch migration [49]. TOPOIIIα has been shown to directly decatenane linked ssDNA circular DNA, the substrate expected to be produced by the BLM branch migration activity [72]. This reaction is stimulated specifically by RMI1 and BLM, but not RMI2 [72]. Finally addition of RMI2 to BLM-TOPOIIIα-RMI1 has been shown to lead to a small stimulation in dHJ dissolution activity [53]; however, this finding could not be verified in a second study [54].

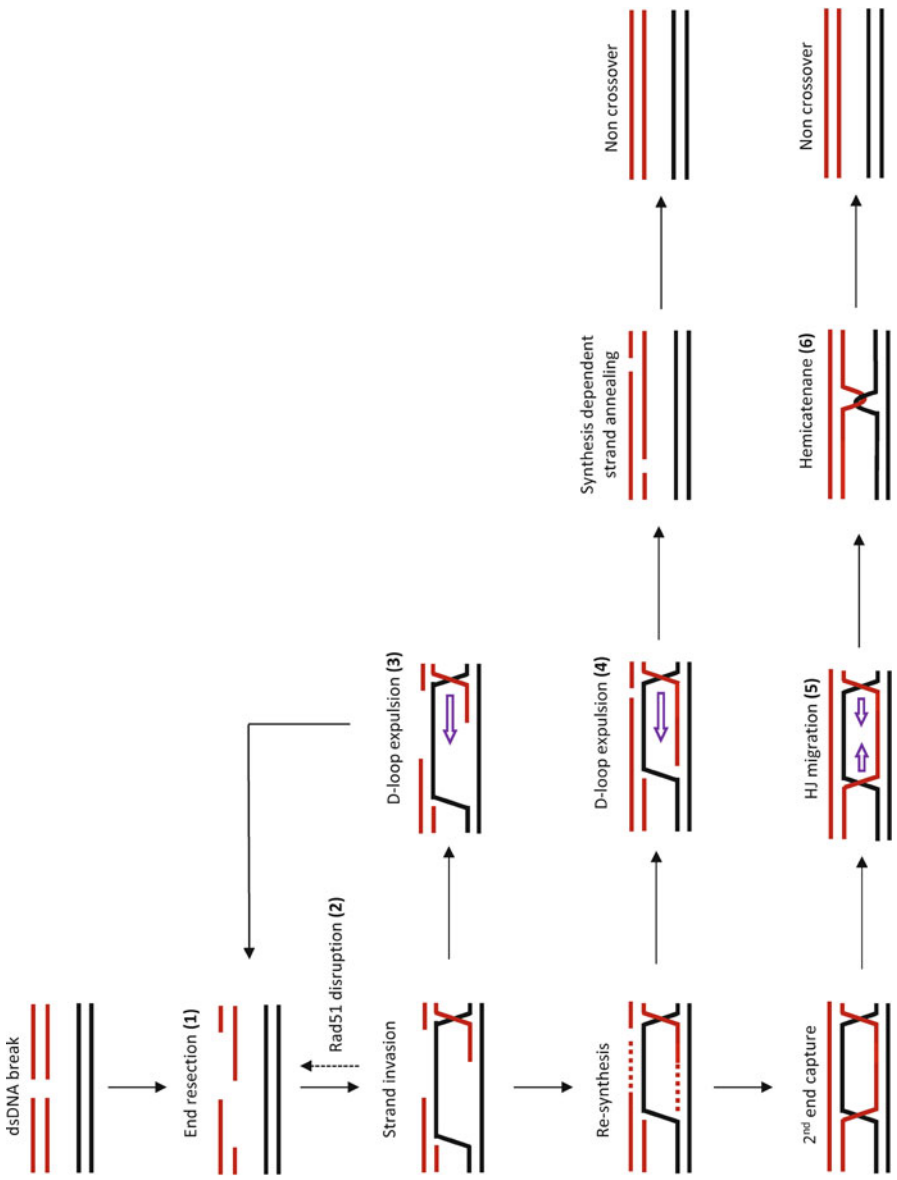
dsDNA break
End resection (1)
Rad51 disruption (2)
Strand invasion
D-loop expulsion (3)
Re-synthesis
D-loop expulsion (4)
Synthesis dependent strand annealing
Non crossover
2nd end capture
HJ migration (5)
Hemicatenane (6)
Non crossover

Fig. 8.3 Putative roles of BLM in DSB repair by homologous recombination. BLM acts as both a pro- and an anti-recombinase, depending on the stage of the homologous recombination process. The DSB (*top left*) is first resected. (1) Extensive end resection can be catalysed by BLM, and is pro-recombinogenic by providing the substrate for strand invasion. BLM also has anti-recombinogenic activities at the early stages prior to DNA synthesis via two different mechanisms (2 and 3). (2) Removal of RAD51 filaments from ssDNA prevents strand invasion and the homology search. (3) Disruption of D-loops prior to DNA synthesis reverses the strand invasion event. After DNA synthesis, BLM acts to promote resolution in a non-crossover fashion by two mechanisms (4–6). (4) Disruption of D-loops prior to second end capture could channel DNA substrates into the synthesis dependent strand-annealing pathway, which exclusively results in non-crossovers. (5) Branch migration of double Holliday junctions, catalysed by BLM, followed by (6) TopIIIα mediated DNA decatenantion, also results exclusively in non-crossovers

Other Sgs1/BLM Functions During Homologous Recombination

Sgs1 and BLM have been shown to play a role in at least three distinct steps during the repair of ssDNA gaps or double stranded breaks (DSBs) via homologous recombination (see Fig. 8.3 for a comprehensive overview). These three steps will be described in turn below:

DNA End-Resection

The first event required in the repair of a DSB via HR is resection of one strand at the dsDNA end, in order to produce an ssDNA stretch for formation of a RAD51 filament prior to strand invasion. The role of RecQ helicases in this process has been most extensively studied in yeast. The DSB break end is initially resected from the 5′ end by Mre11-Rad50-Xrs2 and Sae2, resulting in 50–100 nucleotides of ssDNA [73]. Further processing occurs via two independent pathways catalysed either by the 5′ 3′ nuclease, Exo1, or by Sgs1 together with the Dna2 nuclease/helicase. Both Sgs1 and Dna2 are rapidly recruited to sites of DSBs and gradually move away from the site. The Sgs1-dependent resection subpathway can continue for >28 kb, and requires both the helicase activity of Sgs1 and the nuclease activity of Dna2 [73]. In an *Δexo1* background, deletion of *sgs1* leads to a marked increase in sensitivity to a wide range of DSB inducing drugs, underpinning the in vivo relevance [74]. The resection activity has been successfully reconstituted in vitro, showing that Sgs1, Dna2 and RPA constitute the minimal requirement for resection of DSB ends [75]. Addition of Top3-Rmi1 leads to an ~11-fold stimulation of resection by promoting Sgs1 helicase activity via enhanced DNA affinity [74]. This pathway is conserved in humans; knock-down of BLM leads to an approximately twofold reduction in RPA foci upon DSB induction with camptothecin, as well as a reduction of ATR-mediated CHK1 and CHK2 phosphorylation, which is stimulated by ssDNA [74]. End resection using human proteins has also recently been reconstituted in vitro. BLM, DNA2 and RPA alone are capable of catalysing resection, which is the result of direct interaction between BLM and DNA2 [76]. Processivity is increased by addition of MRE11-RAD50-NBS1, which functions by recruiting BLM-DNA2 to DNA ends [76]. Interestingly BLM also impacts on the second long-range end resection pathway catalysed by EXO1. BLM binds directly to EXO1 and stimulates its resection activity in vitro, independently of functional helicase activity [77]. Further analysis showed that binding to BLM increases the affinity of EXO1 for DNA ends [76].

DNA Strand Invasion and Its Reversal

After the completion of end resection, a free ssDNA 3′ end is generated onto which a RAD51 filament is formed. RAD51 then mediates strand invasion and homology

searching, which allows for synthesis of the lost genetic material. After this early step, the displacement loop (D-loop) so formed can be processed via two HR subpathways: either synthesis-dependent strand-annealing (SDSA), in which the invading ssDNA loop dissociates from the donor template, or via the double Holliday junction pathway, in which second end capture leads to the formation of a covalently closed double Holliday junction structure (reviewed in [78]). BLM has been shown to play a role in both the early and late steps of HR. Analysis of double knock-out mouse ES cells lacking BLM and RAD54, a core HR factor, revealed a role for BLM upstream of RAD54 [79]. Studies in yeast suggest that Sgs1 plays a role as an anti-recombinase in early HR, a function that could be accounted for by direct removal of Rad51 filaments and/or disruption of D-loops from the donor template. *Δsgs1* mutants display a 13-fold increase in recombination between sequences with 91% homology, showing that Sgs1 normally suppresses recombination between divergent sequences [80]. Subsequent work has shown that Sgs1 is required to suppress single-strand annealing between tandem repeats with a 3% sequence diversion [81]. Overexpression of Sgs1 can also rescue the drug sensitivity of *Δsrs2* mutants, a UvrD-like helicase that is known to negatively regulate HR via removal of Rad51 filaments [82]. A genome-wide screen for factors that suppress recombination between naturally duplicated sequences present on multiple yeast chromosomes has been conducted [83]. This study found that, in addition to *SGS1*, deletion of *TOP3* or *RMI1* also leads to an increase in HR-mediated gross chromosomal rearrangement between these diverged sequences [83]. Anti-recombinase activity may thus require an intact RTR complex, despite the fact that helicase activity would seem to be sufficient to catalyse disruption of early HR structures. Finally it is conceivable that Sgs1 could act to channel HR intermediates into the SDSA pathway by disrupting the D-loop after DNA synthesis. However, in a reconstituted in vitro system, Sgs1 was unable to dissociate a D-loop like structure consisting of an ssDNA-Rad51 filament primer extended by Polδ [84].

Roles for Sgs1/BLM in the Late Stages of HR

Sgs1 and BLM play a prominent role in HR by processing late HR intermediates formed by second end capture. The dHJ dissolution pathway provides an elegant in vitro model for how BLM activity could suppress crossovers during HR. Several lines of evidence derived from yeast studies indicate that dHJ dissolution occurs in vivo, at least under some circumstances. Sgs1 suppresses crossovers induced by a DSB by threefold, and this suppression requires helicase activity and the N-terminal Top3 interacting domain [85]. A similar increase in crossovers are seen in Top3-deficient cells, a defect which is epistatic with Sgs1 [85].

Further evidence for a late role for Sgs1 in HR in yeast comes from physical analysis of DNA intermediates formed during HR. In yeast, two-dimensional gel electrophoresis can be applied to directly visualise replication and recombination structures at a specific locus. Using this technique, Liberi et al. showed that Rad51-dependent cruciform structures accumulate in *sgs1* mutants when replication forks

are stalled with MMS [86]. Similar structures accumulate in Top3 [86] and Rmi1 [87, 88] defective cells with the same kinetics, suggesting that their removal requires the entire RTR complex. Subsequent studies have addressed the nature of these cruciform structures by in vivo expression of various heterologous endonucleases in *Δsgs1* and *Δtop3* backgrounds. The Rad51-dependent cruciform structures could be resolved by expression of *E. coli* RusA or the catalytic fragment of human GEN1, $GEN1^{1-527}$, both of which are HJ resolvases in vitro [89]. When expressed in yeast, both RusA and GEN1 did not cut stalled forks or Rad51-independent cruciform structures, suggesting that their in vitro specificity is retained [89]. Further study of the processing of cruciform structures after MMS removal show that, in Rmi1-defective cells, these cruciform structures can eventually be resolved by the Mus81-Mms4 structure specific endonuclease [88]. Taken together, these studies provide evidence that HR-mediated HJ-containing structures accumulate in cells lacking a functional RTR complex. Given that the *S. cerevisiae* RTR complex has been shown to catalyse dHJ dissolution in vitro [49], it seems highly likely that these cruciform structures represent dHJ intermediates that are preferentially resolved by dissolution; however, other non-mutually exclusive explanations are possible (see [90] for further discussion). In cells lacking the RTR complex, such structures are instead cleaved by HJ-resolvases theoretically yielding a 1:1 ratio of crossovers and non-crossovers, which would explain the increased crossover rate observed in *Δsgs1* mutants [85].

Several lines of investigation in vertebrate cells suggest that the role of the RTR complex in the late stages of HR, revealed in yeast, is conserved through evolution. Depletion of RMI2 or TOPOIIIα in human cells leads to an increase in spontaneous chromosome breaks, and RMI1-depleted cells show hypersensitivity to MMS [53]. A second study in chicken DT40 cells showed that inactivation of RMI2 leads to increased SCE frequency, mirroring to the BLM-deficient phenotype in the same assay [54]. A *BLM RMI2* double mutant displayed the same level of SCEs as the *BLM* single mutant, showing that both proteins act in the pathway [54]. Depletion of the MUS81-EME1 or SLX1-SLX4 HJ resolvases in human BLM-deficient cell lines significantly reduces SCE levels, indicating that the increase in SCEs in Bloom's cells occurs through a HJ resolvase-dependent mechanism [91]. Furthermore, depletion of HJ resolvases in Bloom's cells leads to a severe defect in chromosome segregation with chromosome failing to condense and remaining tethered together [91]. Taken together, these data indicate that HR structures in vertebrate cells have the same basic genetic requirements for resolution as in yeast, which suggests that dHJ-like structure is also found in vivo in vertebrate cells.

A Role for RecQ Helicases at Perturbed DNA Replication Forks

DSBs are not the only cellular lesion that may require HR for resolution. HR factors are also implicated in the restart or resolution of stalled replication forks. A conserved feature of both Sgs1 and BLM mutant cells is an increased sensitivity to

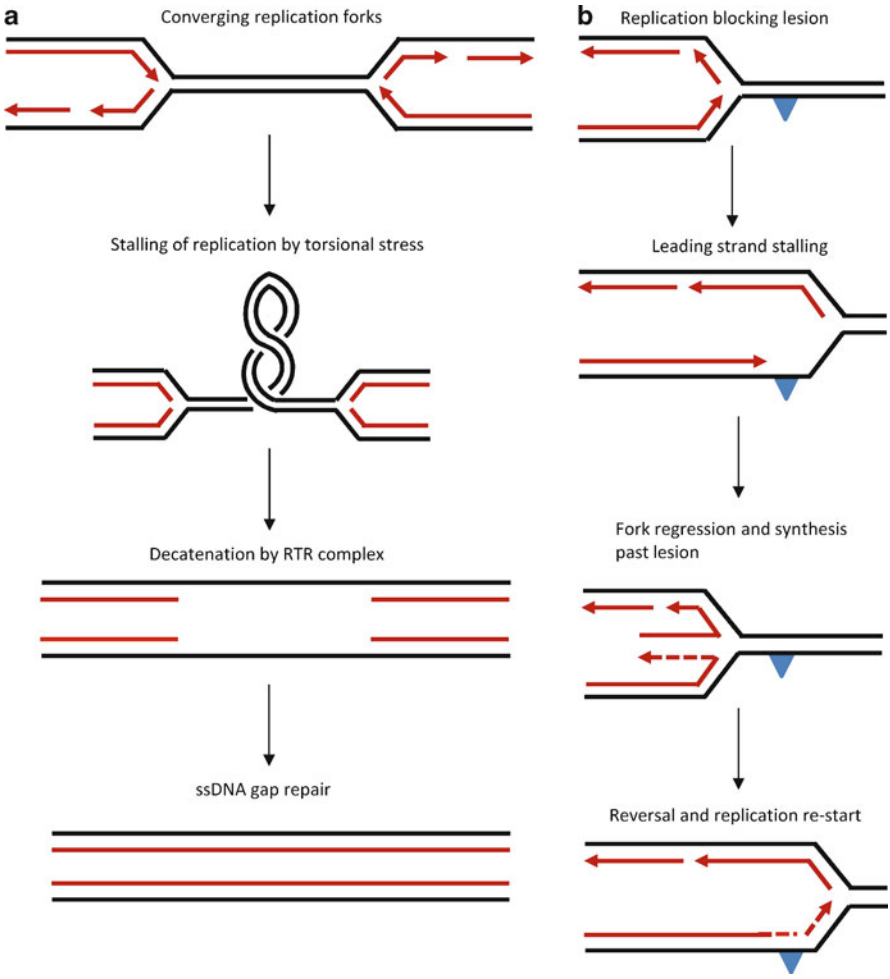

Fig. 8.4 Proposed roles of RecQ helicases during DNA replication. (**a**) Resolution of late replication intermediates. Convergence of two replication forks generates positive supercoiling in front of the replication forks and eventually replication is stalled by torsional stress in the template. The RTR complex could mediate the decatenation of this structure in order to allow separation of the sister chromatids during the anaphase of mitosis. Subsequently, the remaining non-replicated tract is repaired via ssDNA gap filling. (**b**) BLM mediated fork regression. Synthesis of one strand, in this case on the leading strand, is blocked by a DNA adduct, depicted by a *blue triangle*. BLM is proposed to catalyse regression of the fork into a so-called chicken-foot structure, which allows synthesis past the lesion using the nascent lagging strand as the template. Reversal of the chicken-foot beyond the point of the blocking lesion allows DNA synthesis to reassume. The lesion can then be removed later by the relevant repair system

replication stalling agents like hydroxyurea (HU), aphidicolin and MMS, showing that RecQ helicases are required for coping with replication stress. Upon treatment with HU, BLM rapidly accumulates at sites of stalled replication forks [92]. This

re-localisation is dependent on a functional RTR complex and is abrogated by RMI2 knock-down [53]. Similarly Sgs1 also associates with HU-stalled forks [93]. Studies in yeast showed that *Δsgs1* cells fail to keep Polα and Polε associated with replication forks stalled by HU treatment [93]. Helicase deficient Sgs1 cannot suppress this phenotype, suggesting that active remodelling of the stalled fork by Sgs1 is required for extended polymerase retention [93]. Top3 is also required for Polε retention at stalled forks and is epistatic with Sgs1, suggesting that a functional RTR complex is required to process a stalled fork into a stabilised form [94]. Both *Δtop3* and *Δsgs1* cells display defects in replication restart after HU treatment leading to decreased survival [94]. In *mec-100* mutants that lack a functional replication checkpoint, Sgs1 becomes completely essential for Polε and RPA retention at stalled forks [95]. In addition, a drastic 667-fold increase (compared to 4.4-fold in *Δsgs1* single mutants) in chromosomal rearrangements is seen after recovery from 2 h of HU treatment in the double mutant, demonstrating the importance of active modulation of stalled forks in vivo [95].

In human cells BLM co-localises at stalled forks together with the ATR checkpoint kinase, which phosphorylates BLM on threonine T99 and T122 [96]. Cells expressing an unphosphorylatable T99A/T122A mutant form of BLM fail to recover from HU treatment and enter an extended G2/M-arrest [96]. DNA fibre analysis revealed that replication restart after removal of HU or apidicolin is reduced in BLM-deficient cells and cannot be rescued by a helicase-defective BLM mutant, mirroring the results from yeast [97]. The T99A/T122A mutant BLM also showed defective fork restart, showing that checkpoint signals are essential for BLM-mediated fork stability [97].

Recently, RIF1 has been identified as a novel partner of the RTR complex involved in fork restart in vertebrate cells. RIF1 possesses DNA binding activity towards HJs and forked DNA structures [98]. Analysis in chicken cells shows that RIF1 and BLM are recruited to stalled forks with similar kinetics and that RIF1 recruitment is delayed in BLM-deficient cells. Epistasis analysis suggests that both proteins function in the same pathway and are required for efficient fork restart after HU treatment [98]. How RIF1 modulates BLM function at stalled fork, however, awaits more detailed studies. Indeed, the mechanistic details of how Sgs1/BLM stabilise stalled forks are not known. However, one attractive model is that they act by catalysing the regression of stalled forks into a “chicken-foot” structure, thus stabilising the ssDNA by pairing of nascent strands (Fig. 8.4b). In vitro, BLM is capable of regressing between 260 and 300 bp of a model replication fork structure, thus generating a Holliday junction containing “chicken-foot” [99]. Active fork regression has, however, yet to be proven in vivo.

A Role for BLM in Mitosis

BLM has recently been shown to play a novel role in the faithful segregation of sister chromatids in mitosis in unperturbed human cells. During anaphase, BLM localises specifically to a novel class of ultra-fine DNA bridges (UFBs) that connect

sister-chromatids [100]. UFBs cannot be stained by conventional DNA dyes, but immuno-staining revealed that they are almost completely coated by BLM, TOPOIIIα and RMI1, with the recruitment of the latter two depending on BLM. UFBs are present in early anaphase in around 90% of early, unperturbed anaphase cells and their number gradually decreases through anaphase, while the length of the bridge increases. UFBs are also coated by Plk1-interacting checkpoint helicase, PICH [101], which allows for visualisation of UFBs in BLM-deficient cells. In *BLM*$^{-/-}$ cells the number of UFBs is significantly increased, showing that BLM is required for their suppression [100]. The majority of UFBs arise from centromeric DNA and a significant increase is seen upon inactivation of TOPOIIα by inhibitor treatment [100] or depletion [102], suggesting that these bridges consist of catenated dsDNA. The abundance of UFBs at centromeres suggests that these may be physiological structures, possibly acting to assist in centromeric cohesion before the onset of anaphase [103]. A second group of UFBs link chromosomal arms. FISH analysis revealed that these bridges arise from chromosomal fragile sites (CFS), which are difficult to replicate areas of the genome [104]. Induction of replicative stress by aphidicolin, HU or mitomycin C treatment significantly increases the number of cells displaying non-centromeric UFBs and also the average number per cell. This subclass of UFBs is characterised by the presence of a discrete FANCD2 and FANCI focus at each end of the UFB. These FANCD2/I foci arise already in G2 phase, and then in anaphase define where a UFB will form [104]. The RTR complex has previously been shown to form a complex with the five Fanconi Anemia proteins (A, C, E, F, G) that make up part of the FA-core complex in vivo [105]. The FA pathway is activated by aphidicolin and HU and, in addition, it is required to suppress chromosome breakage at CFSs during replicative stress [106]. Moreover, the frequency of replication stress-induced non-centromeric UFBs has been shown to be increased in FANCA, FANCG and FANCI deficient cells, which are all essential for FA pathway function [107]. The presence of both the RTR and FA complexes on these structures suggests that DNA replication/repair is still ongoing at CSFs even as cells enter mitosis. Knock-down of RAD51 does not reduce the frequency of non-centromeric UFBs [104, 108], suggesting that these structures do not represent recombination intermediates. One possible interpretation is that non-centromeric UFBs arise from late replication intermediates in areas where DNA replication has not been fully completed prior to mitosis [103, 109]. As the sister chromatids are pulled apart, hemicatenanes are left at these sites, which require RTR activity for their unlinking. This interpretation is supported by the observation of small RPA tracts within UFBs, showing that at least a subset of these contain some ssDNA [104]. *E. coli* RecQ in conjunction with Top3 and SSB has been shown to specifically catalyse the resolution of converging replication forks in vitro [110]. So far, a similar activity has not been shown for BLM; however, it is tempting to speculate that the RTR complex is recruited to non-centromeric UFBs in order to catalyse the resolution of late replication intermediates and/or hemicatenes in unreplicated DNA (Fig. 8.4a).

Under conditions of replicative stress, 53BP1 foci, which are markers of DNA damage, are formed symmetrically in daughter cells at FSs. These foci persist until the next S-phase, arguing that many daughter cells are “born” with DNA damage

[111]. The formation of 53PB1 foci is significantly increased in BLM-deficient cells, mirroring the situation seen with non-centromeric UFBs [111]. This is highly suggestive of a model where unreplicated CFSs are decatenated by RTR in mitosis and then shielded in the daughter cells by 53BP1 until they can be fully replicated by gap-filling repair in the next S-phase [103]. To date, UFBs have only been observed in human cells, however a potentially similar structure has been observed in *S. pombe* cells arising from a strong replication blocking *lacO*-LacI array [112]. Chromosomal regions equivalent to CFSs, known are replication slow zones, are found in yeast [113]. It remains to be determined if UFB like structures also arise from endogenous replication slow zones under certain conditions or mutant strain backgrounds.

Regulation of BLM by SUMOylation

A large and growing body of work has shown that modification of proteins by the small ubiqutin-like modifier (SUMO) plays a major role in the cellular response to DNA damage (reviewed in [114]). SUMO modification typically regulates subcellular localisation and protein–protein interactions, and provides cells with a fast adaptive response to challenges. Both Sgs1 and BLM are known to be modified by SUMO [115, 116]. SUMOylation was first recognised for BLM, which can be SUMOylated on at least four different lysines, with K331 being a major site [116]. In vitro SUMOylation is dependent on BLM residues 212–237, which probably mediate the interaction with the SUMO conjugating enzyme Ubc9. BLM mutated in two SUMO sites, K317 and K331 (BLM-SD), fails to localise as normal to PML nuclear bodies in unperturbed cells, but instead forms damage-like foci that co-localise with γH2AX in the absence of exogenous DNA damage. Cells expressing the BLM-SD mutant display significantly higher levels of SCEs and micronucleus formation than wild-type BLM-expressing cells, showing that SUMOylation is required for normal BLM function [116]. Further characterisation of the BLM-SD mutant showed that this mutant displays a significant increase in γH2AX foci, DSBs and cell death following HU treatment, suggesting that SUMOylation is required for BLM function at stalled forks [117]. Furthermore, formation of RAD51 foci upon HU treatment is significantly impaired in BLM-SD cells, indicating that the mutant fails to initiate HR repair at stalled and/or broken forks. In vitro, RAD51 preferentially binds to SUMO-BLM over unmodified BLM, which could explain the decrease in focus formation [117].

The dynamics of BLM association with PML-bodies has been closely studied using fluorescence recovery after photobleaching (FRAP). The turnover of BLM in PML bodies is very rapid; the entire pool is exchanged within 1 min [118]. Kinetic modelling suggests that two distinct pool of BLM exists; >80% is exchanged rapidly at the surface, while the remaining protein is retained within PML-bodies for longer time [118]. Taken together the data indicates that SUMOylation regulates multiple aspects of BLM functions in both a pro- and anti-recombinogenic fashion. SUMO-

dependent localisation to PML bodies would sequester BLM and thus be anti-recombinogenic, while SUMOylation at stalled forks would activate HR by facilitating interaction with RAD51. SUMOlyation of Sgs1 has also been observed, with K621 being the preferred site of modification [119]. Sgs1 is specifically SUMOylated in response to treatment with the DNA damaging agents, bleomycin, IR, MMS or EMS, but not treatment with HU or H_2O_2. However, cells expressing SUMOylation-deficient Sgs1 do not display any defects in chromosomal HR function or regulation, but are specifically defective in telomere–telomere recombination [119]. The regulation of Sgs1 by SUMOylation is clearly different from that seen with BLM, and it is possible that, in yeast, SUMOylation instead directs a proportion of Sgs1 to specific telomere function, while not affecting core HR functions.

Concluding Remarks

The RecQ helicase family is one of the most extensively studied groups of proteins. This has led to a burgeoning literature on human RecQ enzymes and their homologs in lower organisms. There has been significant recent progress in understanding how RecQ proteins function during HR and other DNA metabolic processes. However, it would be fair to say that our current knowledge is still quite rudimentary. It seems clear that BLM in human cells fulfils many of the roles of RecQ helicases that are conserved in bacteria and yeast, particularly those that require the action of Top3, RPA and Rmi1. Nevertheless, we really have very little knowledge of the precise roles of the other four human RecQ helicases. Given that WRN and RECQ4 are important for suppression of human disease conditions that are associated with premature cancer development and ageing, it is important that this deficiency is corrected as soon as possible.

Acknowledgements We would like to thank Dr Hocine Mankouri for helpful comments on this article. Work in the authors' laboratory is supported by the Nordea Foundation, The Danish Cancer Society, the Danish Medical Research Council (FSS), The Association for International Cancer Research (AICR) and The Novo Nordisk Foundation.

References

1. Chu WK, Hickson ID. RecQ helicases: multifunctional genome caretakers. Nat Rev Cancer. 2009;9(9):644–54.
2. Bernstein KA, Gangloff S, Rothstein R. The RecQ DNA helicases in DNA repair. Annu Rev Genet. 2010;44:393–417.
3. Monnat Jr RJ. Human RECQ helicases: roles in DNA metabolism, mutagenesis and cancer biology. Semin Cancer Biol. 2010;20(5):329–39.
4. German J, Sanz MM, Ciocci S, Ye TZ, Ellis NA. Syndrome-causing mutations of the BLM gene in persons in the Bloom's Syndrome Registry. Hum Mutat. 2007;28(8):743–53.
5. German J, Archibald R, Bloom D. Chromosomal breakage in a rare and probably genetically determined syndrome of man. Science. 1965;148(3669):506–7.

6. Chaganti RS, Schonberg S, German J. A manyfold increase in sister chromatid exchanges in Bloom's syndrome lymphocytes. Proc Natl Acad Sci USA. 1974;71(11):4508–12.
7. Fairman-Williams ME, Guenther UP, Jankowsky E. SF1 and SF2 helicases: family matters. Curr Opin Struct Biol. 2010;20(3):313–24.
8. Bernstein DA, Keck JL. Domain mapping of Escherichia coli RecQ defines the roles of conserved N- and C-terminal regions in the RecQ family. Nucleic Acids Res. 2003;31(11):2778–85.
9. Bernstein DA, Zittel MC, Keck JL. High-resolution structure of the E.coli RecQ helicase catalytic core. EMBO J. 2003;22(19):4910–21.
10. Saffi J, Pereira VR, Henriques JA. Importance of the Sgs1 helicase activity in DNA repair of Saccharomyces cerevisiae. Curr Genet. 2000;37(2):75–8.
11. Mullen JR, Kaliraman V, Brill SJ. Bipartite structure of the SGS1 DNA helicase in Saccharomyces cerevisiae. Genetics. 2000;154(3):1101–14.
12. Bahr A, De Graeve F, Kedinger C, Chatton B. Point mutations causing Bloom's syndrome abolish ATPase and DNA helicase activities of the BLM protein. Oncogene. 1998;17(20):2565–71.
13. Rong SB, Valiaho J, Vihinen M. Structural basis of Bloom syndrome (BS) causing mutations in the BLM helicase domain. Mol Med. 2000;6(3):155–64.
14. Liu JL, Rigolet P, Dou SX, Wang PY, Xi XG. The zinc finger motif of Escherichia coli RecQ is implicated in both DNA binding and protein folding. J Biol Chem. 2004;279(41):42794–802.
15. Guo RB, Rigolet P, Zargarian L, Fermandjian S, Xi XG. Structural and functional characterizations reveal the importance of a zinc binding domain in Bloom's syndrome helicase. Nucleic Acids Res. 2005;33(10):3109–24.
16. Ren H, Dou SX, Zhang XD, et al. The zinc-binding motif of human RECQ5beta suppresses the intrinsic strand-annealing activity of its DExH helicase domain and is essential for the helicase activity of the enzyme. Biochem J. 2008;412(3):425–33.
17. Pike AC, Shrestha B, Popuri V, et al. Structure of the human RECQ1 helicase reveals a putative strand-separation pin. Proc Natl Acad Sci USA. 2009;106(4):1039–44.
18. Lucic B, Zhang Y, King O, et al. A prominent beta-hairpin structure in the winged-helix domain of RECQ1 is required for DNA unwinding and oligomer formation. Nucleic Acids Res. 2011;39(5):1703–17.
19. Kitano K, Kim SY, Hakoshima T. Structural basis for DNA strand separation by the unconventional winged-helix domain of RecQ helicase WRN. Structure. 2010;18(2):177–87.
20. Huber MD, Duquette ML, Shiels JC, Maizels N. A conserved G4 DNA binding domain in RecQ family helicases. J Mol Biol. 2006;358(4):1071–80.
21. Liu Z, Macias MJ, Bottomley MJ, et al. The three-dimensional structure of the HRDC domain and implications for the Werner and Bloom syndrome proteins. Structure. 1999;7(12):1557–66.
22. Bernstein DA, Keck JL. Conferring substrate specificity to DNA helicases: role of the RecQ HRDC domain. Structure. 2005;13(8):1173–82.
23. Kitano K, Yoshihara N, Hakoshima T. Crystal structure of the HRDC domain of human Werner syndrome protein, WRN. J Biol Chem. 2007;282(4):2717–28.
24. Kim YM, Choi BS. Structure and function of the regulatory HRDC domain from human Bloom syndrome protein. Nucleic Acids Res. 2010;38(21):7764–77.
25. Sato A, Mishima M, Nagai A, et al. Solution structure of the HRDC domain of human Bloom syndrome protein BLM. J Biochem. 2010;148(4):517–25.
26. Karmakar P, Seki M, Kanamori M, et al. BLM is an early responder to DNA double-strand breaks. Biochem Biophys Res Commun. 2006;348(1):62–9.
27. von Kobbe C, Thoma NH, Czyzewski BK, Pavletich NP, Bohr VA. Werner syndrome protein contains three structure-specific DNA binding domains. J Biol Chem. 2003;278(52):52997–3006.
28. Vindigni A, Hickson ID. RecQ helicases: multiple structures for multiple functions? HFSP J. 2009;3(3):153–64.
29. Perry JJ, Yannone SM, Holden LG, et al. WRN exonuclease structure and molecular mechanism imply an editing role in DNA end processing. Nat Struct Mol Biol. 2006;13(5):414–22.

30. Opresko PL, Laine JP, Brosh Jr RM, Seidman MM, Bohr VA. Coordinate action of the helicase and 3' to 5' exonuclease of Werner syndrome protein. J Biol Chem. 2001;276(48):44677–87.
31. Boubriak I, Mason PA, Clancy DJ, Dockray J, Saunders RD, Cox LS. DmWRNexo is a 3'-5' exonuclease: phenotypic and biochemical characterization of mutants of the Drosophila orthologue of human WRN exonuclease. Biogerontology. 2009;10(3):267–77.
32. Capp C, Wu JH, Hsieh TS. Drosophila RecQ4 has a 3 '-5 ' DNA helicase activity that is essential for viability. J Biol Chem. 2009;284(45):30845–52.
33. Abe T, Yoshimura A, Hosono Y, Tada S, Seki M, Enomoto T. The N-terminal region of RECQL4 lacking the helicase domain is both essential and sufficient for the viability of vertebrate cells. Role of the N-terminal region of RECQL4 in cells. Biochim Biophys Acta. 2011;1813(3):473–9.
34. Thangavel S, Mendoza-Maldonado R, Tissino E, et al. Human RECQ1 and RECQ4 helicases play distinct roles in DNA replication initiation. Mol Cell Biol. 2010;30(6):1382–96.
35. Chen CF, Brill SJ. An essential DNA strand-exchange activity is conserved in the divergent N-termini of BLM orthologs. EMBO J. 2010;29(10):1713–25.
36. Umezu K, Nakayama H. RecQ DNA helicase of Escherichia coli. Characterization of the helix-unwinding activity with emphasis on the effect of single-stranded DNA-binding protein. J Mol Biol. 1993;230(4):1145–50.
37. Harmon FG, Kowalczykowski SC. Biochemical characterization of the DNA helicase activity of the Escherichia coli RecQ helicase. J Biol Chem. 2001;276(1):232–43.
38. Shereda RD, Bernstein DA, Keck JL. A central role for SSB in Escherichia coli RecQ DNA helicase function. J Biol Chem. 2007;282(26):19247–58.
39. Shereda RD, Reiter NJ, Butcher SE, Keck JL. Identification of the SSB binding site on E. coli RecQ reveals a conserved surface for binding SSB's C terminus. J Mol Biol. 2009;386(3):612–25.
40. Harmon FG, DiGate RJ, Kowalczykowski SC. RecQ helicase and topoisomerase III comprise a novel DNA strand passage function: a conserved mechanism for control of DNA recombination. Mol Cell. 1999;3(5):611–20.
41. Harmon FG, Kowalczykowski SC. RecQ helicase, in concert with RecA and SSB proteins, initiates and disrupts DNA recombination. Genes Dev. 1998;12(8):1134–44.
42. Gangloff S, McDonald JP, Bendixen C, Arthur L, Rothstein R. The yeast type I topoisomerase Top3 interacts with Sgs1, a DNA helicase homolog: a potential eukaryotic reverse gyrase. Mol Cell Biol. 1994;14(12):8391–8.
43. Ahmad F, Stewart E. The N-terminal region of the Schizosaccharomyces pombe RecQ helicase, Rqh1p, physically interacts with Topoisomerase III and is required for Rqh1p function. Mol Genet Genomics. 2005;273(1):102–14.
44. Fricke WM, Kaliraman V, Brill SJ. Mapping the DNA topoisomerase III binding domain of the Sgs1 DNA helicase. J Biol Chem. 2001;276(12):8848–55.
45. Ui A, Satoh Y, Onoda F, Miyajima A, Seki M, Enomoto T. The N-terminal region of Sgs1, which interacts with Top3, is required for complementation of MMS sensitivity and suppression of hyper-recombination in sgs1 disruptants. Mol Genet Genomics. 2001;265(5):837–50.
46. Chang M, Bellaoui M, Zhang C, et al. RMI1/NCE4, a suppressor of genome instability, encodes a member of the RecQ helicase/Topo III complex. EMBO J. 2005;24(11):2024–33.
47. Chen CF, Brill SJ. Binding and activation of DNA topoisomerase III by the Rmi1 subunit. J Biol Chem. 2007;282(39):28971–9.
48. Wu L, Davies SL, Levitt NC, Hickson ID. Potential role for the BLM helicase in recombinational repair via a conserved interaction with RAD51. J Biol Chem. 2001;276(22):19375–81.
49. Cejka P, Plank JL, Bachrati CZ, Hickson ID, Kowalczykowski SC. Rmi1 stimulates decatenation of double Holliday junctions during dissolution by Sgs1-Top3. Nat Struct Mol Biol. 2010;17(11):1377–82.
50. Wu L, Davies SL, North PS, et al. The Bloom's syndrome gene product interacts with topoisomerase III. J Biol Chem. 2000;275(13):9636–44.
51. Yin J, Sobeck A, Xu C, et al. BLAP75, an essential component of Bloom's syndrome protein complexes that maintain genome integrity. EMBO J. 2005;24(7):1465–76.

52. Raynard S, Zhao W, Bussen W, et al. Functional role of BLAP75 in BLM-topoisomerase IIIalpha-dependent holliday junction processing. J Biol Chem. 2008;283(23):15701–8.
53. Singh TR, Ali AM, Busygina V, et al. BLAP18/RMI2, a novel OB-fold-containing protein, is an essential component of the Bloom helicase-double Holliday junction dissolvasome. Genes Dev. 2008;22(20):2856–68.
54. Xu D, Guo R, Sobeck A, et al. RMI, a new OB-fold complex essential for Bloom syndrome protein to maintain genome stability. Genes Dev. 2008;22(20):2843–55.
55. Wang F, Yang Y, Singh TR, et al. Crystal structures of RMI1 and RMI2, two OB-fold regulatory subunits of the BLM complex. Structure. 2010;18(9):1159–70.
56. Brosh Jr RM, Li JL, Kenny MK, et al. Replication protein A physically interacts with the Bloom's syndrome protein and stimulates its helicase activity. J Biol Chem. 2000;275(31):23500–8.
57. Bergeron KL, Murphy EL, Brown LW, Almeida KH. Critical interaction domains between bloom syndrome protein and RAD51. Protein J. 2011;30(1):1–8.
58. Mohaghegh P, Karow JK, Brosh Jr RM, Bohr VA, Hickson ID. The Bloom's and Werner's syndrome proteins are DNA structure-specific helicases. Nucleic Acids Res. 2001;29(13):2843–9.
59. Bennett RJ, Keck JL, Wang JC. Binding specificity determines polarity of DNA unwinding by the Sgs1 protein of S. cerevisiae. J Mol Biol. 1999;289(2):235–48.
60. Sun H, Karow JK, Hickson ID, Maizels N. The Bloom's syndrome helicase unwinds G4 DNA. J Biol Chem. 1998;273(42):27587–92.
61. Sun H, Bennett RJ, Maizels N. The Saccharomyces cerevisiae Sgs1 helicase efficiently unwinds G-G paired DNAs. Nucleic Acids Res. 1999;27(9):1978–84.
62. Kamath-Loeb A, Loeb LA, Fry M. The werner syndrome protein is distinguished from the bloom syndrome protein by its capacity to tightly bind diverse DNA structures. PLoS One. 2012;7(1):e30189.
63. Karow JK, Constantinou A, Li JL, West SC, Hickson ID. The Bloom's syndrome gene product promotes branch migration of holliday junctions. Proc Natl Acad Sci USA. 2000;97(12):6504–8.
64. Bachrati CZ, Borts RH, Hickson ID. Mobile D-loops are a preferred substrate for the Bloom's syndrome helicase. Nucleic Acids Res. 2006;34(8):2269–79.
65. Bugreev DV, Yu X, Egelman EH, Mazin AV. Novel pro- and anti-recombination activities of the Bloom's syndrome helicase. Genes Dev. 2007;21(23):3085–94.
66. Bugreev DV, Mazina OM, Mazin AV. Bloom syndrome helicase stimulates RAD51 DNA strand exchange activity through a novel mechanism. J Biol Chem. 2009;284(39):26349–59.
67. Wu L, Hickson ID. The Bloom's syndrome helicase suppresses crossing over during homologous recombination. Nature. 2003;426(6968):870–4.
68. Wu L, Chan KL, Ralf C, et al. The HRDC domain of BLM is required for the dissolution of double Holliday junctions. EMBO J. 2005;24(14):2679–87.
69. Bussen W, Raynard S, Busygina V, Singh AK, Sung P. Holliday junction processing activity of the BLM-Topo IIIalpha-BLAP75 complex. J Biol Chem. 2007;282(43):31484–92.
70. Chen SH, Wu CH, Plank JL, Hsieh TS. Essential functions of the C-terminus of Drosophila topoisomerase IIIalpha in double Holliday junction dissolution. J Biol Chem. 2012;287(23):19346–53.
71. Wu L, Bachrati CZ, Ou J, et al. BLAP75/RMI1 promotes the BLM-dependent dissolution of homologous recombination intermediates. Proc Natl Acad Sci USA. 2006;103(11):4068–73.
72. Yang J, Bachrati CZ, Ou J, Hickson ID, Brown GW. Human topoisomerase IIIalpha is a single-stranded DNA decatenase that is stimulated by BLM and RMI1. J Biol Chem. 2010;285(28):21426–36.
73. Zhu Z, Chung WH, Shim EY, Lee SE, Ira G. Sgs1 helicase and two nucleases Dna2 and Exo1 resect DNA double-strand break ends. Cell. 2008;134(6):981–94.
74. Gravel S, Chapman JR, Magill C, Jackson SP. DNA helicases Sgs1 and BLM promote DNA double-strand break resection. Genes Dev. 2008;22(20):2767–72.
75. Cejka P, Cannavo E, Polaczek P, et al. DNA end resection by Dna2-Sgs1-RPA and its stimulation by Top3-Rmi1 and Mre11-Rad50-Xrs2. Nature. 2010;467(7311):112–6.

76. Nimonkar AV, Genschel J, Kinoshita E, et al. BLM-DNA2-RPA-MRN and EXO1-BLM-RPA-MRN constitute two DNA end resection machineries for human DNA break repair. Genes Dev. 2011;25(4):350–62.
77. Nimonkar AV, Ozsoy AZ, Genschel J, Modrich P, Kowalczykowski SC. Human exonuclease 1 and BLM helicase interact to resect DNA and initiate DNA repair. Proc Natl Acad Sci USA. 2008;105(44):16906–11.
78. Li X, Heyer WD. Homologous recombination in DNA repair and DNA damage tolerance. Cell Res. 2008;18(1):99–113.
79. Chu WK, Hanada K, Kanaar R, Hickson ID. BLM has early and late functions in homologous recombination repair in mouse embryonic stem cells. Oncogene. 2010;29(33):4705–14.
80. Myung K, Datta A, Chen C, Kolodner RD. SGS1, the Saccharomyces cerevisiae homologue of BLM and WRN, suppresses genome instability and homeologous recombination. Nat Genet. 2001;27(1):113–6.
81. Sugawara N, Goldfarb T, Studamire B, Alani E, Haber JE. Heteroduplex rejection during single-strand annealing requires Sgs1 helicase and mismatch repair proteins Msh2 and Msh6 but not Pms1. Proc Natl Acad Sci USA. 2004;101(25):9315–20.
82. Mankouri HW, Craig TJ, Morgan A. SGS1 is a multicopy suppressor of srs2: functional overlap between DNA helicases. Nucleic Acids Res. 2002;30(5):1103–13.
83. Putnam CD, Hayes TK, Kolodner RD. Specific pathways prevent duplication-mediated genome rearrangements. Nature. 2009;460(7258):984–9.
84. Sebesta M, Burkovics P, Haracska L, Krejci L. Reconstitution of DNA repair synthesis in vitro and the role of polymerase and helicase activities. DNA Repair. 2011;10(6):567–76.
85. Ira G, Malkova A, Liberi G, Foiani M, Haber JE. Srs2 and Sgs1-Top3 suppress crossovers during double-strand break repair in yeast. Cell. 2003;115(4):401–11.
86. Liberi G, Maffioletti G, Lucca C, et al. Rad51-dependent DNA structures accumulate at damaged replication forks in sgs1 mutants defective in the yeast ortholog of BLM RecQ helicase. Genes Dev. 2005;19(3):339–50.
87. Mankouri HW, Ngo HP, Hickson ID. Shu proteins promote the formation of homologous recombination intermediates that are processed by Sgs1-Rmi1-Top3. Mol Biol Cell. 2007;18(10):4062–73.
88. Ashton TM, Mankouri HW, Heidenblut A, McHugh PJ, Hickson ID. Pathways for Holliday junction processing during homologous recombination in Saccharomyces cerevisiae. Mol Cell Biol. 2011;31(9):1921–33.
89. Mankouri HW, Ashton TM, Hickson ID. Holliday junction-containing DNA structures persist in cells lacking Sgs1 or Top3 following exposure to DNA damage. Proc Natl Acad Sci USA. 2011;108(12):4944–9.
90. Hickson ID, Mankouri HW. Processing of homologous recombination repair intermediates by the Sgs1-Top3-Rmi1 and Mus81-Mms4 complexes. Cell Cycle. 2011;10(18):3078–85.
91. Wechsler T, Newman S, West SC. Aberrant chromosome morphology in human cells defective for Holliday junction resolution. Nature. 2011;471(7340):642–6.
92. Sengupta S, Linke SP, Pedeux R, et al. BLM helicase-dependent transport of p53 to sites of stalled DNA replication forks modulates homologous recombination. EMBO J. 2003;22(5):1210–22.
93. Cobb JA, Bjergbaek L, Shimada K, Frei C, Gasser SM. DNA polymerase stabilization at stalled replication forks requires Mec1 and the RecQ helicase Sgs1. EMBO J. 2003;22(16):4325–36.
94. Bjergbaek L, Cobb JA, Tsai-Pflugfelder M, Gasser SM. Mechanistically distinct roles for Sgs1p in checkpoint activation and replication fork maintenance. EMBO J. 2005;24(2):405–17.
95. Cobb JA, Schleker T, Rojas V, Bjergbaek L, Tercero JA, Gasser SM. Replisome instability, fork collapse, and gross chromosomal rearrangements arise synergistically from Mec1 kinase and RecQ helicase mutations. Genes Dev. 2005;19(24):3055–69.
96. Davies SL, North PS, Dart A, Lakin ND, Hickson ID. Phosphorylation of the Bloom's syndrome helicase and its role in recovery from S-phase arrest. Mol Cell Biol. 2004;24(3):1279–91.

97. Davies SL, North PS, Hickson ID. Role for BLM in replication-fork restart and suppression of origin firing after replicative stress. Nat Struct Mol Biol. 2007;14(7):677–9.
98. Xu D, Muniandy P, Leo E, et al. Rif1 provides a new DNA-binding interface for the Bloom syndrome complex to maintain normal replication. EMBO J. 2010;29(18):3140–55.
99. Ralf C, Hickson ID, Wu L. The Bloom's syndrome helicase can promote the regression of a model replication fork. J Biol Chem. 2006;281(32):22839–46.
100. Chan KL, North PS, Hickson ID. BLM is required for faithful chromosome segregation and its localization defines a class of ultrafine anaphase bridges. EMBO J. 2007;26(14):3397–409.
101. Baumann C, Korner R, Hofmann K, Nigg EA. PICH, a centromere-associated SNF2 family ATPase, is regulated by Plk1 and required for the spindle checkpoint. Cell. 2007;128(1):101–14.
102. Spence JM, Phua HH, Mills W, Carpenter AJ, Porter AC, Farr CJ. Depletion of topoisomerase IIalpha leads to shortening of the metaphase interkinetochore distance and abnormal persistence of PICH-coated anaphase threads. J Cell Sci. 2007;120(pt 22):3952–64.
103. Chan KL, Hickson ID. New insights into the formation and resolution of ultra-fine anaphase bridges. Semin Cell Dev Biol. 2011;22(8):906–12.
104. Chan KL, Palmai-Pallag T, Ying SM, Hickson ID. Replication stress induces sister-chromatid bridging at fragile site loci in mitosis. Nat Cell Biol. 2009;11(6):753–60.
105. Meetei AR, Sechi S, Wallisch M, et al. A multiprotein nuclear complex connects Fanconi anemia and Bloom syndrome. Mol Cell Biol. 2003;23(10):3417–26.
106. Howlett NG, Taniguchi T, Durkin SG, D'Andrea AD, Glover TW. The Fanconi anemia pathway is required for the DNA replication stress response and for the regulation of common fragile site stability. Hum Mol Genet. 2005;14(5):693–701.
107. Vinciguerra P, Godinho SA, Parmar K, Pellman D, D'Andrea AD. Cytokinesis failure occurs in Fanconi anemia pathway-deficient murine and human bone marrow hematopoietic cells. J Clin Invest. 2010;120(11):3834–42.
108. Lahkim Bennani-Belhaj K, Rouzeau S, Buhagiar-Labarchede G, et al. The Bloom syndrome protein limits the lethality associated with RAD51 deficiency. Mol Cancer Res. 2010;8(3):385–94.
109. Chan KL, Hickson ID. On the origins of ultra-fine anaphase bridges. Cell Cycle. 2009;8(19):3065–6.
110. Suski C, Marians KJ. Resolution of converging replication forks by RecQ and topoisomerase III. Mol Cell. 2008;30(6):779–89.
111. Lukas C, Savic V, Bekker-Jensen S, et al. 53BP1 nuclear bodies form around DNA lesions generated by mitotic transmission of chromosomes under replication stress. Nat Cell Biol. 2011;13(3):243–53.
112. Sofueva S, Osman F, Lorenz A, et al. Ultrafine anaphase bridges, broken DNA and illegitimate recombination induced by a replication fork barrier. Nucleic Acids Res. 2011;39(15):6568–84.
113. Cha RS, Kleckner N. ATR homolog Mec1 promotes fork progression, thus averting breaks in replication slow zones. Science. 2002;297(5581):602–6.
114. Dou H, Huang C, Nguyen TV, Lu LS, Yeh ETH. SUMOylation and de-SUMOylation in response to DNA damage. FEBS Lett. 2011;585(18):2891–6.
115. Branzei D, Sollier J, Liberi G, et al. Ubc9-and mms21-mediated sumoylation counteracts recombinogenic events at damaged replication forks. Cell. 2006;127(3):509–22.
116. Eladad S, Ye TZ, Hu P, et al. Intra-nuclear trafficking of the BLM helicase to DNA damage-induced foci is regulated by SUMO modification. Hum Mol Genet. 2005;14(10):1351–65.
117. Ouyang KJ, Woo LL, Zhu JM, Huo DZ, Matunis MJ, Ellis NA. SUMO modification regulates BLM and RAD51 interaction at damaged replication forks. PLOS Biol. 2009;7(12):e1000252.
118. Weidtkamp-Peters S, Lenser T, Negorev D, et al. Dynamics of component exchange at PML nuclear bodies. J Cell Sci. 2008;121(pt 16):2731–43.
119. Lu CY, Tsai CH, Brill SJ, Teng SC. Sumoylation of the BLM ortholog, Sgs1, promotes telomere-telomere recombination in budding yeast. Nucleic Acids Res. 2010;38(2):488–98.

Chapter 9
Roles of DNA Helicases in the Mediation and Regulation of Homologous Recombination

James M. Daley, Hengyao Niu, and Patrick Sung

Abstract Homologous recombination (HR) is an evolutionarily conserved process that eliminates DNA double-strand breaks from chromosomes, repairs injured DNA replication forks, and helps orchestrate meiotic chromosome segregation. Recent studies have shown that DNA helicases play multifaceted roles in HR mediation and regulation. In particular, the *S. cerevisiae* Sgs1 helicase and its human ortholog BLM helicase are involved in not only the resection of the primary lesion to generate single-stranded DNA to prompt the assembly of the HR machinery, but they also function in somatic cells to suppress the formation of chromosome arm crossovers during HR. On the other hand, the *S. cerevisiae* Mph1 and Srs2 helicases, and their respective functional equivalents in other eukaryotes, suppress spurious HR events and favor the formation of noncrossovers via distinct mechanisms. Thus, the functional integrity of the HR process and HR outcomes are dependent upon these helicase enzymes. Since mutations in some of these helicases lead to cancer predisposition in humans and mice, studies on them have clear relevance to human health and disease.

Prologue

By separating the strands in duplex DNA, processing DNA structures, and remodeling nucleoprotein complexes, DNA helicases are indispensable for different facets of DNA metabolism. Here, we review recent research on helicases involved in homologous recombination, one of the two main pathways that eliminates double-strand breaks in DNA. We focus on the RecQ helicases and the Hef-like helicases, which belong to the SF2 helicase superfamily, as well as the SF1 family

J.M. Daley • H. Niu • P. Sung (✉)
Molecular Biophysics and Biochemistry, Yale University School of Medicine,
New Haven, CT, USA
e-mail: patrick.sung@yale.edu

M. Spies (ed.), *DNA Helicases and DNA Motor Proteins*, Advances in Experimental Medicine and Biology, DOI 10.1007/978-1-4614-5037-5_9,

member Srs2. Mutations in RecQ and Hef-like helicases cause several human syndromes that predispose patients to cancer, highlighting the importance of these enzymes in genome maintenance and mutation avoidance.

DNA Double-Strand Break Repair Pathways

Double-strand breaks (DSBs) are extremely toxic because of their propensity to induce genome alterations and rearrangements, including deletions and translocations. DSBs can be eliminated either by nonhomologous DNA end joining (NHEJ) or homologous recombination (HR). During NHEJ, the broken ends are first aligned, processed to reveal microhomology between them, and then ligated [1]. In HR, which is mechanistically much more complex, a homologous DNA sequence, located within either the sister chromatid or the chromosome homolog, is used as the template to direct the repair reaction [2, 3]. Herein, we will focus on the roles of DNA helicases in HR mediation and regulation.

Homologous Repair Pathways

HR-mediated DSB repair is initiated by the nucleolytic degradation of the 5′ strands of the break ends, referred to as DNA end resection. The nucleases Mre11, Exo1, and Dna2 participate in this resection process [4–6]. The 3′ tails derived from resection (Fig. 9.1) are engaged by the Rad51 recombinase, which catalyzes the search for a homologous duplex sequence and the invasion of the sequence to form a DNA joint called the displacement loop, or D-loop [3]. DNA synthesis is initiated from the 3′ end of the invading strand. At this stage, the D-loop structure can be disassembled via the action of a specialized helicase, thus allowing the newly synthesized DNA to anneal with the other 3′ ssDNA tail derived from end resection. This recombination path, termed synthesis-dependent strand annealing (SDSA), yields only noncrossover products (Fig. 9.1). Alternatively, as in the DNA double-strand break repair (DSBR) pathway, the displaced strand in the D-loop structure pairs with the other resected end, forming a DNA intermediate termed the double Holliday junction (dHJ), which is processed endonucleolytically by one of several resolvases (Fig. 9.1) [7]. This type of resolvase-mediated dHJ resolution has the probability of generating chromosome arm crossovers in the recombinants made. As will be discussed at length later, the dHJ can also be resolved by the combined action of a specialized DNA helicase and topoisomerase in a process termed dHJ dissolution to form noncrossover recombinants exclusively (Fig. 9.1). As alluded to above and expounded upon below, helicases play a critical catalytic or regulatory role in nearly every step of the HR reaction, highlighting their importance in genome maintenance.

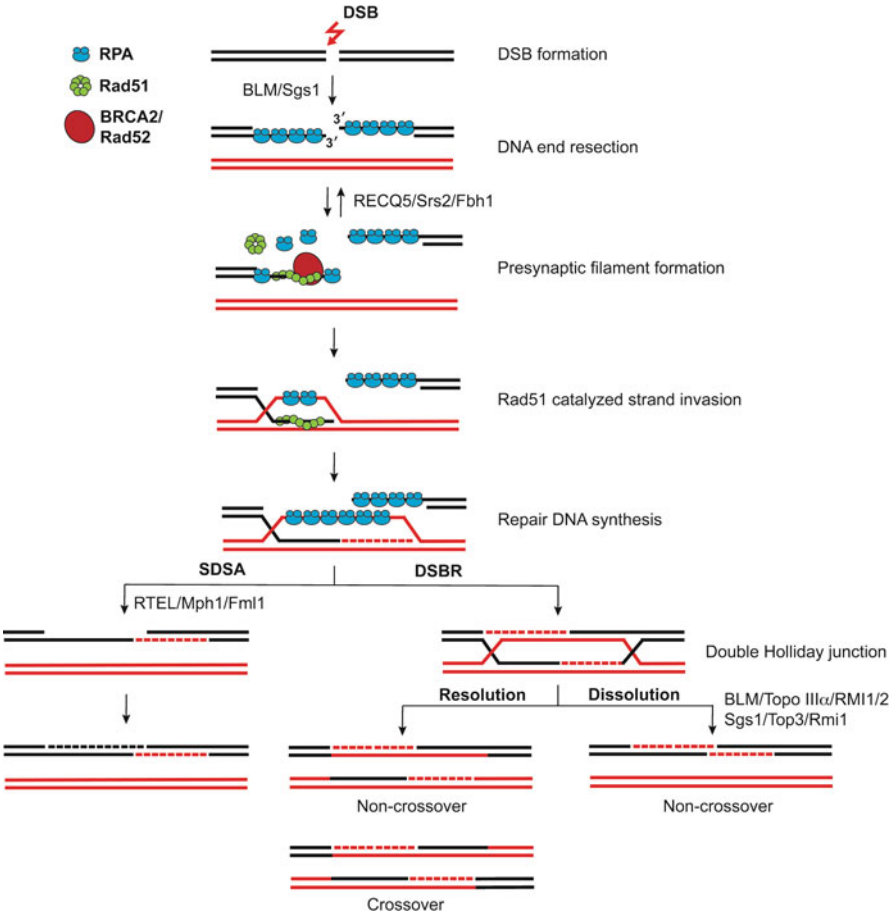

Fig. 9.1 DNA break repair by either the synthesis-dependent strand annealing (*SDSA*) pathway or the double-strand break repair (*DSBR*) pathway. Double-strand breaks induced by DNA damage are first resected to produce 3′ DNA tails, which become coated by the ssDNA-binding protein RPA. Recombination mediator proteins, such as Rad52 in yeast and BRCA2 in humans, promote the exchange of RPA by a helical filament of Rad51. DNA synthesis occurs after strand invasion catalyzed by the Rad51-ssDNA nucleoprotein filament. The resulting DNA joint can be processed through either the SDSA pathway or the DSBR pathway. In the former, the invading strand is ejected by Mph1/FANCM/Fml1 and then becomes annealed with the other ssDNA end. The SDSA pathway generates exclusively noncrossover recombinants. In the DSBR pathway, the second DSB end is captured to yield a double Holliday junction (*dHJ*), which is either resolved by a HJ resolvase to generate crossover or noncrossover products, or it can be dissolved by the concerted action of the Sgs1–Top3–Rmi1 complex in yeast and BLM–Topo IIIα–RMI1/2 complex in humans to generate noncrossover products exclusively

Multifaceted Roles of RecQ Helicases in HR

General Biochemical Properties of the RecQ Helicases

The RecQ family of helicases is named after the founding member, the product of the *E. coli recQ*$^{+}$ gene, which prevents replication fork demise and suppresses illegitimate recombination in bacteria [8]. While five such helicases exist in mammals (BLM, WRN, RECQ1, RECQ4, and RECQ5), Sgs1 is the sole ortholog in *Saccharomyces cerevisiae*. The RecQ helicases share a common domain structure, including a conserved central region of 350–400 residues that harbor the seven classical helicase motifs. Besides this helicase domain, most RecQ helicases also contain the RecQ C-terminal (RQC) domain, believed to mediate protein–protein interactions. The RNase D C-terminal (HRDC) domain (~80 amino acids), which has been implicated in the recognition of various DNA structures, is found in Sgs1, BLM, and WRN but absent in RECQ1, RECQ4, and RECQ5. All RecQ helicases examined to date translocate on ssDNA with a $3' \rightarrow 5'$ polarity.

S. cerevisiae Sgs1

Genetic Characteristics

The *SGS1* gene was isolated as a suppressor of the slow-growth phenotype of mutants of the *TOP3* gene, which encodes a type IA toposiomerase [9]. Sgs1 protein forms a stable complex with Top3 and another protein called Rmi1 [10, 11]. Mutations in *SGS1* also lead to hypersensitivity to different DNA-damaging agents, such as ultraviolet (UV) light and methylmethane sulfonate (MMS), and also to replicative stress caused by exposure to hydroxyurea (HU) [12, 13]. These phenotypes indicate a role of Sgs1 protein in DNA repair and are suggestive of an involvement in replication fork maintenance. Detailed analysis of HR efficiency and pathway choice in mutants has revealed a pro-recombination role of Sgs1 and also a role in the suppression of crossover formation [14–16]. Remarkably, recent genetic and biochemical studies have revealed that Sgs1 also functions in DSB end resection [4–6].

Role of Sgs1 in DNA End Resection

Studies on the genetic requirements and control of DNA end resection are typically conducted in mutants of *RAD51*, which codes for the recombinase enzyme responsible for DNA strand invasion, so as to uncouple DNA resection from the subsequent steps of HR [3, 17]. The Mre11–Rad50–Xrs2 (MRX) complex has long been associated with resection in *S. cerevisiae*. However, the observation that resection is not

abolished in MRX mutants indicated that additional proteins are involved [18]. Recent studies by three groups in *S. cerevisiae* and human cells revealed a multiplicity of resection pathways. Deletion of either *SGS1* or *EXO1*, the latter being a 5′-3′ exonuclease, slows the rate of ssDNA formation several kilobases away from a DSB, but little long-range resection occurs in the *sgs1*Δ *exo1*Δ double mutant [4–6]. Interestingly, the double retains the ability to resect DNA closer to the break site, and further analysis showed that the short-range resection depends on the MRX complex and its companion protein Sae2 [5, 6]. Based on these results, a model was proposed in which the MRX/Sae2 ensemble initiates DSB processing at the break, then parallel pathways involving either Sgs1 or Exo1 conduct extensive resection independently.

The nuclease that functions together with Sgs1 is Dna2 [6], which contains both 5′ flap endonuclease and 5′→3′ helicase activities and functions in Okazaki fragment processing [19, 20]. Interestingly, while the helicase activity of Sgs1 is essential for end resection, that of Dna2 is dispensable [5, 6]. Two groups have reconstituted the Sgs1-Dna2 pathway using purified MRX complex, Sgs1–Top3–Rmi1 complex, Dna2, and the heterotrimeric ssDNA-binding protein RPA [21, 22]. The results from these studies demonstrate that DNA strand separation during resection is mediated by Sgs1, in a manner that is enhanced by the Top3-Rmi1 and MRX complexes [21, 22]. In congruence with genetic observations, although the Dna2 nuclease activity is critical for resection, the Mre11 nuclease activity is dispensable [5, 22]. Interestingly, the topoisomerase activity of Top3, although crucial for the suppression of crossover recombination, is not needed for resection either in cells or in the reconstituted system [22]. Importantly, these studies have unveiled a multifaceted role of RPA. Aside from stimulating Sgs1-mediated DNA unwinding, RPA regulates the Dna2 nuclease activity by promoting 5′ end cleavage while attenuating 3′ cleavage, to help impose the 5′ resection polarity observed [21, 22].

Suppression of Mitotic Crossover Formation by the Sgs1–Top3–Rmi1 Complex

A dramatic increase in crossover recombination is a hallmark phenotype of *sgs1*Δ strains, which stems from altered processing of the dHJ recombination intermediate. Even though crossover events are important for orchestrating the segregation of chromosome homologs in the first cell division during meiosis, they can also lead to chromosomal translocations. By suppressing mitotic crossovers, Sgs1 helps minimize gross chromosome rearrangements and the loss of heterozygosity during DNA repair by HR. Importantly, *top3*Δ and *rmi1*Δ mutants also exhibit elevated HR-associated chromosome crossovers, and genetic analyses have provided evidence for epistasis among these mutants and the *sgs1*Δ mutant [11]. Insights into the anti-crossover activity of the Sgs1–Top3–Rmi1 complex have originated from studies on its human equivalent, the BLM–Topo IIIα–Rmi1–Rmi2 complex (see Section C below) [16, 23]. Specifically, the BLM-associated complex and subsequently the Sgs1 protein ensemble have been shown to possess the ability to dissolve the dHJ intermediate into products that are exclusively noncrossover in nature [24–27].

Role of Sgs1 in Meiotic HR Regulation

Unlike in mitotic cells, HR during meiosis is geared toward the production of crossover products between non-sister homologous chromatids, to ensure the proper segregation of homolog pairs in the first division. A series of protein factors, including Zip1, Zip2, Zip3, Zip4, Mer3, Msh4 and Msh5, constrain the activity of Sgs1 to promote crossover formation [28, 29]. It should be noted that Sgs1 does fulfill important HR regulatory roles during meiosis, by ensuring the proper distribution of crossovers and suppressing the formation of complex DNA joint molecules involving multiple chromatids [30]. It remains to be established whether these meiotic functions of Sgs1 are mediated via dHJ dissolution.

Sgs1 and Homeologous Recombination

Occasionally, recombination can occur between moderately divergent DNA sequences, a process known as "homeologous recombination." Homeologous recombination is actively suppressed via a Sgs1-dependent mechanism. Herein, Sgs1 functions in conjunction with the DNA mismatch repair proteins (mainly the MutSα complex harboring Msh2 and Msh6 proteins) in discriminating against non-identical DNA sequences during HR [31]. Thus, deletion of *SGS1* leads to defects in rejecting heteroduplexes containing divergent sequences [32]. A more recent study has found that when both *SGS1* and *MPH1,* which also codes for a DNA helicase discussed in detail below, are mutated, the resulting strain is further compromised in the ability to discriminate homeology during HR repair [33]. These results suggest that both Sgs1 and Mph1, in an independent fashion, reject heteroduplex intermediates that harbor homeologous sequences.

Bloom Syndrome and the BLM Helicase

Bloom Syndrome and Cellular Phenotypes

BLM is the human RecQ helicase most closely related to Sgs1 in structure and function (see also Chap. 8). Mutations in BLM lead to the rare disease Bloom syndrome (BS). Patients exhibit an abnormally small stature and are highly cancer-prone, with a mean age onset of 24 years [34]. The cancers in BS patients are not restricted to any particular organ or type, indicative of a housekeeping role of BLM in genome maintenance.

Chromosomal aberrations, including chromatid gaps, breaks, and rearrangements, occur frequently in BS [35]. BS cells exhibit an abnormality in HR regulation, manifested as a striking increase in sister chromatid exchanges (SCEs) [35]. Ablation of the BLM gene is lethal in the embryonic stage, but heterozygous animals can be obtained [36, 37]. These BLM+/- animals do not show increased cancer predisposition unless crossed with mice carrying a mutation in the Apc tumor suppressor gene [37].

Biochemical Properties of the BLM Helicase Activity

BLM unwinds a variety of DNA structures including double-stranded DNA with a 3′ overhang, forked structures, bubbles, G quadruplexes, and recombination intermediates such as D-loops and Holliday junctions [38–43]. BLM can also branch migrate Holliday junctions [44–46].

BLM–Topo IIIα–RMI1–RMI2 Complex and its dHJ Dissolution Activity

BLM is stably associated with Topo IIIα, RMI1, and RMI2 in a complex analogous to yeast Sgs1-Top3-Rmi1. Topo IIIα is the ortholog of *S. cerevisiae* Top3, but Rmi2 is not present in *S. cerevisiae* [10, 26, 47, 48]. Importantly, BLM in conjunction with Topo IIIα can dissolve the dHJ in a manner that yields exclusively noncrossover recombinants [16]. In this dHJ dissolution reaction, BLM catalyzes the convergent branch migration of the two Holliday junctions, to process the dHJ into a hemicatenane structure that is resolved by the topoisomerase activity of Topo IIIα [16]. The RMI1–RMI2 complex greatly stimulates the dHJ activity of the BLM–Topo IIIα pair [16, 25, 26, 47], and this functional synergy requires the physical interaction between Rmi1 and Topo IIIα, as revealed by examining mutations in RMI1 that ablate its interaction with Topo IIIα [49–51]. As alluded to earlier, the *S. cerevisiae* Sgs1–Top3–Rmi1 complex also possesses a robust dHJ dissolvase activity [22, 52].

Multifaceted Role of BLM in DNA End Resection

Like Sgs1, BLM cooperates with human DNA2 to promote long-range resection (Fig. 9.2) [4, 53]. As in the case of Sgs1–Dna2, the efficiency of resection mediated by the BLM–DNA2 pair is enhanced by the MRE11–RAD50–NBS1 (MRN) complex, which is the equivalent of *S. cerevisiae* MRX complex [53]. RPA exerts functions in the reconstituted human resection system similar to what have been reported for *S. cerevisiae* RPA, namely, by enhancing BLM-mediated DNA unwinding and imposing a preference for 5′ flap cutting by DNA2 [21, 22, 53]. However, the role of Topo IIIα–Rmi1–Rmi2 in end resection has not yet been examined. Interestingly, BLM also interacts with and enhances the activity of hEXO1 [54]. Thus, in addition to being an integral component of the BLM–DNA2 resection path, BLM may also function in hEXO1-dependent resection.

RECQ5 Helicase and its Role on HR Regulation

Genetic Characterization

RECQ5 has not been linked to a human disease, but its ablation in mice results in cancer susceptibility [55]. RECQ5-deficient cells exhibit elevated SCEs and HR

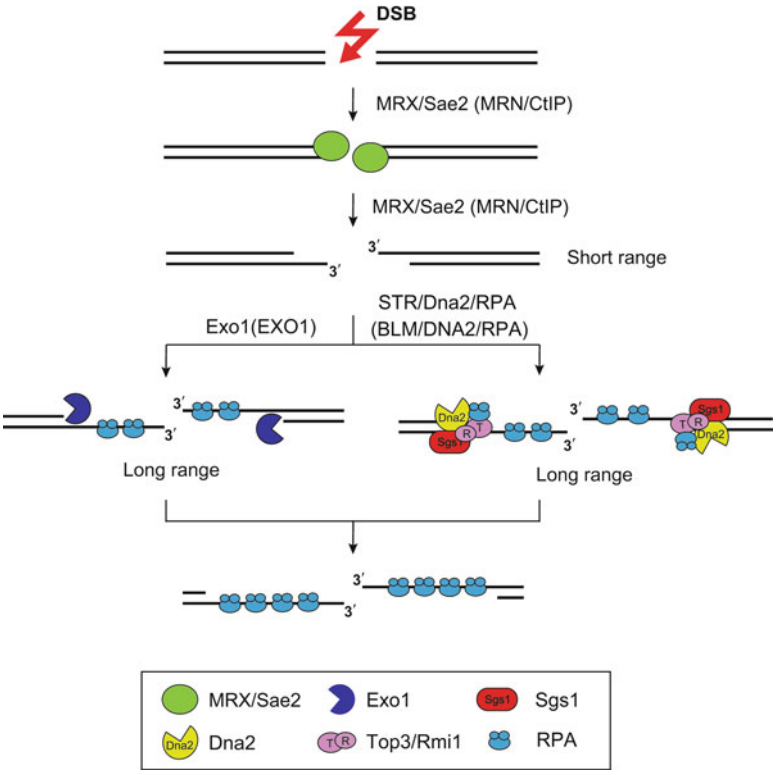

Fig. 9.2 Multiplicity of DNA end resection means. A limited amount of 5′ resection is catalyzed by the MRX–Sae2 complex in yeast or the MRN–CtIP complex in humans. Two parallel pathways are responsible for long-range resection, with one being mediated by Exo1 and the other by the Sgs1 or BLM-associated protein ensemble. *MRX* Mre11-Rad50-Xrs2; *MRN* MRE11-RAD50-NBS1; *STR* Sgs1-Top3-Rmi1

events and are prone to gross chromosomal rearrangements upon genotoxic stress [55, 56]. Depletion of BLM on top of RECQ5 deletion exacerbates the SCE phenotype, indicating that the two proteins function in parallel pathways to regulate HR [55].

Anti-Recombinase Activity of RECQ5

To gain insights into its HR regulatory function, RECQ5 protein was purified and examined in conjunction with the RAD51 recombinase. RECQ5 was found to physically interact with RAD51 and inhibits the recombinase activity of RAD51 [56]. The RAD51 inhibitory activity of RECQ5 is potentiated by RPA. Extensive biochemical analysis and electron microscopy have shown that

RECQ5 displaces RAD51 from ssDNA, in a reaction that is linked to ATP hydrolysis by the former. RPA enhances this anti-recombinase attribute of RECQ5 by preventing the renucleation of RAD51 onto ssDNA [56]. Mutants of RECQ5 impaired for RAD51 interaction have been generated, and characterization of these mutants has furnished evidence that physical interaction with RAD51 is being indispensable for the anti-recombinase function [57]. Together, these findings implicate RECQ5 as a tumor suppressor that acts by preventing inappropriate HR events via the disruption of RAD51-ssDNA nucleoprotein filaments.

Prevention of Transcription-Induced Genome Instability

RECQ5 also associates with RNA polymerase II in a complex distinct from that which harbors RAD51. In this context, RECQ5 seems to be important for minimizing transcription-associated genome instability [58–60]. Thus, loss of RECQ5 leads to the accumulation of spontaneous DSBs during DNA replication that is linked to RNA Pol II transcription [60]. While the specific role of RECQ5 is not yet known in this case, a reasonable assumption is that the helicase activity of RECQ5 unwinds DNA structures or clears DNA of proteins when the transcription and replication machineries collide.

The Hef Family of Helicases

Conservation and Biochemical Properties of Hef

Several conserved DNA helicases/translocases related to archaeal Hef (Helicase-associated endonuclease for fork-structured DNA) have been shown to play an important role in HR regulation. These proteins are members of the SF2 helicase superfamily. *S. cerevisiae* and humans contain one member of this family, Mph1 and FANCM, respectively. The latter is associated with complementation group M of the cancer-prone syndrome Fanconi anemia (FA) [61]. The Hef protein from *Pyrococcus furiosus* contains a conserved helicase domain and a C-terminal endonuclease domain that is structurally related to that found in the nucleases Mus81 and XPF [62]. The crystal structure of the helicase and endonuclease domains of Hef has been solved [63]. Hef is able to process DNA fork and four-way junction structures to produce splayed duplexes [64]. The Hef nuclease, which homodimerizes as revealed in the crystal structure, preferentially cleaves replication fork structures in a manner that is stimulated by the helicase activity [64]. Taken together, these results suggest a role of Hef in processing injured replication forks.

Yeast Mph1 and its HR Regulatory Role

Genetic Characteristics

The yeast *MPH1* gene was identified in a screen for mutants that exhibit a mutator phenotype [65]. Cells lacking Mph1 are hypersensitive to genotoxic chemicals such as MMS, EMS, 4-NQO, and camptothecin [65]. Interestingly, the *mph1*Δ spontaneous mutator phenotype depends on *REV3,* which encodes the catalytic subunit of the translesion synthesis DNA polymerase ζ [66]. Further studies have shown that the *mph1*Δ mutation is epistatic to the HR mutants *rad51*Δ, *rad52*Δ, and *rad55*Δ in terms of spontaneous mutation rates and DNA damage sensitivity [66]. These results suggest that Mph1 functions with HR proteins to promote the error-free bypass of DNA lesions. Additional evidence supporting this premise comes from recent studies on the *S. cerevisiae* Smc5/6 complex, one of the three conserved structural maintenance of chromosomes (SMC) complexes. Mutations in *SMC5* or *SMC6* render yeast cells hypersensitive to agents that interfere with DNA replication, such as HU or MMS. Upon treatment with MMS, accumulation of Rad51-dependent X-shaped DNA intermediates occurs in the *smc5* or *smc6* mutant [67]. Importantly, deletion of *MPH1* or inactivation of the helicase activity of Mph1 protein largely eliminates X-shaped intermediates in *smc5* or *smc6* mutants and suppresses the sensitivity of the mutant cells to HU or MMS [67, 69]. On the other hand, overexpression of *MPH1* further exacerbates some of the phenotypes observed in *smc5/6* mutants [69]. These results suggest that Mph1 functions in HR-mediated replication fork repair, but the activity of Mph1 must be restrained by the Smc5/6 complex to prevent the generation of toxic DNA intermediates.

In a study that examined mutations capable of intensifying the HR regulatory phenotype of *srs2*Δ cells, *MPH1* was discovered as a suppressor of spontaneous unequal SCEs and DNA double-strand break-induced chromosome crossovers [70]. Importantly, Mph1 protein functions in crossover control via a novel mechanism independent of the Srs2 and Sgs1 helicases, which is consistent with the biochemical finding that Mph1 dissociates Rad51-catalyzed D-loops to promote DSB repair via SDSA (see below) [70].

Biochemical Properties of the Mph1 Helicase Activity

While archaeal Hef contains helicase and endonuclease domains, Mph1 has only the helicase domain. Purified Mph1 exhibits a ssDNA-dependent ATPase activity and a 3′-5′ helicase activity that is enhanced by the single-strand DNA-binding protein RPA [71]. Recently, our laboratory and others have demonstrated that Mph1 possesses a robust branch migration activity on replication fork and four-way junction structures and can mediate extensive branch migration of a sigma structure that mimics a DNA replication fork [72, 73]. The biochemical results suggest a role of

Mph1 in processing replication fork structures, similar to Hef. This premise is further supported by the recent finding that cleavage of 5′-flap structures by the Fen1 nuclease, which is needed for Okazaki fragment processing and maturation, is stimulated by Mph1 [72].

D-Loop Dissociative Activity of Mph1

Since genetic studies have implicated *MPH1* in the suppression of crossovers, purified Mph1 was examined for activities relevant for this HR regulatory activity. The protein binds D-loop structures and is particularly adept at unwinding these structures. Importantly, Mph1 dissociates Rad51-made D-loops with high efficiency [70]. D-loop dissociation is linked to ATP hydrolysis by Mph1, as the D209N mutation in the helicase motif II of Mph1 that abolishes its ATPase activity is inactive in this regard [70]. Dissociation of D-loops by Mph1 can explain how it suppresses crossover formation by promoting the SDSA pathway of HR, which only leads to a noncrossover outcome (Fig. 9.1). The *S. pombe* ortholog, Fml1, appears to function similarly [74]. We note that this HR regulatory function of Mph1 distinguishes it in mechanism from Sgs1 and Srs2, which suppress crossover formation by dHJ dissolution (see above) and displacing the Rad51 recombinase from DNA (see below), respectively.

FANCM and its Genetic and Biochemical Properties

As mentioned above, the protein FANCM is the likely human ortholog of Mph1 and Hef [61]. It is part of the large multi-subunit FA complex, which is necessary for the efficient repair of interstrand crosslinks [75]. Like Mph1, FANCM lacks nuclease activity. While FANCM does not possess a classical helicase activity, it can, as in the case of Mph1, utilize its DNA-dependent ATPase activity to translocate along DNA and to promote the migration of Holliday junctions and replication fork reversal [61, 76, 77]. Importantly, FANCM can also efficiently disrupt protein-free D-loops, although it remains to be established whether it can do so within the context of a homologous pairing reaction mediated by Rad51 [77]. As expected, the FANCM-K117R mutant that is defective in ATPase activity is unable to process the Holliday junction or replication fork and is similarly defective in D-loop dissociation [77]. Importantly, FANCM-deficient human and chicken DT40 cells exhibit elevated SCEs, but the phenotype is not as severe as that caused by BLM depletion [78, 79]. Simultaneous ablation of FANCM and BLM does not further increase SCE levels beyond BLM alone, consistent with a role of FANCM in preventing some SCEs in a BLM-dependent manner [78]. It seems reasonable to propose that FANCM favors noncrossover formation during HR via its D-loop dissociative activity.

The Srs2 Helicase and its HR Regulatory Function

SRS2 Identification and Genetic Characteristics

A mutant allele of *SRS2* was identified as a suppressor of the sensitivity of *rad6* and *rad18* mutants, defective in post-replicative DNA repair, to ultraviolet light-induced DNA damage [80]. The suppression depends on HR, and *srs2* mutants show a hyper-recombination phenotype [81, 82]. Taken together, the above genetic observations suggest that Srs2 functions to restrain HR in cells, and an enhanced ability of *srs2* cells to conduct HR can override the DNA repair deficiency of a *rad6* or *rad18* mutation. Mutations in *SRS2* also cause severe synthetic grow defects with mutations in genes that encode factors involved in recombination intermediate processing, such as *SGS1* and *RAD54* [82, 83]. This and other phenotypes of *srs2* mutants can be suppressed by mutating *RAD51* [14]. Interestingly, *Srs2* also attenuates crossover formation by promoting the use of the SDSA pathway, and this occurs independently of *Sgs1* and *Mph1 [*15]. These genetic results reinforce the idea of Srs2 acting as a negative regulator of HR and a promoter of DNA break repair by SDSA.

Anti-Recombinase Activity of Srs2

The mechanism by which Srs2 negatively regulates Rad51-mediated HR was revealed in biochemical studies. Purified Srs2 displays ssDNA-dependent ATPase and 3′-5′ helicase activities and physically interacts with Rad51 [84, 85]. Importantly, the addition of a catalytic quantity of Srs2 to Rad51-mediated homologous DNA pairing reactions strongly inhibits these reactions. Further analysis showed that Srs2 acts by dislodging Rad51 from ssDNA, and that this attribute of Srs2 is enhanced by RPA, which, by occupying ssDNA sites made available as a result of Rad51 eviction, minimizes the reassembly of the Rad51–ssDNA complex [84, 86]. These findings thus provide evidence that Srs2 attenuates HR via dismantling the Rad51-ssDNA complex. Examination of mutant Srs2 proteins that are impaired for complex formation with Rad51 revealed that the efficiency of the anti-recombinase function is dependent on interaction with the later [87, 88]. It has been proposed that interaction of Srs2 with Rad51 triggers ATP hydrolysis within the Rad51 protein filament assembled on ssDNA, causing Rad51 to dissociate from the DNA [87].

Two HR mediators, namely, Rad52 protein and Rad55-Rad57 heterodimer, capable of enhancing the assembly or stability of the Rad51-ssDNA nucleoprotein complex have been described [3]. Rad52 can antagonize the Srs2 anti-recombinase activity by reloading Rad51 onto RPA-coated ssDNA [89], while the Rad55-Rad57 complex attenuates the activity of Srs2 via a direct interaction with it [90].

Anti-Recombinase Function of Srs2 at the DNA Replication Fork

Studies conducted in *S. cerevisiae* have unveiled distinct means of lesion bypass during DNA replication, and the choice of DNA damage tolerance pathway is dependent on the ubiquitination or SUMOylation of the DNA polymerase clamp PCNA [91]. SUMOylation of PCNA also occurs in the absence of exogenously induced DNA damage during S phase. Genetic analysis has shown that SUMO-modified PCNA helps recruit Srs2 to the DNA replication fork, where it inhibits HR by disrupting Rad51 protein filament assembled on ssDNA stemming from fork stalling [91–93]. Srs2 interacts directly with the SUMO-modified form of PCNA, via SIM and PIP motifs located in the C-terminal region of Srs2 that specifically recognize SUMO and PCNA, respectively [92–94]. These findings suggest that SUMO-modified PCNA recruits Srs2 to prevent undesirable HR events from occurring during DNA replication. The high-resolution structure of the C-terminal region of Srs2 bound to SUMO-PCNA has been solved recently [94].

RTEL and its D-Loop Dissociative Properties

To search for the Srs2 equivalent in higher organisms, a genetic screen for synthetic lethality with the *SGS1* ortholog *HIM-6* was performed in *C. elegans*, which led to the identification of RTEL-1, a helicase [95]. RTEL-1 is orthologous to the previously identified murine Rtel protein shown to be a regulator of telomere length [96]. *rtel-1 him-6* double mutant worms show a drastic increase in RAD51 foci, indicating an accumulation of recombination intermediates [95]. Loss of *rtel-1* alone causes sensitivity to DNA-damaging agents and elevated crossover recombination in meiosis [95, 97]. siRNA against human RTEL also leads to increased recombination [95]. In vitro, RTEL can disrupt RAD51-mediated D-loops in a manner that is dependent on RPA, but it cannot disassemble RAD51-ssDNA nucleoprotein filaments, unlike Srs2 and RECQ5 [95, 97]. Thus, RTEL appears to employ the same mechanism as *S. cerevisiae* Mph1 in the regulation of HR [70].

Epilogue

Concerted efforts in model organisms, such as *S. cerevisiae* and *C. elegans*, and companion studies in humans and other vertebrate species have helped identify three distinct means of HR regulation, each of which is mediated by a DNA helicase. These include the disassembly of the RAD51-ssDNA nucleoprotein filament by Srs2/RECQ5, D-loop dissociation by Mph1/RTEL, and dHJ dissolution by the BLM and Sgs1 protein ensembles. These mechanisms function in parallel to ensure that the conservative SDSA mechanism is used predominantly during HR in mitotic cells.

Aside from the known HR regulators as reviewed above, there are tantalizing clues that additional players are involved in HR regulation. Recent evidence suggests that Fbh1, a SF1 helicase that also possesses a ubiquitin E3 ligase activity, may act as an anti-recombinase similar to Srs2 and RECQ5 [98, 99]. The other RecQ family members WRN and RECQ1 may also influence HR (LeRoy et al., 2005; Opresko et al., 2009; Sharma et al., 2005) [46, 100]. Further investigation will be needed to clarify the HR role of these helicases.

References

1. Lieber MR. The mechanism of double-strand DNA break repair by the nonhomologous DNA end-joining pathway. Annu Rev Biochem. 2010;79:181–211.
2. Mimitou EP, Symington LS. Nucleases and helicases take center stage in homologous recombination. Trends Biochem Sci. 2009;34:264–72.
3. San Filippo J, Sung P, Klein H. Mechanism of eukaryotic homologous recombination. Annu Rev Biochem. 2008;77:229–57.
4. Gravel S, Chapman JR, Magill C, Jackson SP. DNA helicases Sgs1 and BLM promote DNA double-strand break resection. Genes Dev. 2008;22:2767–72.
5. Mimitou EP, Symington LS. Sae2, Exo1 and Sgs1 collaborate in DNA double-strand break processing. Nature. 2008;455:770–4.
6. Zhu Z, Chung WH, Shim EY, Lee SE, Ira G. Sgs1 helicase and two nucleases Dna2 and Exo1 resect DNA double-strand break ends. Cell. 2008;134:981–94.
7. Schwartz EK, Heyer WD. Processing of joint molecule intermediates by structure-selective endonucleases during homologous recombination in eukaryotes. Chromosoma. 2011;120:109–27.
8. Hanada K, Ukita T, Kohno Y, Saito K, Kato J, Ikeda H. RecQ DNA helicase is a suppressor of illegitimate recombination in Escherichia coli. Proc Natl Acad Sci USA. 1997;94:3860–5.
9. Gangloff S, McDonald JP, Bendixen C, Arthur L, Rothstein R. The yeast type I topoisomerase Top3 interacts with Sgs1, a DNA helicase homolog: a potential eukaryotic reverse gyrase. Mol Cell Biol. 1994;14:8391–8.
10. Chang M, Bellaoui M, Zhang C, Desai R, Morozov P, Delgado-Cruzata L, Rothstein R, Freyer GA, Boone C, Brown GW. RMI1/NCE4, a suppressor of genome instability, encodes a member of the RecQ helicase/Topo III complex. EMBO J. 2005;24:2024–33.
11. Mullen JR, Nallaseth FS, Lan YQ, Slagle CE, Brill SJ. Yeast Rmi1/Nce4 controls genome stability as a subunit of the Sgs1-Top3 complex. Mol Cell Biol. 2005;25:4476–87.
12. Ii M, Brill SJ. Roles of SGS1, MUS81, and RAD51 in the repair of lagging-strand replication defects in Saccharomyces cerevisiae. Curr Genet. 2005;48:213–25.
13. Onoda F, Seki M, Miyajima A, Enomoto T. Elevation of sister chromatid exchange in Saccharomyces cerevisiae sgs1 disruptants and the relevance of the disruptants as a system to evaluate mutations in Bloom's syndrome gene. Mutat Res. 2000;459:203–9.
14. Gangloff S, Soustelle C, Fabre F. Homologous recombination is responsible for cell death in the absence of the Sgs1 and Srs2 helicases. Nat Genet. 2000;25:192–4.
15. Ira G, Malkova A, Liberi G, Foiani M, Haber JE. Srs2 and Sgs1-Top3 suppress crossovers during double-strand break repair in yeast. Cell. 2003;115:401–11.
16. Wu L, Hickson ID. The Bloom's syndrome helicase suppresses crossing over during homologous recombination. Nature. 2003;426:870–4.
17. Sugawara N, Haber JE. Repair of DNA double strand breaks: in vivo biochemistry. Methods Enzymol. 2006;408:416–29.
18. Krogh BO, Symington LS. Recombination proteins in yeast. Annu Rev Genet. 2004;38:233–71.

19. Bae SH, Seo YS. Characterization of the enzymatic properties of the yeast dna2 Helicase/endonuclease suggests a new model for Okazaki fragment processing. J Biol Chem. 2000;275:38022–31.
20. Budd ME, Choe WC, Campbell JL. DNA2 encodes a DNA helicase essential for replication of eukaryotic chromosomes. J Biol Chem. 1995;270:26766–9.
21. Cejka P, Cannavo E, Polaczek P, Masuda-Sasa T, Pokharel S, Campbell JL, Kowalczykowski SC. DNA end resection by Dna2-Sgs1-RPA and its stimulation by Top3-Rmi1 and Mre11-Rad50-Xrs2. Nature. 2010;467:112–6.
22. Niu H, Chung WH, Zhu Z, Kwon Y, Zhao W, Chi P, Prakash R, Seong C, Liu D, Lu L, et al. Mechanism of the ATP-dependent DNA end-resection machinery from Saccharomyces cerevisiae. Nature. 2010;467:108–11.
23. Chu WK, Hickson ID. RecQ helicases: multifunctional genome caretakers. Nat Rev Cancer. 2009;9:644–54.
24. Cejka P, Kowalczykowski SC. The full-length Saccharomyces cerevisiae Sgs1 protein is a vigorous DNA helicase that preferentially unwinds holliday junctions. J Biol Chem. 2010;285:8290–301.
25. Raynard S, Bussen W, Sung P. A double Holliday junction dissolvasome comprising BLM, topoisomerase IIIalpha, and BLAP75. J Biol Chem. 2006;281:13861–4.
26. Singh TR, Ali AM, Busygina V, Raynard S, Fan Q, Du CH, Andreassen PR, Sung P, Meetei AR. BLAP18/RMI2, a novel OB-fold-containing protein, is an essential component of the Bloom helicase-double Holliday junction dissolvasome. Genes Dev. 2008;22:2856–68.
27. Wu L, Bachrati CZ, Ou J, Xu C, Yin J, Chang M, Wang W, Li L, Brown GW, Hickson ID. BLAP75/RMI1 promotes the BLM-dependent dissolution of homologous recombination intermediates. Proc Natl Acad Sci USA. 2006;103:4068–73.
28. Borner GV, Kleckner N, Hunter N. Crossover/noncrossover differentiation, synaptonemal complex formation, and regulatory surveillance at the leptotene/zygotene transition of meiosis. Cell. 2004;117:29–45.
29. Jessop L, Rockmill B, Roeder GS, Lichten M. Meiotic chromosome synapsis-promoting proteins antagonize the anti-crossover activity of sgs1. PLoS Genet. 2006;2:e155.
30. Oh SD, Lao JP, Hwang PY, Taylor AF, Smith GR, Hunter N. BLM ortholog, Sgs1, prevents aberrant crossing-over by suppressing formation of multichromatid joint molecules. Cell. 2007;130:259–72.
31. Evans E, Sugawara N, Haber JE, Alani E. The Saccharomyces cerevisiae Msh2 mismatch repair protein localizes to recombination intermediates in vivo. Mol Cell. 2000;5:789–99.
32. Sugawara N, Goldfarb T, Studamire B, Alani E, Haber JE. Heteroduplex rejection during single-strand annealing requires Sgs1 helicase and mismatch repair proteins Msh2 and Msh6 but not Pms1. Proc Natl Acad Sci USA. 2004;101:9315–20.
33. Tay YD, Sidebotham JM, Wu L. Mph1 requires mismatch repair-independent and -dependent functions of MutSalpha to regulate crossover formation during homologous recombination repair. Nucleic Acids Res. 2010;38:1889–901.
34. German J, Sanz MM, Ciocci S, Ye TZ, Ellis NA. Syndrome-causing mutations of the BLM gene in persons in the Bloom's Syndrome Registry. Hum Mutat. 2007;28:743–53.
35. Chaganti RS, Schonberg S, German J. A manyfold increase in sister chromatid exchanges in Bloom's syndrome lymphocytes. Proc Natl Acad Sci USA. 1974;71:4508–12.
36. Chester N, Kuo F, Kozak C, O'Hara CD, Leder P. Stage-specific apoptosis, developmental delay, and embryonic lethality in mice homozygous for a targeted disruption in the murine Bloom's syndrome gene. Genes Dev. 1998;12:3382–93.
37. Goss KH, Risinger MA, Kordich JJ, Sanz MM, Straughen JE, Slovek LE, Capobianco AJ, German J, Boivin GP, Groden J. Enhanced tumor formation in mice heterozygous for Blm mutation. Science. 2002;297:2051–3.
38. Bachrati CZ, Borts RH, Hickson ID. Mobile D-loops are a preferred substrate for the Bloom's syndrome helicase. Nucleic Acids Res. 2006;34:2269–79.
39. Mohaghegh P, Karow JK, Brosh Jr RM, Bohr VA, Hickson ID. The Bloom's and Werner's syndrome proteins are DNA structure-specific helicases. Nucleic Acids Res. 2001;29:2843–9.

40. Orren DK, Theodore S, Machwe A. The Werner syndrome helicase/exonuclease (WRN) disrupts and degrades D-loops in vitro. Biochemistry. 2002;41:13483–8.
41. Popuri V, Bachrati CZ, Muzzolini L, Mosedale G, Costantini S, Giacomini E, Hickson ID, Vindigni A. The Human RecQ helicases, BLM and RECQ1, display distinct DNA substrate specificities. J Biol Chem. 2008;283:17766–76.
42. Sharma S, Sommers JA, Choudhary S, Faulkner JK, Cui S, Andreoli L, Muzzolini L, Vindigni A, Brosh Jr RM. Biochemical analysis of the DNA unwinding and strand annealing activities catalyzed by human RECQ1. J Biol Chem. 2005;280:28072–84.
43. Sun H, Karow JK, Hickson ID, Maizels N. The Bloom's syndrome helicase unwinds G4 DNA. J Biol Chem. 1998;273:27587–92.
44. Constantinou A, Tarsounas M, Karow JK, Brosh RM, Bohr VA, Hickson ID, West SC. Werner's syndrome protein (WRN) migrates Holliday junctions and co-localizes with RPA upon replication arrest. EMBO Rep. 2000;1:80–4.
45. Karow JK, Constantinou A, Li JL, West SC, Hickson ID. The Bloom's syndrome gene product promotes branch migration of holliday junctions. Proc Natl Acad Sci USA. 2000;97:6504–8.
46. LeRoy G, Carroll R, Kyin S, Seki M, Cole MD. Identification of RecQL1 as a Holliday junction processing enzyme in human cell lines. Nucleic Acids Res. 2005;33:6251–7.
47. Xu D, Guo R, Sobeck A, Bachrati CZ, Yang J, Enomoto T, Brown GW, Hoatlin ME, Hickson ID, Wang W. RMI, a new OB-fold complex essential for Bloom syndrome protein to maintain genome stability. Genes Dev. 2008;22:2843–55.
48. Yin J, Sobeck A, Xu C, Meetei AR, Hoatlin M, Li L, Wang W. BLAP75, an essential component of Bloom's syndrome protein complexes that maintain genome integrity. EMBO J. 2005;24:1465–76.
49. Bussen W, Raynard S, Busygina V, Singh AK, Sung P. Holliday junction processing activity of the BLM-Topo IIIalpha-BLAP75 complex. J Biol Chem. 2007;282:31484–92.
50. Raynard S, Zhao W, Bussen W, Lu L, Ding YY, Busygina V, Meetei AR, Sung P. Functional role of BLAP75 in BLM-topoisomerase IIIalpha-dependent holliday junction processing. J Biol Chem. 2008;283:15701–8.
51. Yang J, Bachrati CZ, Ou J, Hickson ID, Brown GW. Human topoisomerase IIIalpha is a single-stranded DNA decatenase that is stimulated by BLM and RMI1. J Biol Chem. 2010;285:21426–36.
52. Cejka P, Plank JL, Bachrati CZ, Hickson ID, Kowalczykowski SC. Rmi1 stimulates decatenation of double Holliday junctions during dissolution by Sgs1-Top3. Nat Struct Mol Biol. 2010;17:1377–82.
53. Nimonkar AV, Genschel J, Kinoshita E, Polaczek P, Campbell JL, Wyman C, Modrich P, Kowalczykowski SC. BLM-DNA2-RPA-MRN and EXO1-BLM-RPA-MRN constitute two DNA end resection machineries for human DNA break repair. Genes Dev. 2011;25:350–62.
54. Nimonkar AV, Ozsoy AZ, Genschel J, Modrich P, Kowalczykowski SC. Human exonuclease 1 and BLM helicase interact to resect DNA and initiate DNA repair. Proc Natl Acad Sci USA. 2008;105:16906–11.
55. Hu Y, Lu X, Barnes E, Yan M, Lou H, Luo G. Recql5 and Blm RecQ DNA helicases have nonredundant roles in suppressing crossovers. Mol Cell Biol. 2005;25:3431–42.
56. Hu Y, Raynard S, Sehorn MG, Lu X, Bussen W, Zheng L, Stark JM, Barnes EL, Chi P, Janscak P, et al. RECQL5/Recql5 helicase regulates homologous recombination and suppresses tumor formation via disruption of Rad51 presynaptic filaments. Genes Dev. 2007;21:3073–84.
57. Schwendener S, Raynard S, Paliwal S, Cheng A, Kanagaraj R, Shevelev I, Stark JM, Sung P, Janscak P. Physical interaction of RECQ5 helicase with RAD51 facilitates its anti-recombinase activity. J Biol Chem. 2010;285:15739–45.
58. Islam MN, Fox 3rd D, Guo R, Enomoto T, Wang W. RecQL5 promotes genome stabilization through two parallel mechanisms—interacting with RNA polymerase II and acting as a helicase. Mol Cell Biol. 2010;30:2460–72.
59. Kanagaraj R, Huehn D, MacKellar A, Menigatti M, Zheng L, Urban V, Shevelev I, Greenleaf AL, Janscak P. RECQ5 helicase associates with the C-terminal repeat domain of RNA polymerase II during productive elongation phase of transcription. Nucleic Acids Res. 2010;38:8131–40.

60. Li M, Xu X, Liu Y. The SET2-RPB1 interaction domain of human RECQ5 is important for transcription-associated genome stability. Mol Cell Biol. 2011;31:2090–9.
61. Meetei AR, Medhurst AL, Ling C, Xue Y, Singh TR, Bier P, Steltenpool J, Stone S, Dokal I, Mathew CG, et al. A human ortholog of archaeal DNA repair protein Hef is defective in Fanconi anemia complementation group M. Nat Genet. 2005;37:958–63.
62. Nishino T, Komori K, Ishino Y, Morikawa K. X-ray and biochemical anatomy of an archaeal XPF/Rad1/Mus81 family nuclease: similarity between its endonuclease domain and restriction enzymes. Structure. 2003;11:445–57.
63. Nishino T, Komori K, Tsuchiya D, Ishino Y, Morikawa K. Crystal structure and functional implications of Pyrococcus furiosus hef helicase domain involved in branched DNA processing. Structure. 2005;13:143–53.
64. Komori K, Hidaka M, Horiuchi T, Fujikane R, Shinagawa H, Ishino Y. Cooperation of the N-terminal Helicase and C-terminal endonuclease activities of Archaeal Hef protein in processing stalled replication forks. J Biol Chem. 2004;279:53175–85.
65. Scheller J, Schurer A, Rudolph C, Hettwer S, Kramer W. MPH1, a yeast gene encoding a DEAH protein, plays a role in protection of the genome from spontaneous and chemically induced damage. Genetics. 2000;155:1069–81.
66. Schurer KA, Rudolph C, Ulrich HD, Kramer W. Yeast MPH1 gene functions in an error-free DNA damage bypass pathway that requires genes from Homologous recombination, but not from postreplicative repair. Genetics. 2004;166:1673–86.
67. Choi K, Szakal B, Chen YH, Branzei D, Zhao X. The Smc5/6 complex and Esc2 influence multiple replication-associated recombination processes in Saccharomyces cerevisiae. Mol Biol Cell. 2010;21:2306–14.
68. Chavez A, Agrawal V, Johnson FB. Homologous recombination-dependent rescue of deficiency in the structural maintenance of chromosomes (Smc) 5/6 complex. J Biol Chem. 2011;286:5119–25.
69. Chen YH, Choi K, Szakal B, Arenz J, Duan X, Ye H, Branzei D, Zhao X. Interplay between the Smc5/6 complex and the Mph1 helicase in recombinational repair. Proc Natl Acad Sci USA. 2009;106:21252–7.
70. Prakash R, Satory D, Dray E, Papusha A, Scheller J, Kramer W, Krejci L, Klein H, Haber JE, Sung P, et al. Yeast Mph1 helicase dissociates Rad51-made D-loops: implications for crossover control in mitotic recombination. Genes Dev. 2009;23:67–79.
71. Prakash R, Krejci L, Van Komen S. Anke Schurer K, Kramer W, Sung P. Saccharomyces cerevisiae MPH1 gene, required for homologous recombination-mediated mutation avoidance, encodes a 3′ to 5′ DNA helicase. J Biol Chem. 2005;280:7854–60.
72. Kang YH, Kang MJ, Kim JH, Lee CH, Cho IT, Hurwitz J, Seo YS. The MPH1 gene of Saccharomyces cerevisiae functions in Okazaki fragment processing. J Biol Chem. 2009;284:10376–86.
73. Zheng XF, Prakash R, Saro D, Longerich S, Niu H, Sung P. Processing of DNA structures via DNA unwinding and branch migration by the S. cerevisiae Mph1 protein. DNA Repair (Amst). 2011;10:1034–43.
74. Sun W, Nandi S, Osman F, Ahn JS, Jakovleska J, Lorenz A, Whitby MC. The FANCM ortholog Fml1 promotes recombination at stalled replication forks and limits crossing over during DNA double-strand break repair. Mol Cell. 2008;32:118–28.
75. Kee Y, D'Andrea AD. Expanded roles of the Fanconi anemia pathway in preserving genomic stability. Genes Dev. 2010;24:1680–94.
76. Gari K, Decaillet C, Delannoy M, Wu L, Constantinou A. Remodeling of DNA replication structures by the branch point translocase FANCM. Proc Natl Acad Sci USA. 2008;105:16107–12.
77. Gari K, Decaillet C, Stasiak AZ, Stasiak A, Constantinou A. The Fanconi anemia protein FANCM can promote branch migration of Holliday junctions and replication forks. Mol Cell. 2008;29:141–8.
78. Rosado IV, Niedzwiedz W, Alpi AF, Patel KJ. The Walker B motif in avian FANCM is required to limit sister chromatid exchanges but is dispensable for DNA crosslink repair. Nucleic Acids Res. 2009;37:4360–70.

79. Xue Y, Li Y, Guo R, Ling C, Wang W. FANCM of the Fanconi anemia core complex is required for both monoubiquitination and DNA repair. Hum Mol Genet. 2008;17:1641–52.
80. Lawrence CW, Christensen RB. Metabolic suppressors of trimethoprim and ultraviolet light sensitivities of Saccharomyces cerevisiae rad6 mutants. J Bacteriol. 1979;139:866–76.
81. Nguyen MM, Livingston DM. The effect of a suppressed rad52 mutation on the suppression of rad6 by srs2. Yeast. 1997;13:1059–64.
82. Palladino F, Klein HL. Analysis of mitotic and meiotic defects in Saccharomyces cerevisiae SRS2 DNA helicase mutants. Genetics. 1992;132:23–37.
83. Lee SK, Johnson RE, Yu SL, Prakash L, Prakash S. Requirement of yeast SGS1 and SRS2 genes for replication and transcription. Science. 1999;286:2339–42.
84. Krejci L, Van Komen S, Li Y, Villemain J, Reddy MS, Klein H, Ellenberger T, Sung P. DNA helicase Srs2 disrupts the Rad51 presynaptic filament. Nature. 2003;423:305–9.
85. Van Komen S, Reddy MS, Krejci L, Klein H, Sung P. ATPase and DNA helicase activities of the Saccharomyces cerevisiae anti-recombinase Srs2. J Biol Chem. 2003;278:44331–7.
86. Veaute X, Jeusset J, Soustelle C, Kowalczykowski SC, Le Cam E, Fabre F. The Srs2 helicase prevents recombination by disrupting Rad51 nucleoprotein filaments. Nature. 2003;423:309–12.
87. Antony E, Tomko EJ, Xiao Q, Krejci L, Lohman TM, Ellenberger T. Srs2 disassembles Rad51 filaments by a protein-protein interaction triggering ATP turnover and dissociation of Rad51 from DNA. Mol Cell. 2009;35:105–15.
88. Colavito S, Macris-Kiss M, Seong C, Gleeson O, Greene EC, Klein HL, Krejci L, Sung P. Functional significance of the Rad51-Srs2 complex in Rad51 presynaptic filament disruption. Nucleic Acids Res. 2009;37:6754–64.
89. Burgess RC, Lisby M, Altmannova V, Krejci L, Sung P, Rothstein R. Localization of recombination proteins and Srs2 reveals anti-recombinase function in vivo. J Cell Biol. 2009;185:969–81.
90. Liu J, Renault L, Veaute X, Fabre F, Stahlberg H, Heyer WD. Rad51 paralogues Rad55-Rad57 balance the antirecombinase Srs2 in Rad51 filament formation. Nature. 2011; 479: 245–8.
91. Moldovan GL, Pfander B, Jentsch S. PCNA, the maestro of the replication fork. Cell. 2007;129:665–79.
92. Papouli E, Chen S, Davies AA, Huttner D, Krejci L, Sung P, Ulrich HD. Crosstalk between SUMO and ubiquitin on PCNA is mediated by recruitment of the helicase Srs2p. Mol Cell. 2005;19:123–33.
93. Pfander B, Moldovan GL, Sacher M, Hoege C, Jentsch S. SUMO-modified PCNA recruits Srs2 to prevent recombination during S phase. Nature. 2005;436:428–33.
94. Armstrong AA, Mohideen F, Lima CD. Recognition of SUMO-modified PCNA requires tandem receptor motifs in Srs2. Nature. 2012;483:59–63.
95. Barber LJ, Youds JL, Ward JD, McIlwraith MJ, O'Neil NJ, Petalcorin MI, Martin JS, Collis SJ, Cantor SB, Auclair M, et al. RTEL1 maintains genomic stability by suppressing homologous recombination. Cell. 2008;135:261–71.
96. Ding H, Schertzer M, Wu X, Gertsenstein M, Selig S, Kammori M, Pourvali R, Poon S, Vulto I, Chavez E, et al. Regulation of murine telomere length by Rtel: an essential gene encoding a helicase-like protein. Cell. 2004;117:873–86.
97. Youds JL, Mets DG, McIlwraith MJ, Martin JS, Ward JD, ONeil NJ, Rose AM, West SC, Meyer BJ, Boulton SJ. RTEL-1 enforces meiotic crossover interference and homeostasis. Science. 2010;327:1254–8.
98. Lorenz A, Osman F, Folkyte V, Sofueva S, Whitby MC. Fbh1 limits Rad51-dependent recombination at blocked replication forks. Mol Cell Biol. 2009;29:4742–56.
99. Osman F, Dixon J, Barr AR, Whitby MC. The F-Box DNA helicase Fbh1 prevents Rhp51-dependent recombination without mediator proteins. Mol Cell Biol. 2005;25:8084–96.
100. Opresko PL, Sowd G, Wang H. The Werner syndrome helicase/exonuclease processes mobile D-loops through branch migration and degradation. PLoS One. 2009;4:e4825.

Chapter 10
DNA Helicases in NER, BER, and MMR

Jochen Kuper and Caroline Kisker

Abstract Different DNA repair mechanisms have evolved to protect our genome from modifications caused by endogenous and exogenous agents, thus maintaining the integrity of the DNA. Helicases often play a central role in these repair pathways and have shown to be essential for diverse tasks within these mechanisms. In prokaryotic nucleotide excision repair (NER) for example the two helicases UvrB and UvrD assume vastly different functions. While UvrB is intimately involved in damage verification and acts as an anchor for the other prokaryotic NER proteins UvrA and UvrC, UvrD is required to resolve the post-incision complex leading to the release of UvrC and the incised ssDNA fragment. For the XPD helicase in eukaryotic NER a similar function in analogy to UvrB has been proposed, whereas XPB the second helicase uses only its ATPase activity during eukaryotic NER. In prokaryotic mismatch repair (MMR) UvrD again plays a central role. The different tasks of this protein in the different repair pathways highlight the importance of regulative protein–protein interactions to fine-tune its helicase activity. In other DNA repair pathways the role of the helicases involved is sometimes not as well characterized, and no helicase has so far been described to assume the function of UvrD in eukaryotic MMR. RecQ helicases and FancJ interact with eukaryotic MMR proteins but their involvement in this repair pathway is unclear. Lastly, long-patch base excision repair is linked to the WRN helicase. Many proteins within this pathway interact with the WRN helicase leading to increased activity of the interacting proteins as observed for pol β and FEN-1 or the helicase itself is negatively regulated through the interaction with APE-1. However, compared to the precise functions described for the helicases in the other DNA repair mechanisms the role of WRN in BER remains speculative and requires further analysis.

J. Kuper • C. Kisker (✉)
Rudolf Virchow Center for Experimental Biomedicine, University of Würzburg, Würzburg, Germany
e-mail: jochen.kuper@virchow.uni-wuerzburg.de; caroline.kisker@virchow.uni-wuerzburg.de

M. Spies (ed.), *DNA Helicases and DNA Motor Proteins*, Advances in Experimental Medicine and Biology, DOI 10.1007/978-1-4614-5037-5_10,

Helicases in DNA Repair

The genetic information stored in our DNA is constantly challenged by endogenous and exogenous agents. In order to maintain genomic stability and preserve the genetic information, diverse DNA repair mechanisms have evolved [1]. Within these repair mechanisms DNA helicases assume a pivotal role for successful damage repair. In this chapter the repair mechanisms affecting a single strand of the double-stranded DNA (dsDNA) helix will be discussed in greater detail. Nucleotide excision repair (NER), base excision repair (BER), and MMR all prefer damaged substrates where the damage is usually confined to one of the two DNA strands, leaving the other one as a template for repair. In the case of MMR the situation is more complicated since there is no "real" damage present but mismatched bases have been generated after replication or recombination events. The importance of helicase action and the specific activities of helicases implicated in these pathways differ greatly and in some cases seem to be specifically tailored to a task rather than a more generic unwinding of substrates. All the helicases involved either belong to superfamily 1 (SF1) or superfamily 2 (SF2) helicases. SF1 and SF2 helicases share a common layout consisting of two RecA-like motor domains that are arranged in a tandem repeat and in addition contain other domains contributing to the specific function of the particular protein. The motor domains comprise the composite ATP-binding domain, where ATP hydrolysis takes place and transfers the chemical energy into motion (for a detailed overview, see Chaps. 2 and 3).

Nucleotide Excision Repair

NER is one of the most versatile among the DNA repair pathways [2–5]. Its mechanism is conserved among the kingdoms of life and consists of initial damage recognition, subsequent damage verification, and excision of a ssDNA fragment containing the damaged base (Fig. 10.1). In NER the initial lesion detection is most likely facilitated by an unusual conformation of the DNA backbone, which is subsequently identified by the different damage recognition proteins [6]. However, this process does not seem to be sufficient to confirm the actual presence of a DNA damage. In order to ensure that excision only takes place when a damage is present, a slower kinetic proofreading process is initiated. Within these intricate processes the action of helicases is mandatory for the successful continuation of the repair process. Although the general mechanism of NER is similar between eukaryotes and prokaryotes, the number of proteins and complexities of the different systems varies greatly. Furthermore, the NER process has to be divided into two different mechanisms: (1) global genome repair (GGR) in which the entire genome is actively scanned for lesions and (2) transcription coupled repair (TCR) which is initiated by a stalled RNA polymerase at an actively transcribed gene.

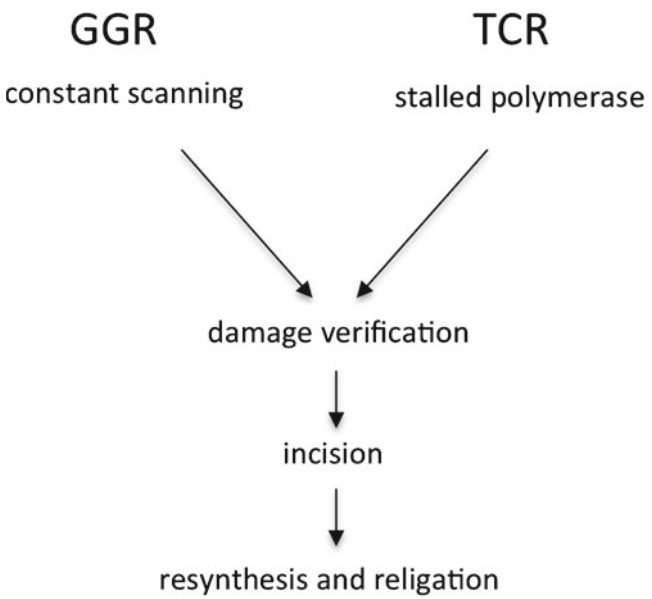

Fig. 10.1 Schematic representation of the two possibilities how a lesion is initially recognized in nucleotide excision repair. In global genome repair (GGR) the genome is scanned by the XPC/HR23B complex in search for damages whereas a stalled RNA polymerase on an actively transcribed gene is the initial signal in transcription coupled repair (TCR) to initiate the repair process. Both mechanisms converge into the same pathway with the recruitment of TFIIH followed by the subsequent steps of damage verification, incision, and resynthesis as well as religation

Both pathways share the same downstream processes after initial damage recognition has been achieved (Fig. 10.1).

Prokaryotic NER

The prokaryotic NER pathway consists of three main proteins named UvrA, UvrB, and UvrC. An additional helicase activity, however, is required for successful repair, which is provided by UvrD (Fig. 10.2). Within prokaryotic NER two essential activities can be associated with helicase activity. One is the actual damage verification process that is carried out by the UvrB protein. The other is the removal of the excised fragment containing the damage and the post-incision complex facilitated by UvrD or PcrA. In *Escherichia coli* this activity is provided by the UvrD protein, in Gram-positive bacteria this role is attributed to the PcrA helicase [7, 8]. UvrB is an SF2 helicase whereas UvrD and PcrA are *bona fide* examples of SF1 helicases. The substrate specificity of UvrB has not been characterized in greater detail but it displays a high affinity for ssDNA (0.5 μM) [9]. UvrD and PcrA have a broader substrate range including duplex DNA but prefer 3′ overhangs and partially

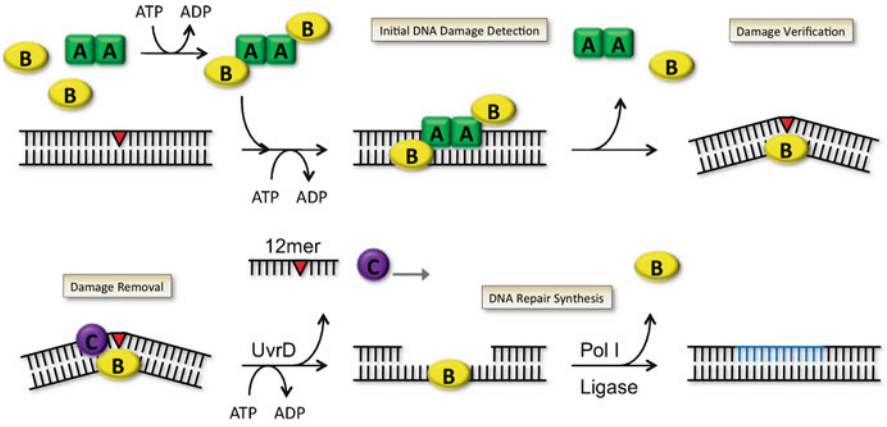

Fig. 10.2 Prokaryotic global genome nucleotide excision repair. UvrA (shown in *green*) forms a homodimer and assembles to a heterotetramer with UvrB (shown in *yellow*). After initial damage detection is achieved by the heterotetrameric complex UvrA dissociates. UvrB stays bound to the DNA and forms the so-called pre-incision complex to which UvrC (shown in *purple*) is recruited. UvrC catalyzes the 3′ and 5′ incisions. Removal of UvrC and the incised ssDNA fragment requires the presence of the helicase UvrD. UvrB stays bound to the DNA until resynthesis is initiated by Pol I and the repair process is completed upon sealing of the nick by DNA ligase

double-stranded DNA containing hairpin structures or flaps, respectively, *in vitro* [10–12]. Although all of the crystal structures available for UvrD and PcrA suggest that they act as monomers, there is evidence suggesting that both helicases have to be activated by another protein or act as multimers to develop full helicase activity *in vitro* [11, 13].

The damage recognition process is carried out by the heterotetrameric $UvrA_2$–$UvrB_2$ complex [14, 15] (Fig. 10.2). This complex consists of the homodimeric ABC ATPase UvrA, and each UvrA monomer provides a UvrB-interacting domain to which one UvrB monomer is bound. This initial damage recognition complex is actively scanning the genome for lesions. UvrA cycles between different nucleotide bound states thus undergoing domain movements that allow the productive binding of a DNA lesion [14]. The UvrA scanning mechanism thus provides a fast initial analysis of the bacterial genome but necessitates a proofreading mechanism prior to excision which is accomplished by the UvrB protein.

The UvrB Helicase

UvrB is an SF2 DEAD-box family helicase that exhibits only weak helicase and ATPase activity [16]. Apart from the classical SF2 RecA-like domains (1a and 3, see also Fig. 10.3) harboring the conserved helicase motifs, UvrB contains three auxiliary domains that most likely aid to its specific function (Fig. 10.3). Domain 1b facilitates additional interactions with the DNA and domains 2 and 4 provide

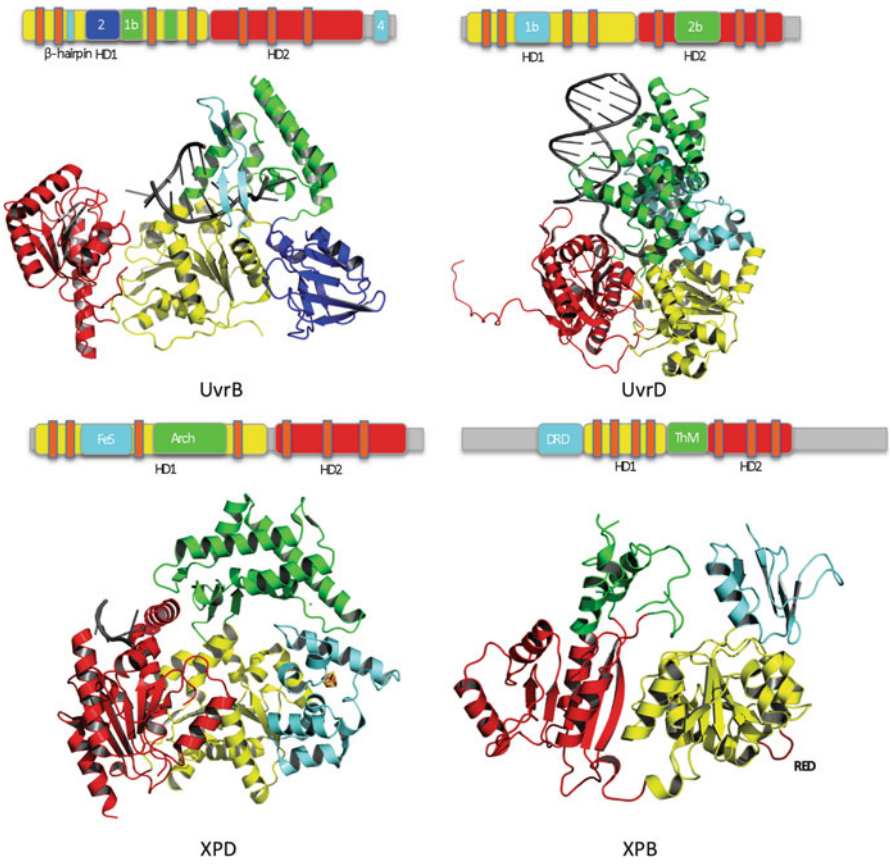

Fig. 10.3 Structures of the helicases involved in pro- and eukaryotic NER. The RecA-like motor domains are shown in all four structures in *yellow* and red, respectively. Above all structures the polypeptides are shown schematically using the same color codes and the helicase motifs are indicated in *orange*. The auxiliary domains are shown in *blue*, *green*, and *cyan*; additional parts are shown in *gray*; and the DNA is shown in *gray* as well

interaction interfaces with other proteins in the NER cascade. Domain 2 exclusively interacts with UvrA, whereas domain 4 interacts with both partners in the NER cascade, UvrA and UvrC [17]. UvrB also contains the so-called N-terminal Q-motif that is present in a number of different functionally unrelated DNA and RNA helicases. The Q-motif is involved in nucleotide binding and positioning which is also exemplified in the UvrB–ATP complex structure [18], where it was shown that N6 and N7 of the adenine form hydrogen bonds to the side chain of the conserved glutamine within the Q-motif thus explaining the specificity for adenine. Another very prominent and unusual feature of UvrB is a so-called β-hairpin that bridges subunits 1a and 1b. The β-hairpin is a structural motif within UvrB that is directly implicated in the damage verification process [18, 19], and several studies showed that specific residues within the β-hairpin are essential for damage

verification [20–22]. In the structure of a UvrB–DNA complex where the DNA substrate adopted a hairpin structure, the β-hairpin directly interacts with the substrate providing a structural basis for the damage verification process [23].

Damage Verification by UvrB

As outlined above, initial damage identification/scanning has to be followed by damage verification to achieve accurate damage detection in NER, thus the presence of a damage has to be verified prior to excision. In prokaryotic NER the three proteins described above have to communicate within this process in order to successfully excise a damaged DNA fragment. The main anchor between the subsequent events is the UvrB helicase. It interacts with both UvrA and UvrC and only dissociates from the DNA once resynthesis of the excised DNA fragment has been initiated. UvrB is thus involved both in the early processes of detection and verification but also guides the endonuclease UvrC to the site where it has to perform the incision reactions [17]. The ATPase and as such also the helicase activity of UvrB are highly regulated by its subdomain 4. Removal of subdomain 4 results in a higher affinity for ssDNA and activation of UvrB's ATPase activity which is further stimulated by the presence of ssDNA [24]. However, its helicase activity seems not to be activated indicating the necessity of another factor which is the UvrA protein. The UvrA–UvrB complex has been shown to display weak helicase activity [25] that can be attributed to the UvrB protein. UvrA interacts with UvrB via UvrB's domain 4 leading to an activation of its ATPase and DNA-binding abilities, while the interaction with domain 2 might ultimately trigger the helicase activity of UvrB. After UvrA has identified the damage, UvrB could be placed up to 80 Å away from the lesion [14] suggesting that UvrB has to unwind the dsDNA until it encounters the damage. However, the exact nature of the handover between UvrB and UvrA has remained elusive so far. It is clear that UvrB uses its destabilizing ability to further unwind a certain stretch of dsDNA until it encounters a damage where it remains bound to the DNA. The damage sensing factor in UvrB is the β-hairpin. The β-hairpin is inserted into the opening of the dsDNA that has been created by UvrA and is subsequently used as a ploughshare to separate the dsDNA as seen in other helicases where a small hairpin- or wedge-like feature is used for this task. The β-hairpin of UvrB, however, is unique in its size and positioning with respect to the helicase scaffold, which has prompted the theory of a padlock mechanism for damage verification [16]. In addition more recent studies revealed that a β-hairpin feature is used in several damage-recognizing proteins as a damage sensor [6]. At the base of the β-hairpin of UvrB several aromatic residues are involved in base-stacking interactions [23] and seem to be essential for proofreading. For example, if either Tyr92 or Tyr93 in the *E. coli* enzyme are mutated to alanine a "lethal" enzyme is generated since nondamaged DNA is incised. However, although the crystal structures of UvrB with a DNA substrate and with ATP have provided a wealth of information on the UvrB action, it is still not clear if the damage resides on the translocated or the nontranslocated strand during the recognition process. The two possibilities will be

described below. The crystal structure of the UvrB–DNA complex indicates a proofreading process where a base is flipped into a hydrophobic pocket during DNA translocation. This pocket could be used for the recognition of a damaged substrate due to sterical hindrance, since it is located between domain 1b and the β-hairpin. This model would also suggest that the damage is located on the translocating strand of the UvrB helicase, which is further supported by data showing that UvrB alone is able to create a pre-incision complex when loaded on a DNA substrate containing a 5′ overhang on the damaged strand [26]. It cannot be excluded, however, that the damage resides on the nontranslocated strand. Tyr95 in the UvrB enzyme form *Bacillus caldotenax* is solvent exposed in the crystal structure and has been implicated in interactions with the damaged base [23, 27]. It has also been shown that a CPD damage is still recognized by photolyase whilst still engaged with UvrB, indicating accessibility of the lesion [28]. Another observation in favor for this theory is the fact that UvrB remains bound to the DNA until it is removed by PolI. This indicates that at least after incision and the removal of the damaged fragment UvrB still interacts with the nondamaged DNA. It is clear, however, that the engagement of UvrB with the lesion creates a trapped state for the helicase, rendering it incapable for further translocation while ATP hydrolysis is maintained. This trapped state triggers increased ATP consumption which is accompanied with the release of UvrA and the recruitment of UvrC for 3′ and 5′ incision. UvrA and UvrC both utilize domain 4 of UvrB as interaction interface. After the incision reaction UvrB remains bound and the next helicase, UvrD is recruited to remove UvrC and the incised ssDNA fragment.

The UvrD Helicase

UvrD is a SF1A helicase (Fig. 10.3) that unlike UvrB fulfills its task in more than one DNA repair process. It consists of four domains that can be grouped into two RecA-like motor domains (1a and 2a) characteristic for SF1 or SF2 helicases and two auxiliary domains that emerge from each motor domain, respectively (1b and 2b). The auxiliary domains are both involved in DNA binding (Fig. 10.3) [29]. Domain 2b can undergo large movements as indicated by a UvrD apo-structure where this domain is rotated by approximately 160° [30] in comparison to the DNA-bound state (Fig. 10.4a). Together with PcrA it is one of the mechanistically most studied helicases and several structures representing different snapshots of the enzymes combined with biochemical data led to deep insights into their helicase translocation mechanisms.

In NER the task of UvrD is to resolve the structures of the post-incision complex leading to the release of UvrC and the lesion containing DNA fragment of about 12 bases marked by the 3′ and 5′ nicks and to enable resynthesis of an unaltered DNA sequence [3]. UvrD contains an N-terminal and an unstructured C-terminal region that interacts with different regions of UvrB. It has been shown that the unstructured C-terminus of UvrD interacts with domains 1a and 2 from UvrB [8]. The N-terminal part of UvrD consisting of domains 1a and 1b interacts with domains 1b and 3 of

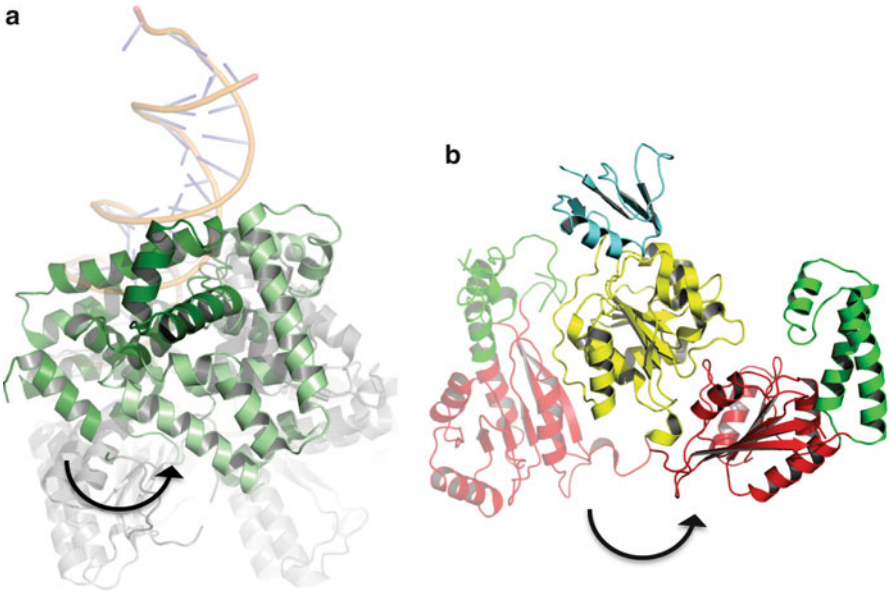

Fig. 10.4 (**a**) Superposition of the UvrD apo-structure onto the DNA-bound structure. To highlight the domain movement only domain 2b is colored (*light green* = apo, *dark green* = DNA-bound structure). The *arrow* indicates the movement of domain 2b which is rotated by approximately 160° upon DNA binding. (**b**) Modeling of the open to the closed state of afXPB. The closed state is achieved by a rotation of approximately 170° around a glycine in the linker region between the two RecA-like domains

UvrB. Truncation of the C-terminal unstructured region of UvrD abolishes the *in vitro* interaction with UvrB but still permits the removal of the post-incision complex *in vitro* [8]. *In vivo* this truncation leads to an increased UV sensitivity of an affected *E. coli* strain [8]. It seems that UvrD's activity is regulated by UvrB to achieve a successful NER event. It has been shown that the UvrA–UvrB complex significantly enhances the activity of UvrD on branch or no branch substrates containing nicks [31]. Although the exact mechanism of UvrD stimulation by either UvrA–UvrB or UvrB remains elusive so far, it displays a striking similarity to one of UvrD's other tasks in MMR where it fulfills a similar task that is triggered by the MutL protein. This mechanism will be described below in greater detail.

Eukaryotic NER

Eukaryotic NER albeit mechanistically similar to prokaryotic NER is infinitely more complex since at least 30 different proteins have been identified that participate in this process [4]. Although there is still some debate about the specific contributions of the individual proteins, a general scheme of action has emerged

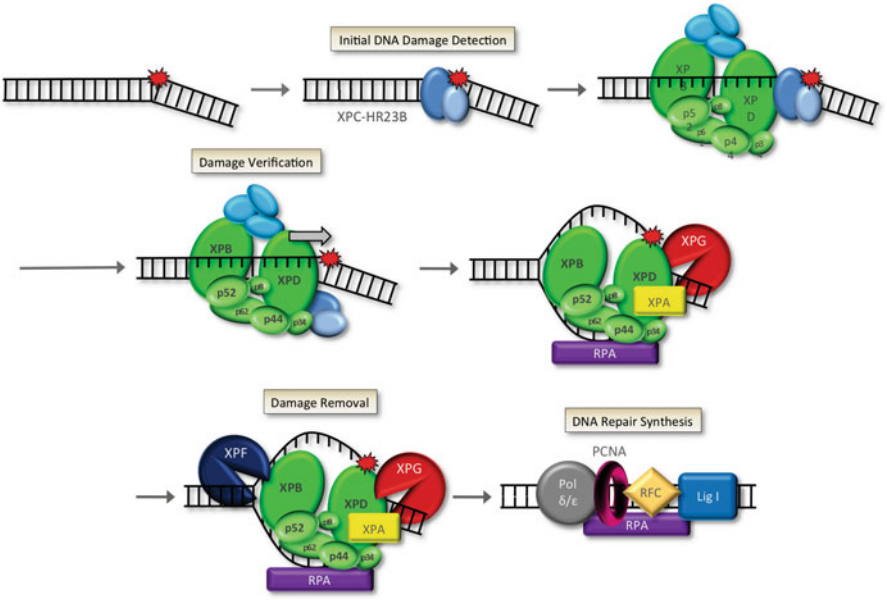

Fig. 10.5 Eukaryotic global genome nucleotide excision repair. Initial damage recognition is achieved by the complex formed between XPC and HR23B, leading to the recruitment of TFIIH. In the subsequent processes the helicase activity of XPD is essential whereas the helicase activity of XPB is not required. XPA most likely triggers the release of the CAK subunit followed by the recruitment of additional factors including the two nucleases XPG and ERCC1/XPF which perform the two incision reactions 3′ and 5′ to the lesion. Repair is completed after resynthesis and sealing of the nick has been achieved

(Fig. 10.5). In the following we will refer to the human GGR–NER pathway and the nomenclature used therein. A damage is initially recognized by the XPC–HR23B complex which subsequently recruits the general transcription factor TFIIH to the site of the lesion. TFIIH consists at this stage of ten subunits, two of the subunits are the helicases XPB and XPD. TFIIH can be divided into a core that harbors the two helicases and five other subunits, and the CAK subunit that consists of the kinase CDK7 in complex with cyclin H and the Mat-1 protein. After the recruitment of TFIIH by XPC the helicase XPB is responsible for the correct loading of TFIIH onto the DNA; however, for this step only the ATPase activity of XPB is required whereas its helicase activity is expendable [32]. After this loading step the helicase activity of XPD is required leading for further unwinding of the DNA presumably until it encounters the damaged site. The arrival of XPA triggers the release of the CAK subunit which leads to the recruitment of further factors and eventually the nucleases catalyzing the incision reactions. The gap is then filled by DNA polymerases δ and κ or DNA polymerase ε bound to PCNA [33]. The nick is eventually sealed by DNA ligase IIIa or DNA ligase I [34].

Structural information on the eukaryotic helicases involved in NER has been scarce, due to the inaccessibility of the proteins to structural studies. However, many archaeal organisms contain XPB and XPD homologs that could be utilized for structural studies and have greatly advanced our understanding of these important helicases. A lack of NER activity results in four different hereditary diseases with severe phenotypes: xeroderma pigmentosum (XP), trichothiodystrophy (TTD), XP combined with Cockayne's syndrome (XP/CS), and cerebro-oculu-facio-skeletal (COFS) syndrome (please also see Chap. 6), thus underlining the importance of this unique DNA repair pathway.

The XPB Helicase

XPB is an SF2A family helicase that consists of four domains. The crystal structure of an XPB homolog from *Archaeoglobus fulgidus* (afXPB) revealed the overall layout of this helicase. AfXPB consists of two RecA-like motor domains (HD1 and HD2), a thumb domain (ThM), and the so-called DRD (damage recognition domain) (Fig. 10.3). In analogy to UvrD the two auxiliary domains emerge each from one of the motor domains. In addition the HD1 domain contains the so-called strictly conserved RED motif that seems to play a key role in DNA unwinding (Fig. 10.3) [35]. The crystal structure revealed an "open" conformation for afXPB that could be modeled into a "closed" form by a rotation of approximately 170° around a glycine in the linker region between HD1 and HD2 (Fig. 10.4b). The "closed" state most likely represents the active state of the helicase that is induced by nucleotide and DNA binding. Studies on the DRD of the human XPB revealed no specific affinity for damaged DNA probably excluding the previously proposed role in damage verification or recognition [36]. However, the importance of the ThM and the RED motif for the role of XPB could be verified. It has been shown that both elements are involved in the DNA-dependent ATPase activity of XPB. These studies also indicated that XPB might not act as a conventional helicase during NER. Based on the results obtained from the crystal structure of afXPB and the mutational analysis of the RED and ThM domains (see above), as well as the analysis of mutants specifically disrupting the helicase or ATPase activity of XPB, it became evident that the helicase activity of XPB is dispensable whereas the ATPase activity is essential for NER. These results led to the proposal that XPB fulfills a role in analogy to the Swi2/Snf family of molecular switches [36]. XPB is the first anchoring point of TFIIH when it is recruited to the lesion by XPC. The proposed domain motion between HD1 and HD2 could be utilized to hook up the complete TFIIH to the site of the lesion. In this process of placing TFIIH the RED motif and the ThM domain are of vital importance.

Being integrated into a large complex like TFIIH the influence of other TFIIH members on XPB has to be considered as well. So far no cross talk has been identified between the two helicases. However, other subunits of TFIIH could modulate the activity of XPB. In *in vitro* experiments so far only p52 seems to directly stimulate the ATPase activity of human XPB suggesting a direct interaction between

these two TFIIH subunits. Human XPB contains an N-terminal extension compared to afXPB. In this extension the two disease causing mutations F99S and T119P, leading to XP/CS and TTD, respectively, are located. Detailed biochemical analysis has shown that these mutations alter the p52-induced ATPase activity which led to the conclusion that this N-terminal part of the protein is involved in the p52–XPB interaction. As a chain of events it has been proposed that after the initial damage recognition has been completed, XPC recruits TFIIH through direct interactions. This triggers a stronger association of TTDA with the TFIIH complex. TTDA is a small subunit (8 kDa) of TFIIH which was only recently discovered but is vital for the repair activity. It has been shown that the presence of NER lesions results in a tighter association of TTDA to TFIIH which is otherwise also present as an isolated subunit in the nucleus and the cytoplasm [37]. TTDA in turn can activate p52, which eventually amplifies XPB's ATPase activity thus achieving a correct loading of TFIIH to the lesion site followed by the concomitant steps in the cascade. This intricate interaction pattern exemplifies how NER helicases are highly regulated parts of larger macromolecular machines.

The XPD Helicase

It has been an enigma of eukaryotic NER why two SF2 helicases with opposite polarities should be necessary for successful damage recognition, verification, and excision. In parallel to the discovery of the role that XPB assumes in the repair pathway great progress has been made towards the elucidation of the function of XPD within TFIIH and in particular during the damage verification process. XPD is an SF2B family helicase. Structural data have been obtained recently by elucidating the structures of XPD homologs from the archaeal organisms *Solfolobus tokodaii* (stXPD), *Sulfolobos acidocaldarius* (saXPD), and *Thermoplasma acidophilum* (taXPD) [38–40]. The crystal structures revealed the overall fold of the XPD protein consisting of two RecA-like domains termed HD1 and HD2 and two auxiliary domains. One of the auxiliary domains was of special interest since it contains an iron sulfur cluster (Fig. 10.3) [41]. The iron sulfur cluster could be readily identified in two of the structures whereas in the third structure this domain was disordered due to oxidation of the cluster leading to a destabilization of the surrounding protein environment. However, the cluster was unambiguously identified as a 4Fe4S cluster (FeS) in the two structures where it was present. The other auxiliary domain was termed arch domain because it builds an arch or bridge-like feature that forms an additional connection between HD1 and the FeS domain thereby creating a pore (Fig. 10.3). XPD also contains a Q-motif at the N-terminus [42]. The overall architecture resembles that of UvrB since both auxiliary domains emerge from HD1 as well and it also contains a Q-motif. Archaeal XPD can readily unwind substrates *in vitro* containing a 5′ overhang, a Y fork, or a bubble [43]. Recently, the structure of taXPD was solved in the presence of a short ssDNA fragment revealing a high-affinity DNA-binding site and also the polarity of the ssDNA strand with

respect to the helicase scaffold. In addition it was shown that ssDNA extends through the pore-like feature created by HD1, the arch domain, and the FeS domain [42].

Within TFIIH the helicase activity of XPD is stimulated by a direct interaction with the p44 subunit of TFIIH. The p44–XPD interaction is mediated via the N-terminus of p44 and the very C-terminus of XPD [44]. Notably, this interaction stimulates only the helicase activity of XPD but not its ATPase activity. XPD also interacts with the CAK subunit via Mat-1, and it was shown to be negatively regulated by the CAK complex [45]. The release of the CAK complex is triggered by the arrival of XPA which allows the NER reaction to proceed [46]. This interaction pattern places XPD in a central position for the regulation of NER, since it is also thought to be involved in the damage verification process (see below). Interestingly, it was shown that the two helicases XPB and XPD fulfill additional roles and have been identified in other macromolecular complexes apart from their role in transcription and NER. Recently it has been shown that XPB is recruited to the centrosome during mitosis [47]. XPD was identified in two other complexes. In the first it forms an independent free complex with the CAK subunit that is also involved in cell cycle regulation and in the second it is part of the MMXD complex where it directly interacts with MIP18 and MMS19 and is involved in chromosome segregation [48–50]. The exact roles of the helicases within these recently identified complexes remain elusive so far. However, these examples underline the high versatility of the two helicases XPD and XPB and also show the importance of protein–protein interactions for helicase action and activity.

The FeS

XPD is also the founding member of a special subgroup of helicases within this family. This subgroup is characterized by the presence of a 4Fe4S (FeS) cluster as an auxiliary cofactor [41] (Fig. 10.6). Other prominent members of this family in humans are represented by the regulator of telomere length helicase (RTEL), Fanconi anemia complementation group J (FancJ), and DDX11 (or hChlR1) [51, 52]. It is very likely that all of these proteins are also 5′–3′ helicases. However, the tasks of these enzymes are diverse and exemplify once again that they should be analyzed in the context of their interaction partners; XPD is involved in NER, chromosome segregation, and transcription [48, 53, 54], DDX11 plays a role in sister chromatid cohesion [55, 56], FancJ is involved in homologous recombination events during double-strand break DNA repair [57], and RTEL participates in maintaining the telomere length or capping [58]. Since all of these helicases share the unusual FeS cluster it is intriguing to speculate whether the cluster just assumes a structural role or whether the electrochemical properties of the FeS cluster participate in the proteins functions and how this could be modulated for the specific tasks of each protein.

The most straightforward assumption for the cluster is a structural role, in which it stabilizes its harboring domain and thereby contributes to the formation of the

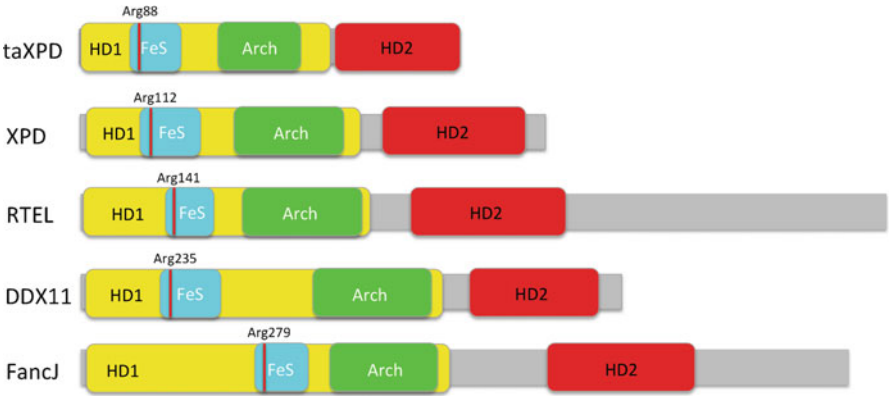

Fig. 10.6 Schematic representation of different SF2B helicases which define a subgroup and are characterized by the presence of a 4Fe4S cluster as an auxiliary cofactor. In addition to XPD (taXPD indicates the XPD protein from *Thermoplasma acidophilum* and XPD the human helicase) the regulator of telomere length helicase (RTEL), Fanconi anemia complementation group J (FancJ), and DDX11 (or hChlR1) are shown

pore. This assumption is clearly supported through biochemical and structural studies. It was shown for saXPD that helicase activity is completely abolished upon loss of the FeS cluster whereas its ATPase activity is not affected [41]. Furthermore, the absence of the FeS cluster harboring domain in the structure of saXPD lacking the FeS cluster indicates the necessity of the cluster for correct folding and stabilization of this domain [38, 39]. In addition the FeS cluster domain harbors the molecular ploughshare enabling XPD to unwind dsDNA [59], thus defining another role for this domain.

However, the described structural roles may be still too simplistic, and an additional function can be envisioned based on the electrochemical properties of the FeS cluster which could act as a sensor of the redox state within the cell and could therefore be required for the correct function of the protein.

Since XPD is involved in NER and has been proposed to play an important role in damage verification, the apparent question arises whether the FeS cluster participates in this process as well. Intriguingly, some similarities can be observed in the FeS cluster containing BER endonucleases EndoIII and MutY [40, 60–62]. In MutY and EndoIII the FeS cluster is located in close vicinity to the DNA backbone and interacts with the DNA via a double arginine motif [61]. It has been proposed that both BER endonucleases utilize their cluster for DNA charge transfer (CT) along the DNA through the π-stacked bases of the DNA. According to this proposal, the FeS cluster is oxidized when it binds to DNA and assumes the FeS^{3+} state. The free electron can then be used for CT [63]. When a damage is encountered along the pathway of the electron the CT becomes short-circuited thus providing an efficient method to identify damaged sites on the DNA (reviewed by [64, 65]). If CT is not disrupted, one protein can reduce the other along the DNA and thus allow them to

disengage from the DNA since they display a reduced affinity for DNA in the FeS^{2+} state. It is likely that the FeS cluster of taXPD, despite the lack of sequence or fold conservation in the FeS cluster domain with respect to the BER enzymes could fulfill a similar role through the highly conserved Arg88 as the double arginine motif in MutY or EndoIII (Fig. 10.6), thus providing the possibility for CT in this protein as well [40]. In strong support of this hypothesis it has been shown very recently that saXPD exhibits a similar DNA-bound redox potential as the BER enzymes MutY and EndoIII [66]. Moreover it could be shown that the current of the signal is increased in the presence of ATP but the potential is not affected. This is most likely related to motions at the protein/DNA interface during the activity cycle of the helicase [66]. Since it has been demonstrated that XPD is tightly bound to damaged DNA [67] and is most likely involved in the damage verification process, the question can be asked whether XPD utilizes the electrochemical properties of the FeS cluster combined with its helicase activity either to sense the damage or for signaling with other NER factors. XPD is able to redistribute on a DNA containing a mismatch in a CT-dependent manner and also communicates with the BER EndoIII via CT [68]. These observations strongly support the notion of CT and the cross talk between different FeS-containing proteins. Interestingly it has been shown that FancJ can also sense oxidative damage in *in vitro* studies in a similar fashion compared to XPD, although the damage is recognized on both strands [69] in FancJ whereas Mathieu et al. showed a preference for the translocating strand in faXPD when a cyclobutane pyrimidine dimer is present [67]. Combined, these observations suggest that the possible CT properties of FeS cluster containing helicases might currently be underestimated. Since all of the above described family members could comprise a comparable layout concerning the FeS cluster domain, the arch domain, and the two RecA-like domains it is tempting to speculate that all family members display similar electrochemical properties when bound to DNA. Intriguingly, all family members are also involved in genomic maintenance or damage detection suggesting that the FeS cluster might not only be a structural feature but also a functional entity for damage detection or signaling.

Prokaryotic Mismatch Repair

The MMR pathway can be divided into three steps: initiation, excision, and repair DNA synthesis [70]. In *E. coli* methyl directed MMR is the main pathway to correct replication errors and faulty recombination events [71]. The MutS homodimer recognizes the mismatched bases in an ATP-dependent fashion. After this initial event the also homodimeric MutL protein is recruited and MutL and MutS form a heterotetrameric complex. This complex activates MutH that is located at the nearest hemimethylated (GATC) site with respect to the mismatch. The activated MutH creates a nick that can be used to separate the parental from the daughter strand. This nick signals the initiation of unwinding by the UvrD helicase in 3′–5′ direction toward the mismatch. UvrD is followed by an exonuclease that degrades the unwound ssDNA strand. Four ssDNA exonucleases are associated with MMR in *E.*

coli: ExoI, ExoVII, ExoX, and RecJ. Depending on the position of the nick, relative to the mismatch, UvrD translocates either on the parental or the daughter strand. Which exonuclease is active depends on the polarity of the mismatched fragment (reviewed in [72]). The resection of the DNA continues well past the mismatch and subsequently DNA polymerase III is recruited to the gap and the resulting nick is sealed by DNA ligase.

UvrD in MMR

As in NER the initial substrate for UvrD is a nicked dsDNA. It seems peculiar that a helicase with a moderate processivity of about 40–50 bp [73, 74] is involved in the unwinding reaction of DNA fragments that can be up to 1–2 kb in size. In NER the fragment that is removed is only about 12 bases long (see above in prokaryotic NER). In analogy to the UvrD stimulation by UvrB the MutL protein stimulates or alters the activity of UvrD to ensure a sufficiently high processivity [72]. *In vitro* studies revealed that MutS, MutL, and UvrD are required on an artificial substrate for proper activation [75]. Similarly to the XPD activation by p44 MutL also stimulates only the helicase activity and not the ATPase activity of UvrD [76]. The interaction site of MutL with UvrD could be mapped to the C-terminus and a region comprising residues 397–438 [77]. The exact interaction sites on UvrD have not been characterized so far.

The enhanced processivity of UvrD is most likely accomplished by an increased affinity of the UvrD–MutL complex for DNA. When one UvrD molecule is loaded it initiates the unwinding reaction and MutL continues to load UvrD monomers that together facilitate an enhanced and more efficient unwinding of the substrate [78]. This observation is well in line with the fact that UvrD is a highly efficient translocase but fails to act as a helicase in its monomeric state; instead the *in vitro* helicase activity requires the presence of a dimer [73]. The MutL-dependent stimulation of UvrD is activated through the presence not the hydrolysis of ATP in MutL which was shown by a MutL variant that was unable to hydrolyze ATP and led to much stronger activation of UvrD [72]. Since MutL displays a rather weak ATPase activity, the system seems to be delicately balanced thus ensuring a reasonable activation of UvrD. A rationale for this limited activation might be the associated exonuclease catalyzing the strand resection. If UvrD would unwind the DNA too fast the nuclease might not be able to keep up resulting in reannealing of the substrate with detrimental effects on the repair process [72]. Also the catalyzed loading would guide UvrD onto the correct strand for the reaction to prevent nonspecific unwinding.

The action of UvrD in MMR and NER is an important example how protein–protein interactions modulate the action of a helicase in order to fulfill a specific task. Helicase action alone would in these cases not be sufficient to maintain the biological function, and the different requirements of UvrD in NER and MMR make this evident. In both cases a partner protein is required to engage UvrD and stimulate its activity; one interaction results in the removal of UvrC and a short DNA fragment, whereas the other results in the unwinding of dsDNA as long as 2 kb.

Eukaryotic MMR

Eukaryotic MMR is highly similar to prokaryotic MMR and employs analogous strategies for damage recognition and repair. Instead of the hemimethylated site eukaryotic MMR requires a nick as starting point after the mismatch has been recognized [71]. MMR deficiency results in hereditary nonpolyposis colorectal cancer that is characterized by a so-called microsatellite instability due to inefficient repair of small insertion deletion loops (IDLs) [70]. As in NER the eukaryotic MMR system follows in principle a similar scheme as the prokaryotic MMR pathway but it is more complicated with respect to the number of proteins and its substrate specificity. There are at least three homologs for MutS which form heterodimers (MutSα [MSH2–MSH6], MutSβ [MSH2–MSH3], and MSH4–MSH5). For MutL the situation is similar and there are also three homologous complexes present: MutLα (MLH1–PMS2), MutLβ (MLH1–PMS1), and MutLγ (MLH1–MLH3). The three different MutS homologs all exhibit different substrate specificities. MutSα seems to recognize both, mismatches and IDLs, whereas MutSβ mainly recognizes IDLs [70]. MSH4–MSH5 is most likely involved in double-strand break repair and also in suppression of nonspecific excision after mismatch removal [70]. There is no known MutH homolog present in eukaryotes which led to the proposal that eukaryotic MMR uses the nicks of Okazaki fragments or the 3′ end of the leading strand during replication as a starting point [79]. Other proteins involved are Exo1, RPA, DNA polymerase δ, RFC, and PCNA [79]. Interestingly no helicase has been directly associated with eukaryotic MMR. In a reconstituted *in vitro* system the above-mentioned components are sufficient to drive a successful MMR reaction [80–82]. However, MMR proteins have been shown to interact with a number of helicases mostly belonging to the RecQ family of helicases [70]. The RecQ helicases belong to the SF2A helicases and contain in addition to the RecA-like domains a domain called RQC (RecQ C-terminal, not present in RecQL4). However, this family is intensively discussed in Chap. 8 and will not be covered here. Another interaction partner is the FancJ helicase [70]. FancJ belongs to the family of FeS-containing helicases described above. Although the interactions have been partly mapped to specific domains and characterized, the involvement of these helicases in MMR remains enigmatic at best and is more likely important in other mechanisms maintaining

Table 10.1 Interactions between different MMR proteins and helicases in eukaryotes

Helicase	Interacting MMR protein(s)
WRN	MutSα, MutSβ, MutLα, RPA
BLM	MutSα, MLH1, RPA
RecQL1	MutSα, MLH1, RPA
FancJ	MLH1

genome stability. Table 10.1 summarizes the different helicases and their respective interaction partners.

BER and WRN Helicase

BER protects the genome from damages caused by oxidation, alkylation, or deamination [83–85]. BER can be divided into two different subpathways: short-patch BER and long-patch BER. Short-patch BER comprises the repair of one base whereas in long-patch BER a longer DNA fragment of several bases is replaced. In principle BER consists of a simple elegant mechanism that is highly conserved between pro- and eukaryotes and only four proteins are required for completion of

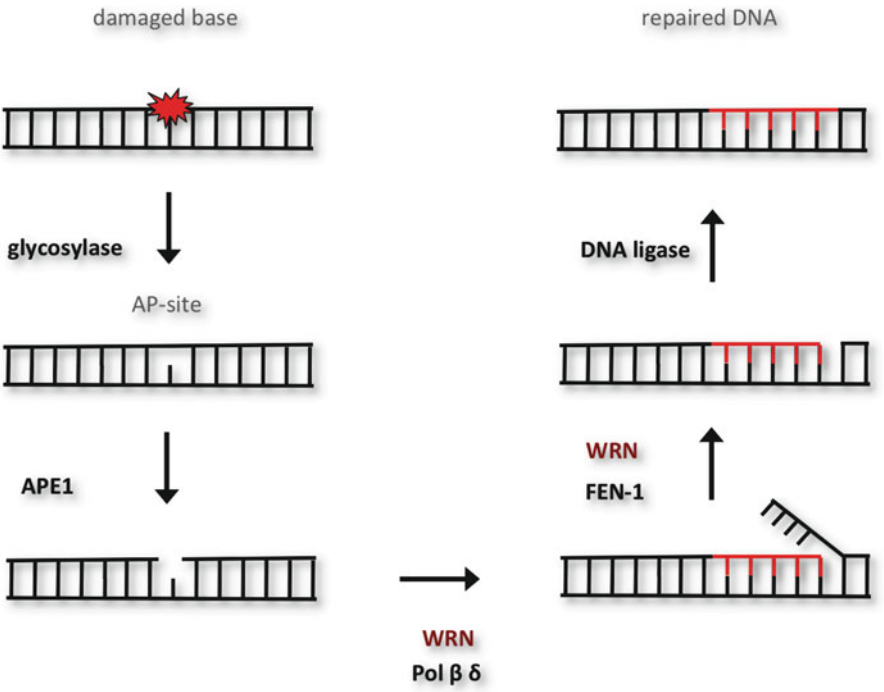

Fig. 10.7 The BER pathway. In short-patch BER damage recognition is achieved by a DNA glycosylase which removes the base by cleavage of the N-glycosidic bond. Subsequently AP endonuclease creates a 5′ nick which is filled by DNA polymerase β and sealed by DNA ligase III. In long-patch BER DNA pol β or δ is recruited to the site created by APE1 and a longer stretch of DNA is unwound which is subsequently a substrate for the endonuclease FEN-1 that specifically recognizes flap structures and is required for long-patch BER. Possible roles of the WRN helicase are indicated. The WRN protein stimulates DNA pol β strand displacement and synthesis in a helicase-dependent manner. In addition WRN is negatively regulated by APE1 thereby impairing unspecific unwinding. Lastly, WRN directly stimulates the activity of FEN-1

repair [86]. At first the DNA damage is recognized by one of the many DNA glycosylases, which is cleaving the N-glycosidic bond thus removing the damage and leaving an apurinic or apyrimidinic site (AP). The AP site is a substrate for the AP-specific endonuclease APE1 which incises the AP site and generates a 3′OH and a 5′-deoxyribose phosphate (5′dRP). In short-patch repair DNA polymerase β removes the 5′dRP and utilizes the 3′ end for replication. The resulting nick is sealed by a DNA ligase (DNA ligase III). In long-patch BER DNA pol β or δ is recruited to the site created by APE1. A longer stretch is then unwound that is subsequently a substrate for the endonuclease FEN-1, which specifically recognizes flap structures and is required for long-patch BER [87–89].

Werner syndrome (WS) is an autosomal recessive disorder that causes segmental progeria and was mapped to the WRN protein. WRN is a SF2A helicase that also contains exonuclease activity. WS patients are characterized by premature development of atrophic skin, thin gray hair, osteoporosis, type II diabetes, cataracts, arteriosclerosis, and cancer [90, 91]. WRN helicase has been shown to interact with many of the proteins involved in BER [92], and it has been suggested that aging is correlated to a defect in the repair of oxidative damage [93–97]. WRN interacts with DNA pol β and δ, PCNA, RPA, and FEN-1 [92]. The WRN helicase activity itself stimulates DNA pol β strand displacement and synthesis [92] in a helicase-dependent manner. WRN is also negatively regulated by APE1 prohibiting unspecific unwinding thus providing a basis for WRN involvement in BER [98]. Also WRN directly stimulates the activity of FEN-1 [92]. The possible roles of WRN helicase are exemplified in Fig. 10.7. However, compared to the precise functions described for the helicases in the other DNA repair mechanisms the role of WRN in BER remains speculative and requires further analysis.

References

1. Lindahl T, Wood RD. Quality control by DNA repair. Science. 1999;286:1897–905.
2. Van Houten B. Nucleotide excision repair in Escherichia coli. Microbiol Rev. 1990;54:18–51.
3. Friedberg EC, Walker GC, Siede W, Wood RD, Schultz RA, Ellenberger T. DNA repair and mutagenesis. Washington, DC: ASM Press; 2006.
4. Gillet LC, Scharer OD. Molecular mechanisms of mammalian global genome nucleotide excision repair. Chem Rev. 2006;106(2):253–76.
5. Sancar A. DNA excision repair. Annu Rev Biochem. 1996;65:43–81.
6. Kuper J, Kisker C. Damage recognition in nucleotide excision DNA repair. Curr Opin Struct Biol. 2012;22(1):88–93.
7. Petit MA, Dervyn E, Rose M, Entian KD, McGovern S, Ehrlich SD, et al. PcrA is an essential DNA helicase of Bacillus subtilis fulfilling functions both in repair and rolling-circle replication. Mol Microbiol. 1998;29(1):261–73.
8. Manelyte L, Guy CP, Smith RM, Dillingham MS, McGlynn P, Savery NJ. The unstructured C-terminal extension of UvrD interacts with UvrB, but is dispensable for nucleotide excision repair. DNA Repair. 2009;8(11):1300–10.
9. Yamagata A, Masui R, Kato R, Nakagawa N, Ozaki H, Sawai H, et al. Interaction of UvrA and UvrB proteins with a fluorescent single-stranded DNA. Implication for slow conformational change upon interaction of UvrB with DNA. J Biol Chem. 2000;275(18):13235–42.

10. Matson SW. Escherichia coli helicase II (urvD gene product) translocates unidirectionally in a 3' to 5' direction. J Biol Chem. 1986;261(22):10169–75.
11. Fischer CJ, Maluf NK, Lohman TM. Mechanism of ATP-dependent translocation of E. coli UvrD monomers along single-stranded DNA. J Mol Biol. 2004;344(5):1287–309.
12. Anand SP, Khan SA. Structure-specific DNA binding and bipolar helicase activities of PcrA. Nucleic Acids Res. 2004;32(10):3190–7.
13. Niedziela-Majka A, Chesnik MA, Tomko EJ, Lohman TM. Bacillus stearothermophilus PcrA monomer is a single-stranded DNA translocase but not a processive helicase in vitro. J Biol Chem. 2007;282(37):27076–85.
14. Pakotiprapha D, Samuels M, Shen K, Hu JH, Jeruzalmi D. Structure and mechanism of the UvrA-UvrB DNA damage sensor. Nat Struct Mol Biol. 2012;19(3):291–8.
15. Verhoeven EE, Wyman C, Moolenaar GF, Goosen N. The presence of two UvrB subunits in the 2002;21(15):4196–205.
16. Theis K, Skorvaga M, Machius M, Nakagawa N, Van Houten B, Kisker C. The nucleotide excision repair protein UvrB, a helicase-like enzyme with a catch. Mutat Res. 2000;460(3–4):277–300.
17. Truglio JJ, Croteau DL, Van Houten B, Kisker C. Prokaryotic nucleotide excision repair: the UvrABC system. Chem Rev. 2006;106(2):233–52.
18. Theis K, Chen PJ, Skorvaga M, Houten BV, Kisker C. Crystal structure of UvrB, a DNA helicase adapted for nucleotide excision repair. EMBO J. 1999;18:6899–907.
19. Van Houten B, Croteau DL, DellaVecchia MJ, Wang H, Kisker C. 'Close-fitting sleeves': DNA damage recognition by the UvrABC nuclease system. Mutat Res. 2005;577(1–2):92–117.
20. Skorvaga M, Theis K, Mandavilli BS, Kisker C, Van Houten B. The beta-hairpin motif of UvrB is essential for DNA binding, damage processing, and UvrC-mediated incisions. J Biol Chem. 2002;277(2):1553–9.
21. Moolenaar GF, Hoglund L, Goosen N. Clue to damage recognition by UvrB: residues in the beta-hairpin structure prevent binding to non-damaged DNA. EMBO J. 2001;20(21):6140–9.
22. Moolenaar GF, Schut M, Goosen N. Binding of the UvrB dimer to non-damaged and damaged DNA: residues Y92 and Y93 influence the stability of both subunits. DNA Repair (Amst). 2005;4(6):699–713.
23. Truglio JJ, Karakas E, Rhau B, Wang H, DellaVecchia MJ, Van Houten B, et al. Structural basis for DNA recognition and processing by UvrB. Nat Struct Mol Biol. 2006;13(4):360–4.
24. Wang H, DellaVecchia MJ, Skorvaga M, Croteau DL, Erie DA, Van Houten B. UvrB domain 4, an autoinhibitory gate for regulation of DNA binding and ATPase activity. J Biol Chem. 2006;281(22):15227–37.
25. Oh EY, Grossman L. Characterization of the helicase activity of the *Escherichia coli* UvrAB protein complex. J Biol Chem. 1989;264:1336–43.
26. Moolenaar GF, Monaco V, van der Marel GA, van Boom JH, Visse R, Goosen N. The effect of the DNA flanking the lesion on formation of the UvrB-DNA preincision complex. Mechanism for the UvrA-mediated loading of UvrB onto a DNA damaged site. J Biol Chem. 2000;275(11):8038–43.
27. Zou Y, Ma H, Minko IG, Shell SM, Yang Z, Qu Y, et al. DNA damage recognition of mutated forms of UvrB proteins in nucleotide excision repair. Biochemistry. 2004;43(14):4196–205.
28. Sancar A, Franklin KA, Sancar GB. Escherichia coli DNA photolyase stimulates uvrABC excision nuclease in vitro. Proc Natl Acad Sci USA. 1984;81(23):7397–401.
29. Lee JY, Yang W. UvrD helicase unwinds DNA one base pair at a time by a two-part power stroke. Cell. 2006;127(7):1349–60.
30. Jia H, Korolev S, Niedziela-Majka A, Maluf NK, Gauss GH, Myong S, et al. Rotations of the 2B sub-domain of E. coli UvrD helicase/translocase coupled to nucleotide and DNA binding. J Mol Biol. 2011;411(3):633–48.
31. Atkinson J, Guy CP, Cadman CJ, Moolenaar GF, Goosen N, McGlynn P. Stimulation of UvrD helicase by UvrAB. J Biol Chem. 2009;284(14):9612–23.
32. Coin F, Oksenych V, Egly JM. Distinct roles for the XPB/p52 and XPD/p44 subcomplexes of TFIIH in damaged DNA opening during nucleotide excision repair. Mol Cell. 2007;26(2):245–56.

33. Ogi T, Limsirichaikul S, Overmeer RM, Volker M, Takenaka K, Cloney R, et al. Three DNA polymerases, recruited by different mechanisms, carry out NER repair synthesis in human cells. Mol Cell. 2010;37(5):714–27.
34. Moser J, Kool H, Giakzidis I, Caldecott K, Mullenders LH, Fousteri MI. Sealing of chromosomal DNA nicks during nucleotide excision repair requires XRCC1 and DNA ligase III alpha in a cell-cycle-specific manner. Mol Cell. 2007;27(2):311–23.
35. Fan L, Arvai AS, Cooper PK, Iwai S, Hanaoka F, Tainer JA. Conserved XPB core structure and motifs for DNA unwinding: implications for pathway selection of transcription or excision repair. Mol Cell. 2006;22(1):27–37.
36. Oksenych V, de Jesus BB, Zhovmer A, Egly JM, Coin F. Molecular insights into the recruitment of TFIIH to sites of DNA damage. EMBO J. 2009;28(19):2971–80.
37. Egly JM, Coin F. A history of TFIIH: two decades of molecular biology on a pivotal transcription/repair factor. DNA Repair. 2011;10(7):714–21.
38. Fan L, Fuss JO, Cheng QJ, Arvai AS, Hammel M, Roberts VA, et al. XPD helicase structures and activities: insights into the cancer and aging phenotypes from XPD mutations. Cell. 2008;133(5):789–800.
39. Liu H, Rudolf J, Johnson KA, McMahon SA, Oke M, Carter L, et al. Structure of the DNA repair helicase XPD. Cell. 2008;133(5):801–12.
40. Wolski SC, Kuper J, Hanzelmann P, Truglio JJ, Croteau DL, Van Houten B, et al. Crystal structure of the FeS cluster-containing nucleotide excision repair helicase XPD. PLoS Biol. 2008;6(6):e149.
41. Rudolf J, Makrantoni V, Ingledew WJ, Stark MJ, White MF. The DNA repair helicases XPD and FancJ have essential iron-sulfur domains. Mol Cell. 2006;23(6):801–8.
42. Kuper J, Wolski SC, Michels G, Kisker C. Functional and structural studies of the nucleotide excision repair helicase XPD suggest a polarity for DNA translocation. EMBO J. 2012;31(2):494–502.
43. Rudolf J, Rouillon C, Schwarz-Linek U, White MF. The helicase XPD unwinds bubble structures and is not stalled by DNA lesions removed by the nucleotide excision repair pathway. Nucleic Acids Res. 2010;38(3):931–41.
44. Coin F, Marinoni JC, Rodolfo C, Fribourg S, Pedrini AM, Egly JM. Mutations in the XPD helicase gene result in XP and TTD phenotypes, preventing interaction between XPD and the p44 subunit of TFIIH. Nat Genet. 1998;20(2):184–8.
45. Sandrock B, Egly JM. A yeast four-hybrid system identifies Cdk-activating kinase as a regulator of the XPD helicase, a subunit of transcription factor IIH. J Biol Chem. 2001;276(38):35328–33.
46. Coin F, Oksenych V, Mocquet V, Groh S, Blattner C, Egly JM. Nucleotide excision repair driven by the dissociation of CAK from TFIIH. Mol Cell. 2008;31(1):9–20.
47. Weber A, Chung HJ, Springer E, Heitzmann D, Warth R. The TFIIH subunit p89 (XPB) localizes to the centrosome during mitosis. Cell Oncol. 2010;32(1–2):121–30.
48. Ito S, Tan LJ, Andoh D, Narita T, Seki M, Hirano Y, et al. MMXD, a TFIIH-independent XPD-MMS19 protein complex involved in chromosome segregation. Mol Cell. 2010;39(4):632–40.
49. Chen J, Larochelle S, Li X, Suter B. Xpd/Ercc2 regulates CAK activity and mitotic progression. Nature. 2003;424(6945):228–32.
50. Li X, Urwyler O, Suter B. Drosophila Xpd regulates Cdk7 localization, mitotic kinase activity, spindle dynamics, and chromosome segregation. PLoS Genet. 2010;6(3):e1000876.
51. Wu Y, Suhasini AN, Brosh Jr RM. Welcome the family of FANCJ-like helicases to the block of genome stability maintenance proteins. Cell Mol Life Sci. 2009;66(7):1209–22.
52. White MF. Structure, function and evolution of the XPD family of iron-sulfur-containing 5'–>3' DNA helicases. Biochem Soc Trans. 2009;37(Pt 3):547–51.
53. Drapkin R, Reardon JT, Ansari A, Huang JC, Zawel L, Ahn K, et al. Dual role of TFIIH in DNA excision repair and in transcription by RNA polymerase II. Nature. 1994;368(6473):769–72.
54. Sung P, Bailly V, Weber C, Thompson LH, Prakash L, Prakash S. Human xeroderma pigmentosum group D gene encodes a DNA helicase. Nature. 1993;365(6449):852–5.
55. Farina A, Shin JH, Kim DH, Bermudez VP, Kelman Z, Seo YS, et al. Studies with the human cohesin establishment factor, ChlR1. Association of ChlR1 with Ctf18-RFC and Fen1. J Biol Chem. 2008;283(30):20925–36.

56. Parish JL, Rosa J, Wang X, Lahti JM, Doxsey SJ, Androphy EJ. The DNA helicase ChlR1 is required for sister chromatid cohesion in mammalian cells. J Cell Sci. 2006;119(pt 23):4857–65.
57. Cantor SB, Bell DW, Ganesan S, Kass EM, Drapkin R, Grossman S, et al. BACH1, a novel helicase-like protein, interacts directly with BRCA1 and contributes to its DNA repair function. Cell. 2001;105(1):149–60.
58. Ding H, Schertzer M, Wu X, Gertsenstein M, Selig S, Kammori M, et al. Regulation of murine telomere length by Rtel: an essential gene encoding a helicase-like protein. Cell. 2004;117(7):873–86.
59. Honda M, Park J, Pugh RA, Ha T, Spies M. Single-molecule analysis reveals differential effect of ssDNA-binding proteins on DNA translocation by XPD helicase. Mol Cell. 2009;35(5):694–703.
60. Fromme JC, Banerjee A, Huang SJ, Verdine GL. Structural basis for removal of adenine mispaired with 8-oxoguanine by MutY adenine DNA glycosylase. Nature. 2004;427(6975):652–6.
61. Guan Y, Manuel RC, Arvai AS, Parikh SS, Mol CD, Miller JH, et al. MutY catalytic core, mutant and bound adenine structures define specificity for DNA repair enzyme superfamily. Nat Struct Biol. 1998;5(12):1058–64.
62. Thayer MM, Ahern H, Xing D, Cunningham RP, Tainer JA. Novel DNA binding motifs in the DNA repair enzyme endonuclease III crystal structure. EMBO J. 1995;14(16):4108–20.
63. Boal AK, Yavin E, Lukianova OA, O'Shea VL, David SS, Barton JK. DNA-bound redox activity of DNA repair glycosylases containing [4Fe-4S] clusters. Biochemistry. 2005;44(23):8397–407.
64. Merino EJ, Boal AK, Barton JK. Biological contexts for DNA charge transport chemistry. Curr Opin Chem Biol. 2008;12(2):229–37.
65. Boal AK, Yavin E, Barton JK. DNA repair glycosylases with a [4Fe-4S] cluster: a redox cofactor for DNA-mediated charge transport? J Inorg Biochem. 2007;101(11–12):1913–21.
66. Mui TP, Fuss JO, Ishida JP, Tainer JA, Barton JK. ATP-stimulated, DNA-mediated redox signaling by XPD, a DNA repair and transcription helicase. J Am Chem Soc. 2011;133:16378–81.
67. Mathieu N, Kaczmarek N, Naegeli H. Strand- and site-specific DNA lesion demarcation by the xeroderma pigmentosum group D helicase. Proc Natl Acad Sci USA. 2010;107:17545–50.
68. Sontz PA, Mui TP, Fuss JO, Tainer JA, Barton JK. DNA charge transport as a first step in coordinating the detection of lesions by repair proteins. Proc Natl Acad Sci USA. 2012;109(6):1856–61.
69. Suhasini AN, Sommers JA, Mason AC, Voloshin ON, Camerini-Otero RD, Wold MS, et al. FANCJ helicase uniquely senses oxidative base damage in either strand of duplex DNA and is stimulated by replication protein A to unwind the damaged DNA substrate in a strand-specific manner. J Biol Chem. 2009;284(27):18458–70.
70. Song L, Yuan F, Zhang Y. Does a helicase activity help mismatch repair in eukaryotes? IUBMB Life. 2010;62(7):548–53.
71. Fukui K. DNA mismatch repair in eukaryotes and bacteria. J Nucleic Acids. 2010;2010:1–6.
72. Matson SW, Robertson AB. The UvrD helicase and its modulation by the mismatch repair protein MutL. Nucleic Acids Res. 2006;34(15):4089–97.
73. Maluf NK, Ali JA, Lohman TM. Kinetic mechanism for formation of the active, dimeric UvrD helicase-DNA complex. J Biol Chem. 2003;278(34):31930–40.
74. Ali JA, Lohman TM. Kinetic measurement of the step size of DNA unwinding by Escherichia coli UvrD helicase. Science. 1997;275(5298):377–80.
75. Dao V, Modrich P. Mismatch-, MutS-, MutL-, and helicase II-dependent unwinding from the single-strand break of an incised heteroduplex. J Biol Chem. 1998;273(15):9202–7.
76. Hall MC, Jordan JR, Matson SW. Evidence for a physical interaction between the Escherichia coli methyl-directed mismatch repair proteins MutL and UvrD. EMBO J. 1998;17(5):1535–41.
77. Hall MC, Matson SW. The Escherichia coli MutL protein physically interacts with MutH and stimulates the MutH-associated endonuclease activity. J Biol Chem. 1999;274(3):1306–12.
78. Mechanic LE, Frankel BA, Matson SW. Escherichia coli MutL loads DNA helicase II onto DNA. J Biol Chem. 2000;275(49):38337–46.
79. Jiricny J. The multifaceted mismatch-repair system. Nat Rev Mol Cell Biol. 2006;7(5):335–46.

80. Zhang Y, Yuan F, Presnell SR, Tian K, Gao Y, Tomkinson AE, et al. Reconstitution of 5'-directed human mismatch repair in a purified system. Cell. 2005;122(5):693–705.
81. Dzantiev L, Constantin N, Genschel J, Iyer RR, Burgers PM, Modrich P. A defined human system that supports bidirectional mismatch-provoked excision. Mol Cell. 2004;15(1):31–41.
82. Genschel J, Modrich P. Mechanism of 5'-directed excision in human mismatch repair. Mol Cell. 2003;12(5):1077–86.
83. Lindahl T. Instability and decay of the primary structure of DNA. Nature. 1993;362(6422):709–15.
84. Sedgwick B, Bates PA, Paik J, Jacobs SC, Lindahl T. Repair of alkylated DNA: recent advances. DNA Repair. 2007;6(4):429–42.
85. Kavli B, Otterlei M, Slupphaug G, Krokan HE. Uracil in DNA–general mutagen, but normal intermediate in acquired immunity. DNA Repair. 2007;6(4):505–16.
86. Kubota Y, Nash RA, Klungland A, Schar P, Barnes DE, Lindahl T. Reconstitution of DNA base excision-repair with purified human proteins: interaction between DNA polymerase beta and the XRCC1 protein. EMBO J. 1996;15(23):6662–70.
87. Kim K, Biade S, Matsumoto Y. Involvement of flap endonuclease 1 in base excision DNA repair. J Biol Chem. 1998;273(15):8842–8.
88. Klungland A, Lindahl T. Second pathway for completion of human DNA base excision-repair: reconstitution with purified proteins and requirement for DNase IV (FEN1). EMBO J. 1997;16(11):3341–8.
89. Robertson AB, Klungland A, Rognes T, Leiros I. DNA repair in mammalian cells: base excision repair: the long and short of it. Cell Mol Life Sci. 2009;66(6):981–93.
90. Martin GM, Oshima J, Gray MD, Poot M. What geriatricians should know about the Werner syndrome. J Am Geriatr Soc. 1999;47(9):1136–44.
91. Martin GM, Oshima J. Lessons from human progeroid syndromes. Nature. 2000;408(6809):263–6.
92. Bohr VA, Deficient DNA. repair in the human progeroid disorder, Werner syndrome. Mutat Res. 2005;577(1–2):252–9.
93. Blank A, Bobola MS, Gold B, Varadarajan S, D Kolstoe D, Meade EH, et al. The Werner syndrome protein confers resistance to the DNA lesions N3-methyladenine and O6-methylguanine: implications for WRN function. DNA Repair. 2004;3(6):629–38.
94. Harrigan JA, Wilson III DM, Prasad R, Opresko PL, Beck G, May A, et al. The Werner syndrome protein operates in base excision repair and cooperates with DNA polymerase beta. Nucleic Acids Res. 2006;34(2):745–54.
95. Imamura O, Fujita K, Itoh C, Takeda S, Furuichi Y, Matsumoto T. Werner and Bloom helicases are involved in DNA repair in a complementary fashion. Oncogene. 2002;21(6):954–63.
96. Szekely AM, Bleichert F, Numann A, Van Komen S, Manasanch E, Ben Nasr A, et al. Werner protein protects nonproliferating cells from oxidative DNA damage. Mol Cell Biol. 2005;25(23):10492–506.
97. Von Kobbe C, May A, Grandori C, Bohr VA. Werner syndrome cells escape hydrogen peroxide-induced cell proliferation arrest. FASEB J. 2004;18(15):1970–2.
98. Ahn B, Harrigan JA, Indig FE, Wilson III DM, Bohr VA. Regulation of WRN helicase activity in human base excision repair. J Biol Chem. 2004;279(51):53465–74.

Chapter 11
Roles for Helicases as ATP-Dependent Molecular Switches

Mark D. Szczelkun

Abstract On the basis of the familial name, a "helicase" might be expected to have an enzymatic activity that unwinds duplex polynucleotides to form single strands. A more encompassing taxonomy that captures alternative enzymatic roles has defined helicases as a sub-class of molecular motors that move directionally and processively along nucleic acids, the so-called "translocases". However, even this definition may be limiting in capturing the full scope of helicase mechanism and activity. Discussed here is another, alternative view of helicases—as machines which couple NTP-binding and hydrolysis to changes in protein conformation to resolve stable nucleo-protein assembly states. This "molecular switch" role differs from the classical view of helicases as molecular motors in that only a single catalytic NTPase cycle may be involved. This is illustrated using results obtained with the DEAD-box family of RNA helicases and with a model bacterial system, the ATP-dependent Type III restriction-modification enzymes. Further examples are discussed and illustrate the wide-ranging examples of molecular switches in genome metabolism.

What Is a Helicase and What Is Its Relationship to a Motor?

As introduced in Chap. 1 [1–5] helicases comprise a large and important group of molecular machines that play numerous roles in genome maintenance. They are modular and are often combined with other domains and enzyme activities. Their diverse roles have arisen from this adaptability [6]. Helicases are commonly perceived as exclusively strand-separation enzymes, unwinding duplex polynucleotides to produce ssDNA or ssRNA as intermediates for genetic processes. It is perhaps less well appreciated that helicases can also play additional roles: as motor enzymes

M.D. Szczelkun (✉)
School of Biochemistry, University of Bristol,
Medical Sciences Building, Bristol, UK
e-mail: mark.szczelkun@bristol.ac.uk

M. Spies (ed.), *DNA Helicases and DNA Motor Proteins*, Advances in Experimental Medicine and Biology, DOI 10.1007/978-1-4614-5037-5_11,

that translocate intact dsDNA (i.e. without any *bona* fide "helicase" activity) [7–9] (Chaps. 12 and 13); or as non-processive molecular switches (i.e. without any *bona* fide "motor" activity) [3, 10–12]. It is the latter role that is the subject of this chapter.

On the basis of bioinformatic analysis, helicases can be identified from the presence of characteristic amino acid motifs and subdivided into Superfamily groups (e.g., SF1, SF2, etc.) [1, 2, 13]. This categorization can, to some extent, help define the activity of these enzymes, i.e., sharing specific motifs with a known and characterised enzyme can be a strong predictor of activity. However, SF definitions cannot always predict whether a helicase will be a true helicase or not. All helicase-based proteins, regardless of their role, are built around a similar core protein architecture [2, 5]; they all contain at least two adjacent RecA-like folds which, in combination with the characteristic motifs, form one or more ATP-binding clefts. A shared mechanistic feature is that ATP binding drives conformational changes that alter the relative positions of the RecA folds which are then coupled to mechanical manipulation of a polynucleotide [14]. Subsequent ATP hydrolysis and ADP/phosphate release allows the enzyme to re-set. This can be viewed as a single kinetic cycle. The question of whether the helicase is a motor or a switch comes down to how this cycle is coupled to the DNA or RNA, and the number of cycles required for the biological role of the enzyme.

An ATP-fuelled molecular motor can be defined on the basis of repetitive ATPase cycles that produce processive and directional movement along a polymer track. For many of the true helicases the underlying motor activity involves directed movement on ssDNA or ssRNA that leads to unwinding of a downstream duplex region. Convincing models have been proposed for how such coupling can occur (see below) [2, 14–17]. For other helicases, the underlying motor activity is coupled to directed movement along intact dsDNA or dsRNA. These helicases are not required to unwind the duplex but instead use the processive motion to remodel polynucleotide structures [18], or nucleoprotein complexes [19], or to move protein domains along a genome (see below) [9]. It has been suggested that the helicases would be better defined as "translocases" first, with a subset being helicases in the true sense [2]. However, there are also helicases being characterised that do not have measureable translocase activity—they do not move directionally along a track—and where even a single catalytic cycle and thus a single ATP may be sufficient for their biological role. These are the helicases acting as molecular switches.

What Is a Molecular Switch and What Is Its Relationship to a Motor?

The concept of a molecular switch is most commonly illustrated based on the activity of the small monomeric GTPases (the G-proteins), for which such activity was first defined [20]. These enzymes can switch between bistable states as a function of GTP hydrolysis and GDP release, and so influence signalling cascades (Fig. 11.1).

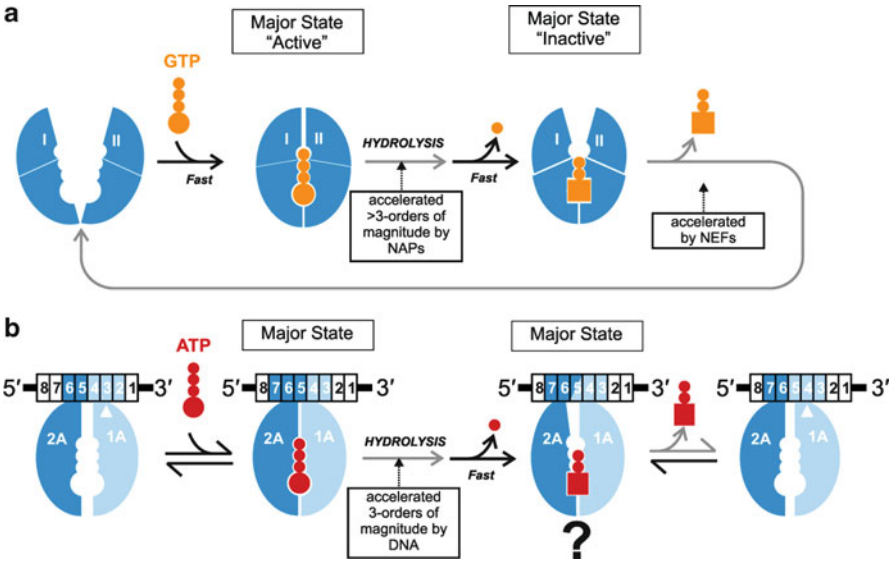

Fig. 11.1 Comparison of the domain motions and metastable states in the kinetic cycles of molecular switches and motors. In both examples the rate-liming transitions are in *grey*. (**a**) Diagrammatic representation of a monomeric small GTPase [20]. The nucleotide-free form of the G-protein has a relaxed and open nucleotide binding cleft. GTP binding to four distinct regions (G-1 to G-4, not shown) by a network of cooperative hydrogen bonds closes the cleft. The G-protein is now "switched on". The cleavage of the β–γ phosphoanhydride bond is rate-limiting but NTPase activating proteins (GAPs) can accelerate this step [25]. Phosphate release is fast, leading to the stable ADP-bound state. Specific residues in G-2 and G-3, Switch I and II respectively, act as phosphate sensors and swing out in response to phosphate release. This partial disordering leads to conformational changes and the G-protein is now "switched off". Dissociation of GDP is rate-limiting but can be accelerated by nucleotide exchange factors (NAPs). At the end of the cycle the protein returns to the nucleotide-free ground state. (**b**) Diagrammatic representation of the ATPase cycle of monomeric PcrA during a single nucleotide step along an ssDNA [14, 26]. The 1A (N-core) and 2A (C-core) RecA folds are shown in *light* and *dark blue*, respectively. For illustrative purposes the connection between the RecA folds and other domains involved in coupling to unwinding is not shown. DNA is shown as a series of *boxes*, with each nucleotide numbered. In the nucleotide-free state, the cleft between the RecA core is open. DNA contacts are made as shown across a 5 nt footprint, with DNA base #3 flipped into an amino acid pocket, shown in 1A (*white triangle*). ATP binding causes domain rotation and closure, altering the DNA contacts including ejecting base #3 from the pocket. ATP hydrolysis is rate-limiting but is accelerated by DNA binding through conformation changes that favours Mg^{2+} binding and a concomitant repositioning of the γ-phosphate [27]. Fast phosphate release following the hydrolysis step leads to a stable ADP-bound state. The structural details of this state are unknown so the cartoon is speculative. Rate-limiting ADP release opens the cleft and rectifies the DNA contacts, with a new base (#4) entering the pocket in 1A. The enzyme has moved one nucleotide 3′-5′ along the DNA

It has been long appreciated that molecular switches and motors share many common features [21, 22]. At one level, there is a common underlying protein fold; they can all be classified as P-loop NTPases [23, 24], α-β proteins that contain five β-strands arranged in a central core sandwiched by α-helices on both sides. This large and

populous grouping can be further divided in two; in one sub-group, which includes the GTPases, the strand leading to the P-loop (containing the Walker A consensus sequence) and the Walker B strand are direct neighbours; in the other sub-group, including the helicases as well as AAA+ and ABC enzymes, there is an additional strand inserted between the P-loop strand and the Walker B strand. Within the GTPase sub-group, motors and switches even share some amino acid motifs [21]; the switch I and II residues of the G-proteins are important sensors of the catalytic state (Fig. 11.1) and equivalent residues are also found in the cytoskeletal kinesin and myosin motors.

At a second level, the switches and motors share mechanistic features, in that they both cycle between metastable states in which nucleotide binding and hydrolysis drive protein conformational changes which can be summarised as the closing and opening of an NTP-binding cleft. For the G-proteins, the major states (those most occupied during the catalytic cycle) are the GTP- and GDP-bound states (corresponding to the "on" and "off" states, respectively, with regards to the activation of downstream signalling partners) [20]. GTP hydrolysis is relatively slow (10^{-2} to 10^{-3} min^{-1}), but is accelerated by many orders of magnitude by interaction with NTPase activating proteins (NAPs). This activation results from the NAPS supplying *in trans* a catalytically important arginine residue (the "arginine finger") that coordinates the γ-phosphate of the bound nucleotide and stabilises the transition state [25]. Phosphate release is then rapid leaving the stable GDP bound state. Rate-limiting GDP release is then accelerated by NDP exchange factors (NEFs) [20]. At physiological GTP concentrations, re-binding is rapid and the nucleotide-free state is short-lived.

The helicases also cycle between metastable states [14]. For example, during translocation on ssDNA, the UvrD/PcrA class of SF1A helicases occupies two major states [26]. ATP hydrolysis is rate-limiting, so that the ATP bound state is long-lived. This step is accelerated by DNA binding [27]. Although the DNA is not an NAP in the G-protein sense—it does not supply a catalytic residue, the equivalent arginine finger residue being found in Motif VI in the C-core RecA fold [15]—it can be considered as such by its overall role. This analogy of the polymer track acting as an NAP for a translocating motor has been forwarded previously [21]. Following the hydrolytic step, phosphate release by the helicase is fast, leading to an ADP-bound state which decays at a similar rate to the hydrolytic step [26]. It is not clear if the DNA acts as a NEF at this stage. Rather than being coupled to "on" and "off" states per se, the ATP cycle is coupled to changes in DNA contacts which drives the motor along the track [14], in this case in a 3′-5′ direction. With changes to the nucleic acid contacts, a similar cycle can also drive a motor in the opposite polarity, 5′-3′ [17].

It could be argued that one feature that distinguishes a motor from a switch is that by the end of the cycle the helicase has advanced one step along a track to a new location, whereas a switch returns to the beginning. Nonetheless, some switches may act as part of larger complexes and at the end of their catalytic cycle may also be in a new state, a later conformational switch being required to dissemble the complex. The difference is that a motor is poised to make a further step. Additionally,

by making multiple directed steps a motor can do work against an increasing load, which can cause alterations in cycle rates or even back steps [28], that may not be observed with switches. Generally speaking, the hydrolytic rates of switches are significantly lower than translocating motors. But caution needs to be used as some *bona fide* helicases are studied in an autoinhibited state. Inclusion of the correct substrate or protein partner is required to unmask a more vigorous ATPase activity. Even so, some motors can have quite modest activated NTPase activities [29].

Clearly, parallels can be drawn at a number of levels between motors and switches. However the textbook view of a helicase is nearly always of an enzyme that ploughs through dsDNA or dsRNA, separating the strands in a stepwise manner. Can a true helicase ever be a single step switch? Or alternatively, could molecular switch activity allow alternative roles for a helicase other than unwinding or translocation? As it turns out, the answer to both these questions can be yes.

DEAD-Box Helicases as Molecular Switches That Unwind and Remodel RNA

The DEAD-box helicases are the largest family of closely related helicases and belong within the SF2 classification [3, 10]. They have a broad genetic remit in RNA metabolism, influencing the folding of RNA and the assembly of RNPs in many processes, including transcription, mRNA splicing, ribosome biogenesis, RNA storage transport and decay, and translation. Whilst other SF2 enzymes are ssRNA translocases (e.g., hepatitis C virus NS3 helicase) [30] and others appear to be dsRNA translocases (e.g., RIG1) [31], there is mounting evidence that the DEAD box helicases act as single-step molecular switches [3, 10]. They can be characterised by up to 12 specific amino acid motifs—the nomenclature of this group deriving from the primary amino acid sequence of the Walker B Motif/Motif II (rather than any allusion to apoptosis or cell death). Structurally they fold to form the familiar dual RecA cores but interact with a bent RNA conformation entirely through sugar-phosphate backbone contacts [32]. Additional RNA interactions can be made by associated RNA recognition motifs (RRMs). They are believed to act as monomeric machines, although they are often found as part of much larger enzyme systems.

Some DEAD box enzymes are *bona fide* helicases—their role in the cell is to unwind short segments of dsRNA. RNA unwinding by these helicases is generally limited to segments of no more than 10–12 bp, consistent with their cellular substrates. As noted above, one of the hallmarks of a translocating motor is directional motion along the polynucleotide track, 3′-5′ or 5′-3′. However, whilst many DEAD box helicases are stimulated by ssRNA overhangs, there is no polarity preference and the ssRNA segments do not even need to be covalently connected to the dsRNA as long as they are proximal in space [33–35]. It appears that the ssRNA merely acts to load the helicase onto the dsRNA. These studies also confirmed that whilst these helicases can unwind dsRNA, they do so without apparent translocation. Instead the strands are pulled apart in a single-step process termed “local strand separation”

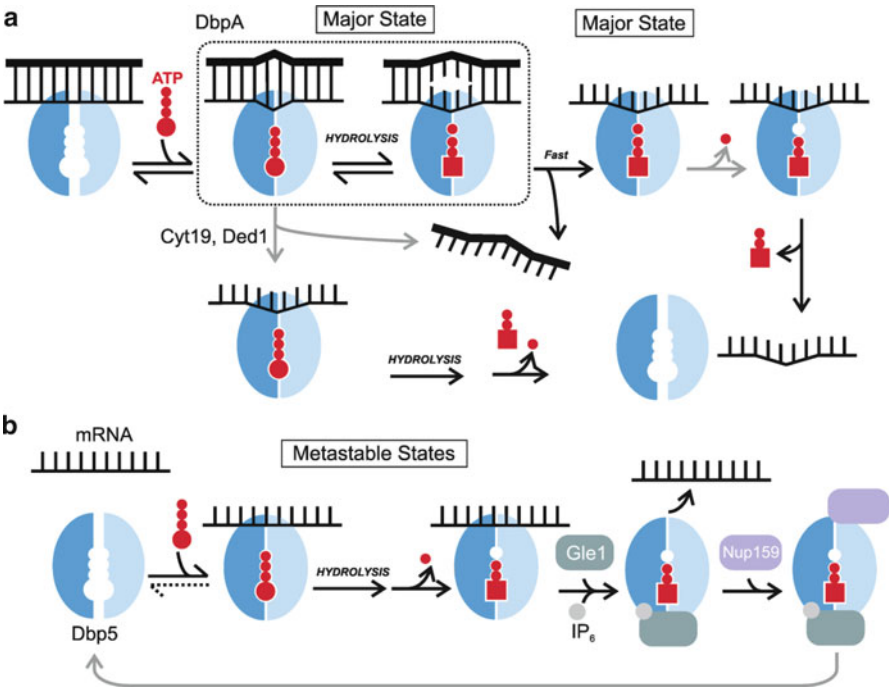

Fig. 11.2 Molecular switch activity of the DEAD box RNA helicases. (**a**) A diagrammatic representation of the ATPase cycle during dsRNA unwinding by DEAD box helicases [3, 37]. The N-core and C-core RecA folds are shown in *light* and *dark blue*, respectively. For illustrative purposes the connection between the RecA folds and other domains involved in RNA and protein binding are not shown. ATP binding to the dsRNA-bound helicase produces domain rotation and closure leading to a stable state in which the RNA is distorted. The route of the next step depends on the enzyme examined. For Cyt19 and Ded1 [34, 35, 38, 40], the ATP binding leads directly to RNA distortion and spontaneous strand separation *without* ATP hydrolysis. The enzyme is then stuck in a metastable ssRNA-ATP state and hydrolysis/product release is required for turnover. Alternatively for DbpA [36, 37], a reversible hydrolytic step cycles between states with different degrees of RNA distortion. The hydrolysed state is sufficiently distorted to allow spontaneous dissociation of the unwound strand. Phosphate release is rate-limiting, leading to a second long-lived state. ADP release is then rapid, allowing dissociation of the second RNA strand and enzyme recycling. (**b**) A molecular clamp role for the Dbp5 helicase and the role of activating factors [3, 45]. Binding of mRNA and ATP by Yeast Dbp5 in the nucleus causes conformation transitions that remodel the RNA and associated proteins. Following transport to the cytoplasm via the nuclear pore (not shown), ATP hydrolysis and phosphate release lead to a metastable ADP·RNA state. Rate-limiting release of the RNA is accelerated by the binding of inositol hexakisphosphate (IP_6) and nuclear pore associated protein Gle1. The rate-limiting release of ADP is then accelerated by binding of nucleoporin Nup159. The protein cofactors are released and Dbp5 recycles to the nucleus

(Fig. 11.2) [35]. DEAD box helicases that remodel RNPs by displacing the protein component appear to also act without necessity for polar translocation and similar mechanisms may be involved [3].

The kinetic cycle of RNA unwinding by a number of DEAD box helicases has been examined with varying degrees of detail [36–40]. For all of these enzymes,

ATP stabilises a tight RNA-binding state. What happens next depends on the enzyme (Fig. 11.2a). For Cyt19, YxiN and Ded1, distortions in the dsRNA in the ATP-bound state cause local strand separation which, given the small number of base pairs, leads to spontaneous strand separation (Fig. 11.2a) [38–40]. The role of ATP hydrolysis is to release the enzyme from the ssRNA to allow another catalytic cycle. Consequently non-hydrolysable ATP analogues can bring about unwinding but not enzyme turnover. The ATPase cycle can also become uncoupled from unwinding, so that the number of ATPs consumed per unwinding event can be >1. Nonetheless the coupling ratio is independent of duplex length, up to a maximum beyond which the enzymes cannot unwind [3]. The actual structural transitions that bring about strand separation have yet to be captured although some specialised roles for protein structural elements have been proposed [41].

In contrast, for the DbpA helicase ATP binding *and* hydrolysis is required for unwinding (Fig. 11.2a) [36, 37]. A reversible ATP hydrolysis step cycles the enzyme between two major states, with the dsRNA being distorted in the ATP-bound state and being partially unwound in the ADP·Pi state. Fast spontaneous dissociation of the partially unwound strand then produces a long-lived ADP·Pi·ssRNA state which decays by rate-limiting phosphate release. The ADP·ssRNA form then rapidly dissociates to turnover the enzyme and release the ssRNA. A similar pathway with slightly different occupancy of the states has been shown for Mss116 [42]. It is argued that unwinding events in the absence of ATP hydrolysis may represent slower off-pathway states that are not accessed under optimised conditions. Thus there are conceptual differences in these models as to the extent of DNA unwinding in the ATP state and whether ATP hydrolysis is required for unwinding in the cell. It remains to be seen whether there is a common mechanism or whether individual enzymes have unique mechanisms where unwinding is either coupled exclusively to ATP hydrolysis, or to either hydrolysis or binding.

As with the G-proteins, the timing of exit from a stable state can be altered. Whilst RNA binding stimulates ATP hydrolysis (possibly acting as an NAP by removing an autoinhibitory domain contact [43]), other proteins factors can inhibit the hydrolysis, extending the lifetime of the ATP·RNA state. By arresting the cycle at this point, an "RNA clamp" can be produced which will only progress when a particular biochemical cue is available [3]. For example, eIF4AIII plays an important role in assembling core protein factors onto the exon-junction complex (EJC) and this role requires ATP binding [44]. The binding by a heterodimer of two of these core factors, MAGOH and Y14, inhibits completion of ATP hydrolysis, possibly at the ADP/Pi release step. This may play a role in maintaining the nucleoprotein complex during export into the cytoplasm.

Alternatively, the DEAD box ATPase may require activation to overcome autoinhibition [3]. For example, Dbp5 which is involved in the remodelling of nucleoproteins on mRNA and assists in its export from the nucleus, needs to interact with inositol hexakisphosphate, and the protein cofactors Gle1 and Nup159 in the cytoplasm to facilitate mRNA release and enzyme turnover following ATP hydrolysis (Fig. 11.2b) [45]. These factors can be considered as NEFs, facilitating exit from a tightly-bound product state.

The DEAD box helicases are a fascinating example of the diversification of helicase function and mechanism. As more of this enzyme family is examined, the number of roles is likely to also increase, promising to reveal additional roles for helicase domains. It will be important to pursue in-depth structural analysis of the different states during the catalytic cycle, to identify how the switch between those states can be accelerated or inhibited to elicit cellular control.

The Bacterial RM Enzymes as Models for Helicase-Driven Long-Range Motion on DNA

Restriction-modification (RM) enzymes are widely distributed in the kingdom Monera and defend against bacteriophage infection [46, 47]. They can be classified into different "Types" on the basis of gene composition, cofactor requirements and mechanism [48]; the Type I and III RM enzymes both contain domains with SF2 helicase motifs and folds [49, 50]. (It should be noted that there are nonetheless distinctive differences in the sequences of the motifs and in the arrangement of domain insertions in the RecA fold) [50]. Type I enzymes consist of a core methyltransferase (MTase), comprised of HsdM and HsdS subunits in the ratio M_2S_1, and two HsdR subunits [51–53]. The HsdR polypeptides are the fusions of an endonuclease domain, an SF2 helicase domain and an MTase-interaction domain [50, 54, 55].

The Type III enzymes have a similar architecture, consisting of two core Mod MTase subunits and either one or two Res subunits, the latter containing the helicase-nuclease domains [56, 57]. The nuclease activities of both Type I and III enzymes are ATP-dependent—mutations in the characteristic SF2 motifs prevent both ATP and DNA hydrolysis [58–60]. The role of the helicase domains is to facilitate the long-range communication between pairs of RM enzymes, which may occur over many thousands of base pairs. This communication event is required to trigger the cleavage activity and has likely evolved as a "double-check" mechanism to help prevent accidental cleavage of host DNA when unmodified recognition sites arise, i.e. two or more unmodified sites must be present to allow cleavage [61].

The Type I and III systems were the first RM enzymes to be purified in 1968 and were shown to require ATP for DNA cleavage [62–69], although it was more than 20 years before they were identified as having helicase domains [49]. It was noted early on that the ATPase activity of the Type III enzymes was >1,000-fold lower than the Type I enzymes [68, 70], although it was unclear if ATP hydrolysis or just ATP binding was required by the Type III enzymes. Both Types recognised asymmetric sequences but cleaved DNA at non-specific loci which in some cases could be thousands of base pairs distant from the site [71]. On this basis a role for ATP hydrolysis in moving the enzymes along DNA was suggested as early as 1974 [72]. Subsequent EM analysis with the Type I enzymes provided evidence for the formation of DNA loops, and a model for motion on DNA by loop translocation was formulated (Fig. 11.3) [73–76]. In this model a Type I RM enzyme forms a tightly bound complex with its recognition site whilst an HsdR subunit is attached on

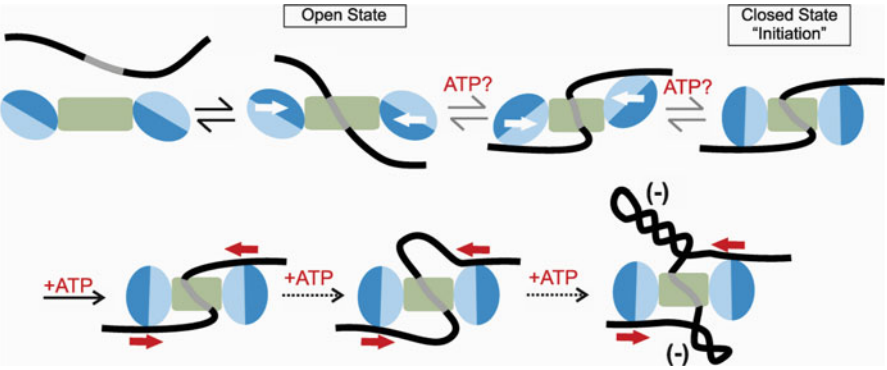

Fig. 11.3 Helicase domains in Type I restriction-modification enzymes catalyse dsDNA translocation. The mechanism of helicase-dependent dsDNA translocation for the Type I RM enzymes [9, 53, 73–76, 81, 83, 97]. Initial recognition of an asymmetric specific DNA site (*grey box*) by the MTase domain (*green box*) loads the monomeric helicases (HsdR, *blue circle*) onto the adjacent DNA on both sides of the site. This open conformation then changes to the closed conformation, producing the initiation state. This transition may or may not require ATP binding/hydrolysis. In the initiation state, each helicase starts to translocate away from the complex, principally using contacts to the 3′-5′ strand of intact dsDNA, whilst the MTase remains bound at the site. Each helicase acts as an independent motor, using one ATP to move 1 bp. As translocation continues, two different-sized expanding loops of DNA are produced. Because the helicase moves in 1–2 bp steps, the DNA is rotated during translocation and the expanding loops are negatively supercoiled. Upon collision with a converging Type I enzyme, the nuclease domains are activated to cleave DNA at the distant collision site (not shown) [77]

either side of the complex. The helicase domains of the HsdR subunits then start to translocate along the DNA away from the site, so pumping the DNA into two expanding loops of negatively supercoiled DNA (Fig. 11.3). Cleavage occurs when two converging motors collide [77].

The loop translocation model has been robustly demonstrated for the Type I enzymes using in vivo assays [78, 79], and both ensemble and single molecule assays [9, 80–83]. However, no evidence for strand separation has been found and translocation on interstrand crosslinked DNA has been taken as evidence that the Type I enzymes are monomeric dsDNA translocases, i.e. they move on intact duplex DNA [9], similar to the chromatin remodelling enzymes (Chap. 13). One ATP was required to move one base pair [81], suggesting that similar domain motions drive dsDNA motion as suggested for ssDNA motion by the SF1 unwinding enzymes (Fig. 11.1b). This 1:1 coupling explains the high ATPase activity of Type I enzymes, since cleavage often requires DNA communication between a pair of sites over thousands of base pairs, hence requiring the consumption of thousands of ATPs.

The mechanism of long-range communication for the Type III enzymes has proven much more elusive [11, 84]. Early work was hampered by the low ATPase activity and difficulties in coupling ATPase rates with cleavage rates. This was partly a problem with the use of DNA substrates with different numbers and arrangements of sites, but was subsequently clarified when DNA cleavage was shown to strictly require a pair of recognition sequence in inverted repeat orientation (i.e.

arranged head-to-head or tail-to-tail), with sites in direct repeat (i.e. head-to-tail) resistant to hydrolysis [85–87]. The sites need to be on the same DNA but could be thousands of base pairs apart [88]. This is a form of "site orientation selectivity" as also observed in some recombinases where DNA topology rather than ATP is used to bias the interactions.

The production of homogeneous Type III enzyme preparations of sufficient activity in the 1990s allowed the absolute requirement for ATP hydrolysis to be confirmed [85]. The communication between a pair of sites was tested by binding a Lac repressor between the sites [85]. This inhibited cleavage, suggesting a 1-D route for communication. By analogy with the Type I communication scheme, it was proposed that Type III RM enzymes communicate via a loop translocation mechanism in which the helicase domains (in Res) translocate in one direction from the site whilst the DNA recognition domain (in Mod) remains at the site. Rather than the bidirectional model shown in Fig. 11.3, it was expected that translocation would have a defined polarity based on the recognition site orientation. A related model based on stepwise translocation without looping has also been suggested [89].

Evidence supporting a role for DNA loop formation during translocation has been obtained using Atomic Force Microscopy [90–92]. However, other ensemble and single molecule experiments have, despite much effort, been unable to corroborate the formation of loops. In particular, a magnetic tweezers assay showed that DNA stretched by up to 1.5 pN is cleaved at a rate equivalent to that of relaxed DNA without evidence for the formation of loops of >1 s lifetime [93]. Regardless of loop formation, it has also not been possible to find any other evidence for processive dsDNA translocation [87, 93, 94]. Firstly, although the movement along DNA of many *bona fide* dsDNA translocases can be measured using the triplex displacement assay [80], Type III enzymes do not displace the triplexes and, in fact, can by-pass them efficiently [93]. Secondly, the recurrent problem with applying translocation schemes is that the ATPase activity is lower than expected [11]. For example, PstII hydrolyses ~40 ATP/min yet can cut a DNA with two sites 1,100 bp apart in <10 s [95]. For a translocation model this equates to ~80 bp moved per ATP, a ratio not easily reconciled to dsDNA translocation models based on our current understanding of helicase structure and the coupling of metastable states to the nucleic acid track. Thirdly, it is difficult to explain based on unidirectional translocation how the Type III enzymes can achieve their reported site orientation selectivity [11].

The magnetic tweezers study also revealed another important observation [93]. In the microscope flow cell where a linear DNA is attached at one end to a glass surface and at the other end to a magnetic bead, endonuclease activity was as efficient as freely diffusing plasmid DNA. In comparison, linear DNA in bulk solution was a poor substrate for endonuclease activity unless the DNA ends were "capped", for example with a bulky protein moiety. This suggested that DNA ends were a site of accelerated dissociation from the DNA, despite the fact that they were distant from the recognition sites and located both up- and downstream. These results suggested that motion on DNA was bidirectional. However, for the Type I enzymes, bidirectional loop translocation results in cleavage that is independent of relative site orientation [96, 97].

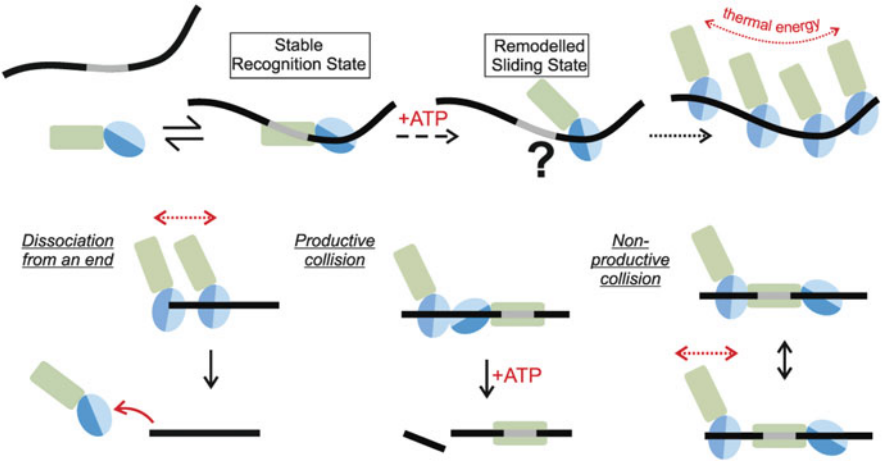

Fig. 11.4 Possible role for the helicase domains in the Type III restriction-modification enzymes as a molecular switch that initiates DNA sliding [11, 93]. (*Upper panels*) Recognition of an asymmetric specific DNA site by the Mod subunits (*green rectangle*) leads to directional loading of the helicase Res subunit(s) (*blue ellipsoid*) onto the adjacent non-specific DNA on *one side* of the site. This forms a stable recognition state that activates ATP hydrolysis, leading to a conformational switch into the sliding mode, shown here as release of Mod from the site (although the exact details are unknown). ATP hydrolysis is no longer required as motion is random, driven by thermal energy. Because the Res subunit does not release the DNA, the directionality of the original loading orientation is maintained (note the order of the blue segments). (*Lower panels*) Upon reaching a free DNA end, the motor can lose DNA contacts and dissociate more rapidly than from internal sites. Upon reaching another Type III enzyme bound to a site *in the opposite* orientation, interaction of the Res subunits and further ATP hydrolysis produces DNA cleavage, the motor at the site cutting the "top" strand, the sliding motor cutting the "bottom" strand. This produces a dsDNA break 25–27 bp away from one side of the site. Upon reaching another Type III enzyme bound to a site *in the same* orientation, the Res subunits cannot interact correctly and DNA cleavage cannot occur

To account for these observations a new model was proposed in which the Type III helicase domain acts a molecular switch rather than a processive translocase (Fig. 11.4) [11, 93]. In this model the role of ATP hydrolysis is to enable a conformational switch from a specific DNA binding mode into a non-specific "DNA sliding" mode. Sliding is a process in which a protein remains bound to DNA, most likely via weak electrostatic interactions, but where the activation energy to move from one site to an adjacent site without releasing the DNA is less than ~2•$k_B T$ [98–100]. Sliding is therefore thermally activated, and results in both "backwards" and "forwards" steps with equal probability (assuming a uniform energy landscape, which may not always be the case on DNA).

Upon hydrolysing ATP, the Type III enzyme leaves its site, and starts to move randomly on the DNA (Fig. 11.4). Because sliding is thermally activated and thus directionally randomised, on linear DNA the enzyme will occasionally approach a DNA end. If uncapped, the enzyme will dissociate and thus cleavage is less efficient as the total sliding lifetime (the time to search for another Type III enzyme) is shorter (Fig. 11.4). Occasionally the enzyme will collide with a second Type III

enzyme bound to a site. Where this enzyme is correctly oriented, further ATP hydrolysis leads to DNA cleavage (Fig. 11.4) [56]. Because ATP is only consumed at initiation and cleavage, and sliding requires no chemical input, the ATPase rates will appear low and independent of distance [93]. Where collision occurs with an incorrectly oriented enzyme (Fig. 11.4), the Res subunits cannot interact and cleavage is not activated. Collisions between sliding enzymes away from their sites is either rare (due to the large differences in rates for initiation and sliding) [93] or non-productive. The role of the ATP hydrolysis at the cleavage step may be a check to ensure that one enzyme is bound to a site.

The sliding model is consistent with much of the published data in the literature, and provides a straightforward explanation for site orientation selectivity as well as for cleavage site preference [11, 94]. The notable exceptions are the AFM studies which support a more important role for DNA loop formation and DNA translocation [84, 90–92]. These anomalies remain to be reconciled. To provide direct demonstration of DNA sliding, single molecule fluorescence microscopy has been used to observe single labelled proteins. Similar studies are now underway with the Type III RM enzymes (Ralf Seidel and Friedrich Schwarz, unpublished data).

At a fundamental level, almost every protein that interacts with DNA will do so via multiple interactions with random non-specific sites and will move between those sites by "facilitated-diffusion" [101, 102]. DNA Sliding is one pathway for facilitated-diffusion and there has been a heated debate as to its relative contribution compared to alternative 3-D routes ("hopping", "jumping", etc.) [102, 103]. A central criticism of sliding is that it is an inefficient way to get from A to B. Because there is a quadratic dependence between the numbers of steps needed to move a given distance, sliding could be inexorably slow. However, measurements of putative 1-D sliding events suggest stepping rates of 1×10^7–1×10^9 min^{-1} [100, 104–106]. Returning to the PstII example [95], this would correspond to 0.6–30 s to move 1,100 bp between the sites. This is similar to what Type I motors can achieve using fewer, but slower, directed steps and only by consuming thousands of additional ATPs.

Even if sliding is fast, the off-rate must be correspondingly slow, e.g., PstII would need to remain on the DNA long enough to take the ~1.2×10^6 steps required to move 1,100 bp. Many obligatory sliding factors, such as the replication processivity factors, achieve high processivity by forming a ring structure clamped around the DNA [107]. It is tempting to speculate that whilst sliding may only play a short-range role in searching for a site [103], when communication must occur with a defined orientation and initiate from a defined location, the sliding process must be licensed by ATP binding and hydrolysis (see below).

The question of how conformational changes in the Type III helicase domain(s) produce the switch from recognition to sliding remains open. It is possible that the ATPase activity is used to assemble a toroidal protein structure to increase DNA binding lifetime whilst reducing DNA contacts. It may be that the helicase subunits form the clamp (Fig. 11.4). Recent data suggests that only a single Res subunit is required for efficient cleavage activity [57], and monomeric "sliding clamps" do exist [104]. Alternatively, the helicase may act to remodel the methyltransferase

domain. There is currently no X-ray crystallographic structure of a Type III RM enzyme. Although there are differences in the helicase motifs between the Type I and III enzymes [50], it is likely that the helicase domains will look similar. Only a structure of the full protein complex bound to dsDNA will suffice in explaining how a helicase can produce an efficient sliding machine.

Other ATPases with Switch and Clamp Roles

There are many other examples of NTP hydrolysing protein machines for which it is difficult to explain a role for chemical energy in producing directional stepwise translocation, and in which molecular switch roles have instead been invoked [12, 108]. Some of these are closely related to the RecA-based NTPases and share structural folds [23], for example the ABC transporter family. Others such as the GHKL (gyrase, Hsp90, histidine kinase, MutL) superfamily are unrelated to the canonical ATP binding folds [24]. Some of these ATPases collaborate with helicases as part of larger nucleoprotein complexes. A noteworthy observation is that many of these switch mechanisms seem to involve protein complexes with multiple ATP binding sites [12]. Whilst some nucleotide may be required for hydrolysis, others may be used in purely allosteric roles.

Of particular relevance to the developing story of the Type III RM sliding mechanism are the bacterial mismatch repair proteins MutL (GHKL family ATPase) and MutS (ABC family ATPase) and their eukaryotic homologues [109, 110]. In both proteins the nucleotide binding pockets are composite being formed by the sharing of catalytic residues from separate domains across a dimer interface [111, 112]. Thus binding of one or two nucleotides bridge the dimers, and initiate changes in protein–protein and protein–DNA interactions, with hydrolysis and ADP/Pi release allowing turnover of the interactions. Recognition of the base pair mismatch by a MutS dimer requires ATP and may result in the formation of a sliding clamp [113]. This state allows stable binding and communication between the mismatch and the strand scission site which may be thousands of base pairs away. ATP-bound MutL interacts with the MutS–DNA complex, later acting to load and activate the UvrD helicase at the strand scission [109, 110]. The exact sequential series of ATP binding/hydrolysis steps in the complete repair pathway is unclear, and, similarly to the Type III enzymes, more needs to be done to test the robustness of the sliding mechanism over other roles for the ATP switch of MutS.

Also of relevance to the Type III RM enzymes are the clamp loaders—the γ/τ complex in bacteria and the replication factor–C (RFC) in eukaryotes—which act to load sliding clamp processivity factors onto DNA [107]. Here is a clear-cut example of the necessity for an energy input (from the loader) in order to establish a hyperstable and correctly oriented sliding state (the clamp). Acting as a molecular switch, ATP binding is sufficient to stabilise the clamp–clamp loader complex and support loading of the clamp around DNA [114]. To release the clamp and recycle the loader however requires DNA-stimulated hydrolysis of three ATPs [107, 115]. The clamp

loaders are classified as AAA+ proteins, a broad and diverse family of ATPases with roles in many cellular processes [116]. Typically they assemble into hexamers, although the clamp loader complexes are pentameric. A great many AAA+ proteins act as molecular switches regulated by the binding of target substrate which activates the NTPase activity via a "glutamate switch" [108]. However, other AAA+ enzymes—for example RuvB [117] and HPV E2 helicase [118]—are *bona fide* processive ssDNA and dsDNA translocases. Nevertheless, as discussed above, the same underlying processes probably produce the different activities.

Another example of multiple ATPase modules within one complex is the bacterial UvrAB complex which operates in nucleotide excision repair and in which a molecular switch may act to load a helicase [119] (see also Chap. 10). UvrA (ABC family ATPase) is a DNA damage sensor which forms a homodimer where each monomer contains two composite ABC modules [120]. Therefore there are four possible ATP binding/hydrolysis centres. This arrangement differs from the MutS example above in that ATP binding does not directly act to tether the monomers in the dimer, but likely regulates dimerization indirectly. The functional significance of ATP binding and hydrolysis and the role of the resulting conformational changes in UvrA are not entirely clear. It is likely that cycles of ATP binding, hydrolysis and release allow handoff between damage recognition and replacement with the second ATPase module, the SF2 helicase UvrB, but the precise details remain to be resolved.

Summary and Outlook

A perplexing feature of many molecular switches is that the hydrolysis of the high energy phosphoanhydride bond of a nucleoside triphosphate is required to drive reactions that appear energetically neutral or even favourable. For example, there are plenty of examples of restriction enzymes that can readily cut DNA without requiring ATP hydrolysis [47]. What then might be the role of NTP binding and hydrolysis in a molecular switch?

There are recurring themes in the above systems that help to provide answers to this question: (1) Directionality—ATP hydrolysis drives the reaction in one direction through the cycle by helping to interchange hyperstable intermediate states; (2) Positioning—a requirement for activation of sequential ATP binding, hydrolysis and product release ensures that the next reaction step only occurs when the complex is present at the correct location and/or that the correct protein cofactors are present; (3) Timing—the hydrolysis step can act as a molecular clock, ensuring that the next step is held up until the suitable conditions are met. One conclusion therefore is that an NTP-switch allows a finer level of metabolic control.

As more helicases are studied in molecular detail, fascinating new mechanisms and roles are being revealed. The future challenges come in dealing with the increasing molecular complexity—especially, in determining the reaction mechanism when there are multiple ATP binding sites. Carefully designed and clever

combinations of ensemble and single molecule experiments will be required to allow complete biological processes to be followed in real time.

Acknowledgements I thank Ralf Seidel, Steve Halford, Dale Wigley, Mark Dillingham, Nigel Savery, Julia Toth, Fiona Diffin and Kara van Aelst for discussions about helicases and restriction enzymes and for experimental assistance.

References

1. Wu CG, Spies M. Overview: what are DNA helicases? DNA helicases and DNA motor proteins. 2012.
2. Singleton MR, Dillingham MS, Wigley DB. Structure and mechanism of helicases and nucleic acid translocases. Annu Rev Biochem. 2007;76:23–50.
3. Linder P, Jankowsky E. From unwinding to clamping - the DEAD box RNA helicase family. Nat Rev Mol Cell Biol. 2011;12(8):505–16.
4. Pyle AM. Translocation and unwinding mechanisms of RNA and DNA helicases. Annu Rev Biophys. 2008;37:317–36.
5. Caruthers JM, McKay DB. Helicase structure and mechanism. Curr Opin Struct Biol. 2002; 12(1):123–33.
6. Singleton MR, Wigley DB. Multiple roles for ATP hydrolysis in nucleic acid modifying enzymes. EMBO J. 2003;22(18):4579–83.
7. Durr H, Flaus A, Owen-Hughes T, Hopfner KP. Snf2 family ATPases and DExx box helicases: differences and unifying concepts from high-resolution crystal structures. Nucleic Acids Res. 2006;34(15):4160–7.
8. Ryan DP, Owen-Hughes T. Snf2-family proteins: chromatin remodellers for any occasion. Curr Opin Chem Biol. 2011;15(5):649–56.
9. Stanley LK, Seidel R, van der Scheer C, Dekker NH, Szczelkun MD, Dekker C. When a helicase is not a helicase: dsDNA tracking by the motor protein EcoR124I. EMBO J. 2006;25(10):2230–9.
10. Jankowsky E. RNA helicases at work: binding and rearranging. Trends Biochem Sci. 2011; 36(1):19–29.
11. Szczelkun MD, Friedhoff P, Seidel R. Maintaining a sense of direction during long-range communication on DNA. Biochem Soc Trans. 2010;38(2):404–9.
12. Szczelkun MD. Translocation, switching and gating: potential roles for ATP in long-range communication on DNA by Type III restriction endonucleases. Biochem Soc Trans. 2011; 39(2):589–94.
13. Gorbalenya AE, Koonin EV. Helicases: amino acid sequence comparisons and structure-function relationships. Curr Opin Struct Biol. 1993;3:419–29.
14. Soultanas P, Wigley DB. Unwinding the 'Gordian knot' of helicase action. Trends Biochem Sci. 2001;26(1):47–54.
15. Velankar SS, Soultanas P, Dillingham MS, Subramanya HS, Wigley DB. Crystal structures of complexes of PcrA DNA helicase with a DNA substrate indicate an inchworm mechanism. Cell. 1999;97(1):75–84.
16. Dillingham MS, Wigley DB, Webb MR. Demonstration of unidirectional single-stranded DNA translocation by PcrA helicase: measurement of step size and translocation speed. Biochemistry. 2000;39(1):205–12.
17. Saikrishnan K, Powell B, Cook NJ, Webb MR, Wigley DB. Mechanistic basis of 5'-3' translocation in SF1B helicases. Cell. 2009;137(5):849–59.
18. Singleton MR, Scaife S, Wigley DB. Structural analysis of DNA replication fork reversal by RecG. Cell. 2001;107(1):79–89.

19. Savery NJ. The molecular mechanism of transcription-coupled DNA repair. Trends Microbiol. 2007;15(7):326–33.
20. Wittinghofer A, Vetter IR. Structure-function relationships of the G domain, a canonical switch motif. Annu Rev Biochem. 2011;80:943–71.
21. Vale RD. Switches, latches, and amplifiers: common themes of G proteins and molecular motors. J Cell Biol. 1996;135(2):291–302.
22. Goody RS, Hofmann-Goody W. Exchange factors, effectors, GAPs and motor proteins: common thermodynamic and kinetic principles for different functions. Eur Biophys J. 2002;31(4):268–74.
23. Leipe DD, Koonin EV, Aravind L. Evolution and classification of P-loop kinases and related proteins. J Mol Biol. 2003;333(4):781–815.
24. Thomsen ND, Berger JM. Structural frameworks for considering microbial protein- and nucleic acid-dependent motor ATPases. Mol Microbiol. 2008;69(5):1071–90.
25. Ahmadian MR, Stege P, Scheffzek K, Wittinghofer A. Confirmation of the arginine-finger hypothesis for the GAP-stimulated GTP-hydrolysis reaction of Ras. Nat Struct Biol. 1997;4(9):686–9.
26. Toseland CP, Martinez-Senac MM, Slatter AF, Webb MR. The ATPase cycle of PcrA helicase and its coupling to translocation on DNA. J Mol Biol. 2009;392(4):1020–32.
27. Soultanas P, Dillingham MS, Velankar SS, Wigley DB. DNA binding mediates conformational changes and metal ion coordination in the active site of PcrA helicase. J Mol Biol. 1999;290(1):137–48.
28. Carter NJ, Cross RA. Kinesin's moonwalk. Curr Opin Cell Biol. 2006;18(1):61–7.
29. Deaconescu AM, Chambers AL, Smith AJ, et al. Structural basis for bacterial transcription-coupled DNA repair. Cell. 2006;124(3):507–20.
30. Cheng W, Arunajadai SG, Moffitt JR, Tinoco Jr I, Bustamante C. Single-base pair unwinding and asynchronous RNA release by the hepatitis C virus NS3 helicase. Science. 2011;333(6050):1746–9.
31. Myong S, Cui S, Cornish PV, et al. Cytosolic viral sensor RIG-I is a 5'-triphosphate-dependent translocase on double-stranded RNA. Science. 2009;323(5917):1070–4.
32. Sengoku T, Nureki O, Nakamura A, Kobayashi S, Yokoyama S. Structural basis for RNA unwinding by the DEAD-box protein Drosophila Vasa. Cell. 2006;125(2):287–300.
33. Bordeleau ME, Matthews J, Wojnar JM, et al. Stimulation of mammalian translation initiation factor eIF4A activity by a small molecule inhibitor of eukaryotic translation. Proc Natl Acad Sci USA. 2005;102(30):10460–5.
34. Yang Q, Jankowsky E. The DEAD-box protein Ded1 unwinds RNA duplexes by a mode distinct from translocating helicases. Nat Struct Mol Biol. 2006;13(11):981–6.
35. Yang Q, Del Campo M, Lambowitz AM, Jankowsky E. DEAD-box proteins unwind duplexes by local strand separation. Mol Cell. 2007;28(2):253–63.
36. Henn A, Cao W, Hackney DD, De La Cruz EM. The ATPase cycle mechanism of the DEAD-box rRNA helicase, DbpA. J Mol Biol. 2008;377(1):193–205.
37. Henn A, Cao W, Licciardello N, Heitkamp SE, Hackney DD, De La Cruz EM. Pathway of ATP utilization and duplex rRNA unwinding by the DEAD-box helicase, DbpA. Proc Natl Acad Sci USA. 2011;107(9):4046–50.
38. Liu F, Putnam A, Jankowsky E. ATP hydrolysis is required for DEAD-box protein recycling but not for duplex unwinding. Proc Natl Acad Sci USA. 2008;105(51):20209–14.
39. Aregger R, Klostermeier D. The DEAD box helicase YxiN maintains a closed conformation during ATP hydrolysis. Biochemistry. 2009;48(45):10679–81.
40. Chen Y, Potratz JP, Tijerina P, Del Campo M, Lambowitz AM, Russell R. DEAD-box proteins can completely separate an RNA duplex using a single ATP. Proc Natl Acad Sci USA. 2008;105(51):20203–8.
41. Del Campo M, Lambowitz AM. Structure of the yeast DEAD box protein Mss116p reveals two wedges that crimp RNA. Mol Cell. 2009;35(5):598–609.
42. Cao W, Coman MM, Ding S, et al. Mechanism of Mss116 ATPase reveals functional diversity of DEAD-Box proteins. J Mol Biol. 2011;409(3):399–414.

43. Collins R, Karlberg T, Lehtio L, et al. The DEXD/H-box RNA helicase DDX19 is regulated by an a-helical switch. J Biol Chem. 2009;284(16):10296–300.
44. Ballut L, Marchadier B, Baguet A, Tomasetto C, Seraphin B, Le Hir H. The exon junction core complex is locked onto RNA by inhibition of eIF4AIII ATPase activity. Nat Struct Mol Biol. 2005;12(10):861–9.
45. Montpetit B, Thomsen ND, Helmke KJ, Seeliger MA, Berger JM, Weis K. A conserved mechanism of DEAD-box ATPase activation by nucleoporins and InsP6 in mRNA export. Nature. 2011;472(7342):238–42.
46. Wilson GG, Murray NE. Restriction and modification systems. Annu Rev Genet. 1991;25:585–627.
47. Roberts RJ, Vincze T, Posfai J, Macelis D. REBASE–a database for DNA restriction and modification: enzymes, genes and genomes. Nucleic Acids Res. 2010;38(database issue):D234–6.
48. Roberts RJ, Belfort M, Bestor T, et al. A nomenclature for restriction enzymes, DNA methyltransferases, homing endonucleases and their genes. Nucleic Acids Res. 2003;31(7):1805–12.
49. Gorbalenya AE, Koonin EV. Endonuclease (R) subunits of type-I and type-III restriction-modification enzymes contain a helicase-like domain. FEBS Lett. 1991;291(2):277–81.
50. McClelland SE, Szczelkun MD. The type I and III restriction endonucleases: structural elements in the molecular motors that process DNA. Nucleic Acids Mol Biol. 2004;14:111–35.
51. Dryden DT, Cooper LP, Thorpe PH, Byron O. The in vitro assembly of the EcoKI type I DNA restriction/modification enzyme and its in vivo implications. Biochemistry. 1997;36(5):1065–76.
52. Janscak P, Dryden DT, Firman K. Analysis of the subunit assembly of the typeIC restriction-modification enzyme EcoR124I. Nucleic Acids Res. 1998;26(19):4439–45.
53. Kennaway CK, Taylor JE, Song CF, et al. Structure and operation of the DNA-translocating type I DNA restriction enzymes. Genes Dev. 2012;26(1):92–104.
54. Obarska-Kosinska A, Taylor JE, Callow P, Orlowski J, Bujnicki JM, Kneale GG. HsdR subunit of the type I restriction-modification enzyme EcoR124I: biophysical characterisation and structural modelling. J Mol Biol. 2008;376(2):438–52.
55. Lapkouski M, Panjikar S, Janscak P, et al. Structure of the motor subunit of type I restriction-modification complex EcoR124I. Nat Struct Mol Biol. 2009;16(1):94–5.
56. Janscak P, Sandmeier U, Szczelkun MD, Bickle TA. Subunit assembly and mode of DNA cleavage of the type III restriction endonucleases EcoP1I and EcoP15I. J Mol Biol. 2001;306(3):417–31.
57. Wyszomirski KH, Curth U, Alves J, et al. Type III restriction endonuclease EcoP15I is a heterotrimeric complex containing one Res subunit with several DNA-binding regions and ATPase activity. Nucleic Acids Res. 2012;40:3610–22.
58. Davies GP, Powell LM, Webb JL, Cooper LP, Murray NE. EcoKI with an amino acid substitution in any one of seven DEAD-box motifs has impaired ATPase and endonuclease activities. Nucleic Acids Res. 1998;26(21):4828–36.
59. Webb JL, King G, Ternent D, Titheradge AJ, Murray NE. Restriction by EcoKI is enhanced by co-operative interactions between target sequences and is dependent on DEAD box motifs. EMBO J. 1996;15(8):2003–9.
60. Saha S, Rao DN. Mutations in the Res subunit of the EcoPI restriction enzyme that affect ATP-dependent reactions. J Mol Biol. 1997;269(3):342–54.
61. Halford SE, Gowers DM, Sessions RB. Two are better than one. Nat Struct Biol. 2000;7(9):705–7.
62. Linn S, Arber W. Host specificity of DNA produced by Escherichia coli, X. In vitro restriction of phage fd replicative form. Proc Natl Acad Sci USA. 1968;59(4):1300–6.
63. Meselson M, Yuan R. DNA restriction enzyme from E. coli. Nature. 1968;217(5134):1110–4.
64. Roulland-Dussoix D, Boyer HW. The Escherichia coli B restriction endonuclease. Biochim Biophys Acta. 1969;195(1):219–29.

65. Eskin B, Linn S. The deoxyribonucleic acid modification and restriction enzymes of Escherichia coli B. II. Purification, subunit structure, and catalytic properties of the restriction endonuclease. J Biol Chem. 1972;247(19):6183–91.
66. Eskin B, Linn S. The deoxyribonucleic acid modification and restriction enzymes of Escherichia coli B. J Biol Chem. 1972;247(19):6192–6.
67. Haberman A. The bacteriophage P1 restriction endonuclease. J Mol Biol. 1974;89(4): 545–63.
68. Reiser J, Yuan R. Purification and properties of the P15 specific restriction endonuclease from Escherichia coli. J Biol Chem. 1977;252(2):451–6.
69. Kauc L, Piekarowicz A. Purification and properties of a new restriction endonuclease from Haemophilus influenzae Rf. Eur J Biochem. 1978;92(2):417–26.
70. Yuan R, Hamilton DL, Hadi SM, Bickle TA. Role of ATP in the cleavage mechanism of the EcoP15 restriction endonuclease. J Mol Biol. 1980;144(4):501–19.
71. Horiuchi K, Zinder ND. Cleavage of bacteriophage fl DNA by the restriction enzyme of Escherichia coli B. Proc Natl Acad Sci USA. 1972;69(11):3220–4.
72. Shulman MJ. Model for wandering restriction enzymes. Nature. 1974;252(5478):76–8.
73. Rosamond J, Endlich B, Linn S. Electron microscopic studies of the mechanism of action of the restriction endonuclease of Escherichia coli B. J Mol Biol. 1979;129(4):619–35.
74. Yuan R, Hamilton DL, Burckhardt J. DNA translocation by the restriction enzyme from E. coli K. Cell. 1980;20(1):237–44.
75. Endlich B, Linn S. The DNA restriction endonuclease of Escherichia coli B. II. Further studies of the structure of DNA intermediates and products. J Biol Chem. 1985;260(9):5729–38.
76. Endlich B, Linn S. The DNA restriction endonuclease of Escherichia coli B. I. Studies of the DNA translocation and the ATPase activities. J Biol Chem. 1985;260(9):5720–8.
77. Studier FW, Bandyopadhyay PK. Model for how type I restriction enzymes select cleavage sites in DNA. Proc Natl Acad Sci USA. 1988;85(13):4677–81.
78. Davies GP, Kemp P, Molineux IJ, Murray NE. The DNA translocation and ATPase activities of restriction-deficient mutants of Eco KI. J Mol Biol. 1999;292(4):787–96.
79. Garcia LR, Molineux IJ. Translocation and specific cleavage of bacteriophage T7 DNA in vivo by EcoKI. Proc Natl Acad Sci USA. 1999;96(22):12430–5.
80. Firman K, Szczelkun MD. Measuring motion on DNA by the type I restriction endonuclease EcoR124I using triplex displacement. EMBO J. 2000;19(9):2094–102.
81. Seidel R, Bloom JG, Dekker C, Szczelkun MD. Motor step size and ATP coupling efficiency of the dsDNA translocase EcoR124I. EMBO J. 2008;27(9):1388–98.
82. Seidel R, Bloom JG, van Noort J, et al. Dynamics of initiation, termination and reinitiation of DNA translocation by the motor protein EcoR124I. EMBO J. 2005;24(23):4188–97.
83. Seidel R, van Noort J, van der Scheer C, et al. Real-time observation of DNA translocation by the type I restriction modification enzyme EcoR124I. Nat Struct Mol Biol. 2004;11(9):838–43.
84. Dryden DT, Edwardson JM, Henderson RM. DNA translocation by type III restriction enzymes: a comparison of current models of their operation derived from ensemble and single-molecule measurements. Nucleic Acids Res. 2011;39(11):4525–31.
85. Meisel A, Mackeldanz P, Bickle TA, Kruger DH, Schroeder C. Type III restriction endonucleases translocate DNA in a reaction driven by recognition site-specific ATP hydrolysis. EMBO J. 1995;14(12):2958–66.
86. Meisel A, Bickle TA, Kruger DH, Schroeder C. Type III restriction enzymes need two inversely oriented recognition sites for DNA cleavage. Nature. 1992;355(6359):467–9.
87. van Aelst K, Toth J, Ramanathan SP, Schwarz FW, Seidel R, Szczelkun MD. Type III restriction enzymes cleave DNA by long-range interaction between sites in both head-to-head and tail-to-tail inverted repeat. Proc Natl Acad Sci USA. 2011;107(20):9123–8.
88. Peakman LJ, Szczelkun MD. DNA communications by Type III restriction endonucleases–confirmation of 1D translocation over 3D looping. Nucleic Acids Res. 2004;32(14):4166–74.
89. Raghavendra NK, Rao DN. Unidirectional translocation from recognition site and a necessary interaction with DNA end for cleavage by Type III restriction enzyme. Nucleic Acids Res. 2004;32(19):5703–11.

90. Crampton N, Roes S, Dryden DT, Rao DN, Edwardson JM, Henderson RM. DNA looping and translocation provide an optimal cleavage mechanism for the type III restriction enzymes. EMBO J. 2007;26(16):3815–25.
91. Crampton N, Yokokawa M, Dryden DT, et al. Fast-scan atomic force microscopy reveals that the type III restriction enzyme EcoP15I is capable of DNA translocation and looping. Proc Natl Acad Sci USA. 2007;104(31):12755–60.
92. Reich S, Gossl I, Reuter M, Rabe JP, Kruger DH. Scanning force microscopy of DNA translocation by the Type III restriction enzyme EcoP15I. J Mol Biol. 2004;341(2):337–43.
93. Ramanathan SP, van Aelst K, Sears A, et al. Type III restriction enzymes communicate in 1D without looping between their target sites. Proc Natl Acad Sci USA. 2009;106(6):1748–53.
94. Schwarz FW, van Aelst K, Toth J, Seidel R, Szczelkun MD. DNA cleavage site selection by Type III restriction enzymes provides evidence for head-on protein collisions following 1D bidirectional motion. Nucleic Acids Res. 2011;39(18):8042–51.
95. Sears A, Peakman LJ, Wilson GG, Szczelkun MD. Characterization of the Type III restriction endonuclease PstII from Providencia stuartii. Nucleic Acids Res. 2005;33(15):4775–87.
96. Szczelkun MD, Janscak P, Firman K, Halford SE. Selection of non-specific DNA cleavage sites by the type IC restriction endonuclease EcoR124I. J Mol Biol. 1997;271(1):112–23.
97. Szczelkun MD, Dillingham MS, Janscak P, Firman K, Halford SE. Repercussions of DNA tracking by the type IC restriction endonuclease EcoR124I on linear, circular and catenated substrates. EMBO J. 1996;15(22):6335–47.
98. Slutsky M, Mirny LA. Kinetics of protein-DNA interaction: facilitated target location in sequence-dependent potential. Biophys J. 2004;87(6):4021–35.
99. Givaty O, Levy Y. Protein sliding along DNA: dynamics and structural characterization. J Mol Biol. 2009;385(4):1087–97.
100. Blainey PC, van Oijen AM, Banerjee A, Verdine GL, Xie XS. A base-excision DNA-repair protein finds intrahelical lesion bases by fast sliding in contact with DNA. Proc Natl Acad Sci USA. 2006;103(15):5752–7.
101. von Hippel PH, Berg OG. Facilitated target location in biological systems. J Biol Chem. 1989;264(2):675–8.
102. Halford SE, Marko JF. How do site-specific DNA-binding proteins find their targets? Nucleic Acids Res. 2004;32(10):3040–52.
103. Halford SE. An end to 40 years of mistakes in DNA-protein association kinetics? Biochem Soc Trans. 2009;37(Pt 2):343–8.
104. Komazin-Meredith G, Mirchev R, Golan DE, van Oijen AM, Coen DM. Hopping of a processivity factor on DNA revealed by single-molecule assays of diffusion. Proc Natl Acad Sci USA. 2008;105(31):10721–6.
105. Bonnet I, Biebricher A, Porte PL, et al. Sliding and jumping of single EcoRV restriction enzymes on non-cognate DNA. Nucleic Acids Res. 2008;36(12):4118–27.
106. Lin Y, Zhao T, Jian X, et al. Using the bias from flow to elucidate single DNA repair protein sliding and interactions with DNA. Biophys J. 2009;96(5):1911–7.
107. Kelch BA, Makino DL, O'Donnell M, Kuriyan J. How a DNA polymerase clamp loader opens a sliding clamp. Science. 2011;334(6063):1675–80.
108. Zhang X, Wigley DB. The 'glutamate switch' provides a link between ATPase activity and ligand binding in AAA+ proteins. Nat Struct Mol Biol. 2008;15(11):1223–7.
109. Iyer RR, Pluciennik A, Burdett V, Modrich PL. DNA mismatch repair: functions and mechanisms. Chem Rev. 2006;106(2):302–23.
110. Kunkel TA, Erie DA. DNA mismatch repair. Annu Rev Biochem. 2005;74:681–710.
111. Ban C, Junop M, Yang W. Transformation of MutL by ATP binding and hydrolysis: a switch in DNA mismatch repair. Cell. 1999;97(1):85–97.
112. Obmolova G, Ban C, Hsieh P, Yang W. Crystal structures of mismatch repair protein MutS and its complex with a substrate DNA. Nature. 2000;407(6805):703–10.
113. Jeong C, Cho WK, Song KM, et al. MutS switches between two fundamentally distinct clamps during mismatch repair. Nat Struct Mol Biol. 2011;18(3):379–85.

114. Seybert A, Wigley DB. Distinct roles for ATP binding and hydrolysis at individual subunits of an archaeal clamp loader. EMBO J. 2004;23(6):1360–71.
115. Sakato M, Zhou Y, Hingorani MM. ATP binding and hydrolysis-driven rate-determining events in the RFC-catalyzed PCNA clamp loading reaction. J Mol Biol. 2012;416(2):176–91.
116. Erzberger JP, Berger JM. Evolutionary relationships and structural mechanisms of AAA+ proteins. Annu Rev Biophys Biomol Struct. 2006;35:93–114.
117. George H, Kuraoka I, Nauman DA, Kobertz WR, Wood RD, West SC. RuvAB-mediated branch migration does not involve extensive DNA opening within the RuvB hexamer. Curr Biol. 2000;10(2):103–6.
118. Enemark EJ, Joshua-Tor L. Mechanism of DNA translocation in a replicative hexameric helicase. Nature. 2006;442(7100):270–5.
119. Truglio JJ, Croteau DL, Van Houten B, Kisker C. Prokaryotic nucleotide excision repair: the UvrABC system. Chem Rev. 2006;106(2):233–52.
120. Pakotiprapha D, Inuzuka Y, Bowman BR, et al. Crystal structure of Bacillus stearothermophilus UvrA provides insight into ATP-modulated dimerization, UvrB interaction, and DNA binding. Mol Cell. 2008;29(1):122–33.

Chapter 12
The FtsK Family of DNA Pumps

Gaëlle Demarre, Elisa Galli, and François-Xavier Barre

Abstract Interest for proteins of the FtsK family initially arose from their implication in many primordial processes in which DNA needs to be transported from one cell compartment to another in eubacteria. In the first section of this chapter, we address a list of the cellular functions of the different members of the FtsK family that have been so far studied. Soon after their discovery, interest for the FstK proteins spread because of their unique biochemical properties: most DNA transport systems rely on the assembly of complex multicomponent machines. In contrast, six FtsK proteins are sufficient to assemble into a fast and powerful DNA pump; the pump transports closed circular double stranded DNA molecules without any covalent-bond breakage nor topological alteration; transport is oriented despite the intrinsic symmetrical nature of the double stranded DNA helix and can occur across cell membranes. The different activities required for the oriented transport of DNA across cell compartments are achieved by three separate modules within the FtsK proteins: a DNA translocation module, an orientation module and an anchoring module. In the second part of this chapter, we review the structural and biochemical properties of these different modules.

Introduction

In eukaryotic cells, the existence of active mechanisms for the transport of DNA was inferred from the observation of chromosomes during mitosis in the early twentieth century (see [1] for a review). It was soon after realized that spindle microtubules provide both the scaffold and the driving force for it. In brief, spindle microtubules attach to a complex protein structure, the kinetochore, which is assembled on a specific

G. Demarre • E. Galli • F. Barre (✉)
Centre de Génétique Moléculaire, CNRS,
Gif sur Yvette, Cedex, France
e-mail: gaelle.demarre@cgm.cnrs-gif.fr; elisa.galli@cgm.cnrs-gif.fr;
barre@cgm.cnrs-gif.fr

M. Spies (ed.), *DNA Helicases and DNA Motor Proteins*, Advances in Experimental Medicine and Biology, DOI 10.1007/978-1-4614-5037-5_12,

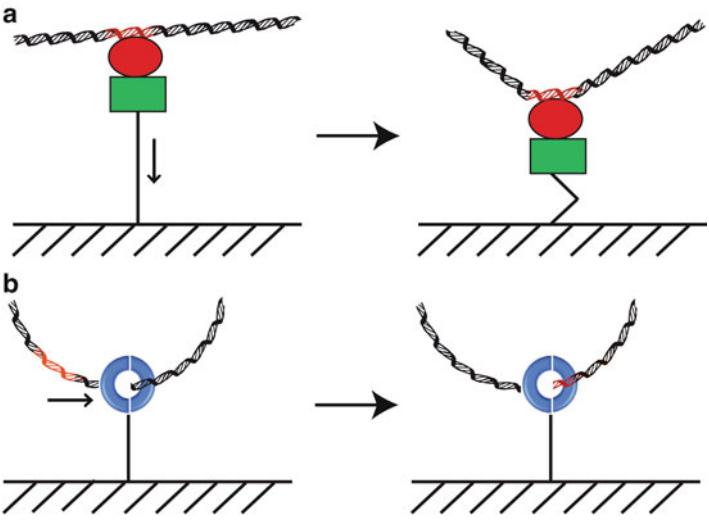

Fig. 12.1 Two main strategies for the transport of DNA. (**a**) DNA on a leash. A DNA binding protein (*red*) polymerizes over a specific DNA motif (*red*). The following recruitment of a motor protein (*green*) provides the partitioning force, pushing or pulling the DNA in a specific direction. (**b**) Pumping DNA. The motor protein (*blue*) is anchored to a fix position and directionally translocates on DNA. A DBA segment is depicted in *red* to indicate the orientation of translocation

chromosomal region, the centromere. Chromosomes are then pushed/pulled by tubulin polymerization/depolymerization in connection with the activity of kinesin and dynein cytoskeletal motors. Many bacterial plasmids and chromosomes harbour conceptually equivalent DNA transport machineries, the partition systems (see [2, 3] for a review): repeated DNA sequence motifs serve as nucleation sites for the polymerization of a dedicated DNA binding protein, resulting in the formation of a nucleoprotein complex through which the driving force generated by a motor protein, generally an ATPase, is transmitted (Fig. 12.1a). However, bacteria also possess a conceptually different chromosomal transport machinery, in which the driving force is provided by the direct contact of a motor protein with the DNA molecule: the motor protein, which runs along the DNA molecule similarly to DNA helicases or translocases, behaves as a DNA pump because it is anchored to a fixed position within the cell (Fig. 12.1b). Interest for this DNA transport machinery initially arose from its crucial importance for the equal partition of genetic information between the mother cell and the prespore during sporulation in *Bacillus subtilis* [4, 5], between sister cells during chromosome dimer resolution in *Escherichia coli* [6, 7] and between cell filaments during the conjugative transfer of some plasmids in streptomyces [8, 9]. However, the discovery of the unique structural and biochemical properties of this transport system very soon raised a considerable interest for the study of its mode of action per se: (i) the DNA pumps transport DNA across nearly [10] or fully closed [9, 11, 12] cell membranes, which is reminiscent of classical conjugation and of natural transformation; (ii) however, circular double stranded DNA molecules are transferred without any

covalent-bond breakage and little alteration to the topology of the molecule [13] whereas a single DNA strand is transported after the introduction of a nick during natural transformation and conjugation; (iii) despite the intrinsic symmetrical nature of the double stranded DNA helix, transport is oriented [14–17]; (iv) most DNA transport systems rely on the assembly of complex multicomponent machines. In contrast, the DNA pumps consist of a single multifunctional protein, which defines a specific family of P-loop NTPase: the FtsK family.

In this chapter, we first address a list of the biological observations made on the cellular functions of the different members of the FtsK family that have been so far studied. Second, we review the structural and biochemical properties of these proteins that explain their cellular activities.

Cellular Functions Performed by the FtsK Family of Proteins

Interest for the FtsK family of proteins arose from the realization that it is implicated in many primordial processes in which DNA needs to be transported from one cell compartment to another in eubacteria.

Sporulation

The first member of the FtsK family to be characterized was the *Bacillus subtilis* SpoIIIE protein, which is essential for sporulation (Fig. 12.2a). At the onset of sporulation, the cell divides asymmetrically at one cell pole over a partially segregated copy of the chromosome, trapping only one-third of it in the forespore. This allows for the activation of specific transcription factors in each cell compartment. Initially, σ^F is activated in the forespore, followed by σ^E in the mother cell, then σ^G is activated in the forespore and finally σ^K in the mother cell (see [18] for a review). During spore development, SpoIIIE localizes at the division septum [19] where it serves to pump the remaining 70% of the chromosome into the forespore [4, 5, 20]. A beautiful feature of SpoIIIE-dependent DNA transport is that the two arms of the chromosome are simultaneously pumped into the forespore [11]. Septal localization depends on the presence of trapped DNA, which acts as an anchor for the nucleation of the pump [11, 21]. Initial studies suggested that SpoIIIE acted as a DNA exporter and that the direction of transport depended on its specific assembly on the mother cell side of the septum [22, 23]. However, later studies demonstrated that the orientation is primarily dictated by the DNA sequence itself [15, 17]. Spore development is accompanied by a strong distortion of the division septum, which curves out to eventually engulf the smaller cell. Engulfment is completed by the loss of attachment between the forespore and the mother cell. SpoIIIE is implicated in the engulfment process [24], at least in part because it promotes membrane fusion [25]. SpoIIIE also promotes membrane fusion during cytokinesis [26], which led to the idea that it transports DNA across fused septal membranes by creating a pore [11, 12].

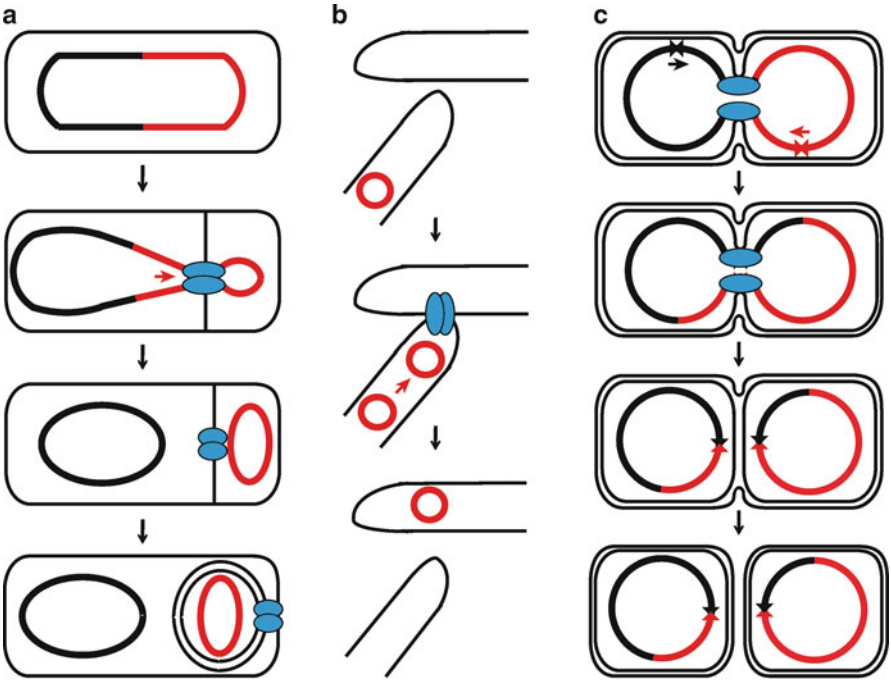

Fig. 12.2 The three main functions attributed to members of the FtsK family of proteins. (**a**) Sporulation. SpoIIIE (*blue*) localizes on trapped DNA at the polar septum and pumps one copy of the chromosome from the mother cell into the forespore. The mother cell membrane then surrounds the forespore in a process called engulfment. (**b**) Conjugation. TraB (*blue*) localizes to the hyphal tips of the mycelia and mediates the transfer of plasmid DNA between two mycelial streptomycetes. (**c**) Cell proliferation. FtsK (*blue*) localizes at the division site where it directionally translocates septally trapped DNA and is involved in chromosome dimer resolution. The two sister chromatids are shown in *red* and *black* to emphasize the position of the crossover that resulted from homologous recombination events. The two *dif* sites of the chromosome dimer are indicated by two *inverted triangles*

Conjugation

Proteins of the FtsK family are also implicated in the conjugative transfer of numerous plasmids from mycelial streptomycetes (Fig. 12.2b). In contrast to most conjugative elements, which rely on Type IV secretion systems, these plasmids are transferred in the dsDNA form [8]. A single plasmid-encoded protein, hereafter referred to as TraB, is sufficient to promote conjugal plasmid transfer [27]. The plasmidic TraB proteins localize to the hyphal tips of the mycelia, where plasmid transfer occurs [27]. They specifically recognize and bind to the dsDNA of their cognate conjugative plasmid [9] and are able to translocate along dsDNA [27]. In addition, they form pores in lipid bilayers [9].

Cell Proliferation

In addition to sporulation and conjugation, proteins of the FtsK family serve for the segregation of chromosomal DNA during vegetative growth, which probably explains their presence in the genome of most bacteria [28, 29]. The paradigm of these proteins is *E. coli* FtsK. FtsK was first identified as a cell division protein [30]. It interacts with many other cell division proteins [31], most notably with FtsZ, which targets it to midcell at an early stage of septum formation, right after FtsA [32–35]. FtsK is essential for cell division in *E. coli*. In its absence, late cell division proteins fail to localize to the septum [36], but the viability of null mutants is restored in cells overexpressing late cell division proteins such as FtsQ [37]. Recent studies further suggest that FtsK might be implicated in a checkpoint to control the final stages of cell division when DNA remains trapped in the septum [38, 39]. Initially, the involvement of FtsK in the transport of septally trapped chromosomes was guessed from the microscopic observation of cells carrying *ftsK* truncations [34]. However, chromosomal DNA is rarely trapped in the closing septum in *E. coli*, and FtsK-dependent DNA transport becomes crucial for cell proliferation only when septum localization and nucleoid organization are altered [39, 40]. Indeed, DNA transport by FtsK is normally limited to cells harbouring a chromosome dimer in *E. coli* [10, 41, 42]. As a consequence, most of our knowledge on FtsK derives from the discovery of its role in chromosome dimer resolution [6, 7]. Chromosome dimers are created by odd numbers of crossovers due to homologous recombination between circular chromosomes. They block chromosome segregation and remain trapped in the dividing septum (Fig. 12.2c). FtsK loads on dimer DNA in the regions where replication terminates [43]. Chromosome dimer resolution depends on the addition of a crossover at *dif*, a 28 bp site located at the opposite of the origin of replication, by two related tyrosine recombinases, XerC and XerD. FtsK plays two roles in the process [44]. First, it brings together the two *dif* sites carried by the dimer at midcell by pumping the DNA in an oriented manner [6, 14, 45]. The orientation of translocation is dictated by the sequence of the DNA [14, 46]. Second, it activates recombination at *dif* via a direct interaction with the XerCD complex [47–51]. The *Haemophilus influenzae*, *Vibrio cholerae* and *Lactococcus lactis* FtsK homologs are similarly implicated in the activation of Xer recombination [28, 50, 52]. Evidence has also been found that the *V. cholerae* and *L. lactis* FtsK homologs can follow DNA sequence polarity [28, 53]. Two FtsK homologs are encoded in the genome of *B. subtilis*, SpoIIIE and SftA [54, 55]. Both are implicated in chromosome segregation during vegetative cell division [54, 55], notably because they synergistically affect dimer resolution, presumably by positioning the *dif* sites in close proximity [56]. However, it is important to stress that the role of FtsK proteins during vegetative cell division is probably not restricted to chromosome dimer resolution. Because of the helical nature of DNA, replication of circular chromosomes results in the formation of two catenated molecules. In *E. coli*, the chromosome dimer resolution system is able to remove catenation links when the activity of TopoIV, the major cellular decatenase, is compromised [57, 58]. In addition, *E. coli*

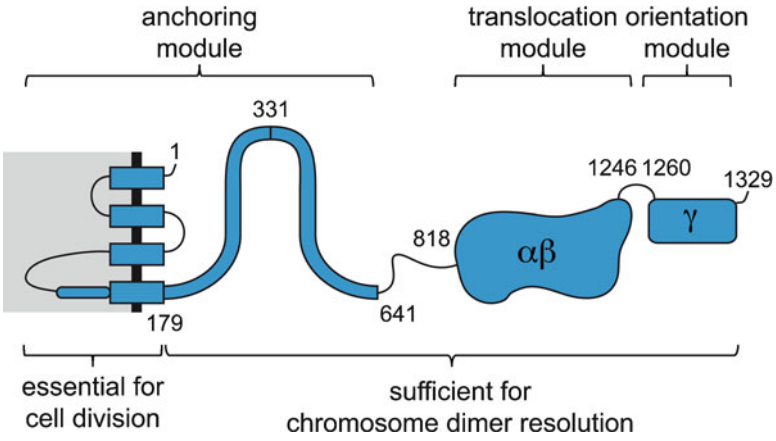

Fig. 12.3 Structure of the *E. coli* FtsK protein. *Numbers* indicate the aa residue at the beginning or end of each the different FtsK modules

FtsK has been directly implicated in the stimulation of the Topo IV activity [59–61]. In *Caulobacter crescentus*, FtsK is essential for chromosome segregation [62]. Results from the lab suggest that *V. cholerae* FtsK processes chromosomal DNA in the absence of chromosome dimers (Demarre and Barre, unpublished data).

Structural and Functional Analysis of the FtsK Family of Proteins

As can be seen from the wide range of cellular activities in which they are implicated, proteins of the FtsK family are multifunctional. This is reflected in their primary structure, the different activities being achieved by separate domains. Three modules can be delineated in the protein: a DNA translocation module, an orientation module and an anchoring/pore formation module. Most of what we have learned on the different modules of the FtsK family of proteins was obtained from studies of *E. coli* FtsK [50] and we will use the *E. coli* FtsK nomenclature to refer to each of these modules (Fig. 12.3a). The *E. coli* FtsK anchoring module, $FtsK_N$, consists of the first 641 N-terminal aa residues of the protein [38]. The orientation module, $FtsK_\gamma$, consists of the last 69 C-terminal aa residues of the protein [63]. A long ~200 aa residue linker, rich in proline and glutamine, and a short ~15 aa flexible linker separate the translocation module of the protein, $FtsK_{\alpha\beta}$ [64], from $FtsK_N$ and $FtsK_\gamma$, respectively.

The DNA Translocation Module

$FtsK_{\alpha\beta}$ belongs to the P-loop NTPase superfamily (CL0023). Members of this superfamily are characterized by a conserved nucleotide phosphate-binding motif,

the P-loop or Walker A motif, and a Walker B motif, whose first acidic residue serves to coordinate the Mg^{2+} cation involved in NTP hydrolysis. $FtsK_{\alpha\beta}$ is structurally related to proteins of the type IV secretion systems (T4SS), the TrwB-like proteins involved in the conjugal transfer of plasmids and the archeal HerA bi-directional DNA helicases, suggesting that a common DNA pumping mechanism might be operational in both cellular and viral genome segregation [65]. $FtsK_{\alpha\beta}$ functions as a multimer [51], like TrwB [66]. However, $FtsK_{\alpha\beta}$ defines a specific structural family (Pfam 01580) of very powerful ATP-dependent translocases [20, 51] that do not unwind DNA but translocate along it [13]. Indeed, peptides encompassing the complete translocation modules of *E. coli* FtsK and *B. subtilis* SpoIIIE translocate at over 5 kb/s and against a stall force of over 60 pN at room temperature [67, 68]. At 37 °C, the velocity of the *E. coli* translocation module increases to 17.5 kb/s [69]. In vivo, the full length proteins can strip off proteins from the DNA on their passage [70, 71]. In vitro, FtsK can displace various roadblocks such as triplex oligonucleotides, streptavidin attached on biotinylated DNA and fork DNA structures [72–74]. A notable exception is its inability to displace the Xer recombinases, which fits with its role in chromosome dimer resolution [75].

Understanding of the DNA pumping mechanism of FtsK came with the determination of the structure of the *Pseudomonas aeruginosa* $FtsK_{\alpha\beta}$ module. It crystallized as a hexamer, forming a closed ring of 120 Å in outer diameter and a central annulus of 30 Å in diameter, which is large enough to encompass the double stranded DNA helix [64]. Electron microscopy, ultracentrifugation analysis, millisecond-resolution biochemical experiments and the higher activity of covalent dimers and trimers confirm the hexameric structure of the FtsK pumps [64, 73, 74, 76]. In vitro, hexamerization depends on protein concentration and on the presence of DNA but not on ATP [64], which fits with in vivo studies on the timing of activity of the FtsK pumps and on the conditions of assembly of the SpoIIIE pumps [21, 77].

Structural studies suggested a rotary inchworm model of translocation, in which each subunit sequentially translocates of ~1.6 bp by hydrolyzing a single ATP molecule [64]. Millisecond-resolution biochemical experiments agree with a 2 bp step size for each subunit [73], which implies that each subunit of the hexamer only needs to contact DNA every ~12 bp. This is close to the helical pitch of the DNA helix. It fits with the observation that FtsK translocates along the DNA with minimal perturbations to the supercoil density before or after the motor [13]. A nicety of this rotational behaviour is that it would minimize in vivo disturbance to the chromosomal supercoil density.

However, recent studies challenged the rotary inchworm model. Xer recombination activation of FtsK on short synthetic dsDNA substrates harbouring ssDNA gaps between the FtsK loading site and *dif* suggests that FtsK can bypass gaps of up to 30 nucleotides during translocation [72]. Covalent trimers with a catalytic mutation in the central subunit were found to form hexamers with two mutated subunits that had robust ATPase activity, activated XerCD recombination at *dif* and displayed wild-type translocation velocity [74]. In contrast, they had lost much of their capacity to displace triplex oligonucleotides, or streptavidin linked to biotin-DNA during translocation along DNA, suggesting that they could not work against high forces [74]. Based on

these results, the authors suggested an escort model of translocation, as proposed for some hexameric ring helicases [78]. In this model, ATPase-driven allosteric changes of a single subunit drive similar conformational changes in the five non-active subunits in a domino-like fashion, which moves the whole hexamer forward. Thus, maximum speed can be achieved with a single active subunit. In contrast, the maximal force against which the motor can fight depends on the number of active subunits. An analogy can be drawn with rugby. During open phases of the game, the speed at which the ball advances in the field is given by the speed of the player that carries the ball, his/her teammates remaining at his/her back to recover the ball in case of interception by the opposing team. In other phases of the game, the players bind together to form a maul or a ruck. The team then advances thanks to the combined strength of all the members that are engaged in the maul or rug against the other team.

The Orientation Module

In *E. coli*, the activity of the chromosome dimer resolution site, *dif,* is restricted to the terminus of the chromosome, the region where replication normally terminates [79]. The terminus is organized into a specific chromosomal domain by the MatP/*matS* site-specific system, independently from the replication termination process [80–83]. It is the last part of the chromosome to be segregated away from midcell and it has therefore the highest risk of being trapped in the septum. Correspondingly, it seems to be the loading region of FtsK in *E. coli* [43, 84]. However, the activity of *dif* is restricted to a small zone within the terminus [79], located at the junction of the two replichores of the chromosome [45, 85, 86]. This is because FtsK translocation is oriented by 8 bp polar sequence motifs, the KOPS (for FtsK-orienting polar sequences), which are repeated on the two replichores and point towards *dif* [14]. KOPS directly orient the direction of translocation [14, 16, 68]. They are recognized by FtsKγ [87], which adopts a winged helix-turn-helix (wHTH) structure [63] and binds to KOPS motifs as a trimer [76]. FtsK does not need KOPS to load on DNA [67] and it was proposed in early models that KOPS served as translocation blocks. However, it is now clear that they dictate the direction of translocation by promoting the oriented loading of FtsK [46, 69, 73]. The role of KOPS is reminiscent of the role of the Chi motif, which controls homologous recombination [88, 89]. Motifs unrelated to the *E. coli* Chi motif but with a similar role in homologous recombination have been reported in other bacteria [90–92].

The consensus sequence of the *E. coli* KOPS is 5′-GGGNACCC-3′ [14]. Such sequences are also repeated and highly skewed on the two replichores of many bacterial circular chromosomes, such as on the two *V. cholerae* chromosomes [28]. In this particular case, genetic evidence has been obtained that they are recognized by the *V. cholerae* FtsK protein via its gamma domain [28]. However, the *E. coli* consensus is not universal. Different over-represented and highly skewed sequences have been co-opted to serve as KOPS in other species. For instance, the *L. lactis* FtsK protein recognizes the 5′-GAAGAAG-3′ motif [53]. Nevertheless, the presence

of a sequence-specific DNA binding domain is a conserved feature of the FtsK family. For instance, translocation of *B. subtilis* SpoIIIE is oriented by the 5′-GAGAAGGG-3′ polar DNA sequence motif [15]. Even more strikingly, the γ domain of the TraB protein of the *Streptomyces venezuelae* pSVH1 conjugative plasmid specifically binds to repeated 8 bp motifs, 5′-GACCCGGA-3′ [9].

Oriented translocation by FtsK sorts sister chromosomes on either side of the septum, which finally allows the formation of a recombination synapse by bringing the two *dif* sites carried by chromosome dimers together. In addition, FtsK promotes a complete Xer recombination reaction at *dif* by reversing the catalytic state of XerC and XerD in the synaptic complex. In the absence of FtsK, Holliday Junctions (HJs) are created and resolved back to the original substrate in cycles of XerC-mediated strand exchanges [6]. FtsK presumably modifies the conformation of the recombinational complex, allowing XerD to mediate a first pair of strand exchanges, creating a new HJ intermediate that is resolved into crossing over by XerC-strand exchanges [6, 28, 51]. Because FtsK is a DNA translocase, it was initially believed that activation of Xer recombination was a consequence of the topological changes translocation could impose on the DNA globally. Indeed, this may well be the case in some species like *L. lactis* [52]. However, *E. coli* FtsK does not require to translocate on DNA over long distances to activate Xer recombination [46, 49]. It can also activate recombination across single stranded gaps [72]. A functional study of FtsK revealed a species-specific interaction between FtsKγ and the Xer recombinases [50], which led to the discovery of a functional interaction between FtsKγ and XerD [48]. Indeed, addition of FtsKγ in the absence of the translocase domain is sufficient to promote Xer recombination, clearly separating Xer activation from translocation [47]. Thus, *E. coli* FtsKγ plays two roles in Xer recombination.

The Anchoring Module

E. coli FtsK is anchored to the inner membrane by four transmembrane segments at its N-terminus [93]. Likewise, four transmembrane helices are predicted on the N-terminus of FtsK in most other bacterial species. In addition, four transmembrane helices are also present at the N-terminus of *B. subtilis* SpoIIIE. Similarly, all TraB proteins contain predicted N-terminal transmembrane helices [9]. However, given the fluidity of membranes, it is doubtful that transmembrane domains could be sufficient for the anchoring of pumps working against high forces. Neither are they essential since an N-terminal truncation of *E. coli* FtsK lacking all four transmembrane helices, $FtsK_{179–1329}$, is able to resolve chromosome dimers as efficiently as the full length protein [10]. In addition, a second FtsK/SpoIIIE-like protein is encoded in the genome of *B. subtilis*: SftA [54, 55]. SftA participates in chromosome segregation during vegetative cell division, notably to resolve chromosome dimers. SftA lacks any predicted transmembrane helices, just like $FtsK_{179–1329}$ [38].

What provides the anchoring of the FtsK family of pumps? *E. coli* FtsK is an essential component of the cell division machinery. It interacts with both early

(FtsZ) and late (FtsQ, FtsL and FtsW) cell division proteins through multiple regions ($FtsK_{1–179}$, $FtsK_{179–331}$ and $FtsK_{332–641}$), which anchors it to the septum [31, 38]. Even though a detailed map of molecular interactions is still lacking in *B. subtilis*, a similar scenario is probably true for SftA, which colocalizes with FtsZ at nascent division sites [54, 55], and for SpoIIIE, which targets to the septum of both tvegetative and sporulating cells in the presence of trapped DNA. In contrast, evidence has been obtained that the TraB proteins of the Streptomycetes conjugative plasmids localize at the hyphal tips of the mycelium through as yet unknown molecular interactions [27].

What is the function of the transmembrane helices found on most proteins of the FtsK family? SpoIIIE was reported to transport DNA across fused septal membranes during sporulation in *B. subtilis* [11]. Along with its involvement in membrane fission [12], it suggests that it pumps DNA through a pore or a channel. This is also very likely for the conjugative plasmid DNA transfer observed in the Streptomycetes. Correspondingly, spontaneously insertion of the pSVH1 TraB protein into membranes was shown to create ionic channels [9]. Deletion of the transmembrane region of the protein abolished this phenomenon, strongly suggesting that the transmembrane domain of SpoIIIE and TraB are implicated in pore formation. The topological similarity between the integral transmembrane domains of SpoIIIE and *E. coli* FtsK and the presence of a small patch of 36% of identity around their fourth transmembrane helix [94] suggested that $FtsK_{1–179}$ could also be involved in pore formation. However, fully efficient chromosome dimer resolution was observed in *E. coli* cells lacking the integral membrane domain of FtsK, indicating that pore formation is extremely rarely required [10]. This was all the more surprising as constriction initiation seems required for DNA translocation, which would leave little time for it before septum closure [77]. However, multiple regions along the FtsK protein are implicated in the progress of cell division [38, 41] and inactivation of FtsK translocation led to aberrant cell morphologies in *E. coli* cells carrying chromosomes with highly asymmetric replichores [39]. It is therefore tempting to speculate that there is a reciprocal control between DNA translocation and septum constriction, FtsK translocation serving as a DNA sensor to delay septum closure until the end of chromosome segregation.

Perspectives

Our understanding of the structure and function of the DNA pumps of the FtsK family has profited from a combination of genetics, cellular biology, biochemical and biophysical studies, including single molecule experiments. Many of our initial questions on this family of protein have been answered. However, several of them remain to be solved and numerous additional questions have been raised with each advance.

1. The translocation module of FtsK proteins, FtsKαβ, belongs to the P-loop NTPase superfamily. It assembles into a ring-shape hexameric motor with a

central opening [64] through which dsDNA is pumped at a high speed and against strong forces [67–69]. The hexameric motor does not follow the helical groove of the DNA helix so that little distortion of DNA superhelicity is introduced during translocation [13]. Energy for translocation comes from ATP hydrolysis. However, motors carrying several ATPase-deficient subunits still translocate at a high speed, albeit against lower forces [74]. This could be explained by an escort mechanism of translocation. However, we still lack structural and biochemical knowledge on the contacts made by each FtsKαβ subunit with dsDNA during translocation, on the allosteric changes driven by ATP binding, ATP hydrolysis and ADP release of a single subunit, and on how such changes can affect the DNA contacts made by the other subunits.

2. Orientation of translocation relies on the adjunction of a site-specific DNA binding domain, FtsKγ, to FtsKαβ, which serves to load the motor in a specific orientation on specific repeated DNA motifs (Fig. 12.4, [46, 63, 87]). Although it remained a matter of debate and controversy for a long time, it is now widely admitted that FtsK motors do not recognize the orientation motifs in the course of translocation, whether they are in the correct or opposite orientation with respect to the direction of translocation of the motor (Fig. 12.4). What prevents FtsKγ from contacting DNA during translocation? Future work will need to assess the properties of FtsK motors lacking the FtsKγ module or carrying modules that cannot recognize the motifs.
3. The DNA molecules that are transported by FtsK pumps are circular, which creates a topological problem for their loading and unloading, and for the completion of DNA transport across membranes. Both in vivo and in vitro experiments suggest that the *E. coli* FtsKαβ hexamerizes only at high concentration and in the presence of DNA [21, 64, 73], which explains how it can load on circular DNA molecules (Fig. 12.4). However, it remains to be understood how FtsK pumps fall apart at the end of translocation. Is the disassembly passive or is there a specific active mechanism? In this aspect, it is interesting to note that *E. coli* FtsK stops translocating when it encounters XerC and XerD at *dif* [75]. In contrast, it seems to be able to eject most other DNA binding proteins [70, 71]. As FtsKγ interacts with XerD [48], it is tempting to imagine that contacts with the recombinases affect the stability of the motor, thereby facilitating its unloading at the end of translocation (Fig. 12.4). Understanding how motors unload is all the more important for DNA pumps that transport DNA across a membrane pore, like SpoIIIE and TraB, since the membrane creates a physical barrier for the transfer of DNA [9, 11]. Two models have been proposed for the transport of circular DNA molecule across fully closed membranes. In the first one, a pore for a single DNA duplex is formed by the six integral domain of hexameric pumps (Fig. 12.5a). Two pumps are required for the simultaneous transfer of the two dsDNA arms of a single circular DNA molecule [11]. Translocation stops when the DNA pumps collide against each other. The motors then unload and the two pores fuse to allow for the passage of the remaining dsDNA segment by a passive mechanism. In the second model, it is proposed that the integral domains of dozens of FtsK proteins create a channel large enough to accommodate two DNA

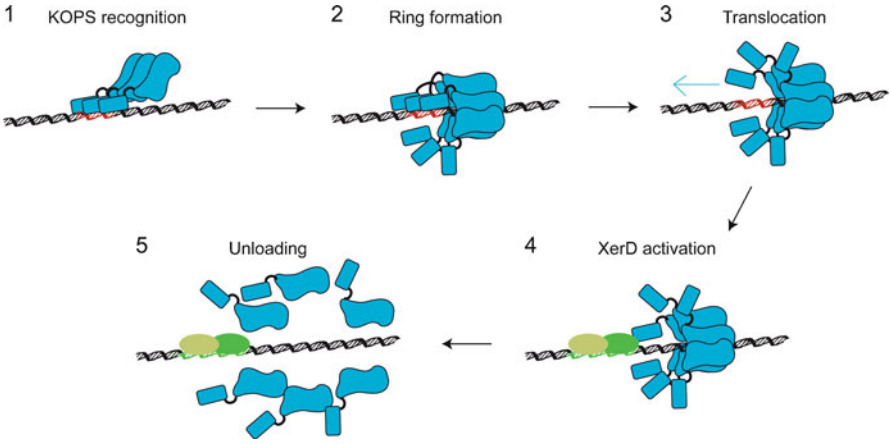

Fig. 12.4 Assembly and disassembly of the FtsK pumps. (1) Oriented loading on KOPS. Three FtsKγ bind one KOPS (in *red*). (2) Hexamerization of FtsKαβ. (3) Translocation. FtsKγ domains do not contact the DNA. The *blue arrow* shows the orientation of the translocation. (4) XerD activation. When the FtsK hexamer reaches XerCD (respectively in *light* and *dark green*) bound to *dif* site (*green* DNA), translocation is stopped, allowing one FtsKγ domain to interact with XerD. (5) Unloading of the pump via the disassembly of the FtsK hexamer

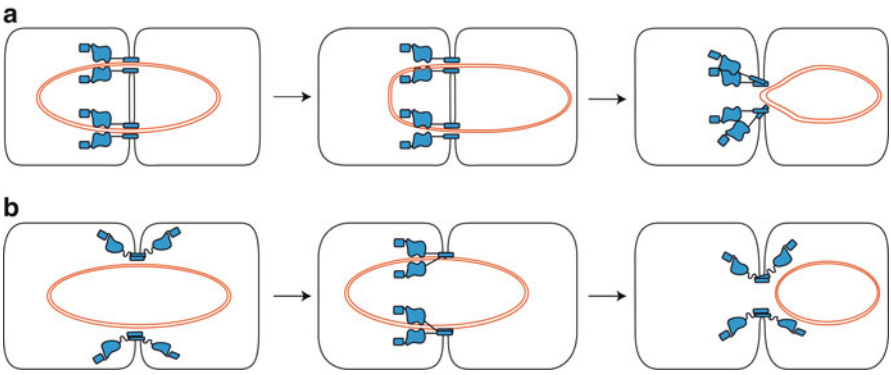

Fig. 12.5 Topology of the pores formed by FtsK pumps. (**a**) The one pore-one pump model. (**b**) The one channel-multiple pumps model

duplexes (Fig. 12.5a). Several hexameric pumps are connected to this DNA channel and they take charge of the DNA molecule simultaneously. An advantage of this model is that it can be applied to proteins that create pores like TraB and SpoIIIE, but also to proteins for which pore formation is dispensable like FtsK and SftA. Transport of chromosomes across an incompletely formed septum is compatible with the observation that active SpoIIIE molecules are only found on the side of the septum from which DNA is exported [17, 22, 23]: because of the expected inertia of chromosomes, FtsKαβ modules should initially move away from the septum after loading. This movement should persist until the

linker arms are fully extended so that they should end up on the side from which DNA is exported (Fig. 12.5b).

4. Excision of small DNA cassettes inserted in the *E. coli* chromosome between two directly repeated *dif* sites has been used to estimate the frequency of activation of Xer recombination by FtsK in vivo, and hence the timing and zone of activity of the FtsK pumps [45, 77]. The frequency of *dif*-cassette excision drops when homologous recombination is abolished [6, 77, 95] suggesting that *E. coli* FtsK loads very infrequently on monomeric chromosomes and that its role is mainly restricted to chromosome dimer resolution. Likewise, FtsK has been shown to control the XerCD/*dif* dimer resolution system of *V. cholerae*, *H. influenzae* and Lactococci [28, 50, 52, 96]. SpoIIIE was shown to participate, together with SftA, in chromosome dimer resolution in *B. subtilis* [56]. However, translocation by *E. coli* FtsK seems to be also required when TopoIV activity is compromised [57, 61], when the organization and/or the packaging of the chromosome are altered [39, 40] or when chromosome replication is affected [97]. In addition, FtsK translocation seems to be essential in *C. crescentus* [62]. In *V. cholerae,* we got evidence that it loads on monomeric chromosomes as frequently as on dimeric chromosomes (G. Demarre and F.-X. Barre, unpublished results). Correspondingly, cells harbouring FtsK mutants deficient in translocation are much sicker than cells in which Xer recombination is compromised (G. Demarre and F.-X. Barre, unpublished results). Therefore, we believe that the role of FtsK translocation is not limited to chromosome dimer resolution and that studying other model organisms should help us gain further insight into its multiple functions.
5. Finally, we would like to emphasize our lack of knowledge on the mechanisms that coordinate the activity of the FtsK family of proteins with the other cellular processes. In *E. coli*, excision of *dif*-cassettes was found to occur shortly before or commensurate with septum closure [77]. Septum formation is a complex process that involves the ordered recruitment of more than a dozen proteins. FtsK is recruited to the septum at an early stage of septum assembly, corresponding to the recruitment and stabilization of a ring of the tubulin-like FtsZ protein, but no visible constriction at midcell [32, 33]. Constriction occurs during the second stage of septum formation, after the recruitment of proteins involved in the synthesis and degradation of the peptidoglycan (Fig. 12.6). Thus, *E. coli* FtsK activity seems to be delayed with respect to its septal recruitment, which leaves little time for chromosome dimer resolution before cell fission (Fig. 12.6, green arrow). This is all the more intriguing as dimer resolution does not depend on the integral domain of the protein, ruling out models in which it would form a pore to pass chromosomal DNA through closed septal membranes [10]. However, *E. coli* FtsK participates in the recruitment and stabilization of the peptidoglycan synthesis and degradation machinery [30, 41] and could delay septum closure until chromosome segregation is achieved [38, 39]. Correspondingly, SpoIIIE seems to be implicated in membrane fusion [12]. Thus, FtsK is ideally suited to create a cell cycle checkpoint, which would serve as a last safeguard to avoid division over partially segregated chromosomes (Fig. 12.6, red arrow). Recent

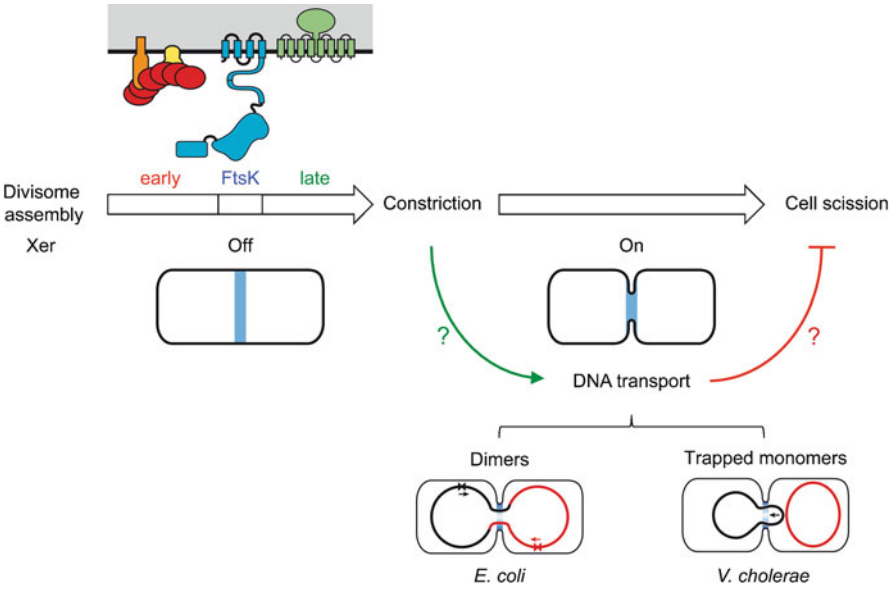

Fig. 12.6 Integration between cell division and chromosome segregation. In the scheme of the different divisome proteins, three early cell division proteins, FtsZ, FtsA and ZipA, are shown in *red*, *orange* and *yellow*, respectively, and two late cell division proteins, FtsI and FtsW, are shown in *green*

progress has unravelled a variety of regulatory circuits that help synchronize DNA synthesis, chromosome segregation and cell division in bacteria (see [98] for a review). Most of them are not conserved or are effected by divergent machineries. For instance, different machineries serve to delay septum formation in the rod shaped *E. coli* and *B. subtilis* bacteria when DNA damages trigger the SOS response or when unsegregated DNA is still present at midcell. Likewise, the *minCD* system inhibits random septum formation along the long axis of the *E. coli* and *B. subtilis* rods by different mechanisms. In *C. crescentus*, the *minCD* system itself is functionally replaced by an interaction between an inhibitor of septation and a system controlling the position of the region surrounding the origin of replication of the chromosome. In contrast, the FtsK checkpoint could be a general feature of the bacterial cell cycle. Therefore, future studies should aim at deciphering the molecular mechanisms that allow for the control of the DNA translocation activity of FstK during septation and at establishing the existence and the generality of a checkpoint mechanism that could reciprocally control the progress of septation (Fig. 12.6).

Acknowledgements We would like to acknowledge financial support from the Agence Nationale pour la Recherche [ANR-09-BLAN-0258] and from the European Research Council under the European Community's Seventh Framework Programme [FP7/2007-2013 Grant Agreement no. 281590].

References

1. Mitchison TJ, Salmon ED. Mitosis: a history of division. Nat Cell Biol. 2001;3(1):E17–21.
2. Bouet JY, Nordstrom K, Lane D. Plasmid partition and incompatibility–the focus shifts. Mol Microbiol. 2007;65(6):1405–14.
3. Schumacher MA. Structural biology of plasmid partition: uncovering the molecular mechanisms of DNA segregation. Biochem J. 2008;412(1):1–18.
4. Wu LJ, Lewis PJ, Allmansberger R, Hauser PM, Errington J. A conjugation-like mechanism for prespore chromosome partitioning during sporulation in Bacillus subtilis. Genes Dev. 1995;9(11):1316–26.
5. Wu LJ, Errington J. Bacillus subtilis spoIIIE protein required for DNA segregation during asymmetric cell division. Science. 1994;264(5158):572–5.
6. Barre FX, et al. FtsK functions in the processing of a Holliday junction intermediate during bacterial chromosome segregation. Genes Dev. 2000;14(23):2976–88.
7. Steiner W, Liu G, Donachie WD, Kuempel P. The cytoplasmic domain of FtsK protein is required for resolution of chromosome dimers. Mol Microbiol. 1999;31(2):579–83.
8. Possoz C, Ribard C, Gagnat J, Pernodet JL, Guerineau M. The integrative element pSAM2 from Streptomyces: kinetics and mode of conjugal transfer. Mol Microbiol. 2001;42(1):159–66.
9. Vogelmann J, et al. Conjugal plasmid transfer in Streptomyces resembles bacterial chromosome segregation by FtsK/SpoIIIE. EMBO J. 2011;30(11):2246–54.
10. Dubarry N, Barre FX. Fully efficient chromosome dimer resolution in Escherichia coli cells lacking the integral membrane domain of FtsK. EMBO J. 2010;29(3):597–605.
11. Burton BM, Marquis KA, Sullivan NL, Rapoport TA, Rudner DZ. The ATPase SpoIIIE transports DNA across fused septal membranes during sporulation in Bacillus subtilis. Cell. 2007;131(7):1301–12.
12. Fleming TC, et al. Dynamic SpoIIIE assembly mediates septal membrane fission during Bacillus subtilis sporulation. Genes Dev. 2010;24(11):1160–72.
13. Saleh OA, Bigot S, Barre FX, Allemand JF. Analysis of DNA supercoil induction by FtsK indicates translocation without groove-tracking. Nat Struct Mol Biol. 2005;12(5):436–40.
14. Bigot S, et al. KOPS: DNA motifs that control E. coli chromosome segregation by orienting the FtsK translocase. EMBO J. 2005;24(21):3770–80.
15. Ptacin JL, et al. Sequence-directed DNA export guides chromosome translocation during sporulation in Bacillus subtilis. Nat Struct Mol Biol. 2008;15(5):485–93.
16. Levy O, et al. Identification of oligonucleotide sequences that direct the movement of the Escherichia coli FtsK translocase. Proc Natl Acad Sci U S A. 2005;102(49):17618–23.
17. Becker EC, Pogliano K. Cell-specific SpoIIIE assembly and DNA translocation polarity are dictated by chromosome orientation. Mol Microbiol. 2007;66(5):1066–79.
18. Piggot PJ, Hilbert DW. Sporulation of Bacillus subtilis. Curr Opin Microbiol. 2004;7(6):579–86.
19. Wu LJ, Errington J. Septal localization of the SpoIIIE chromosome partitioning protein in Bacillus subtilis. EMBO J. 1997;16(8):2161–9.
20. Bath J, Wu LJ, Errington J, Wang JC. Role of bacillus subtilis SpoIIIE in DNA transport across the mother cell-prespore division septum. Science. 2000;290(5493):995–7.
21. Ben-Yehuda S, Rudner DZ, Losick R. Assembly of the SpoIIIE DNA translocase depends on chromosome trapping in Bacillus subtilis. Curr Biol. 2003;13(24):2196–200.
22. Sharp MD, Pogliano K. Role of cell-specific SpoIIIE assembly in polarity of DNA transfer. Science. 2002;295(5552):137–9.
23. Sharp MD, Pogliano K. MinCD-dependent regulation of the polarity of SpoIIIE assembly and DNA transfer. EMBO J. 2002;21(22):6267–74.
24. Sharp MD, Pogliano K. An in vivo membrane fusion assay implicates SpoIIIE in the final stages of engulfment during Bacillus subtilis sporulation. Proc Natl Acad Sci U S A. 1999;96(25):14553–8.
25. Sharp MD, Pogliano K. The membrane domain of SpoIIIE is required for membrane fusion during Bacillus subtilis sporulation. J Bacteriol. 2003;185(6):2005–8.
26. Liu NJ, Dutton RJ, Pogliano K. Evidence that the SpoIIIE DNA translocase participates in membrane fusion during cytokinesis and engulfment. Mol Microbiol. 2006;59(4):1097–113.

27. Reuther J, Gekeler C, Tiffert Y, Wohlleben W, Muth G. Unique conjugation mechanism in mycelial streptomycetes: a DNA-binding ATPase translocates unprocessed plasmid DNA at the hyphal tip. Mol Microbiol. 2006;61(2):436–46.
28. Val M-E, et al. FtsK-dependent dimer resolution on multiple chromosomes in the pathogen Vibrio cholerae. PLoS Genet. 2008;4(9):e1000201.
29. Kono N, Arakawa K, Tomita M. Comprehensive prediction of chromosome dimer resolution sites in bacterial genomes. BMC Genomics. 2011;12(1):19.
30. Begg KJ, Dewar SJ, Donachie WD. A new Escherichia coli cell division gene, ftsK. J Bacteriol. 1995;177(21):6211–22.
31. Di Lallo G, Fagioli M, Barionovi D, Ghelardini P, Paolozzi L. Use of a two-hybrid assay to study the assembly of a complex multicomponent protein machinery: bacterial septosome differentiation. Microbiology. 2003;149(Pt 12):3353–9.
32. Yu XC, Tran AH, Sun Q, Margolin W. Localization of cell division protein FtsK to the Escherichia coli septum and identification of a potential N-terminal targeting domain. J Bacteriol. 1998;180(5):1296–304.
33. Wang L, Lutkenhaus J. FtsK is an essential cell division protein that is localized to the septum and induced as part of the SOS response. Mol Microbiol. 1998;29(3):731–40.
34. Liu G, Draper GC, Donachie WD. FtsK is a bifunctional protein involved in cell division and chromosome localization in Escherichia coli. Mol Microbiol. 1998;29(3):893–903.
35. Draper GC, McLennan N, Begg K, Masters M, Donachie WD. Only the N-terminal domain of FtsK functions in cell division. J Bacteriol. 1998;180(17):4621–7.
36. Chen JC, Beckwith J. FtsQ, FtsL and FtsI require FtsK, but not FtsN, for co-localization with FtsZ during Escherichia coli cell division. Mol Microbiol. 2001;42(2):395–413.
37. Geissler B, Margolin W. Evidence for functional overlap among multiple bacterial cell division proteins: compensating for the loss of FtsK. Mol Microbiol. 2005;58(2):596–612.
38. Dubarry N, Possoz C, Barre FX. Multiple regions along the Escherichia coli FtsK protein are implicated in cell division. Mol Microbiol. 2010;78(1088–1100):1088–100.
39. Lesterlin C, Pages C, Dubarry N, Dasgupta S, Cornet F. Asymmetry of chromosome Replichores renders the DNA translocase activity of FtsK essential for cell division and cell shape maintenance in Escherichia coli. PLoS Genet. 2008;4(12):e1000288.
40. Yu XC, Weihe EK, Margolin W. Role of the C terminus of FtsK in Escherichia coli chromosome segregation. J Bacteriol. 1998;180(23):6424–8.
41. Bigot S, Corre J, Louarn J, Cornet F, Barre FX. FtsK activities in Xer recombination, DNA mobilization and cell division involve overlapping and separate domains of the protein. Mol Microbiol. 2004;54(4):876–86.
42. Recchia GD, Aroyo M, Wolf D, Blakely G, Sherratt DJ. FtsK-dependent and -independent pathways of Xer site-specific recombination. EMBO J. 1999;18(20):5724–34.
43. Deghorain M, et al. A defined terminal region of the E. coli chromosome shows late segregation and high FtsK activity. PLoS One. 2011;6(7):e22164.
44. Capiaux H, Lesterlin C, Perals K, Louarn JM, Cornet F. A dual role for the FtsK protein in Escherichia coli chromosome segregation. EMBO Rep. 2002;3(6):532–6.
45. Perals K, Cornet F, Merlet Y, Delon I, Louarn JM. Functional polarization of the Escherichia coli chromosome terminus: the dif site acts in chromosome dimer resolution only when located between long stretches of opposite polarity. Mol Microbiol. 2000;36(1):33–43.
46. Bigot S, Saleh OA, Cornet F, Allemand JF, Barre FX. Oriented loading of FtsK on KOPS. Nat Struct Mol Biol. 2006;13(11):1026–8.
47. Grainge I, Lesterlin C, Sherratt DJ. Activation of XerCD-dif recombination by the FtsK DNA translocase. Nucleic Acids Res. 2011;39(12):5140–8.
48. Yates J, et al. Dissection of a functional interaction between the DNA translocase, FtsK, and the XerD recombinase. Mol Microbiol. 2006;59(6):1754–66.
49. Massey TH, Aussel L, Barre F-X, Sherratt DJ. Asymmetric activation of Xer site-specific recombination by FtsK. EMBO Rep. 2004;5(4):399–404.
50. Yates J, Aroyo M, Sherratt DJ, Barre FX. Species specificity in the activation of Xer recombination at dif by FtsK. Mol Microbiol. 2003;49(1):241–9.

51. Aussel L, et al. FtsK is a DNA motor protein that activates chromosome dimer resolution by switching the catalytic state of the XerC and XerD recombinases. Cell. 2002;108(2):195–205.
52. Nolivos S, Pages C, Rousseau P, Le Bourgeois P, Cornet F. Are two better than one? Analysis of an FtsK/Xer recombination system that uses a single recombinase. Nucleic Acids Res. 2010;38(19):6477–89.
53. Nolivos S, et al. Co-evolution of segregation guide DNA motifs and the FtsK translocase in bacteria: identification of the atypical Lactococcus lactis KOPS motif. Nucleic Acids Res. 2012;40:5535–45.
54. Kaimer C, Gonzalez-Pastor JE, Graumann PL. SpoIIIE and a novel type of DNA translocase, SftA, couple chromosome segregation with cell division in Bacillus subtilis. Mol Microbiol. 2009;74(4):810–25.
55. Biller SJ, Burkholder WF. The Bacillus subtilis SftA (YtpS) and SpoIIIE DNA translocases play distinct roles in growing cells to ensure faithful chromosome partitioning. Mol Microbiol. 2009;74(4):790–809.
56. Kaimer C, Schenk K, Graumann PL. Two DNA translocases synergistically affect chromosome dimer resolution in Bacillus subtilis. J Bacteriol. 2011;193(6):1334–40.
57. Grainge I, et al. Unlinking chromosome catenanes in vivo by site-specific recombination. EMBO J. 2007;26(19):4228–38.
58. Ip SC, Bregu M, Barre FX, Sherratt DJ. Decatenation of DNA circles by FtsK-dependent Xer site-specific recombination. EMBO J. 2003;22(23):6399–407.
59. Bigot S, Marians KJ. DNA chirality-dependent stimulation of topoisomerase IV activity by the C-terminal AAA+ domain of FtsK. Nucleic Acids Res. 2010;38(9):3031–40.
60. Espeli O, Levine C, Hassing H, Marians KJ. Temporal regulation of topoisomerase IV activity in E. coli. Mol Cell. 2003;11(1):189–201.
61. Espeli O, Lee C, Marians KJ. A physical and functional interaction between Escherichia coli FtsK and topoisomerase IV. J Biol Chem. 2003;278(45):44639–44.
62. Wang SC, West L, Shapiro L. The bifunctional FtsK protein mediates chromosome partitioning and cell division in Caulobacter. J Bacteriol. 2006;188(4):1497–508.
63. Sivanathan V, et al. The FtsK gamma domain directs oriented DNA translocation by interacting with KOPS. Nat Struct Mol Biol. 2006;13(11):965–72.
64. Massey TH, Mercogliano CP, Yates J, Sherratt DJ, Lowe J. Double-stranded DNA translocation: structure and mechanism of hexameric FtsK. Mol Cell. 2006;23:457–69.
65. Iyer LM, Makarova KS, Koonin EV, Aravind L. Comparative genomics of the FtsK-HerA superfamily of pumping ATPases: implications for the origins of chromosome segregation, cell division and viral capsid packaging. Nucleic Acids Res. 2004;32(17):5260–79.
66. Gomis-Ruth FX, et al. The bacterial conjugation protein TrwB resembles ring helicases and F1-ATPase. Nature. 2001;409(6820):637–41.
67. Saleh OA, Perals C, Barre FX, Allemand JF. Fast, DNA-sequence independent translocation by FtsK in a single-molecule experiment. EMBO J. 2004;23(12):2430–9.
68. Pease PJ, et al. Sequence-directed DNA translocation by purified FtsK. Science. 2005;307(5709):586–90.
69. Lee JY, Finkelstein IJ, Crozat E, Sherratt DJ, Greene EC. Single-molecule imaging of DNA curtains reveals mechanisms of KOPS sequence targeting by the DNA translocase FtsK. Proc Natl Acad Sci U S A. 2012;109(17):6531–6.
70. Marquis KA, et al. SpoIIIE strips proteins off the DNA during chromosome translocation. Genes Dev. 2008;22(13):1786–95.
71. Lau IF, et al. Spatial and temporal organization of replicating Escherichia coli chromosomes. Mol Microbiol. 2003;49(3):731–43.
72. Bonne L, Bigot S, Chevalier F, Allemand JF, Barre FX. Asymmetric DNA requirements in Xer recombination activation by FtsK. Nucleic Acids Res. 2009;37(7):2371–80.
73. Graham JE, Sherratt DJ, Szczelkun MD. Sequence-specific assembly of FtsK hexamers establishes directional translocation on DNA. Proc Natl Acad Sci U S A. 2010;107(47):20263–8.
74. Crozat E, et al. Separating speed and ability to displace roadblocks during DNA translocation by FtsK. EMBO J. 2010;29(8):1423–33.

75. Graham JE, Sivanathan V, Sherratt DJ, Arciszewska LK. FtsK translocation on DNA stops at XerCD-dif. Nucleic Acids Res. 2009;38(1):72–81.
76. Lowe J, et al. Molecular mechanism of sequence-directed DNA loading and translocation by FtsK. Mol Cell. 2008;31(4):498–509.
77. Kennedy SP, Chevalier F, Barre FX. Delayed activation of Xer recombination at dif by FtsK during septum assembly in Escherichia coli. Mol Microbiol. 2008;68(4):1018–28.
78. Enemark EJ, Joshua-Tor L. Mechanism of DNA translocation in a replicative hexameric helicase. Nature. 2006;442(7100):270–5.
79. Cornet F, Louarn J, Patte J, Louarn JM. Restriction of the activity of the recombination site dif to a small zone of the Escherichia coli chromosome. Genes Dev. 1996;10(9):1152–61.
80. Mercier R, et al. The MatP/matS site-specific system organizes the terminus region of the E. coli chromosome into a macrodomain. Cell. 2008;135(3):475–85.
81. Espeli O, Mercier R, Boccard F. DNA dynamics vary according to macrodomain topography in the E. coli chromosome. Mol Microbiol. 2008;68(6):1418–27.
82. Lesterlin C, Mercier R, Boccard F, Barre FX, Cornet F. Roles for replichores and macrodomains in segregation of the Escherichia coli chromosome. EMBO Rep. 2005;6:557–62.
83. Valens M, Penaud S, Rossignol M, Cornet F, Boccard F. Macrodomain organization of the Escherichia coli chromosome. EMBO J. 2004;23(21):4330–41.
84. Meile JC, et al. The terminal region of the E. coli chromosome localises at the periphery of the nucleoid. BMC Microbiol. 2011;11(1):28.
85. Corre J, Patte J, Louarn JM. Prophage lambda induces terminal recombination in Escherichia coli by inhibiting chromosome dimer resolution. An orientation-dependent cis-effect lending support to bipolarization of the terminus. Genetics. 2000;154(1):39–48.
86. Corre J, Louarn JM. Evidence from terminal recombination gradients that FtsK uses replichore polarity to control chromosome terminus positioning at division in Escherichia coli. J Bacteriol. 2002;184(14):3801–7.
87. Ptacin JL, Nollmann M, Bustamante C, Cozzarelli NR. Identification of the FtsK sequence-recognition domain. Nat Struct Mol Biol. 2006;13(11):1023–5.
88. Spies M, et al. A molecular throttle: the recombination hotspot chi controls DNA translocation by the RecBCD helicase. Cell. 2003;114(5):647–54.
89. Taylor AF, Schultz DW, Ponticelli AS, Smith GR. RecBC enzyme nicking at Chi sites during DNA unwinding: location and orientation-dependence of the cutting. Cell. 1985;41(1):153–63.
90. Sourice S, Biaudet V, El Karoui M, Ehrlich SD, Gruss A. Identification of the Chi site of Haemophilus influenzae as several sequences related to the Escherichia coli Chi site. Mol Microbiol. 1998;27(5):1021–9.
91. El Karoui M, et al. Orientation specificity of the Lactococcus lactis chi site. Genes Cells. 2000;5(6):453–61.
92. El Karoui M, Biaudet V, Schbath S, Gruss A. Characteristics of Chi distribution on different bacterial genomes. Res Microbiol. 1999;150(9–10):579–87.
93. Dorazi R, Dewar SJ. Membrane topology of the N-terminus of the Escherichia coli FtsK division protein. FEBS Lett. 2000;478(1–2):13–8.
94. Barre FX. FtsK and SpoIIIE: the tale of the conserved tails. Mol Microbiol. 2007;66(5):1051–5.
95. Perals K, et al. Interplay between recombination, cell division and chromosome structure during chromosome dimer resolution in Escherichia coli. Mol Microbiol. 2001;39(4):904–13.
96. Le Bourgeois P, et al. The unconventional Xer recombination machinery of Streptococci/Lactococci. PLoS Genet. 2007;3(7):e117.
97. McCool JD, Sandler SJ. Effects of mutations involving cell division, recombination, and chromosome dimer resolution on a priA2::kan mutant. Proc Natl Acad Sci U S A. 2001;98(15):8203–10.
98. Thanbichler M. Synchronization of chromosome dynamics and cell division in bacteria. Cold Spring Harb Perspect Biol. 2010;2(1):a000331.

Chapter 13
ATP-Dependent Chromatin Remodeling

Jaya Yodh

Abstract In the eukaryotic nucleus, processes of DNA metabolism such as transcription, DNA replication, and repair occur in the context of DNA packaged into nucleosomes and higher order chromatin structures. In order to overcome the barrier presented by chromatin structures to the protein machinery carrying out these processes, the cell relies on a class of enzymes called chromatin remodeling complexes which catalyze ATP-dependent restructuring and repositioning of nucleosomes. Chromatin remodelers are large multi-subunit complexes which all share a common SF2 helicase ATPase domain in their catalytic subunit, and are classified into four different families—SWI/SNF, ISWI, CHD, INO80—based on the arrangement of other domains in their catalytic subunit as well as their non-catalytic subunit composition. A large body of structural, biochemical, and biophysical evidence suggests chromatin remodelers operate as histone octamer-anchored directional DNA translocases in order to disrupt DNA–histone interactions and catalyze nucleosome sliding. Remodeling mechanisms are family-specific and depend on factors such as how the enzyme engages with nucleosomal and linker DNA, features of DNA loop intermediates, specificity for mono- or oligonucleosomal substrates, and ability to remove histones and exchange histone variants. Ultimately, the biological function of chromatin remodelers and their genomic targeting in vivo is regulated by each complex's subunit composition, association with chromatin modifiers and histone chaperones, and affinity for chromatin signals such as histone posttranslational modifications.

J. Yodh (✉)
Department of Physics, University of Illinois at Urbana-Champaign,
Urbana, IL, USA
e-mail: jyodh@illinois.edu

M. Spies (ed.), *DNA Helicases and DNA Motor Proteins*, Advances in Experimental Medicine and Biology, DOI 10.1007/978-1-4614-5037-5_13,

Chromatin: The Physiological Substrate for DNA Metabolism

The eukaryotic nucleus is faced with the challenge of containing chromosomal DNA approximately 2 m in length. This topological barrier is solved via packaging of DNA into chromatin nucleoprotein structures. The nucleosome is the fundamental structural unit of chromatin, comprising 145–147 bp of DNA wrapped 1.65 times in a left-handed superhelical spiral around a core histone octamer complex [1]. This octamer is comprised of two copies of each of four core histone proteins, H2A, H2B, H3, and H4, that assembles from a $(H3–H4)_2$ tetramer flanked on either side by a H2A–H2B dimer (Fig. 13.1a).

The individual core histone proteins each contain a globular histone fold domain (80–90 amino acids) that shows strong structural homology across evolution despite little sequence conservation. The histone fold consists of two short helices flanking a longer central α-helix, and provides the structural basis for dimer formation within the octamer by head-to-tail association of the fold portion of two chains in a characteristic hand-shake motif [2]. The core histones also contain evolutionarily conserved N- and C-terminal tail domains (20–35 residues) which are random coil in structure and contain many basic residues responsible for intra-nucleosomal electrostatic tail–DNA interaction as well as inter-nucleosomal tail–DNA and tail–tail interactions in higher-order structures. The histone tails contain conserved residues that are subject to posttranslational modifications (PTMs) such as acetylation, methylation, phosphorylation, and ubiquitylation which are involved in epigenetic regulation of gene expression.

Details of histone–histone and histone–DNA interactions have been revealed through crystal structures of canonical and variant nucleosome core particles (NCPs) [3]. One of the key features is a twofold symmetry around a dyad axis originating at the half-way point in the DNA sequence. The $(H3–H4)_2$ tetramer interacts with the single DNA helix dyad region through a 4-helix H3–H3′ bundle, and H2A–H2B dimers interact with the two DNA helices on the face opposite the dyad. While the interactions between the dimers are relatively minor, dimer–tetramer interaction interfaces are formed by a H2B–H4 4-helix bundle and by the H2A docking domain and the opposite arm of the tetramer [1, 4].

In terms of histone–DNA interactions, there are 14 superhelical (SHL) regions of interaction between the histone core and the minor groove of DNA (numbered 0.5–6.5 in either direction from the dyad (0)). These interactions are not sequence-specific and involve main chain and side chain phosphate interactions, additional ionic interactions, arginine insertion, and water-mediated H-bonds [3]. Crystal structures with satellite palindromic and 601 nucleosome positioning sequences [5] provide evidence for intrinsic site-specific 1 bp stretching at SHL ±2 and SHL ±5 which likely will affect recognition by regulatory proteins [4]. Another key factor in nucleosome positioning is the sequence propensity for highly flexible base pair steps. In vitro selection studies on nucleosome positioning sequences revealed enrichment of TA di-nucleotides at positions requiring maximal bending/compression of the minor groove. One particular narrow minor groove is achieved at SHL

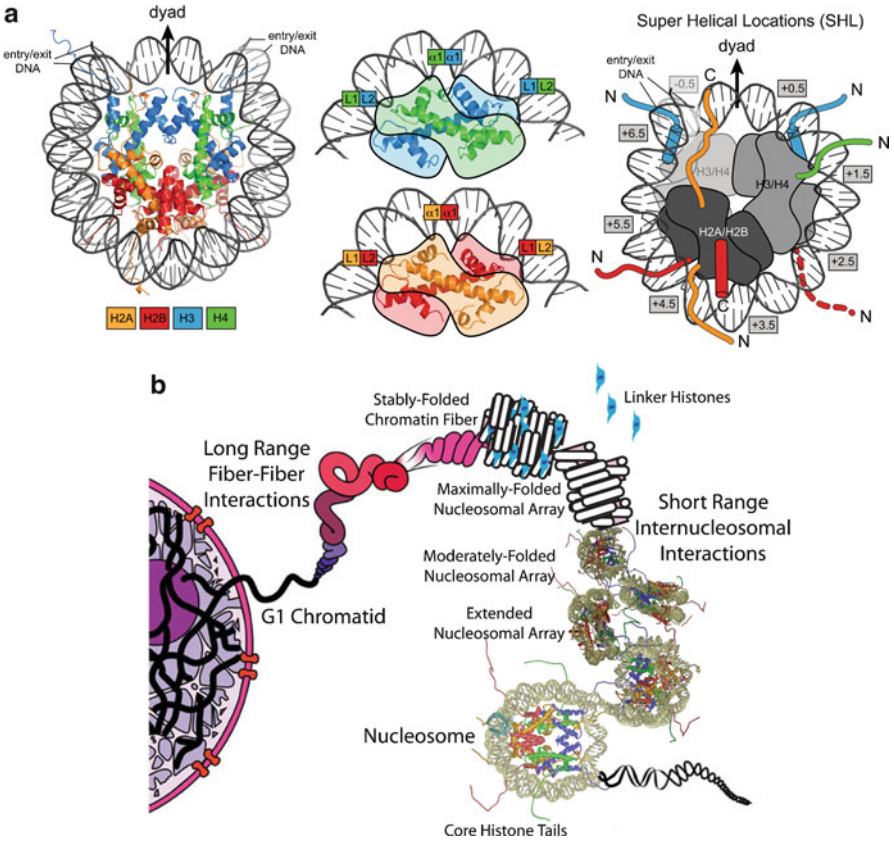

Fig. 13.1 Nucleosome and chromatin structure. (**a**) Features of the nucleosome core particle (NCP). (*Left*) Crystal structure of the NCP [1]. DNA (146 bp) wraps in left-handed superhelix around an octamer of core histones (H2A (*yellow*), H2B (*red*), H3 (*blue*), H4 (*green*)), that is composed of a two H2A–H2B dimers which flank a central $(H3–H4)_2$ tetramer (comprised of two H3–H4 dimers). The tetramer contacts the dyad, the twofold axis of symmetry centered halfway through the DNA. (*Center*) Each histone dimer in the nucleosome contacts three consecutive minor grooves, with the central contact made by α1 helix of each histone in the dimer (α1–α1 motif) and the two side contacts made by loops positioned before helix 2 of one histone and helix 3 of the other histone in the dimer (L1–L2 motif), thus contacting all 12 minor grooves in the nucleosome. (*Right*) Nucleosome superhelical locations (SHL) are defined as alternating regions where DNA major and minor grooves face the histone core. Starting from the dyad, defined as SHL0, consecutive major grooves are labeled SHL +1, +2, etc. (and SHL −1, −2 in the opposite direction), while minor grooves are similarly labeled SHL ±0.5, ±1.5, etc. Therefore, H3/H4 dimers coordinate SHL ±0.5, ±1.5, ±2.5—the three minor grooves on either side of dyad, while H2A/H2B dimers contact SHL ±3.5, ±4.5, ±5.5. The N- and C-terminal tails of the core histones (*colored lines*) are unstructured and shown projecting from the nucleosome core. Additional minor groove contacts are also shown for the H3 N-terminal tail and helix (*blue*). See text for further details. Reprinted from [89] with permission from Elsevier Limited. (**b**) Levels of DNA compaction in eukaryotes range from naked DNA to fully condensed chromatid, with the nucleosome as the fundamental structural unit. The first intermediate structure is the extended nucleosomal array or 10-nm fiber in which nucleosomes are spaced by ~200 bp. Histone N-terminal tail–tail and tail–DNA interactions facilitate formation of a moderately folded nucleosomal array. Addition of linker histones and other chromatin-binding proteins promotes maximal folding of the nucleosomal array and formation of the 30-nm fiber via short-range internucleosomal interactions. Long-range fiber–fiber interactions eventually compact the chromatin fiber an additional 500-fold into the transcriptionally inert metaphase chromosome. See text for further details. Reprinted from [19] with permission from Elsevier Limited

±1.5 via a unique histone sugar clamp motif, and this region likely is responsible for positioning power of TTTAA elements in vitro (601 NCPs [5] contain this sequence at SHL ±1.5) and TATAA sequence in vivo [6]. In terms of unwrapping potential, single-molecule experiments involving force-induced unzipping of nucleosomal DNA revealed three major regions of unwrapping with the most force required to unzip interactions at the dyad and less force required to unwrap exterior arms, consistent with fewer histone–DNA contacts in these regions [7].

The nucleosome itself is dynamic and can adopt various noncanonical conformations (reviewed in [8, 9]) including structural isomers containing histone variants, or sub-nucleosomal particles such as the "tetrasome" and "di-tetrasome" (which contain only the $(H3–H4)_2$ tetramer), and the "hexasome" which has lost one H2A/H2B dimer. These structures are relevant to the idea of "open" nucleosome states, recently supported by a single-molecule fluorescence study identifying a salt-induced nucleosome unwrapping intermediate in which the dimer/tetramer interface is disrupted but the dimers are still associated with DNA [10]. Super-nucleosomal particles have also been proposed such as the "altosome"—asymmetric dinucleosomes with partially loosened DNA [11, 12], and "reversome"—chromatin fibers containing histone octamers with DNA wrapped in a right-handed supercoil (R-octasome) [13]. Centromeric chromatin has been associated with "hemisomes"—heterotypic tetrasomes with one copy each of the core histones, with H3 replaced by the centromeric variant, CENH3 [14]. Noncanonical nucleosome conformations are typically achieved during transcription or nucleosome assembly through the action of histone chaperones, chromatin remodeling complexes, and chromatin modifying enzymes (see sections "Families of Chromatin Remodelers," "ATP-Dependent Activities of Chromatin Remodelers and Mechanisms for Chromatin Mobilization," and "Regulation of Chromatin Remodeler Activity: Genomic Targeting and Interplay with Histone Modifications and Modifiers").

In the eukaryotic cell, the nucleosome (6 nm height × 10 nm width) provides the fundamental unit for condensation into higher order structures (shown schematically in Fig. 13.1b) (reviewed in [15–19]). Two major types of chromatin fibers have been observed in interphase chromatin. The 10-nm diameter "beads-on-a-string" fiber spaces nucleosome "beads" every ~200 bp connected by linker DNA. In vitro models for this fiber have been reconstituted with 2–48 nucleosomes on arrays of repeated nucleosome positioning sequences and have been subject of several structural, biochemical, and biophysical studies. The 10-nm fiber is essentially an "unfolded" fiber observed experimentally and it is probably less relevant in vivo. Condensation of the unfolded fiber into the more physiologically relevant 30-nm diameter fiber (~40-fold compaction from naked DNA) is achieved via an intrinsic folding pathway involving core histones (specifically H4 N-terminal domain) and linker histone (H1/H5) [16]. Electron microscopy (EM) studies of accurately positioned 48-mer arrays as well as models based on tetranucleosome crystal structure provide evidence that the nucleosomal arrays within the 30-nm fiber are organized as a zig-zag two-start helix as opposed to a one-start solenoid model [20]. The 30-nm fiber undergoes an additional ~500-fold level of compaction in order to pack into the fully condensed and transcriptionally inert metaphase chromosome

(reviewed in [21]). Models for intermediate tertiary structures include the (1) radial-loop protein scaffold [21], (2) chromonema fiber [21], and (3) random-chain (beaded), based on microscopy studies of extracted metaphase chromosomes, tandem arrays in live cells, and native chromatin in live cells [22].

The large majority of interphase chromatin consists of decondensed, transcriptionally active euchromatin in the form of nucleosomal arrays (10- and 30-nm fibers) that undergo dynamic rearrangements between various secondary and tertiary structures [16]. Transcription is enabled through these structural dynamics in chromatin fibers through the action of chromatin remodelers and epigenetic regulation (e.g., histone PTMs) that allow, for example, promoter regions to be nucleosome-free. The remaining interphase chromatin is transcriptionally inert and sequestered into various heterochromatin structures such as telomeric and centromeric DNA. Recently, a number of studies have implicated architectural nucleosome-binding proteins such as MeCP2, MENT, Polycomb, and HP1 in forming unique 30-nm fiber repressive secondary structures present in more condensed heterochromatin [16]. The next sections ("Families of Chromatin Remodelers," "ATP-Dependent Activities of Chromatin Remodelers and Mechanisms for Chromatin Mobilization," and "Regulation of Chromatin Remodeler Activity: Genomic Targeting and Interplay with Histone Modifications and Modifiers") will focus on the energy-dependent activity of chromatin remodeling complexes which are largely responsible for nucleosomal structural dynamics, rearrangements and genomic positioning during transcription, and other DNA metabolic processes.

Families of Chromatin Remodelers

Genome packaging dynamics are dictated by a number of requirements of the eukaryotic cell. Some examples include (1) correct positioning of nucleosomes after DNA replication, (2) exposure of promoter sequences during transcription, (3) DNA and RNA polymerase activity in the face of nucleosomes, and (4) action of DNA repair and recombination machinery in a chromatin context. Such processes typically require displacement, component restructuring, and unwrapping/repositioning of nucleosomes, which are achieved through the ATP-dependent action of a class of enzymes called chromatin remodelers [23, 24]. Depending on the enzyme and cellular process, remodeling can lead to varying outcomes that promote either chromatin decondensation or condensation.

There are four evolutionarily conserved families of multi-subunit chromatin remodeling complexes—SWI/SNF, ISWI, CHD, INO80—which all share a common ATP hydrolyzing catalytic domain that allows for energy-dependent alterations in histone–DNA interactions [23, 24]. Each family's ATPase or catalytic subunit has a common bipartite DExx and HELICc domain structure present in the SWI/SNF subfamily (named after first remodeler discovered) of the SF2 DNA helicase superfamily [25] (also see Chap. 3). Each family is distinguished by the presence of unique domains inserted between and flanking these two regions of the ATPase

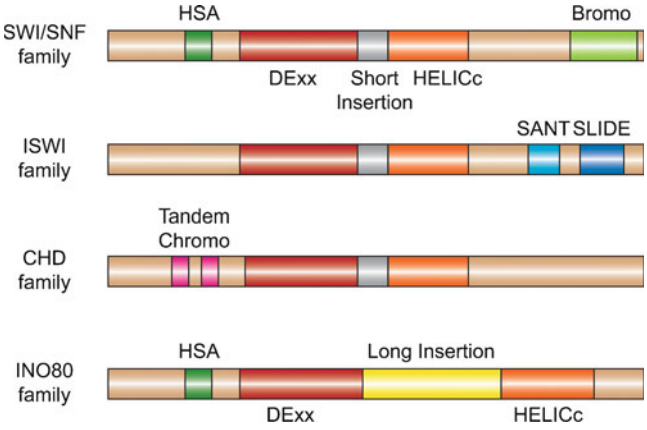

Fig. 13.2 Families of chromatin remodelers. (**a**) All chromatin remodelers contain a catalytic subunit with an SWI/SNF ATPase domain comprised of a DExx and HELICc motifs found in Superfamily 2 (SF2) DNA helicases. The ATPase domain provides the motor for DNA translocation around the histone octamer. Remodeling complexes are further divided into four major families based on the unique domains present in the catalytic subunit. The SWI/SNF family has an N-terminal helicase-SANT (HSA) and C-terminal Bromo domain flanking its ATPase domains. The ISWI family has a SANT-SLIDE domain in its C-terminus. The CHD family possesses tandem chromo-domains upstream of its ATPase domain. The INO80 family contains an HSA domain upstream of its ATPase, and unlike the other three families which have a short insertion between their two ATPase motifs, the INO80 family has a long insertion. See text for further details. Reproduced from [24] with permission of *Annual Reviews*

subunit (Fig. 13.2a). Unique domains in the catalytic as well as associated subunits confer specialized functions to the remodeler depending on the cellular context. For example, while all remodeling complexes display enhanced affinity for nucleosomes, how they are targeted to nucleosomal regions depends on factors such as specific recognition of nucleosomal DNA and PTMs and interactions with specific transcription factors and chromatin modifiers. Family-specific domains in the catalytic subunit are also responsible for interaction with other subunits in the complex and allosteric regulation of activity. The subunit composition of the four families including species orthologues is listed in Table 13.1 and described below.

The SWI/SNF family [24, 26–29], discovered through *S. cerevisiae* screening for suppression of transcriptional mutants with a *swi*tching defective/*s*ucrose *n*on-*f*ermenting phenotype, comprises 8–14 subunits forming two types of complexes (yeast SWI/SNF and RSC; drosophila BAP/PBAP; human BAF/PBAF) around one of two related catalytic subunits (*S. cerevisiae* Swi2/Snf2 and Sth1; drosophila BRM/Brahma; human BRM/BRG1). Both ATPase subunits have an N-terminal helicase-SANT (HSA) domain that interacts with actin-related proteins (ARP subunits), and a C-terminal Bromo/poly-Bromo domain that interacts with acetylated histones, contributing to promoter targeting. In higher eukaryotes but not yeast, β-actin is also a subunit of the remodeling complex, and has been postulated to act as a nucleotide exchange factor for the ATPase subunit in human BAF [30]. SWI/SNF remodeling

Table 13.1 Remodeler composition and orthologous subunits: subunit composition is shown of the major remodeling complexes in each of the four families in yeast, drosophila, and humans

Family and composition		Model organisms									
		Yeast		Fly			Human				
SWI/SNF	Complex	**SWI/SNF**	**RSC**	**BAP**	**PBAP**		**BAF**		**PBAF**		
	ATPase	Swi2/Snf2	Sth1	BRM/Brahma			hBRM or BRG1		BRG1		
	Non-catalytic homologous subunits	Swi1/Adr6		Osa/eyelid	Polybromo BAP170		BAF250/hOSA1		BAF180 BAF200		
		Swi3 Swp73 Snf5	Rsc8/Swh3 Rsc6 Sfh1	MOR/BAP155 BAP60 SNR1/BAP45 BAP111/dalao BAP55 or BAP47			BAF155, BAF170 BAF60a or b or c hSNF5/BAF47/INI1 BAF57 BAF53a or b				
		Arp7, Arp9		Actin			β–actin				
	Unique	Note 1	Note 2								
ISWI	Complex	**ISW1a**	**ISW1b**	**ISW2**	**NURF**	**CHRAC**	**ACF**	**NURF**	**CHRAC**	**ACF**	
	ATPase	Isw1		Isw2	ISWI			SNF2L	SNF2H*		
	Non-catalytic homologous subunits			Itc1	NURF301	ACF1 CHRAC14 CHRAC16		BPTF	hACF1/WCRF180 hCHRAC17 hCHRAC15		
					NURF55/p55			RbAp46 or 48			
	Unique	Ioc3	Ioc2, 4		NURF38						
CHD	Complex		**CHD1**		**CHD1**	**Mi-2/NuRD**		**CHD1**	**NuRD**		
	ATPase		Chd1		dCHD1	dMi-2		CHD1	Mi-2α/CHD3, Mi-2β/CHD4		
	Non-catalytic homologous subunits					dMBD2/3 dMTA dRPD3 p55 p66/68			MBD3 MTA1,2,3 HDAC1,2 RbAp46 or 48 p66αβ		
	Unique								DOC-1?		
INO80	Complex	**INO80**		**SWR1**	**Pho-dINO80**	**Tip60**		**INO80**	**SRCAP**	**TRRAP/Tip60**	
	ATPase	Ino80		Swr1	dIno80	Domino		hIno80	SRCAP	p400	
	Non-catalytic homologous subunits	Rvb1,2			Reptin, Pontin			RUVBL1,2/Tip49a,b			
		Arp5,8	Arp6		dArp5,8	BAP55		Arp5,8	Arp6	Actin	
		Arp4,Actin1			dActin1	Actin87E		BAF53a			
		Taf14	Yaf9			dGAS41			GAS41		
		Ies2,6						hIes2,6			
			Swc4/Eaf2			dDMAP1			DMAP1		
			Swc2/Vps72			dYL-1			YL-1		
			Bdf1			dBrd8				Brd8/TRC/p120	
			H2AZ,H2B			H2Av,H2B			H2AZ,H2B		
			Swc6/Vps71						ZnF-HIT1		
						dTra1				TRRAP	
						dTip60				Tip60	
						dMRG15				MRG15,MRGX	
						dEaf6				FLJ11730	
						dMRGBP				MRGBP	
						E(Pc)				EPC1,EPC-like	
						dING3				ING3	
	Unique	Ies1,3-5,Nhp10		Swc3,5,7	Pho			Note 3			

Note 1: Swp82,Taf14,Snf6,Snf11
Note 2: Rsc1 or Rsc2,Rsc3-5,7,9,10,30,Htl1,Ldb7,Rtt102
Note 3: Amida,NFRKB,MCRS1,UCH37,FLJ90652,FLJ20309
*In addition, SNF2H associates respectively with Tip5, RSF1, WSTF to form **NoRC**, **RSF** and **WICH** remodelers

See text for further details. Reproduced (pre-print version) from [24] with permission of *Annual Reviews*

complexes mainly function in promoting gene expression (and dsDNA break repair in the case of rad54p), producing multiple outcomes via DNA translocation and topological changes including octamer ejection, dimer displacement and exchange, nucleosome sliding, and disome formation (see section “ATP-Dependent Activities

of Chromatin Remodelers and Mechanisms for Chromatin Mobilization"). They do not have roles in chromatin assembly during DNA replication.

The ISWI (*i*mitation *swi*tch) family of remodelers [23, 24, 31] are smaller compared to SWI/SNF with only 2–4 subunits. The three major ISWI complexes (yeast ISW1a/ISW1b/ISW2; NURF, CHRAC, and ACF in drosophila and humans) are assembled around two related catalytic subunits (*S. cerevisiae* Isw1/Iswi2; drosophila ISWI; human SNF2L/SNF2H). The ATPase subunit has unique C-terminal, adjacent SANT (ySIW2, yADA2, hNCoR, hTFIIIB), and SLIDE (SANT-like ISWI) domains that are responsible for recognition of the nucleosome through interactions with nucleosomal and linker DNA and histone tails. The remaining subunits offer additional domains including DNA-binding motifs in hCHRAC and dNURF301, and plant homeodomains (PDH), and bromodomains (hBPTF, hACF1). ISWI mainly functions in nucleosome spacing via sliding. Its ability to bind linker DNA and nucleosomal DNA on either side of the nucleosome is postulated to allow nucleosome centering on the DNA. While ACF and CHRAC have roles in chromatin assembly and transcription repression, NURF leads to transcriptional activation via randomizing nucleosome spacing.

The CHD remodeler family is named after the catalytic subunit domains—*c*hromodomain, *h*elicase, and *D*NA binding [23, 24, 30]. The simplest remodeler in this family, CHD1, is comprised of a single catalytic subunit (Chd1) across species (although it can be oligomeric in higher organisms). In higher eukaryotes, the NuRD complex contains up to ten subunits assembled around the catalytic subunit Mi-2. In both Chd1 and Mi-2 catalytic subunits, two tandem chromo-domains N-terminal to the ATPase region are involved in recognition of methylated H3 tails. Large variability exists in cellular functions of CHD remodelers—some activate transcription through nucleosome repositioning or removal, while others such as vertebrate Mi2/NuRD are involved in transcriptional repression via histone deacetylase (HDAC1/2) and methyl CpG-binding domains (MBD).

The INO80 chromatin remodelers comprise the most complex family in terms of subunit composition across species [24, 32]. Unlike the other three remodeler families, the INO80 family catalytic subunit is defined by a much longer insertion between the two regions to which two types of its protein subunits bind—(1) actin-binding protein (ARP) and (2) Rvb1,2 helicase-related (AAA-ATPase) proteins. The ATPase subunit also has an N-terminal HSA domain for binding actin and ARPs, other subunits found in the remodelers of this family. INO80 has multiple functions in transcriptional activation (via subunit histone acetylase (HAT) activity) as well as DNA repair. Similar to the ISWI remodeler family, INO80 remodelers interact with extranucleosomal DNA in order to mobilize nucleosomes. In addition, the yeast SWR1 and related drosophila Tip60 and human SRCAP complexes are unique in that they contain histone H2A variant H2A.Z and histone H2B as subunits and are able to catalyze the exchange of the canonical H2A–H2B dimer with the variant containing H2A.Z, a structural change associated with both transcriptional activation and silencing [33].

ATP-Dependent Activities of Chromatin Remodelers and Mechanisms for Chromatin Mobilization

Chromatin Remodelers Are Not Bona-Fide Helicase Enzymes

The bipartite ATPase domain of chromatin remodelers is homologous to that found in SF2 DNA helicases containing helicase motifs I–III in the subdomain I and helicase motifs IV–VI in subdomain II ([24] see also Chap. 3). Like DNA helicases, chromatin remodelers demonstrate DNA-dependent ATPase activity and in all cases it is also nucleosomal DNA-dependent. However, only the Mi-2 and ISWI families display higher activation of ATP hydrolysis with nucleosomal DNA as a cofactor relative to free DNA. Despite the sequence homology to DNA helicases, chromatin remodelers are unable to catalyze ATP-dependent separation of DNA strands in vitro [34], consistent with the absence of a strand-separation "pin" motif found in helicases [35, 36]. However, depending on the remodeler family, a number of other ATP-dependent activities have been reported for chromatin remodeling complexes and their catalytic subunits by themselves. These activities include translocation or sliding of the histone octamer relative to DNA, and displacement or exchange of core histone components (Fig. 13.3). These are discussed below in terms of mechanisms to yield outcomes such as nucleosome repositioning/spacing, restructuring, and removal.

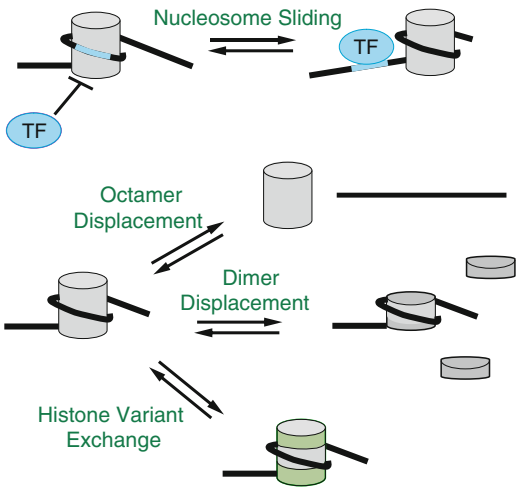

Fig. 13.3 Modes of nucleosome remodeling. Chromatin remodelers recognize the nucleosome and catalyze energy-dependent activities such as DNA translocation around the histone octamer (i.e., nucleosome sliding) and displacement/exchange of core histone components (histone dimers, octamers, and variants). Depending on the particular remodeler and the cellular context, these activities will yield different outcomes, for example, nucleosome repositioning to enable exposure of DNA-binding sites to transcription factors (TF), nucleosome phased spacing to enable heterochromatin formation, and nucleosome restructuring and removal. Adapted and reprinted by permission from Macmillan Publishers Ltd: *Nature Structural and Molecular Biology* [87]

Interaction of Chromatin Remodelers with DNA and the Nucleosome

Where and how chromatin remodelers interact with the nucleosome is critical to understanding their mechanisms of nucleosome remodeling. One of the first locations to be explored for nucleosome binding was the DNA entry/exit point and evidence suggesting this was reported for SWI/SNF complexes that displayed a propensity to bind 4-way-junctions [37]. ACF remodeling complex was also mapped to the nucleosome entry/exit region [38]. Further investigations ultimately revealed that the ATPase domain binds to an internal site within the nucleosome. Critical to this conclusion were reports that ssDNA gaps two helical turns from the dyad (SHL ±2) impeded nucleosome sliding by ISW2 and SWI/SNF [39], RSC [40], as well as NURF [41]. This was consistent with footprinting studies showing that one of the binding sites for ISWI2 is the internal position SHL2 site within the nucleosome [42] and that SWI/SNF [39] and RSC [40] bound to this region also.

Multilobed structures of the large remodeling complexes, SWI/SNF and RSC, have been reconstructed from EM images and place a single nucleosome within a central cavity with the "translocase"-binding site at the internal SHL2 position and the DNA entry/exit regions and the dyad partially exposed (Fig. 13.4a) [43–45]. In the SWI/SNF study [45], DNA footprinting showed SWI/SNF protected one DNA gyre, covering 50 bp from the nucleosome entry site (DNA-binding domain [DBD]) to two helical turns from the dyad (translocase domain). Bartholomew and colleagues [46] have recently discovered a key difference in how SWI/SNF and ISWI translocase domains engage the internal SH2 nucleosome-binding site. Using site-specific crosslinking and footprinting methods, they showed that Isw2 binds the outer face of the DNA superhelix via the cleft between its ATPase subdomains, while Snf2 intercalates between the octamer and the DNA via a region external to the cleft. These differences may account for the ability of SWI/SNF to break more histone–DNA interactions upon engaging the nucleosome relative to ISWI [39].

Thus, DNA–histone mapping and structural studies revealed that SWI/SNF and RSC bound nucleosomal DNA from the near-dyad to near-end region. In contrast, the smaller ISWI complexes protect not only the internal SHL2 position but also extra-chromosomal linker DNA (Fig. 13.4b) [41, 42, 47–49]. From a combination of DNA photoaffinity crosslinking and peptide mapping methods, Bartholomew and colleagues delineated interactions for the SHL2 with the DEXD box of the catalytic subunit Isw2p, the entry-exit region with the HAND domain of Isw2p and subunit Ict1p, and the extrachromosomal DNA with Ict1, Isw2 (Sant-Slide domain), and subunit Dpb4p (Fig. 13.4b) [42, 47, 49]. NURF (drosophila ISWI) was also mapped via footprinting to bind both the stretch of linker DNA as well as an internal SHL2 site, with H4 N-terminal tails required for the near-dyad interactions [41]. The capacity to interact with DNA outside the nucleosome core is also consistent with reports showing linker length dependence on nucleosome sliding activity (discussed in section "Chromatin Remodelers Reposition and Space Nucleosomes") by this remodeling family [50–53]. The ability to engage the nucleosome at both internal and extra-nucleosomal DNA sites is postulated to allow ISWI-type remodelers to center nucleosome within a DNA sequence.

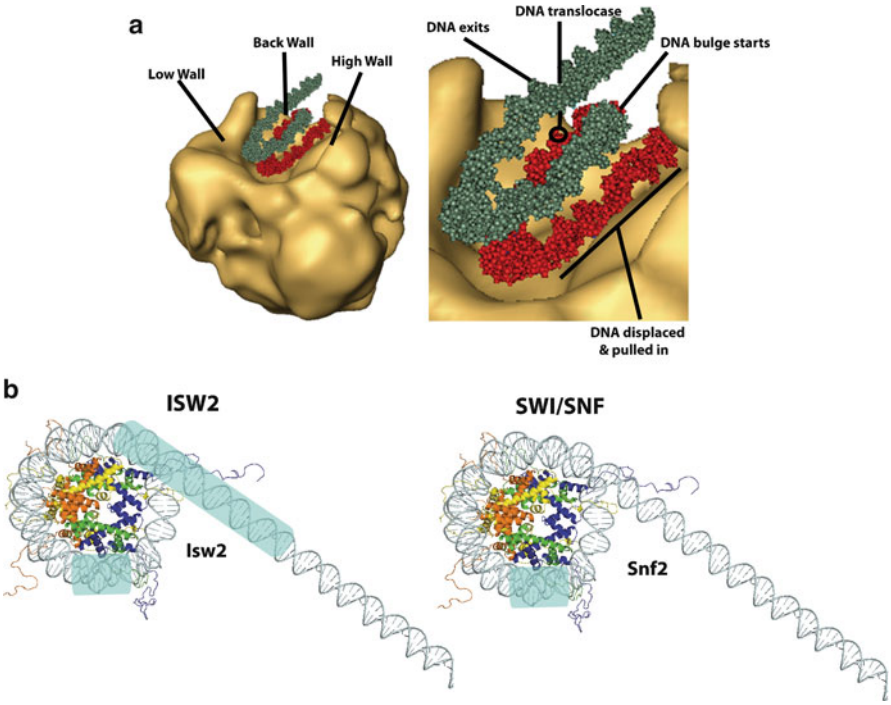

Fig. 13.4 Nucleosome binding by SWI/SNF and ISWI chromatin remodelers. (**a**) Model of SWI/SNF (tan) binding to the nucleosome in a central cavity based on EM, footprinting and crosslinking studies. The histone core is omitted from this depiction. One gyre of nucleosomal DNA (*red*) faces the interior of the remodeler cavity, while the other gyre (*grey*) is more exposed facing the exterior of the trough. The mapped translocase domain is predicted to pull the DNA proximal to the high wall in towards the nucleosome dyad axis where the bulge will form. Other predictions based on this model include (1) the high wall may protect the "pulled" DNA from completely unraveling, (2) the bulge will form in an area not protected by SWI/SNF and propagate to an area with less steric hindrance along the low wall, and (3) SWI/SNF can only bind one nucleosome at a time. (**b**) Comparison of remodeler-nucleosomal DNA contacts for ISW2 and SWI/SNF chromatin remodeler families' respective catalytic subunits, Isw2 (*left*) and Snf2 (*right*). Contacts were mapped by site-directed DNA crosslinking (highlighted in *blue*). While Snf2 interacts with SHL2 site only, Isw2 interacts with both SHL2 and extrachromosomal DNA starting at the entry site. See text for further details. Reprinted from [27] with permission from Elsevier Limited

Chromatin Remodelers Catalyze dsDNA Translocation, Generating Loops and Superhelical Tension in DNA

While remodelers do not separate strands, per se, the homology of their ATPase domain with that of DNA helicases led to exploration of their capacity to function as ATP-dependent DNA motors and catalyze DNA translocation. The engagement of different remodelers with the nucleosome at the internal SHL2 position suggested that the ATPase motor or "translocase" domain acted at this site, disrupting

DNA–histone interactions through DNA translocation with generation of DNA distortions such as loops and topological strain.

Early studies investigating remodeler translocation demonstrated that SWI/SNF [54], Rad54 [54], RSC [55], and ISWI [56] possess an ATP-dependent ability to displace a short oligonucleotide from a triple helix, suggesting an ability to translocate [56] along one of the dsDNA strands. A 3′–5′ polarity of translocation was confirmed by inhibition of strand displacement when gaps were placed in a 3′–5′ tracking strand [40, 55, 56]. Observation of DNA-length dependence of ATP hydrolysis activity by RSC and its ATPase motor, Sth1 [55], and ISWI [56] provided indirect evidence for ATPase-promoted DNA translocation.

An initial exploration of how remodelers impact DNA supercoiling was carried out by Owen-Hughes and colleagues [57] by measuring ATP-dependent cruciform generation from an $[AT]_{34}$ repeat construct. Consistent with their DNA cofactor dependence of ATP hydrolysis, hBRG1 and SWI/SNF created cruciforms on both naked and nucleosomal DNA constructs, whereas Mi-2 and ISWI activities were specific to nucleosomal DNA. SWI/SNF was also demonstrated to transiently induce ATP-dependent supercoiling in a mini-circle system [58]. RSC remodeling measured by restriction enzyme accessibility was less effective on nucleosomes with positioned nicks, indicating both DNA twist and translocation are involved in remodeling [55]. A role for torsional strain was observed for ISWI but not SWI/SNF in that nucleosome movement from an internal position was prevented by single nicks at this near-dyad site for ISWI but not SWI/SNF [39].

Subsequently, single-molecule systems provided more direct observation of translocation activity for the Snf2 remodeler family. Translocation on dsDNA by hRad54 protein was implicated by an atomic force microscopy (AFM) analysis of hRad54–DNA complexes containing unconstrained supercoils in the presence of ATP [59]. A flow-based optical trap assay was used to examine fluorescently labeled Rad54p [60] move along a dsDNA track. Rad54 translocation along λ DNA was ATP-dependent, highly processive at 300 bp/s and did not involve looping. A homologue, Rdh54, was shown using total internal reflection fluorescence microscopy to catalyze highly processive translocation-coupled loop extrusion on naked DNA, creating large 6 kb DNA loops [61]. In a separate study [62] using magnetic tweezers, RSC complex was shown to catalyze ATP-dependent reductions in DNA length of naked DNA—translocating at 200 bp/s for an average of 420 s at very low tension (0.3 pN). These DNA shortenings were accompanied by generation of DNA loops and superhelical tension, and were postulated to reflect rapid and reversible DNA translocation events. Recently Zhang and colleagues [63] applied a high resolution optical tweezers-tethered translocase system to remeasure translocation on naked DNA by the RSC catalytic subunit, and discovered it could translocate against forces up to 30 pN as a highly processive motor with a small step size (2 bp) with multiple modes of loop formation. A similar activity was reported for SWI/SNF and RSC using an optical trap system; however in this case, the ATP-dependent reversible DNA shortening events were observed on oligonucleosomal DNA (containing 1–4 nucleosomes) at tensions between 1 and 6 pN and against forces up to 12 pN. In this system, SWI/SNF was able to catalyze sequential reversible shortening

events, indicating more processive translocation (13 bp/s), and DNA looping was reflected by the variation in DNA length reductions (average size of 100 bp) [64]. Support for DNA loop formation was also noted for ACF in which remodeling produced increased DNA accessibility at regions bordering the nucleosome as measured by an ethidium bromide intercalation assay [38], suggesting a "loop recapture model" for DNA movement along the nucleosome (see section "Physical Models for Remodeler-Promoted DNA Movement Around the Octamer").

Chromatin Remodelers Reposition and Space Nucleosomes

Nucleosome mobilization by chromatin remodelers has been probed traditionally by monitoring changes in DNA accessibility of nucleases, restriction enzymes, and transcription factors upon ATP-dependent remodeling. For example, SWI/SNF ATP-dependent remodeling activity was discovered by DNaseI footprinting studies demonstrating facilitation of transcription factor binding to their cognate sites when incorporated into mononucleosomes [65, 66].

The main biochemical methods to address remodeler-promoted nucleosome movement include nucleosome mapping by indirect end labeling in vivo and nucleosome mapping by site-directed mapping and gel shifts in vitro [67, 68]. Early studies using DNA photoaffinity labeling showed that after remodeling and ATP hydrolysis, the RSC and SWI/SNF contacts within the nucleosome undergo multiple changes such as displacement of catalytic subunits from the nucleosomal DNA surface [69]. In a photochemical mapping study, SWI/SNF peeled as much as 50 bp from the ends of a mononucleosome [70], arguing for a stable remodeled product which contains a loop at the entry-exit site. Footprinting and restriction enzyme accessibility assays showed that RSC catalytic subunit Sth1 engaged the nucleosome at a position 2 helical turns from the dyad and moved the nucleosomal DNA from this location [40]. Photoaffinity DNA crosslinking assays with nucleosomes containing ssDNA gaps at different locations later confirmed that SWI/SNF and ISWI translated nucleosomes from an internal site SHL-2 with a 50 bp and 10 bp step size, respectively [39]. Nuclease mapping studies revealed Rad54 bidirectionally repositioned nucleosomes in an ATP-dependent manner [71]; however its rate of translocation was much faster relative to its nucleosome sliding activity indicating that translocation may not be the rate-limiting event in sliding [60].

Wang and colleagues [72] examined how SWI/SNF altered histone–DNA interactions using an elegant optical trap-based DNA unzipping assay on a mononucleosome. They discovered that after SWI/SNF ATP-dependent remodeling, the nucleosome retained its canonical nucleosome disruption force signature with three regions of interaction (two centered at ~50 bp away from dyad and one centered at the dyad); however the distribution of nucleosome positioning was shifted continuously by ~28 bp bidirectionally around the original (unremodeled) position. Furthermore, the remodeling events were transient and did not result in any permanent change in the histone composition. A later study [73] applying a single-molecule

methyltransferase accessibility assay (MapIT) to study remodeling also showed a broad distribution of DNA accessibility for SWI/SNF remodeled nucleosomes; however this was mainly due to large heterogeneity in bidirectional translational positioning accompanied by loss of canonical histone–DNA contacts. In contrast, ISWI nucleosome repositioning was unidirectional and generally preserved the canonical structure [74, 75, 76].

Recently, native RSC- and Mi2-mediated nucleosome positioning over long distances was examined using high resolution PAGE on mononucleosomes situated on DNA with long arms [77]. In contrast to bidirectional remodeling observed for SWI/SNF [72, 73], both remodelers showed a strong sequence dependence of the initial direction of translocation. At limiting ATP, RSC was able to reposition the nucleosome in 20 bp steps within the 601 positioning sequence and at more processive rates outside the 601, indicating remodeling processivity is likely influenced by DNA sequence.

Along with information garnered regarding the propensity to reposition nucleosomes and the directionality and step size of remodeling, family-specific features have also been observed regarding the ability to regularly space nucleosomes. A major example is the ISWI family of remodelers which is known to space nucleosomes in transcriptionally silenced regions. The capacity to space nucleosomes by remodelers is related to their ability to bind and be activated by extrachromosomal DNA and to operate as a dimer, as in the case of ACF. As mentioned in section "Interaction of Chromatin Remodelers with DNA and the Nucleosome," ISWI remodelers are distinguished from the SWI/SNF family based on their ability to bind extrachromosomal DNA. This ability turned out to be important for activity as the ATPase activity for ISWI was stimulated by linker DNA [56]. ISWI2 had an absolute requirement for 20 bp of linker DNA for remodeling and additional 43 bp of flanking DNA stimulated activity [42]. Furthermore, increasing linker lengths stimulated nucleosome sliding by ISWI2, and the remodeler could discriminate between linker DNA lengths such that on substrates with two DNA arms, it preferred to bind the longer arm and remodeled the nucleosome towards the center. Further analysis showed that ISW2 cannot move the nucleosome closer than 11 bp from the DNA end, and ssDNA gaps in the linker and entry regions did not impede remodeling, indicating no requirement for torsional strain [52]. A similar ability of ISW1a, b, and Isw2, as well as Chd1 (catalytic subunit of the CHD family) to center nucleosomes through preferential binding to longer linker DNA, with a loss of remodeling activity at linkers <15 bp (for all but Isw1b) was observed by Owen Hughes and colleagues [78]. This combined work led to the idea that remodelers that act as "nucleosome spacing factors" do so by centering the nucleosome within a DNA fragment. The leading model suggests ISWI preferentially binds longer linker DNA and moves the nucleosome towards the center, and repeats this cycle on alternate sides until the linker DNA is too short to remodel further (see section "Physical Models for Remodeler-Promoted DNA Movement Around the Octamer").

A major difference between the repositioning activity of two ISWI complexes in yeast—ISW1a and ISW2—is that the former but not the latter can space nucleosomes

at a set distance of 175 bp. Bartholomew and colleagues conducted an investigation {48} using high resolution nucleosome mapping, site-specific DNA crosslinking, and nucleosome-binding assays that showed this difference in spacing ability was attributed to the fact that ISW1a requires binding 33 bp of only one arm of linker DNA in order to retain its interactions with the internal site, but loses this interaction and stops remodeling when it protects both linker arms. In contrast, ISW2 has a different preference for extrachromosomal DNA at the entry/exit that results in lack of spacing ability. Further analysis of the yeast ISWI proteins helped delineate stages of remodeling by spacing factors [51]. In particular, a role for ATP hydrolysis in formation of a committed ISW1a and ISW2-nucleosome complex was observed that involved transitioning from an initial complex only protecting linker DNA to one protecting over one complete turn of the nucleosomal DNA, with an important role played by the Dbp4 subunit in destabilizing histone–DNA contacts 15 bp away from the ATPase domain.

Recently, the INO80 remodeling complex involved in transcriptional activation and DNA repair was also investigated [79] for its linker DNA requirements. A minimum of 33–43 bp linker DNA and H2A but not H4 tails were required for remodeling by Ino80. On di- and tri-nucleosomal arrays, it moved nucleosomes towards each other, stopping at 30 bp linker DNA to achieve a repeat length of 177 bp.

Human ACF, ATP-dependent chromatin assembly factor, helps form regularly spaced arrays in transcriptionally silenced chromatin [80, 81]. ACF was shown using ExoIII mapping to move nucleosomes by 50 bp from end to center positions [38]. In a bulk FRET-based nucleosome repositioning assay, ACF remodeling was activated by increasing linker DNA lengths such that ACF kinetically discriminated between flanking DNA lengths in order to center nucleosomes [50]. Using a single-molecule FRET assay in which FRET donor and acceptors were placed respectively on surface-tethered end-positioned nucleosome and exit linker DNA of varying lengths, Zhuang and colleagues [82] provided evidence for ACF-catalyzed nucleosome "centering" within a DNA fragment. To prove the nucleosome was actually being translocated in this system, ssDNA gaps were incorporated within 2–3 helical turns from the dyad to "stall" the nucleosome and FRET decrease was directly proportional to gap-dyad distance. Translocation of an end-positioned nucleosome was interrupted by well-defined kinetic pauses consistent with unidirectional repositioning by an ACF monomer, while that of a center-positioned nucleosome was processive and bidirectional, consistent with ACF operating as a dimer with each monomer binding on either side of the nucleosome as observed in EM reconstructions of SNF2h bound nucleosomes [83, 84] and proposed in FCS studies showing that ACF had four DNA-binding sites [38].

Physical Models for Remodeler-Promoted DNA Movement Around the Octamer

Through these studies, several models of how chromatin remodelers move DNA around the histone octamer have been formulated. The basic tenet is that the remod-

eler interacts specifically at SHL2 through its translocase domain and also at a region closer to the linker DNA through a separate DBD. The remodeler either moves along the DNA around the nucleosome or remains fixed at the near-dyad site and catalyzes directional propagation of a DNA bulge and/or twist around the nucleosome [40]. The end result is either a transient disruption in DNA–histone contacts resulting in a transient increase in accessibility of nucleosomal DNA (i.e., loosening), or a more permanent disruption of contacts, resulting in a change in the translational position or "sliding" of the nucleosome.

Original models for remodeler-induced histone core movement relative to DNA invoked a "twist diffusion" model in which thermal fluctuation-induced twist of linker DNA would be propagated around the histone octamer surface in 1 bp steps, changing both the rotational and translational phasing of the nucleosome. This model was supported by structural findings that the nucleosome can accommodate a single bp insertion or deletion at certain locations [1, 85]. Twist diffusion became less favored with a report that remodeling by ISWI moved nucleosomes in 10 bp steps, thus maintaining the rotational phasing of the nucleosomes [39] and that physical barriers such as hairpins and streptavidin beads, which should impede rotation during sliding, did not affect remodeling by SWI/SNF [86] and ACF [38].

An alternative, generally favored model is the "bulge propagation" model in which a longer segment of DNA is detached from the linker DNA region and transfers to the histone core, forming a loop which propagates around the octamer surface, breaking and reforming histone–DNA contacts until the loop reaches the opposite linker, effectively translating the nucleosome position by a distance defined by the size of the loop. Figure 13.5a provides a schematic view of the bulge propagation model for SWI/SNF and ISWI remodelers based on their nucleosome binding and DNA translocation features [53]. As SWI/SNF protects an extensive region of DNA, it is predicted to create larger bulges of 50 bp via translocation by its catalytic subunit anchored at the SHL2 position. ISWI, on the other hand, is predicted to generate a smaller ~10 bp bulge achieved through concerted action of its two binding sites at the internal site and linker DNA. Propagation of the bulge in a unidirectional manner beyond the region between the entry and internal site would require the release of the SHL2 contact.

Figure 13.5b shows an alternative "1+10" ratchet model for SWI/SNF and ISWI DNA translocation that invokes an "inchworm" type movement proposed for many SF1 and SF2 DNA helicases [87]. In this model, the remodeler contacts the nucleosome at SHL2 through its translocase domain (tr) and near the proximal linker DNA via a DBD which are connected through a flexible hinge region (H). The Tr domain binds tightly to the near-dyad position and initially tracks 1 bp towards the dyad. The DBD is initially bound to any helical repeat position between the dyad and the proximal linker (ISWI will be closer to linker than SWI/SNF). Once Tr catalyzes 1 bp movement, the DBD moves and binds tightly to a position 1 helical repeat away from Tr. This causes Tr to weaken its dyad interaction, promoting a conformational change in DBD so that it moves back to its original position, pulling with it a 10 bp loop of DNA which ultimately will pass thru Tr. Tr will reengage and the cycle continues, thus enabling "inchworm" like propagation of an

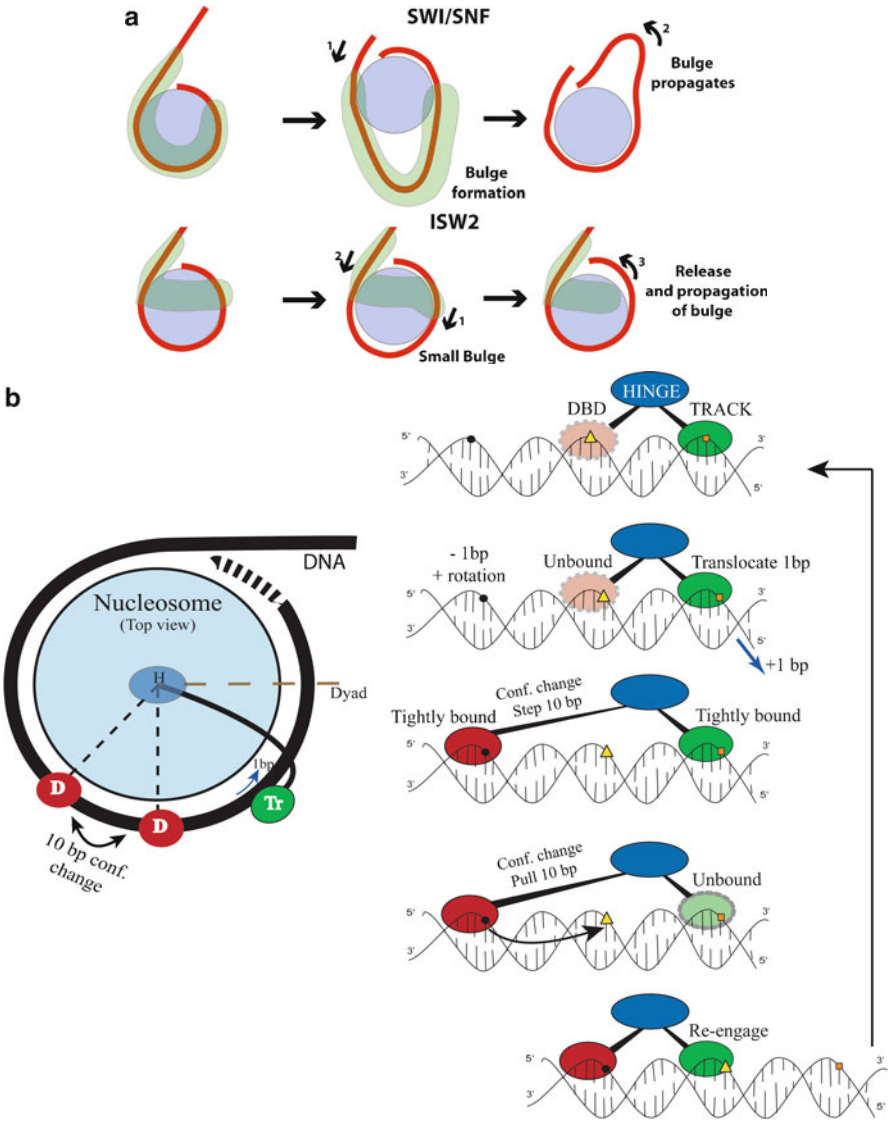

Fig. 13.5 Proposed mechanisms for DNA translocation around the nucleosome by chromatin remodelers. (**a**) Models for SWI/SNF and ISWI chromatin remodeling via bulge propagation. Proposed models are based on differences reported between SWI/SNF and RSC with regard to remodeler interactions with histones and nucleosomal DNA as well as features of DNA translocation. Depictions: histone octamer (*grey shaded circle*), nucleosomal DNA (*red line*), footprint of remodeler on nucleosome (*shaded green*). (*Top*) SWI/SNF is anchored at SHL2 but has extensive interactions with nucleosomal DNA providing more potential to generate a large DNA bulge (~50 bp) that is propagated around the nucleosome (*arrows 1 and 2*). (*Bottom*) ISW2 has two contact points with the nucleosome at SHL2 and the entry site/extrachromosomal DNA which

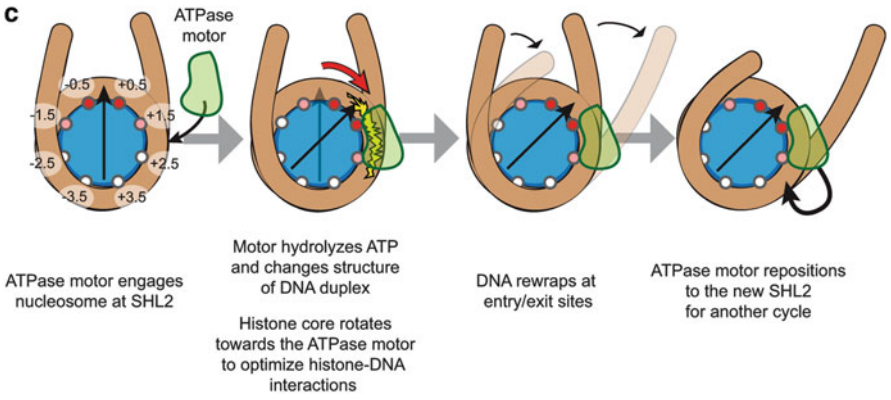

Fig. 13.5 (continued) work in concert to create a smaller (10 bp) bulge between the two binding sites (*arrows 1 and 2*) due to torsional strain created at the internal site being offset by pulling of opposite linker towards the nucleosome. Bulge propagation and DNA translocation is achieved only upon release of the internal contact (*arrow 3*). Reprinted from [53] with permission from Elsevier Limited. (**b**) Modified "inchworm" (1+10 ratchet) model for IWSI/SWI/SNF remodeling shown as a nucleosome top-view rendition (*left*) and as a translocation cycle (*right*). Remodeler contacts the nucleosome at SHL2 through its translocase domain (tr) and at the linker DNA via a DNA-binding domain (DBD) which are connected through a flexible hinge region (H). In this schematic, the tr domain is anchored while the DBD domain (shown bound 10 bp from dyad) alternates between two conformations, with fixed positions of each domain depicted as a triangle and square. See text for further details. Reprinted by permission from Macmillan Publishers Ltd: *Nature Structural and Molecular Biology* [87]. (**c**) Alternative model for nucleosome sliding involving rotation of the histone core. This model postulates that upon binding SHL2 by the ATPase motor (*green*), the DNA structure is altered (*yellow*) in such a way as to promote repositioning of energetically important contacts at the dyad (*black arrow*) towards the remodeler. This is achieved by rotation of the histone core within the DNA wrap (*red arrow*), effectively translocating the DNA by one minor groove while maintaining rotational positioning. To continue the cycle, the motor domain repositions itself at the new SHL2 site. Reprinted from [89] with permission from Elsevier Limited

11 bp loop around the nucleosome involving sequential release of domains at both binding sites. In this model, the DBD domain serves as an internal "ratchet" to promote directional translocation of DNA towards the dyad, taking into account the torsional strain created by the translocase domain [87].

The bulge propagation model is supported by detection of DNA looping during remodeling using single-molecule techniques; however the variation in loop size may reflect remodeler variation in translocation step size and force generation. For example the difference in repositioning intervals for SWI/SNF (50 bp) vs. ISWI (10 bp) may reflect differences in bulge size, stopping points, and disruption severity for these two remodelers [39]. A similar "loop recapture" model was proposed for the ACF remodeling complex based on studies mapping its binding to the nucleosome entry/exit region, introducing a DNA loop at this position which propagates around the histone octamer resulting in nucleosome repositioning [38]. Another variation on this model was put forth based on intranucleosomal crosslinking

studies suggesting that intermediates in SWI/SNF- and RSC-remodeling contain an additional internal loop which is threaded through the nucleosome [88].

A third model recently put forth suggests that the remodeling does not involve DNA movement, but instead the histone octamer rotates relative to stationary DNA [89] (Fig. 13.5c). The tenets of this model are that upon binding of the ATPase domain to SHL2, it alters the histone–DNA contacts in this region. The octamer tries to maintain optimal histone–DNA contacts by rotating its dyad α1–α1 and L1–L2 contacts towards the remodeler by one minor groove register, thus achieving translational repositioning without changing rotational position. The swiveling of the histone core may be facilitated by high density of basic residues in that region of the octamer including a single Arg that intercalates into the minor groove.

Physical Models for Remodeler-Promoted Nucleosome Spacing

Two different mechanistic models for spacing of nucleosomes have been proposed based on structural studies of ACF complex and ISWI complexes bound to nucleosomes [90] (Fig. 13.6). ACF catalytic subunit, Snf2h, was shown by Narlikar group [84, 91] to bind a nucleosome as a dimer with each monomer flanking one gyre of DNA (Fig. 13.6 left), but only one of them has ATP bound, allowing it to bind to its cognate H4 N-terminal tail and linker DNA. If the longer linker side is bound by ATP-bound ACF monomer, it will be activated for ATP-dependent translocation, drawing linker DNA into the nucleosome and propagating around the nucleosome via a loop recapture mechanism. The opposite linker DNA will subsequently increase in length, leading to stimulation of the ATP hydrolysis by the second monomer and translocation in the opposite direction. The end result is a tug of war between the directions of DNA movement around the nucleosome, ultimately centering the nucleosome.

A different mechanism for ISW1a nucleosome spacing was derived from a combination of crystal structure and cryoEM reconstructions of ISW1a lacking its ATPase domain (ISW1a(ΔATPase))±DNA or with nucleosomes with linkers of 45 and 29 bp [92] (Fig. 13.6 right). Interestingly, ISW1a bound as a monomer to the nucleosome with two linkers of 45 and 29 bp, but in the presence of a nucleosome with a single 45 bp linker, it bound as a dimer bridging the two nucleosomes. Each ISW1a(ΔATPase) bound only linker DNA and the entry/exit region, with ISW1a near the proximal nucleosome bound in the opposite orientation to that of the monomeric species. These results suggested that the true substrate for ISW1a may be a di-nucleosome, and ISW1a acts as a "protein ruler" setting the distance between two adjacent mononucleosomes. The schematic shows the HSS domain of the ISW1 a ATPase and Ioc3 accessory subunit bound to linker DNA between the two nucleosomes with the ATPase domain on the SHL2 region of the "mobile nucleosome." Ioc3 bridges that linker DNA to the distal linker on the "static" nucleosome. Translocation pulls linker DNA into the mobile nucleosome, bringing the two nucleosomes closer to each other and stops once the static nucleosome interacts with the Ioc3 subunit, thus defining a target length between nucleosomes which is reflective of its role in generating regularly spaced nucleosomal arrays.

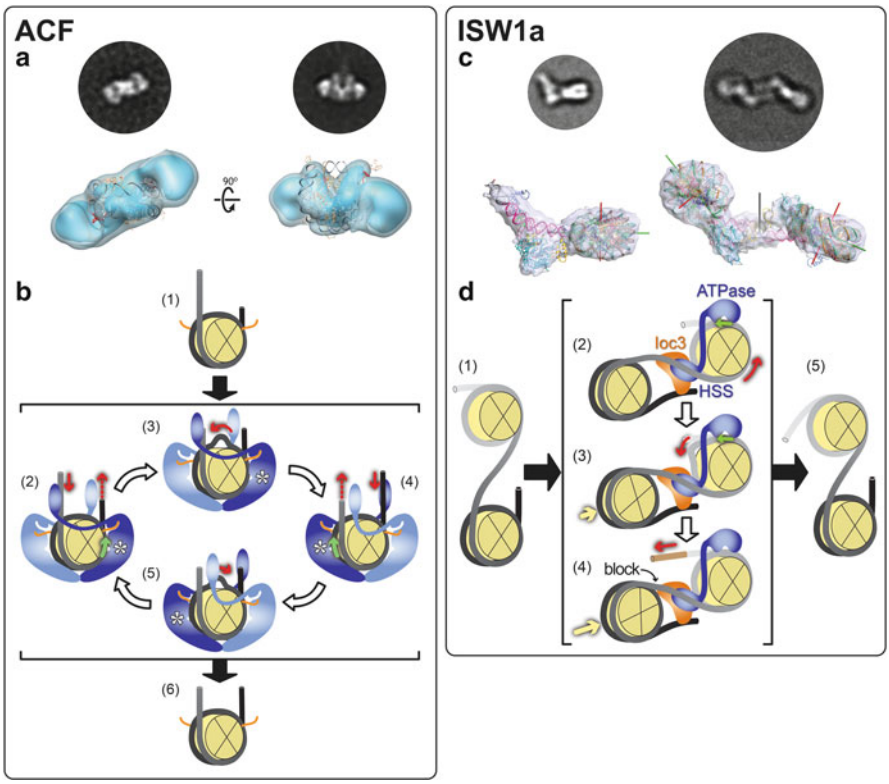

Fig. 13.6 Remodeling mechanisms proposed for ISWI family chromatin remodelers. *Left: human ACF* (**a**) Electron microscopy reconstructions of two SNF2h monomers bound to a single nucleosome at SHL +2 and −2. (**b**) Proposed mechanism for nucleosome centering by ACF based on [84]. (Stages 1–6) Two ACF monomers (inactive ATP-unbound (*light blue*) and active ATP-bound (*dark blue*)) bind on either side of the nucleosome (histone octamer (*yellow cylinder*); nucleosomal DNA (*grey tubing*)). The active monomer binds its cognate H4 N-terminal tail (*orange lines*), allowing it to interact with the longer linker DNA. This stimulates translocation (*green arrow*) from the ATPase-binding site (*) pulling the longer linker DNA into and around the nucleosome, releasing at the other end (stages 2–3, *red arrows*). The opposite linker will subsequently increase in length, activating the other ACF monomer for translocation in the opposite direction (stages 4–5). The cycle will repeat until the nucleosome is centered (stage 6). *Right: S. cerevisiae ISW1a*: (**c**) Combined EM/crystal structures resolved for ISW1a without its catalytic domain (ISW1a(ΔATPase)) [92] bound to a nucleosome with 45 and 29 bp linkers (*left*) and with a single 45 bp linker (*right*). In the dual linker structure, the HSS domain of the catalytic subunit and the Ioc3 subunit bind so as to bridge the two linkers. In the single-linker structure, a twofold symmetric dimeric particle containing two ISW1a(ΔATPase) bound to two orientations of the nucleosome. (**d**) (Stages 1–5) depict a schematic model proposed for di-nucleosome spacing by ISW1a, with the ATPase domain modeled at SHL2 of the "mobile" nucleosome, the HSS domain bound to linker DNA of the "mobile" nucleosome, and the Ioc3 subunit bridging the mobile nucleosome linker and static nucleosome distal linker. ISW1a becomes activated for translocation and pulls linker DNA bridging the two nucleosomes towards the mobile nucleosome. Eventually, Ioc3 interaction with the static nucleosome will prevent further translocation and determine a fixed spacing distance between nucleosomes. See text for further details. Reprinted from [90] with permission from Elsevier Limited

Chromatin Remodelers Catalyze Dimer Release and Exchange in Mononucleosomes

Several biochemical studies have addressed the possibility of dimer loss during remodeling. One study showed SWI/SNF remodeling was transient and not impeded by octamer crosslinking [86]. The histone chaperone and centromere-associated chromatin remodeling factor, FACT, was shown to generate hexameric particles [93]. Owen-Hughes and colleagues [94] detected ATP-dependent exchange of histone dimers between chromatin fragments by SWI/SNF and RSC but not ISWI. Beato and colleagues [95] demonstrated dimer exchange by SWI/SNF in a sequence-dependent manner in the MMTV promoter system. In another study, nucleoplasmin-mediated stimulation of SWI/SNF promotion of GAL4 nucleosome binding provided indirect evidence for dimer transfer during remodeling [96]. An observation of SWI/SNF-remodeled sub-nucleosomal size particles species was made using MAP-IT accessibility assays [73]. In contrast, single-molecule mononucleosome unzipping studies showed that SWI/SNF did not promote histone dimer removal since remodeling did not result in a tetrasome disruption signature [72].

Certain members of INO80 family, yeast SWR1, drosophila Tip60, and human SRCAP complexes, are unique amongst the Snf2 ATPase remodelers in their ability to catalyze exchange of canonical H2A/H2B dimers with H2A.Z/H2B dimers [97]. This ability correlates with the fact that histone H2A.Z is one of the subunits in these complexes, and it is clearly a major function of these complexes. The incorporation of H2A.Z in chromatin does not alter canonical nucleosome structure [98], and most likely these remodelers are targeted to regions of the genome that require H2A.Z for multiple functions such as prevention of heterochromatin spreading [32].

Chromatin Remodeler Activity in an Oligonucleosome Context: Disome Formation, Dimer and Octamer Eviction, and DNA Bridging

A unique product of chromatin remodeling that has been reported is an altered dimer of nucleosomes or disome, which constrains fewer negative supercoils than normal. Using biochemical assays [99] and AFM [100], it was shown that hSWI/SNF remodeled nucleosomes were converted into a disome containing 60 bp of loosened DNA. Other similarly "altered" nucleosomes were reported upon RSC remodeling [101] and SWI/SNF remodeling [70]. The ability to form disomes was postulated to facilitate ATP-dependent octamer transfer in trans by these remodelers [102]. Extension of these studies to polynucleosomal arrays revealed disome and altered disome (altosome) species created by SWI/SNF remodeling that offer new avenues for transcriptional regulation [11, 12].

Solution AFM recognition imaging experiments [103] provided evidence that H2A was released from SWI/SNF remodeled polynucleosomal arrays. Bartholemew and colleagues [104] have examined SWI/SNF remodeling on di- and tri-nucleosomal templates and observe two stage loss of an octamer (1 dimer followed by entire octamer). The octamer eviction from oligonucleosomes does not require any acceptor DNA or histone chaperone, in contrast to mononucleosome disassembly by SWI/SNF/RSC which is observed in the presence of Asf1 or Nap1 [105]. Mapping of repositioned nucleosomes is consistent with a model that SWI/SNF moves proximal nucleosomes towards the end of the template, displacing the distal octamer. These results are consistent with an AFM imaging study of di-nucleosomes [106] in which overlapping of nucleosomes can promote dimer removal.

Very recently, the first single-molecule investigation of an ISWI family remodeler, specifically yeast Iswi1a motor, was carried out using a combination of transmission EM (TEM) and magnetic tweezers [107]. Strikingly, in an ATP-independent manner, Isw1a bound in a dynamic manner to naked DNA with high cooperativity, forming both intra- and inter-molecular DNA bridges that assemble into a "DNA zipper." On a single nucleosome with long linker arms, Isw1a ATP-dependent remodeling was shown by TEM to involve bridging of extranucleosomal DNA on each arm, stimulating repositioning. Taking into account a recent structural model in which ISWIa acts as "protein ruler" that determines the spacing between two adjacent nucleosomes [92], the TEM/single molecule study supports a "conveyer belt" model for Isw1a remodeling in which Isw1a units forming the DNA zipper act as "wheels" in the presence of ATP to translocate the DNA like a chain in a conveyer belt (Fig. 13.7).

Regulation of Chromatin Remodeler Activity: Genomic Targeting and Interplay with Histone Modifications and Modifiers

The diversity in composition, activities, and mechanisms of chromatin remodeling complexes is critical for their ultimate cellular function in regulating transcription and other DNA metabolic processes. Layered upon this are two additional factors—histone modifications and histone modifying enzymes—that regulate their activity in order to targeting remodeling complexes to relevant genomic regions and control whether they facilitate chromatin decondensation or condensation.

Histone Modifications as Signals to Regulating Chromatin Remodeling Activity

PTMs of histones occur at specific residues located primarily in the unstructured N-terminal tails of the core histones. PTMs are catalyzed by histone acetyltransferases (HATs), histone deacetylases (HDACs), histone methyltransferases, and demethylases along with histone-specific phosphorylation, ubiquitilation, ribosylation and

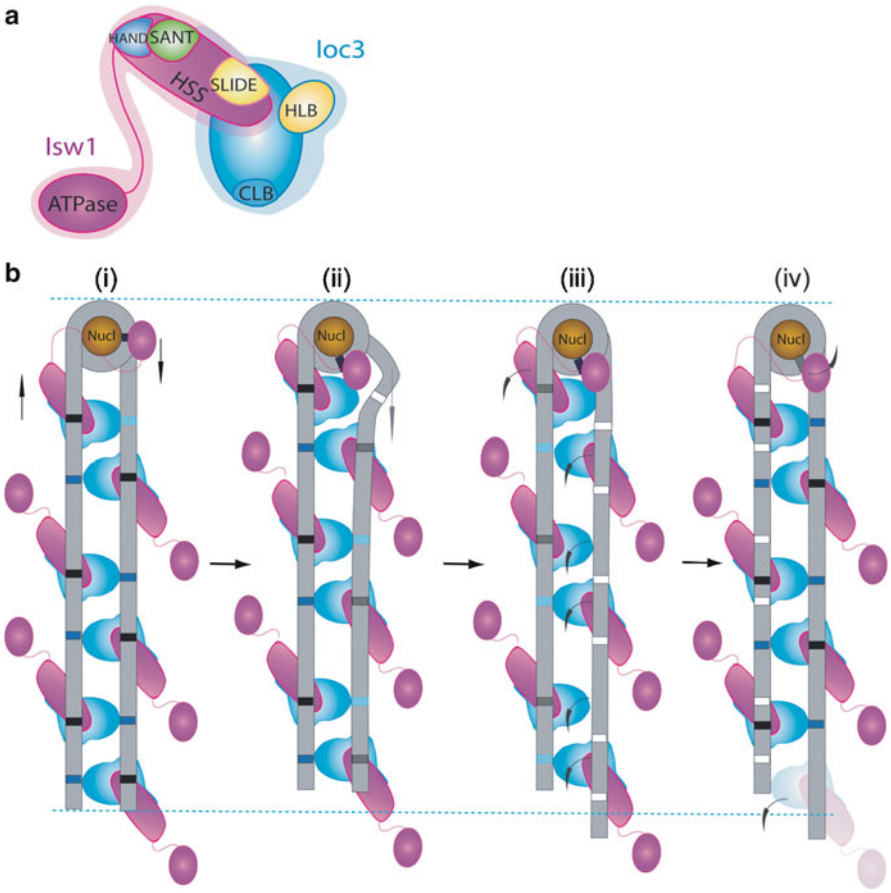

Fig. 13.7 Bridging of nucleosomal DNA by ISW1a: Conveyer belt model for remodeling. (**a**) Drawing of Isw1a protein based on [92]. ATPase domain (*magenta*) is separated from the HSS domain by a flexible linker, and HSS in turn interacts with Ioc3 subunit. (**b**) "Conveyer belt" model for Isw1a remodeling on nucleosomal DNA based on magnetic tweezer/TEM studies [107]. (Stage i) Starting from single nucleosome with sufficient flanking DNA, ISW1a could nucleate fiber formation by ATP-dependent bridging/zippering of the two DNA arms. (Stages ii–iv) ISW1a engaged at the nucleosome, catalyzes ATP-dependent translocation of linker DNA, creating a distortion in the DNA that weakens its Ioc3/Isw1–DNA interaction (interaction site changes from *dark blue* to *light blue*). In response, the remaining ISW1a molecules continue ATP-dependent translocation, serving as wheels in a DNA conveyer belt, such that one DNA arm length increases while the other shortens, and the number of DNA bridges decreases (interaction sites become white upon release of Isw1a subdomains). See text for further details. Reprinted from [107] under the terms of the Creative Commons Attribution License

other enzyme modifiers [108]. The resultant PTMs serve as "histone marks" that serve as epitopes for recognition by "reader" modules within chromatin remodeling complexes and other protein machinery, targeting them to specific regions of the genome in particular cellular contexts (i.e., DNA repair, gene activation or silencing, etc.). In addition, histone PTMs can have structural consequences both in terms of NCP

dynamics and in terms of higher order structure (e.g., [109]). These features determine a "histone code" such that different combinations of histone PTM patterns correlate with specific gene expression outcomes [110]. An example of global epigenetic effects for histone H3 include tri-methylation at Lysine 4, 9, or 27 respectively associated with gene activation, heterochromatin formation, and gene repression [108].

The impact of histone tails and PTMs on remodeling has been explored via numerous genetic and biochemical studies (reviewed in [108, 111]). Owen-Hughes and colleagues utilized a peptide ligation strategy to investigate H3- and H4-specific tail histone modifications [112] and discovered remodeler-specific outcomes for different reaction steps. For example, H3-tetraAc but not H4 tetra-Ac increased RSC remodeling rate by lowering the K_m for nucleosome cofactor in the ATPase reaction, thus impacting substrate binding. In contrast, H4-tetraAc increased the k_{cat} with no impact on K_m for Isw2 and Chd1 remodeling. This was consistent with reports demonstrating loss of ISWI ATPase and remodeling activity by removal of the H4 terminus [113, 114].

Chromatin remodelers are thus impacted by histone PTMs in two major ways—they serve as signals for recognition and recruitment of remodelers as well as allosteric effectors of catalytic activity by remodelers. Remodelers are not only recruited by PTM signals, but also via other signals such as histone variants, nonhistone proteins, DNA sequence, DNA methylation, and chromatin-associated RNAs [115] (see Fig. 13.8a). In addition, these signals can also regulate the kinetic steps of the remodeling event which has been modeled by Rippe and colleagues [115] to comprise equilibrium binding of the remodeler to the target sequence, initiation of remodeling involving formation of a high-energy intermediate (e.g., DNA loop), ATP-dependent translocation (the catalytic step), and termination of remodeling. Binding affinities can be modulated in a DNA sequence-independent way such as a change in the H3 or H4 modification that directly changes affinity of the remodeler for the substrate [112], or in a sequence-dependent manner as has been observed for nucleosome positioning by Chd1 and ACF [116]. Rates of catalysis for both the translocation and ATP hydrolysis reactions are affected by chromatin marks as mentioned earlier [112–114]. In addition to tail effects, histone variants and binding domains also regulate catalysis—for example, H2A.Z containing nucleosomes increased the translocation rate of mammalian ISWI relative to canonical H2A [117], and the double chromodomain of Chd1 discriminates between inhibitory naked DNA vs. stimulatory nucleosomal DNA cofactors in its ATPase reaction [118].

Targeting of Chromatin Remodelers to the Genome: Epitope Recognition by Protein-Binding Domains and Target Search Mechanisms

The chromatin remodeling complexes have evolved as macromolecular machines which include a wide range of noncatalytic subunits and domains. Evolutionarily, this serves two purposes: (1) improving efficiency by allowing coupling of reactions

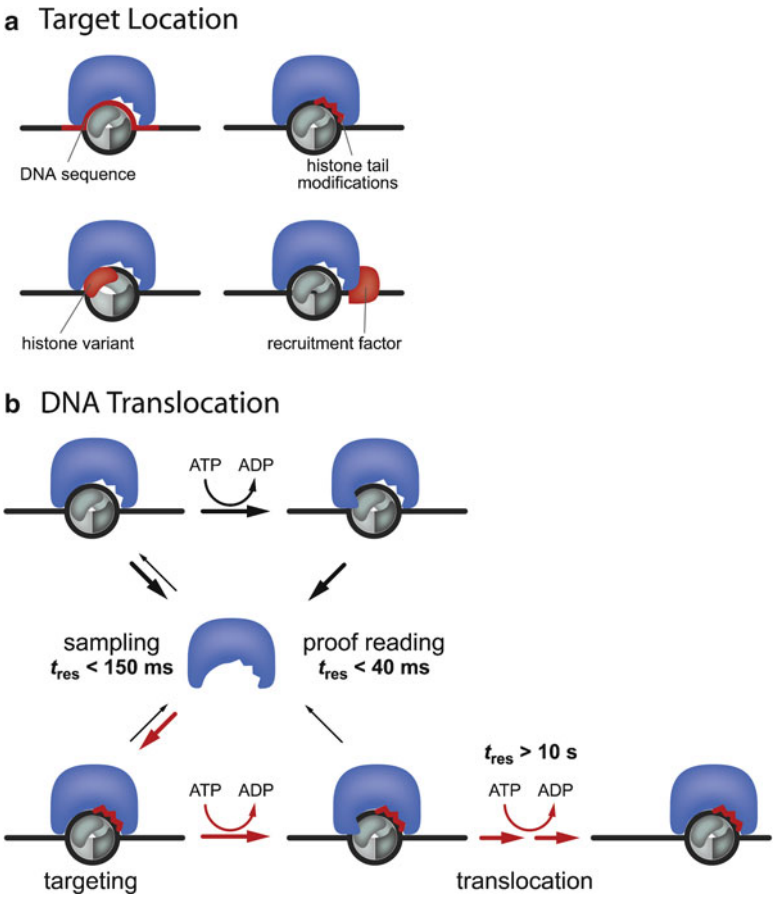

Fig. 13.8 Target location and continuous sampling mechanism for ISWI remodeler translocation. (**a**) Chromatin remodelers are targeted to genomic locations by recognition of specific signals such as DNA sequence and methylation, histone tail modifications, histone variants, and recruitment factors such as histone modifying enzymes. (**b**) ISWI remodeling involves transient binding and continuous sampling of nucleosome-binding sites for the appropriate target. Target discrimination is achieved through signal recognition and kinetic proofreading. Remodeler residence times and kinetic proofreading times are based on [129] and [128], respectively. With appropriate signal recognition, the remodeler can proceed along a successful translocation pathway (*red arrows*). See text for further details. Reprinted from [31] with permission from John Wiley and Sons

in a remodeling event and (2) diversification of function through multiple combinatorial assemblies. Examples of the latter include alterations in remodeler subunit composition to control development as in the case of mammalian BAF subunit usage regulating neuronal differentiation, identification of human chromatin remodeler subunits as tumor suppressors [30], and the synergistic and sequential action of different "reader" domains in recognition, creation, and, removal of different histone PTMs during remodeling [111].

Three types of chromatin remodeling complex protein domains that "read" PTM histone "marks" include bromodomains that interact specifically with acetylated tails [119], chromodomains and PHD fingers that interact with methylated lysines (reviewed in [120]). In these cases, these protein interaction domains are part of subunits within a chromatin remodeler, histone modifier, and/or other protein factor that recognizes the epigenetic mark. As an example, SWI/SNF interacts with SAGA-acetylated H3 and H4 tails via the bromodomain in its catalytic subunit, which stimulates retention and remodeling at promoter nucleosomes, and ultimately the displacement of SAGA HAT complex from these promoters [111]. Another example of PTM-mediated complex targeting for gene expression is recruitment of the NURF complex for activation of Hox genes in vertebrate development via recognition of H3K4me3 by the PHD domain of its BPTF noncatalytic subunit [121].

In addition to transcription, histone modifications also play a role in DNA replication and repair. In replication, PTMs associate with histone chaperones—proteins that assemble, exchange, and remove histones from the nucleosome [122] and histone modifiers to aid in deposition and maturation of chromatin at replication forks. One of many examples involves newly synthesized histones which contain H3K56Ac and H4K5K12diAc. These are created and delivered as Ac-H3.1-H4 tetramers via the histone chaperone ASF in conjunction with different HATS (HAT1 and Rtt109) to chromatin assembly factor CAF-1. CAF-1, in turn, is recruited to the leading and lagging strands by PCNA [105, 122–124]. Both histone variants and modifications are important for double-strand break (DSB) repair via chromatin remodeler activity. In particular, INO80 and SWR1 complexes are recruited to DSBs via binding to phosphorylated H2AX or γ-H2AX. This is postulated to aid in further recruitment of homologous recombination-mediated DNA repair factors in the case of INO80, and non-homologous end—joining repair factors in the case of SWR1 [125].

In all of these processes, the chromatin remodeler must be directed to the appropriate substrate/region within the genome. Localization of remodelers, chromatin modifiers, and chromatin epigenetic marks to different regions of the genome has been mapped primarily using CHIP-based technology [126, 127]. More recently, multi-scale fluorescence fluctuation microscopy (FCS, FRAP) technologies have been used to monitor diffusion and binding kinetics of the ISWI family of chromatin remodelers in live mammalian cells [31, 115, 128, 129]. The latter studies were used to formulate a model for ISWI remodeler target search involving "continuous sampling" of all nucleosomes in the genome for signals that mark them for remodeling (i.e., translocation). The target search is postulated to involve both 1D diffusion along chromatin fibers and 3D diffusion in space and occur on a minute time scale. Factors controlling the search by continuous sampling include remodeler concentration and nucleosome-binding affinity (regulated by chromatin signals discussed above, Fig. 13.8a), the propensity for unproductive collisions, and the residence time required for remodeler to identify the target (Fig. 13.8b). The fluorescence studies on ISWI determined the remodeler was present in high abundance (μM levels) in the nucleus and while it bound tran-

siently with 100 ms residence times in G1/2 phase, a significantly larger fraction accumulated rapidly and became immobilized at replication foci during S phase and at DNA repair sites. Hence, in the presence of the appropriate signal (e.g., DNA repair sites), ISWI remodelers were capable of fast target location with an average sampling time of tens of seconds. In addition to sampling, ATP-dependent kinetic proofreading [83, 130] may also be part of the targeting scheme for ISWI remodelers.

Concluding Remarks

In the last two decades, a combination of genetic, biochemical, structural, single-molecule, and live cell biophysical studies has provided an emerging picture of chromatin remodeling complexes which share certain sequence and mechanistic features, namely a SWI/SNF catalytic ATPase domain that allows for engagement with the nucleosome and catalysis of directional dsDNA translocation around the histone octamer. Depending on the cellular context and remodeler-specific features, different remodeling outcomes are produced in vivo such as production of regularly spaced arrays in heterochromatin stretches by ISWI families or removal of promoter-bound nucleosomes to allow transcription by SWI/SNF family remodelers. To understand more fully how these genomic outcomes are achieved through the action of chromatin remodeling complexes will require further investigation and advances in structural, theoretical, biophysical single-molecule, and live cell approaches.

Some additional areas of exploration pertaining to remodeler translocation mechanisms include (1) how the catalytic subunit recognizes the internal SHL2 position, (2) single-molecule analysis of SWR1/INO80 translocation as this family does not have same processivity requirements as SWI/SNF, and also high resolution (<5 bp) single-molecule analysis of SWI/SNF/ISWI remodeling, and (3) the structure and composition of remodeling intermediates especially with regard to removal/exchange/transfer of histone dimers and octamers. Higher resolution EM reconstructions should provide more structural information on large complex organization and CHD and INO80 complexes. While progress has been made on how remodelers function at the mononucleosome and di-nucleosome level and with nucleosomal arrays, experimental systems should be adapted to study how chromatin remodelers work on higher order structures like native chromatin fibers that contain histone H1. This is especially pertinent because of the combinatorial nature of the histone code and the fact that remodeler "reader" modules often work cooperatively with other modules to recognize multiple features within or bridging many nucleosomes [111]. Lastly, genetics and genome mapping studies have revealed that the specificity in biological functions of chromatin remodelers lies in their subunit usage. Thus, it is critical to continue to investigate the mechanistic and regulatory roles of individual subunits within chromatin remodelers to help elucidate differences between members of different families and subfamilies.

References

1. Luger K, Mader AW, Richmond RK, Sargent DF, Richmond TJ. Crystal structure of the nucleosome core particle at 2.8 A resolution. Nature. 1997;389:251–60.
2. Arents G, Moudrianakis EN. The histone fold: a ubiquitous architectural motif utilized in DNA compaction and protein dimerization. Proc Natl Acad Sci U S A. 1995;92:11170–4.
3. Andrews AJ, Luger K. Nucleosome structure(s) and stability: variations on a theme. Annu Rev Biophys. 2011;40:99–117.
4. Tan S, Davey CA. Nucleosome structural studies. Curr Opin Struct Biol. 2011;21:128–36.
5. Lowary PT, Widom J. New DNA sequence rules for high affinity binding to histone octamer and sequence-directed nucleosome positioning. J Mol Biol. 1998;276:19–42.
6. Wu B, Mohideen K, Vasudevan D, Davey CA. Structural insight into the sequence dependence of nucleosome positioning. Structure. 2010;18:528–36.
7. Hall MA, Shundrovsky A, Bai L, Fulbright RM, Lis JT, Wang MD. High-resolution dynamic mapping of histone-DNA interactions in a nucleosome. Nat Struct Mol Biol. 2009;16:124–9.
8. Lavelle C, Prunell A. Chromatin polymorphism and the nucleosome superfamily: a genealogy. Cell Cycle. 2007;6:2113–9.
9. Zlatanova J, Bishop TC, Victor JM, Jackson V, van Holde K. The nucleosome family: dynamic and growing. Structure. 2009;17:160–71.
10. Bohm V, Hieb AR, Andrews AJ, Gansen A, Rocker A, Toth K, et al. Nucleosome accessibility governed by the dimer/tetramer interface. Nucleic Acids Res. 2011;39:3093–102.
11. Ulyanova NP, Schnitzler GR. Human SWI/SNF generates abundant, structurally altered dinucleosomes on polynucleosomal templates. Mol Cell Biol. 2005;25:11156–70.
12. Ulyanova NP, Schnitzler GR. Inverted factor access and slow reversion characterize SWI/SNF-altered nucleosome dimers. J Biol Chem. 2007;282:1018–28.
13. Bancaud A, Wagner G, Conde ESN, Lavelle C, Wong H, Mozziconacci J, et al. Nucleosome chiral transition under positive torsional stress in single chromatin fibers. Mol Cell. 2007;27:135–47.
14. Dalal Y, Furuyama T, Vermaak D, Henikoff S. Structure, dynamics, and evolution of centromeric nucleosomes. Proc Natl Acad Sci U S A. 2007;104:15974–81.
15. Woodcock CL, Ghosh RP. Chromatin higher-order structure and dynamics. Cold Spring Harb Perspect Biol. 2010;2:a000596.
16. Luger K, Hansen JC. Nucleosome and chromatin fiber dynamics. Curr Opin Struct Biol. 2005;15:188–96.
17. Li G, Reinberg D. Chromatin higher-order structures and gene regulation. Curr Opin Genet Dev. 2011;21:175–86.
18. Tremethick DJ. Higher-order structures of chromatin: the elusive 30 nm fiber. Cell. 2007;128:651–4.
19. Chakravarthy S, Park YJ, Chodaparambil J, Edayathumangalam RS, Luger K. Structure and dynamic properties of nucleosome core particles. FEBS Lett. 2005;579:895–8.
20. Dorigo B, Schalch T, Kulangara A, Duda S, Schroeder RR, Richmond TJ. Nucleosome arrays reveal the two-start organization of the chromatin fiber. Science. 2004;306:1571–3.
21. Belmont AS. Mitotic chromosome scaffold structure: new approaches to an old controversy. Proc Natl Acad Sci U S A. 2002;99:15855–7.
22. Muller WG, Rieder D, Kreth G, Cremer C, Trajanoski Z, McNally JG. Generic features of tertiary chromatin structure as detected in natural chromosomes. Mol Cell Biol. 2004;24:9359–70.
23. Smith CL, Peterson CL. ATP-dependent chromatin remodeling. Curr Top Dev Biol. 2005;65:115–48.
24. Clapier CR, Cairns BR. The biology of chromatin remodeling complexes. Annu Rev Biochem. 2009;78:273–304.

25. Fairman-Williams ME, Guenther UP, Jankowsky E. SF1 and SF2 helicases: family matters. Curr Opin Struct Biol. 2010;20:313–24.
26. Hopfner KP, Gerhold CB, Lakomek K, Wollmann P. Swi2/Snf2 remodelers: hybrid views on hybrid molecular machines. Curr Opin Struct Biol. 2012;22:225–33.
27. Hota SK, Bartholomew B. Diversity of operation in ATP-dependent chromatin remodelers. Biochim Biophys Acta. 2011;1809:476–87.
28. Kasten MM, Clapier CR, Cairns BR. SnapShot: chromatin remodeling: SWI/SNF. Cell. 2009;144(310):e311.
29. Liu N, Balliano A, Hayes JJ. Mechanism(s) of SWI/SNF-induced nucleosome mobilization. Chembiochem. 2011;12:196–204.
30. Hargreaves DC, Crabtree GR. ATP-dependent chromatin remodeling: genetics, genomics and mechanisms. Cell Res. 2011;21:396–420.
31. Erdel F, Rippe K. Chromatin remodelling in mammalian cells by ISWI-type complexes—where, when and why? FEBS J. 2011;278:3608–18.
32. Bao Y, Shen X. INO80 subfamily of chromatin remodeling complexes. Mutat Res. 2007;618:18–29.
33. Guillemette BT, Bataille AR, Gévry N, Adam M, Blanchette M, Robert FO, et al. Variant histone H2A.Z is globally localized to the promoters of inactive yeast genes and regulates nucleosome positioning. PLoS Biol. 2005;3:e384.
34. Durr H, Flaus A, Owen-Hughes T, Hopfner KP. Snf2 family ATPases and DExx box helicases: differences and unifying concepts from high-resolution crystal structures. Nucleic Acids Res. 2006;34:4160–7.
35. Durr H, Korner C, Muller M, Hickmann V, Hopfner KP. X-ray structures of the Sulfolobus solfataricus SWI2/SNF2 ATPase core and its complex with DNA. Cell. 2005;121:363–73.
36. Singleton MR, Dillingham MS, Wigley DB. Structure and mechanism of helicases and nucleic acid translocases. Annu Rev Biochem. 2007;76:23–50.
37. Quinn J, Fyrberg AM, Ganster RW, Schmidt MC, Peterson CL. DNA-binding properties of the yeast SWI/SNF complex. Nature. 1996;379:844–7.
38. Strohner R, Wachsmuth M, Dachauer K, Mazurkiewicz J, Hochstatter J, Rippe K, et al. A 'loop recapture' mechanism for ACF-dependent nucleosome remodeling. Nat Struct Mol Biol. 2005;12:683–90.
39. Zofall M, Persinger J, Kassabov SR, Bartholomew B. Chromatin remodeling by ISW2 and SWI/SNF requires DNA translocation inside the nucleosome. Nat Struct Mol Biol. 2006;13:339–46.
40. Saha A, Wittmeyer J, Cairns BR. Chromatin remodeling through directional DNA translocation from an internal nucleosomal site. Nat Struct Mol Biol. 2005;12:747–55.
41. Schwanbeck R, Xiao H, Wu C. Spatial contacts and nucleosome step movements induced by the NURF chromatin remodeling complex. J Biol Chem. 2004;279:39933–41.
42. Kagalwala MN, Glaus BJ, Dang W, Zofall M, Bartholomew B. Topography of the ISW2-nucleosome complex: insights into nucleosome spacing and chromatin remodeling. EMBO J. 2004;23:2092–104.
43. Chaban Y, Ezeokonkwo C, Chung WH, Zhang F, Kornberg RD, Maier-Davis B, et al. Structure of a RSC-nucleosome complex and insights into chromatin remodeling. Nat Struct Mol Biol. 2008;15:1272–7.
44. Leschziner AE, Saha A, Wittmeyer J, Zhang Y, Bustamante C, Cairns BR, et al. Conformational flexibility in the chromatin remodeler RSC observed by electron microscopy and the orthogonal tilt reconstruction method. Proc Natl Acad Sci U S A. 2007;104:4913–8.
45. Dechassa ML, Zhang B, Horowitz-Scherer R, Persinger J, Woodcock CL, Peterson CL, et al. Architecture of the SWI/SNF-nucleosome complex. Mol Cell Biol. 2008;28:6010–21.
46. Dechassa ML, Hota SK, Sen P, Chatterjee N, Prasad P, Bartholomew B. Disparity in the DNA translocase domains of SWI/SNF and ISW2. Nucleic Acids Res. 2012;40:4412–21.
47. Dang W, Kagalwala MN, Bartholomew B. The Dpb4 subunit of ISW2 is anchored to extranucleosomal DNA. J Biol Chem. 2007;282:19418–25.

48. Gangaraju VK, Bartholomew B. Dependency of ISW1a chromatin remodeling on extranucleosomal DNA. Mol Cell Biol. 2007;27:3217–25.
49. Dang W, Bartholomew B. Domain architecture of the catalytic subunit in the ISW2-nucleosome complex. Mol Cell Biol. 2007;27:8306–17.
50. Yang JG, Madrid TS, Sevastopoulos E, Narlikar GJ. The chromatin-remodeling enzyme ACF is an ATP-dependent DNA length sensor that regulates nucleosome spacing. Nat Struct Mol Biol. 2006;13:1078–83.
51. Gangaraju VK, Prasad P, Srour A, Kagalwala MN, Bartholomew B. Conformational changes associated with template commitment in ATP-dependent chromatin remodeling by ISW2. Mol Cell. 2009;35:58–69.
52. Zofall M, Persinger J, Bartholomew B. Functional role of extranucleosomal DNA and the entry site of the nucleosome in chromatin remodeling by ISW2. Mol Cell Biol. 2004;24:10047–57.
53. Gangaraju VK, Bartholomew B. Mechanisms of ATP dependent chromatin remodeling. Mutat Res. 2007;618:3–17.
54. Jaskelioff M, Van Komen S, Krebs JE, Sung P, Peterson CL. Rad54p is a chromatin remodeling enzyme required for heteroduplex DNA joint formation with chromatin. J Biol Chem. 2003;278:9212–8.
55. Saha A, Wittmeyer J, Cairns BR. Chromatin remodeling by RSC involves ATP-dependent DNA translocation. Genes Dev. 2002;16:2120–34.
56. Whitehouse I, Stockdale C, Flaus A, Szczelkun MD, Owen-Hughes T. Evidence for DNA translocation by the ISWI chromatin-remodeling enzyme. Mol Cell Biol. 2003;23:1935–45.
57. Havas K, Flaus A, Phelan M, Kingston R, Wade PA, Lilley DM, et al. Generation of superhelical torsion by ATP-dependent chromatin remodeling activities. Cell. 2000;103:1133–42.
58. Gavin I, Horn PJ, Peterson CL. SWI/SNF chromatin remodeling requires changes in DNA topology. Mol Cell. 2001;7:97–104.
59. Solinger JA, Kiianitsa K, Heyer WD. Rad54, a Swi2/Snf2-like recombinational repair protein, disassembles Rad51:dsDNA filaments. Mol Cell. 2002;10:1175–88.
60. Amitani I, Baskin RJ, Kowalczykowski SC. Visualization of Rad54, a chromatin remodeling protein, translocating on single DNA molecules. Mol Cell. 2006;23:143–8.
61. Prasad TK, Robertson RB, Visnapuu ML, Chi P, Sung P, Greene EC. A DNA-translocating Snf2 molecular motor: Saccharomyces cerevisiae Rdh54 displays processive translocation and extrudes DNA loops. J Mol Biol. 2007;369:940–53.
62. Lia G, Praly E, Ferreira H, Stockdale C, Tse-Dinh YC, Dunlap D, et al. Direct observation of DNA distortion by the RSC complex. Mol Cell. 2006;21:417–25.
63. Sirinakis G, Clapier CR, Gao Y, Viswanathan R, Cairns BR, Zhang Y. The RSC chromatin remodelling ATPase translocates DNA with high force and small step size. EMBO J. 2011;30:2364–72.
64. Zhang Y, Smith CL, Saha A, Grill SW, Mihardja S, Smith SB, et al. DNA translocation and loop formation mechanism of chromatin remodeling by SWI/SNF and RSC. Mol Cell. 2006;24:559–68.
65. Imbalzano AN, Kwon H, Green MR, Kingston RE. Facilitated binding of TATA-binding protein to nucleosomal DNA. Nature. 1994;370:481–5.
66. Kwon H, Imbalzano AN, Khavari PA, Kingston RE, Green MR. Nucleosome disruption and enhancement of activator binding by a human SW1/SNF complex. Nature. 1994;370:477–81.
67. Hota SK, Bartholomew B. Approaches for studying nucleosome movement by ATP-dependent chromatin remodeling complexes. Methods Mol Biol. 2012;809:367–80.
68. Hota SK, Dechassa ML, Prasad P, Bartholomew B. Mapping protein-DNA and protein-protein interactions of ATP-dependent chromatin remodelers. Methods Mol Biol. 2012;809:381–409.
69. Sengupta SM, VanKanegan M, Persinger J, Logie C, Cairns BR, Peterson CL, et al. The interactions of yeast SWI/SNF and RSC with the nucleosome before and after chromatin remodeling. J Biol Chem. 2001;276:12636–44.
70. Kassabov SR, Zhang B, Persinger J , Bartholomew B. Sucleosome . Mol Cell. 2003;11: 391-403.

71. Alexeev A, Mazin A, Kowalczykowski SC. Rad54 protein possesses chromatin-remodeling activity stimulated by the Rad51-ssDNA nucleoprotein filament. Nat Struct Biol. 2003;10:182–6.
72. Shundrovsky A, Smith CL, Lis JT, Peterson CL, Wang MD. Probing SWI/SNF remodeling of the nucleosome by unzipping single DNA molecules. Nat Struct Mol Biol. 2006;13:549–54.
73. Bouazoune K, Miranda TB, Jones PA, Kingston RE. Analysis of individual remodeled nucleosomes reveals decreased histone-DNA contacts created by hSWI/SNF. Nucleic Acids Res. 2009;37:5279–94.
74. Kassabov SR, Henry NM, Zofall M, Tsukiyama T, Bartholomew B. High-resolution mapping of changes in histone-DNA contacts of nucleosomes remodeled by ISW2. Mol Cell Biol.2002;22:7524–34.
75. Hamiche A, Sandaltzopoulos R, Gdula DA, Wu C. ATP-dependent histone octamer sliding mediated by the chromatin remodeling complex NURF. Cell. 1999;97:833–42.
76. Langst G, Bonte EJ, Corona DF, Becker PB. Nucleosome movement by CHRAC and ISWI without disruption or trans-displacement of the histone octamer. Cell. 1999;97:843–52.
77. van Vugt JJ, de Jager M, Murawska M, Brehm A, van Noort J, Logie C. Multiple aspects of ATP-dependent nucleosome translocation by RSC and Mi-2 are directed by the underlying DNA sequence. PLoS One. 2009;4:e6345.
78. Stockdale C, Flaus A, Ferreira H, Owen-Hughes T. Analysis of nucleosome repositioning by yeast ISWI and Chd1 chromatin remodeling complexes. J Biol Chem. 2006;281:16279–88.
79. Udugama M, Sabri A, Bartholomew B. The INO80 ATP-dependent chromatin remodeling complex is a nucleosome spacing factor. Mol Cell Biol. 2011;31:662–73.
80. Fyodorov DV, Blower MD, Karpen GH, Kadonaga JT. Acf1 confers unique activities to ACF/CHRAC and promotes the formation rather than disruption of chromatin in vivo. Genes Dev. 2004;18:170–83.
81. Ito T, Bulger M, Pazin MJ, Kobayashi R, Kadonaga JT. ACF, an ISWI-containing and ATP-utilizing chromatin assembly and remodeling factor. Cell. 1997;90:145–55.
82. Blosser TR, Yang JG, Stone MD, Narlikar GJ, Zhuang X. Dynamics of nucleosome remodelling by individual ACF complexes. Nature. 2009;462:1022–7.
83. Narlikar GJ. A proposal for kinetic proof reading by ISWI family chromatin remodeling motors. Curr Opin Chem Biol. 2010;14:660–5.
84. Racki LR, Yang JG, Naber N, Partensky PD, Acevedo A, Purcell TJ, et al. The chromatin remodeller ACF acts as a dimeric motor to space nucleosomes. Nature. 2009;462:1016–21.
85. Ong MS, Richmond TJ, Davey CA. DNA stretching and extreme kinking in the nucleosome core. J Mol Biol. 2007;368:1067–74.
86. Aoyagi S, Narlikar G, Zheng C, Sif S, Kingston RE, Hayes JJ. Nucleosome remodeling by the human SWI/SNF complex requires transient global disruption of histone-DNA interactions. Mol Cell Biol. 2002;22:3653–62.
87. Cairns BR. Chromatin remodeling: insights and intrigue from single-molecule studies. Nat Struct Mol Biol. 2007;14:989–96.
88. Liu N, Peterson CL, Hayes JJ. SWI/SNF- and RSC-catalyzed nucleosome mobilization requires internal DNA loop translocation within nucleosomes. Mol Cell Biol. 2011;31:4165–75.
89. Bowman GD. Mechanisms of ATP-dependent nucleosome sliding. Curr Opin Struct Biol. 2010;20:73–81.
90. Leschziner AE. Electron microscopy studies of nucleosome remodelers. Curr Opin Struct Biol. 2011;21:709–18
91. Racki LR, Narlikar GJ. ATP-dependent chromatin remodeling enzymes: two heads are not better, just different. Curr Opin Genet Dev. 2008;18:137–44.
92. Yamada K, Frouws TD, Angst B, Fitzgerald DJ, DeLuca C, Schimmele K, et al. Structure and mechanism of the chromatin remodelling factor ISW1a. Nature. 2011;472:448–53.
93. Belotserkovskaya R, Oh S, Bondarenko VA, Orphanides G, Studitsky VM, Reinberg D. FACT facilitates transcription-dependent nucleosome alteration. Science. 2003;301:1090–3.

94. Bruno M, Flaus A, Stockdale C, Rencurel C, Ferreira H, Owen-Hughes T. Histone H2A/H2B dimer exchange by ATP-dependent chromatin remodeling activities. Mol Cell. 2003;12:1599–606.
95. Vicent GP, Nacht AS, Smith CL, Peterson CL, Dimitrov S, Beato M. DNA instructed displacement of histones H2A and H2B at an inducible promoter. Mol Cell. 2004;16:439–52.
96. Cote J, Quinn J, Workman JL, Peterson CL. Stimulation of GAL4 derivative binding to nucleosomal DNA by the yeast SWI/SNF complex. Science. 1994;265:53–60.
97. Mizuguchi G, Shen X, Landry J, Wu WH, Sen S, Wu C. ATP-driven exchange of histone H2AZ variant catalyzed by SWR1 chromatin remodeling complex. Science. 2004;303:343–8.
98. Suto RK, Clarkson MJ, Tremethick DJ, Luger K. Crystal structure of a nucleosome core particle containing the variant histone H2A.Z. Nat Struct Biol. 2000;7:1121–4.
99. Schnitzler G, Sif S, Kingston RE. Human SWI/SNF interconverts a nucleosome between its base state and a stable remodeled state. Cell. 1998;94:17–27.
100. Schnitzler GR, Cheung CL, Hafner JH, Saurin AJ, Kingston RE, Lieber CM. Direct imaging of human SWI/SNF-remodeled mono- and polynucleosomes by atomic force microscopy employing carbon nanotube tips. Mol Cell Biol. 2001;21:8504–11.
101. Lorch Y, Cairns BR, Zhang M, Kornberg RD. Activated RSC-nucleosome complex and persistently altered form of the nucleosome. Cell. 1998;94:29–34.
102. Phelan ML, Schnitzler GR, Kingston RE. Octamer transfer and creation of stably remodeled nucleosomes by human SWI-SNF and its isolated ATPases. Mol Cell Biol. 2000;20:6380–9.
103. Bash R, Wang H, Anderson C, Yodh J, Hager G, Lindsay SM, et al. AFM imaging of protein movements: histone H2A-H2B release during nucleosome remodeling. FEBS Lett. 2006;580:4757–61.
104. Dechassa ML, Sabri A, Pondugula S, Kassabov SR, Chatterjee N, Kladde MP, et al. SWI/SNF has intrinsic nucleosome disassembly activity that is dependent on adjacent nucleosomes. Mol Cell. 2010;38:590–602.
105. Park YJ, Luger K. Histone chaperones in nucleosome eviction and histone exchange. Curr Opin Struct Biol. 2008;18:282–9.
106. Engeholm M, de Jager M, Flaus A, Brenk R, van Noort J, Owen-Hughes T. Nucleosomes can invade DNA territories occupied by their neighbors. Nat Struct Mol Biol. 2009;16:151–8.
107. De Cian A, Praly E, Ding F, Singh V, Lavelle C, Le Cam E, et al. ATP-independent cooperative binding of yeast Isw1a to bare and nucleosomal DNA. PLoS One. 2012;7:e31845.
108. Kouzarides T. Chromatin modifications and their function. Cell. 2007;128:693–705.
109. Shogren-Knaak M, Ishii H, Sun J-M, Pazin MJ, Davie JR, Peterson CL. Histone H4-K16 acetylation controls chromatin structure and protein interactions. Science. 2006;311:844–7.
110. Gardner KE, Allis C, Strahl BD. Operating on chromatin, a colorful language where context matters. J Mol Biol. 2011;409:36–46.
111. Suganuma T, Workman JL. Signals and combinatorial functions of histone modifications. Annu Rev Biochem. 2011;80:473–99.
112. Ferreira H, Flaus A, Owen-Hughes T. Histone modifications influence the action of Snf2 family remodelling enzymes by different mechanisms. J Mol Biol. 2007;374:563–79.
113. Clapier CR, Langst G, Corona DF, Becker PB, Nightingale KP. Critical role for the histone H4 N terminus in nucleosome remodeling by ISWI. Mol Cell Biol. 2001;21:875–83.
114. Clapier CR, Nightingale KP, Becker PB. A critical epitope for substrate recognition by the nucleosome remodeling ATPase ISWI. Nucleic Acids Res. 2002;30:649–55.
115. Erdel F, Krug J, Langst G, Rippe K. Targeting chromatin remodelers: signals and search mechanisms. Biochim Biophys Acta. 2011;1809:497–508.
116. Rippe K, Schrader A, Riede P, Strohner R, Lehmann E, Langst G. DNA sequence- and conformation-directed positioning of nucleosomes by chromatin-remodeling complexes. Proc Natl Acad Sci U S A. 2007;104:15635–40.
117. Goldman JA, Garlick JD, Kingston RE. Chromatin remodeling by imitation switch (ISWI) class ATP-dependent remodelers is stimulated by histone variant H2A.Z. J Biol Chem. 2010;285:4645–51.

118. Hauk G, McKnight JN, Nodelman IM, Bowman GD. The chromodomains of the Chd1 chromatin remodeler regulate DNA access to the ATPase motor. Mol Cell. 2010;39:711–23.
119. Hassan AH, Awad S, Al-Natour Z, Othman S, Mustafa F, Rizvi TA. Selective recognition of acetylated histones by bromodomains in transcriptional co-activators. Biochem J. 2007;402:125–33.
120. Glatt S, Alfieri C, Muller CW. Recognizing and remodeling the nucleosome. Curr Opin Struct Biol. 2011;21:335–41.
121. Wysocka J, Swigut T, Xiao H, Milne TA, Kwon SY, Landry J, et al. A PHD finger of NURF couples histone H3 lysine 4 trimethylation with chromatin remodelling. Nature. 2006;442:86–90.
122. Das C, Tyler JK, Churchill ME. The histone shuffle: histone chaperones in an energetic dance. Trends Biochem Sci. 2010;35:476–89.
123. Ransom M, Dennehey BK, Tyler JK. Chaperoning histones during DNA replication and repair. Cell. 2010;140:183–95.
124. Alabert C, Groth A. Chromatin replication and epigenome maintenance. Nat Rev Mol Cell Biol. 2012;13:153–67.
125. Morrison AJ, Shen X. Chromatin remodelling beyond transcription: the INO80 and SWR1 complexes. Nat Rev Mol Cell Biol. 2009;10:373–84.
126. Jayani RS, Ramanujam PL, Galande S. Studying histone modifications and their genomic functions by employing chromatin immunoprecipitation and immunoblotting. Methods Cell Biol. 2010;98:35–56.
127. Truax AD, Greer SF. ChIP and Re-ChIP assays: investigating interactions between regulatory proteins, histone modifications, and the DNA sequences to which they bind. Methods Mol Biol. 2012;809:175–88.
128. Erdel F, Rippe K. Binding kinetics of human ISWI chromatin-remodelers to DNA repair sites elucidate their target location mechanism. Nucleus. 2012;2:105–12.
129. Erdel F, Schubert T, Marth C, Langst G, Rippe K. Human ISWI chromatin-remodeling complexes sample nucleosomes via transient binding reactions and become immobilized at active sites. Proc Natl Acad Sci U S A. 2010;107:19873–8.
130. Blossey R, Schiessel H. Kinetic proofreading of gene activation by chromatin remodeling. HFSP J. 2008;2:167–70.
131. Leschziner AE. Electron microscopy studies of nucleosome remodelers. Curr Opin Struct Biol. 2011;21:709–18.

ERRATUM

Structure and Mechanisms of SF1 DNA Helicases

Kevin D. Raney, Alicia K. Byrd, and Suja Aarattuthodiyil

M. Spies (ed.), *DNA Helicases and DNA Motor Proteins*, Advances in Experimental Medicine and Biology, DOI 10.1007/978-1-4614-5037-5_2,

DOI 10.1007/978-1-4614-5037-5_14

1. The author sequence in the chapter opening page should be in the below order. Suja Aarattuthodiyil, Alicia K. Byrd, Kevin D. Raney
2. Kevin D. Raney should be the corresponding author for this Chapter 2.

The online version of the original chapter can be found at http://dx.doi.org/10.1007/978-1-4614-5037-5_2

Index

M. Spies (ed.), *DNA Helicases and DNA Motor Proteins*, Advances in Experimental Medicine and Biology, DOI 10.1007/978-1-4614-5037-5,